ESTIMATING THE HISTORICAL TIMESPAN OF ARCHAEOLOGICAL PHENOMENA

Abdulrahman Sulaiman Al-Ruzaiza

A Thesis Submitted to the

University of Glasgow

for the Degree of

Doctor of Philosophy (Ph.D)

Faculty of Science

Department of Statistics

November, 1994

© *Abdulrahman Sulaiman Al-Ruzaiza, 1994*

ProQuest Number: 13834219

All rights reserved

INFORMATION TO ALL USERS
The quality of this reproduction is dependent upon the quality of the copy submitted.

In the unlikely event that the author did not send a complete manuscript
and there are missing pages, these will be noted. Also, if material had to be removed,
a note will indicate the deletion.

ProQuest 13834219

Published by ProQuest LLC (2019). Copyright of the Dissertation is held by the Author.

All rights reserved.
This work is protected against unauthorized copying under Title 17, United States Code
Microform Edition © ProQuest LLC.

ProQuest LLC.
789 East Eisenhower Parkway
P.O. Box 1346
Ann Arbor, MI 48106 – 1346

Thesis
9974
Copy 2

GLASGOW
UNIVERSITY
LIBRARY

In the name of Allah
the merciful the compassionate

To those who sacrifice for me

To my Mother;

To my Father;

To my Wife;

and To my children

To you all, I would like to dedicate this thesis.

Abstract

When a reasonably representative selection of material can be collected from an archaeological event (eg. a particular site or culture), it is often of interest to archaeologists to derive a credible historical range, based on radiocarbon measurements, for the event. Using the concept of the floruit of a culture suggested by Ottaway (1973), this thesis provides a contribution in this sphere, by which a set of calibrated dates is used to provide a calendar range (*i.e.* floruit estimate) for the archaeological event.

The thesis consists of three subsequent parts, each corresponding to a different aspect of this problem. Part one (chapter 2) deals with the basic calibration problem that uses a radiocarbon date to predict the corresponding calendar date. Part two (chapters 3-5 inclusive) considers the development and applications of five methods for estimating the floruit of an archaeological event. Part three (chapter 6) considers the question of temporal overlap between two archaeological cultures.

Chapter **1** is a general introduction to this thesis and gives a brief background to archaeological contexts and to radiocarbon dating. Definitions of the problems involved in the thesis are given and the pursued aims outlined.

Chapter **2** is concerned with the calibration problem and the fitting of the calibration curve. A non-parametric regression is used to fit the calibration curve and a Kernel method based on the regression estimator of Watson (1964) is employed. The technique of calibration of a single radiocarbon date is

reviewed and the provision of point and interval estimates for calibrated dates is discussed with consideration of the problem of multiple point estimates.

In Chapter **3**, the definition of the floruit is given and the idea of a quartile interval is considered and employed in development of five methods of floruit estimation. Three of these methods require only pencil, paper and the calibration curve to be applied, while the other two seek to estimate a frequency distribution underlying the archaeological event. A non-parametric kernel density estimation is used to construct an estimate for this frequency distribution. A cross-validation method is used to choose the smoothing parameter but, as it is not entirely satisfactory, alternative weighting methods are considered. Chapter **4** involves a simulation study to investigate the performance of the floruit interval estimation methods presented in the previous chapter over different parts of the calibration curve. Data are simulated from Normal, Skewed and Bimodal distribution functions for different combinations of sample sizes and Inter-Quartile Ranges (I.Q.R.) of the underlying frequency distribution. The performance of the five methods are compared according to four statistical criteria. Simulation results indicate that density estimation methods are superior to the others. In Chapter **5**, the performance of the five methods are compared by applying them to a selection of groups of real radiocarbon dates collected from different archaeological cultures. The effect of several factors on the floruit estimates are considered in these applications and the results for each are summarised and discussed.

Chapter **6** propounds two different approaches to quantify the degree of temporal overlap between two archaeological cultures on the basis of a set of radiocarbon dates from each culture. One is based on the proportional overlap between their frequency distributions, while the other is based on the time overlap between their floruits. Applications of these methods on real data are presented and discussed.

Finally, Chapter **7** outlines the conclusions from the preceding chapters and suggests some ideas for further work.

Table of Contents

Acknowledgements

First of all, I praise Allah who furnished me with health and strength to complete this work and without whom it would not have been completed.

Secondly, I owe a debt of gratitude to many people for providing me with every possible assistance, statistical or otherwise, during the period of my research.

On the top of the list, I would like to express my deep appreciation and gratitude to my supervisor Mr. ***Tom C. Aitchison*** for suggesting the topic of this research and for his advice, encouragement and patience throughout the period of this study.

I would also like to thank Professor ***Barbara S. Ottaway***, of the University of Sheffield, for kindly providing the data analysed in this thesis.

I wish to extend my thanks to Professor ***Ian Ford***; Head of the department, the staff members and to the fellow research students for providing me with very comfortable working environment.

I am indebted to many friends in Glasgow and Riyadh for the support they have given me. In particular, I would like to express my gratitude to Mr. ***Jasim Al-Najmawi*** and Mr. ***Abdulaziz Al-Jaser*** who were generous in their time and assistance to ease my mind from some of the family onus.

My heartfelt thanks are due to my parents and to my older brother ***'Ibrahim'*** for all their help, guidance and support, not just for the duration of my research, but in whatever I have attempted to do.

My final acknowledgement is a word of special thanks reserved for my wife for her magnificent devotion to her family and for her continuous understanding, encouragement, moral support and patience without which this research would have been made infinitely more difficult.

Abdulrahman S. Al-Ruzaiza

November, 1994.

List of Tables

Chapter 4 *Simulation Study*

List of Figures

Chapter 3 *Floruit Estimation Methods*

Chapter 4 *Simulation Study* *105*

Chapter 6 *Overlap of Archaeological Cultures*

Chapter 1

General Introduction

1.1 Introduction

Studying man's past is the main interest of archaeological science. The only information available to the archaeologist is the material remains of man's past cultures which have been left behind. These remains consist of types of artefacts which are encountered, often during extensive excavations, in different places such as pit or trench levels, caches, house floors or graves (Michels; 1973). There are a number of archaeological techniques that can be used to link these artefacts to past events which can be linked, in turn, with contexts and features by using processes of logic such as stratigraphic levels and post holes (Bowman; 1990). With the use of typology (the study of changes in pottery, tools, etc.) artefacts from one site can also be linked to those of another site or culture.

With the surviving architectural remains and the artefacts found within the culture, the archaeologist can describe the structure of the culture and its nature along with discerning the pattern of settlement and the human activities which may have taken place in the culture. For example, Galgenberg is a site of the Late Neolithic Cham culture situated in the Bavarian Alpenvorland in southern Germany which was excavated by Dr. Barbara Ottaway during the period of 1981-1986. Different types of materials and artefacts were collected from the site and used by the archaeologist to study the structure and the nature of the Galgenberg site in addition to dating it. Some of these artefacts are flint, implements and ornaments of bone and antler, stone tool, pottery and ceramic which are shown in figures 1.1a-f (Ottaway; 1988).

The main aim of this thesis is to estimate the *duration* of an archaeological phenomenon such as the occupation of a settlement or a cultural group. Therefore the dating of artefacts from such a phenomenon can be used to determine the period of time to which the phenomenon belongs.

The acceptance of radiocarbon dating (developed by Libby and his associates (Arnold and Libby; 1949)) as a chronological technique some forty years ago (Ralph; 1971) brought it to considerable usage in archaeological science. Unfortunately not all artefacts found can be radiocarbon dated but in many such circumstances a reasonably representative selection of material can be collected from a dig for radiocarbon dating. Archaeologists would (on the basis of such radiocarbon measurements) like to quote credible historical dates for the existence of the particular phenomenon. Due to long-term and short-term variations in atmospheric radiocarbon, the radiocarbon dates do not represent the true historical dates. Accordingly, a calibration procedure is required to refer the radiocarbon dates to their true historical dates. There are various methods established for the calibration of a single radiocarbon date

(Aitchison *et al.*; 1989) but the problem of collating, calibrating and summarising a group of radiocarbon dates remains an open question. A relatively simplistic approach to this problem has already been attempted (Aitchison, Ottaway and Scott; 1990). The main objective throughout this work is basically to clarify the specific nature and definition of this problem and to present in a practical manner a statistical basis to its solution by means of radiocarbon calibration. In the next section a brief background to the involved subject of radiocarbon dating is given. A more extensive background can be found elsewhere (Ralph; 1971, Fleming; 1976 and Olsson; 1991).

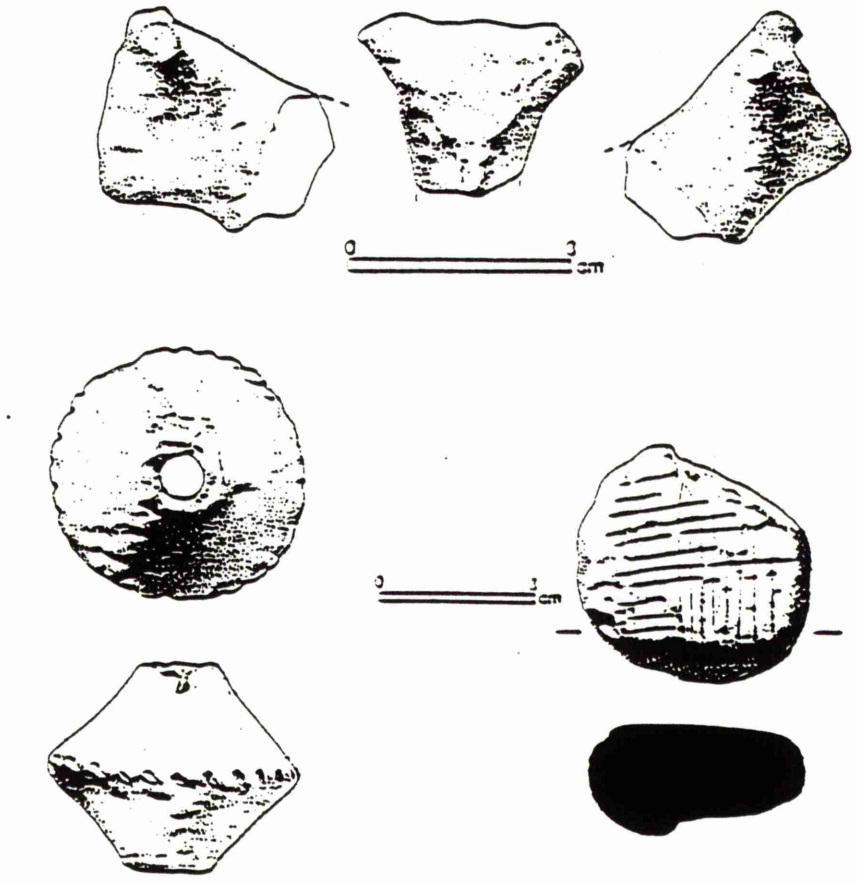

a) A zoomorphic head, a spindle whorl and an incised disc.

Figure 1.1a : Some of the archaeological materials taken from the *Cham* enclosure *Galgenberg* (Ottaway; 1988).

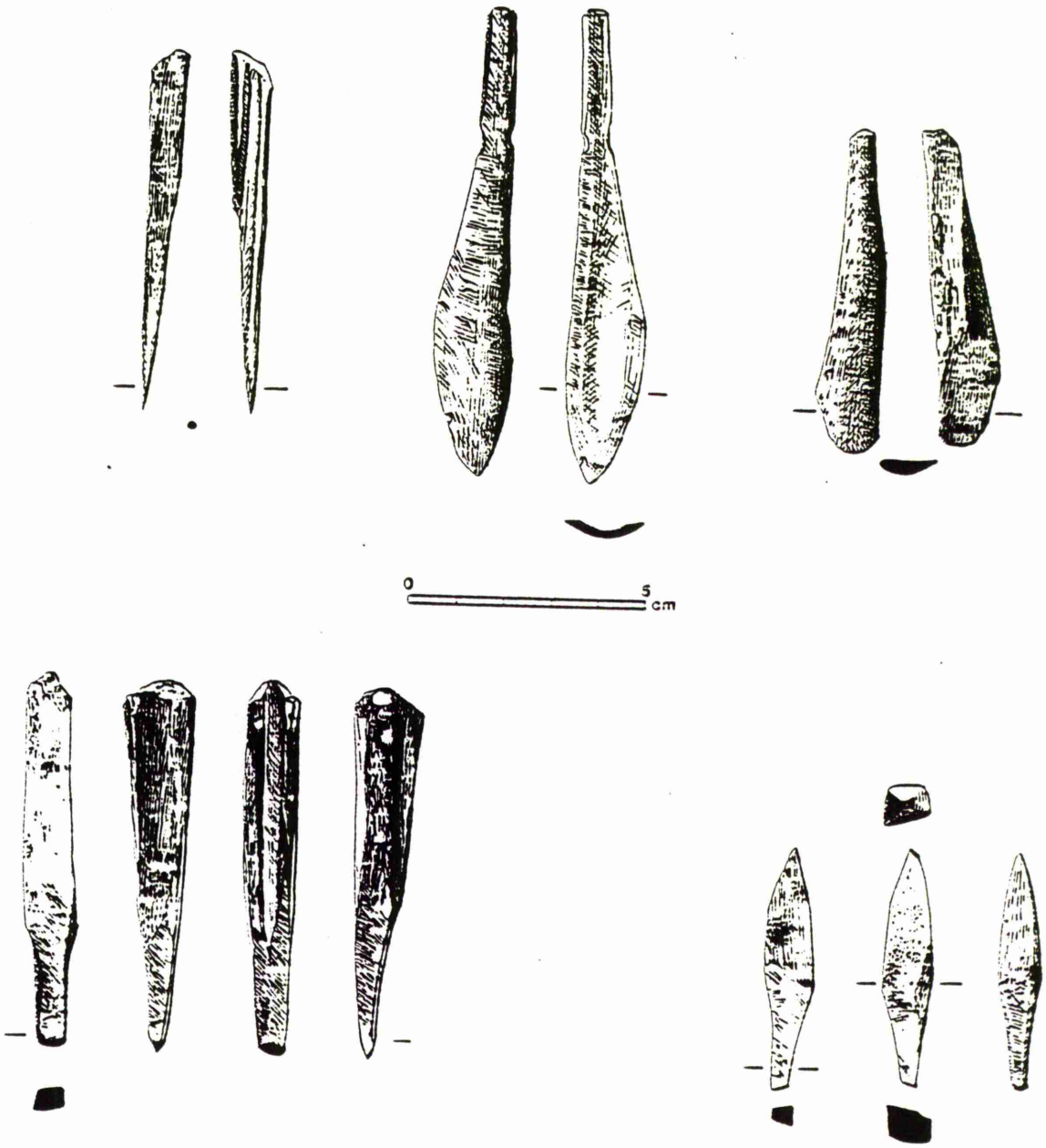

b) *Cham* bone implements.

Figure 1.1b : Some of the archaeological materials taken from the *Cham* enclosure *Galgenberg* (Ottaway; 1988).

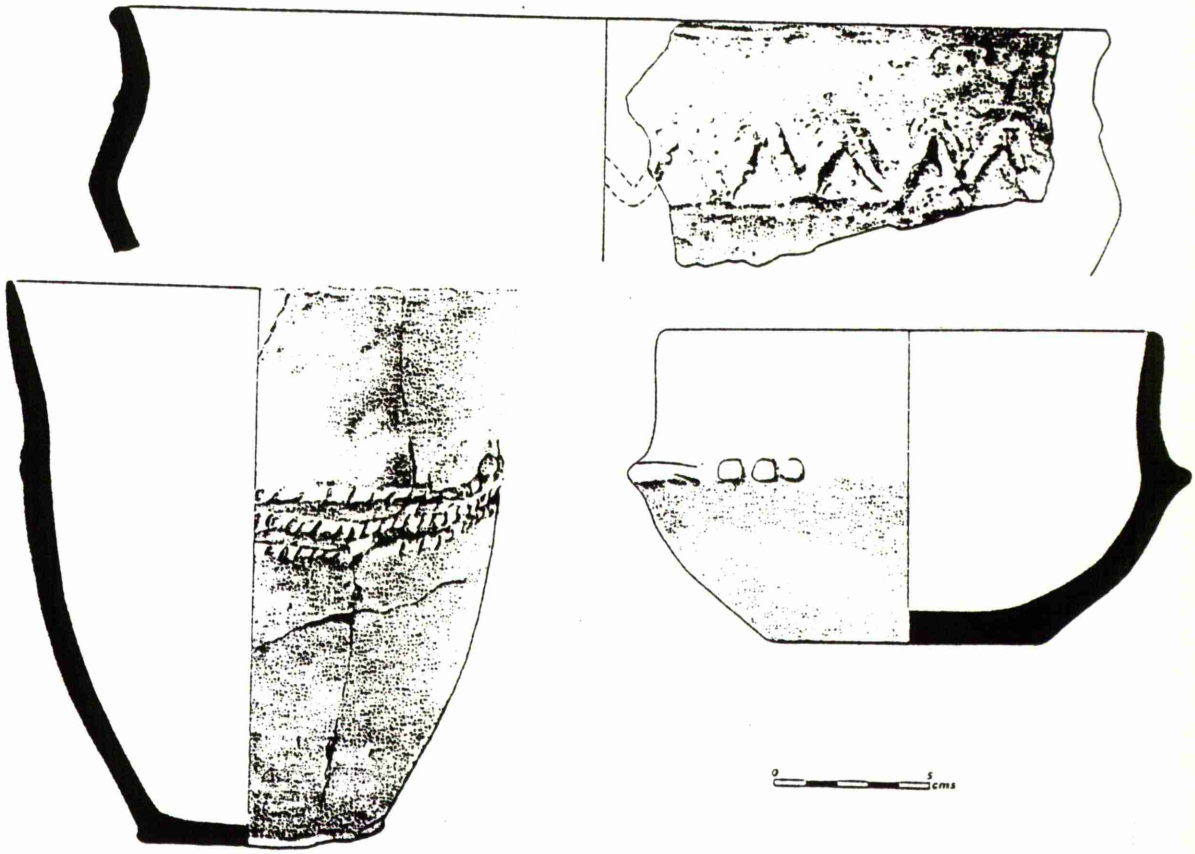

c) Characteristics *Cham* pottery

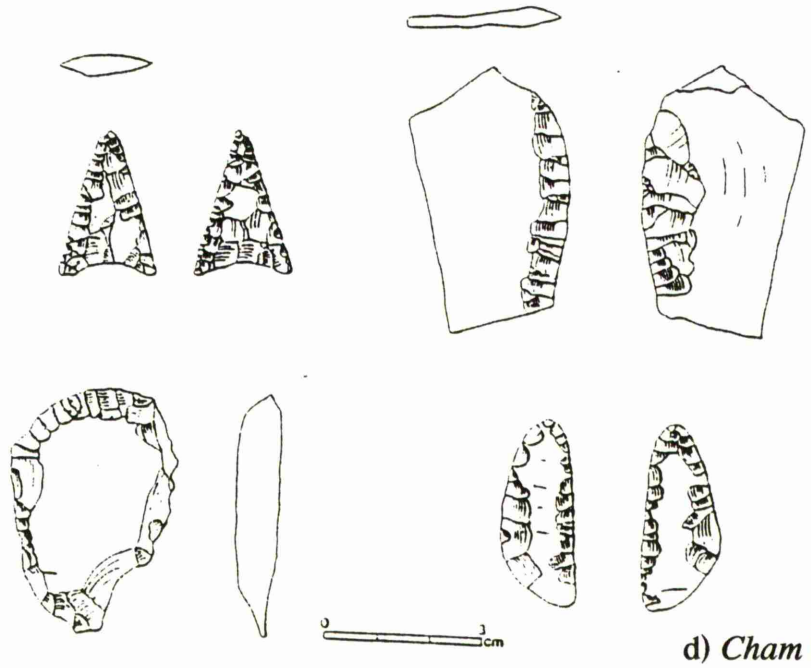

d) *Cham* flint implements

Figure 1.1 c&d : Some of the archaeological materials taken from the *Cham* enclosure *Galgenberg* (Ottaway; 1988).

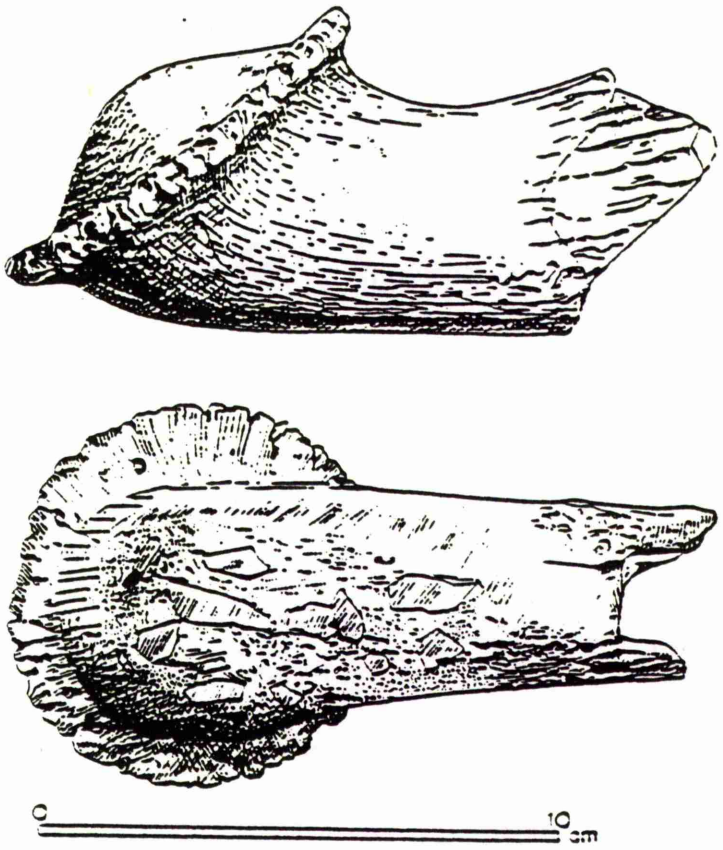

e) A shafthole antler tool.

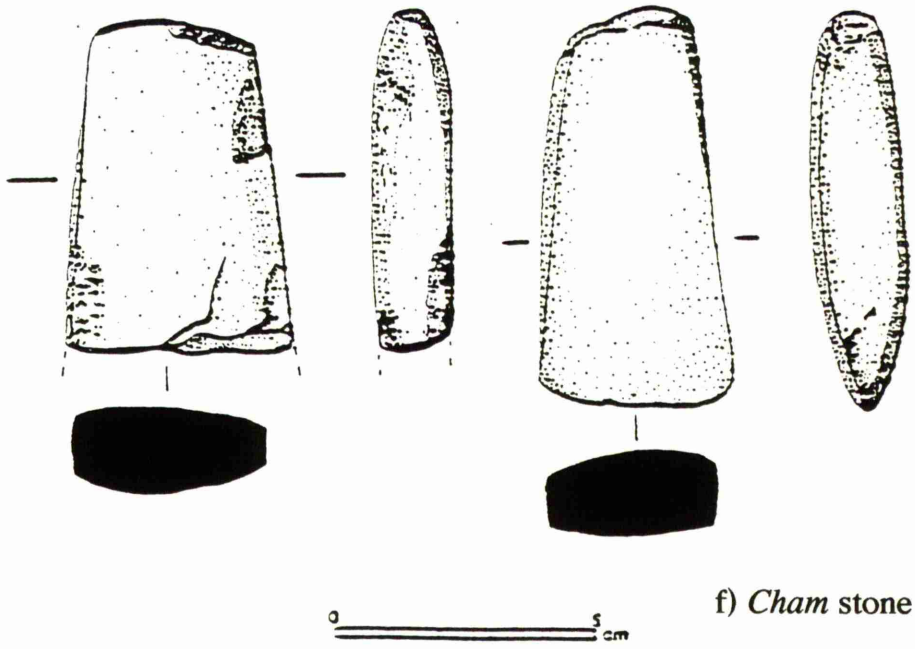

f) *Cham* stone axes.

Figure 1.1 e&f : Some of the archaeological materials taken from the *Cham* enclosure *Galgēnberg* (Ottaway; 1988).

1.2 Background to Radiocarbon Dating

Formation of radiocarbon occurs in the upper atmosphere when nitrogen atoms react with neutrons and mix rapidly with carbon dioxide. Due to the mechanism of photosynthesis all living plants absorb this (radioactive) carbon dioxide and in turn animals eat plants which makes them very weakly radioactive. Under such equilibrium conditions any amount of radiocarbon which decays away is continually replenished from the atmosphere while the organism still alive. As soon as the organism dies, it no longer breaths and ceases to acquire additional radiocarbon from the atmosphere which means its radiocarbon concentration is no longer replaced but starts to decrease slowly. The radiocarbon concentration decreases exponentially, and the loss rate of radioactivity is defined by the half-life estimated as 5568±30 years (Godwin; 1962).

1.2.1 Radiocarbon Decay and Age Measurement

The production of a radiocarbon date involves physical and chemical techniques which attempt to evaluate the concentration of the remaining radiocarbon in any sample collected, while the conversion of this measurement to radiocarbon years involves conventional methods which are followed by radiocarbon laboratories throughout the world (Harkness, 1975). There is no intention to cover the chemical techniques here; it is quite sufficient to highlight briefly the calculation of a radiocarbon date.

The exponential decay curve of radiocarbon may be expressed by the following equation (Clark, 1979)

$$A_m = A(x)\, e^{-\lambda x}$$

where A_m is the amount of radiocarbon in the sample when it is measured; $A(x)$ represents the original amount of radiocarbon in the sample when it died x years ago;

and λ denotes the decay constant and equals $(log_e 2/z)$ where z is the half-life of radiocarbon " in years ".

Solving the above equation with respect to x gives

$$x = \frac{1}{\lambda} log_e \left(\frac{A(x)}{A_m} \right)$$

the desired radiocarbon date which is normally reported with an associated standard error in years BP, where BP stand for 'Before Present' taken to be 1950 AD. The standard error emphasises the random nature of radioactive decay.

1.2.2 Datable Materials

In general organic material can be radiocarbon dated and the selection of such material should give preference to consideration of the amount of material available. This means a reliable date can be obtained from a small piece of material with a high carbon content, while large amounts are required for material containing low carbon content (Michels; 1973).

Some of the more common materials for radiocarbon dating are Charcoal, Wood, Peat, Bones, Ivory, Shells, Organic matter mixed with earth, Sediments, lake Marls, deep sea and lake Cores and Pottery.

1.3 The Problem and the Pursued Aims

On the basis of a group of radiocarbon dates from artefacts from one or more sites, the problem of estimating the timespan of an archaeological cultural group on the historical time scale is extremely important for archaeologists.

At the beginning there are two assumptions essential to any analysis attempting to estimate the timespan of an archaeological culture. The first is that there is a frequency distribution, with respect to the historical time scale, of all possible artefacts or objects from the culture which might be sampled. The second obviously assumes that the actual *datable* artefacts sampled by the archaeologist constitute a reasonably representative sample from this frequency distribution *i.e.* from the culture.

One important summary of such a frequency distribution is the ***Floruit***. This is conceptually defined as the most prolific period in the culture. It was first suggested by Ottaway (1973) and is defined mathematically as the two quartiles of the frequency distribution underlying the culture. In other words the floruit consists of the lower and upper quartiles of the frequency distribution *i.e.* it covers the middle 50% of artefacts from the culture as illustrated in figure 1.2.

Accordingly, the major aims of this work are to :-

- Use a suitable calibration curve to calibrate the radiocarbon dates into the historical time scale with an estimate of the standard error at each calibrated historical date.
- Develop the floruit estimation methods proposed in Aitchison *et al.* (1990) to provide point and interval estimates for the floruit.
- Compare and judge the performance of all the available methods of floruit estimation through a large simulation study.
- Apply these different methods to a large selection of data from real cultures to assess the difference in the methods.

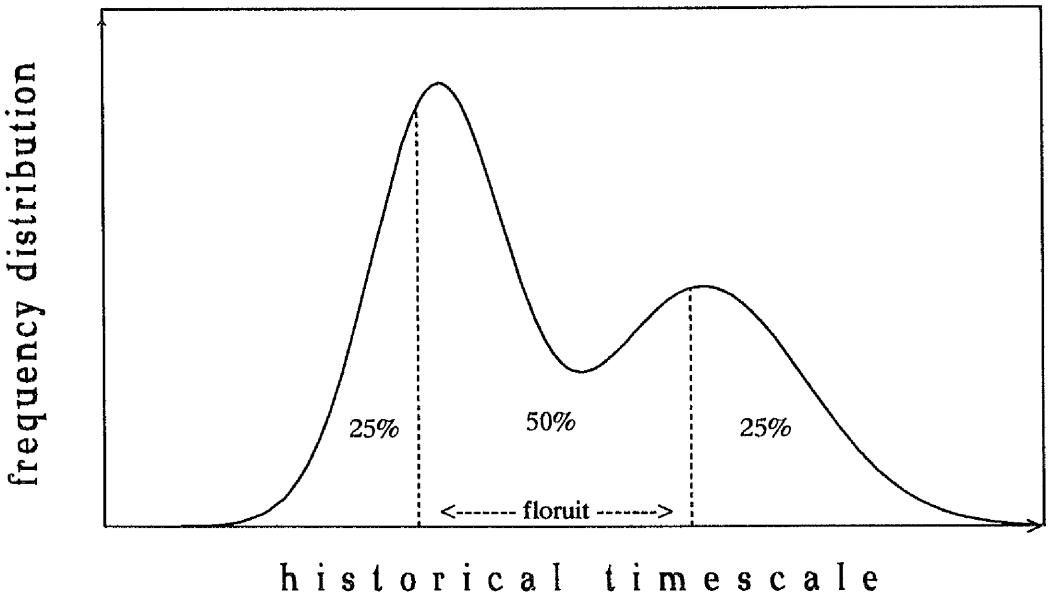

Figure 1.2 : Diagrammatic representation for the definition of the floruit of a culture.

Moreover, in the comparison of archaeological cultures, the relation of radiocarbon dates obtained from one archaeological culture to the radiocarbon dates obtained from other culture is vital to ascertain the correct chronological order of events. It is important to archaeologist to know if the occupation of settlement in one site or culture was or was not coeval with another culture in different part of the world. In other words, the archaeologists wishes to decide whether or not there is a temporal overlap between neighbouring cultures where "neighbouring" is in the geographical sense.

Accordingly the other major aim of this thesis is to produce methods to determine whether or not two distinct archaeological cultures might be contemporaneous. Briefly, the second pursued aim of this work is to:-

- Investigate the degree of overlap between two archaeological cultures.

1.4 Chapter Layout of the Thesis

This thesis is divided into three sections, each relating to a different aspect of the problems mentioned above.

The first part of the thesis, ***chapter two***, is concerned with the calibration problem. It deals with the use of a suitable non-parametric regression procedure to produce the calibration of a single radiocarbon date in terms of (multiple) potential historical dates and their appropriate standard errors.

The second section (***chapters three, four and five***) deals with floruit estimation methods and investigate their performance and applicability. ***Chapter three*** introduces five methods of floruit estimation. These methods are divided into two types. The first type involves simple ad hoc methods which require only pen and paper to provide the estimation of the floruit. The second type consists of highly computational methods based on the estimation of the frequency distribution underlying the culture. ***Chapter four*** investigates the performance of the five floruit estimation methods through a large scale simulation study. This study covers the performance of the five methods over different parts of the calibration curve. Four statistical criteria are used in the simulations to compare the performance of the five methods. ***Chapter five*** applies the five floruit estimation methods to a wide selection of real examples from archaeologically interesting cultures to illustrate their applicability. Various factors which may influence the floruit estimates such as sample size, outlier date, shape and degree of smoothing of the calibration curve are considered in these applications.

The third major part of this thesis, ***chapter six***, is concerned with the problem of measuring the temporal overlap between two neighbouring archaeological cultures. Two distinct methods are proposed. The first measures the proportional overlap using density estimation functions of the two cultures while the second measures the time overlap between the floruits of the two cultures.

Chapter **2**

Calibration of A Single Radiocarbon Date

2.1 Introduction

To interpret a radiocarbon age of an archaeological artefact in terms of its true historical age , a suitable calibration procedure must be employed. Since the first method for dating was established by Libby and his co-worker (Arnold and Libby;1949, Libby;1955), several authors, (Houtermans; 1971, Clark; 1975, Neftel; 1980, Klein *et al*; 1982) have attempted different methods to solve this problem. Recently a review for the current calibration methods for single and replicate radiocarbon dates has been published by a group of people (Aitchison *et al*; 1989).

The essential aim of this chapter is to review such procedures to enable one to estimate credible true historical ages (with appropriate errors) from which the reported radiocarbon ages may have been generated.

The essential ingredients required for the calibration exercise can be briefly summarized as follows(Aitchison and Scott; 1987):

1) a data source consisting of (successive) samples of known true historical age with corresponding measured radiocarbon ages ;

2) a suitable curve fitting approach to model the dependence of the radiocarbon age on its true historical age ;

and 3) a suitable calibration method for the radiocarbon ages to the true historical ages.

The above elements constitute the basis for the calibration mechanism, and these will be highlighted and described in this chapter.

2.2 The Data Source for the Calibration Curve — The Irish Oaks Data

The fundamental element in the construction of the calibration curve is the series of samples of known true historical age with corresponding measured radiocarbon ages. Since the radiocarbon measurements involve physical techniques, such as synthesis and counting, they are not precise in estimating the radiocarbon age and hence there will be an error associated with each radiocarbon age *i.e.* all the radiocarbon ages are reported as years "**BP**" in the form "**age ±error BP**" where **BP** stand for 'Before Present' i.e. before 1950 AD and error denotes one estimated standard error of the radiocarbon age measurement.

Initially a series of Bristlecone Pine some 8000 years long was established in the 1960's as the basis for constructing calibration curves(Bowman; 1990). More recently the series based on European oak and measured in the 'high precision' laboratories established by many people over the last fifteen years

(Pearson *et al*; 1977, Bruns *et al*; 1980, Stuiver; 1982, Pearson *et al*; 1983 and 1986) has effectively superseded the Bristlecone Pine series.

The source of the data used in this work to estimate the relationship between the radiocarbon ages and true historical ages and then to construct the calibration curve is a series of "high precision" radiocarbon measurements of Irish oaks containing 355 samples of known true historical ages ,**T**, with corresponding measured radiocarbon age , **X** , and its associated error , σ_x , from **AD 1840** to **5210 BC** taken from Pearson *et al* (1986).

These data are taken since they are likely to prove the most readily accessible and widely used source for such purposes. It should be noted however none of the theoretical work involved in this thesis depends at all on this particular source and the same ideas could be easily applied to any other such source as required.

2.3 Functional Form of the Relationship Between Radiocarbon Age (x) and Historical Age (t)

Since, at least for the data source, the historical ages are fixed and assumed known but there is variability in the reported radiocarbon ages, it is natural therefore to model the conditional relationship of **X** given **T**.

The most straightforward choice for such a relationship is to take

$$x = f(t) + \varepsilon$$

where the error ε is assumed to be normally distributed with zero mean and constant variance independent of the value of t.

The next step is to either assume a parametric or a non-parametric form for $f(t)$ *i.e.* the expected value of **X** given **T**= t.

The parametric approach involves the specification of the conditional mean of the relationship in either a linear, quadratic or polynomial regression form, and then uses least squares to estimate the parameters of the underlying specified model. For examples of this method in the radiocarbon context see Damon *et al* (1974),or Klein *et al* (1980). On the other hand the non-parametric approach does not make any overt assumption to the specified form of the relationship between the two variables except that the underlying curve is 'smooth'.

Although it is clear from figure (2.1) that the general form of the relationship is monotonic and indeed almost linear, there are sufficient significant short term deviations from linearity or 'wiggles' as they are often called in the radiocarbon literature to force one into assuming that the relationship is in fact highly complex and this requires the use of the non-parametric approach. Indeed one of the basic assumptions in the calculation of radiocarbon dates, namely that the concentration of the radiocarbon in the atmosphere is constant from year to year, is certainly untrue, even before the Industrial Revolution, so that annual fluctuations in the atmospheric radiocarbon concentration will themselves necessitate short term deviations from linearity. A final reason for this choice is that it is more flexible and allows the data itself to dictate the shape of the relationship.

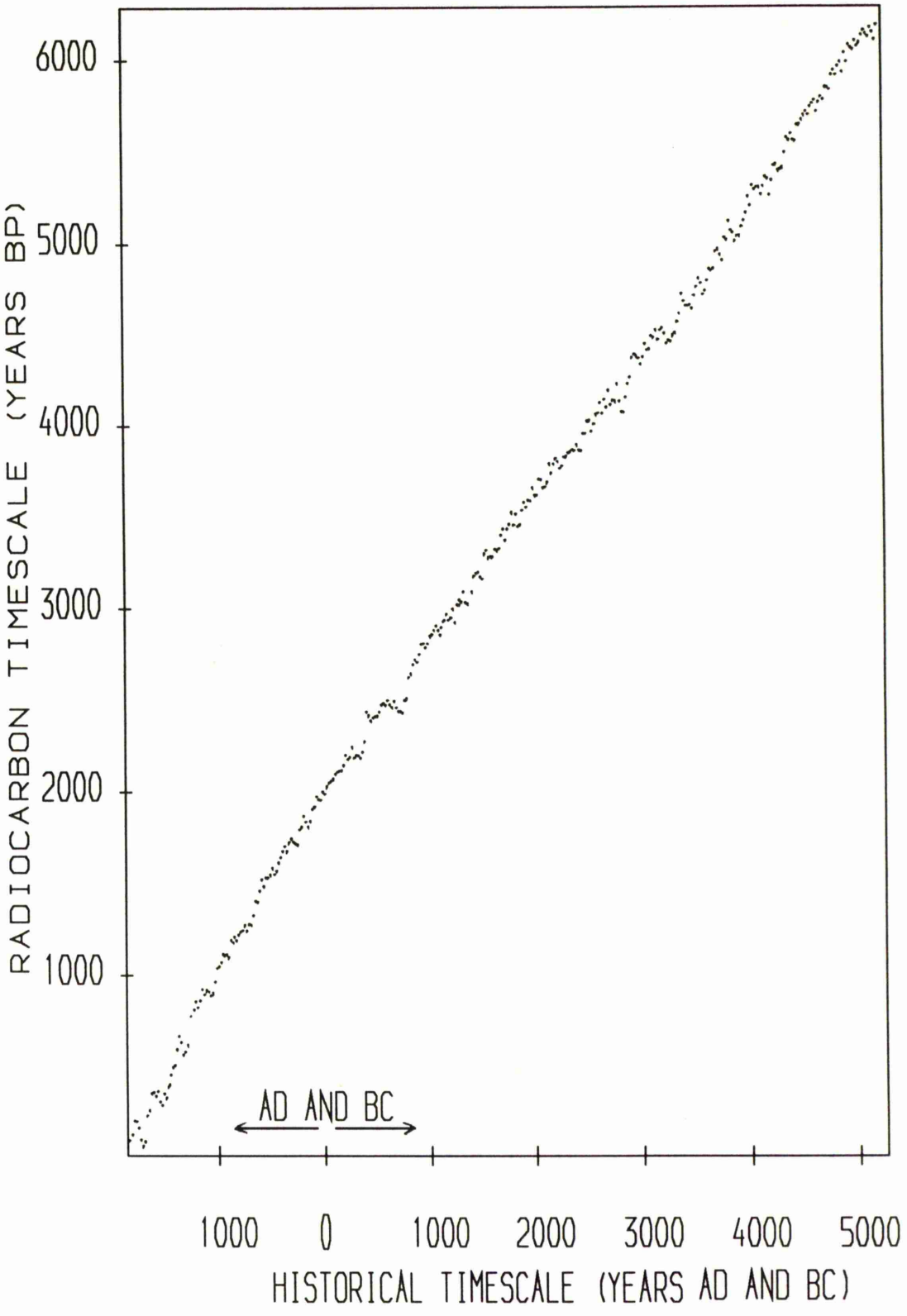

Figure 2.1 : Scatter plot for the Irish oaks data showing true historical ages versus radiocarbon dates.

2.4 Fitting the Calibration Curve

Here a non-parametric regression method has been used to fit the Irish oaks data, *i.e.* the only information available about the functional dependence of the radiocarbon ages on the true historical ages is that it is a smooth function.

So if the data $\{(t_i, x_i)\ ;\ i=1,2,.....,n\}$ consists of historical age t_i and corresponding radiocarbon age x_i with estimated standard error σ_i then the model is

$$x_i = f(t_i) + \varepsilon_i \qquad i=1,2,.....,n \qquad .....(2.1)$$

where $f(t)$ is the 'unknown' radiocarbon calibration curve at time t, ε_i is the variability induced by radiocarbon dating and these are assumed to be independent random variables each with zero mean and a standard error of σ_i.

As the exact form of the radiocarbon calibration curve, $f(t)$, is unknown, then the first task is to provide an estimate, $\hat{f}(t)$, and take account of the error which must be associated with this estimate.

In general, there are in fact various approaches to non-parametric regression many of these such as, smoothing splines (Neftel; 1980), fourier smoothing (Houtermans; 1971, Klein *et al*; 1982) and convoluted smoothing (Clark; 1975) have been already employed in the radiocarbon context. These methods have recently been compared by Aitchison and Scott (1987) and they found that the differences between fitting the various non-parametric regression methods on the same data are really not very substantial and that the choice of smoothing parameter is more crucial than the choice of the method itself.

Here Kernel methods are employed basically because they are computationally very simple and an estimate of the error in the fitted curve is easily derivable (conditional of course on the choice of smoothing parameter)

unlike some of the other methods. The technique adopted here is based on the Kernel regression estimator of Watson (1964).

The basic form of the kernel estimator is

$$\hat{f}(t) = \sum_{i=1}^{n} x_i \; w_i(t) \qquad .....(2.2)$$

where $w_i(t)$ is a "weight function" involving a smoothing parameter λ (to be determined) , and can be defined as follow

$$w_i(t) \propto \frac{1}{\sigma_i} \; exp\left(-\frac{1}{2}\left(\frac{(t-t_i)}{\lambda\,\sigma_i}\right)^2\right) \qquad i=1,2,.....,n$$

$$\text{subject to} \qquad \sum_{i=1}^{n} w_i(t) = 1$$

Clearly, the estimate is expressed as a simple weighted average of the radiocarbon dates with the weights determined by how far the age t, under consideration, is from each of the 'data source' historical ages t_i and the magnitude of the corresponding errors σ_i (*i.e.* a weighted average of the , x_i , where the weights decrease as t_i gets further from t).

2.5 Choosing the Smoothing Parameter

The smoothing parameter plays a very important role in determining the shape or smoothness of the fitted calibration curve, $\hat{f}(t)$. The final estimate of the shape of the curve depends more critically on the smoothing parameter choice ,λ , than the mathematical form of the weight function w, which makes the choice of λ crucial .

As an illustration of this, figure 2.2 shows different estimates of the calibration curve for the Irish oaks data based on different choices of λ. When λ is small (e.g. λ =0.5) then one is close to linearly interpolating the data but

when λ is large (e.g. λ =5.0) then one is beginning to over smooth (possibly) the curve, and indeed if one lets λ =20.0 then this will reduce to linear regression and eventually towards $\hat{f}(t)$ simply reducing to a weighted average of the x_i, namely

$$\frac{\sum_{i=1}^{n} \frac{x_i}{\sigma_i^2}}{\sum_{i=1}^{n} \frac{1}{\sigma_i^2}}$$

One automatic way to choose λ is to allow the data itself to assess the amount of smoothing required (*i.e.* a data dependent choice). This can be done through the method of cross-validation (Clark; 1977).

The basic idea of cross-validation can be described briefly in the following steps :

- *Step 1* Choose a starting value of the smoothing parameter λ (typically a small value which just about linearly interpolates the data),
- *Step 2* Omit one of the data points $\{(t_i, x_i),\ i=1,2,.....,n\}$,
- *Step 3* Evaluate the predicted value $\hat{x}_i = \hat{f}_{-i}(t_i)$ for x_i based on the remaining data points, where , $\hat{f}_{-i}(t_i)$ is the estimated function without the omitted pair involved ,
- *Step 4* Repeat steps 2 and 3 for all data points and calculate the cross-validation mean square error, that is

$$CV(\lambda) = \frac{1}{n} \sum_{i=1}^{n} \{x_i - \hat{f}_{-i}(t_i)\}^2$$ for the particular value of λ

- *Step 5* Repeat the process for a different value of the smoothing parameter λ and repeat steps 2,3 and 4, until a 'sensible' range of values of λ has been covered.

In this sense therefore the optimal choice for the smoothing parameter λ is the one which minimizes the cross-validation mean square error (*i.e.* minimizes $\mathbf{CV}(\lambda)$ over the range of λ considered suitable).

This method has been applied to the available data and the best value of smoothing parameter found to be equal to **1.37.** Once the smoothing parameter for the estimated calibration curve is chosen, attention is turned towards the amount of the uncertainty associated with the fitted curve $\hat{f}(t)$.

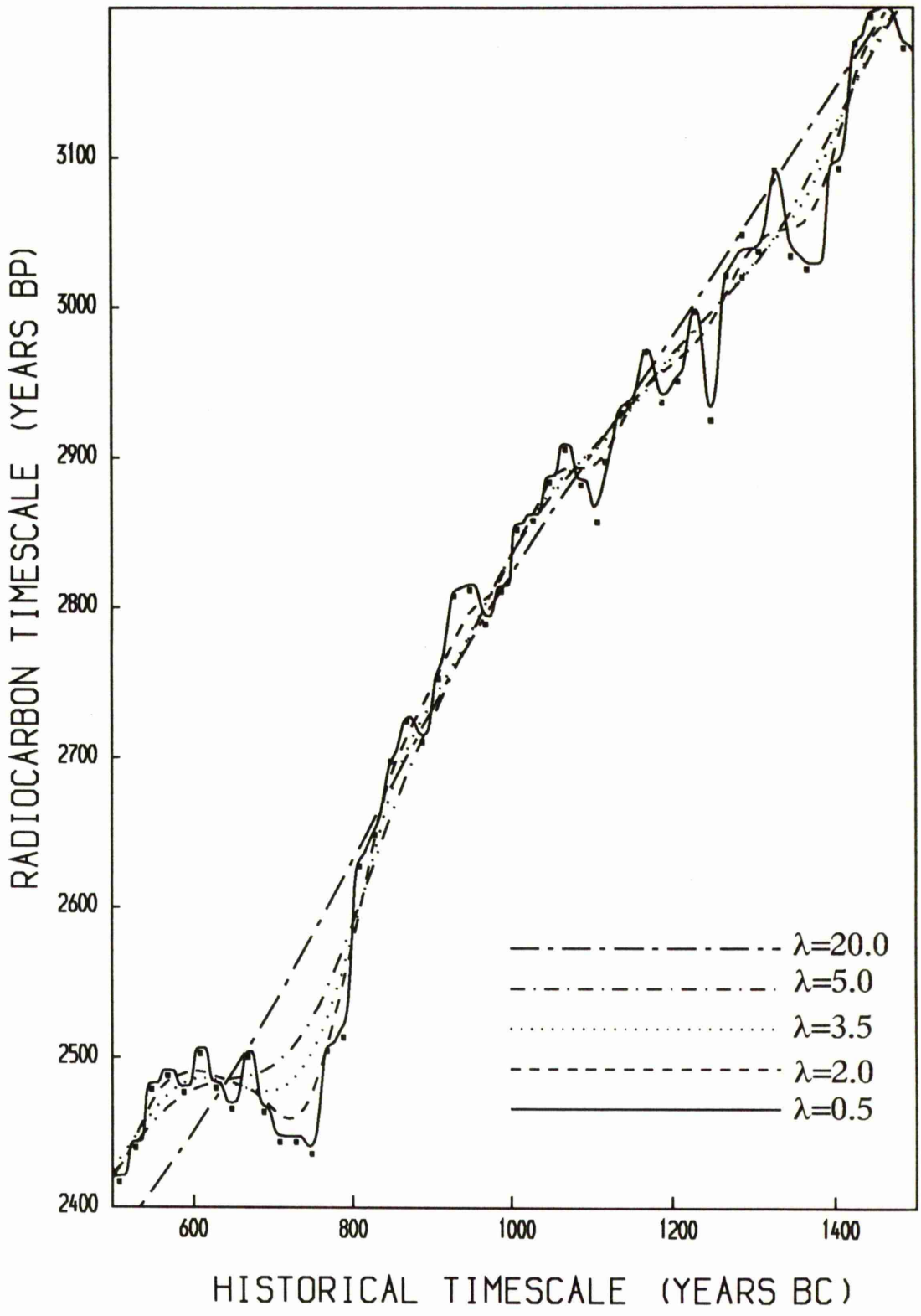

Figure 2.2 : Part from different estimates of the calibration curve for the Irish oaks data based on different choices of smoothing parameter.

2.6 Estimation of the Uncertainty on the Calibration Curve

As mentioned above, every radiocarbon age is accompanied by an error term (one standard deviation) which expresses the precision of its measurement. This quoted error is based on a number of factors including the counting error of the radioactive decay, synthesis of benzene, quenching and fractionation.

The role of the quoted error is important because of its influence on the uncertainty in the fitted calibration curve. Experimental studies from both normal and high precision laboratories based on replicate studies have found the quoted error to be a gross underestimate of the actual measurement error. For instance, Clark(1975) analysed data of relating radiocarbon age and calendar age obtained from different laboratories and recommend that the quoted error must doubled to be more realistic. Pardi and Marcus(1977) conclude that the true error approximately equal to four times those quoted. International replicate studies (International Study Group; 1982 and 1983) based on a large number of laboratories world-wide also indicate that the quoted errors do not reflect the actual true error by a factor of 2 or 3.

For the data used in the construction of the calibration curve Stuiver and Pearson (1986) suggests an overall error equal to **1.6** times the quoted error for the Radiocarbon age . This value was chosen as a rough estimate of an appropriate multiplier for the quoted (counting) error to make into a more realistic overall error which takes into account all sources of errors, and from here all radiocarbon errors will be corrected to be equal to **1.6** times the quoted value.

Finally since the estimated calibration curve was

$$\hat{f}(t) = \sum_{i=1}^{n} x_i \, w_i(t)$$

its variance will be

$$Var\left\{\hat{f}(t)\right\} = Var\left\{\sum_{i=1}^{n} x_i \, w_i(t)\right\}$$

$$= \sum_{i=1}^{n} \sigma_i^2 \left\{ w_i(t) \right\}^2 \qquad \text{(all conditional on choice of } \lambda)$$

$$= \hat{\sigma}_c^2(t) \qquad \text{.....(2.3)}$$

where $w_i(t)$ as before but with the σ_i replaced by $1.6\,\sigma_i$.

This will vary across the true historical time scale. Figure 2.3 shows that generally speaking (based on the assumed radiocarbon errors) the form of the calibration curve is well estimated at least on the larger scale. However figures 2.3A to 2.3H show the local detail and one can see more clearly when the curve is assumed to be less precisely estimated (e.g. in the range 700 to 300 AD) .

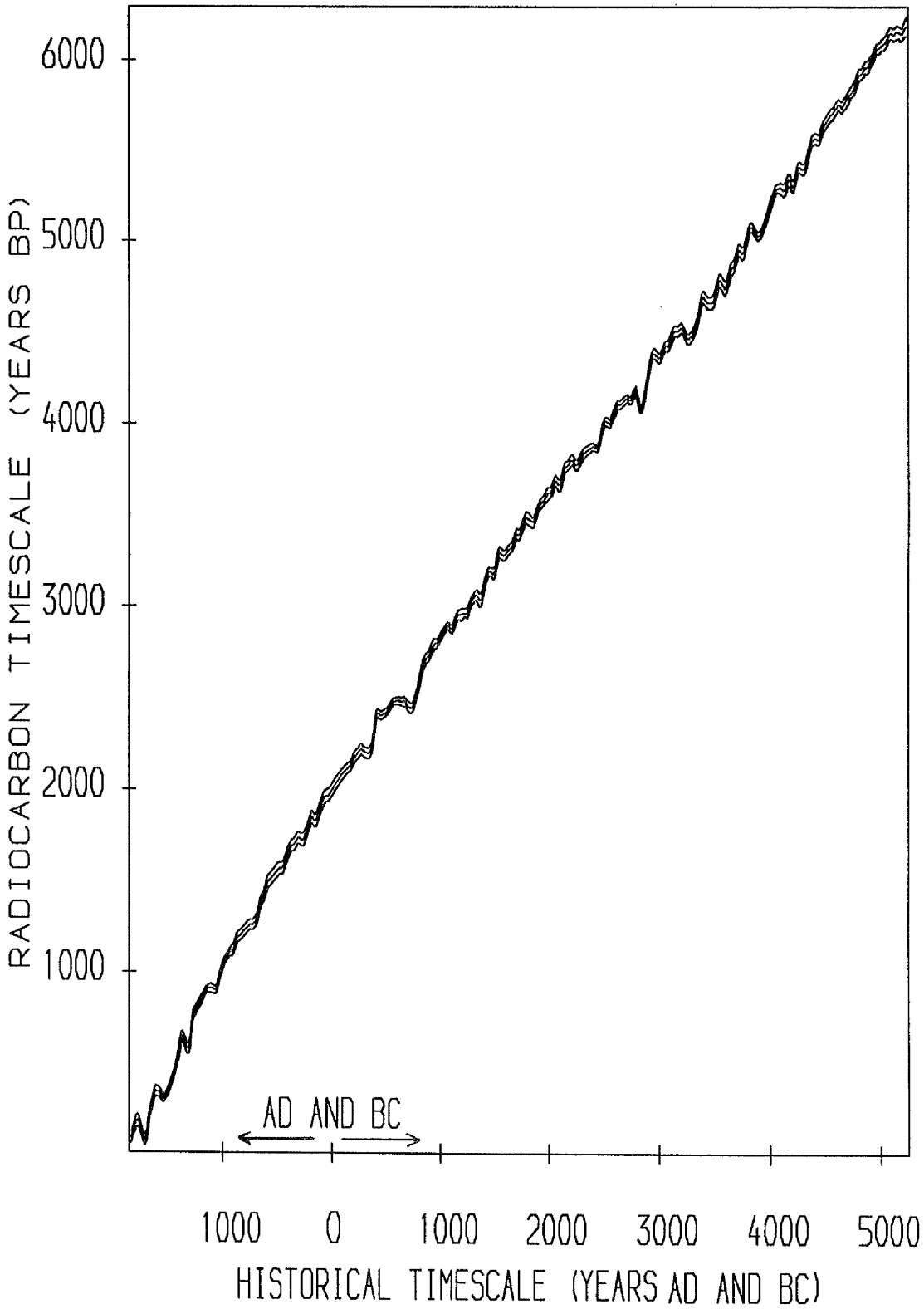

Figure 2.3 :- Estimate of the calibration curve for the Irish oaks data with the estimation of its uncertainty.

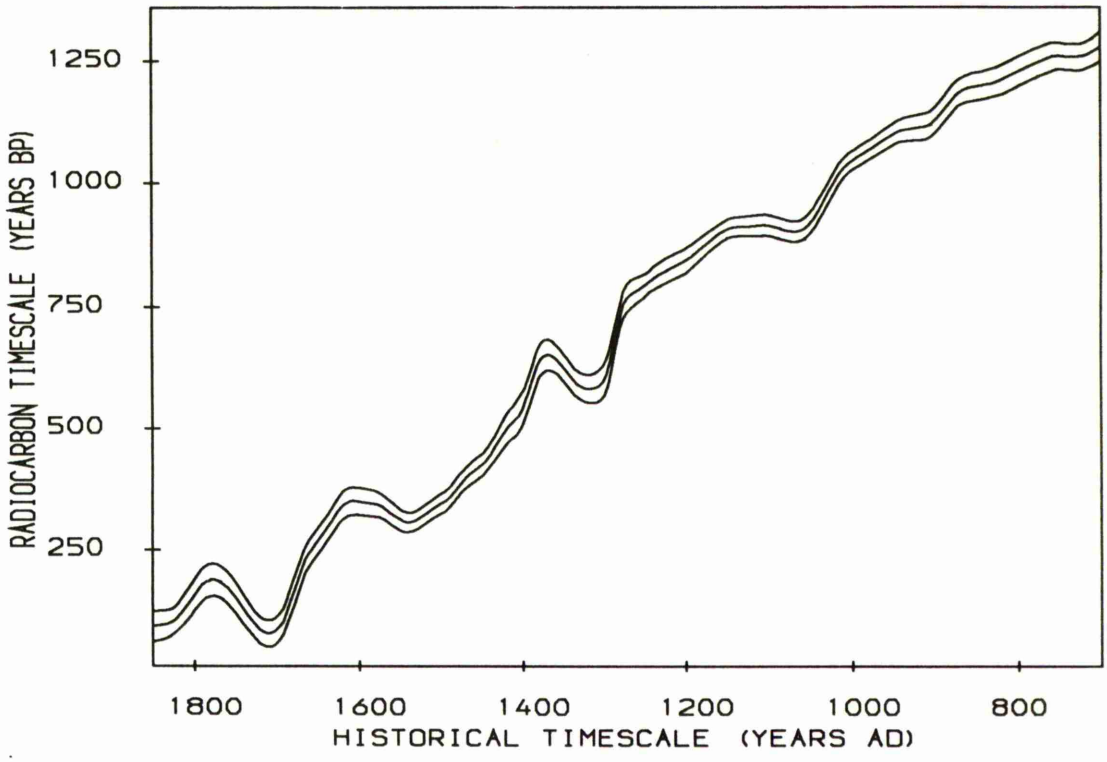

Figure 2.3 (a)

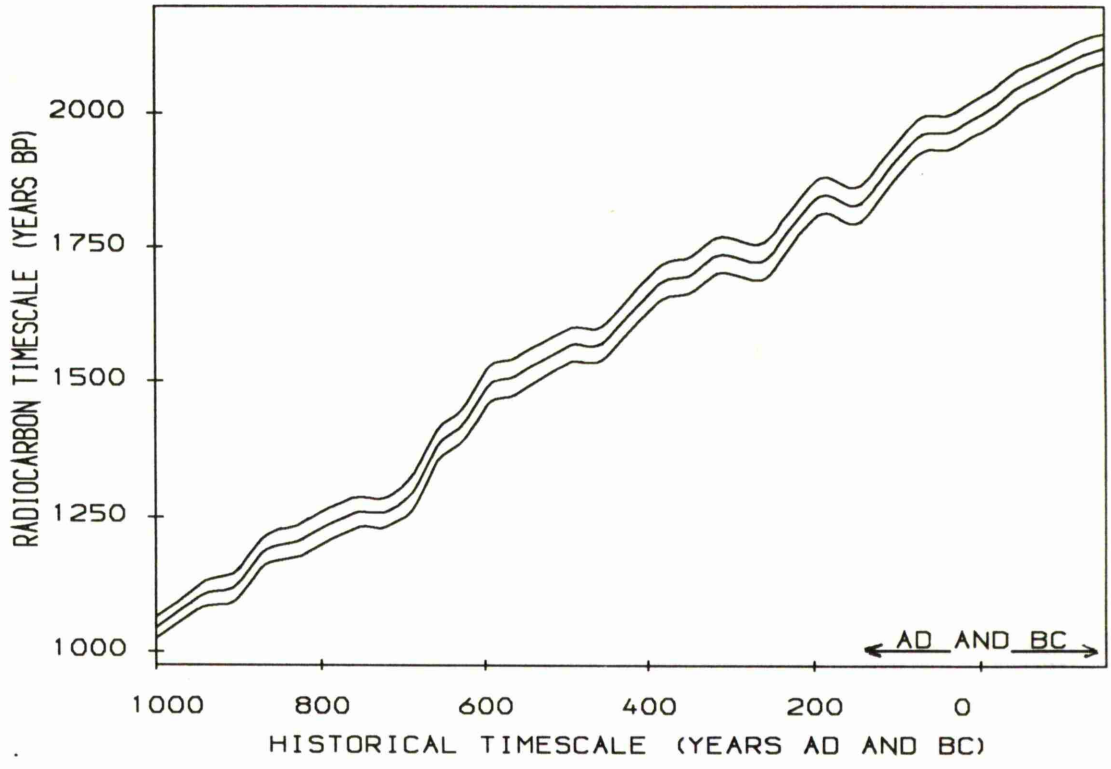

Figure 2.3 (b)

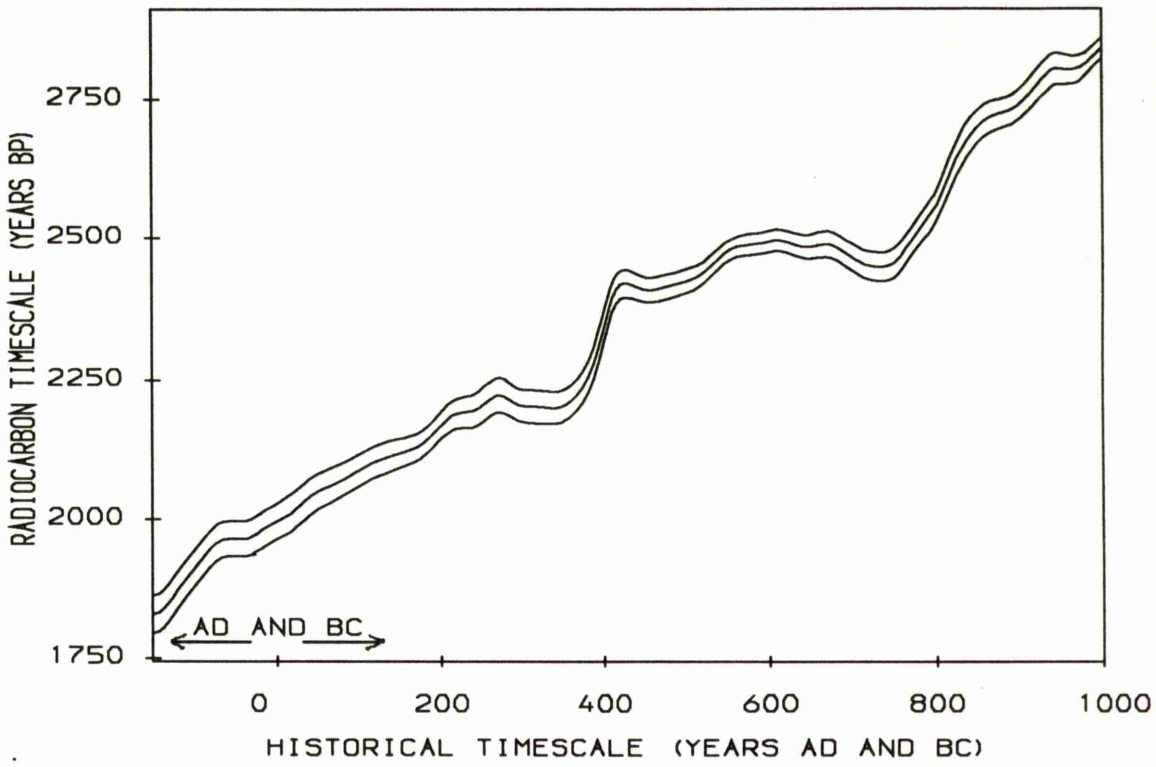

Figure 2.3 (c)

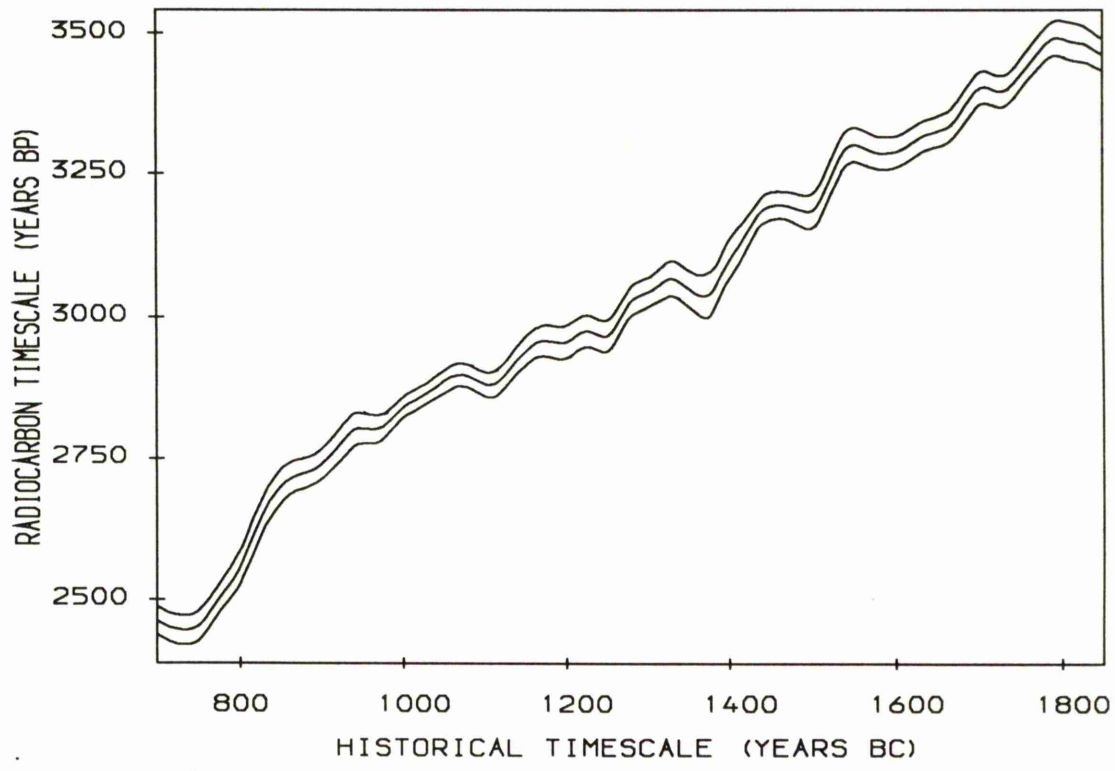

Figure 2.3 (d)

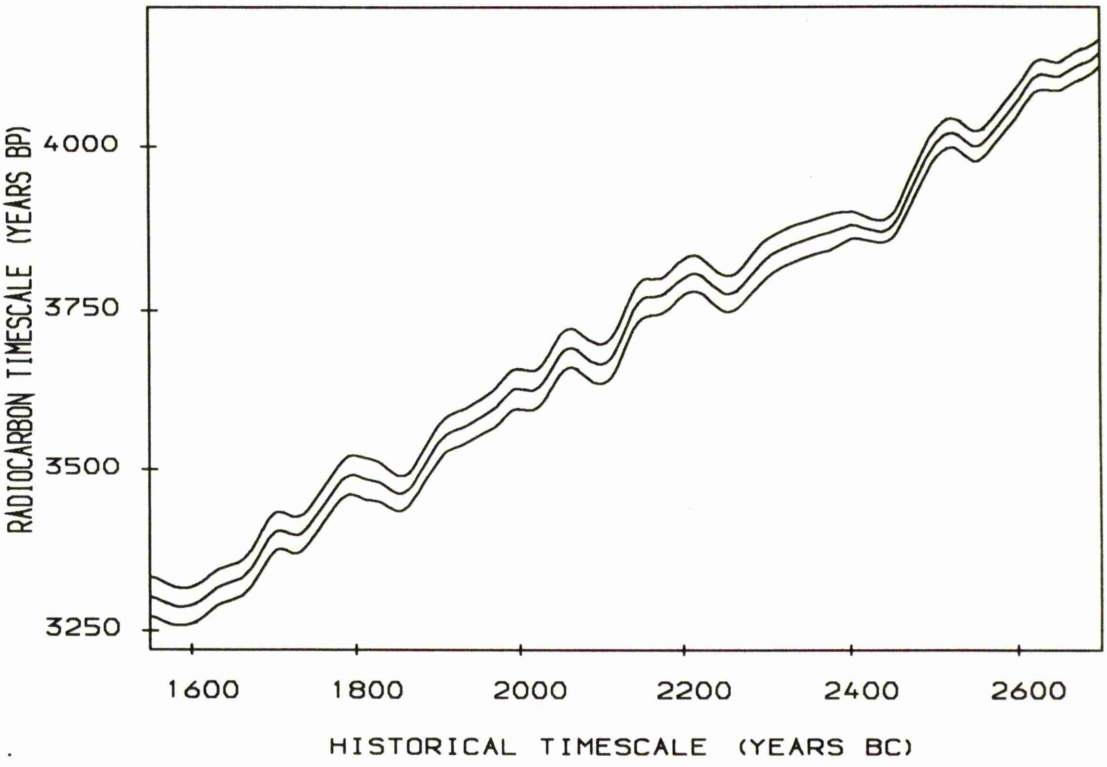

Figure 2.3 (e)

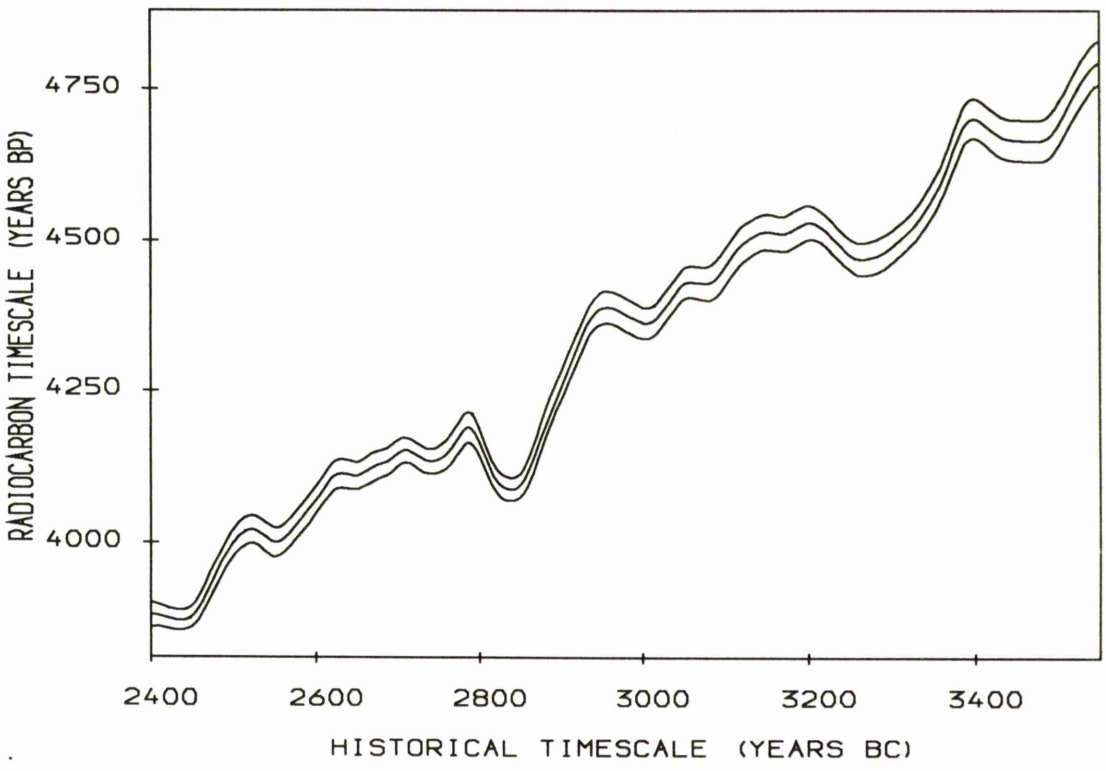

Figure 2.3 (f)

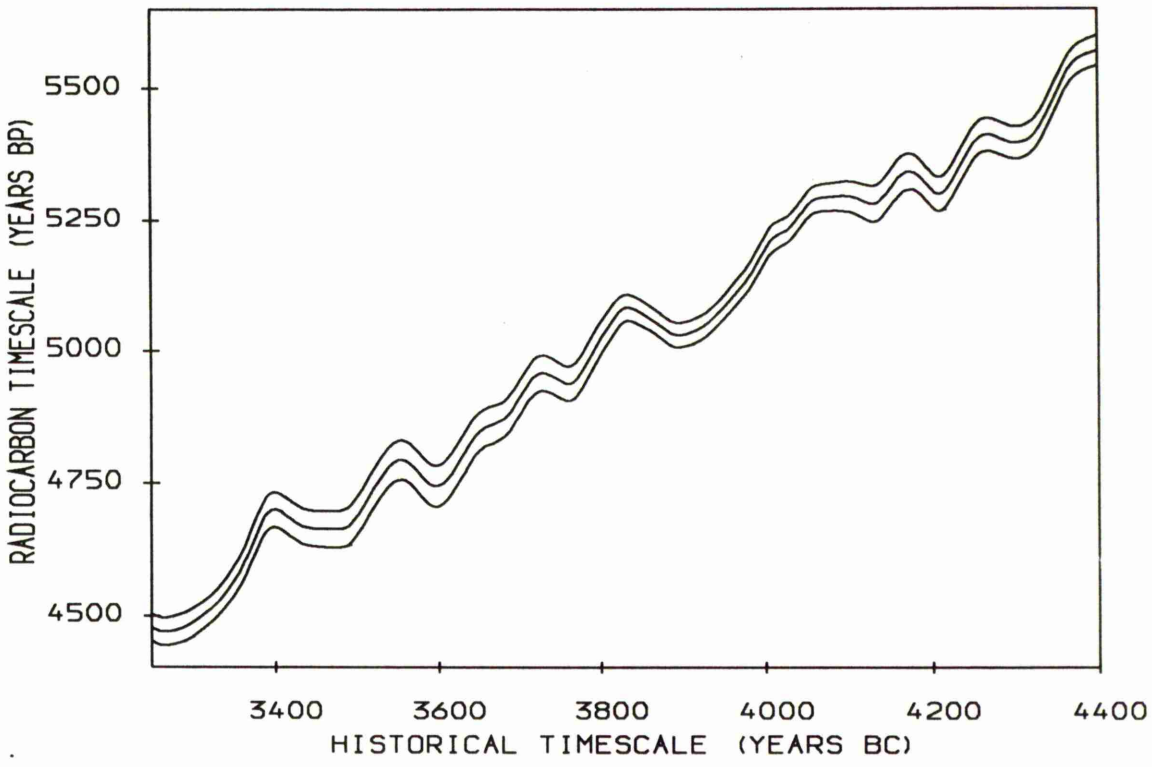

Figure 2.3 (g)

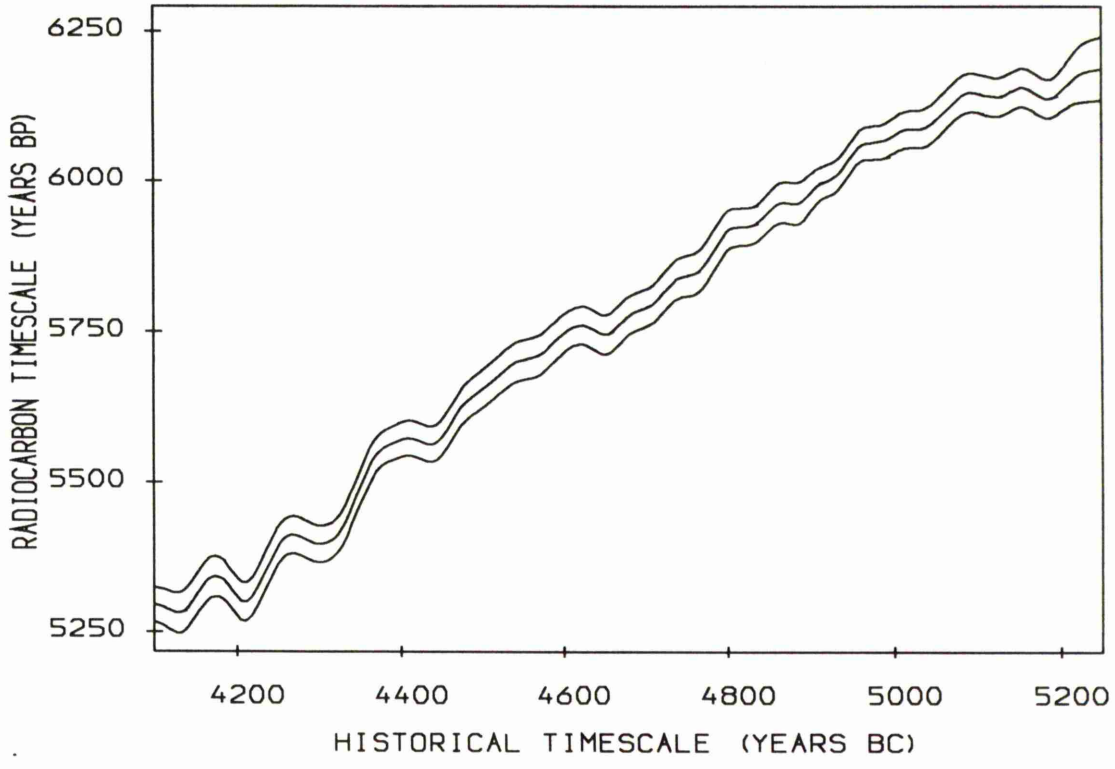

Figure 2.3 (h)

2.7 Radiocarbon Dates for Calibration

There are basically three different contexts where radiocarbon measurements are calibrated to provide point and interval estimates on the historical timescale. These are

1) a single radiocarbon measurement from an artefact or site;

2) a set of replicate radiocarbon measurements from the same material (eg. artefact)

and 3) a group of radiocarbon measurements from different materials from the same historical population.

The main emphasis of this thesis is the analysis of groups of radiocarbon dates (*i.e.* with the last type of data) which are assumed to be representative of an archaeological culture and the object as discussed in chapter one is to provide point and interval estimates for the floruit (the most prolific period in the culture) of each culture individually. Before this is dealt with directly, a review of how to calibrate a single radiocarbon date (or indeed a series of replicate dates) both from the view of point and interval estimation is carried out.

2.8 Calibration of A Single Date — Point Estimation

For the measured radiocarbon age y with standard error σ_y, the problem is to estimate the unknown true historical age, say u, for it. Due to the lack of monotonicity in the pattern of the calibration curve (commonly known as wiggles), the calibration of a single radiocarbon age is often non-trivial even if $f(t)$ is known rather than just $\hat{f}(t)$ and there was no error in the radiocarbon age y. In this section the provision of a point estimate for the true historical age u is considered in detail.

As shown in figures (2.3a to 2.3h) there are 'wiggly' sections of the calibration curve which provide multiple values of u which could correspond to the observed radiocarbon date

i.e. multiple solutions of the equation

$$y=f(u) \qquad \text{..... (2.4)}$$

although obviously in practice one have to solve the equation

$$y=\hat{f}(u) \qquad \text{..... (2.5)}$$

for all possible solutions of u. Now let the solutions to (2.5) be

$$\hat{u}_1,\hat{u}_2,.....,\hat{u}_k \qquad \text{with} \qquad \hat{u}_j=\hat{f}_j^{-1}(y) \qquad j=1,.....,k$$

where k is an odd integer number and the $\hat{f}_j^{-1}(.)$ are the appropriate inverse functions.

These estimated true ages can be evaluated through a computer search over the range of historical ages if a suitable software is available (or graphically otherwise) by intersecting the y value in the radiocarbon age axis with the fitted curve ,$\hat{f}(u)$, then projecting down onto the true historical age axis. This is illustrated in figure (2.4).

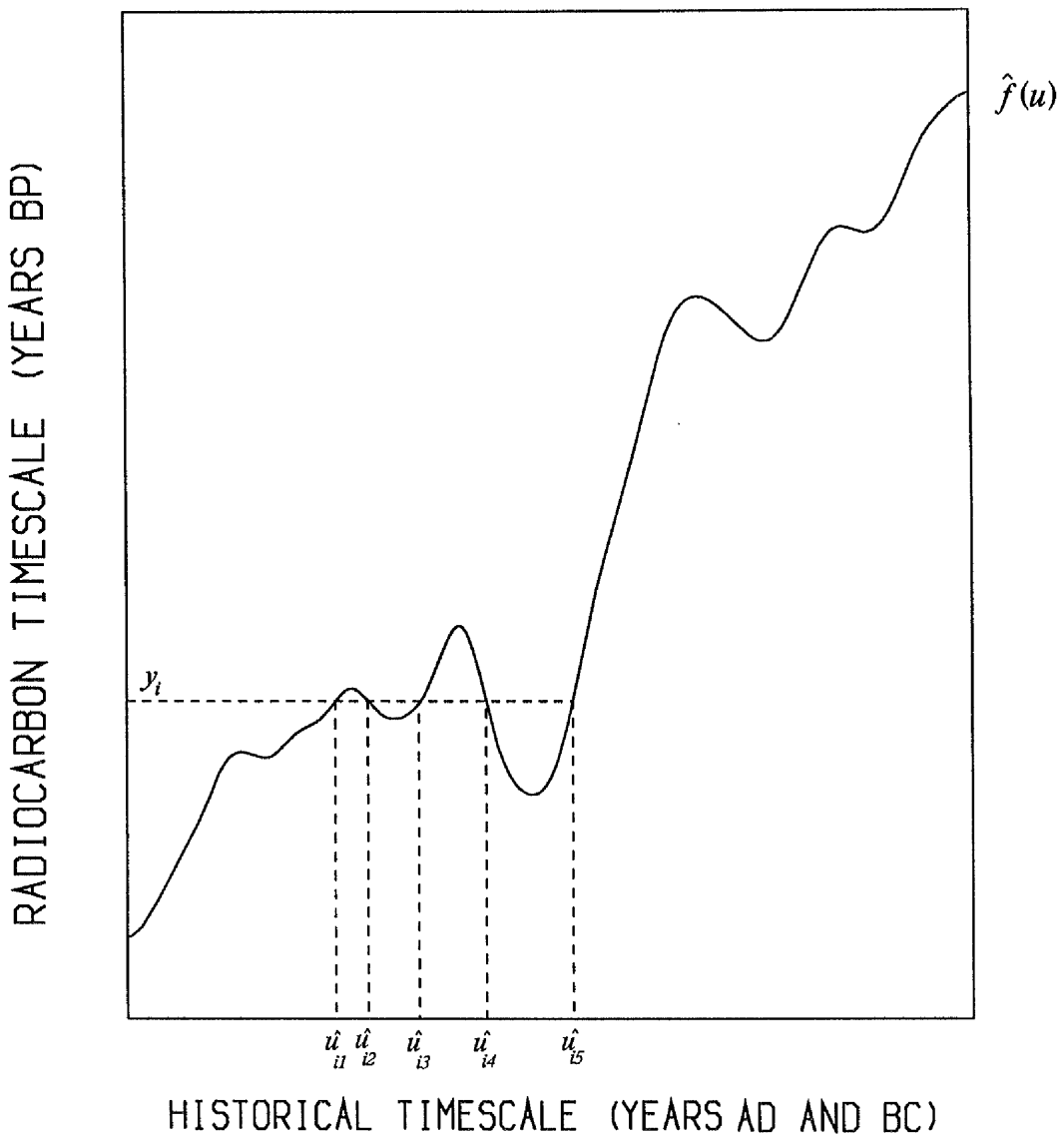

Figure 2.4 : Illustrative diagram for the calibration of a radiocarbon date y_i which corresponds to five historical ages u_{i1} - u_{i5}.

On its own the point estimate however gives no indication of the precision of the true historical age estimation and so it is necessary to incorporate in the 'overall answer' the uncertainty (*i.e.* error) in both y and $\hat{f}(\cdot)$ to provide an interval estimate for the historical age.

2.9 Calibration of A Single Date — Interval Estimation

Interval estimation of the estimated historical age u can be obtained through one or other of several different approaches based on suitable approximations. Initially two situations are considered as to whether the calibration is carried out on a monotonic or non-monotonic section of the calibration curve. Both will be considered in two cases depending on whether or not the variance, $\hat{\sigma}_c^2(u)$, is assumed constant.

To illustrate the difficulties and pitfalls involved in constructing an interval estimate for u with some prescribed confidence (usually 95%) it is useful to consider first the corresponding problem in simple linear regression.

2.9.1 The Simple Linear Case

If a linear model $f(t) = \alpha + \beta t$ had been fitted to the data then a pivotal function for u would be

$$\frac{y-(\hat{\alpha}+\hat{\beta}u)}{\sqrt{\sigma_y^2+\hat{\sigma}_c^2(u)}} \sim t(n-2) \qquad \text{....(2.6)}$$

where $$\hat{\sigma}_c^2(u) = \hat{\sigma}^2\left(\frac{1}{n}+\frac{(u-\bar{t})^2}{S_{tt}}\right) ;$$

$$\hat{\sigma}^2 = \frac{\sum_{i=1}^{n}\left(x_i-\hat{f}(t_i)\right)^2}{n-2} \quad \text{and} \quad S_{tt} = \sum_{i=1}^{n}(t_i-\bar{t})^2$$

i.e. the pivotal function is of the form

$$\frac{y-\hat{f}(u)}{\sqrt{\sigma_y^2+\hat{\sigma}_c^2(u)}} \sim t(n-2) \qquad \text{.....(2.7)}$$

Now from equation (2.6) above, if u in the vicinity of $\bar{t}$ (or if S_{tt} is very large) then $\hat{\sigma}_c^2(u)$ is effectively constant, at say $\hat{\sigma}_c^2$, and an approximate

95% C.I. for u would be obtained as:

$$I(u) = \left\{ u: \left| \frac{y-(\hat{\alpha} + \hat{\beta}\, u)}{\sigma^*} \right| \leq t(n-2; 0.975) \right\}$$

with $\sigma^* = \sqrt{\sigma_y^2 + \hat{\sigma}_c^2}$

$$\Rightarrow \quad I(u) = \left\{ u: \quad u \in \frac{y-\hat{\alpha}}{\hat{\beta}} \pm \frac{t(n-2; 0.975)\ \sigma^*}{\hat{\beta}} \right\}$$

$$\Rightarrow \quad I(u) = \left\{ u: \quad u \in \hat{f}^{-1}(y) \pm \frac{t(n-2; 0.975)\ \sigma^*}{\hat{f}'(u)} \right\} \qquad .....(2.8)$$

since here $f(u) = \alpha + \beta u$

and $f'(u) = \beta$ for all u

2.9.2 The Non-parametric Regression Case — Monotonic Sections of the Curve

Now the assumption of linearity is dropped and consideration centres on monotonic sections of the calibration curve. This will be considered in the cases of $\hat{\sigma}_c^2(u)$ being assumed constant and otherwise.

2.9.2.1 Monotonic Sections with Constant Variance

The case of non-parametric regression with effectively a one-to-one relationship between the radiocarbon age and the historical age is considered. Equation (2.7) can be adapted to provide an approximate pivotal function for u although the actual choice of degrees of freedom for the t distribution is rather arbitrary since the smoothed function $\hat{f}(u)$ involves no specific parameters. Thus in such situations (i.e. monotonic increasing parts of the curve) the approximate pivotal function for u is given by

$$\frac{y-\hat{f}(u)}{\sqrt{\sigma_y^2 + \hat{\sigma}_c^2(u)}} \sim N(0, 1)$$

resulting in an approximate 95% C.I. for u of the form

$$I(u) = \left\{ u: \quad \left| \frac{y - \hat{f}(u)}{\sqrt{\sigma_y^2 + \sigma_c^2(u)}} \right| < N(0,1;0.975) \right\}$$

with again $\sigma^* = \sqrt{\sigma_y^2 + \sigma_c^2}$ and $\sigma_c^2(u) = \sigma_c^2$ assumed constant over the range of the calibration, the approximate 95% C.I for u will be of the form

$$I(u) = \left\{ u: \quad \left| \frac{y - \hat{f}(u)}{\sigma^*} \right| < N(0,1;0.975) \right\}$$

Then $$I(u) = \left\{ u: \quad \hat{f}(u) \in y \pm 1.96\ \sigma^* \right\}$$

Thus $$I(u) = \left\{ \hat{f}^{-1}(y - 1.96\ \sigma^*), \hat{f}^{-1}(y + 1.96\ \sigma^*) \right\} \qquad .....(2.9)$$

The geometric form of this interval is illustrated in figure (2.5).

As a further approximation a Taylor expansion of the function $\hat{f}^{-1}$ can be used to rewrite equation (2.9) as follows:-

Using the basic result that

$$g(w+h) \cong g(w) + h\, g'(w)$$

where $$g = \hat{f}^{-1} \quad , \quad w = y$$

and apply this first with $h = +1.96\ \sigma^*$ and then $h = +1.96\ \sigma^*$. This gives

$$\hat{f}^{-1}(y + 1.96\sigma^*) \cong \hat{f}^{-1}(y) + 1.96\ \sigma^* \left\{ \hat{f}^{-1}(y) \right\}'$$

and $$\hat{f}^{-1}(y - 1.96\sigma^*) \cong \hat{f}^{-1}(y) - 1.96\ \sigma^* \left\{ \hat{f}^{-1}(y) \right\}'$$

and since under normal regularity conditions

$$\left\{ \hat{f}^{-1}(y) \right\}' = \frac{1}{\hat{f}'(u)}$$

these reduce to $\hat{f}^{-1}(y \pm 1.96\ \sigma^*) \cong \hat{f}^{-1}(y) \pm 1.96 \dfrac{\sigma^*}{\hat{f}'(u)}$

and hence equation (2.9) becomes

$$I(u) = \left\{ u: \quad \hat{f}^{-1}(y) \pm 1.96 \frac{\sigma^*}{\hat{f}'(u)} \right\}$$

i.e.

$$I(u) = \left\{ u: \quad \hat{u} \pm 1.96 \frac{\sigma^*}{\hat{f}'(u)} \right\} \qquad \text{.....(2.10)}$$

which is the same form as equation (2.8) for the linear case. Note that $\hat{u} = \hat{f}^{-1}(y)$ and $\hat{\sigma}_c^2(u)$ does not depend on u, and in practice, of course, replace u by $\hat{u}$ in the function $\hat{f}'(u)$.

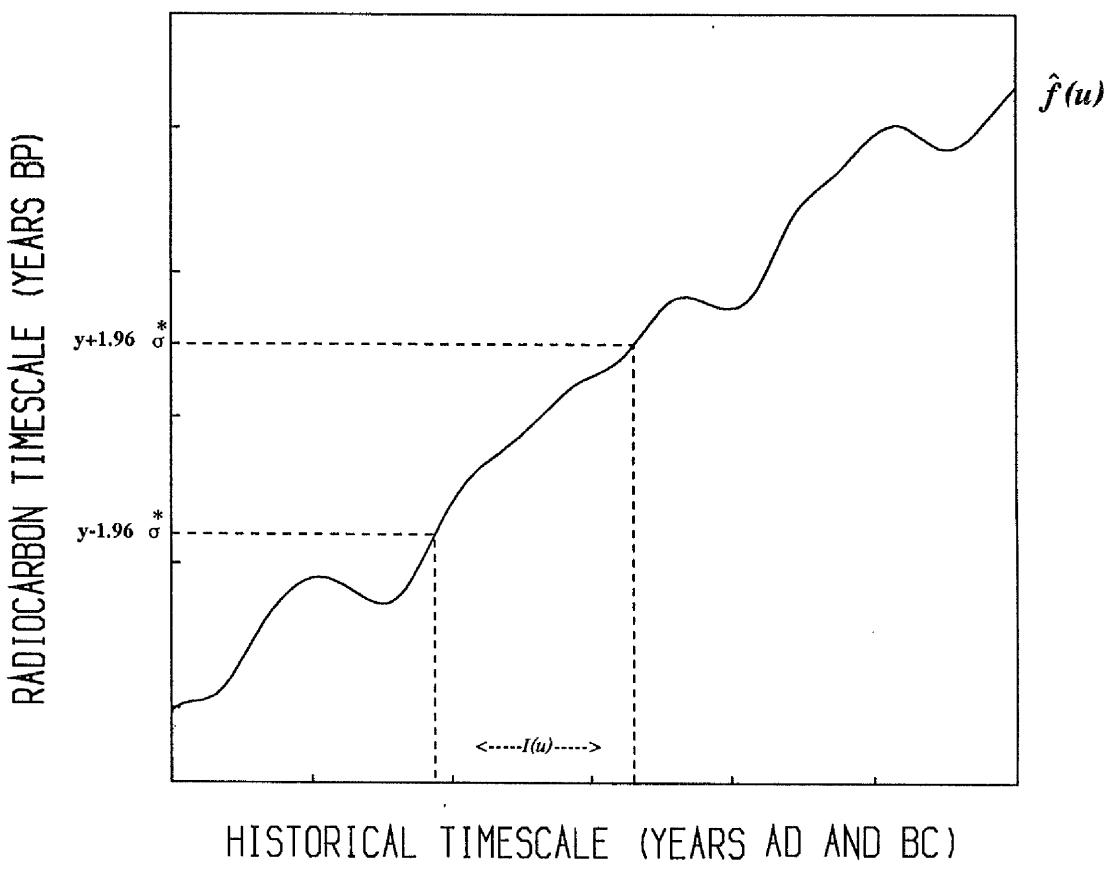

Figure 2.5 :- Diagrammatic representation shows the interval of the calibrated historical age when the variance of the curve is constant.

2.9.2.2 Monotonic Sections with Non-Constant Variance

Now return to the general case when $\hat{\sigma}_c^2(u)$ is not constant but there is still basically a one-to-one relationship between the radiocarbon age and the historical age. The pivotal function is exactly the same as before and results in an approximate 95% confidence interval of

$$I(u) = \left\{ u: \quad \left| \frac{y - \hat{f}(u)}{\sqrt{\sigma_y^2 + \hat{\sigma}_c^2(u)}} \right| < 1.96 \right\}$$

however this interval is computationally awkward to evaluate and can only be produced by carrying out a computer search over all (sensible) values of u to ascertain the set of values of u for which the observed radiocarbon age y falls in the interval

$$\left\{ \hat{f}(u) - 1.96\sqrt{\sigma_y^2 + \hat{\sigma}_c^2(u)} \ , \ \hat{f}(u) + 1.96\sqrt{\sigma_y^2 + \hat{\sigma}_c^2(u)} \right\} .$$

Since $\hat{\sigma}_c^2(u)$ now depends upon u one neat approximation available is to replace the constant σ^* in (2.10) by $\sqrt{\sigma_y^2 + \hat{\sigma}_c^2(\hat{u})}$ to get the interval of the form

$$I(u) = \left\{ u: \quad \hat{u} \pm 1.96 \ \frac{\sqrt{\sigma_y^2 + \hat{\sigma}_c^2(\hat{u})}}{\hat{f}'(\hat{u})} \right\} \qquad .....(2.11)$$

Now consider the following approximations to the exact calibration. The main reasons for this are firstly to employ a graphical approach to provide the interval (of considerable appeal to archaeologist who wishes to carry out the calibration him/herself) and secondly to generate some ideas and illustrate some results essential for the reminder of this thesis where the case of using multiple dates to estimate the duration of a culture is considered.

In practical terms the interval can be provided graphically by drawing a horizontal line parallel to the historical age axis at a height y . Where this

straight line cuts the prediction band curves $\left\{\hat{f}(u) \pm 1.96\sqrt{\sigma_y^2 + \hat{\sigma}_c^2(u)}\right\}$, drop perpendiculars onto the historical axis to give the lower and upper bounds for the 95% C.I. for the estimated historical age u as illustrated in figure (2.6).

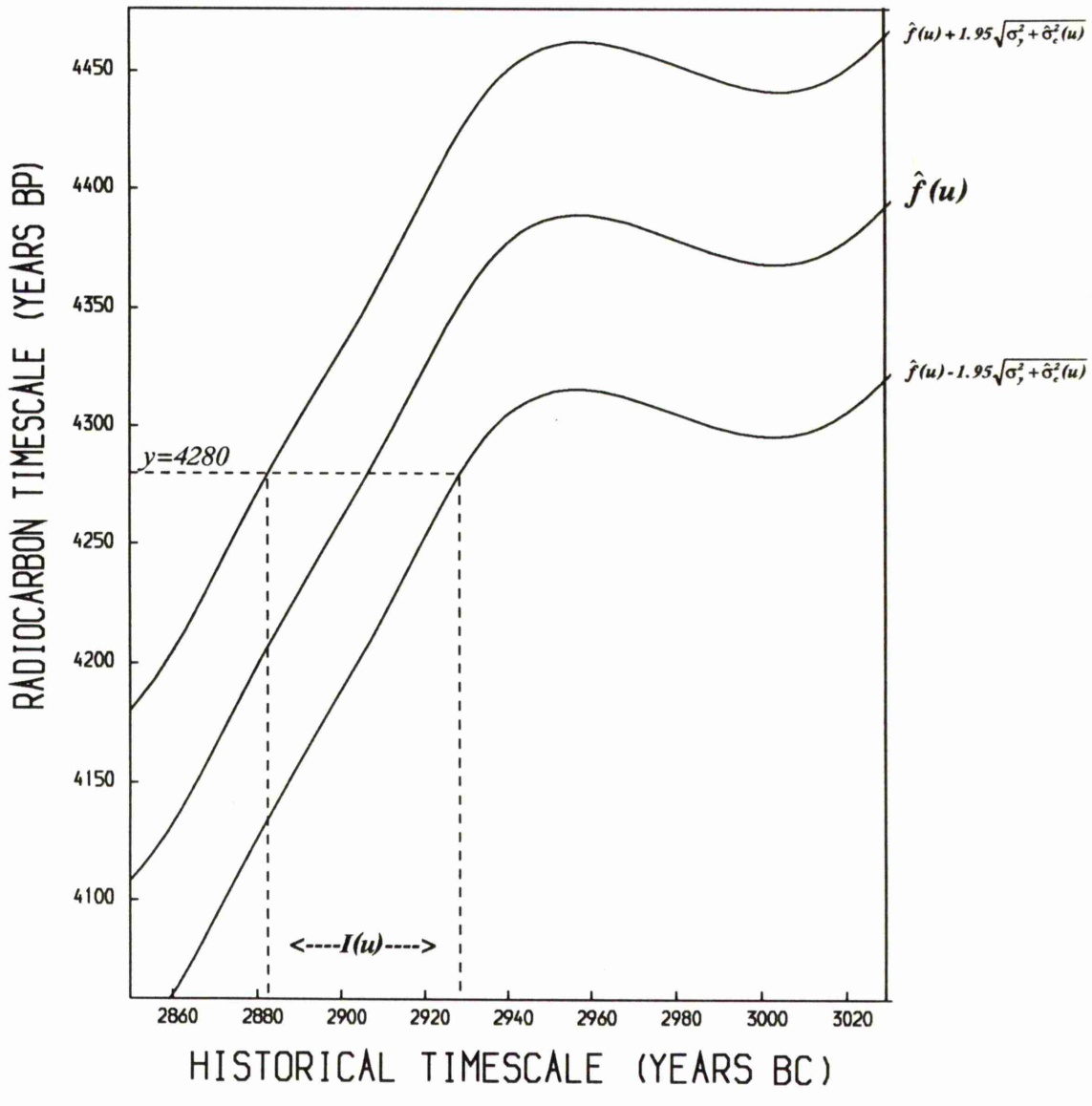

Figure 2.6 :- Production of 95% confidence interval for the historical age using the first approximation.

The major drawback to this is that the prediction bands have to be altered for each different value of σ_y. This means that in a sense every radiocarbon date to be calibrated requires a completely new set of prediction bands. Clearly this is unsatisfactory if the calibration is being carried out by hand. To overcome this, one approximation (Neftel; 1980) is to use the confidence bands for the calibration curve $\hat{f}(u)+r\,\hat{\sigma}_c(u)$ and $\hat{f}(u)-r\,\hat{\sigma}_c(u)$ and intersect them with the two lines $y\text{-}r\sigma_y$ and $y+r\sigma_y$ respectively with r=2 to give the approximate 95% C.I. for u. Aitchison and Scott (1987) found this interval is far too wide for even approximate 95% confidence and by a geometric argument they deduce that the value of r should be 1.5 to get approximate 95% C.I.'s for u (figure 2.7).

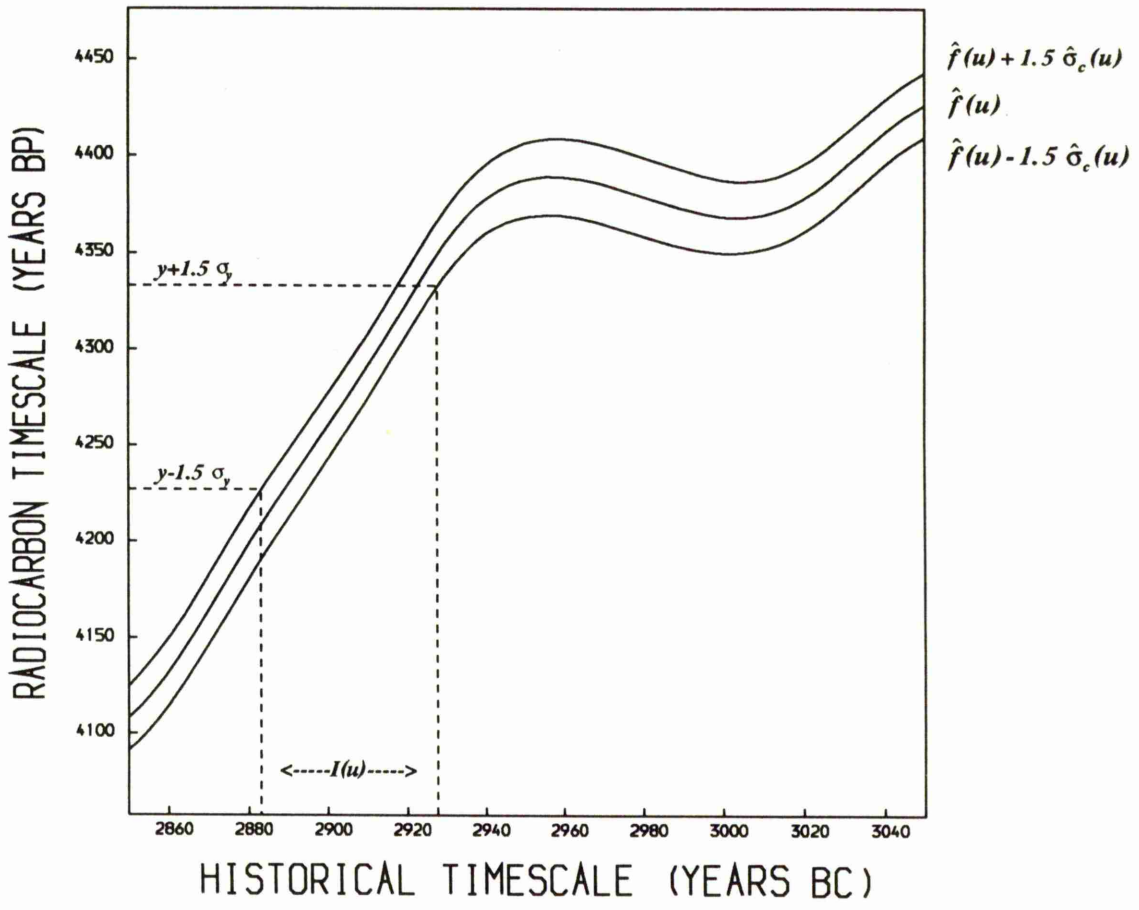

Figure 2.7 : Production of 95% confidence interval for the calibrated historical age.

Strictly speaking the interval is of the form

$$I(u) = \{u: \quad y - r\sigma_y < \hat{f}(u) + r\hat{\sigma}_c(u) \quad \text{and} \quad y + r\sigma_y > \hat{f}(u) - r\hat{\sigma}_c(u)\} \quad .....(2.12)$$

i.e. a range resulting in end points which are the solutions of the equations

$$y - r\sigma_y = \hat{f}(u) + r\hat{\sigma}_c(u)$$

and

$$y + r\sigma_y = \hat{f}(u) - r\hat{\sigma}_c(u)$$

respectively which can then be written as the solutions of

$$\hat{f}(u) = y \pm r\{\sigma_y + \hat{\sigma}_c(u)\}$$

and hence

$$u = \hat{f}^{-1}\{y \pm r(\sigma_y + \hat{\sigma}_c(u))\}$$

Thus exploiting the Taylor series expansion of $\hat{f}^{-1}$ used in section (2.9.2.1) provides the approximation

$$I(u) = \left\{u: \quad u \in \hat{f}^{-1}(y) \pm \frac{r(\sigma_y + \hat{\sigma}_c(u)}{\hat{f}'(u)}\right\} \quad .....(2.13)$$

Replacing u by $\hat{u}$ on the right hand side of this result merely requires the evaluation of $\hat{f}^{-1}(y) = \hat{u}$ and then simply replacing u by $\hat{u}$ in the functions $\hat{\sigma}_c(u)$ and $\hat{f}'(u)$ *i.e.* the only graphical information required is the inverse of the fitted calibration curve at y and its variance and slope at this point.

In summary therefore one only requires a set of curves (i.e. confidence bands for the curve) unlike the 'exact but numerically or graphically awkward method' described at the start of this section.

2.9.2.3 Illustrative Example

To clarify these ideas and approximations consider the following example:-

In a calibration of a single radiocarbon date *y=4280 B.P.* (with standard error 35 years) which corresponds to one historical date $\hat{u}$ *=2906 B.C.*, the

above approximations will be employed to provide an approximate 95% confidence interval for the historical date and their results will be compared.

In order to compare the graphical approximations with the computational approximations (based on the Taylor expansion) the derivative $\hat{f}'(\cdot)$ and the variance of the calibration curve $\hat{\sigma}_c(\cdot)$ at the point $\hat{u}$ should be evaluated and they are equal to 3.141 and 178 respectively.

For the first approximation find the two values of u which satisfy

$$y = \hat{f}(u) + 1.96\sqrt{\sigma_y^2 + \hat{\sigma}_c^2(u)}$$

and $$y = \hat{f}(u) - 1.96\sqrt{\sigma_y^2 + \hat{\sigma}_c^2(u)} \ .$$

The solutions of these are 2883 BC and 2929 BC respectively which are provided graphically as illustrated in figure (2.6) and confirmed by computer search over a range of historical ages u.

For the approximation based on the Taylor expansion of the function $\hat{f}^{-1}$ in the first approximation, substitute the values of $\hat{u}$, σ_y^2, $\hat{\sigma}_c^2(\hat{u})$ and $\hat{f}'(\hat{u})$ into equation (2.11). The corresponding interval is

$$I(u) = \left\{u: \quad \hat{u} \pm 1.96 \ \frac{\sqrt{\sigma_y^2 + \hat{\sigma}_c^2(\hat{u})}}{\hat{f}'(\hat{u})}\right\}$$

$$= \left\{u: \quad 2906 \pm 1.96 \ \frac{\sqrt{(35)^2 + 178}}{3.141}\right\}$$

$$= \{2883, 2930\} \text{ BC.}$$

For the other approximation (Neftel; 1980, Aitchison and Scott; 1987) which use the graphical approach illustrated in figure (2.7) find the two values of u which are the solutions of the equations

$$y - 1.5\ \sigma_y = \hat{f}(u) + 1.5\ \hat{\sigma}_c(u)$$

and $$y+1.5\ \sigma_y = \hat{f}(u) - 1.5\ \hat{\sigma}_c(u)$$

These values are 2883 BC and 2928 BC respectively.

For the last approximation based on the Taylor expansion, again substitute the values of $\hat{u}$, σ_y, $\hat{\sigma}_c(\hat{u})$ and $\hat{f}'(\hat{u})$ into equation (2.13) and obtained the required interval, that is

$$I(u) = \left\{u: \quad \hat{u} \pm \frac{1.5\ (\sigma_y + \hat{\sigma}_c(\hat{u})}{\hat{f}'(\hat{u})}\right\}$$

$$= \left\{u: \quad 2906 \pm \frac{1.5\ (35+\sqrt{178}}{3.141}\right\}$$

$$= \{2883\ ,\ 2929\}\ \text{BC}.$$

All of these intervals are rounded to the nearest decade and collected in the table below .

Approximations		95% Confidence Interval for $\hat{u}$
First approximation	Graphical (figure 2.6)	2880 - 2930 BC
	Taylor expansion (equation 2.11)	2880 - 2930 BC
Neftel and Aitchison & Scott approximation	Graphical (figure 2.7)	2880 - 2930 BC
	Taylor expansion (equation 2.13)	2880 - 2930 BC

Obviously there are no differences amongst these intervals which suggest that the above approximations will provide effectively the same interval when the calibration is carried out on monotonic sections of the curve.

2.9.3 The Non-parametric Regression Case — Non-monotonic Sections of the Curve

As discussed in the previous section the methods basically extend to the case of multiple point estimates *i.e.* in situations where the calibration curve is wiggly. In this case the required interval will be the union of the intervals of the multiple date estimates or the combination of more than one interval if the intervals of the multiple date estimates overlap.

Therefore, for the exact calibration method the general case of approximate 95% confidence interval for u is of the form

$$I_{\bullet}(u) = \left\{ u: \left| \frac{y - \hat{f}(u)}{\sqrt{\sigma_y^2 + \hat{\sigma}_c^2(u)}} \right| < 1.96 \right\}$$

which can be written as the union of all the intervals which together constitute the required interval for u and is of the form

$$I_{\bullet}(u) = \bigcup_{i=1}^{k} I_i(u)$$

where k is the number of historical ages corresponding to the radiocarbon date y.

In the following sub-sections the two situations where $\sigma_c^2(u)$ is assumed constant or not will be considered.

2.9.3.1 Non-monotonic Sections with Constant Variance

When the variance $\hat{\sigma}_c^2(u)$ is constant over the range of the calibration the resulting form of the approximate 95% C.I. will be

$$I_{\bullet}(u) = \left\{ u: \left| \frac{y - \hat{f}(u)}{\sigma^*} \right| < 1.96 \right\} \qquad .....(2.14)$$

with again $\sigma^* = \sqrt{\sigma_y^2 + \sigma_c^2}$ and $\hat{\sigma}_c^2(u) = \sigma_c^2$ assumed constant.

Now the required interval for u is of the form

$$I_{\bullet}(u) = \bigcup_{i=1}^{k} I_i(u)$$

with $I_i(u) = \left\{u: \quad \hat{f}_i^{-1}\left(\hat{f}(u) - 1.96\ \sigma^*\right) < u < \hat{f}_i^{-1}\left(\hat{f}(u) + 1.96\ \sigma^*\right)\right\}$ .....(2.15)

using each inverse function in turn.

To illustrate this, consider the case shown in figure (2.8) where there are three historical ages corresponding to the radiocarbon date and the required interval for u will be the union of the three intervals of these historical dates

i.e. $$I_{\bullet}(u) = \bigcup_{i=1}^{3} I_i(u)$$

Since two of the intervals $I_2(u)$ and $I_3(u)$ intersect to provide a combined interval $I_{23}(u)$ then there are two disjoint intervals which together provide the required interval estimate for $I_{\bullet}(u)$

i.e. $$I_{\bullet}(u) = I_1(u) \cup I_{23}(u)$$

Now applying the approximation based on the Taylor expansion to each disjoint interval gives

$$I_i(u) \cong \left\{u: \quad \hat{u}_i - 1.96\frac{\sigma^*}{\hat{f}'(\hat{u}_i)}, \quad \hat{u}_i + 1.96\frac{\sigma^*}{\hat{f}'(\hat{u}_i)}\right\} \qquad .....(2.16)$$

Thus the two intervals shown in figure (2.8) can be then evaluated as

$$I_1(u) = \left\{u: \quad \hat{u}_1 \pm 1.96\frac{\sigma^*}{\hat{f}_1'(\hat{u}_1)}\right\}$$

and $$I_{23}(u) = \left\{u: \quad \hat{u}_2 - 1.96\frac{\sigma^*}{\hat{f}_2'(\hat{u}_2)}, \quad \hat{u}_3 + 1.96\frac{\sigma^*}{\hat{f}_3'(\hat{u}_3)}\right\}$$

Since the variance $\hat{\sigma}_c^2(u)$ is constant and $\hat{u}_i$ can be evaluated from the inverse function $\hat{f}_i^{-1}(y)$ then the method only requires the value of $\hat{f}'(\hat{u}_i)$ to produce the required interval for the historical age u.

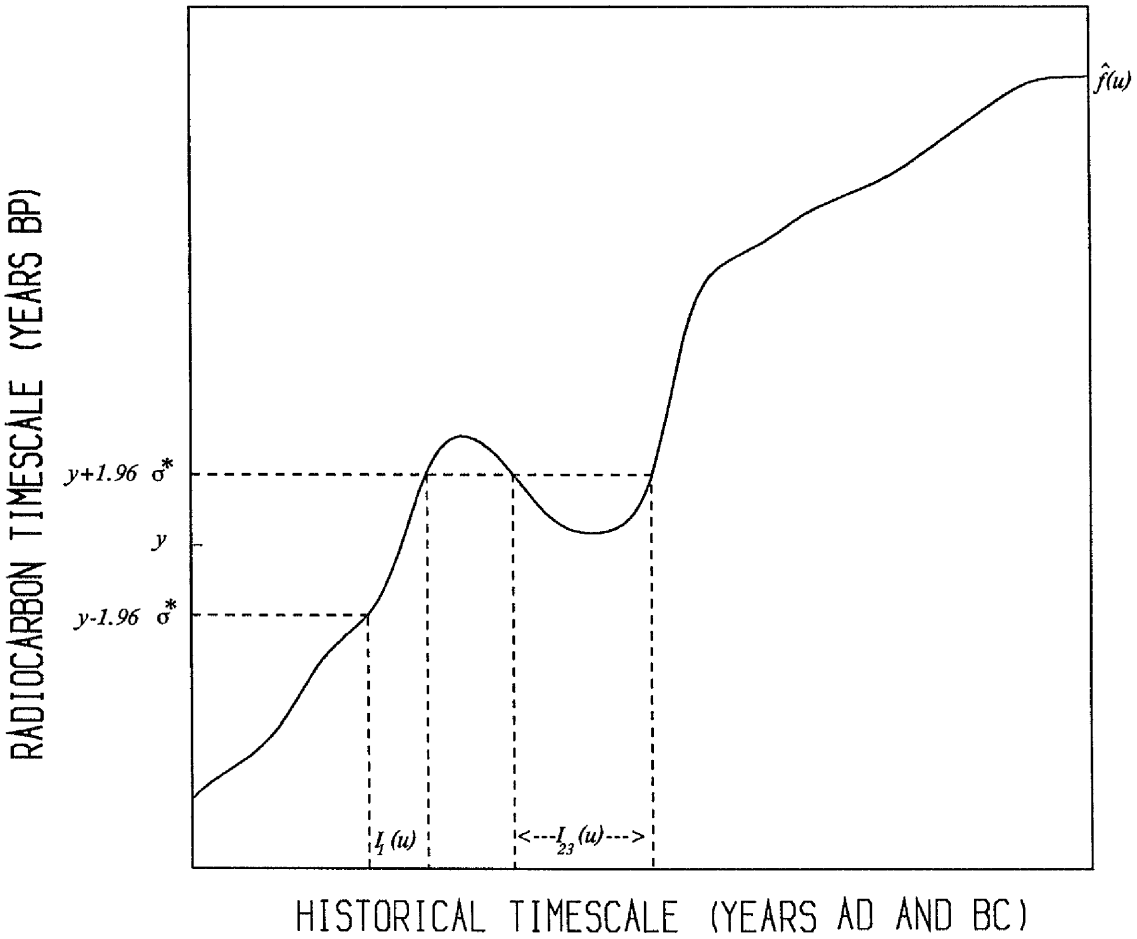

Figure 2.8 : Graphical illustration for the two disjoint intervals which together constitute the required interval estimate $\boldsymbol{I_\bullet(u)}$.

2.9.3.2 Non-monotonic Sections with Non-Constant Variance

If one looks back to the general case and considers the situation where the variance $\hat{\sigma}_c^2(u)$ is not constant there is still the same pivotal function as before resulting in an approximate 95% C.I of

$$I_{\bullet}(u) = \left\{ u: \left| \frac{y - \hat{f}(u)}{\sqrt{\sigma_y^2 + \hat{\sigma}_c^2(u)}} \right| < 1.96 \right\} \qquad .....(2.17)$$

where $\hat{\sigma}_c^2(u)$ now depends on u.

As before equation (2.17) can be written as the union of all the intervals which together constitute the required interval for the historical age u and only replace the constant σ^* in (2.15) and (2.16) above by $\sqrt{\sigma_y^2 + \hat{\sigma}_c^2(\hat{u})}$ to get

$$I_i(u) = \left\{ u: \quad \hat{f}_i^{-1}\{\hat{f}(u) - 1.96\sqrt{\sigma_y^2 + \hat{\sigma}_c^2(u)}\} < u < \hat{f}_i^{-1}\{\hat{f}(u) + 1.96\sqrt{\sigma_y^2 + \hat{\sigma}_c^2(u)}\} \right\}$$

Again by using each inverse function in turn as shown in figure (2.9).

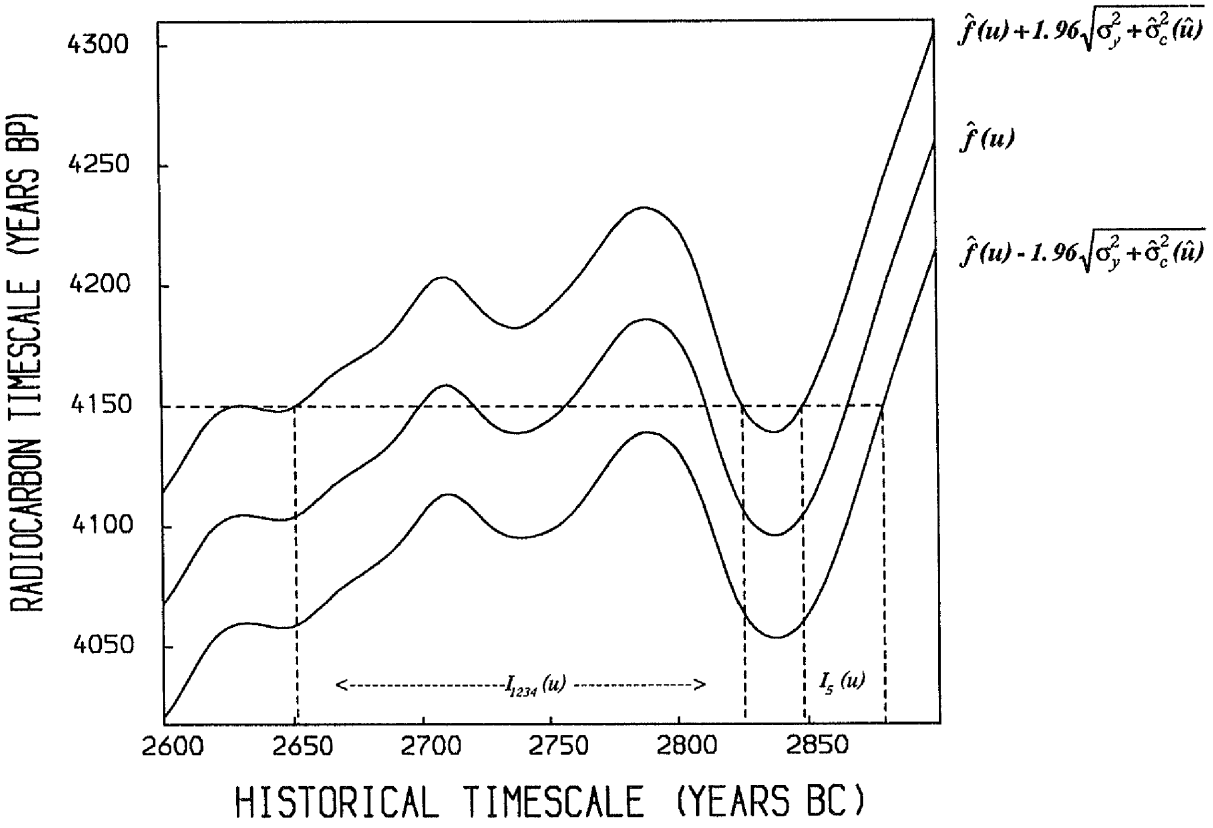

Figure 2.9 : Diagram of the two disjoint intervals which constitute the 95% confidence interval for the calibrated historical age.

Now applying the approximation based on the Taylor expansion to each disjoint interval as before gives

$$I_i(u) \cong \left\{u: \quad \hat{u}_i - 1.96\frac{\sqrt{\sigma_y^2+\hat{\sigma}_c^2(\hat{u}_i)}}{\hat{f}'(\hat{u}_i)} < u < \hat{u}_i + 1.96\frac{\sqrt{\sigma_y^2+\hat{\sigma}_c^2(\hat{u}_i)}}{\hat{f}'(\hat{u}_i)}\right\} \quad .....(2.18)$$

which is computationally more appealing since it requires only $\hat{f}'(\hat{u}_i)$ and $\hat{\sigma}_c^2(\hat{u}_i)$.

Although an alternative approximation similar to that described earlier in sub-section (2.9.2.2) uses the solutions of the equations

$$y \pm r\,\sigma_y = \hat{f}(u) \mp r\hat{\sigma}_c(u)$$

to provide an interval of the form

$$I_i(u) \cong \left\{u: \quad \hat{u}_i - \frac{r\,(\sigma_y+\hat{\sigma}_c(\hat{u}_i))}{\hat{f}'(\hat{u}_i)} \;,\; \hat{u}_i + \frac{r\,(\sigma_y+\hat{\sigma}_c(\hat{u}_i))}{\hat{f}'(\hat{u}_i)}\right\} \quad .....(2.19)$$

where $r=1.5$ gives an approximate 95% confidence interval for u as illustrated in figure (2.10)

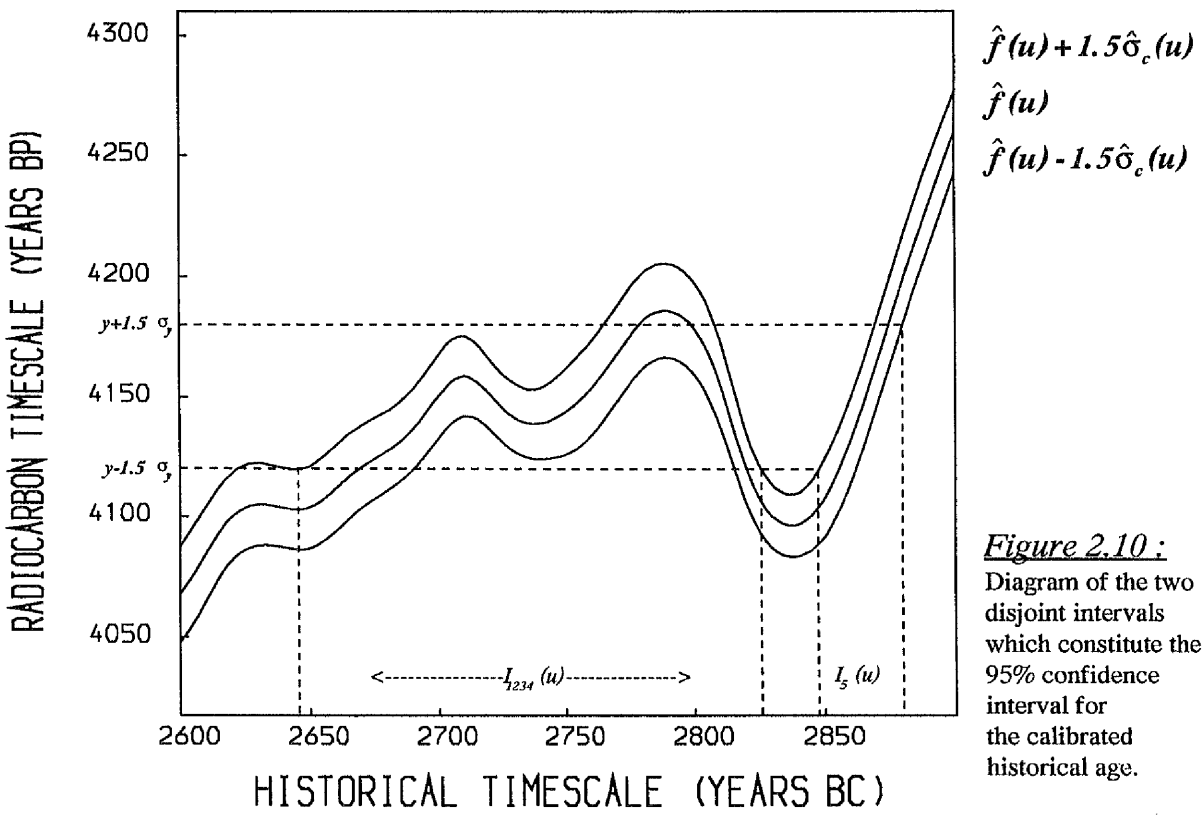

Figure 2.10 : Diagram of the two disjoint intervals which constitute the 95% confidence interval for the calibrated historical age.

2.9.3.3 Illustrative Example

This sub-section will attempt to clarify the above ideas by employing them to provide an approximate 95% confidence interval for a single calibrated historical age where the calibration has been made on a wiggly (non-monotonic) part of the curve and the resulting intervals will be compared.

For the first approximation where the prediction bands for the calibration curve are $\hat{f}(u) \pm 1.96\sqrt{\sigma_y^2 + \hat{\sigma}_c^2(u)}$, consider the case shown in figure (2.9) where the radiocarbon date y=*4150 BP* (with standard error 20 years) has been calibrated and there are five historical dates which may have generated this radiocarbon date. These are 2700, 2720, 2755, 2810 and 2865 BC and four of their intervals $I_1(u), I_2(u), I_3(u)$ and $I_4(u)$ intersect to give a combined interval $I_{1234}(u)$, so that two disjoint intervals constitute the required interval estimate of the form

$$I_{\bullet}(u) = I_{1234}(u) \cup I_5(u)$$

with

$$I_{\bullet}(u) = \left\{ u: \left| \frac{y - \hat{f}(u)}{\sigma_y^2 + \hat{\sigma}_c^2(u)} \right| < 1.96 \right\}$$

these result in the two intervals as follows:-

$$I_{1234}(u) = \{2650\text{-}2825\} \text{ BC}$$

and

$$I_5(u) = \{2850\text{-}2880\} \text{ BC.}$$

Now using the approximation based on Taylor expansion give

$$I_{1234}(u) \approx \left\{ u: \quad \hat{u}_1 - 1.96 \frac{\sqrt{\sigma_y^2 + \hat{\sigma}_c^2(\hat{u}_1)}}{\hat{f}'(\hat{u}_1)} \;,\; \hat{u}_4 + 1.96 \frac{\sqrt{\sigma_y^2 + \hat{\sigma}_c^2(\hat{u}_4)}}{\hat{f}'(\hat{u}_4)} \right\}$$

$$= \{2665\text{-}2825\} \text{ BC.}$$

whereas

$$I_5(u) \approx \left\{ u: \quad \hat{u}_5 \pm 1.96 \frac{\sqrt{\sigma_y^2 + \hat{\sigma}_c^2(\hat{u}_5)}}{\hat{f}'(\hat{u}_5)} \right\}$$

$$= \{2850\text{-}2880\} \text{ BC.}$$

For the second order approximation (Neftel; 1980, Aitchison and Scott; 1987) it is clear from figure (2.10) that the required interval will be the same form as the form above and the two intervals

$I_{1234}(u)$=*{2645-2825} BC* and $I_5(u)$=*{2845-2880} BC*

will constitute the required interval for the historical age u.

For the approximation based on Taylor expansion for this approximation will give the intervals of the forms

$$I_{1234}(u) \approx \left\{ u_1 - \frac{1.5(\sigma_y + \hat{\sigma}_e(\hat{u}_1))}{\hat{f}'(\hat{u}_1)}, u_4 + \frac{1.5(\sigma_y + \hat{\sigma}_e(\hat{u}_4))}{\hat{f}'(\hat{u}_4)} \right\}$$

$$= \{2665\text{-}2825\} \text{ BC}$$

and $$I_5(u) \approx \left\{ \hat{u}_5 \pm \frac{1.5(\sigma_y + \hat{\sigma}_e(\hat{u}_5))}{\hat{f}'(\hat{u}_5)} \right\}$$

$$= \{2850\text{-}2880\} \text{ BC.}$$

Now summarise the above results to the nearest decades in the following table:-

Approximations		95% Confidence Interval for $\hat{u}$,	
		$I_{1234}(u)$	$I_5(u)$
First approximation	Graphical (figure 2.9)	2650 - 2830 BC	2850 - 2880 BC
	Taylor expansion (equation 2.18)	2660 - 2830 BC	2850 - 2880 BC
Neftel and Aitchison & Scott approximation	Graphical (figure 2.10)	2640 - 2830 BC	2840 - 2880 BC
	Taylor expansion (equation 2.19)	2660 - 2830 BC	2850 - 2880 BC

Comparing the resulted intervals together shows no real difference among these approximations. All the graphical methods gave nearly the same intervals while the approximations based on Taylor expansion usually seem to be identical in most cases. This example helps to assure that any of the above approximations can be used to provide the approximate 95% confidence interval for a calibrated historical date.

2.9.4 Interpretation from a Standard Error Viewpoint

As can be seen from the previous discussion each of the estimates of the true historical age will have a "standard error" associated to it, say ***Se(u)***, and this can be justified as follows:

Since the corresponding true historical age $\hat{u}$ for the radiocarbon age y can be evaluated by solving this equation

$$y = \hat{f}(\hat{u}) \qquad \text{for all } \hat{u}$$

then $$\hat{u} = \hat{f}^{-1}(y)$$

with variance $$Var(\hat{u}) = Var\{\hat{f}^{-1}(y)\}$$

Next, the $Var\{\hat{f}^{-1}(y)\}$ can be approximated by means of a Taylor expansion (Lindley; 1965) to give

$$Var\left\{\hat{f}^{-1}(y)\right\} \cong Var(y)\left\{\hat{f}'^{-1}(y)\right\}^2$$

i.e. $$Var(\hat{u}) \cong Var(y)\left\{\hat{f}'^{-1}(y)\right\}^2 = \frac{Var(y)}{\left\{\hat{f}'(\hat{u})\right\}^2} \qquad .....(2.20)$$

since $$\hat{f}'^{-1}(y) = \frac{1}{\hat{f}'(\hat{u})}$$

To combine the error of the radiocarbon measurement with the error of the fitted curve refer to the original regression model $y = \hat{f}(u) + \varepsilon$ and calculate the variance of y as

$$Var(y) = Var\{\hat{f}(u)\} + Var(\varepsilon)$$

$$\Rightarrow \quad Var(y) = \hat{\sigma}_c^2(u) + \sigma_y^2$$

So effectively use this in (2.20) to give

$$Var(\hat{u}) \cong \frac{\left\{\hat{\sigma}_c^2(\hat{u}) + \sigma_y^2\right\}}{\left\{\hat{f}'(\hat{u})\right\}^2}$$

$$\Rightarrow \quad Se(\hat{u}) \cong \frac{\sqrt{\hat{\sigma}_c^2(\hat{u}) + \sigma_y^2}}{\hat{f}'(\hat{u})}$$

Now it is clear from the above that there are three factors involved in the "error" associated with each of the estimates of true historical age:-

1) The error in the corresponding radiocarbon dates σ_y ;

2) The amount of uncertainty in the fitted curve at that point $\hat{\sigma}_c(\hat{u})$,

and 3) The slope or steepness of the curve at that point $\hat{f}'(\hat{u})$.

The simple interpretation of the above is that when the curve is steep (*i.e.* $|f'(.)|$ is large) then $Se(\hat{u})$ will be small and hence a fairly precise estimate of that value of u will be obtained. Conversely, when the curve is flat (*i.e.* $|f'(.)|$ is small) then $Se(\hat{u})$ will be large and hence there will result a less precise estimate of that value of u.

For example, the resulted interval of the historical age from calibrating the radiocarbon date y=*3860* BP is much wider than the resulted interval of the historical age from calibrating the radiocarbon date y=*4300* BP (see Figure 2.11 for illustration of both cases).

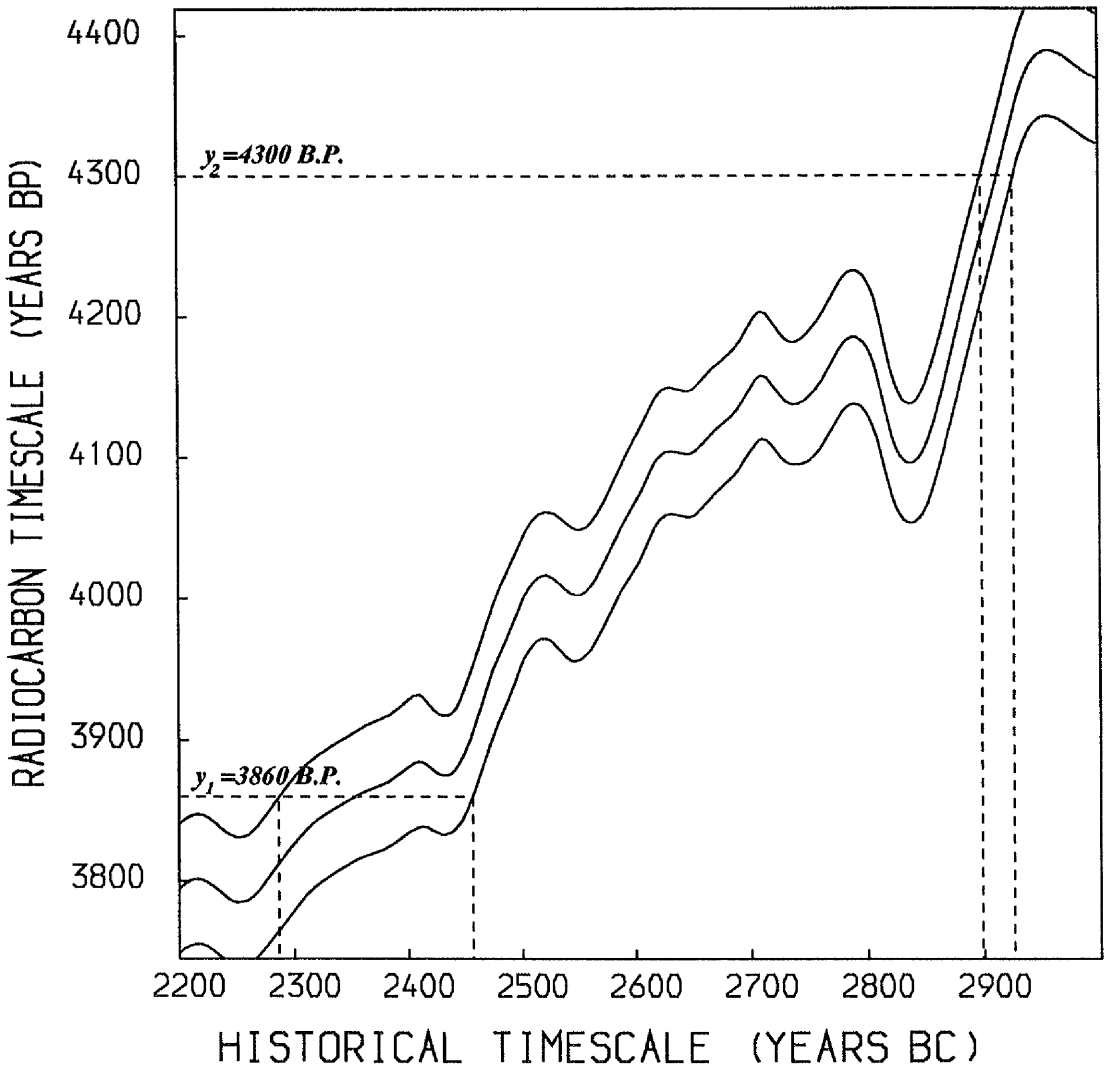

Figure 2.11 : Diagrammatic representation shows the magnitude of the error in the calibrated age when the calibration curve is steep or flat.

One problem in providing approximations to the 95% C.I. for ***u*** is that unreasonably large intervals can occur. This happens occasionally when the calibration is carried out on flat parts of the curve and the derivative of the curve at ***u*** is very small. In such instances perhaps the best approach would be the graphical methods since they do not take account of the derivative of the curve at the historical age ***u***.

2.10 Replicate Dates from the Same Source

It is important to note that the calibration of replicate dates from the same source (i.e. more than one radiocarbon measurement made on a single sample) are dealt with in a fashion identical to that used in the previous sections for a single date.

The appropriate method of combining replicate dates $y_1, y_2, \ldots\ldots, y_m$ from the same unknown u with errors $\sigma_{y_1}, \sigma_{y_2}, \ldots\ldots, \sigma_{y_m}$ is to weight them according to their errors

$$i.e. \qquad \bar{y}_w = \frac{\sum_{i=1}^{m} \frac{y_i}{\sigma^2_{y_i}}}{\sum_{i=1}^{m} \frac{1}{\sigma^2_{y_i}}} \qquad \text{with error} \qquad \sigma_w = \sqrt{\frac{1}{\sum_{i=1}^{m} \frac{1}{\sigma^2_{y_i}}}}$$

then simply use $\bar{y}_w$ in above in place of y with σ_y replaced by σ_w in the intervals of the previous sections (Ward and Wilson; 1981).

2.11 Summary

This chapter has been almost entirely concerned with discussion of the fitting of the radiocarbon calibration curve and the method of calibration. A brief history of the data used in the construction of the curve was given. The requirements of parametric and non-parametric regression for the curve fitting were considered and the flexibility of non-parametric regression made it preferable to a parametric approach in spite of the problem of the choice of the smoothing parameter.

A Kernel based estimator was used to provide a fitted calibration curve with the smoothing parameter chosen by cross-validation. An estimate of the standard error of the curve was then evaluated after correction by a multiplier to make more realistic the quoted errors of the radiocarbon dates .

The major emphasis in this chapter has been to review the technique of calibration of a single radiocarbon date and to discuss the provision of point and interval estimates for the calibrated date (historical age). The problem of multiple point estimates was highlighted and the major factors involved in the uncertainty of the true historical age were found to be a realistic estimate of the error in the data as will as the error in the curve and the slope of the curve in the region of the calibration.

In the next chapter the case of multiple dates from a culture is considered and the results of this chapter are exploited to obtain a sensible density estimate of $p(t)$ based on combinations of multiple point estimates which is why it was useful to illustrate calibration in this way for a single date.

Chapter 3

Floruit Estimation Methods

3.1 Introduction

With the help of radiocarbon dating , archaeologists would like to be able to date the duration of an archaeological phenomenon such as the occupation of a settlement, or the duration of a particular culture group. In the previous chapter a review of the mechanism for the calibration of single radiocarbon date was carried out, but summarising and presenting a group of radiocarbon dates has particular difficulties arising from the fact that the artefacts being dated might come not only from different sites but from different temporal horizons *i.e* they may span a possibly wide range of time. Accordingly instead of estimating a specific date of historical interest one must attempt to summarise the samples of radiocarbon dated material in the form of a historical range within which the settlement or culture flourished. The work in this chapter and the next two chapters is an attempt to extend

and develop the approach proposed in Aitchison, Ottaway and Scott (1990) and this chapter will be devoted to discuss various approaches which will provide such a summary for an archaeological culture when a reasonably representative selection of artefacts or material can be collected from this culture.

3.2 Definition of the Problem

Assume there are a sample of radiocarbon dates

$$y_1, y_2, \ldots\ldots\ldots, y_n$$

with their associated errors

$$\sigma_1, \sigma_2, \ldots\ldots\ldots, \sigma_n$$

where n is the number of artefacts sampled from a culture. The major question which arises is how to summarise this group of radiocarbon dates on the historical timescale?. Several answers have been proposed to this question such as a simple average (Quitta; 1967, Neustupny;1968) which has been criticised for insufficient information about each single date (Waterbolk; 1971, Ottaway; 1973). Geyh and de Maret (1982) suggested the use of sample histograms. One simple attempt to get around the difficulties that the dates may have been drawn from a period spanning hundreds of historical years is to use the extremes of the calibrated single dates as an overall summary of the phenomenon. Unfortunately this method is effectively useless and undesirable because the larger the sample size for one archaeological phenomenon, the larger the final range will be in addition to the neglect of any statistical information contained within the series of measurements (Ottaway; 1986).

In order to date the duration of any cultural group, it is essential to begin with two assumptions. The first one is that there is a frequency

distribution (with respect to the historical timescale) of all possible artefacts or materials from the phenomenon which might be sampled by the archaeologists. The second one is that the actual artefacts or materials sampled by the archaeologists are, as far as is practical, a reasonably representative sample from this frequency distribution.

The main emphasis in the proposed approach to this problem will be to concentrate on the concept of the Floruit of a culture suggested by Ottaway (1973) which can be considered as an effective summary of such a frequency distribution. The Floruit is defined conceptually to be the most prolific period in the culture and mathematically to be the 25th and 75th percentiles (or the time between the lower and upper quartiles) of the frequency distribution of the radiocarbon ages of artefacts were produced from the culture. Using this definition for the floruit leads to the use of the sample quartiles (quartile interval estimator) to estimate the floruit of a culture through the estimation of the lower quartile, say $\eta_{0.25}$, and upper quartile, say $\eta_{0.75}$,

with $\int_{-\infty}^{\eta_{0.25}} p(t)dt = 0.25$ and $\int_{-\infty}^{\eta_{0.75}} p(t)dt = 0.75$

for the lower and upper quartiles respectively. $p(t)$ is the frequency distribution underlying the culture where t is historical time (Figure 3.1 shows the theoretical frequency distribution of radiocarbon ages of artefacts sampled from a culture and the definition of the floruit of the culture).

Before moving onward, it should be noticed the difference between the duration and floruit of an archaeological culture. The duration of a culture means the period of time from the beginning to the end of the culture, while its floruit is as defined above.

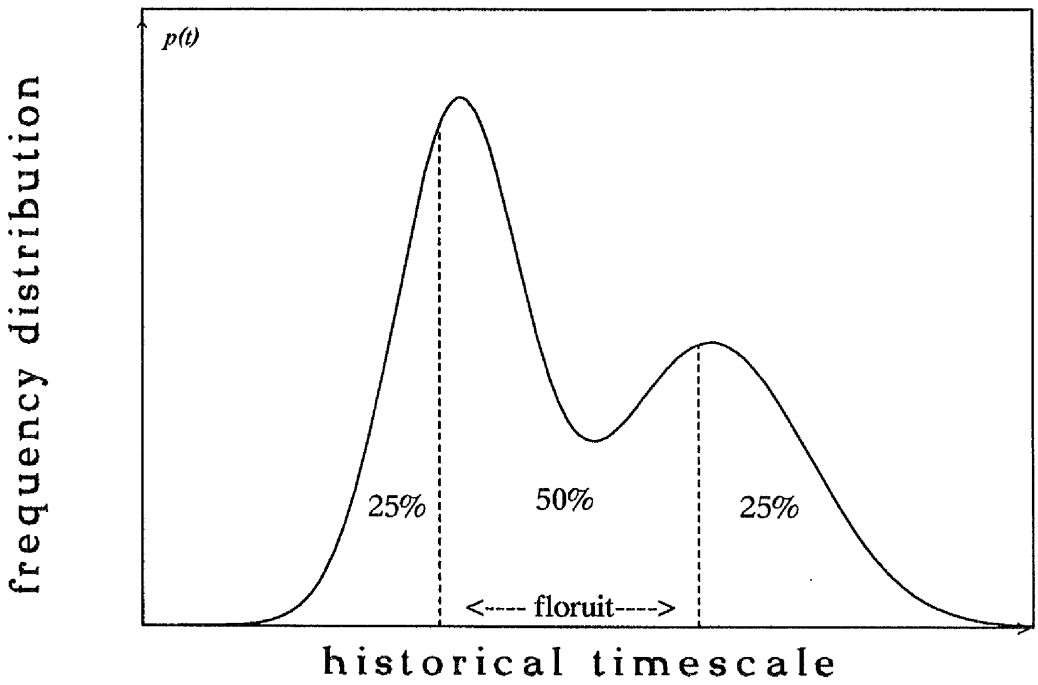

Figure 3.1 : Diagrammatic representation of the definition of a floruit.

3.3 Difficulties of the Floruit Estimation

The methods of floruit point and interval estimation which are described in this chapter are divided into two types. Firstly simple ad hoc pen and paper methods are considered and then more formal methods involving the use of density estimation (these are highly computational methods).

In practice the questions which need to be considered before solving the floruit estimation problem are :-

1) How does one provide an interval estimate for the Floruit ?

2) How does the calibration issue enter the Floruit estimation problem? Does one calibrate the radiocarbon dates first or construct an interval on the radiocarbon dates and then calibrate ?

Throughout this work these points will be highlighted.

3.4 Advantages of the Quartile Interval Estimator

There are a number of advantages to be gained from using the quartile interval estimator (Q.I.E.) defined here as $\hat{\eta}_{0.25}$ and $\hat{\eta}_{0.75}$ to estimate the cultural floruit. First of all, the sample quartiles are very easy to calculate (the method of calculation is given in section 3.5).

The second advantage is that the quartile interval is a very useful summary for the frequency distribution and can provide a very simple diagrammatic summary.

The third advantage is that the quartile interval estimator is stable and fairly insensitive to the addition of a few more observations, *i.e.* the effect on the quartile interval will be small if one or two more observations are available. For instance in the case of one new observation added being an extreme value the quartile interval will not be very greatly affected *i.e.* it avoids giving excessive weight to outlying observations.

3.4.1 Point Estimation

In general the quartile interval estimator (*i.e* a point estimate of the floruit) tells us relatively little and gives no idea of the precision of the estimate of the floruit of the culture. The main reason for this is that the quoted radiocarbon dating errors are not included in the calculation and hence all the radiocarbon dates are treated with equal weight. In other words there is no consideration is taken of the uncertainty in the radiocarbon dates (Aitchison, Ottaway and Scott, 1990). For this reason estimating the floruit by using point estimation alone will be insufficient and one should concentrate on the provision of an interval estimation of the quartiles as a means of providing an interval estimate of the floruit of a culture.

3.4.2 Interval Estimation

The most sensible way to improve the point estimation of the cultural floruit is to provide an interval estimate for the sample quartiles by, roughly speaking, providing a joint confidence statement with a lower bound for the lower quartile and a higher bound for the upper quartile. Naturally this will contain the point estimate for the quartiles and will be much more likely to contain the true floruit of the culture than the range of the point estimates themselves.

3.5 Pen and Paper Methods

This section deals with the simple ad hoc methods which require only pen and paper to provide the estimation of the floruit of the culture. Initially the general problem of calculating the point estimate for the quartiles of a random sample is treated, then a method for producing an interval estimate and finally the floruit estimation problem itself.

3.5.1 General Problem of Quartile Estimation from a Sample

a) Point Estimate for the Quartiles

For a random variable Z from which z_1 ,....., z_n , are independent and identically distributed realisations, there are three quartiles which divide the population into quarters, or four equal parts. These are called the lower quartile, median and upper quartile. The lower quartile is the number for which 25% of the population have values of the random variable less than or equal. The median is the number which divides the population into two equal parts. The upper quartile is the number for which 75% of the population have values of the random variables less than. In other words, the 100p, or the percentiles, of the distribution, $p(z)$, of Z which divide the

population into 100 equal parts can be defined as η_p which satisfies

$$P\{Z < \eta_p\} = p$$

where p is a real number between 0 and 1 (see figure 3.2).

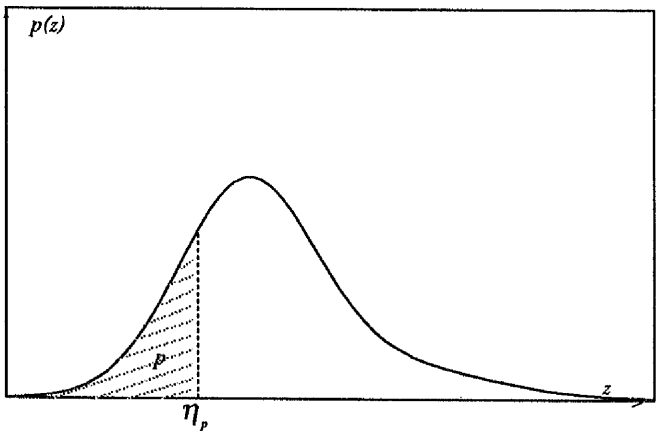

Figure 3.2 : Diagrammatic representation of the definition of a percentile.

The simplest way to determine a point estimate for the population quartile from a given sample is summarised in the following steps:

- Arrange the sample in ascending order from the smallest value to the largest value and allocate the rank to each observation to satisfy

$$z_{(1)} \leq z_{(2)} \leq \ldots\ldots\ldots\ldots \leq z_{(n)}$$

- Evaluate the number $Q = \dfrac{\delta n + 2}{4}$ in the ordered sample with $\delta = 1$ for the lower quartile and $\delta = 3$ for the upper quartile.
- If the resulting Q is an integer, then the quartile coincides with the sample value of rank Q. If the resulted Q is a fraction, then the quartile lies between two sample values and can be evaluated using the following formula

$$\hat{\eta}_p = z_{(i)} + (Q - i)\{z_{(i+1)} - z_{(i)}\} \qquad \ldots\ldots(3.1)$$

for p=0.25 and p=0.75 for the lower quartile and upper quartile respectively, where i is the largest integer not exceeding Q, $z_{(i)}$ and $z_{(i+1)}$ is the $(i)^{th}$ and the $(i+1)^{th}$ values in the order statistics. If the resulting Q falls on or between the ranks of tied values then the sample quartile is taken to be the common value of the ties.

b) Interval Estimate for the Quartiles

To extend this approach to provide a joint confidence interval for the population quartiles $\eta_{0.25}$ and $\eta_{0.75}$, find two values, the lower bound $\hat{\eta}_L$ for $\eta_{0.25}$ and upper bound $\hat{\eta}_U$ for $\eta_{0.75}$ such that

$$p(\hat{\eta}_L < \eta_{0.25} \text{ and } \eta_{0.75} < \hat{\eta}_U) = 1-\alpha \qquad .....(3.2)$$

where $1-\alpha$ is the required confidence coefficient for some chosen value $0<\alpha<1$.

The two values $\hat{\eta}_L$ and $\hat{\eta}_U$ can be evaluated by obtaining the confidence interval for both lower and upper quartiles and then take the lower bound of the lower quartile and the upper bound of the upper quartile as a joint confidence interval for the quartiles.

The method of providing a confidence interval for any population percentile is described and explored in detail by Noether (1967), Gibbons (1971) and Mood *et. al* (1974), and only a brief explanation will be given here.

The simplest way to construct a confidence interval for any population percentile η_p is to use a smaller value of the order statistics, say $z_{(r)}$, than $\hat{\eta}_p$ and a larger value of the order statistics, say $z_{(s)}$, than $\hat{\eta}_p$ such that

$$P(z_{(r)} < \eta_p < z_{(s)}) = 1-\alpha$$

where $1 \le r < s \le n$. The event $z_{(r)} < \eta_p$ means that r of the n observations are less than $\hat{\eta}_p$ and it occurs if and only if either $z_{(r)} < \eta_p < z_{(s)}$ or $z_{(s)} < \eta_p$ happened.

Since the last two events are mutually exclusive then for all $r<s$

$$P(z_{(r)} < \eta_p) = P(z_{(r)} < \eta_p < z_{(s)}) + P(z_{(s)} < \eta_p)$$

which can be rewritten as

$$P(z_{(r)} < \eta_p < z_{(s)}) = P(z_{(r)} < \eta_p) - P(z_{(s)} < \eta_p) \qquad .....(3.3)$$

The two probabilities $P(z_{(r)} < \eta_p)$ and $P(z_{(s)} < \eta_p)$ can be expressed as the sum of the last $(n\text{-}r+1)$ and $(n\text{-}s+1)$ terms of the binomial probability distribution with parameter p respectively. Therefore equation (3.3) can be rewritten as follows

$$P(z_{(r)} < \eta_p < z_{(s)}) = \sum_{i=r}^{n} \binom{n}{i} p^i (1-p)^{n-i} - \sum_{i=s}^{n} \binom{n}{i} p^i (1-p)^{n-i}$$

$$= \sum_{i=r}^{s-1} \binom{n}{i} p^i (1-p)^{n-i} \qquad .....(3.4)$$

and taking this equal to 0.05 and solve for r and s to obtain the confidence interval $(z_{(r)}, z_{(s)})$ for η_p from the order statistics.

Thus a $100(1\text{-}\alpha)\%$ confidence interval for η_p can be obtained by a suitable choice for r and s using the binomial distribution. For a small sample size $(n \leq 20)$ a binomial distribution table can be used to choose r and s. For a large sample size $(n > 20)$ the binomial distribution can be approximated to the normal distribution with mean np and variance $np(1\text{-}p)$ by using the approximation based on the Central Limit Theorem (Conover, 1971) and r and s can be evaluated as follow

$$r = np + \psi_{\frac{\alpha}{2}} \sqrt{np(1-p)} \qquad .....(3.5)$$

and

$$s = np + \psi_{1-\frac{\alpha}{2}} \sqrt{np(1-p)} \qquad .....(3.6)$$

where ψ_α is the quantile of the standard normal random variable Ψ, selected so $p(\Psi < \psi_\alpha) = \alpha$ and $p(\Psi > \psi_\alpha) = 1-\alpha$.

p is some specified number between zero and one (0.25 for the lower quartile and 0.75 for the upper quartile).

In practice r and s will not be integers and the actual values of $z_{(r)}$ and $z_{(s)}$ will be obtained using the weight formula as before, that is

$$z_{(r)} = z_{(r^*)} + (z_{(r^*+1)} - z_{(r^*)})(r - r^*) \qquad .....(3.7)$$

where r^* is the largest integer not exceeding r, $z_{(r^*)}$ and $z_{(r^*+1)}$ are the r^{*th} and $(r^*+1)^{th}$ values in the order statistics. Similarly, r replaced with s in the formula (3.7) to obtain the s^{th} order statistics $z_{(s)}$. Then the interval estimate for the population quartiles is the interval with the end points $\hat{\eta}_L$ and $\hat{\eta}_U$ where $\hat{\eta}_L$ is the value of the order statistics $z_{(r)}$ for the lower quartile $\eta_{0.25}$ and $\hat{\eta}_U$ is the value of the order statistics $z_{(s)}$ for the upper quartile $\eta_{0.75}$.

Therefore

$$P(\hat{\eta}_L < \eta_{0.25} \text{ and } \eta_{0.75} < \hat{\eta}_U) = 1 - \alpha \qquad .....(3.8)$$

provides an approximate $100(1-\alpha)\%$ joint confidence interval, namely $(\hat{\eta}_L , \hat{\eta}_U)$, for the population quartiles *i.e.* $(\eta_{0.25} , \eta_{0.75})$.

c) Example

This is an illustrative example which will illustrate how to calculate the point and interval estimates for the population quartiles from a random sample using the above strategy. The data used is a random sample of 21 observations as follows:-

2220 2050 1950 2280 2130 1950 2020 2350 2060 2370 2210
2080 2110 2130 2190 2250 2140 2260 2310 2150 2350

The first step in obtaining the estimates is to arrange the sample in ascending order and allocate the appropriate rank to each observation as follows:-

$1950_{(1.5)}$	$1950_{(1.5)}$	$2020_{(3)}$	$2050_{(4)}$	$2060_{(5)}$	$2080_{(6)}$	$2110_{(7)}$
$2130_{(8.5)}$	$2130_{(8.5)}$	$2140_{(10)}$	$2150_{(11)}$	$2190_{(12)}$	$2210_{(13)}$	$2220_{(14)}$
$2250_{(15)}$	$2260_{(16)}$	$2280_{(17)}$	$2310_{(18)}$	$2350_{(19.5)}$	$2350_{(19.5)}$	$2370_{(21)}$

where the values in subscript brackets are the rankes.

The next step is to find the positions of the quartiles in the order statistics which in this case are $\frac{21+2}{4}=5.75$ for the lower quartile and $\frac{3(21)+2}{4}=16.25$ for the upper quartile. Since both these numbers are not integers, then the value of the lower quartile lies between the sample values ranked 5 and 6 and the value of the upper quartile lies between the sample values ranked 16 and 17 with appropriate weights determined by the values 5.75 and 16.25.

Finally, to estimate the lower quartile $\eta_{0.25}$ substitute Q with 5.75, i with 5, z_i with 2060 and z_{i+1} with 2080 in the above formula (3.1) and the resulting estimate for the lower quartile is equal

$$\hat{\eta}_{0.25} = 2060 + (5.75-5)(2080-2060)$$
$$= 2075$$

Similarly, to estimate the upper quartile $\eta_{0.75}$ substitute Q with 16.25, i with 16, z_i with 2260 and z_{i+1} with 2280 again in the same formula (3.1) to obtain the estimate of the upper quartile as

$$\hat{\eta}_{0.75} = 2260 + (16.25-16)(2280-2260)$$
$$= 2265 .$$

Thus the point estimate for the quartiles of the sample is (2075,2265).

To provide an approximate 95% joint confidence interval for the quartiles compute r and s as discussed above for both quartiles. First for the lower quartile at α=0.05

$$r = (21)(0.25) + (-1.96)\sqrt{(21)(0.25)(0.75)}$$
$$=5.25\text{-}3.9 = 1.35$$

and $$s = (21)(0.25) + (1.96)\sqrt{(21)(0.25)(0.75)}$$

$$=5.25 + 3.9 = 9.15$$

Therefor, the two order statistics $z_{(r)}$ and $z_{(s)}$ for the lower quartile can be obtained by using the weight formula (3.7) above with $r^* = 1$ and $s^* = 9$. So the value for the lower bound of the lower quartile is

$$\hat{\eta}_L = z_{(1.35)} = z_{(1)} + (1.35 - 1)(z_{(2)} - z_{(1)})$$

$$=1950+0.35(1950-1950)=1950$$

and the value for the upper bound of the lower quartile is

$$\hat{\eta}_U = z_{(9.15)} = z_{(9)} + (9.15 - 9)(z_{(10)} - z_{(9)})$$

$$=2130+0.15(2140-2130)=2131.5$$

This means that the approximate 95% confidence interval for the value of the ***lower quartile*** of the population is ***(1950,2140)***.

Similarly for the upper quartile one can get $r=11.85$ and $s=19.65$ and again using the same weight formula (3.7) with $r^* = 11$ and $s^* = 19$ one can obtain the two order statistics $z_{(r)}$ and $z_{(s)}$ for the upper quartile. So the value for the lower bound of the upper quartile is

$$\hat{\eta}_L = z_{(11.85)} = z_{(11)} + (11.85 - 11)(z_{(12)} - z_{(11)})$$

$$=2150+0.85(2190-2150)=2184$$

and the value for the upper bound of the upper quartile is

$$\hat{\eta}_U = z_{(19.65)} = z_{(19)} + (19.65 - 19)(z_{(20)} - z_{(19)})$$

$$=2350+0.65(2350-2350)=2350$$

which means the approximate 95% confidence interval for the ***upper quartile*** of the population is ***(2190,2350)***.

Finally, to provide an approximate 95% confidence interval for the quartile interval (*i.e.* joint confidence interval for the quartiles) take the

lower bound of the interval estimate of lower quartile and the upper bound of the interval estimate of the upper quartile which can be written in the following form

$$P(\eta_{0.25} > 1950) = 0.975$$

and

$$P(\eta_{0.75} < 2350) = 0.975$$

so merging them together produces

$$P(1950 < \eta_{0.25} \quad \text{and} \quad \eta_{0.75} < 2350) = 0.95$$

i.e. the approximate 95% confidence interval for the ***quartile interval*** of the population is ***(1950,2350)*** with the corresponding point estimate for the quartile interval is (2075 , 2265) *i.e.* a much narrower interval.

3.5.2 Methods of Providing an Interval Estimate for the Floruit

In this section two versions of pen and paper methods are introduced. The basic idea of these methods is to define the extended quartile interval (E.Q.I) as an interval estimate for the floruit by the incorporation of the quoted dating errors of each of the sample of radiocarbon dates. Then apply the strategy of the previous section to these augmented dates. In the first version use the uncalibrated dates to calculate the extended quartile interval for the sample of radiocarbon dates and then calibrate the resulting interval to the historical timescale. In the second version calibrate the radiocarbon dates to the historical timescale and then calculate the extended quartile interval based on these calibrated dates.

3.5.2.1 Method A —

Calibration of the E.Q.I. of the Radiocarbon Dates

For this method calculate the extended radiocarbon dates ($Ey_1, Ey_2, \ldots\ldots\ldots, Ey_n$) for the given group of radiocarbon dates ($y_1, y_2, \ldots\ldots\ldots, y_n$) by including their errors ($\sigma_1, \sigma_2, \ldots\ldots\ldots, \sigma_n$), using the following formula

$$Ey_i = y_i + d\sigma_i$$

for a suitable choice of d , where d is a quantile of a standard normal random variable. Then evaluate the quartile interval for the extended dates and calibrate the result to the historical timescale. This can be done by constructing two series (lower and upper series) for the radiocarbon dates. In the first series calculate the lower extension series, say $\hat{\xi}_i$, for the radiocarbon dates with d equal to the lower quartile of the standard normal distribution (d=-0.6745)

i.e. $\hat{\xi}_i = y_i - 0.6745\ \sigma_i$ i=1,2,.....,n.

In the second series, calculate the upper extension series, say $\hat{\zeta}_i$, for the radiocarbon dates with d equal to the upper quartile of the standard normal distribution (d=0.6745)

i.e. $\hat{\zeta}_i = y_i + 0.6745\,\sigma_i$ $i=1,2,\ldots\ldots\ldots,n.$

thereafter, evaluate the lower quartile in the lower series and call it the extended lower quartile, say $E\hat{\eta}_{0.25}$, for the radiocarbon dates. In the upper series evaluate the upper quartile and call it the extended upper quartile, say $E\hat{\eta}_{0.75}$, for the radiocarbon dates. The two extended quartile estimates $E\hat{\eta}_{0.25}$ and $E\hat{\eta}_{0.75}$ will give the extended quartile interval (E.Q.I.) for the radiocarbon dates. The final step is to calibrate the resulting (E.Q.I.) into the historical timescale conservatively *i.e.* if several historical dates conform to the (E.Q.I.) in the radiocarbon timescale, the calibrated values which give the widest interval must be taken as the interval estimate for the floruit (an illustration of this is given in figure 3.3). The following two examples are given to illustrate this approach practically.

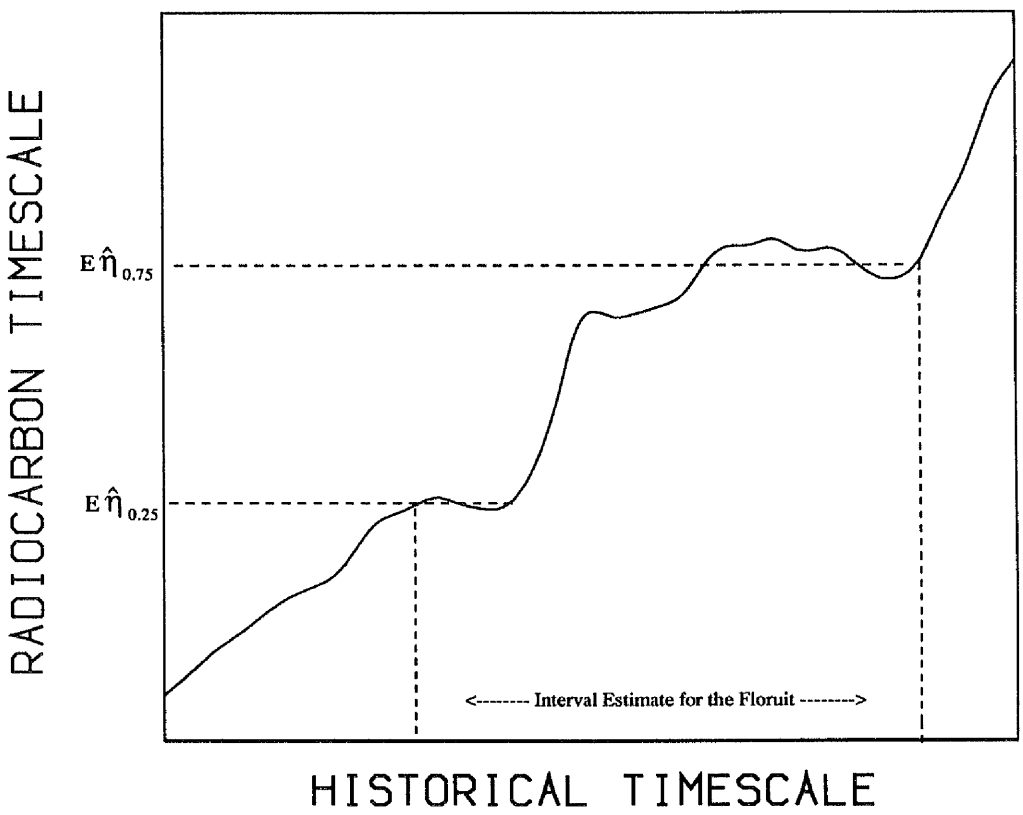

Figure 3.3 : Calibration of the E.Q.I. of the radiocarbon dates conservatively.

Example (1)

A sample of 35 radiocarbon dates were taken from the *Pfyn* culture (found in present-day *Switzerland*) is used in this example to provide an interval estimate for the true floruit of the *Pfyn* culture using the above strategy. The radiocarbon dates are shown in table (3.1) with their associated errors in addition to the lower and the upper series.

Since the sample size is equal to 35, then the lower quartile is found at the 9.25^{th} position and the upper quartile is found at the 26.75^{th} position. Since both positions are not integers, use formula (3.1) to evaluate the E.Q.I. for the radiocarbon dates which in this case is (4741 , 5205) years BP. The interval estimate for the floruit of the *Pfyn* culture will be obtained by calibrating the resulted E.Q.I. of the radiocarbon dates to the historical timescale (as discussed in previous chapter). So the interval estimate of the floruit obtained, and rounded to the nearest decade, is (3520 , 4000) years BC.

Example (2)

The data used in this example is a sample of 38 radiocarbon dates taken from *Sâone-Rhône* culture (situated in Switzerland) and shown in table (3.2) with their associated errors together with the two series. The quartiles are found at the 10^{th} and 29^{th} positions. The E.Q.I. for the radiocarbon dates is thus (3953 , 4261) years BP. As before calibrate the E.Q.I. to the historical timescale and the interval estimate for the floruit of the *Sâone-Rhône* culture found is (2480 , 2900) years BC.

y_i	σ_i	Lower series ($\hat{\xi}_i$)	Rank	Upper series ($\hat{\zeta}_i$)	Rank
4690	150	4588	2	4792	4
4690	200	4555	1	4825	9
4735	130	4647	3	4823	8
4750	100	4682	5	4818	7
4750	60	4709	6	4791	2
4750	60	4709	7	4791	3
4755	40	4728	8	4782	1
4765	40	4738	9	4792	5
4780	150	4678	4	4882	11
4790	40	4763	11	4817	6
4800	40	4773	12	4827	10
4850	150	4748	10	4952	14
4875	50	4841	13	4909	12
4910	100	4842	14	4978	16
4915	40	4888	16	4942	13
4930	70	4882	15	4978	15
4940	70	4892	17	4988	17
4965	40	4938	19	4992	18
4980	70	4932	18	5028	19
4990	60	4949	20	5031	20
5020	40	4993	22	5047	21
5030	45	4999	24	5061	22
5040	60	4999	23	5081	23
5060	100	4992	21	5128	24
5100	70	5052	26	5148	25
5100	70	5052	27	5148	26
5140	130	5052	28	5228	29
5160	120	5079	29	5241	30
5170	70	5122	30	5218	27
5180	170	5065	28	5295	32
5180	70	5132	31	5228	28
5200	70	5152	32	5248	31
5280	60	5239	33	5321	33
5320	60	5279	34	5361	34
5415	60	5374	35	5456	35

Table 3.1: Radiocarbon dates, y_i, (years BP) from *Pfyn* culture with their associated errors, σ_i, and the two series constructed (Note that : $\hat{\xi}_i$ rounded down to the previous integer and $\hat{\zeta}_i$ rounded up to the next integer).

y_i	σ_i	Lower series ($\hat{\xi}_i$)	Rank	Upper series ($\hat{\zeta}_i$)	Rank
3900	100	3832	1	3968	1
3900	100	3832	2	3968	2
3960	120	3879	3	4041	4
3970	100	3902	5	4038	3
3990	100	3922	7	4058	5
4000	120	3919	6	4081	8
4000	150	3898	4	4102	11
4000	100	3932	8	4068	6
4010	100	3942	9	4078	7
4020	100	3952	10	4088	9
4030	100	3962	11	4098	10
4060	100	3992	12	4128	13
4077	70	4029	17	4125	12
4080	100	4012	13	4148	14
4080	100	4012	14	4148	15
4090	90	4029	16	4151	17
4100	90	4039	18	4161	18
4100	120	4019	15	4181	20
4103	70	4055	20	4151	16
4129	70	4081	24	4177	19
4130	100	4062	21	4198	21
4140	140	4045	19	4235	25
4140	100	4072	22	4208	22
4160	100	4092	26	4228	23
4160	120	4079	23	4241	28
4160	110	4085	25	4235	24
4170	100	4102	28	4238	26
4180	120	4099	27	4261	29
4191	70	4143	31	4239	27
4200	110	4125	29	4275	30
4210	100	4142	30	4278	31
4230	110	4155	32	4305	32
4260	100	4192	34	4328	33
4280	160	4172	33	4388	37
4290	120	4209	35	4371	35
4300	100	4232	37	4368	34
4300	110	4225	36	4375	36
4320	110	4245	38	4395	38

Table 3.2: Radiocarbon dates, y_i, (years BP) from *Sâone-Rhône* culture with their associated errors, σ_i, and the two series constructed (Note that : $\hat{\xi}_i$ rounded down to the previous integer and $\hat{\zeta}_i$ rounded up to the next integer).

3.5.2.2 Method B —

Calculation of the E.Q.I. Based on the Calibrated Dates

This method will be concerned with the calibration of each radiocarbon date y_i into the historical timescale individually and the evaluation of all the possible values of these which might have generated the radiocarbon date with their standard error (derived in chapter two).

i.e. find $\hat{u}_{ij} = \hat{f}_j^{-1}(y_i)$ $j = 1,\ldots\ldots,k_i$ and $i = 1,\ldots\ldots,n$

where k_i is the odd number of historical dates correspond to the i^{th} radiocarbon date, and where $\hat{f}_j^{-1}$ is the inverse function, then compute the standard error as

$$\sigma(\hat{u}_{ij}) = \frac{\sqrt{\sigma_i^2 + \hat{\sigma}_c^2(\hat{u}_{ij})}}{\hat{f}'(\hat{u}_{ij})}$$

The next step is to calculate the E.Q.I. for the historical dates as the required interval estimate for the floruit. Here there are two obvious alternatives using either fractional weighting (method B1) or a weighted average of the $\hat{u}_{ij}$ for $j = 1,\ldots.. k_i$ (method B2).

3.5.2.3 Method B1 : Fractional Weighting

This method uses a fractional weighting scheme which gives an appropriate weight to each calibrated date and then estimates the quartiles from these historical dates and their weights.

If the uncalibrated date (radiocarbon date) corresponds to only one calibrated date (historical date) then the calibrated date will given weight equal to one. If the uncalibrated date (radiocarbon date) corresponds to three calibrated dates (historical dates) then each of the three calibrated dates will given weight equal to one third *i.e.* $\frac{1}{3}$. In general every calibrated date $\hat{u}_{ij}$ will be given weight equal to $\frac{1}{k_i}$.

The E.Q.I. for the calibrated dates is evaluated as before from the extended calibrated dates $E\hat{u}_{ij}$ as calculated before

i.e. $E\hat{u}_{ij} = \hat{u}_{ij} + d\,\sigma(\hat{u}_{ij}) \qquad j = 1,\ldots\ldots, k_i \qquad$ and $\qquad i = 1,\ldots\ldots, n$

for a suitable choice of d , where d is the quantile of a standard normal distribution.

Following the same procedure as in method *A*, construct two series. In the first series, calculate the lower extension series for the calibrated dates with d=*-0.6745* (the lower quartile of the standard normal distribution) as follows

$$\hat{\xi}_{ij} = \hat{u}_{ij} - 0.6745\ \sigma(\hat{u}_{ij})$$

and in the second series, calculate the upper extension series for the calibrated dates with d=*0.6745* (the upper quartile of the standard normal distribution) as follows

$$\hat{\zeta}_{ij} = \hat{u}_{ij} + 0.6745\ \sigma(\hat{u}_{ij})$$

In both series, the extensions $\hat{\xi}_{ij}$ and $\hat{\zeta}_{ij}$ will be given weight equal to $\frac{1}{k_i}$, ordered in ascending order from youngest date to the oldest date, evaluate the appropriate ranks for the quartiles as before and use the weights to count into the appropriate $\hat{\xi}_{(ij)}$ and $\hat{\zeta}_{(ij)}$ based on these appropriate ranks.

From the first series calculate the lower quartile of the weighted dates as discussed above and call it the extended lower quartile, say $E\hat{\eta}_{0.25}$, for the calibrated dates while in the second series calculate the upper quartile of the weighted dates and call it the extended upper quartile, say $E\hat{\eta}_{0.75}$, for the calibrated dates. The two extended quartiles $E\hat{\eta}_{0.25}$ and $E\hat{\eta}_{0.75}$ for the calibrated dates will provide the interval estimate of the floruit.

3.5.2.4 Method B2 : Weighted Average

Instead of fractional weighting of all the calibrated dates used in method ***B1*** above use the weighted averages of the calibrated dates to calculate the historical date quartiles. If one single radiocarbon date corresponds to multiple historical dates, then combine the historical dates together and take their average by weighting them according to their associated errors $\hat{\sigma}(\hat{u}_{ij})$ as follows

$$\bar{u}_{i\bullet} = \frac{\sum_{j=1}^{k_i} \frac{\hat{u}_{ij}}{\hat{\sigma}^2(\hat{u}_{ij})}}{\sum_{j=1}^{k_i} \frac{1}{\hat{\sigma}^2(\hat{u}_{ij})}} \qquad i=1,2,.....,n$$

and the error $\hat{\sigma}_{i\bullet}$ on the pooled mean is given by

$$\hat{\sigma}_{i\bullet} = \sqrt{\frac{1}{\sum_{j=1}^{k_i} \frac{1}{\hat{\sigma}^2(\hat{u}_{ij})}}}$$

Then similar to previous methods, calculate the extended calibrated dates $(E\bar{u}_{1\bullet}, E\bar{u}_{2\bullet}, ..., E\bar{u}_{n\bullet})$ as follows

$$E\bar{u}_{i\bullet} = \bar{u}_{i\bullet} + d\,\hat{\sigma}_{i\bullet} \qquad i = 1,2,.....,n$$

where d is as before. Now evaluate the E.Q.I. by constructing the two series as before and calculate the lower extension for each $\bar{u}_{i\bullet}$ in the first series with $d=-0.6745$

i.e. compute $\hat{\xi}_{i\bullet} = \bar{u}_{i\bullet} - 0.6745\,\hat{\sigma}_{i\bullet}$

and calculate the upper extension for each $\bar{u}_{i\bullet}$ in the second series with $d=0.6745$

i.e. compute $\hat{\zeta}_{i\bullet} = \bar{u}_{i\bullet} + 0.6745\,\hat{\sigma}_{i\bullet}$

Finally apply the same ideas as before to calculate the extended lower quartile in the first series while in the second series calculate the extended upper quartile to provide the interval estimate for the floruit.

Example (3)

In this example the data sets from the previous examples, 1 and 2, will be used and methods ***B1*** and ***B2*** applied to evaluate the extended quartile intervals for the calibrated dates to provide the intervals estimates for the floruits.

The first data set (*Pfyn* culture) has 61 possible historical dates calibrated from the 35 radiocarbon dates taken from the culture. These data are shown in table (3.3) with the two series constructed for the fractional weighting method and in table (3.4) with the two series constructed for the weighted average method. The other data set (*Sâone-Rhône* culture) has 72 possible historical dates calibrated from the 38 radiocarbon dates taken from the culture. Table (3.5) shows the data with the two series constructed for the fractional weighting method and table (3.6) shows the data with the two series constructed for the weighted average method. As before the quartiles are found at 9.25^{th} and 26.75^{th} positions for the *Pfyn* data and at 10^{th} and 29^{th} position for the *Sâone-Rhône* data. The resulting E.Q.I.'s for the calibrated dates which will provide the intervals estimates for the floruits are summarised, and rounded to the nearest decade, in the following table:-

Culture	Method	Extended Quartile Interval
Pfyn	Fractional Weighting (B1)	3550 - 4010
	Weighted Average (B2)	3550 - 4010
Sâone-Rhône	Fractional Weighting (B1)	2500 - 2910
	Weighted Average (B2)	2500 - 2900

y_i	k_i	$\hat{t}_{ij}$	$Se(\hat{t}_{ij})$	$\hat{\xi}_{ij}$	$\hat{\zeta}_{ij}$	ω_{ij}
4690	3	3387	114	3310(4)	3464(1)	0.33
		3414	190	3285(3)	3543(3)	0.33
		3499	110	3424(6)	3574(10)	0.33
4690	3	3387	152	3284(2)	3490(2)	0.33
		3414	256	3241(1)	3587(11)	0.33
		3499	147	3399(5)	3599(13)	0.33
4735	1	3517	82	3461(8)	3573(9)	1
4750	3	3524	67	3478(10)	3570(8)	0.33
		3588	75	3537(21)	3639(19)	0.33
		3603	67	3557(26)	3649(23)	0.33
4750	3	3524	41	3496(11)	3552(6)	0.33
		3588	93	3525(17)	3651(24)	0.33
		3603	112	3527(19)	3679(27)	0.33
4750	3	3524	41	3496(12)	3552(7)	0.33
		3588	93	3525(18)	3651(25)	0.33
		3603	112	3527(20)	3679(28)	0.33
4755	3	3526	29	3506(15)	3546(4)	0.33
		3584	46	3552(24)	3616(15)	0.33
		3608	48	3575(27)	3641(20)	0.33
4765	3	3530	31	3509(16)	3551(5)	0.33
		3578	38	3552(23)	3604(14)	0.33
		3614	34	3591(28)	3637(17)	0.33
4780	3	3538	149	3437(7)	3639(18)	0.33
		3569	152	3465(9)	3671(26)	0.33
		3621	100	3553(25)	3689(29)	0.33
4790	3	3545	70	3497(13)	3593(12)	0.33
		3560	82	3504(14)	3616(16)	0.33
		3625	26	3607(29)	3643(21)	0.33
4800	1	3629	25	3612(30)	3646(22)	1
4850	1	3653	160	3545(22)	3761(35)	1
4875	1	3682	56	3644(31)	3720(31)	1

y_i	k_i	$\hat{t}_{ij}$	$Se(\hat{t}_{ij})$	$\hat{\xi}_{ij}$	$\hat{\zeta}_{ij}$	ω_{ij}
4910	1	3699	59	3659(32)	3739(33)	1
4915	1	3701	24	3684(35)	3718(30)	1
4930	1	3707	46	3675(34)	3739(32)	1
4940	3	3711	55	3673(33)	3749(34)	0.33
		3754	64	3710(36)	3798(37)	0.33
		3761	67	3715(37)	3807(38)	0.33
4965	1	3778	24	3761(39)	3795(36)	1
4980	1	3783	38	3757(38)	3809(40)	1
4990	1	3786	33	3763(40)	3809(39)	1
5020	1	3798	28	3779(44)	3817(41)	1
5030	1	3802	32	3780(45)	3824(42)	1
5040	3	3806	42	3777(43)	3835(43)	0.33
		3881	89	3820(47)	3942(45)	0.33
		3915	144	3817(46)	4013(50)	0.33
5060	3	3815	70	3767(42)	3863(44)	0.33
		3864	147	3764(41)	3964(46)	0.33
		3935	110	3860(48)	4010(49)	0.33
5100	1	3958	65	3914(49)	4002(47)	1
5100	1	3958	65	3914(50)	4002(48)	1
5140	1	3979	90	3918(51)	4040(55)	1
5160	1	3987	66	3942(53)	4032(54)	1
5170	1	3990	37	3965(54)	4015(51)	1
5180	1	3994	89	3933(52)	4055(56)	1
5180	1	3994	37	3969(55)	4019(52)	1
5200	1	4001	45	3970(56)	4032(53)	1
5280	1	4051	57	4011(57)	4089(57)	1
5320	3	4154	46	4122(58)	4186(58)	0.33
		4194	49	4160(59)	4228(59)	0.33
		4222	39	4195(60)	4249(60)	0.33
5415	1	4324	55	4286(61)	4362(61)	1

Table 3.3: Estimates of historical dates (years BC) corresponding to each radiocarbon date (years BP), their estimated standard errors, lower series ($\hat{\xi}_{ij}$) ,upper series ($\hat{\zeta}_{ij}$) and their weights (ω_{ij}) from *Pfyn* culture (Note that : $\hat{\xi}_{ij}$ rounded down to the previous integer and $\hat{\zeta}_{ij}$ rounded up to the next integer).

y_i	k_i	$\hat{t}_{ij}$	$Se(\hat{t}_{ij})$	$\bar{t}_{i\bullet}$	$Se(\bar{t}_{i\bullet})$	$\hat{\xi}_{ij}$	$\hat{\zeta}_{ij}$
4690	3	3387	114	3440	74	3390(2)	3490(1)
		3414	190				
		3499	110				
4690	3	3387	152	3440	98	3373(1)	3507(2)
		3414	256				
		3499	147				
4735	1	3517	82	3517	82	3461(3)	3573(6)
4750	3	3524	67	3541	40	3543(8)	3597(8)
		3588	75				
		3603	67				
4750	3	3524	41	3541	35	3517(4)	3565(3)
		3588	93				
		3603	112				
4750	3	3524	41	3541	35	3517(5)	3565(4)
		3588	93				
		3603	112				
4755	3	3526	29	3555	22	3540(7)	3570(5)
		3584	46				
		3608	48				
4765	3	3530	31	3571	20	3557(10)	3585(7)
		3578	38				
		3614	34				
4780	3	3538	149	3589	73	3539(6)	3639(10)
		3569	152				
		3621	100				
4790	3	3545	70	3611	23	3595(11)	3627(9)
		3560	82				
		3625	26				
4800	1	3629	25	3629	25	3612(12)	3646(11)
4850	1	3653	160	3653	160	3545(9)	3761(16)
4875	1	3682	56	3682	56	3644(13)	3720(13)

y_i	k_i	$\hat{t}_{ij}$	$Se(\hat{t}_{ij})$	$\bar{t}_{i\bullet}$	$Se(\bar{t}_{i\bullet})$	$\hat{\xi}_{ij}$	$\hat{\zeta}_{ij}$
4910	1	3699	59	3699	59	3659(14)	3739(15)
4915	1	3701	24	3701	24	3684(16)	3718(12)
4930	1	3707	46	3707	46	3675(15)	3738(14)
4940	3	3711	55	3738	35	3714(17)	3762(17)
		3754	64				
		3761	67				
4965	1	3778	24	3778	24	3761(19)	3795(18)
4980	1	3783	38	3783	38	3757(18)	3809(20)
4990	1	3786	33	3786	33	3763(20)	3809(19)
5020	1	3798	28	3798	28	3779(21)	3817(21)
5030	1	3802	32	3802	32	3780(22)	3824(22)
5040	3	3806	42	3826	36	3801(23)	3851(23)
		3881	89				
		3915	144				
5060	3	3815	70	3851	55	3813(24)	3889(24)
		3864	147				
		3935	110				
5100	1	3958	65	3958	65	3914(25)	4002(25)
5100	1	3958	65	3958	65	3914(26)	4002(26)
5140	1	3979	90	3979	90	3918(27)	4040(31)
5160	1	3987	66	3987	66	3942(29)	4032(30)
5170	1	3990	37	3990	37	3965(30)	4015(27)
5180	1	3994	89	3994	89	3933(28)	4054(32)
5180	1	3994	37	3994	37	3969(31)	4019(28)
5200	1	4001	45	4001	45	3970(32)	4032(29)
5280	1	4051	57	4051	57	4012(33)	4090(33)
5320	3	4154	46	4193	25	4176(34)	4210(34)
		4194	49				
		4222	39				
5415	1	4324	55	4324	55	4286(35)	4362(35)

Table 3.4: Estimates of historical dates (years BC) corresponding to each radiocarbon date (years BP), their estimated standard errors, weighted averages ($\bar{t}_{i\bullet}$), standard error of the averages, lower series ($\hat{\xi}_{ij}$) and upper series ($\hat{\zeta}_{ij}$) from *Pfyn* culture (Note that : $\hat{\xi}_{ij}$ rounded down to the previous integer and $\hat{\zeta}_{ij}$ rounded up to the next integer.)

y_i	k_i	$\hat{t}_{ij}$	$Se(\hat{t}_{ij})$	$\hat{\xi}_{ij}$	$\hat{\zeta}_{ij}$	ω_{ij}
3900	1	2461	62	2419(2)	2503(1)	1
3900	1	2461	62	2419(3)	2503(2)	1
3960	1	2482	73	2432(6)	2532(4)	1
3970	1	2485	65	2441(9)	2529(3)	1
3990	1	2494	75	2443(10)	2545(5)	1
4000	1	2499	104	2428(4)	2570(7)	1
4000	1	2499	130	2411(1)	2587(9)	1
4000	1	2499	87	2440(8)	2558(6)	1
4010	3	2506	114	2429(5)	2583(8)	0.33
		2538	135	2446(11)	2630(12)	0.33
		2562	127	2476(13)	2648(16)	0.33
4020	3	2515	112	2439(7)	2591(10)	0.33
		2527	118	2447(12)	2607(11)	0.33
		2569	102	2500(14)	2638(13)	0.33
4030	1	2575	96	2510(15)	2640(14)	1
4060	1	2594	98	2527(16)	2661(20)	1
4077	1	2602	57	2563(21)	2641(15)	1
4080	1	2604	77	2552(18)	2656(18)	1
4080	1	2604	77	2552(19)	2656(19)	1
4090	3	2610	68	2564(23)	2656(17)	0.33
		2835	35	2811(51)	2859(46)	0.33
		2842	31	2821(53)	2863(48)	0.33
4100	3	2615	83	2559(20)	2671(21)	0.33
		2823	101	2754(39)	2892(53)	0.33
		2852	86	2793(50)	2911(61)	0.33
4100	3	2615	110	2540(17)	2690(23)	0.33
		2823	134	2732(38)	2914(62)	0.33
		2852	114	2775(45)	2929(66)	0.33
4103	3	2618	80	2564(22)	2672(22)	0.33
		2821	63	2777(48)	2863(47)	0.33
		2855	52	2819(52)	2891(52)	0.33
4129	3	2678	93	2615(26)	2741(24)	0.33
		2810	35	2786(49)	2834(35)	0.33
		2864	20	2850(64)	2878(49)	0.33
4130	3	2678	108	2605(25)	2751(25)	0.33
		2810	50	2776(47)	2844(41)	0.33
		2864	29	2844(57)	2884(50)	0.33
4140	5	2693	168	2579(24)	2807(28)	0.2
		2727	161	2618(28)	2836(38)	0.2
		2752	148	2652(29)	2852(44)	0.2
		2807	64	2763(42)	2851(43)	0.2
		2867	60	2826(54)	2908(59)	0.2
4140	5	2693	113	2616(27)	2770(26)	0.2
		2727	101	2658(30)	2796(27)	0.2
		2752	87	2693(31)	2811(29)	0.2
		2807	46	2775(46)	2839(39)	0.2
		2867	29	2847(61)	2886(51)	0.2
4160	3	2767	79	2713(35)	2821(30)	0.33
		2801	47	2769(44)	2833(34)	0.33
		2872	40	2845(59)	2899(55)	0.33
4160	3	2767	95	2702(32)	2832(33)	0.33
		2801	56	2763(41)	2839(40)	0.33
		2872	48	2839(55)	2905(58)	0.33
4160	3	2767	87	2708(34)	2826(32)	0.33
		2801	51	2766(43)	2836(37)	0.33
		2872	44	2842(56)	2902(57)	0.33
4170	3	2772	72	2723(36)	2821(31)	0.33
		2798	54	2761(40)	2835(36)	0.33
		2874	40	2847(60)	2901(56)	0.33
4180	3	2777	103	2707(33)	2847(42)	0.33
		2794	94	2730(37)	2858(45)	0.33
		2877	48	2844(58)	2910(60)	0.33
4191	1	2879	29	2859(67)	2899(54)	1
4200	1	2882	47	2850(62)	2914(63)	1
4210	1	2885	45	2854(66)	2916(64)	1
4230	1	2891	56	2853(65)	2929(65)	1
4260	1	2901	56	2863(68)	2939(67)	1
4280	1	2907	84	2850(63)	2964(72)	1
4290	1	2911	61	2869(69)	2953(70)	1
4300	1	2914	48	2881(71)	2947(68)	1
4300	1	2914	53	2878(70)	2950(69)	1
4320	1	2920	51	2885(72)	2955(71)	1

Table 3.5: Estimates of historical dates (years BC) corresponding to each radiocarbon date (years BP), their estimated standard errors, lower series ($\hat{\xi}_{ij}$) ,upper series ($\hat{\zeta}_{ij}$) and their weights (ω_{ij}) from *Sâone-Rhône* culture (Note that $\hat{\xi}_{ij}$ rounded down to the previous integer and $\hat{\zeta}_{ij}$ rounded up to the next integer.)

y_i	k_i	$\hat{t}_{ij}$	$Se(\hat{t}_{ij})$	$\bar{t}_{i\bullet}$	$Se(\bar{t}_{i\bullet})$	$\hat{\xi}_{ij}$	$\hat{\zeta}_{ij}$
3900	1	2461	62	2461	62	2419(2)	2503(1)
3900	1	2461	62	2461	62	2419(3)	2503(2)
3960	1	2482	73	2482	73	2432(5)	2532(4)
3970	1	2485	65	2485	65	2441(7)	2529(3)
3990	1	2494	75	2494	75	2443(8)	2545(5)
4000	1	2499	104	2499	104	2428(4)	2570(7)
4000	1	2499	130	2499	130	2411(1)	2587(10)
4000	1	2499	87	2499	87	2440(6)	2558(6)
4010	3	2506	114	2533	72	2484(9)	2582(8)
		2538	135				
		2562	127				
4020	3	2515	112	2539	64	2495(10)	2583(9)
		2527	118				
		2569	102				
4030	1	2575	96	2575	96	2510(11)	2640(11)
4060	1	2594	98	2593	98	2527(12)	2661(15)
4077	1	2602	57	2602	57	2564(15)	2640(12)
4080	1	2604	77	2604	77	2552(13)	2656(13)
4080	1	2604	77	2604	77	2552(14)	2656(14)
4090	3	2610	68	2815	22	2800(20)	2830(19)
		2835	35				
		2842	31				
4100	3	2615	83	2754	51	2719(17)	2789(16)
		2823	101				
		2852	86				
4100	3	2615	110	2754	68	2708(16)	2800(17)
		2823	134				
		2852	114				
4103	3	2618	80	2797	36	2772(18)	2822(18)
		2821	63				
		2855	52				
4129	3	2678	93	2845	17	2833(28)	2857(26)
		2810	35				
		2864	20				
4130	3	2678	108	2841	25	2824(27)	2858(27)
		2810	50				
		2864	29				

y_i	k_i	$\hat{t}_{ij}$	$Se(\hat{t}_{ij})$	$\bar{t}_{i\bullet}$	$Se(\bar{t}_{i\bullet})$	$\hat{\xi}_{ij}$	$\hat{\zeta}_{ij}$
4140	5	2693	168	2818	39	2791(19)	2845(20)
		2727	161				
		2752	148				
		2807	64				
		2867	60				
4140	5	2693	113	2831	23	2815(25)	2847(21)
		2727	101				
		2752	87				
		2807	46				
		2867	29				
4160	3	2767	79	2833	28	2814(23)	2852(22)
		2801	47				
		2872	40				
4160	3	2767	95	2833	34	2810(21)	2856(25)
		2801	56				
		2872	48				
4160	3	2767	87	2833	31	2812(22)	2854(23)
		2801	51				
		2872	44				
4170	3	2772	72	2835	29	2815(24)	2855(24)
		2798	54				
		2874	40				
4180	3	2777	103	2848	39	2821(26)	2875(28)
		2794	94				
		2877	48				
4191	1	2879	29	2879	29	2859(33)	2899(29)
4200	1	2882	47	2882	47	2850(29)	2914(30)
4210	1	2885	45	2885	45	2854(32)	2916(31)
4230	1	2891	56	2891	56	2853(31)	2929(32)
4260	1	2901	56	2901	56	2863(34)	2939(33)
4280	1	2907	84	2907	84	2850(30)	2964(38)
4290	1	2911	61	2911	61	2869(35)	2952(36)
4300	1	2914	48	2914	48	2881(37)	2947(34)
4300	1	2914	53	2914	53	2878(36)	2950(35)
4320	1	2920	51	2920	51	2885(38)	2955(37)

Table 3.6: Estimates of historical dates (years BC) corresponding to each radiocarbon date (years BP), their estimated standard errors, weighted averages ($\bar{t}_{i\bullet}$), standard error of the average, lower series ($\hat{\xi}_{ij}$) and upper series ($\hat{\zeta}_{ij}$) from *Sâone-Rhône* culture (Note that : $\hat{\xi}_{ij}$ rounded down to the previous integer and $\hat{\zeta}_{ij}$ rounded up to the next integer.)

3.6 Computational Methods

The preceding section has been concerned with simple ad hoc pen and paper methods to provide point and interval estimates for the floruit. This section deals with the problem in a more formal way using computational methods which involve the estimate of a density function underlying the culture.

At the start of this section remember the two assumptions from section 3.2 which underlay any formal approach to the problem and redefine the problem here.

The two assumptions were

a) There is a frequency distribution of all possible artefacts from the culture or phenomenon from which the sample is drawn.

and b) These sampled artefacts are assumed to be a reasonably representative sample from this frequency distribution.

In order to estimate the floruit of the culture (as defined early) first estimate the frequency distribution , say $p(t)$, underlying the culture where t is the historical time and hence its lower quartile $\eta_{0.25}$ and upper quartile $\eta_{0.75}$ which constitute the floruit.

The data available to provide inferences about the two quartiles $\eta_{0.25}$ and $\eta_{0.75}$ are the radiocarbon dates

$$y_1, y_2, \ldots\ldots\ldots\ldots, y_n$$

and their associated errors

$$\sigma_1, \sigma_2, \ldots\ldots\ldots\ldots, \sigma_n$$

where n is the number of artefacts sampled.

Since each of the radiocarbon dates , y_i , has been produced from a true but unknown historical age , t_i , from the underlying probability density

function (p.d.f.) $p(t)$, then the relationship between the radiocarbon dates and the historical ages is

$$y_i = f(t_i) + \varepsilon_i$$

where $\varepsilon_i \sim N(0, \sigma_i^2)$ and all the ε_i are assumed independent. This model is the basis to enable one to provide estimates $\hat{t}_{ij}$ for the historical ages which might have generated the observed radiocarbon dates y_i based on the estimated calibration function $\hat{f}(.)$.

Once such estimates $\hat{t}_{ij}$ for $j = 1,....., k_i$ and $i = 1,....., n$ have been provided then attempt an estimate of the frequency distribution $p(t)$ underlying the culture and finally estimate the lower quartile and upper quartile ($\eta_{0.25}$, $\eta_{0.75}$) of $p(t)$ as an estimate of the floruit itself.

3.7 Density Estimation

One of the basic concepts in statistics is the probability density function (p.d.f) which is a very useful tool for exploring the distribution structure of an unknown population. For a set of observed data points, assumed to have been sampled from an unknown population, the fundamental problem is the estimation of the distribution function or the density function of the population from which the sample has been drawn.

There are two approaches to density estimation, parametric and non-parametric. In the parametric approach a rigid assumption will be made about the family of distributions from which the observed data is assumed to have arisen. For example, the data may be assumed to have been sampled from a population adequately described by some (unknown) member of the normal family. This assumption requires the estimate of one or more population parameters such as the mean and variance in the case of the normal.

In contrast to the parametric approach, the non-parametric approach does not involve the assumption of a family of distributions or the investigation of the population parameters. Virtually the only basic assumption in the non-parametric approach is that the underlying p.d.f. is "smooth" in a mathematical sense. Here the data are allowed to speak for themselves in determining the estimate of the probability density function to a much greater extent than by imposing a specific parametric model upon them.

The existing methods of non-parametric density estimation for both univariate and multivariate cases such as histogram, naive estimator, kernel estimator, orthogonal series and many others have been described by, for example, Prakasa Rao (1983) and Silverman (1986). Here the method based on kernel density estimation which was first suggested by Rosenblatt (1956) and then developed later by Whittle (1958) and Parzen (1962) will be used because it has a wide applicability, involves only simple calculation and is straight forward to apply. This choice does not mean that the kernel method is necessarily the best in all circumstances, although it would be surprising if the method did not prove more than adequate.

Now for convenience consider the general form of the kernel estimator in the following section and then it application to the estimated calibrated dates $\hat{t}_{ij}$ in order to provide the estimate of the frequency distribution underlying the historical culture or phenomenon (section 3.7.2) which will be used to provide the floruit estimate for the culture.

3.7.1 General Kernel Density Estimator

For a random sample, $t_1, t_2, \ldots\ldots, t_n$, drawn from a population with probability density function $p(t)$, the aim of kernel density estimation is to provide such an estimate $\hat{p}(t)$ for the function $p(t)$.

The kernel density estimator $\hat{p}(t)$ can be written in the form

$$\hat{p}(t) = \frac{1}{n\lambda} \sum_{i=1}^{n} K\left(\frac{t - t_i}{\lambda}\right) \qquad .....(3.6)$$

where K(.) is a smooth so-called kernel function, usually a symmetric probability density function and λ is a smoothing parameter which controls the width of K(.) and hence the degree of smoothness of the function $\hat{p}(t)$. In other word the shape of the contribution to $\hat{p}(.)$ centred at each observation is determined by the kernel function while the smoothing parameter λ determines their width. The kernel estimator $\hat{p}(t)$ is produced from the summation of the protuberances (see figure 3.4 for illustration).

In fact the value of smoothing parameter λ is the important element and is widely held to be far more crucial in determining the shape of the density function more than the choice of K(.) itself (Silverman; 1986). Methods of choosing the smoothing parameter will be considered later (section 3.8).

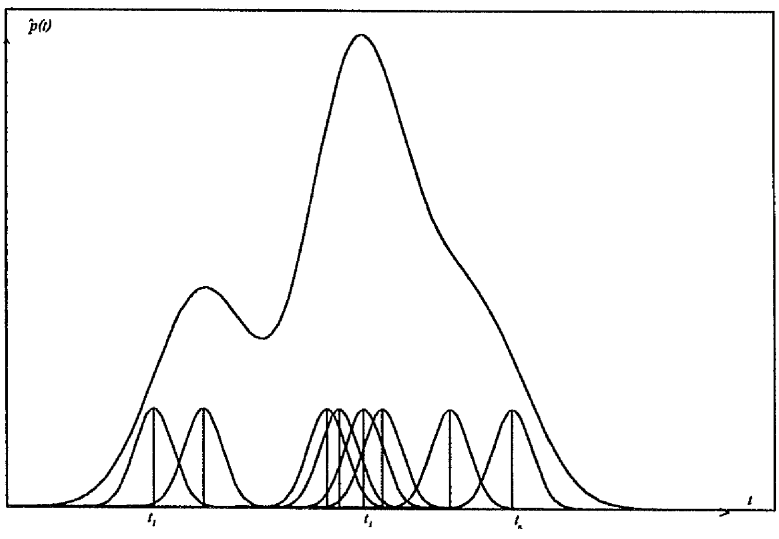

Figure 3.4 : Definition of Kernel estimate showing individual kernels.

3.7.2 Estimation of the Frequency Distribution Underlying a Culture

In order to estimate the frequency distribution underlying a culture, combine the calibrated historical dates $\hat{t}_{ij}$ (already estimated in section 2.8) by using a form of kernel density estimation technique based on the estimated standard errors $Se(\hat{t}_{ij})$ (section 2.9) as weights.

In this case the estimate, $\hat{p}(t)$, of the frequency distribution $p(t)$ will take this form

$$\hat{p}(t) = \frac{1}{n\lambda} \sum_{i=1}^{n} \frac{1}{k_i} \sum_{j=1}^{k_i} K\left(\frac{t - \hat{t}_{ij}}{\lambda Se(\hat{t}_{ij})} \right) \qquad .....(3.7)$$

where k_i is the (odd) number of possible historical dates corresponding to the i^{th} sample of the observed radiocarbon dates, y_i . K(.) is chosen to be a normal kernel density with smoothing parameter λ chosen by an appropriate data-dependent method (section 3.8). In general the value of λ is crucial and different for each separate group of radiocarbon dates (i.e. from each separate phenomenon). The above estimator, $\hat{p}(t)$, implies that at any value, t, in the historical timescale it is a weighted average of kernel functions centred at each of the $\hat{t}_{ij}$ respectively. The further away t is from $\hat{t}_{ij}$ then, generally speaking, the less influence $\hat{t}_{ij}$ has on the estimate of the frequency distribution at t (although the estimated standard error of the calibrated dates $\hat{t}_{ij}$ also plays an important role in this influence).

3.8 Choosing the Smoothing Parameter

While the choice of the kernel function K(.) and the value of the smoothing parameter λ are necessary for density estimates, it is generally accepted in density estimation that the problem of choosing the smoothing parameter λ (called the window width in some literature) is more crucial than the choice of kernel function K(.). Figure 3.5 illustrates the effect of different values of the

smoothing parameter for a set of data taken from a bimodal distribution. When λ is chosen too small the spikes appear at the observations (i.e. we are under smoothing the data), while if λ is chosen too large then the true nature of the distribution can disappear (i.e. over smoothed).

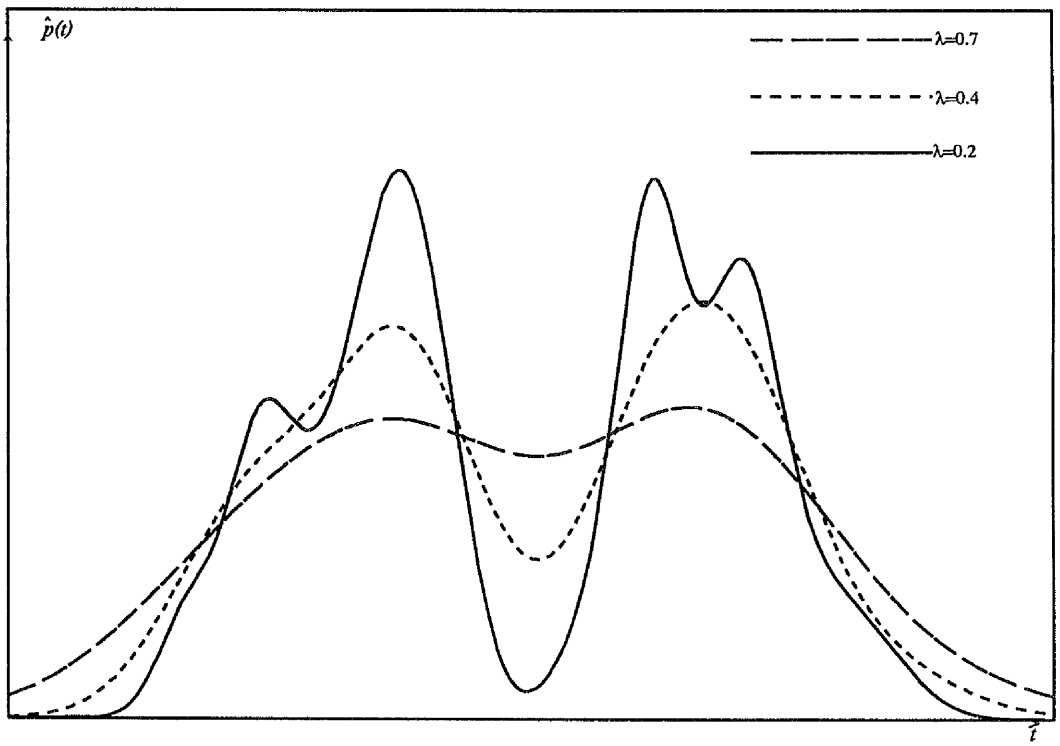

Figure 3.5 : Effect of different values of the smoothing parameter on density estimation.

Various methods have been proposed for the choice of the smoothing parameter. These either involve a subjective choice by plotting the density function for various values of the smoothing parameter (Scott *et al.*; 1977) which is used for purposes of exploratory data analysis or an "objective" (automatic) choice which uses the data to provide an appropriate value of the smoothing parameter when using density estimation for presenting conclusions. Several authors have discussed and compared the methods of choosing the smoothing parameter, for a review see for example Bowman (1981), Silverman

(1986) and Park and Marron (1990). There is no intention to go into theoretical details of these methods and compare them in this work. The goal here is to employ some of the existing methods to provide a reasonable choice for the smoothing parameter λ .

3.8.1 Cross-validation Method

One of the most popular approaches in choosing the smoothing parameter was suggested by Habbema, Hermans and Van der Broek (1974) and by Duin (1976) using a maximum likelihood approach.

When maximising the likelihood function (as a function of λ)

$$\prod_{i=1}^{n} \hat{p}(t_i) \qquad .....(3.8)$$

the solution is $\lambda = 0$ which is unsatisfactory because the estimate will contain a spike placed at each data point. Habbema et al and Duin resolved this by choosing λ to maximise

$$\prod_{i=1}^{n} \hat{p}_{-i}(t_i) \qquad .....(3.9)$$

where $\hat{p}_{-i}(t_i)$ is the density estimate at the point t_i constructed from all the data points except t_i . This approach which leads (not always) to a reasonable degree of smoothing was shown by Titterington (1980) to be a cross-validatory choice in the sense of Stone (1974).

Since the maximum of the log likelihood function occurs at the maximum of the likelihood function then maximise

$$\frac{1}{n} \sum_{i=1}^{n} log\ \hat{p}_{-i}(t_i) \qquad .....(3.10)$$

with respect to λ

For practical convenience the cross-validation technique will be described briefly in the following steps using the definition in (3.7).

i.e. maximise

$$CV(\lambda) = \frac{1}{n} \sum_{i=1}^{n} \frac{1}{k_i} \sum_{j=1}^{k_i} log\ \hat{p}_{-ij}(\hat{t}_{ij}) \qquad .....(3.11)$$

- *Step 1* choose a small starting value of the smoothing parameter λ .
- *Step 2* Omit one of the calibrated dates $\hat{t}_{ij}$ $i=1,.....,n$ and $j=1,.....,k_i$.
- *Step 3* Evaluate the log likelihood function, $log\ \hat{p}_{-ij}(\hat{t}_{ij})$, for $\hat{t}_{ij}$ based on the remaining calibrated dates, where $\hat{p}_{-ij}(\bullet)$ is as defined in (3.9) above.
- *Step 4* Repeat step 2 and 3 for all calibrated dates and calculate the cross-validation function which is averaged over each choice of omitted $\hat{t}_{ij}$ to obtain

$$CV(\lambda) = \frac{1}{n} \sum_{i=1}^{n} \frac{1}{k_i} \sum_{j=1}^{k_i} log\ \hat{p}_{-ij}(\hat{t}_{ij}) \qquad \text{for the particular value of } \lambda$$

- *Step 5* Repeat the process for a different value of the smoothing parameter λ and repeat steps 2,3 and 4 until a sensible range of values of λ has been covered.

Finally, the optimal choice of λ for the likelihood cross-validation is then the value of λ which maximises the function $CV(\lambda)$ for the calibrated dates.

The method of likelihood cross-validation has the advantages that it is a completely automatic method for choosing the smoothing parameter and does not present severe computational difficulties. In general, the method of cross-validation has proved to be useful in the control of the degree of smoothing

when estimating non-parametrically an unknown probability density function. This does not means that the cross-validation method is the best in all circumstances. It leads sometimes to an unsatisfactory choice for the smoothing parameter (either under or over smoothing the function) because it is a data-dependent method (*i.e.* a different value for the smoothing parameter for each different data set). To illustrate this further, the following examples are considered.

3.8.1.1 Illustrative Examples

Cross-validation was applied to the previous data sets (the *Pfyn* and *Sâone-Rhône* cultures). The historical dates of both data cultures have been used to construct the density functions underlying the two cultures using normal kernel functions.

In the *Pfyn* data cross-validation produces a smoothing parameter of 1.2 which produces a density estimate underlying the culture which looks reasonably smoothed and is shown in figure (3.6a). For the *Sâone-Rhône* data the smoothing parameter chosen by cross-validation is 0.14 which produces a density estimate underlying the culture which appears under smoothed and is shown in figure (3.7a). This is clearly an unsatisfactory representation of the data.

In an attempt to overcome the unsatisfactory choice produced by the cross-validation method, alternative methods for the choice of smoothing parameter are considered in the next section.

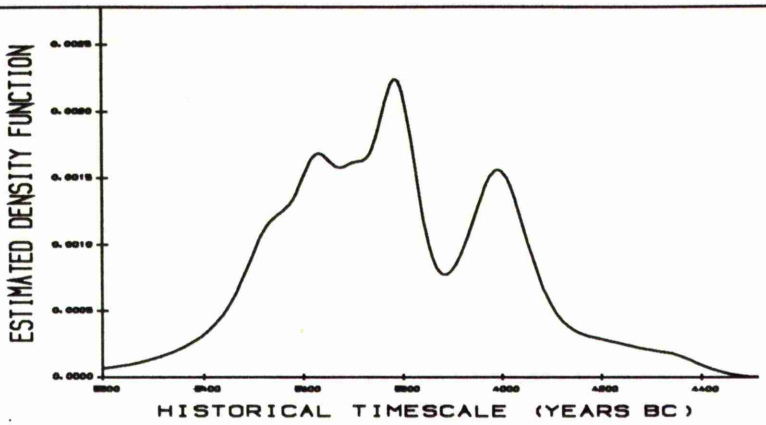

Figure 3.6a :

Density estimate of the true frequency distribution for the *Pfyn* culture (λ=1.2).

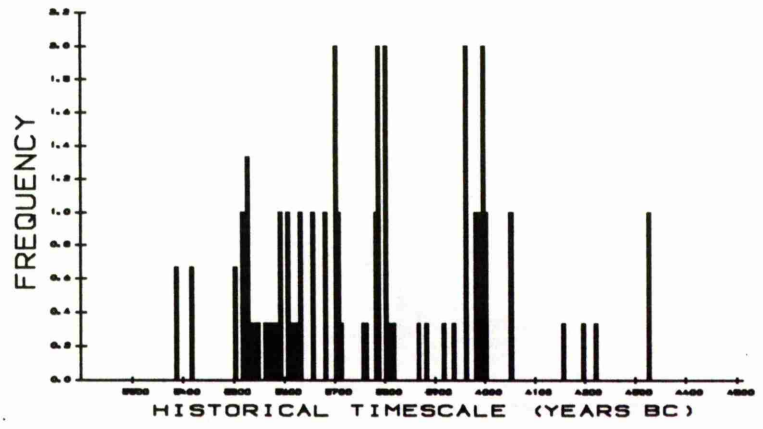

Figure 3.6b :

Histograms for the calibrated historical dates for the *Pfyn* culture.

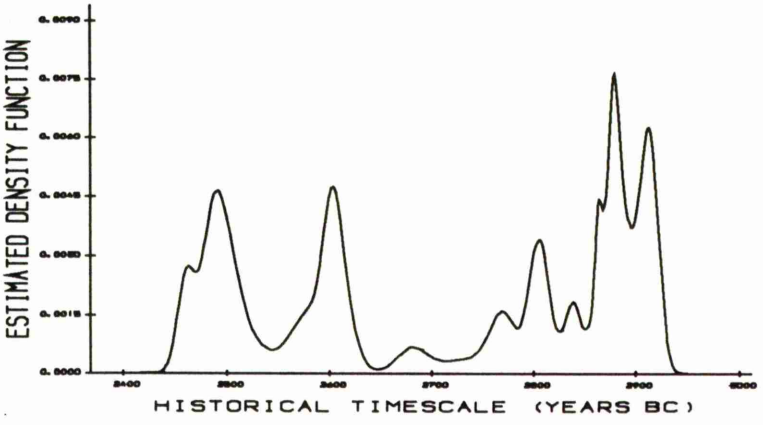

Figure 3.7a :

Density estimate of the true frequency distribution for the *Sâone-Rhône* culture (λ=0.14).

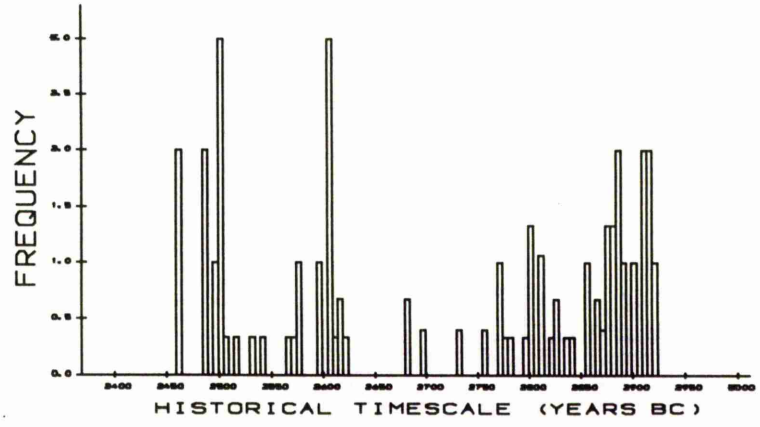

Figure 3.7b:

Histograms for the calibrated historical dates for the *Sâone-Rhône* culture.

3.8.2 Alternative Methods

Epanechnikov (1969) shows that an optimal choice for the smoothing parameter based on normal kernels can be obtained to approximately minimise the estimate of the mean integrated squared error. The optimal smoothing parameter can be regarded as a proportional to the standard deviation, say σ, of the true density.

The approximated formula for the optimal choice of the smoothing parameter, say λ_{opt}, using the normal kernel would be

$$\lambda_{opt} = \left(\frac{4}{3n}\right)^{\frac{1}{5}} \sigma \qquad .....(3.12)$$

where λ_{opt} replaces the quantity $\lambda Se(\hat{t}_{ij})$ in formula (3.7) above and the estimate $\hat{p}(t)$ of the frequency distribution $p(t)$ becomes

$$\hat{p}(t) = \frac{1}{n\,\lambda_{opt}} \sum_{i=1}^{n} \frac{1}{k_i} \sum_{j=1}^{k_i} K\left(\frac{t-\hat{t}_{ij}}{\lambda_{opt}}\right) \qquad .....(3.13)$$

To actually compute λ_{opt} for a set of data, it is generally necessary to estimate the standard deviation from the data and then to substitute the estimate in formula (3.12) above. This choice of λ_{opt} tends to perform well if the data is distributed normally and tends to over-smooth when used with bimodal or multimodal data (Silverman, 1986).

If every historical date was calibrated from different radiocarbon date (*i.e.* every single radiocarbon date y_i corresponds to one historical date t_i only) and the radiocarbon and hence historical dates have equal standard errors, then the standard deviation used in (3.12) can be calculated in the usual way

i.e. $$\hat{\sigma} = \sqrt{\frac{\sum_{i=1}^{n}(t_i - \bar{t})^2}{n}}$$

In practice of course, there is generally more than one possible historical date which may have produced the observed radiocarbon date (dependent on how wiggly the calibration curve is in the neighbourhood of the historical date). Also the standard errors for the radiocarbon dates and hence historical dates are almost always not equal. In this case one have to weight each historical date $\hat{t}_{ij}$ (*i.e.* inversely to its standard error $Se(\hat{t}_{ij})$) and then calculate the standard deviation for the weighted dates.

Two different *ad hoc* approaches have been used to estimate the smoothing parameter λ_{opt} based on approximately the same idea. Roughly speaking both methods are based on weighting in some fashion the historical dates according to their standard errors and then calculating some equivalent formula to the standard deviation for these weighted dates. The formula for these *ad hoc* approaches, say ***w1*** and ***w2***, are given below together with a rationalisation of the thinking behind the choice of weights.

The first possibility (***w1***) considered for estimation of the smoothing parameter was to base the standard deviation on the weighted averages of a multiple historical dates which might be calibrated from a single radiocarbon date. This has been achieved by using the following formula to evaluate the weighted averages, say $\bar{u}_{i\bullet}$, for the possible multiple dates

$$\bar{u}_{i\bullet} = \frac{\sum_{j=1}^{k_i} \frac{\hat{t}_{ij}}{Se(\hat{t}_{ij})}}{\sum_{j=1}^{k_i} \frac{1}{Se(\hat{t}_{ij})}}$$

and then calculate the standard deviation for $\bar{u}_{i\bullet}$ as follows

$$\hat{\sigma}_1 = \sqrt{\frac{\sum_{i=1}^{n} (\bar{u}_{i\bullet} - \bar{u}_{\bullet\bullet})^2}{n}} \qquad .....(3.14)$$

where $$\bar{u}_{\bullet\bullet} = \frac{\sum_{i=1}^{n} \bar{u}_{i\bullet}}{n}$$

Unfortunately, this approach does not perform well at all and generally produces large estimates for the smoothing parameter and hence tends to grossly over-smooth the data. The reason for this is because the weighted averages $\bar{u}_{i\bullet}$ have different standard errors.

The other possibility (*w2*) considered in the estimation of the smoothing parameter was as follows :-

Let $u_{ij} = \frac{\hat{t}_{ij}}{Se(\hat{t}_{ij})}$ (which will have a constant variance for all i and j).

Compute the standard deviation for the u_{ij} (which will be substituted for σ in the above formula (3.12) to evaluate the smoothing parameter) by using the following formula :-

$$\hat{\sigma}_2 = \sqrt{\frac{\sum_{i=1}^{n} \frac{1}{k_i} \sum_{j=1}^{k_i} (u_{ij} - \bar{u}_{\bullet\bullet})^2}{n}} \qquad .....(3.15)$$

which gives the weight $\frac{1}{k_i}$ to the sum of squares $\sum_{j=1}^{k_i} (u_{ij} - \bar{u}_{\bullet\bullet})^2$,

where $$\bar{u}_{\bullet\bullet} = \frac{\sum_{i=1}^{n} \frac{1}{k_i} \sum_{j=1}^{k_i} u_{ij}}{n}$$

Compared to the previous method this approach tends to produce smaller values of the smoothing parameter. In general this method works reasonably well and can provide more sensible smoothing (in some cases) than the method of cross-validation.

3.8.2.1 Illustrative Examples

The methods described in the previous section were applied to the *Pfyn* and *Sâone-Rhône* data sets and the resulting choices of the smoothing parameter are

Method used	Values of the smoothing parameter	
	Pfyn data	*Sâone-Rhône* data
(*w1*)	110.1	83.7
(*w2*)	31.51	16.5

Figure 3.8 shows the plots of the density function underlying the *Pfyn* culture using both methods. As mentioned earlier one can see that method *w2* tends to under-smooth the density function, while method *w1* has over-smoothed the function. The plots of the density function underlying the *Sâone-Rhône* culture using both methods are shown in figure 3.9. While method *w1* over-smooths, method *w2* provide reasonable smoothing (but possibly under-smoothed).

Comparing the resulting estimates of $p(t)$ for method *w1* with that of the cross-validation method (see figure 3.6 for the *Pfyn* data and figure 3.7 for the *Sâone-Rhône* data) show that, method *w2* performed moderately well in the case of *Sâone-Rhône* data set and provide better smoothing for the density function underlying the culture than the cross-validation method which is clearly under-smoothed the density function. For the *Pfyn* culture although cross-validation has produced a smoother density function estimate, *w2* also produced a reasonable level of smoothing. So, at least in these two examples, one of the smoothing methods based on the $\hat{t}_{ij}$ and their standard errors do as well as if not better than the cross-validation based technique.

Accordingly the later approach (*w2*) will be considered together with the cross-validation method in the estimation of the density function underlying a culture, while the first approach (*w1*) will be eliminated since it produces large

values of the smoothing parameter and hence over-smooths the density function.

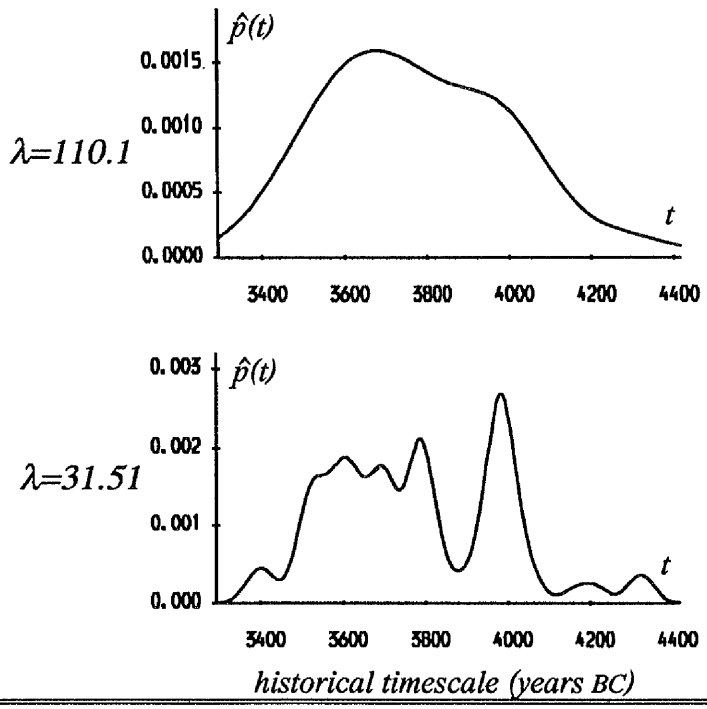

Figure 3.8 :

Density estimates underlying the *Pfyn* data with smoothing parameter obtained by the weighting methods.

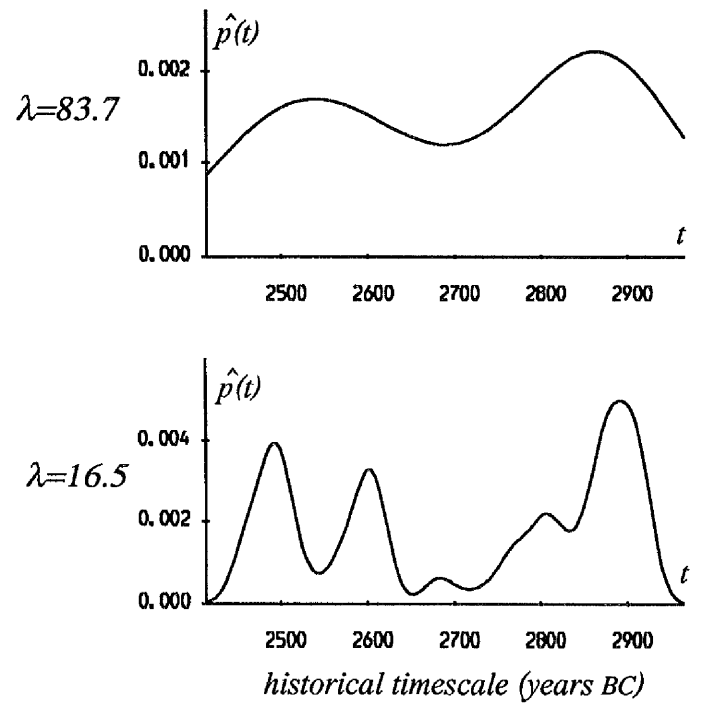

Figure 3.9:

Density estimates underlying the *Sâone-Rhône* data with smoothing parameter obtained by the weighting methods.

3.9 Floruit Estimation

With an appropriate choice for the smoothing parameter, the density function (frequency distribution), $\hat{p}(t)$, underlying a culture can be estimated. Once the density estimate is obtained one can turnover attention to the main goal of this chapter which is concerned with the estimation of the floruit for an archaeological culture or phenomenon.

3.9.1 Point Estimate for the Floruit

A very simple way to provide the point estimate for the floruit of a culture is to obtain an estimate of the cumulative distribution function (c.d.f.), $\hat{F}(t)$, of the frequency distribution by integrating the kernel estimator of the density underlying the culture and hence derive estimates of the quartiles directly.

The estimate of the c.d.f. of $\hat{p}(t)$ is

$$\hat{F}(t) = \int_{-\infty}^{t} \hat{p}(u)\, du$$

i.e. the proportion of artefacts or materials accumulated up to historical time *t*. (in practice '$-\infty$' means any point prior to the existence of any aspect of the culture).

In mathematical terms the estimate $\hat{F}(t)$ can be written as

$$\hat{F}(t) = \frac{1}{n}\sum_{i=1}^{n}\frac{1}{k_i}\sum_{j=1}^{k_i}\Phi\left(\frac{t-\hat{t}_{ij}}{\lambda\, Se(\hat{t}_{ij})}\right) \qquad .....(3.16)$$

with the smoothing parameter, λ, chosen by the cross-validation method and as

$$\hat{F}(t) = \frac{1}{n}\sum_{i=1}^{n}\frac{1}{k_i}\sum_{j=1}^{k_i}\Phi\left(\frac{t-\hat{t}_{ij}}{\lambda}\right) \qquad .....(3.17)$$

if the smoothing parameter, λ, is chosen by the ad hoc (weighting) method.

$\Phi(\bullet)$ is the cumulative distribution function for the standard normal distribution.

The next step is the estimate of the floruit which can be obtained from the solutions of $\hat{F}(t) = 0.25$ and $\hat{F}(t) = 0.75$ respectively to give $\hat{\eta}_{0.25}$ and $\hat{\eta}_{0.75}$ as the estimates of the lower and upper quartiles respectively. Figure 3.10 shows a diagrammatic representation for the floruit estimate which can be obtained graphically by intersecting the two values 0.25 and 0.75 in the c.d.f. axis with the function $\hat{F}(t)$ then projecting down onto the true historical timescale axis. The resulting "point" estimate of the floruit is $(\hat{\eta}_{0.25}, \hat{\eta}_{0.75})$.

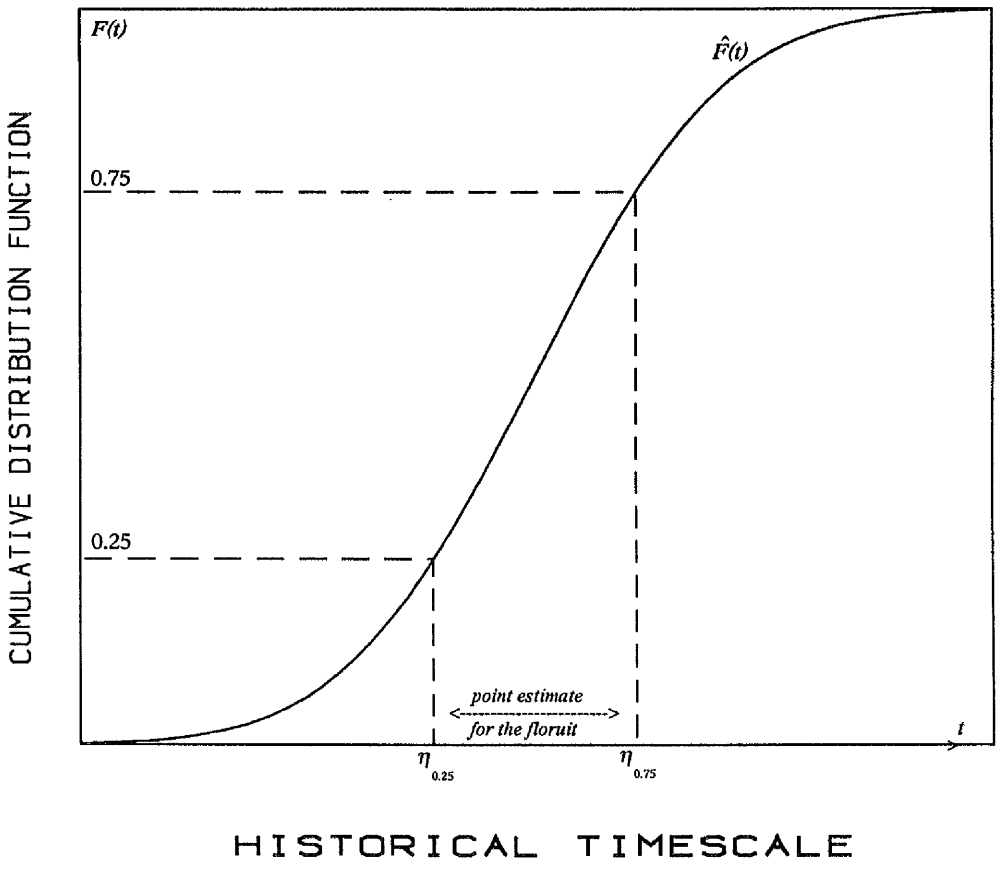

Figure 3.10 : Diagrammatic representation for the floruit estimate.

3.9.2 Interval Estimate for the Floruit

Although a 'point' estimate of the floruit is desirable, it is preferable to give some idea of its accuracy and this can be achieved through the production of an interval estimate. A number of possible techniques for constructing interval estimate for the floruit can be adopted. The method adopted in this work is to use an approximate pivotal function for the true cumulative distribution function $F(t)$ at each possible historical time t based on the estimate $\hat{F}(t)$ itself (Aitchison *et al*; 1991).

One obvious possible choice of approximate pivotal function for $F(t)$ (Azzalini; 1981) is given by

$$\frac{\hat{F}(t)-F(t)}{\sqrt{\frac{F(t)\{1-F(t)\}}{n}}} \overset{\cdot}{\sim} N(0,1)$$

resulting in an approximate 95% confidence interval for $F(t)$ of the form

$$I\{F(t)\}=\left\{F(t): \quad \left|\frac{\hat{F}(t)-F(t)}{\sqrt{\frac{F(t)\{1-F(t)\}}{n}}}\right| < N(0,1;0.975)\right\}$$

Although in practice it may will be reasonable to replace $F(t)\{1\text{-}F(t)\}$ above by $\hat{F}(t)\{1-\hat{F}(t)\}$, which results in the interval

$$I\{F(t)\}=\left\{F(t): \quad F(t) \in \hat{F}(t) \pm 1.96\sqrt{\frac{\hat{F}(t)\{1-\hat{F}(t)\}}{n}}\right\} \qquad .....(3.18)$$

This is clearly illustrated in figure 3.11 where $\hat{F}(t)$ is the middle band with the corresponding 95% confidence intervals for the true $F(t)$ "surrounding" it.

The remaining step in providing the approximate 95% confidence interval for the floruit is to use the confidence bands $\hat{F}(t) \pm 1.96\sqrt{\frac{\hat{F}(t)\{1-\hat{F}(t)\}}{n}}$ for the true $F(t)$ and intersect them with the two lines 0.25 and 0.75 respectively to give lower and upper bounds $(\hat{\eta}_L, \hat{\eta}_U)$ for the approximate 95% confidence interval for the true floruit (see figure 3.11 for illustration). Obviously this method allows that any other choice of percentage confidence can be adopted as required.

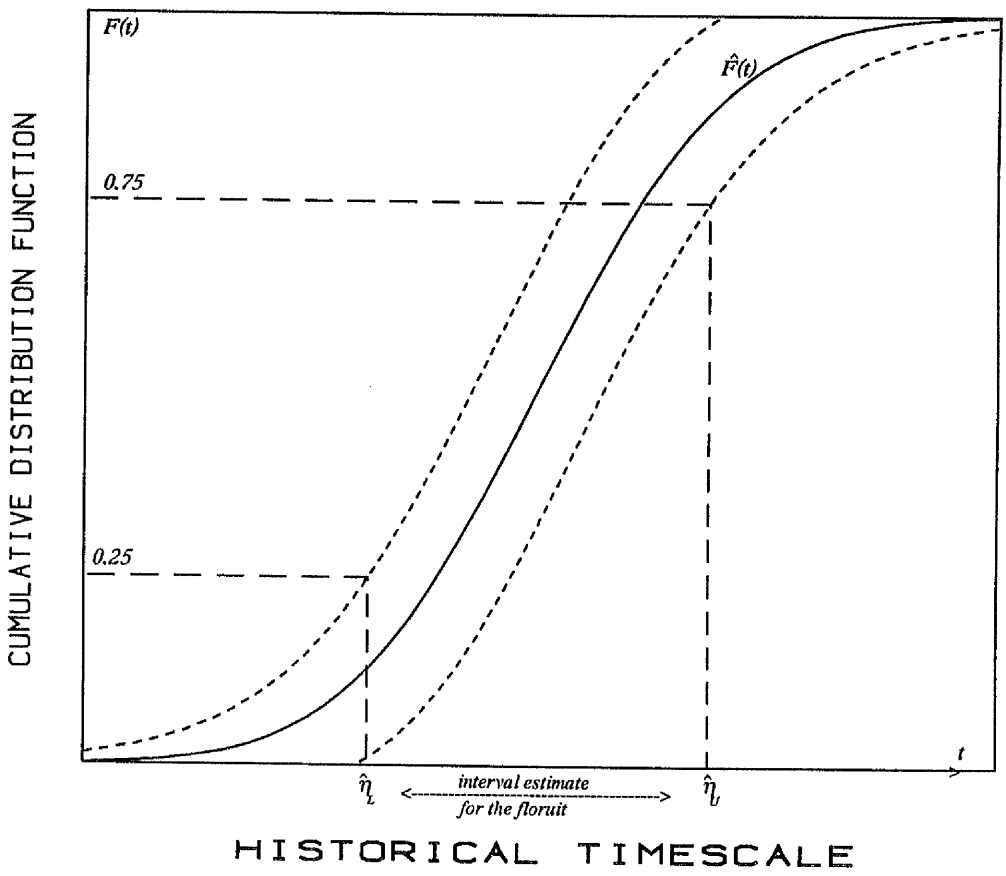

Figure 3.11 : Diagrammatic representation of the production of an interval estimate of the floruit .

Clearly there are also several possible choices of approximate pivotal function for *F(t)*- most of which are similar to these used in the production of an interval estimate for Binomial parameter. For example, to escape the problem of an interval estimate lying outside of the range [0,1] then one can use the logistic based result that if $x \sim Bi[n,\theta]$ then

$$\frac{\log\frac{x}{n-x} - \log\frac{\theta}{1-\theta}}{\sqrt{\frac{1}{x}+\frac{1}{n-x}}} \overset{\cdot}{\sim} N(o,1)$$

to produce an induced interval for θ. For the c.d.f. context replace θ by *F(t)* and $\frac{x}{n}$ by $\hat{F}(t)$. This interval will have the merit of always lying inside the interval [0,1] unlikely the previous.

Mathematically, the lowest value $\hat{\eta}_L$ of *t* whose (vertical) interval estimate for *F(t)* contains 0.25 can be obtained by solving the quadratic equation

$$0.25 = F(t) + 1.96\sqrt{\frac{F(t)\{1-F(t)\}}{n}} \qquad .....(3.19)$$

and the highest value $\hat{\eta}_U$ of *t* whose (vertical) interval estimate for *F(t)* contains 0.75 can be obtained by solving the equation

$$0.75 = F(t) - 1.96\sqrt{\frac{F(t)\{1-F(t)\}}{n}} \qquad .....(3.20)$$

An alternative approximation for the pivotal function is based on assuming that the vertical width of the confidence bands for *F(t)* will not be radically different at $t = \eta_{0.25}$ and at $t = \eta_{0.75}$. Effectively this means replacing *F(t)* or $\hat{F}(t)$ in the denominator by 0.25 for the production of $\hat{\eta}_{0.25}$ and similarly by 0.75 for the production of $\hat{\eta}_{0.75}$.

i.e. the approximate pivotal function used to provide $\hat{\eta}_L$ is

$$\frac{\hat{F}(t) - F(t)}{\sqrt{\frac{0.25(1-0.25)}{n}}} \sim N(0,1)$$

this results in an approximate 95% confidence interval for $F(t)$ of the form

$$I\{F(t)\} = \left\{ F(t): \quad F(t) \in \hat{F}(t) \pm 1.96 \sqrt{\frac{0.25(1-0.25)}{n}} \right\} \qquad .....(3.21)$$

Note : it is necessary in such a double approximation to ensure that n should be at least **12.**

The interval estimate for the floruit becomes the solutions of the following equations instead

$$0.25 = \hat{F}(t) + 1.96 \sqrt{\frac{0.25(1-0.25)}{n}}$$

for the lowest value of t

i.e. $$\hat{\eta}_L = \hat{F}^{-1} \left\{ 0.25 - 1.96 \sqrt{\frac{0.25(1-0.25)}{n}} \right\}$$

and $$0.75 = \hat{F}(t) - 1.96 \sqrt{\frac{0.75(1-0.75)}{n}}$$

for the highest value of t

i.e. $$\hat{\eta}_U = \hat{F}^{-1} \left\{ 0.75 + 1.96 \sqrt{\frac{0.75(1-0.75)}{n}} \right\}$$

This is clearly the simplest computational method for providing an interval estimate for the floruit as it requires only the estimate $\hat{F}$.

3.9.3 Illustrative Examples

To illustrate the above approach practically consider the two data sets given earlier (*Pfyn* and *Sâone-Rhône* data) and provide point estimates for the true floruit for both cultures with corresponding 95% confidence intervals. As discussed above these are based on estimating the cumulative distribution function which is necessary for estimation of the floruit. This can be achieved easily by integrating the estimate of the density function underlying each culture and constructing a confidence band around the estimate. The cumulative distribution function is the middle band shown in Figures 3.12 to 3.15 with the interval estimates for the true $F(t)$ surrounding it. Reading off the point and interval estimates for the true quartiles of the frequency distribution of both cultures give the results summarised in table (3.7) as point estimates with corresponding approximate 95% confidence intervals for the floruits of the two cultures.

Culture	Method	Smoothing parameter	Point Estimate (years BC)	Interval Estimate (years BC)
Pfyn	Cross-Validation	1.21	3620 - 3960	3540 - 4030
	Weighting (*w1*)	110.1	3600 - 3950	3520 - 4050
	Weighting (*w2*)	31.51	3610 - 3960	3540 - 4010
Sâone-Rhône	Cross-Validation	0.14	2560 - 2880	2490 - 2900
	Weighting (*w1*)	83.7	2550 - 2870	2490 - 2920
	Weighting (*w2*)	16.5	2550 - 2880	2490 - 2900

Table 3.7 : Point estimates with approximate 95% confidence intervals, rounded to the nearest decade, for the floruits of the *Pfyn* and *Sâone-Rhône* cultures.

Due to the over-smoothed density function caused by the weighting method (*w1*), it will now be clear that this method gives the widest interval estimates compared to the other method. While the cross-validation method seems identical with the weighting method (*w2*) in the case of *Sâone-Rhône* data, it produced a wider interval for the *Pfyn* data.

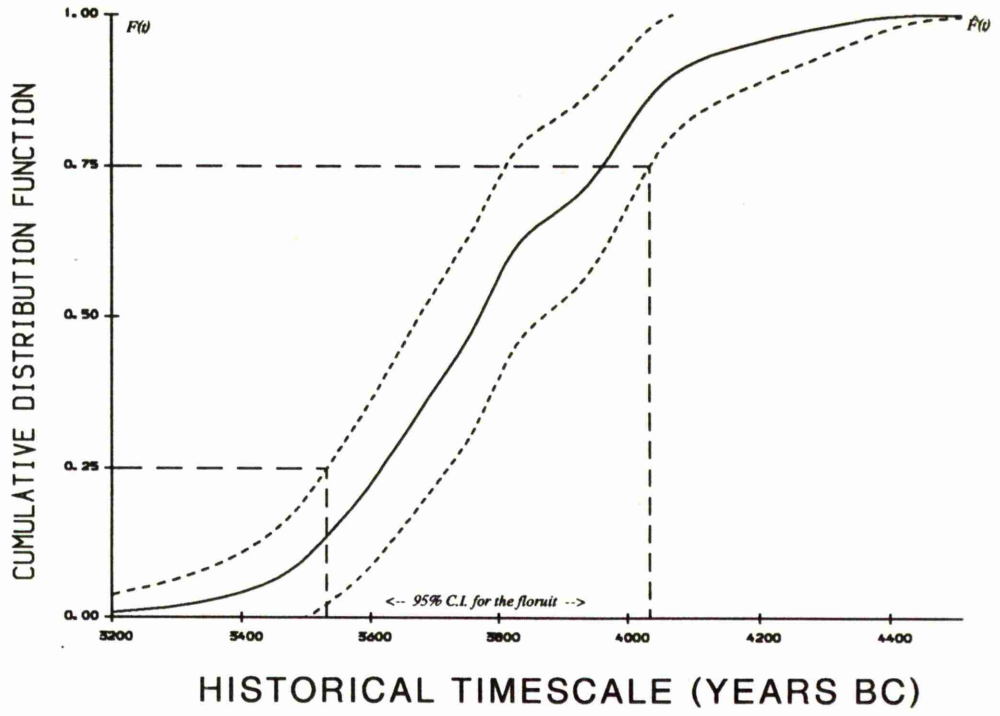

Figure 3.12 : Production of the interval estimate of the floruit for the *Pfyn* culture using method of cross-validation to smooth the density function.

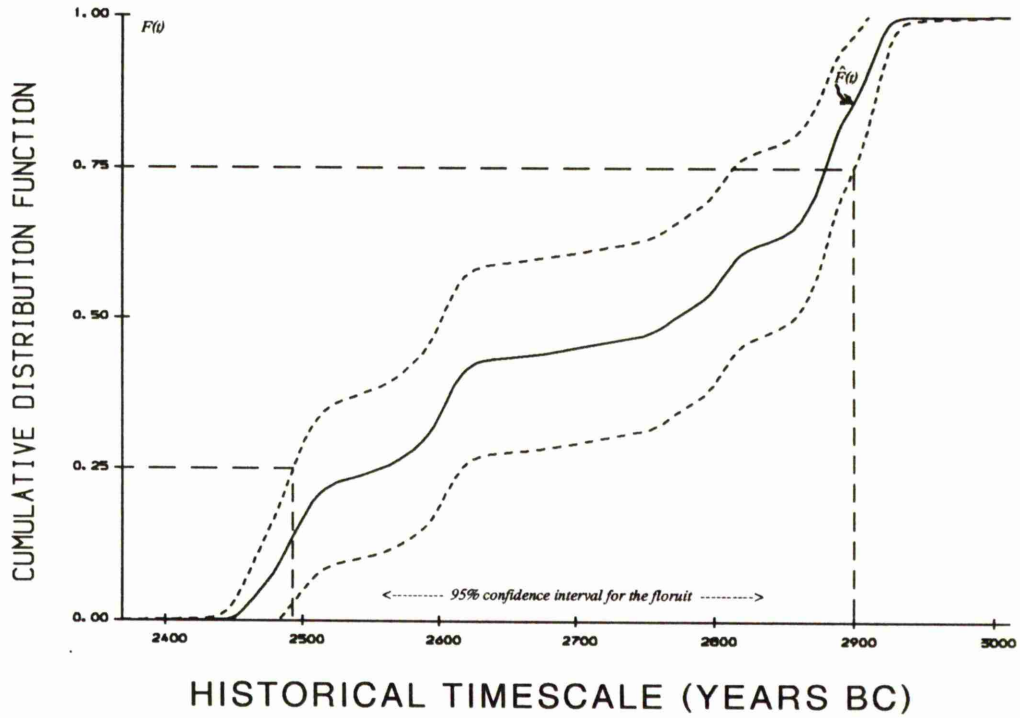

Figure 3.13 : Production of the interval estimate of the floruit for the *Sâone-Rhône* culture using the method of cross-validation to smooth the density function.

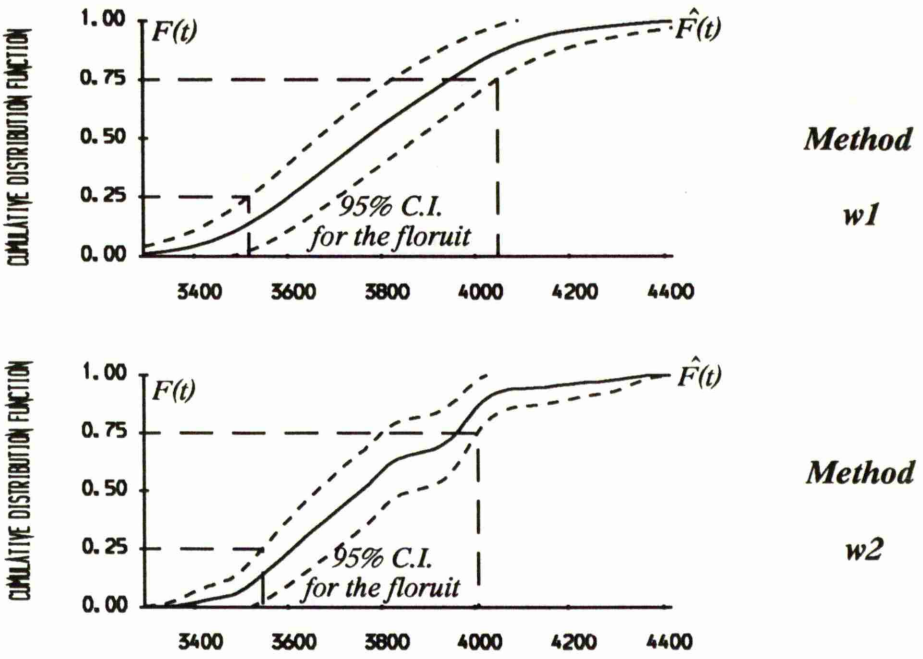

Figure 3.14 : Production of the interval estimate of the floruit for the *Pfyn* culture using the weighting methods to smooth the density function.

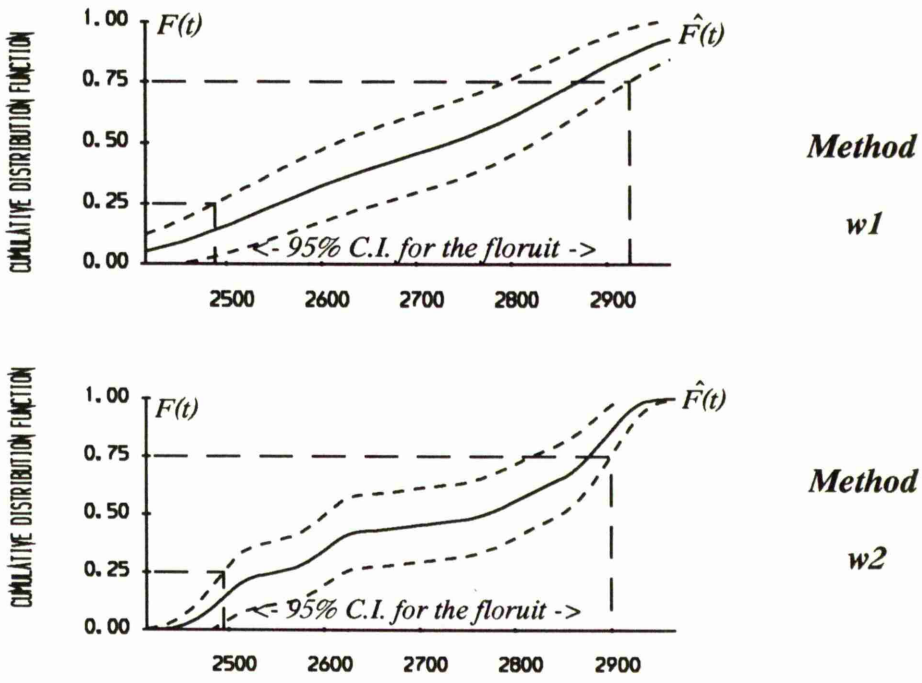

Figure 3.15 : Production of the interval estimate of the floruit for the *Sâone-Rhône* culture using the weighting methods to smooth the density function.

3.10 Summary

In this chapter, the concept of the floruit of an archaeological culture was defined. The purpose has been to provide procedures to enable one to produce an interval estimate of the floruit based on a chosen confidence coefficient. Some advantages of using the quartile interval were given. Methods of floruit estimation were introduced and discussed.

The earlier part of the chapter focused attention on the simple pen and paper methods and the general problem of quartile estimation was reviewed with numerical examples given.

The reminder of the chapter was concerned with highly computational methods which require the estimate of the frequency distribution underlying a culture. The technique of density estimation was reviewed and kernel density estimation used to provide an estimate for the frequency distribution underlying a culture. Although a cross-validation method has been used to choose the smoothing parameter, it was found not to be entirely satisfactory and alternative methods using weighted formulae have been considered.

The main concern of this chapter is floruit estimation which has been presented in detail based on the estimation of the cumulative distribution function (obtained by integration from the estimation of the density function taking into account the uncertainty in such an estimate).

In the next chapter, the properties of each of these methods will be investigated in a large scale simulation studies for different population distributions with different sample sizes. The aim of such is to identify which, if any, of the methods achieve the chosen confidence as well as being as narrow as possible.

Chapter 4

Simulation Study

4.1 Introduction

The emphasis in the preceding chapter was on introducing and presenting various methods which use the sample data in different manners to provide estimates for the floruit of an archaeological culture with an approximate 95% confidence interval for the floruit. This chapter is an investigation of the performance of these methods. The most effective way of achieving this is through a simulation study in which large numbers of simulations are carried out over a wide variety of cases with known floruits covering a large range of different underlying scenarios.

4.2 Preparing a Simulation Study

To avoid potential confusion, the five methods of providing an interval estimate for the floruit that were presented in the previous chapter are :-

Method A: The conservative calibration of the Extended Quartile Interval (E.Q.I.) based on the radiocarbon dates (section 3.5.2.1).

Method B: The Extended Quartile Interval (E.Q.I.) for the calibrated dates (historical dates) based on the fractional weighting scheme (section 3.5.2.3).

Method C: The Extended Quartile Interval (E.Q.I.) for the calibrated dates (historical dates) based on the weighted averages approach (section 3.5.2.4).

Method D: This represents the interval estimate for the floruit using the density estimation technique with variance approximated by $\frac{\hat{F}(t)\{1-\hat{F}(t)\}}{n}$ for the estimated cumulative distribution function (section 3.9.2).

Method E: This represents the interval estimate for the floruit using the density estimation technique with variance replaced by $\frac{(0.25)(0.75)}{n}$ for the estimated cumulative distribution function (section 3.9.2).

The purpose of this study is to compare and judge the performance of these alternative methods.

The true underlying artefact distribution and hence true floruit are taken in simulation to be centred at four specific points relative to areas of the calibration curve which are respectively linear, flat, steep and wiggly in order to investigate the effect of the curve shape on the floruit estimate. The particular parts of the curve which are used in the simulations are centred at the following ***historical*** dates :

Year 700 AD where the calibration curve is relatively ***linear*** which indicates that every radiocarbon date calibrated on this part corresponds to a single historical date (figure 4.1).

Year 500 BC where the curve is relatively ***flat*** for calibration and this can cause a large standard error on the calibrated dates (figure 4.2).

Year 2850 BC where the calibration curve is ***steep*** and ***wiggly*** which is likely to produce multiple historical dates for every radiocarbon date calibrated on this part (figure 4.3).

Year 3200 BC where the calibration curve is ***flat*** and ***wiggly*** which is likely to produce multiple historical dates with large standard errors for every radiocarbon date calibrated on this part (figure 4.4).

To ensure that the simulations results are not specific to a particular distribution and not specific to a particular sample size, the true underlying artefacts are taken to be distributed about the chosen points above according to one of three density functions:

i) a Normal distribution

ii) a Skewed distribution

iii) a Bimodal distribution

with sample sizes of 20, 50 and 100 for each distribution.

In order to simulate reasonable values for the radiocarbon dates of artefacts it is essential first to simulate true historical dates. In the following sub-sections the techniques for simulating true historical dates from these assumed distributions on the historical timescale are described. The choice of parameters for such distributions are investigated first based on particular choices of 'true' quartiles.

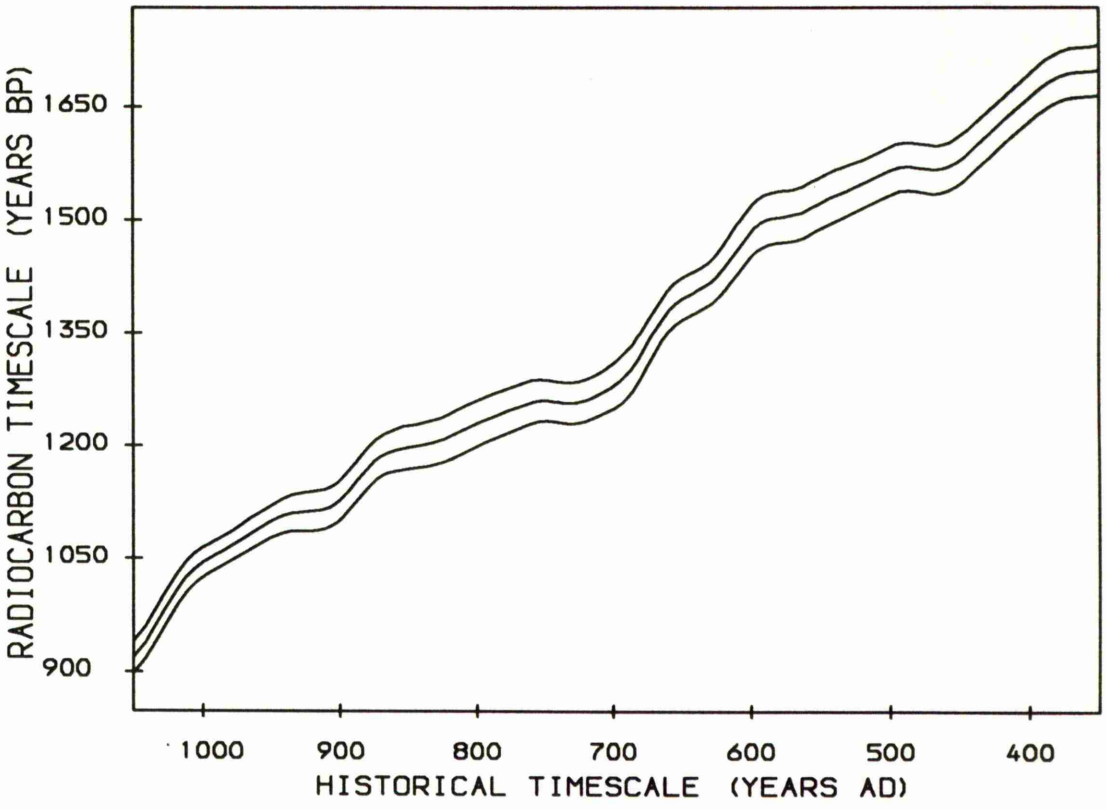

Figure 4.1 : ***Linear*** **part of the calibration curve used in the simulation study.**

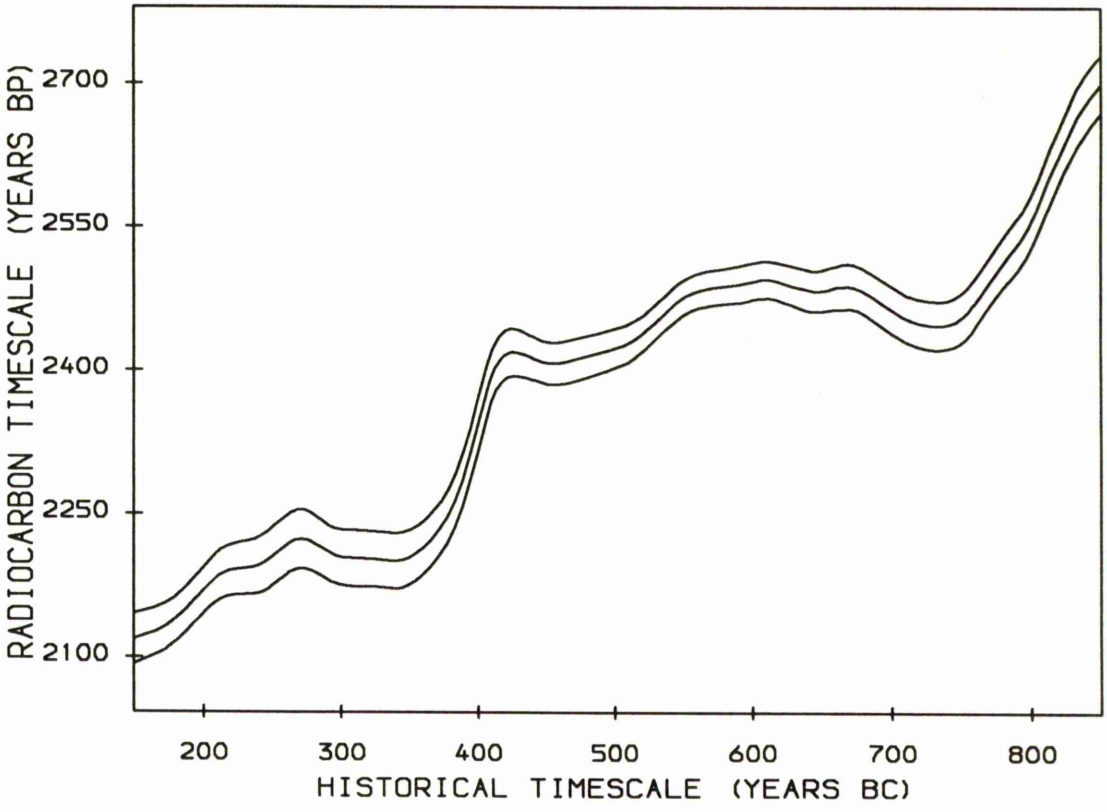

Figure 4.2 : ***Flat*** **part of the calibration curve used in the simulation study.**

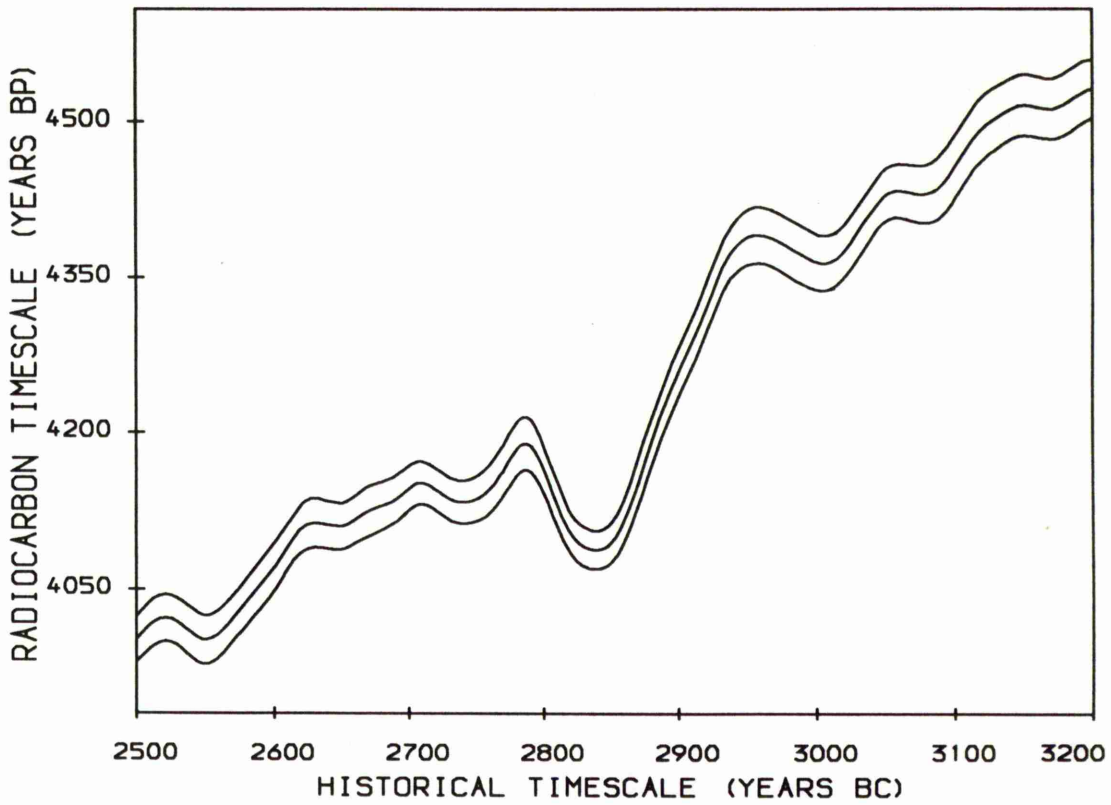

Figure 4.3 : ***steep*** and ***wiggly*** part of the calibration curve used in the simulation study.

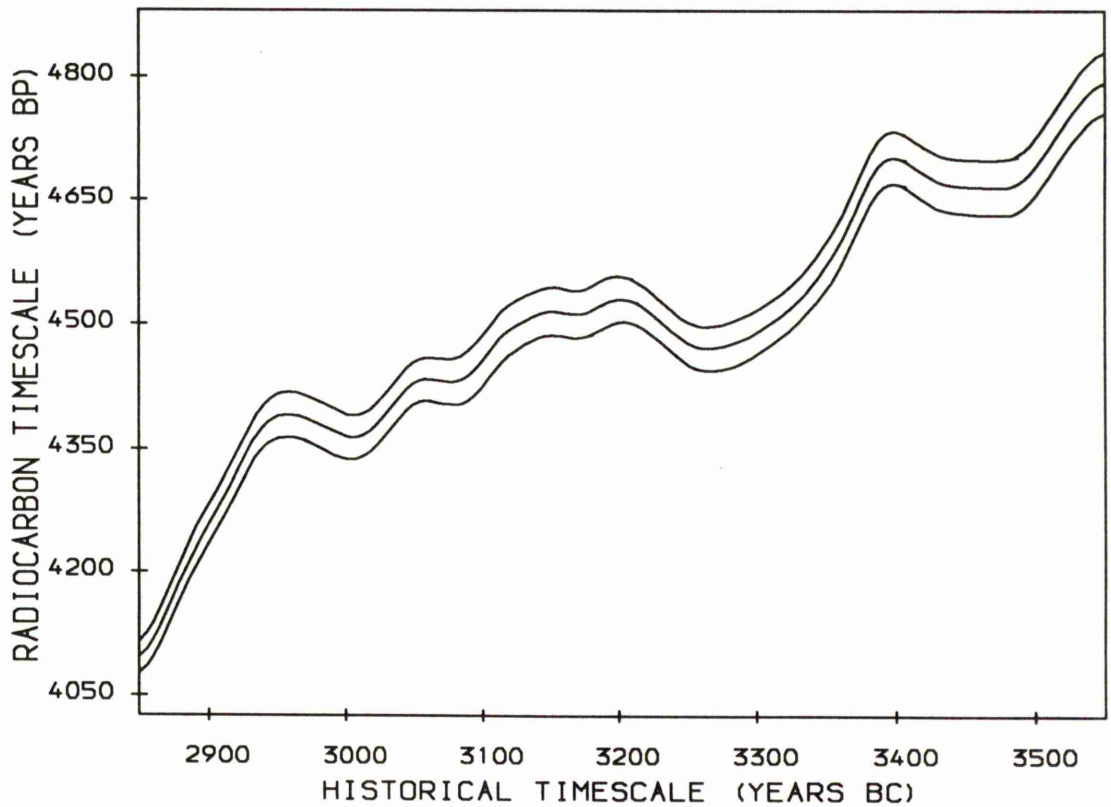

Figure 4.4 : ***Flat*** and ***wiggly*** part of the calibration curve used in the simulation study

4.2.1 Simulation from Normal Distribution

The true historical dates, t_i, can be simulated from any Normal distribution by using the probability density function of the standard Normal distribution in the following form:

$$t_i = \text{mean} + \sigma * z_i$$

where, z_i is a random variable generated randomly from the standard normal distribution and σ is the underlying standard deviation of the assumed artefact distribution. The mean takes the values of the historical dates chosen earlier as the centres of the chosen parts of the calibration curve *i.e.* 700 AD, 500 BC, 2850 BC and 3200 BC.

σ is taken to be equal to 50, 150 and 450 respectively in different simulation corresponding to approximate inter quartile ranges (I.Q.R.) of *70*, *200* and *600* respectively since the I.Q.R. of a Normal distribution is $\frac{4}{3}\sigma$ (density function plots of these choices are displayed in figure 4.5a). These choices of quartiles seem to reflect short, medium and long term cultural durations as seen in archaeological contexts.

4.2.2 Simulation from Skewed and Bimodal Distributions

To simulate true historical dates, t_i, from a Skewed and Bimodal distributions the following form can be used:

$$t_i = \text{mean} + u_i$$

where the means are as above and u_i is a random observation taken from a mixture of two normal distributions which are defined in the following form:

$$u \equiv f N\{-\mu, \sigma^2\} + (1-f)\, N\left\{\mu, (\tfrac{3}{2}\sigma)^2\right\}$$

i.e. a mixture of two Normal distributions, 2μ apart with a mixing proportion of f. The choice of more variability in the right hand part is obviously quite arbitrary but again is an attempt to mirror situations seen in real archaeological contexts.

The density function of u can therefore be written in the form:

$$p(u) = \frac{f}{\sigma\sqrt{2\pi}} exp\left\{-\frac{1}{2}\left(\frac{u+\mu}{\sigma}\right)^2\right\} + \frac{(1-f)}{\frac{3}{2}\sigma\sqrt{2\pi}} exp\left\{-\frac{1}{2}\left(\frac{u-\mu}{\frac{3}{2}\sigma}\right)^2\right\}$$

Here if one takes $\mu = \sigma$ this will give Skewed distributions, while taking $\mu = 2\sigma$ provides Bimodal distributions. In both cases a mixing proportion of $f=0.5$ was used.

The inter quartile ranges (I.Q.R.) for all Skewed and Bimodal distributions have been taking again as *70, 200* and *600* years. The resulting choices for μ and σ corresponding to these choices of I.Q.R. are given in the following table :-

Distribution	μ	σ	I.Q.R
Skewed	31	31	70
	89	89	200
	266	266	600
Bimodal	35	17.5	70
	100	50	200
	300	150	600

The density function plots for these choices are shown in figures 4.5b&c. Once the parameters have been chosen for the required simulation distribution as one of the cases specified in this or the previous section the procedure of simulating n observations can be summarized in three steps:

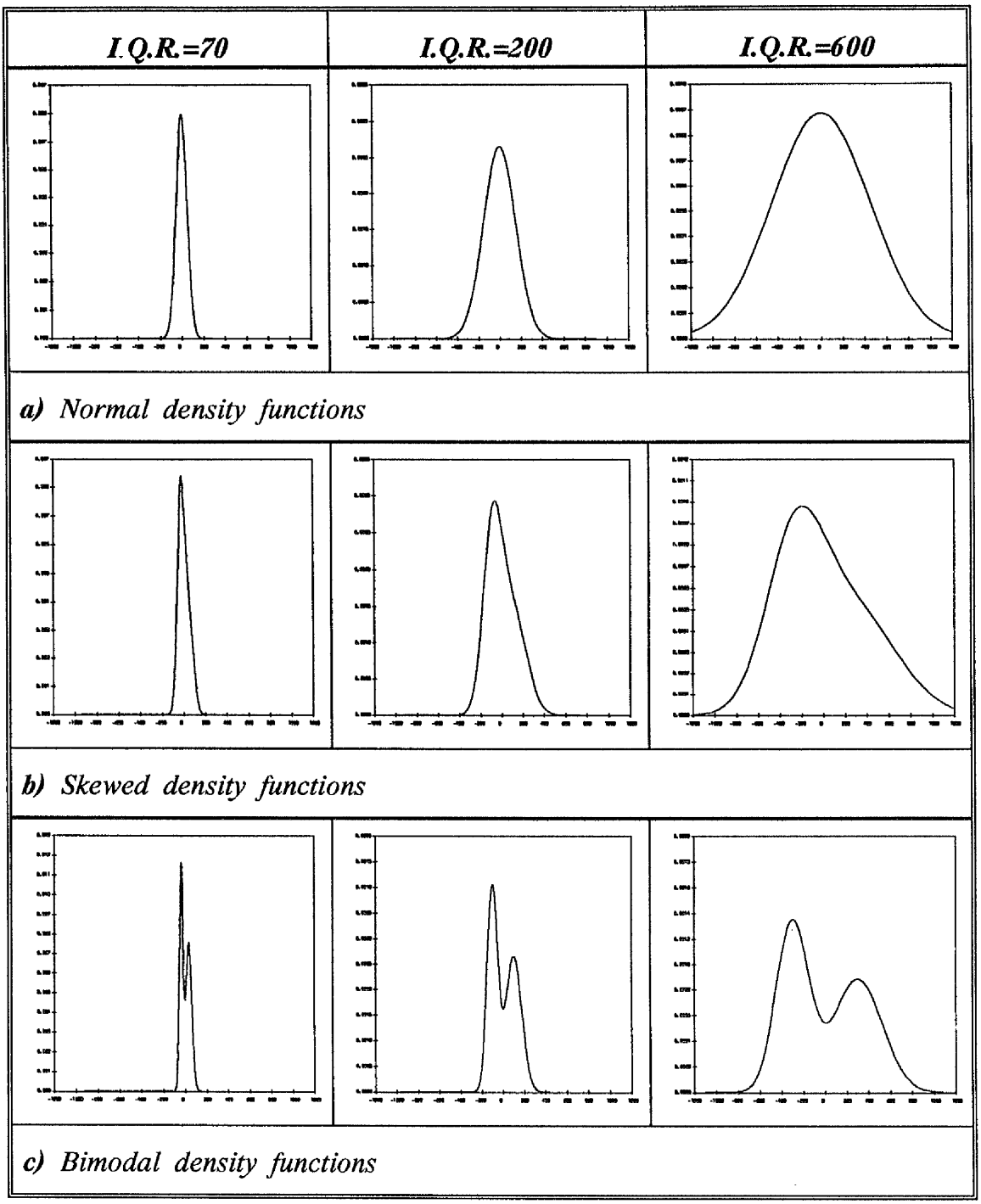

Figure 4.5 : Plots of the density functions used in the simulations.

- *step 1* Construct the cumulative distribution function $P(u) = P\{U \leq u\}$, where U is the random variable involved. This can be done simply by graphically plotting the function.

  i.e. $$P(u) = \int_{-\infty}^{u} p(v)dv$$

- *step 2* Generate n uniform variates from the range [0,1].

- *step 3* Set $P(u)$ equal to each of the uniform variates in turn and solve numerically or graphically for u.

This procedure is illustrated in figure 4.6 for the case where the uniform variate happens to be 0.43. These values of u are then the observations from the assumed artefact distribution under the chosen set of assumptions of shape, I.Q.R. and the centre of the distribution.

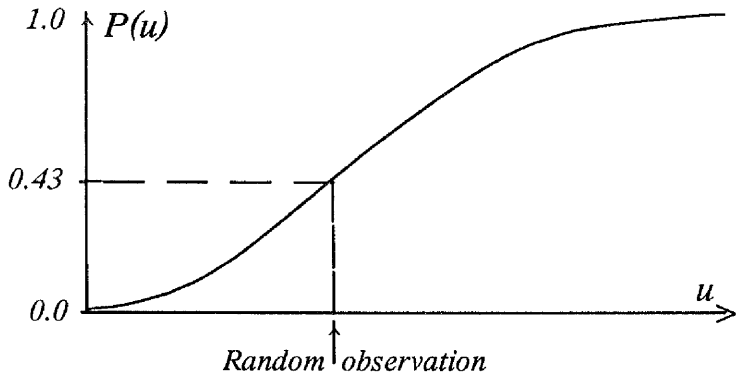

Figure 4.6 : Illustration of procedure for obtaining a random observation from a given probability distribution.

Overall therefore the components of the assumed underlying artefact distribution for the simulations are:-

a) The centre of the distribution (*i.e.* 700 AD, 500 BC, 2850 BC or 3200 BC).

b) The shape of the distribution (*i.e.* Normal, Skewed or Bimodal).

c) The Inter-Quartile Range of the distribution (*i.e.* 70, 200 or 600 years).

4.3 Criteria Used to Judge the Methods

For the interval estimators four statistical criteria have been defined to investigate the performance of the methods used.

These criteria are :

- *The Coverage* Defined to be the fraction of the true population quartiles (*i.e.* floruit) covered by the interval estimate.
- *The Wastage* Defined to be the fraction of the interval estimate of the floruit which does not overlap the true population quartiles.
- *The Population Coverage* Defined to be the area under the distribution curve between the end points of the interval estimate of the floruit.

These criteria are evaluated for each simulation and then summarised over a large number of simulations. The further criterion is

- *The Confidence* Defined as the fraction of the number of simulations in which the interval estimate covers the true floruit completely *i.e.* the fraction of times the coverage=1.

For example, if the true quartiles are *tq1* and *tq2* and the interval estimate of the sample quartiles are *sq1* and *sq2* then the above criteria are calculated as follow:

$$Coverage = \begin{cases} 1.0 & \text{if}(sq1 \le tq1 \text{ and } sq2 \ge tq2) \\ \dfrac{tq2 - sq1}{tq2 - tq1} & \text{if}(tq1 \le sq1 \le tq2 \text{ and } sq2 \ge tq2) \\ \dfrac{sq2 - tq1}{tq2 - tq1} & \text{if}(tq1 \le sq2 \le tq2 \text{ and } tq1 \ge sq1) \\ \dfrac{sq2 - sq1}{tq2 - tq1} & \text{if}(tq1 \le sq1 \text{ and } sq2 \le tq2) \\ 0.0 & \text{if}(sq1 \ge tq2 \text{ or } sq2 \le tq1) \end{cases}$$

$$Wastage = \begin{cases} 1.0 & \text{if } (sq1 \ge tq2 \text{ or } sq2 \le tq1) \\ \dfrac{sq2 - tq2}{sq2 - sq1} & \text{if } (tq1 \le sq1 \le tq2 \text{ and } sq2 \ge tq2) \\ \dfrac{tq1 - sq1}{sq2 - sq1} & \text{if } (tq1 \le sq2 \le tq2 \text{ and } tq1 \ge sq1) \\ \dfrac{(tq1 - sq1) + (sq2 - tq2)}{sq2 - sq1} & \text{if } (sq1 \le tq1 \text{ and } sq2 \ge tq2) \\ 0.0 & \text{if } (tq1 \le sq1 \text{ and } sq2 \le tq2) \end{cases}$$

$$Population\ Coverage = \int_{sq1}^{sq2} p(u)\, du$$

$$Confidence = \frac{\{number\ of\ coverages = 1.0\}}{number\ of\ simulations}$$

The performance of the methods of floruit estimation can be judged when the simulations are carried out and the long-run proportions of Coverage, Wastage and Population Coverage evaluated and the Confidence estimated.

Clearly the best method will be the method which will generally have a high Coverage (*i.e.* close to one) with high Confidence, low average Wastage (*i.e.* close to zero) and Population Coverage close to half (since the quartiles are estimated half of the population lie between these).

4.4 The Simulation Procedure

For each combination of centre, shape and interquartile range of the assumed underlying artefact distributions a total of 1000 simulations were carried out for each choice of sample size (*i.e.* 20, 50 or 100). To explain how the simulations were actually performed a brief description of the construction of the simulation program follows :

- *step 1* Evaluate the true population quartiles

  i.e. the true floruit.

- *step 2* Simulate the set of historical dates t_i, where $i=1,.....,n$ from the assumed true distribution.

- *step 3* Evaluate the corresponding expected radiocarbon date y_i for each t_i using the fitted relationship between radiocarbon dates and historical dates described in section 2.4

  i.e. evaluate $y_i = \hat{f}(u_i)$

- *step 4* Simulate the associated errors σ_i for the radiocarbon dates from a uniform distribution (the associated errors σ for the radiocarbon dates considered in this study were between 50 and 100 which reflect the belief that the actual radiocarbon errors reported are for the most part in this range).

- *step 5* Use the set of simulated pairs of y_i and σ_i , apply each of the five methods of floruit estimation and calculate the Coverage, Wastage and Population Coverage for each method. (Also note whether or not the coverage equals 1).

- *step 6* Repeat steps 2 to 5 one thousand times.

- *step 7* Summarise the Coverage, Wastage and Population Coverage for each method (by a three numbers summary of median and quartiles). Then estimate the Confidence for each method.

For each of the five methods, the Lower quartile, Median and Upper quartile for the results of 1000 simulations are presented in tables 4.1 to 4.15 for the Coverage, Wastage and Population Coverage. The results for the Confidence for the five methods are given in tables 4.16 to 4.20 .

Before discussion of the simulation results (section 4.5) it is convenient to represent the results graphically. For each distribution (Normal, Skewed and Bimodal) the plots of the Median of the 1000 simulations for the Coverage, Wastage and Population coverage with the plots of the estimated Confidence are shown in figures 4.7 to 4.26 to judge the performance of each of the five methods over the different parts of the calibration curve for the combinations of sample size and the Inter-Quartile Range (I.Q.R.).

Distribution	I.Q.R.	Curve Centred at Year 700 AD			Curve Centred at Year 500 BC		
		n=20	n=50	n=100	n=20	n=50	n=100
Normal	70	1.0 1.0 1.0	1.0 1.0 1.0	1.0 1.0 1.0	1.0 1.0 1.0	1.0 1.0 1.0	1.0 1.0 1.0
	200	0.961 1.0 1.0	1.0 1.0 1.0	1.0 1.0 1.0	1.0 1.0 1.0	1.0 1.0 1.0	1.0 1.0 1.0
	600	0.820 0.956 1.0	0.947 0.997 1.0	0.981 1.0 1.0	0.954 1.0 1.0	1.0 1.0 1.0	1.0 1.0 1.0
Skewed	70	1.0 1.0 1.0	1.0 1.0 1.0	1.0 1.0 1.0	1.0 1.0 1.0	1.0 1.0 1.0	1.0 1.0 1.0
	200	0.931 1.0 1.0	0.998 1.0 1.0	1.0 1.0 1.0	0.989 1.0 1.0	1.0 1.0 1.0	1.0 1.0 1.0
	600	0.836 0.936 0.986	0.922 0.963 1.0	0.949 0.975 1.0	0.938 0.987 1.0	0.975 1.0 1.0	0.999 1.0 1.0
Bimodal	70	1.0 1.0 1.0	1.0 1.0 1.0	1.0 1.0 1.0	1.0 1.0 1.0	1.0 1.0 1.0	1.0 1.0 1.0
	200	0.959 1.0 1.0	1.0 1.0 1.0	1.0 1.0 1.0	1.0 1.0 1.0	1.0 1.0 1.0	1.0 1.0 1.0
	600	0.912 0.977 1.0	0.959 1.0 1.0	0.987 1.0 1.0	0.986 1.0 1.0	1.0 1.0 1.0	1.0 1.0 1.0

Distribution	I.Q.R.	Curve Centred at Year 2850 BC			Curve Centred at Year 3200 BC		
		n=20	n=50	n=100	n=20	n=50	n=100
Normal	70	1.0 1.0 1.0	1.0 1.0 1.0	1.0 1.0 1.0	1.0 1.0 1.0	1.0 1.0 1.0	1.0 1.0 1.0
	200	0.907 1.0 1.0	1.0 1.0 1.0	1.0 1.0 1.0	1.0 1.0 1.0	1.0 1.0 1.0	1.0 1.0 1.0
	600	0.896 1.0 1.0	0.937 1.0 1.0	1.0 1.0 1.0	0.941 0.985 1.0	0.982 1.0 1.0	0.999 1.0 1.0
Skewed	70	1.0 1.0 1.0	1.0 1.0 1.0	1.0 1.0 1.0	1.0 1.0 1.0	1.0 1.0 1.0	1.0 1.0 1.0
	200	0.883 1.0 1.0	1.0 1.0 1.0	1.0 1.0 1.0	1.0 1.0 1.0	1.0 1.0 1.0	1.0 1.0 1.0
	600	0.845 1.0 1.0	0.979 1.0 1.0	1.0 1.0 1.0	0.880 0.937 1.0	0.928 0.979 1.0	0.945 1.0 1.0
Bimodal	70	1.0 1.0 1.0	1.0 1.0 1.0	1.0 1.0 1.0	1.0 1.0 1.0	1.0 1.0 1.0	1.0 1.0 1.0
	200	0.904 1.0 1.0	1.0 1.0 1.0	1.0 1.0 1.0	1.0 1.0 1.0	1.0 1.0 1.0	1.0 1.0 1.0
	600	0.901 1.0 1.0	0.935 1.0 1.0	1.0 1.0 1.0	0.957 0.999 1.0	0.994 1.0 1.0	1.0 1.0 1.0

Table 4.1 : Lower quartile, Median and Upper quartile for the ***Coverage*** of method *A* over 1000 simulations and over different parts of the calibration curve for the combination of distribution, I.Q.R. and sample size.

Distribution	I.Q.R.	Curve Centred at Year 700 AD			Curve Centred at Year 500 BC		
		n=20	n=50	n=100	n=20	n=50	n=100
Normal	70	1.0 1.0 1.0	1.0 1.0 1.0	1.0 1.0 1.0	1.0 1.0 1.0	1.0 1.0 1.0	1.0 1.0 1.0
	200	1.0 1.0 1.0	1.0 1.0 1.0	1.0 1.0 1.0	1.0 1.0 1.0	1.0 1.0 1.0	1.0 1.0 1.0
	600	0.873 0.996 1.0	1.0 1.0 1.0	1.0 1.0 1.0	0.823 1.0 1.0	1.0 1.0 1.0	1.0 1.0 1.0
Skewed	70	1.0 1.0 1.0	1.0 1.0 1.0	1.0 1.0 1.0	1.0 1.0 1.0	1.0 1.0 1.0	1.0 1.0 1.0
	200	1.0 1.0 1.0	1.0 1.0 1.0	1.0 1.0 1.0	1.0 1.0 1.0	1.0 1.0 1.0	1.0 1.0 1.0
	600	0.865 0.987 1.0	0.979 1.0 1.0	0.997 1.0 1.0	0.917 1.0 1.0	1.0 1.0 1.0	1.0 1.0 1.0
Bimodal	70	1.0 1.0 1.0	1.0 1.0 1.0	1.0 1.0 1.0	1.0 1.0 1.0	1.0 1.0 1.0	1.0 1.0 1.0
	200	1.0 1.0 1.0	1.0 1.0 1.0	1.0 1.0 1.0	1.0 1.0 1.0	1.0 1.0 1.0	1.0 1.0 1.0
	600	0.923 1.0 1.0	1.0 1.0 1.0	1.0 1.0 1.0	0.905 1.0 1.0	1.0 1.0 1.0	1.0 1.0 1.0

Distribution	I.Q.R.	Curve Centred at Year 2850 BC			Curve Centred at Year 3200 BC		
		n=20	n=50	n=100	n=20	n=50	n=100
Normal	70	1.0 1.0 1.0	1.0 1.0 1.0	1.0 1.0 1.0	1.0 1.0 1.0	1.0 1.0 1.0	1.0 1.0 1.0
	200	0.899 0.981 1.0	0.966 1.0 1.0	0.995 1.0 1.0	1.0 1.0 1.0	1.0 1.0 1.0	1.0 1.0 1.0
	600	0.831 0.978 1.0	0.966 1.0 1.0	0.996 1.0 1.0	0.823 0.988 1.0	0.988 1.0 1.0	1.0 1.0 1.0
Skewed	70	1.0 1.0 1.0	1.0 1.0 1.0	1.0 1.0 1.0	1.0 1.0 1.0	1.0 1.0 1.0	1.0 1.0 1.0
	200	0.845 0.953 1.0	0.946 1.0 1.0	0.975 1.0 1.0	1.0 1.0 1.0	1.0 1.0 1.0	1.0 1.0 1.0
	600	0.806 0.957 1.0	0.935 1.0 1.0	0.971 1.0 1.0	0.820 0.945 0.987	0.934 0.971 0.992	0.959 0.976 0.990
Bimodal	70	1.0 1.0 1.0	1.0 1.0 1.0	1.0 1.0 1.0	1.0 1.0 1.0	1.0 1.0 1.0	1.0 1.0 1.0
	200	0.853 0.958 1.0	0.950 1.0 1.0	0.989 1.0 1.0	1.0 1.0 1.0	1.0 1.0 1.0	1.0 1.0 1.0
	600	0.812 0.982 1.0	0.966 1.0 1.0	0.988 1.0 1.0	0.834 1.0 1.0	0.990 1.0 1.0	1.0 1.0 1.0

Table 4.2 : Lower quartile, Median and Upper quartile for the ***Coverage*** of method ***B*** over 1000 simulations and over different parts of the calibration curve for the combination of distribution, I.Q.R. and sample size.

Distribution	I.Q.R.	Curve Centred at Year 700 AD			Curve Centred at Year 500 BC		
		n=20	n=50	n=100	n=20	n=50	n=100
Normal	70	1.0 1.0 1.0	1.0 1.0 1.0	1.0 1.0 1.0	1.0 1.0 1.0	1.0 1.0 1.0	1.0 1.0 1.0
	200	1.0 1.0 1.0	1.0 1.0 1.0	1.0 1.0 1.0	1.0 1.0 1.0	1.0 1.0 1.0	1.0 1.0 1.0
	600	0.872 0.994 1.0	1.0 1.0 1.0	1.0 1.0 1.0	0.797 1.0 1.0	1.0 1.0 1.0	1.0 1.0 1.0
Skewed	70	1.0 1.0 1.0	1.0 1.0 1.0	1.0 1.0 1.0	1.0 1.0 1.0	1.0 1.0 1.0	1.0 1.0 1.0
	200	1.0 1.0 1.0	1.0 1.0 1.0	1.0 1.0 1.0	1.0 1.0 1.0	1.0 1.0 1.0	1.0 1.0 1.0
	600	0.864 0.984 1.0	0.979 1.0 1.0	0.997 1.0 1.0	0.866 1.0 1.0	1.0 1.0 1.0	1.0 1.0 1.0
Bimodal	70	1.0 1.0 1.0	1.0 1.0 1.0	1.0 1.0 1.0	1.0 1.0 1.0	1.0 1.0 1.0	1.0 1.0 1.0
	200	1.0 1.0 1.0	1.0 1.0 1.0	1.0 1.0 1.0	1.0 1.0 1.0	1.0 1.0 1.0	1.0 1.0 1.0
	600	0.922 1.0 1.0	1.0 1.0 1.0	1.0 1.0 1.0	0.870 1.0 1.0	1.0 1.0 1.0	1.0 1.0 1.0

Distribution	I.Q.R.	Curve Centred at Year 2850 BC			Curve Centred at Year 3200 BC		
		n=20	n=50	n=100	n=20	n=50	n=100
Normal	70	1.0 1.0 1.0	1.0 1.0 1.0	1.0 1.0 1.0	1.0 1.0 1.0	1.0 1.0 1.0	1.0 1.0 1.0
	200	0.678 0.917 1.0	0.690 0.994 1.0	0.790 0.971 1.0	1.0 1.0 1.0	1.0 1.0 1.0	1.0 1.0 1.0
	600	0.759 0.933 1.0	0.907 0.998 1.0	0.980 1.0 1.0	0.814 0.929 1.0	0.887 1.0 1.0	0.984 1.0 1.0
Skewed	70	1.0 1.0 1.0	1.0 1.0 1.0	1.0 1.0 1.0	1.0 1.0 1.0	1.0 1.0 1.0	1.0 1.0 1.0
	200	0.626 0.887 1.0	0.645 0.916 0.997	0.700 0.943 1.0	1.0 1.0 1.0	1.0 1.0 1.0	1.0 1.0 1.0
	600	0.738 0.930 1.0	0.913 0.982 1.0	0.957 1.0 1.0	0.806 0.921 0.981	0.844 0.956 0.981	0.935 0.967 0.984
Bimodal	70	1.0 1.0 1.0	1.0 1.0 1.0	1.0 1.0 1.0	1.0 1.0 1.0	1.0 1.0 1.0	1.0 1.0 1.0
	200	0.643 0.783 0.975	0.667 0.707 0.962	0.676 0.722 0.975	1.0 1.0 1.0	1.0 1.0 1.0	1.0 1.0 1.0
	600	0.762 0.931 1.0	0.914 0.992 1.0	0.977 1.0 1.0	0.824 0.948 1.0	0.863 1.0 1.0	0.937 1.0 1.0

Table 4.3 : Lower quartile, Median and Upper quartile for the ***Coverage*** of method ***C*** over 1000 simulations and over different parts of the calibration curve for the combination of distribution, I.Q.R. and sample size.

Distribution	I.Q.R.	Curve Centred at Year 700 AD						Curve Centred at Year 500 BC					
		n=20			n=50			n=100			n=20			n=50			n=100		
Normal	70	1.0	1.0	1.0	1.0	1.0	1.0	1.0	1.0	1.0	1.0	1.0	1.0	1.0	1.0	1.0	1.0	1.0
	200	1.0	1.0	1.0	1.0	1.0	1.0	1.0	1.0	1.0	1.0	1.0	1.0	1.0	1.0	1.0	1.0	1.0
	600	1.0	1.0	1.0	1.0	1.0	1.0	1.0	1.0	1.0	1.0	1.0	1.0	1.0	1.0	1.0	1.0	1.0
Skewed	70	1.0	1.0	1.0	1.0	1.0	1.0	1.0	1.0	1.0	1.0	1.0	1.0	1.0	1.0	1.0	1.0	1.0
	200	1.0	1.0	1.0	1.0	1.0	1.0	1.0	1.0	1.0	1.0	1.0	1.0	1.0	1.0	1.0	1.0	1.0
	600	0.992	1.0	1.0	0.996	1.0	1.0	0.989	1.0	1.0	1.0	1.0	1.0	1.0	1.0	1.0	1.0	1.0
Bimodal	70	1.0	1.0	1.0	1.0	1.0	1.0	1.0	1.0	1.0	1.0	1.0	1.0	1.0	1.0	1.0	1.0	1.0
	200	1.0	1.0	1.0	1.0	1.0	1.0	1.0	1.0	1.0	1.0	1.0	1.0	1.0	1.0	1.0	1.0	1.0
	600	1.0	1.0	1.0	1.0	1.0	1.0	1.0	1.0	1.0	1.0	1.0	1.0	1.0	1.0	1.0	1.0	1.0

Distribution	I.Q.R.	Curve Centred at Year 2850 BC						Curve Centred at Year 3200 BC					
		n=20			n=50			n=100			n=20			n=50			n=100		
Normal	70	1.0	1.0	1.0	1.0	1.0	1.0	1.0	1.0	1.0	1.0	1.0	1.0	1.0	1.0	1.0	1.0	1.0
	200	1.0	1.0	1.0	1.0	1.0	1.0	1.0	1.0	1.0	1.0	1.0	1.0	1.0	1.0	1.0	1.0	1.0
	600	1.0	1.0	1.0	1.0	1.0	1.0	1.0	1.0	1.0	1.0	1.0	1.0	1.0	1.0	1.0	1.0	1.0
Skewed	70	1.0	1.0	1.0	1.0	1.0	1.0	1.0	1.0	1.0	1.0	1.0	1.0	1.0	1.0	1.0	1.0	1.0
	200	1.0	1.0	1.0	1.0	1.0	1.0	1.0	1.0	1.0	1.0	1.0	1.0	1.0	1.0	1.0	1.0	1.0
	600	1.0	1.0	1.0	1.0	1.0	1.0	1.0	1.0	1.0	1.0	1.0	1.0	1.0	1.0	0.981	1.0	1.0
Bimodal	70	1.0	1.0	1.0	1.0	1.0	1.0	1.0	1.0	1.0	1.0	1.0	1.0	1.0	1.0	1.0	1.0	1.0
	200	1.0	1.0	1.0	1.0	1.0	1.0	1.0	1.0	1.0	1.0	1.0	1.0	1.0	1.0	1.0	1.0	1.0
	600	1.0	1.0	1.0	1.0	1.0	1.0	1.0	1.0	1.0	1.0	1.0	1.0	1.0	1.0	1.0	1.0	1.0

Table 4.4 : Lower quartile, Median and Upper quartile for the ***Coverage*** of method ***D*** over 1000 simulations and over different parts of the calibration curve for the combination of distribution, I.Q.R. and sample size.

Distribution	I.Q.R.	Curve Centred at Year 700 AD			Curve Centred at Year 500 BC		
		n=20	n=50	n=100	n=20	n=50	n=100
Normal	70	1.0 1.0 1.0	1.0 1.0 1.0	1.0 1.0 1.0	1.0 1.0 1.0	1.0 1.0 1.0	1.0 1.0 1.0
	200	1.0 1.0 1.0	1.0 1.0 1.0	1.0 1.0 1.0	1.0 1.0 1.0	1.0 1.0 1.0	1.0 1.0 1.0
	600	1.0 1.0 1.0	1.0 1.0 1.0	1.0 1.0 1.0	1.0 1.0 1.0	1.0 1.0 1.0	1.0 1.0 1.0
Skewed	70	1.0 1.0 1.0	1.0 1.0 1.0	1.0 1.0 1.0	1.0 1.0 1.0	1.0 1.0 1.0	1.0 1.0 1.0
	200	1.0 1.0 1.0	1.0 1.0 1.0	1.0 1.0 1.0	1.0 1.0 1.0	1.0 1.0 1.0	1.0 1.0 1.0
	600	1.0 1.0 1.0	1.0 1.0 1.0	1.0 1.0 1.0	1.0 1.0 1.0	1.0 1.0 1.0	1.0 1.0 1.0
Bimodal	70	1.0 1.0 1.0	1.0 1.0 1.0	1.0 1.0 1.0	1.0 1.0 1.0	1.0 1.0 1.0	1.0 1.0 1.0
	200	1.0 1.0 1.0	1.0 1.0 1.0	1.0 1.0 1.0	1.0 1.0 1.0	1.0 1.0 1.0	1.0 1.0 1.0
	600	1.0 1.0 1.0	1.0 1.0 1.0	1.0 1.0 1.0	1.0 1.0 1.0	1.0 1.0 1.0	1.0 1.0 1.0

Distribution	I.Q.R.	Curve Centred at Year 2850 BC			Curve Centred at Year 3200 BC		
		n=20	n=50	n=100	n=20	n=50	n=100
Normal	70	1.0 1.0 1.0	1.0 1.0 1.0	1.0 1.0 1.0	1.0 1.0 1.0	1.0 1.0 1.0	1.0 1.0 1.0
	200	1.0 1.0 1.0	1.0 1.0 1.0	1.0 1.0 1.0	1.0 1.0 1.0	1.0 1.0 1.0	1.0 1.0 1.0
	600	1.0 1.0 1.0	1.0 1.0 1.0	1.0 1.0 1.0	1.0 1.0 1.0	1.0 1.0 1.0	1.0 1.0 1.0
Skewed	70	1.0 1.0 1.0	1.0 1.0 1.0	1.0 1.0 1.0	1.0 1.0 1.0	1.0 1.0 1.0	1.0 1.0 1.0
	200	1.0 1.0 1.0	1.0 1.0 1.0	1.0 1.0 1.0	1.0 1.0 1.0	1.0 1.0 1.0	1.0 1.0 1.0
	600	1.0 1.0 1.0	1.0 1.0 1.0	1.0 1.0 1.0	1.0 1.0 1.0	1.0 1.0 1.0	1.0 1.0 1.0
Bimodal	70	1.0 1.0 1.0	1.0 1.0 1.0	1.0 1.0 1.0	1.0 1.0 1.0	1.0 1.0 1.0	1.0 1.0 1.0
	200	1.0 1.0 1.0	1.0 1.0 1.0	1.0 1.0 1.0	1.0 1.0 1.0	1.0 1.0 1.0	1.0 1.0 1.0
	600	1.0 1.0 1.0	1.0 1.0 1.0	1.0 1.0 1.0	1.0 1.0 1.0	1.0 1.0 1.0	1.0 1.0 1.0

Table 4.5 : Lower quartile, Median and Upper quartile for the ***Coverage*** of method ***E*** over 1000 simulations and over different parts of the calibration curve for the combination of distribution, I.Q.R. and sample size.

Distribution	I.Q.R.	Curve Centred at Year 700 AD			Curve Centred at Year 500 BC		
		n=20	n=50	n=100	n=20	n=50	n=100
Normal	70	$_{0.715}^{0.740}{}_{0.760}$	$_{0.732}^{0.745}{}_{0.755}$	$_{0.738}^{0.745}{}_{0.752}$	$_{0.832}^{0.836}{}_{0.839}$	$_{0.833}^{0.836}{}_{0.838}$	$_{0.834}^{0.835}{}_{0.837}$
	200	$_{0.346}^{0.445}{}_{0.518}$	$_{0.356}^{0.421}{}_{0.474}$	$_{0.378}^{0.423}{}_{0.458}$	$_{0.511}^{0.527}{}_{0.630}$	$_{0.516}^{0.528}{}_{0.623}$	$_{0.520}^{0.528}{}_{0.616}$
	600	$_{0.062}^{0.233}{}_{0.323}$	$_{0.074}^{0.216}{}_{0.255}$	$_{0.076}^{0.203}{}_{0.232}$	$_{0.112}^{0.211}{}_{0.307}$	$_{0.137}^{0.199}{}_{0.256}$	$_{0.135}^{0.185}{}_{0.232}$
Skewed	70	$_{0.664}^{0.699}{}_{0.721}$	$_{0.688}^{0.704}{}_{0.717}$	$_{0.697}^{0.706}{}_{0.714}$	$_{0.803}^{0.807}{}_{0.811}$	$_{0.805}^{0.807}{}_{0.810}$	$_{0.806}^{0.808}{}_{0.809}$
	200	$_{0.304}^{0.409}{}_{0.487}$	$_{0.312}^{0.381}{}_{0.453}$	$_{0.321}^{0.370}{}_{0.417}$	$_{0.474}^{0.503}{}_{0.606}$	$_{0.471}^{0.494}{}_{0.594}$	$_{0.473}^{0.491}{}_{0.590}$
	600	$_{0.158}^{0.231}{}_{0.314}$	$_{0.148}^{0.193}{}_{0.276}$	$_{0.136}^{0.178}{}_{0.245}$	$_{0.130}^{0.210}{}_{0.296}$	$_{0.127}^{0.182}{}_{0.246}$	$_{0.128}^{0.166}{}_{0.214}$
Bimodal	70	$_{0.695}^{0.725}{}_{0.745}$	$_{0.716}^{0.732}{}_{0.743}$	$_{0.724}^{0.734}{}_{0.741}$	$_{0.824}^{0.828}{}_{0.831}$	$_{0.826}^{0.828}{}_{0.830}$	$_{0.827}^{0.829}{}_{0.830}$
	200	$_{0.324}^{0.409}{}_{0.473}$	$_{0.329}^{0.390}{}_{0.439}$	$_{0.335}^{0.388}{}_{0.424}$	$_{0.512}^{0.527}{}_{0.622}$	$_{0.517}^{0.526}{}_{0.546}$	$_{0.519}^{0.526}{}_{0.537}$
	600	$_{0.061}^{0.210}{}_{0.256}$	$_{0.062}^{0.144}{}_{0.232}$	$_{0.057}^{0.110}{}_{0.214}$	$_{0.118}^{0.188}{}_{0.250}$	$_{0.117}^{0.171}{}_{0.217}$	$_{0.129}^{0.168}{}_{0.200}$

Distribution	I.Q.R.	Curve Centred at Year 2850 BC			Curve Centred at Year 3200 BC		
		n=20	n=50	n=100	n=20	n=50	n=100
Normal	70	$_{0.797}^{0.831}{}_{0.840}$	$_{0.800}^{0.827}{}_{0.837}$	$_{0.802}^{0.808}{}_{0.835}$	$_{0.804}^{0.842}{}_{0.848}$	$_{0.836}^{0.843}{}_{0.846}$	$_{0.840}^{0.843}{}_{0.845}$
	200	$_{0.524}^{0.574}{}_{0.616}$	$_{0.531}^{0.552}{}_{0.597}$	$_{0.538}^{0.550}{}_{0.573}$	$_{0.532}^{0.548}{}_{0.628}$	$_{0.538}^{0.546}{}_{0.563}$	$_{0.540}^{0.546}{}_{0.555}$
	600	$_{0.241}^{0.286}{}_{0.352}$	$_{0.259}^{0.287}{}_{0.311}$	$_{0.273}^{0.290}{}_{0.306}$	$_{0.168}^{0.236}{}_{0.342}$	$_{0.169}^{0.201}{}_{0.296}$	$_{0.171}^{0.192}{}_{0.285}$
Skewed	70	$_{0.762}^{0.803}{}_{0.814}$	$_{0.765}^{0.777}{}_{0.811}$	$_{0.768}^{0.774}{}_{0.808}$	$_{0.765}^{0.814}{}_{0.821}$	$_{0.772}^{0.816}{}_{0.819}$	$_{0.811}^{0.816}{}_{0.818}$
	200	$_{0.472}^{0.536}{}_{0.577}$	$_{0.484}^{0.511}{}_{0.557}$	$_{0.487}^{0.503}{}_{0.543}$	$_{0.480}^{0.499}{}_{0.595}$	$_{0.490}^{0.501}{}_{0.597}$	$_{0.490}^{0.497}{}_{0.592}$
	600	$_{0.208}^{0.251}{}_{0.358}$	$_{0.206}^{0.235}{}_{0.302}$	$_{0.212}^{0.232}{}_{0.263}$	$_{0.182}^{0.276}{}_{0.344}$	$_{0.160}^{0.244}{}_{0.304}$	$_{0.176}^{0.222}{}_{0.284}$
Bimodal	70	$_{0.787}^{0.819}{}_{0.831}$	$_{0.790}^{0.800}{}_{0.829}$	$_{0.792}^{0.798}{}_{0.828}$	$_{0.792}^{0.835}{}_{0.840}$	$_{0.829}^{0.835}{}_{0.839}$	$_{0.831}^{0.836}{}_{0.838}$
	200	$_{0.497}^{0.540}{}_{0.593}$	$_{0.523}^{0.540}{}_{0.565}$	$_{0.529}^{0.542}{}_{0.553}$	$_{0.526}^{0.541}{}_{0.558}$	$_{0.535}^{0.542}{}_{0.552}$	$_{0.539}^{0.544}{}_{0.549}$
	600	$_{0.228}^{0.281}{}_{0.312}$	$_{0.246}^{0.279}{}_{0.300}$	$_{0.266}^{0.285}{}_{0.298}$	$_{0.166}^{0.209}{}_{0.321}$	$_{0.159}^{0.187}{}_{0.262}$	$_{0.167}^{0.183}{}_{0.209}$

Table 4.6 : Lower quartile, Median and Upper quartile for the ***Wastage*** of method *A* over 1000 simulations and over different parts of the calibration curve for the combination of distribution, I.Q.R. and sample size.

Distribution	I.Q.R.	Curve Centred at Year 700 AD			Curve Centred at Year 500 BC		
		n=20	n=50	n=100	n=20	n=50	n=100
Normal	70	$0.764\ ^{0.786}\ _{0.803}$	$0.778\ ^{0.792}\ _{0.801}$	$0.785\ ^{0.793}\ _{0.799}$	$0.846\ ^{0.849}\ _{0.852}$	$0.847\ ^{0.849}\ _{0.851}$	$0.848\ ^{0.849}\ _{0.850}$
	200	$0.425\ ^{0.498}\ _{0.564}$	$0.430\ ^{0.468}\ _{0.539}$	$0.440\ ^{0.470}\ _{0.520}$	$0.547\ ^{0.563}\ _{0.592}$	$0.554\ ^{0.566}\ _{0.584}$	$0.560\ ^{0.570}\ _{0.582}$
	600	$0.114\ ^{0.239}\ _{0.332}$	$0.120\ ^{0.203}\ _{0.289}$	$0.129\ ^{0.178}\ _{0.249}$	$0.161\ ^{0.267}\ _{0.345}$	$0.180\ ^{0.264}\ _{0.309}$	$0.179\ ^{0.252}\ _{0.291}$
Skewed	70	$0.717\ ^{0.750}\ _{0.770}$	$0.743\ ^{0.758}\ _{0.768}$	$0.751\ ^{0.761}\ _{0.767}$	$0.819\ ^{0.823}\ _{0.826}$	$0.821\ ^{0.823}\ _{0.825}$	$0.822\ ^{0.823}\ _{0.825}$
	200	$0.380\ ^{0.469}\ _{0.533}$	$0.377\ ^{0.435}\ _{0.508}$	$0.386\ ^{0.423}\ _{0.491}$	$0.501\ ^{0.520}\ _{0.562}$	$0.509\ ^{0.525}\ _{0.546}$	$0.515\ ^{0.529}\ _{0.545}$
	600	$0.118\ ^{0.244}\ _{0.324}$	$0.074\ ^{0.206}\ _{0.260}$	$0.077\ ^{0.181}\ _{0.232}$	$0.187\ ^{0.261}\ _{0.340}$	$0.193\ ^{0.233}\ _{0.292}$	$0.194\ ^{0.226}\ _{0.265}$
Bimodal	70	$0.744\ ^{0.770}\ _{0.790}$	$0.766\ ^{0.780}\ _{0.790}$	$0.774\ ^{0.783}\ _{0.789}$	$0.839\ ^{0.842}\ _{0.845}$	$0.841\ ^{0.842}\ _{0.844}$	$0.841\ ^{0.842}\ _{0.844}$
	200	$0.405\ ^{0.464}\ _{0.533}$	$0.419\ ^{0.449}\ _{0.498}$	$0.425\ ^{0.445}\ _{0.477}$	$0.546\ ^{0.562}\ _{0.587}$	$0.553\ ^{0.565}\ _{0.579}$	$0.559\ ^{0.568}\ _{0.578}$
	600	$0.112\ ^{0.190}\ _{0.286}$	$0.115\ ^{0.154}\ _{0.237}$	$0.115\ ^{0.146}\ _{0.199}$	$0.156\ ^{0.248}\ _{0.310}$	$0.157\ ^{0.229}\ _{0.279}$	$0.163\ ^{0.214}\ _{0.265}$

Distribution	I.Q.R.	Curve Centred at Year 2850 BC			Curve Centred at Year 3200 BC		
		n=20	n=50	n=100	n=20	n=50	n=100
Normal	70	$0.808\ ^{0.821}\ _{0.832}$	$0.816\ ^{0.822}\ _{0.827}$	$0.818\ ^{0.822}\ _{0.826}$	$0.807\ ^{0.826}\ _{0.837}$	$0.820\ ^{0.828}\ _{0.833}$	$0.825\ ^{0.828}\ _{0.832}$
	200	$0.423\ ^{0.516}\ _{0.595}$	$0.443\ ^{0.500}\ _{0.570}$	$0.470\ ^{0.498}\ _{0.572}$	$0.482\ ^{0.532}\ _{0.583}$	$0.494\ ^{0.518}\ _{0.579}$	$0.498\ ^{0.518}\ _{0.571}$
	600	$0.161\ ^{0.274}\ _{0.349}$	$0.156\ ^{0.262}\ _{0.316}$	$0.152\ ^{0.257}\ _{0.306}$	$0.086\ ^{0.204}\ _{0.299}$	$0.094\ ^{0.178}\ _{0.233}$	$0.101\ ^{0.145}\ _{0.221}$
Skewed	70	$0.761\ ^{0.788}\ _{0.801}$	$0.783\ ^{0.792}\ _{0.799}$	$0.787\ ^{0.792}\ _{0.797}$	$0.768\ ^{0.794}\ _{0.807}$	$0.787\ ^{0.797}\ _{0.803}$	$0.794\ ^{0.798}\ _{0.803}$
	200	$0.412\ ^{0.483}\ _{0.557}$	$0.416\ ^{0.459}\ _{0.533}$	$0.426\ ^{0.459}\ _{0.540}$	$0.428\ ^{0.483}\ _{0.538}$	$0.439\ ^{0.467}\ _{0.533}$	$0.443\ ^{0.467}\ _{0.528}$
	600	$0.132\ ^{0.266}\ _{0.354}$	$0.104\ ^{0.249}\ _{0.278}$	$0.101\ ^{0.224}\ _{0.270}$	$0.083\ ^{0.201}\ _{0.313}$	$0.047\ ^{0.165}\ _{0.230}$	$0.054\ ^{0.147}\ _{0.194}$
Bimodal	70	$0.786\ ^{0.811}\ _{0.821}$	$0.807\ ^{0.813}\ _{0.819}$	$0.810\ ^{0.814}\ _{0.819}$	$0.796\ ^{0.818}\ _{0.828}$	$0.810\ ^{0.820}\ _{0.825}$	$0.816\ ^{0.820}\ _{0.824}$
	200	$0.298\ ^{0.486}\ _{0.555}$	$0.340\ ^{0.460}\ _{0.508}$	$0.351\ ^{0.458}\ _{0.499}$	$0.477\ ^{0.509}\ _{0.572}$	$0.488\ ^{0.504}\ _{0.536}$	$0.495\ ^{0.505}\ _{0.530}$
	600	$0.148\ ^{0.228}\ _{0.318}$	$0.141\ ^{0.187}\ _{0.287}$	$0.141\ ^{0.183}\ _{0.278}$	$0.076\ ^{0.166}\ _{0.244}$	$0.079\ ^{0.120}\ _{0.211}$	$0.091\ ^{0.115}\ _{0.176}$

Table 4.7 : Lower quartile, Median and Upper quartile for the ***Wastage*** of method ***B*** over 1000 simulations and over different parts of the calibration curve for the combination of distribution, I.Q.R. and sample size.

Distribution	I.Q.R.	Curve Centred at Year 700 AD			Curve Centred at Year 500 BC		
		n=20	n=50	n=100	n=20	n=50	n=100
Normal	70	$_{0.763}^{0.786}{}_{0.803}$	$_{0.778}^{0.792}{}_{0.800}$	$_{0.784}^{0.793}{}_{0.799}$	$_{0.835}^{0.845}{}_{0.848}$	$_{0.842}^{0.846}{}_{0.848}$	$_{0.843}^{0.846}{}_{0.848}$
	200	$_{0.425}^{0.498}{}_{0.563}$	$_{0.429}^{0.468}{}_{0.539}$	$_{0.439}^{0.470}{}_{0.519}$	$_{0.517}^{0.549}{}_{0.568}$	$_{0.536}^{0.551}{}_{0.564}$	$_{0.544}^{0.553}{}_{0.562}$
	600	$_{0.113}^{0.224}{}_{0.319}$	$_{0.119}^{0.189}{}_{0.279}$	$_{0.125}^{0.171}{}_{0.231}$	$_{0.140}^{0.257}{}_{0.340}$	$_{0.154}^{0.254}{}_{0.300}$	$_{0.157}^{0.230}{}_{0.282}$
Skewed	70	$_{0.717}^{0.749}{}_{0.769}$	$_{0.742}^{0.758}{}_{0.768}$	$_{0.751}^{0.760}{}_{0.767}$	$_{0.804}^{0.818}{}_{0.823}$	$_{0.815}^{0.820}{}_{0.822}$	$_{0.817}^{0.820}{}_{0.822}$
	200	$_{0.380}^{0.468}{}_{0.531}$	$_{0.376}^{0.433}{}_{0.508}$	$_{0.385}^{0.423}{}_{0.491}$	$_{0.469}^{0.505}{}_{0.538}$	$_{0.488}^{0.505}{}_{0.523}$	$_{0.494}^{0.507}{}_{0.522}$
	600	$_{0.104}^{0.228}{}_{0.312}$	$_{0.070}^{0.197}{}_{0.248}$	$_{0.072}^{0.160}{}_{0.222}$	$_{0.178}^{0.256}{}_{0.332}$	$_{0.183}^{0.225}{}_{0.283}$	$_{0.184}^{0.216}{}_{0.256}$
Bimodal	70	$_{0.743}^{0.770}{}_{0.790}$	$_{0.766}^{0.780}{}_{0.790}$	$_{0.773}^{0.783}{}_{0.789}$	$_{0.826}^{0.838}{}_{0.842}$	$_{0.835}^{0.839}{}_{0.841}$	$_{0.837}^{0.840}{}_{0.841}$
	200	$_{0.404}^{0.463}{}_{0.532}$	$_{0.418}^{0.448}{}_{0.495}$	$_{0.423}^{0.444}{}_{0.475}$	$_{0.504}^{0.547}{}_{0.566}$	$_{0.524}^{0.549}{}_{0.562}$	$_{0.538}^{0.551}{}_{0.560}$
	600	$_{0.108}^{0.177}{}_{0.267}$	$_{0.113}^{0.152}{}_{0.228}$	$_{0.114}^{0.144}{}_{0.190}$	$_{0.144}^{0.235}{}_{0.302}$	$_{0.143}^{0.211}{}_{0.275}$	$_{0.152}^{0.199}{}_{0.257}$

Distribution	I.Q.R.	Curve Centred at Year 2850 BC			Curve Centred at Year 3200 BC		
		n=20	n=50	n=100	n=20	n=50	n=100
Normal	70	$_{0.728}^{0.813}{}_{0.829}$	$_{0.804}^{0.816}{}_{0.823}$	$_{0.809}^{0.816}{}_{0.821}$	$_{0.794}^{0.816}{}_{0.831}$	$_{0.803}^{0.824}{}_{0.829}$	$_{0.818}^{0.825}{}_{0.828}$
	200	$_{0.265}^{0.476}{}_{0.550}$	$_{0.117}^{0.461}{}_{0.509}$	$_{0.170}^{0.403}{}_{0.487}$	$_{0.462}^{0.506}{}_{0.556}$	$_{0.485}^{0.501}{}_{0.540}$	$_{0.489}^{0.502}{}_{0.524}$
	600	$_{0.131}^{0.226}{}_{0.323}$	$_{0.141}^{0.187}{}_{0.281}$	$_{0.139}^{0.183}{}_{0.265}$	$_{0.062}^{0.159}{}_{0.280}$	$_{0.069}^{0.129}{}_{0.201}$	$_{0.073}^{0.119}{}_{0.169}$
Skewed	70	$_{0.623}^{0.775}{}_{0.795}$	$_{0.699}^{0.783}{}_{0.793}$	$_{0.756}^{0.784}{}_{0.791}$	$_{0.756}^{0.782}{}_{0.801}$	$_{0.768}^{0.793}{}_{0.799}$	$_{0.783}^{0.794}{}_{0.798}$
	200	$_{0.241}^{0.448}{}_{0.518}$	$_{0.140}^{0.428}{}_{0.469}$	$_{0.148}^{0.392}{}_{0.445}$	$_{0.405}^{0.452}{}_{0.508}$	$_{0.427}^{0.447}{}_{0.488}$	$_{0.433}^{0.448}{}_{0.476}$
	600	$_{0.102}^{0.243}{}_{0.327}$	$_{0.084}^{0.183}{}_{0.270}$	$_{0.080}^{0.157}{}_{0.240}$	$_{0.035}^{0.173}{}_{0.277}$	$_{0.036}^{0.088}{}_{0.194}$	$_{0.036}^{0.079}{}_{0.166}$
Bimodal	70	$_{0.694}^{0.802}{}_{0.817}$	$_{0.790}^{0.806}{}_{0.815}$	$_{0.799}^{0.808}{}_{0.814}$	$_{0.784}^{0.807}{}_{0.822}$	$_{0.793}^{0.816}{}_{0.821}$	$_{0.805}^{0.816}{}_{0.820}$
	200	$_{0.075}^{0.357}{}_{0.512}$	$_{0.021}^{0.242}{}_{0.470}$	$_{0.023}^{0.126}{}_{0.382}$	$_{0.447}^{0.492}{}_{0.534}$	$_{0.478}^{0.493}{}_{0.512}$	$_{0.485}^{0.496}{}_{0.511}$
	600	$_{0.115}^{0.186}{}_{0.284}$	$_{0.109}^{0.159}{}_{0.237}$	$_{0.123}^{0.152}{}_{0.209}$	$_{0.059}^{0.123}{}_{0.210}$	$_{0.061}^{0.100}{}_{0.156}$	$_{0.063}^{0.099}{}_{0.133}$

Table 4.8 : Lower quartile, Median and Upper quartile for the ***Wastage*** of method *C* over 1000 simulations and over different parts of the calibration curve for the combination of distribution, I.Q.R. and sample size.

Distribution	I.Q.R.	Curve Centred at Year 700 AD			Curve Centred at Year 500 BC		
		n=20	n=50	n=100	n=20	n=50	n=100
Normal	70	$0.732\ ^{0.759}\ 0.794$	$0.703\ ^{0.734}\ 0.749$	$0.689\ ^{0.716}\ 0.732$	$0.833\ ^{0.838}\ 0.842$	$0.830\ ^{0.833}\ 0.836$	$0.828\ ^{0.830}\ 0.832$
	200	$0.472\ ^{0.544}\ 0.601$	$0.381\ ^{0.444}\ 0.505$	$0.349\ ^{0.404}\ 0.443$	$0.530\ ^{0.613}\ 0.668$	$0.517\ ^{0.532}\ 0.621$	$0.509\ ^{0.518}\ 0.529$
	600	$0.334\ ^{0.417}\ 0.485$	$0.248\ ^{0.329}\ 0.386$	$0.220\ ^{0.258}\ 0.332$	$0.325\ ^{0.410}\ 0.493$	$0.250\ ^{0.312}\ 0.366$	$0.215\ ^{0.260}\ 0.310$
Skewed	70	$0.691\ ^{0.722}\ 0.763$	$0.660\ ^{0.694}\ 0.711$	$0.644\ ^{0.677}\ 0.694$	$0.804\ ^{0.809}\ 0.814$	$0.801\ ^{0.804}\ 0.807$	$0.799\ ^{0.802}\ 0.804$
	200	$0.447\ ^{0.513}\ 0.577$	$0.346\ ^{0.415}\ 0.492$	$0.303\ ^{0.366}\ 0.413$	$0.505\ ^{0.608}\ 0.636$	$0.474\ ^{0.505}\ 0.598$	$0.460\ ^{0.473}\ 0.554$
	600	$0.329\ ^{0.412}\ 0.480$	$0.269\ ^{0.328}\ 0.379$	$0.210\ ^{0.282}\ 0.323$	$0.321\ ^{0.409}\ 0.492$	$0.238\ ^{0.309}\ 0.377$	$0.201\ ^{0.256}\ 0.306$
Bimodal	70	$0.709\ ^{0.741}\ 0.768$	$0.684\ ^{0.717}\ 0.734$	$0.665\ ^{0.700}\ 0.718$	$0.825\ ^{0.829}\ 0.834$	$0.823\ ^{0.826}\ 0.828$	$0.821\ ^{0.823}\ 0.825$
	200	$0.406\ ^{0.490}\ 0.560$	$0.327\ ^{0.399}\ 0.451$	$0.298\ ^{0.340}\ 0.395$	$0.525\ ^{0.565}\ 0.661$	$0.512\ ^{0.525}\ 0.545$	$0.505\ ^{0.513}\ 0.523$
	600	$0.255\ ^{0.334}\ 0.394$	$0.166\ ^{0.244}\ 0.282$	$0.091\ ^{0.155}\ 0.235$	$0.249\ ^{0.328}\ 0.394$	$0.187\ ^{0.240}\ 0.288$	$0.160\ ^{0.194}\ 0.234$

Distribution	I.Q.R.	Curve Centred at Year 2850 BC			Curve Centred at Year 3200 BC		
		n=20	n=50	n=100	n=20	n=50	n=100
Normal	70	$0.809\ ^{0.838}\ 0.850$	$0.797\ ^{0.806}\ 0.825$	$0.791\ ^{0.796}\ 0.802$	$0.813\ ^{0.841}\ 0.851$	$0.799\ ^{0.810}\ 0.835$	$0.795\ ^{0.800}\ 0.809$
	200	$0.562\ ^{0.618}\ 0.675$	$0.517\ ^{0.555}\ 0.594$	$0.477\ ^{0.528}\ 0.550$	$0.548\ ^{0.577}\ 0.640$	$0.520\ ^{0.544}\ 0.560$	$0.469\ ^{0.523}\ 0.539$
	600	$0.338\ ^{0.436}\ 0.504$	$0.302\ ^{0.331}\ 0.405$	$0.284\ ^{0.308}\ 0.334$	$0.323\ ^{0.427}\ 0.491$	$0.239\ ^{0.305}\ 0.386$	$0.196\ ^{0.244}\ 0.297$
Skewed	70	$0.780\ ^{0.811}\ 0.828$	$0.764\ ^{0.774}\ 0.796$	$0.757\ ^{0.764}\ 0.770$	$0.773\ ^{0.808}\ 0.823$	$0.763\ ^{0.774}\ 0.802$	$0.758\ ^{0.765}\ 0.774$
	200	$0.522\ ^{0.581}\ 0.654$	$0.481\ ^{0.520}\ 0.559$	$0.443\ ^{0.484}\ 0.509$	$0.499\ ^{0.539}\ 0.616$	$0.475\ ^{0.499}\ 0.531$	$0.425\ ^{0.475}\ 0.493$
	600	$0.361\ ^{0.434}\ 0.485$	$0.264\ ^{0.342}\ 0.386$	$0.237\ ^{0.262}\ 0.326$	$0.352\ ^{0.426}\ 0.486$	$0.242\ ^{0.318}\ 0.390$	$0.196\ ^{0.240}\ 0.301$
Bimodal	70	$0.798\ ^{0.827}\ 0.839$	$0.788\ ^{0.796}\ 0.811$	$0.782\ ^{0.787}\ 0.793$	$0.800\ ^{0.833}\ 0.843$	$0.789\ ^{0.799}\ 0.824$	$0.784\ ^{0.790}\ 0.796$
	200	$0.516\ ^{0.582}\ 0.633$	$0.465\ ^{0.528}\ 0.563$	$0.437\ ^{0.488}\ 0.529$	$0.523\ ^{0.555}\ 0.582$	$0.452\ ^{0.522}\ 0.542$	$0.426\ ^{0.474}\ 0.523$
	600	$0.302\ ^{0.339}\ 0.421$	$0.259\ ^{0.301}\ 0.321$	$0.213\ ^{0.277}\ 0.300$	$0.249\ ^{0.332}\ 0.408$	$0.183\ ^{0.229}\ 0.277$	$0.133\ ^{0.189}\ 0.216$

Table 4.9 : Lower quartile, Median and Upper quartile for the ***Wastage*** of method ***D*** over 1000 simulations and over different parts of the calibration curve for the combination of distribution, I.Q.R. and sample size.

Distribution	I.Q.R.	Curve Centred at Year 700 AD			Curve Centred at Year 500 BC		
		n=20	n=50	n=100	n=20	n=50	n=100
Normal	70	$0.772\ 0.808\ 0.835$	$0.728\ 0.745\ 0.759$	$0.704\ 0.725\ 0.737$	$0.839\ 0.844\ 0.854$	$0.832\ 0.835\ 0.837$	$0.829\ 0.831\ 0.833$
	200	$0.570\ 0.633\ 0.669$	$0.433\ 0.489\ 0.546$	$0.376\ 0.425\ 0.463$	$0.632\ 0.674\ 0.707$	$0.526\ 0.548\ 0.641$	$0.513\ 0.522\ 0.537$
	600	$0.453\ 0.517\ 0.576$	$0.306\ 0.368\ 0.425$	$0.237\ 0.282\ 0.354$	$0.448\ 0.518\ 0.583$	$0.297\ 0.358\ 0.413$	$0.238\ 0.286\ 0.330$
Skewed	70	$0.740\ 0.781\ 0.815$	$0.685\ 0.706\ 0.722$	$0.662\ 0.685\ 0.699$	$0.811\ 0.817\ 0.827$	$0.803\ 0.806\ 0.809$	$0.800\ 0.803\ 0.805$
	200	$0.543\ 0.602\ 0.640$	$0.398\ 0.480\ 0.518$	$0.329\ 0.389\ 0.445$	$0.622\ 0.646\ 0.681$	$0.485\ 0.581\ 0.619$	$0.464\ 0.479\ 0.578$
	600	$0.440\ 0.505\ 0.568$	$0.311\ 0.370\ 0.416$	$0.255\ 0.295\ 0.348$	$0.450\ 0.518\ 0.576$	$0.289\ 0.357\ 0.413$	$0.230\ 0.283\ 0.325$
Bimodal	70	$0.756\ 0.793\ 0.822$	$0.708\ 0.730\ 0.744$	$0.681\ 0.709\ 0.724$	$0.831\ 0.836\ 0.843$	$0.825\ 0.828\ 0.830$	$0.822\ 0.824\ 0.826$
	200	$0.535\ 0.588\ 0.632$	$0.380\ 0.442\ 0.494$	$0.316\ 0.370\ 0.414$	$0.563\ 0.667\ 0.690$	$0.521\ 0.536\ 0.622$	$0.509\ 0.517\ 0.527$
	600	$0.359\ 0.424\ 0.473$	$0.234\ 0.267\ 0.347$	$0.122\ 0.208\ 0.245$	$0.352\ 0.425\ 0.482$	$0.228\ 0.276\ 0.331$	$0.177\ 0.215\ 0.252$

Distribution	I.Q.R.	Curve Centred at Year 2850 BC			Curve Centred at Year 3200 BC		
		n=20	n=50	n=100	n=20	n=50	n=100
Normal	70	$0.841\ 0.853\ 0.877$	$0.803\ 0.815\ 0.836$	$0.794\ 0.799\ 0.805$	$0.847\ 0.855\ 0.871$	$0.805\ 0.821\ 0.842$	$0.797\ 0.803\ 0.814$
	200	$0.633\ 0.682\ 0.736$	$0.546\ 0.579\ 0.614$	$0.504\ 0.539\ 0.561$	$0.583\ 0.650\ 0.679$	$0.537\ 0.556\ 0.576$	$0.492\ 0.531\ 0.544$
	600	$0.470\ 0.528\ 0.588$	$0.320\ 0.385\ 0.433$	$0.297\ 0.316\ 0.361$	$0.450\ 0.518\ 0.583$	$0.280\ 0.354\ 0.432$	$0.215\ 0.267\ 0.323$
Skewed	70	$0.818\ 0.837\ 0.860$	$0.771\ 0.784\ 0.812$	$0.760\ 0.767\ 0.773$	$0.815\ 0.828\ 0.846$	$0.770\ 0.785\ 0.813$	$0.761\ 0.768\ 0.779$
	200	$0.594\ 0.659\ 0.710$	$0.510\ 0.549\ 0.580$	$0.464\ 0.494\ 0.526$	$0.546\ 0.623\ 0.662$	$0.494\ 0.514\ 0.570$	$0.453\ 0.483\ 0.500$
	600	$0.456\ 0.519\ 0.568$	$0.317\ 0.370\ 0.429$	$0.248\ 0.294\ 0.345$	$0.449\ 0.519\ 0.568$	$0.294\ 0.373\ 0.424$	$0.214\ 0.272\ 0.329$
Bimodal	70	$0.833\ 0.844\ 0.867$	$0.793\ 0.804\ 0.826$	$0.784\ 0.790\ 0.796$	$0.838\ 0.848\ 0.862$	$0.795\ 0.808\ 0.833$	$0.787\ 0.792\ 0.800$
	200	$0.597\ 0.649\ 0.696$	$0.509\ 0.551\ 0.586$	$0.452\ 0.512\ 0.538$	$0.565\ 0.595\ 0.660$	$0.499\ 0.539\ 0.555$	$0.438\ 0.497\ 0.530$
	600	$0.355\ 0.432\ 0.497$	$0.291\ 0.316\ 0.336$	$0.244\ 0.288\ 0.306$	$0.345\ 0.438\ 0.495$	$0.212\ 0.263\ 0.316$	$0.162\ 0.202\ 0.231$

Table 4.10 : Lower quartile, Median, and Upper quartile for the ***Wastage*** of method ***E*** over 1000 simulations and over different parts of the calibration curve for the combination of distribution, I.Q.R. and sample size.

Distribution	I.Q.R.	Curve Centred at Year 700 AD			Curve Centred at Year 500 BC		
		n=20	n=50	n=100	n=20	n=50	n=100
Normal	70	$0.917^{0.949}_{0.969}$	$0.940^{0.955}_{0.969}$	$0.944^{0.957}_{0.963}$	$0.981^{0.985}_{0.988}$	$0.982^{0.985}_{0.987}$	$0.983^{0.985}_{0.987}$
	200	$0.638^{0.722}_{0.797}$	$0.673^{0.737}_{0.784}$	$0.698^{0.750}_{0.784}$	$0.750^{0.770}_{0.927}$	$0.760^{0.775}_{0.922}$	$0.765^{0.778}_{0.917}$
	600	$0.484^{0.547}_{0.619}$	$0.514^{0.573}_{0.619}$	$0.528^{0.575}_{0.611}$	$0.518^{0.582}_{0.634}$	$0.554^{0.592}_{0.623}$	$0.561^{0.589}_{0.615}$
Skewed	70	$0.879^{0.917}_{0.940}$	$0.901^{0.921}_{0.938}$	$0.907^{0.921}_{0.934}$	$0.985^{0.988}_{0.993}$	$0.987^{0.989}_{0.991}$	$0.987^{0.989}_{0.991}$
	200	$0.634^{0.704}_{0.795}$	$0.673^{0.723}_{0.780}$	$0.690^{0.727}_{0.764}$	$0.701^{0.739}_{0.924}$	$0.713^{0.741}_{0.919}$	$0.722^{0.744}_{0.916}$
	600	$0.475^{0.553}_{0.623}$	$0.516^{0.566}_{0.619}$	$0.536^{0.568}_{0.612}$	$0.529^{0.589}_{0.648}$	$0.550^{0.589}_{0.628}$	$0.563^{0.589}_{0.615}$
Bimodal	70	$0.952^{0.984}_{0.994}$	$0.968^{0.984}_{0.991}$	$0.978^{0.984}_{0.991}$	$1.0^{1.0}_{1.0}$	$1.0^{1.0}_{1.0}$	$1.0^{1.0}_{1.0}$
	200	$0.692^{0.764}_{0.886}$	$0.731^{0.822}_{0.879}$	$0.752^{0.831}_{0.873}$	$0.797^{0.832}_{0.994}$	$0.810^{0.840}_{0.874}$	$0.820^{0.840}_{0.865}$
	600	$0.505^{0.572}_{0.664}$	$0.529^{0.581}_{0.658}$	$0.537^{0.576}_{0.644}$	$0.553^{0.633}_{0.689}$	$0.582^{0.638}_{0.679}$	$0.600^{0.639}_{0.669}$

Distribution	I.Q.R.	Curve Centred at Year 2850 BC			Curve Centred at Year 3200 BC		
		n=20	n=50	n=100	n=20	n=50	n=100
Normal	70	$0.868^{0.904}_{0.935}$	$0.887^{0.909}_{0.927}$	$0.899^{0.914}_{0.927}$	$0.999^{0.999}_{1.000}$	$0.999^{1.000}_{1.000}$	$0.999^{1.000}_{1.000}$
	200	$0.689^{0.850}_{0.895}$	$0.828^{0.851}_{0.878}$	$0.839^{0.852}_{0.867}$	$0.824^{0.839}_{0.924}$	$0.832^{0.840}_{0.852}$	$0.836^{0.841}_{0.848}$
	600	$0.521^{0.632}_{0.666}$	$0.591^{0.648}_{0.665}$	$0.642^{0.654}_{0.664}$	$0.519^{0.581}_{0.648}$	$0.568^{0.588}_{0.653}$	$0.577^{0.589}_{0.651}$
Skewed	70	$0.842^{0.877}_{0.904}$	$0.858^{0.877}_{0.895}$	$0.863^{0.877}_{0.890}$	$0.996^{0.997}_{0.998}$	$0.997^{0.997}_{0.998}$	$0.997^{0.998}_{0.998}$
	200	$0.698^{0.823}_{0.878}$	$0.810^{0.830}_{0.873}$	$0.816^{0.830}_{0.854}$	$0.800^{0.814}_{0.918}$	$0.812^{0.820}_{0.922}$	$0.815^{0.820}_{0.919}$
	600	$0.529^{0.594}_{0.657}$	$0.579^{0.601}_{0.651}$	$0.591^{0.604}_{0.642}$	$0.518^{0.579}_{0.669}$	$0.527^{0.606}_{0.666}$	$0.541^{0.611}_{0.663}$
Bimodal	70	$0.893^{0.938}_{0.966}$	$0.918^{0.943}_{0.962}$	$0.925^{0.943}_{0.958}$	$1.0^{1.0}_{1.0}$	$1.0^{1.0}_{1.0}$	$1.0^{1.0}_{1.0}$
	200	$0.695^{0.921}_{0.950}$	$0.911^{0.928}_{0.946}$	$0.920^{0.932}_{0.943}$	$0.885^{0.908}_{0.923}$	$0.904^{0.913}_{0.922}$	$0.909^{0.915}_{0.920}$
	600	$0.557^{0.687}_{0.739}$	$0.604^{0.716}_{0.739}$	$0.708^{0.724}_{0.738}$	$0.550^{0.617}_{0.705}$	$0.572^{0.618}_{0.675}$	$0.594^{0.618}_{0.660}$

Table 4.11 : Lower quartile, Median and Upper quartile for the ***Population Coverage*** of method ***A*** over 1000 simulations and over different parts of the calibration curve for the combination of distribution, I.Q.R. and sample size.

Distribution	I.Q.R.	Curve Centred at Year 700 AD			Curve Centred at Year 500 BC		
		n=20	n=50	n=100	n=20	n=50	n=100
Normal	70	0.951 0.983 0.992	0.978 0.988 0.992	0.984 0.989 0.991	0.990 0.992 0.995	0.991 0.992 0.994	0.991 0.992 0.994
	200	0.709 0.770 0.850	0.736 0.768 0.839	0.749 0.780 0.834	0.777 0.806 0.861	0.794 0.817 0.850	0.802 0.821 0.844
	600	0.508 0.575 0.646	0.549 0.586 0.644	0.559 0.585 0.625	0.509 0.599 0.662	0.574 0.630 0.659	0.586 0.627 0.652
Skewed	70	0.917 0.962 0.978	0.959 0.969 0.977	0.962 0.970 0.975	0.994 0.995 0.998	0.994 0.996 0.997	0.995 0.996 0.997
	200	0.703 0.764 0.843	0.728 0.762 0.836	0.738 0.767 0.827	0.733 0.777 0.851	0.758 0.795 0.836	0.771 0.802 0.833
	600	0.506 0.573 0.643	0.525 0.581 0.624	0.532 0.576 0.612	0.536 0.624 0.674	0.589 0.630 0.665	0.607 0.631 0.654
Bimodal	70	0.977 0.998 1.0	0.996 0.999 1.0	0.998 0.999 1.0	1.0 1.0 1.0	1.0 1.0 1.0	1.0 1.0 1.0
	200	0.767 0.828 0.937	0.811 0.845 0.912	0.821 0.850 0.896	0.838 0.884 0.947	0.860 0.895 0.935	0.873 0.900 0.932
	600	0.547 0.611 0.694	0.583 0.615 0.675	0.592 0.615 0.652	0.552 0.660 0.734	0.616 0.680 0.732	0.631 0.676 0.723

Distribution	I.Q.R.	Curve Centred at Year 2850 BC			Curve Centred at Year 3200 BC		
		n=20	n=50	n=100	n=20	n=50	n=100
Normal	70	0.912 0.942 0.959	0.931 0.948 0.958	0.938 0.948 0.956	0.999 1.0 1.0	1.0 1.0 1.0	1.0 1.0 1.0
	200	0.629 0.708 0.835	0.696 0.725 0.859	0.713 0.737 0.878	0.800 0.837 0.870	0.817 0.834 0.868	0.820 0.835 0.866
	600	0.490 0.581 0.656	0.548 0.615 0.660	0.562 0.626 0.663	0.494 0.560 0.614	0.536 0.570 0.612	0.545 0.566 0.608
Skewed	70	0.877 0.908 0.929	0.901 0.915 0.926	0.904 0.915 0.924	0.998 0.999 0.999	0.999 0.999 0.999	0.999 0.999 0.999
	200	0.578 0.704 0.820	0.694 0.725 0.857	0.714 0.742 0.864	0.770 0.810 0.845	0.786 0.809 0.844	0.790 0.810 0.843
	600	0.494 0.574 0.640	0.527 0.597 0.634	0.544 0.599 0.630	0.484 0.546 0.604	0.498 0.547 0.577	0.504 0.545 0.566
Bimodal	70	0.947 0.975 0.988	0.965 0.978 0.986	0.969 0.979 0.984	1.0 1.0 1.0	1.0 1.0 1.0	1.0 1.0 1.0
	200	0.516 0.706 0.809	0.632 0.738 0.799	0.710 0.753 0.820	0.915 0.931 0.940	0.929 0.935 0.940	0.932 0.936 0.939
	600	0.498 0.601 0.710	0.567 0.628 0.706	0.604 0.640 0.710	0.484 0.581 0.654	0.542 0.583 0.638	0.560 0.583 0.621

Table 4.12 : Lower quartile, Median and Upper quartile for the ***Population Coverage*** of method ***B*** over 1000 simulations and over different parts of the calibration curve for the combination of distribution, I.Q.R. and sample size.

Distribution	I.Q.R.	Curve Centred at Year 700 AD			Curve Centred at Year 500 BC		
		n=20	n=50	n=100	n=20	n=50	n=100
Normal	70	0.951 0.983 0.992	0.978 0.988 0.992	0.984 0.989 0.991	0.989 0.991 0.994	0.990 0.991 0.993	0.990 0.991 0.993
	200	0.708 0.769 0.850	0.735 0.768 0.837	0.748 0.779 0.832	0.766 0.785 0.826	0.778 0.794 0.818	0.787 0.800 0.816
	600	0.506 0.572 0.640	0.547 0.580 0.638	0.557 0.582 0.615	0.493 0.584 0.652	0.560 0.617 0.650	0.572 0.614 0.644
Skewed	70	0.917 0.962 0.978	0.958 0.969 0.977	0.962 0.970 0.975	0.993 0.995 0.997	0.994 0.995 0.996	0.994 0.995 0.996
	200	0.701 0.763 0.841	0.728 0.762 0.835	0.737 0.766 0.827	0.714 0.749 0.811	0.736 0.759 0.797	0.747 0.767 0.793
	600	0.502 0.566 0.638	0.523 0.575 0.612	0.530 0.568 0.604	0.518 0.609 0.664	0.576 0.625 0.656	0.599 0.625 0.646
Bimodal	70	0.977 0.998 1.0	0.996 0.999 1.0	0.998 0.999 1.0	1.0 1.0 1.0	1.0 1.0 1.0	1.0 1.0 1.0
	200	0.765 0.827 0.936	0.811 0.845 0.910	0.821 0.850 0.896	0.822 0.859 0.906	0.842 0.868 0.901	0.854 0.875 0.898
	600	0.543 0.604 0.680	0.582 0.613 0.668	0.592 0.613 0.646	0.518 0.635 0.723	0.602 0.660 0.725	0.620 0.660 0.717

Distribution	I.Q.R.	Curve Centred at Year 2850 BC			Curve Centred at Year 3200 BC		
		n=20	n=50	n=100	n=20	n=50	n=100
Normal	70	0.845 0.917 0.949	0.908 0.937 0.951	0.927 0.940 0.950	0.996 1.0 1.0	0.999 1.0 1.0	1.0 1.0 1.0
	200	0.475 0.640 0.735	0.450 0.662 0.723	0.492 0.664 0.720	0.768 0.817 0.853	0.809 0.821 0.847	0.812 0.822 0.837
	600	0.455 0.540 0.628	0.510 0.569 0.633	0.548 0.582 0.634	0.455 0.533 0.592	0.483 0.547 0.586	0.521 0.552 0.579
Skewed	70	0.817 0.882 0.917	0.867 0.900 0.917	0.890 0.906 0.916	0.995 0.998 0.999	0.998 0.999 0.999	0.999 0.999 0.999
	200	0.405 0.623 0.723	0.410 0.635 0.721	0.423 0.650 0.725	0.732 0.786 0.828	0.775 0.793 0.821	0.781 0.794 0.815
	600	0.461 0.546 0.619	0.513 0.562 0.622	0.527 0.566 0.606	0.455 0.522 0.582	0.467 0.520 0.558	0.490 0.520 0.550
Bimodal	70	0.876 0.952 0.981	0.939 0.967 0.981	0.960 0.973 0.981	1.0 1.0 1.0	1.0 1.0 1.0	1.0 1.0 1.0
	200	0.341 0.515 0.716	0.302 0.456 0.714	0.310 0.417 0.680	0.865 0.921 0.933	0.921 0.928 0.934	0.926 0.930 0.934
	600	0.458 0.561 0.655	0.526 0.599 0.658	0.565 0.611 0.658	0.463 0.538 0.622	0.475 0.558 0.605	0.506 0.566 0.591

Table 4.13 : Lower quartile, Median and Upper quartile for the ***Population Coverage*** of method ***C*** over 1000 simulations and over different parts of the calibration curve for the combination of distribution, I.Q.R. and sample size.

Distribution	I.Q.R.	Curve Centred at Year 700 AD			Curve Centred at Year 500 BC		
		n=20	n=50	n=100	n=20	n=50	n=100
Normal	70	0.932 0.960 0.983	0.924 0.949 0.963	0.916 0.937 0.949	0.982 0.986 0.991	0.980 0.983 0.986	0.980 0.981 0.984
	200	0.741 0.837 0.890	0.704 0.760 0.812	0.682 0.734 0.770	0.769 0.905 0.957	0.764 0.784 0.920	0.759 0.771 0.786
	600	0.652 0.731 0.797	0.620 0.666 0.722	0.602 0.630 0.679	0.661 0.723 0.790	0.624 0.665 0.704	0.606 0.635 0.668
Skewed	70	0.900 0.934 0.986	0.895 0.916 0.937	0.886 0.904 0.918	0.986 0.990 0.994	0.985 0.988 0.990	0.984 0.986 0.988
	200	0.734 0.827 0.896	0.702 0.759 0.816	0.678 0.722 0.758	0.734 0.927 0.947	0.722 0.775 0.921	0.710 0.730 0.878
	600	0.662 0.738 0.798	0.624 0.680 0.725	0.599 0.648 0.689	0.670 0.738 0.803	0.622 0.669 0.719	0.609 0.640 0.671
Bimodal	70	0.967 0.989 0.997	0.957 0.979 0.990	0.944 0.971 0.983	1.0 1.0 1.0	1.0 1.0 1.0	1.0 1.0 1.0
	200	0.765 0.897 0.969	0.739 0.834 0.895	0.725 0.784 0.847	0.824 0.918 0.998	0.814 0.841 0.886	0.807 0.825 0.848
	600	0.682 0.743 0.841	0.611 0.677 0.723	0.568 0.615 0.670	0.692 0.758 0.838	0.648 0.694 0.743	0.623 0.659 0.693

Distribution	I.Q.R.	Curve Centred at Year 2850 BC			Curve Centred at Year 3200 BC		
		n=20	n=50	n=100	n=20	n=50	n=100
Normal	70	0.902 0.938 0.990	0.892 0.915 0.937	0.882 0.900 0.915	0.999 1.0 1.0	0.999 0.999 1.0	0.999 0.999 0.999
	200	0.811 0.899 0.946	0.802 0.852 0.890	0.752 0.834 0.856	0.837 0.864 0.929	0.820 0.839 0.856	0.793 0.825 0.836
	600	0.670 0.746 0.812	0.655 0.680 0.734	0.648 0.665 0.684	0.641 0.718 0.798	0.615 0.658 0.719	0.594 0.622 0.657
Skewed	70	0.879 0.915 0.997	0.864 0.886 0.912	0.854 0.871 0.889	0.996 0.998 0.999	0.996 0.997 0.998	0.996 0.997 0.997
	200	0.796 0.880 0.949	0.802 0.844 0.882	0.770 0.818 0.839	0.816 0.851 0.932	0.803 0.822 0.849	0.772 0.806 0.819
	600	0.680 0.748 0.807	0.624 0.683 0.726	0.608 0.627 0.684	0.655 0.746 0.814	0.600 0.667 0.736	0.571 0.609 0.660
Bimodal	70	0.939 0.968 0.995	0.915 0.943 0.964	0.905 0.925 0.941	1.0 1.0 1.0	1.0 1.0 1.0	1.0 1.0 1.0
	200	0.797 0.941 0.986	0.767 0.920 0.952	0.744 0.890 0.929	0.900 0.924 0.961	0.891 0.908 0.923	0.882 0.896 0.907
	600	0.719 0.770 0.857	0.685 0.739 0.762	0.658 0.717 0.739	0.668 0.744 0.842	0.622 0.660 0.717	0.590 0.626 0.652

Table 4.14 : Lower quartile, Median and Upper quartile for the ***Population Coverage*** of method ***D*** over 1000 simulations and over different parts of the calibration curve for the combination of distribution, I.Q.R. and sample size.

Distribution	I.Q.R.	Curve Centred at Year 700 AD			Curve Centred at Year 500 BC		
		n=20	n=50	n=100	n=20	n=50	n=100
Normal	70	$0.963\ 0.985\ 0.999$	$0.940\ 0.957\ 0.970$	$0.923\ 0.942\ 0.953$	$0.986\ 0.991\ 0.997$	$0.982\ 0.984\ 0.987$	$0.980\ 0.982\ 0.984$
	200	$0.859\ 0.923\ 0.951$	$0.745\ 0.797\ 0.851$	$0.709\ 0.753\ 0.786$	$0.912\ 0.960\ 0.974$	$0.772\ 0.805\ 0.938$	$0.763\ 0.776\ 0.798$
	600	$0.758\ 0.820\ 0.873$	$0.651\ 0.706\ 0.755$	$0.616\ 0.645\ 0.703$	$0.753\ 0.817\ 0.874$	$0.657\ 0.696\ 0.738$	$0.620\ 0.653\ 0.682$
Skewed	70	$0.936\ 0.988\ 0.999$	$0.907\ 0.926\ 0.947$	$0.893\ 0.909\ 0.923$	$0.989\ 0.994\ 0.998$	$0.986\ 0.989\ 0.991$	$0.984\ 0.987\ 0.988$
	200	$0.850\ 0.913\ 0.944$	$0.738\ 0.806\ 0.840$	$0.698\ 0.740\ 0.781$	$0.937\ 0.953\ 0.961$	$0.736\ 0.906\ 0.937$	$0.715\ 0.739\ 0.905$
	600	$0.769\ 0.825\ 0.873$	$0.670\ 0.720\ 0.755$	$0.616\ 0.665\ 0.703$	$0.766\ 0.837\ 0.884$	$0.659\ 0.705\ 0.752$	$0.625\ 0.658\ 0.688$
Bimodal	70	$0.990\ 0.998\ 1.0$	$0.968\ 0.985\ 0.993$	$0.953\ 0.974\ 0.985$	$1.0\ 1.0\ 1.0$	$1.0\ 1.0\ 1.0$	$1.0\ 1.0\ 1.0$
	200	$0.920\ 0.977\ 0.993$	$0.802\ 0.879\ 0.930$	$0.743\ 0.819\ 0.865$	$0.897\ 0.998\ 0.999$	$0.827\ 0.859\ 0.995$	$0.812\ 0.831\ 0.857$
	600	$0.769\ 0.868\ 0.920$	$0.665\ 0.701\ 0.799$	$0.586\ 0.644\ 0.680$	$0.785\ 0.859\ 0.916$	$0.686\ 0.728\ 0.787$	$0.640\ 0.677\ 0.712$

Distribution	I.Q.R.	Curve Centred at Year 2850 BC			Curve Centred at Year 3200 BC		
		n=20	n=50	n=100	n=20	n=50	n=100
Normal	70	$0.932\ 0.975\ 1.0$	$0.903\ 0.925\ 0.946$	$0.888\ 0.905\ 0.919$	$1.0\ 1.0\ 1.0$	$0.999\ 1.0\ 1.0$	$0.999\ 0.999\ 0.999$
	200	$0.907\ 0.953\ 0.975$	$0.843\ 0.873\ 0.911$	$0.794\ 0.844\ 0.864$	$0.868\ 0.939\ 0.960$	$0.834\ 0.849\ 0.873$	$0.810\ 0.831\ 0.841$
	600	$0.766\ 0.825\ 0.887$	$0.672\ 0.719\ 0.762$	$0.657\ 0.672\ 0.705$	$0.739\ 0.817\ 0.876$	$0.644\ 0.690\ 0.756$	$0.605\ 0.638\ 0.675$
Skewed	70	$0.912\ 0.997\ 1.0$	$0.875\ 0.897\ 0.929$	$0.859\ 0.876\ 0.894$	$0.998\ 0.999\ 1.0$	$0.997\ 0.998\ 0.998$	$0.996\ 0.997\ 0.997$
	200	$0.896\ 0.946\ 0.982$	$0.828\ 0.871\ 0.900$	$0.797\ 0.826\ 0.853$	$0.850\ 0.940\ 0.960$	$0.817\ 0.835\ 0.893$	$0.794\ 0.812\ 0.825$
	600	$0.783\ 0.837\ 0.888$	$0.666\ 0.719\ 0.764$	$0.616\ 0.658\ 0.701$	$0.769\ 0.835\ 0.885$	$0.644\ 0.719\ 0.767$	$0.587\ 0.629\ 0.687$
Bimodal	70	$0.968\ 0.994\ 1.0$	$0.929\ 0.953\ 0.974$	$0.911\ 0.931\ 0.946$	$1.0\ 1.0\ 1.0$	$1.0\ 1.0\ 1.0$	$1.0\ 1.0\ 1.0$
	200	$0.940\ 0.988\ 0.998$	$0.887\ 0.939\ 0.976$	$0.798\ 0.911\ 0.935$	$0.926\ 0.958\ 0.998$	$0.903\ 0.918\ 0.933$	$0.889\ 0.902\ 0.912$
	600	$0.783\ 0.867\ 0.912$	$0.726\ 0.756\ 0.778$	$0.682\ 0.729\ 0.746$	$0.752\ 0.853\ 0.929$	$0.649\ 0.699\ 0.760$	$0.609\ 0.638\ 0.665$

Table 4.15 : Lower quartile, Median and Upper quartile for the ***Population Coverage*** of method ***E*** over 1000 simulations and over different parts of the calibration curve for the combination of distribution, I.Q.R. and sample size.

Distribution	I.Q.R.	Curve Centred at Year 700 AD			Curve Centred at Year 500 BC		
		n=20	n=50	n=100	n=20	n=50	n=100
Normal	70	0.977	1.0	1.0	0.999	1.0	1.0
	200	0.635	0.812	0.878	0.955	0.999	1.0
	600	0.335	0.483	0.628	0.562	0.776	0.908
Skewed	70	0.959	0.998	1.0	0.998	1.0	1.0
	200	0.578	0.746	0.822	0.709	0.835	0.922
	600	0.214	0.285	0.309	0.431	0.563	0.734
Bimodal	70	0.967	0.998	1.0	1.0	1.0	1.0
	200	0.661	0.792	0.895	0.975	0.996	1.0
	600	0.399	0.554	0.669	0.647	0.838	0.956
Distribution	I.Q.R.	Curve Centred at Year 2850 BC			Curve Centred at Year 3200 BC		
		n=20	n=50	n=100	n=20	n=50	n=100
Normal	70	0.992	1.0	1.0	1.0	1.0	1.0
	200	0.729	0.840	0.931	0.994	1.0	1.0
	600	0.519	0.704	0.884	0.389	0.569	0.730
Skewed	70	0.994	0.999	1.0	1.0	1.0	1.0
	200	0.723	0.855	0.925	0.963	0.998	1.0
	600	0.525	0.717	0.867	0.308	0.409	0.514
Bimodal	70	0.989	1.0	1.0	1.0	1.0	1.0
	200	0.701	0.843	0.939	0.991	1.0	1.0
	600	0.521	0.681	0.844	0.478	0.651	0.778

Table 4.16 : Simulation results for the estimated ***Confidence*** for method ***A*** over different parts of the calibration curve for the combination of distribution, I.Q.R. and sample size.

Distribution	I.Q.R.	Curve Centred at Year 700 AD			Curve Centred at Year 500 BC		
		n=20	n=50	n=100	n=20	n=50	n=100
Normal	70	0.990	1.0	1.0	0.997	1.0	1.0
	200	0.833	0.973	0.997	0.982	0.999	1.0
	600	0.492	0.754	0.893	0.600	0.833	0.930
Skewed	70	0.977	0.999	1.0	0.996	1.0	1.0
	200	0.812	0.969	0.998	0.886	0.988	0.999
	600	0.414	0.563	0.699	0.601	0.825	0.955
Bimodal	70	0.979	0.999	1.0	0.998	1.0	1.0
	200	0.823	0.973	0.993	0.978	0.998	1.0
	600	0.561	0.793	0.918	0.659	0.880	0.965
Distribution	I.Q.R.	Curve Centred at Year 2850 BC			Curve Centred at Year 3200 BC		
		n=20	n=50	n=100	n=20	n=50	n=100
Normal	70	0.991	1.0	1.0	0.985	1.0	1.0
	200	0.465	0.595	0.722	0.982	1.0	1.0
	600	0.438	0.572	0.729	0.443	0.693	0.850
Skewed	70	0.985	1.0	1.0	0.986	1.0	1.0
	200	0.397	0.518	0.627	0.976	1.0	1.0
	600	0.408	0.537	0.681	0.208	0.219	0.196
Bimodal	70	0.989	1.0	1.0	0.987	1.0	1.0
	200	0.372	0.525	0.694	0.983	1.0	1.0
	600	0.437	0.535	0.665	0.530	0.723	0.816

Table 4.17: Simulation results for the estimated ***Confidence*** for method ***B*** over different parts of the calibration curve for the combination of distribution, I.Q.R. and sample size.

Distribution	I.Q.R.	Curve Centred at Year 700 AD			Curve Centred at Year 500 BC		
		n=20	n=50	n=100	n=20	n=50	n=100
Normal	70	0.990	1.0	1.0	0.992	1.0	1.0
	200	0.831	0.972	0.997	0.964	0.997	1.0
	600	0.484	0.753	0.891	0.528	0.782	0.887
Skewed	70	0.974	0.999	1.0	0.993	1.0	1.0
	200	0.808	0.968	0.998	0.846	0.972	0.997
	600	0.407	0.562	0.694	0.555	0.782	0.931
Bimodal	70	0.979	0.999	1.0	0.993	0.999	1.0
	200	0.823	0.971	0.997	0.964	0.998	1.0
	600	0.553	0.789	0.917	0.574	0.796	0.928
Distribution	I.Q.R.	Curve Centred at Year 2850 BC			Curve Centred at Year 3200 BC		
		n=20	n=50	n=100	n=20	n=50	n=100
Normal	70	0.904	0.992	1.0	0.966	0.996	1.0
	200	0.316	0.302	0.359	0.921	0.997	1.0
	600	0.359	0.497	0.645	0.304	0.524	0.674
Skewed	70	0.832	0.921	0.970	0.958	0.997	0.999
	200	0.265	0.241	0.297	0.891	0.990	1.0
	600	0.344	0.451	0.577	0.206	0.222	0.203
Bimodal	70	0.872	0.986	1.0	0.961	0.995	1.0
	200	0.207	0.157	0.178	0.924	0.994	1.0
	600	0.370	0.449	0.578	0.369	0.546	0.642

Table 4.18 : Simulation results for the estimated ***Confidence*** for method ***C*** over different parts of the calibration curve for the combination of distribution, I.Q.R. and sample size.

Distribution	I.Q.R.	Curve Centred at Year 700 AD			Curve Centred at Year 500 BC		
		n=20	n=50	n=100	n=20	n=50	n=100
Normal	70	0.979	0.998	1.0	0.998	1.0	1.0
	200	0.860	0.881	0.882	0.974	0.998	1.0
	600	0.818	0.851	0.879	0.900	0.938	0.969
Skewed	70	0.963	0.998	0.998	1.0	1.0	1.0
	200	0.827	0.841	0.839	0.856	0.868	0.866
	600	0.743	0.736	0.684	0.854	0.864	0.927
Bimodal	70	0.970	0.996	0.999	1.0	1.0	1.0
	200	0.825	0.838	0.828	0.987	0.998	1.0
	600	0.831	0.837	0.854	0.916	0.946	0.977
Distribution	I.Q.R.	Curve Centred at Year 2850 BC			Curve Centred at Year 3200 BC		
		n=20	n=50	n=100	n=20	n=50	n=100
Normal	70	0.996	1.0	1.0	0.998	1.0	1.0
	200	0.850	0.851	0.826	0.994	1.0	1.0
	600	0.855	0.877	0.904	0.818	0.893	0.921
Skewed	70	0.999	1.0	1.0	1.0	1.0	1.0
	200	0.844	0.874	0.844	0.978	0.999	1.0
	600	0.883	0.924	0.947	0.764	0.759	0.675
Bimodal	70	0.998	1.0	1.0	1.0	1.0	1.0
	200	0.792	0.785	0.775	0.997	0.999	1.0
	600	0.857	0.821	0.857	0.858	0.890	0.893

Table 4.19 : Simulation results for the estimated ***Confidence*** for method ***D*** over different parts of the calibration curve for the combination of distribution, I.Q.R. and sample size.

Distribution	I.Q.R.	Curve Centred at Year 700 AD			Curve Centred at Year 500 BC		
		n=20	n=50	n=100	n=20	n=50	n=100
Normal	70	0.997	1.0	1.0	1.0	1.0	1.0
	200	0.958	0.937	0.907	0.993	0.998	1.0
	600	0.951	0.911	0.921	0.973	0.972	0.983
Skewed	70	0.991	0.998	0.999	1.0	1.0	1.0
	200	0.949	0.900	0.890	0.948	0.921	0.906
	600	0.925	0.849	0.770	0.961	0.928	0.952
Bimodal	70	0.998	0.999	1.0	1.0	1.0	1.0
	200	0.943	0.912	0.872	0.998	0.999	1.0
	600	0.947	0.906	0.907	0.976	0.972	0.981
Distribution	I.Q.R.	Curve Centred at Year 2850 BC			Curve Centred at Year 3200 BC		
		n=20	n=50	n=100	n=20	n=50	n=100
Normal	70	1.0	1.0	1.0	0.998	1.0	1.0
	200	0.950	0.911	0.884	0.998	1.0	1.0
	600	0.929	0.950	0.931	0.946	0.942	0.953
Skewed	70	1.0	1.0	1.0	1.0	1.0	1.0
	200	0.922	0.927	0.876	0.995	1.0	1.0
	600	0.956	0.958	0.962	0.905	0.842	0.757
Bimodal	70	1.0	1.0	1.0	1.0	1.0	1.0
	200	0.921	0.865	0.824	0.999	0.999	1.0
	600	0.932	0.897	0.892	0.955	0.938	0.924

Table 4.20 : Simulation results for the estimated ***Confidence*** for method ***E*** over different parts of the calibration curve for the combination of distribution, I.Q.R. and sample size.

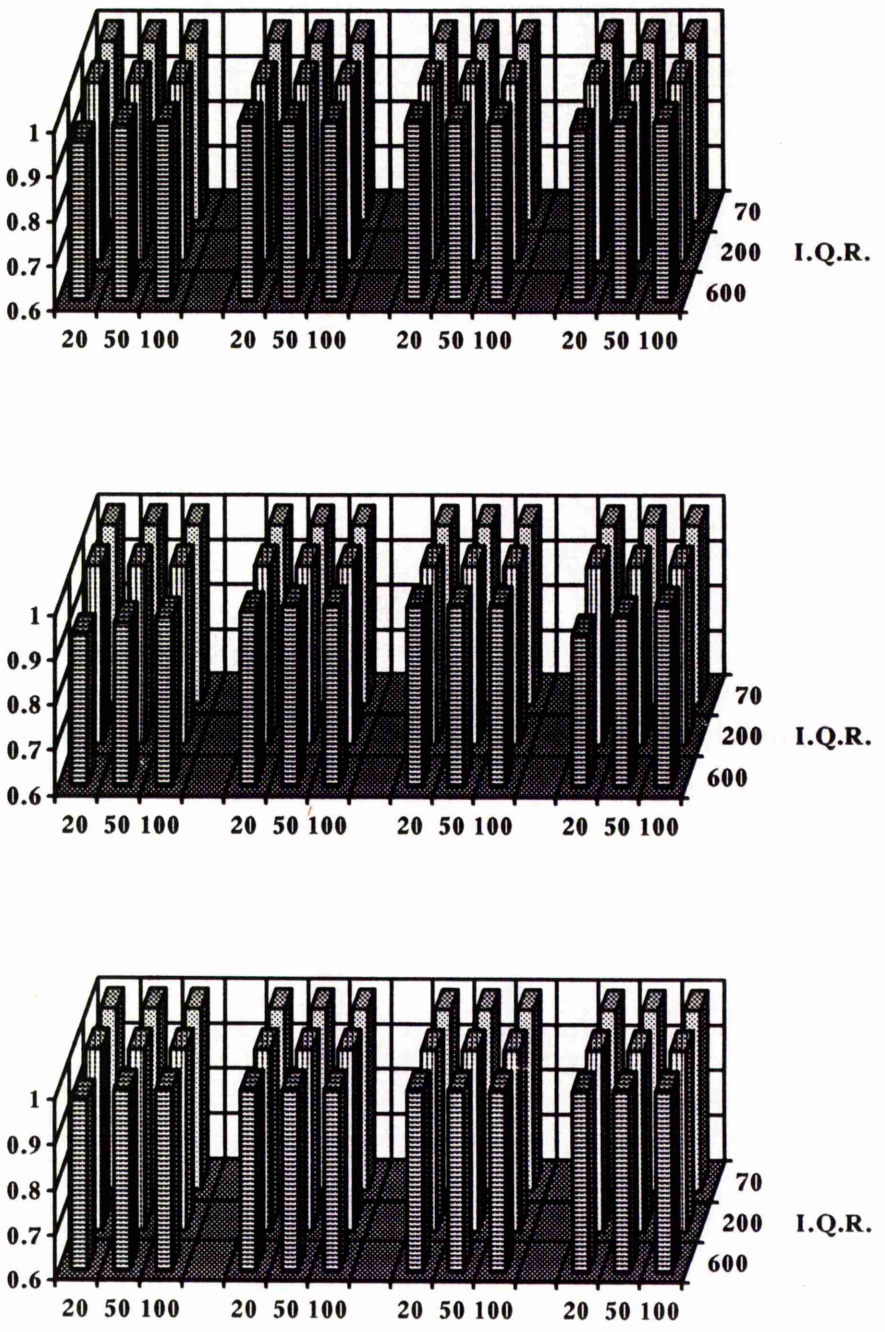

Figure 4.7 : Bar charts for the ***median*** of the ***Coverage*** of method ***A*** from a 1000 simulations.

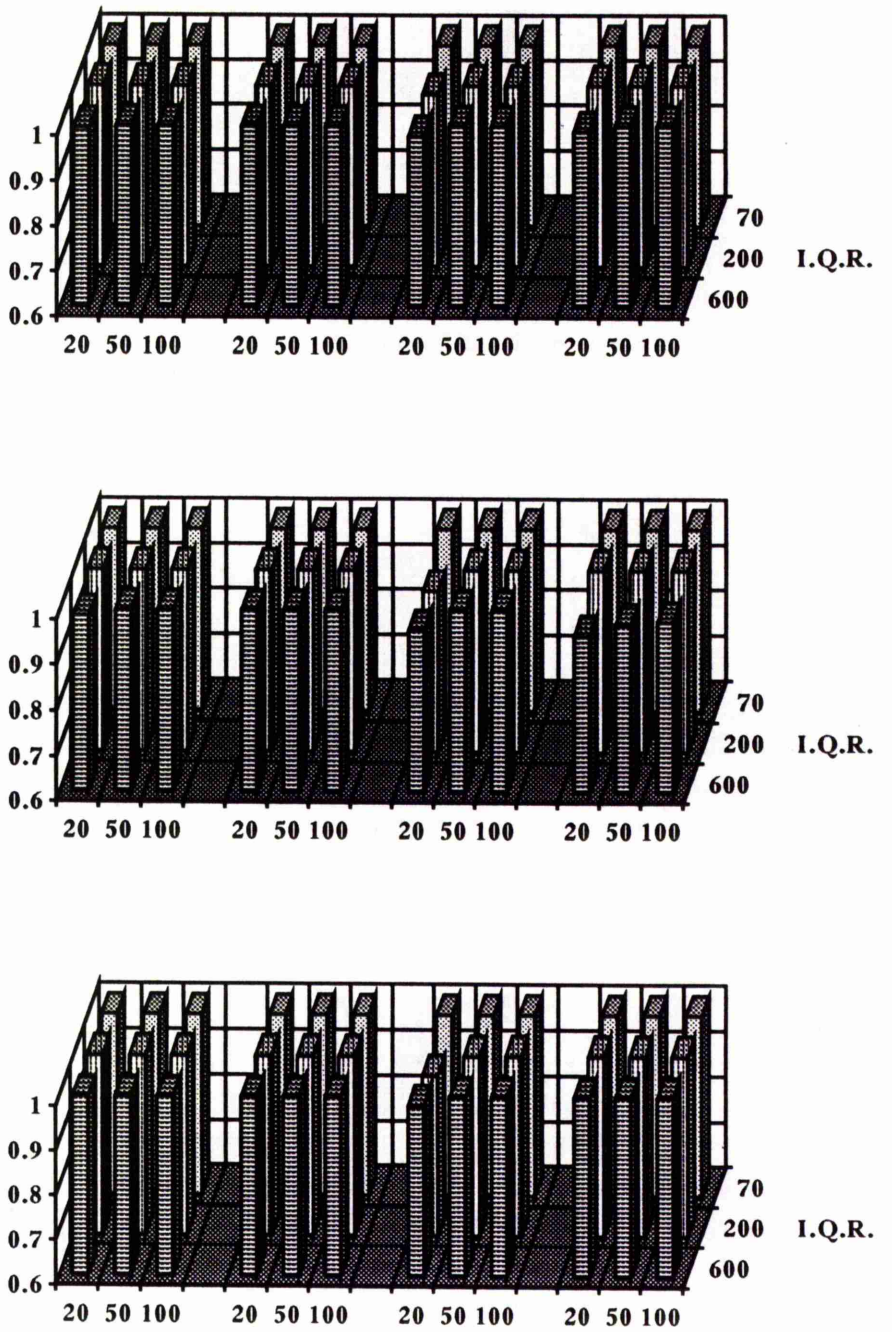

Figure 4.8 : Bar charts for the ***median*** of the ***Coverage*** of method ***B*** from a 1000 simulations.

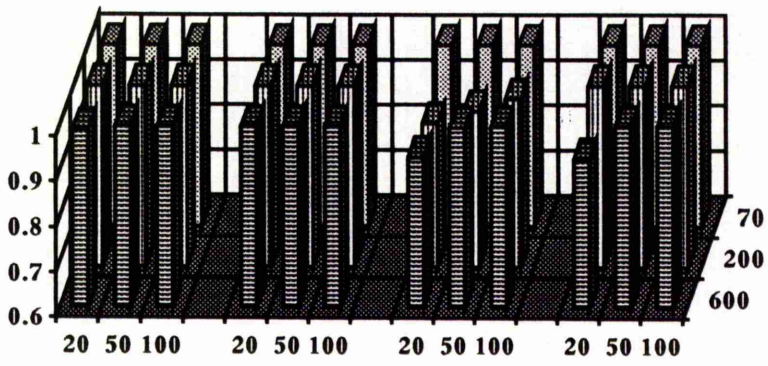

Normal Distribution

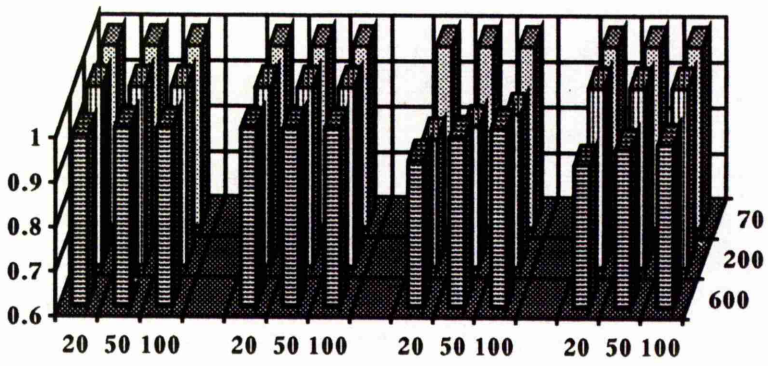

Skewed Distribution

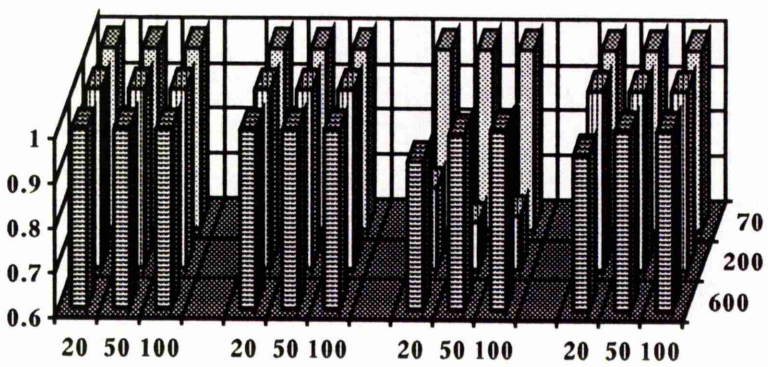

Bimodal Distribution

Years 700 AD 500 BC 2850 BC 3200 BC

Figure 4.9 : Bar charts for the ***median*** of the ***Coverage*** of method ***C*** from a 1000 simulations.

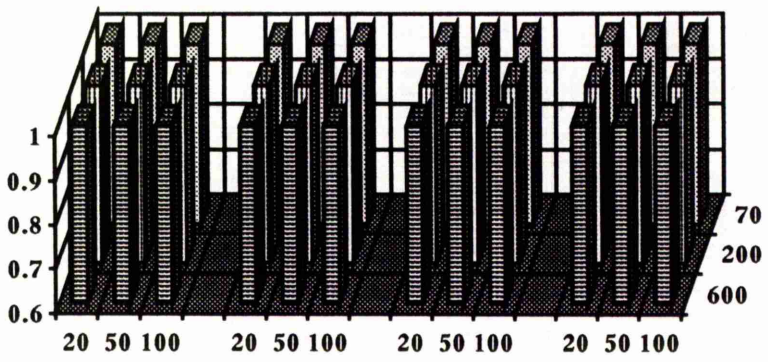

Normal Distribution

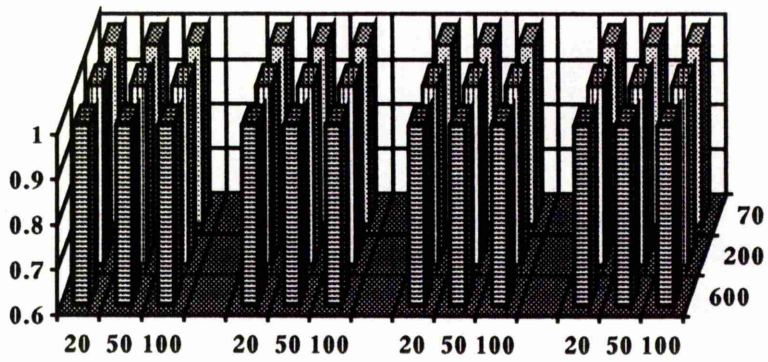

Skewed Distribution

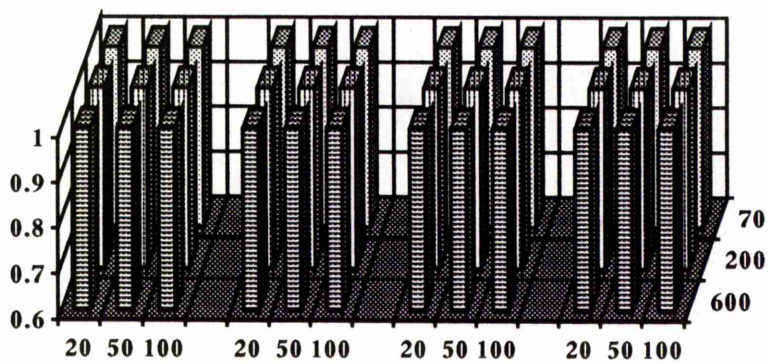

Bimodal Distribution

Years 700 AD 500 BC 2850 BC 3200 BC

Figure 4.10 : Bar charts for the ***median*** of the ***Coverage*** of method ***D*** from a 1000 simulations.

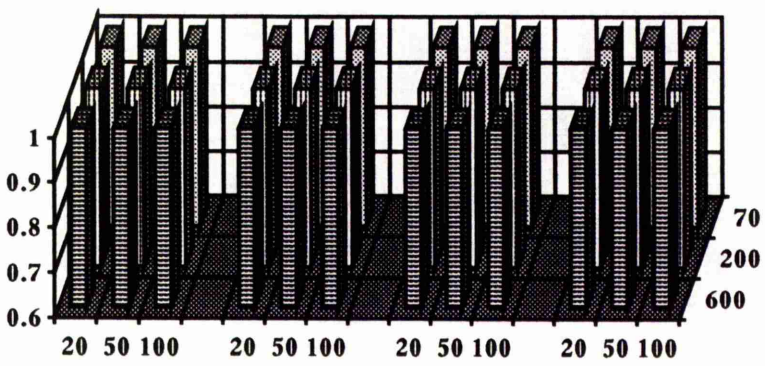

Normal Distribution

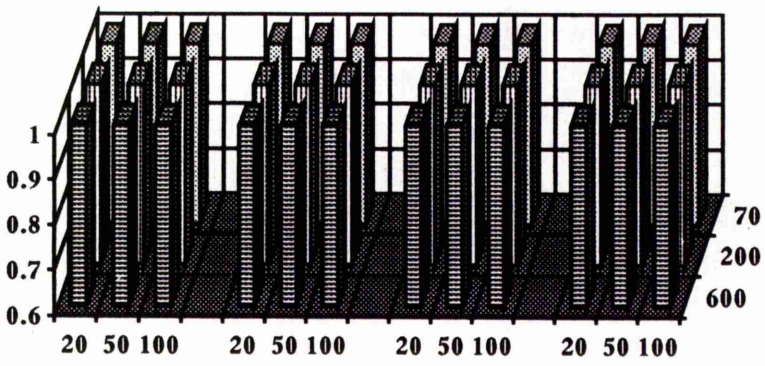

Skewed Distribution

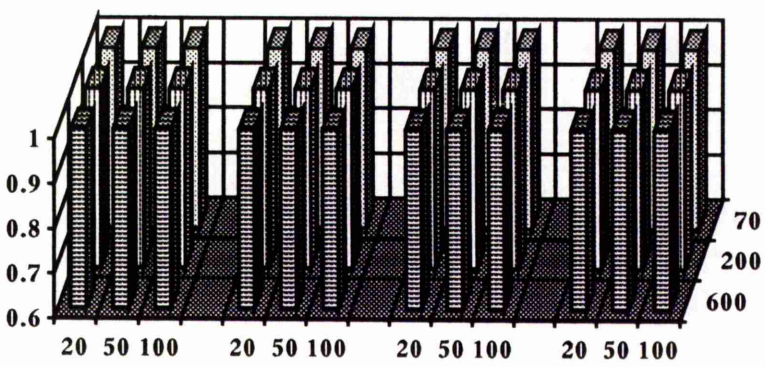

Bimodal Distribution

Years 700 AD 500 BC 2850 BC 3200 BC

Figure 4.11 : Bar charts for the ***median*** of the ***Coverage*** of method ***E*** from a 1000 simulations.

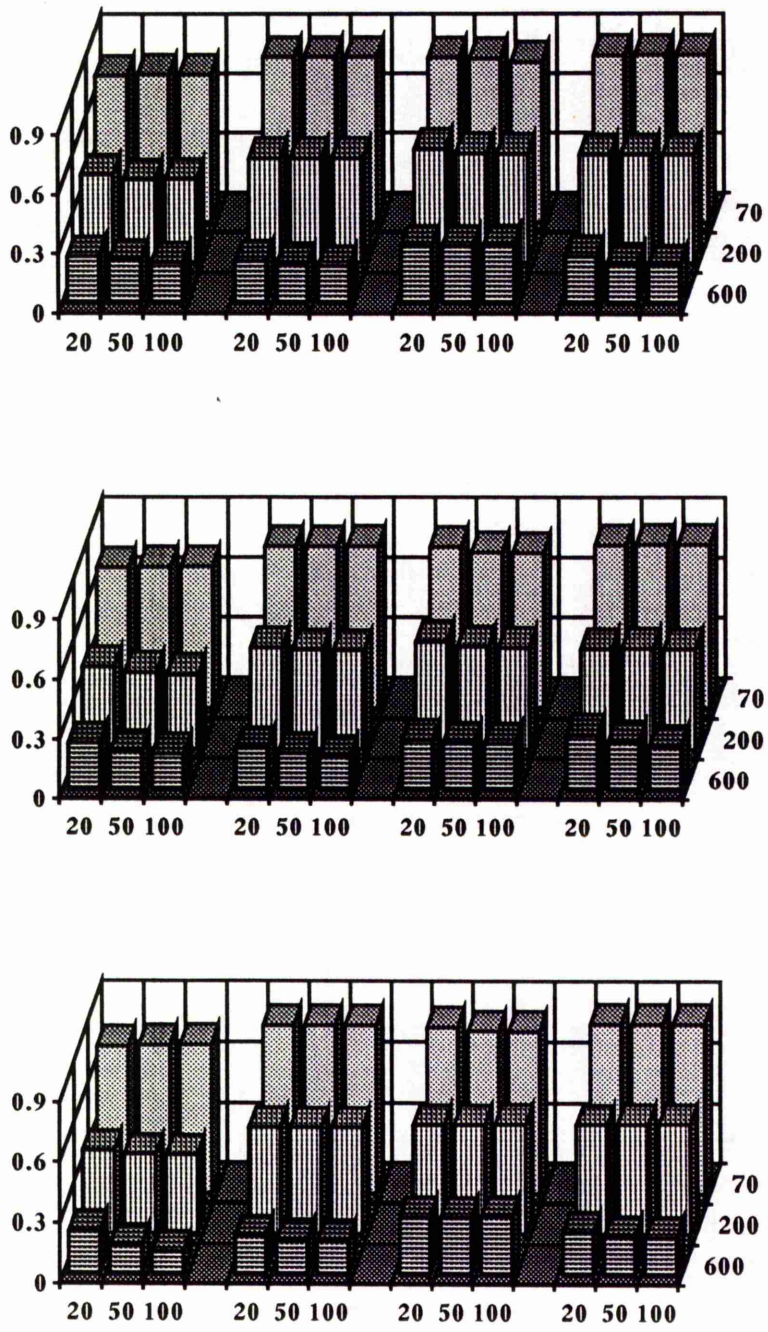

Figure 4.12 : Bar charts for the ***median*** of the ***Wastage*** of method ***A*** from a 1000 simulations.

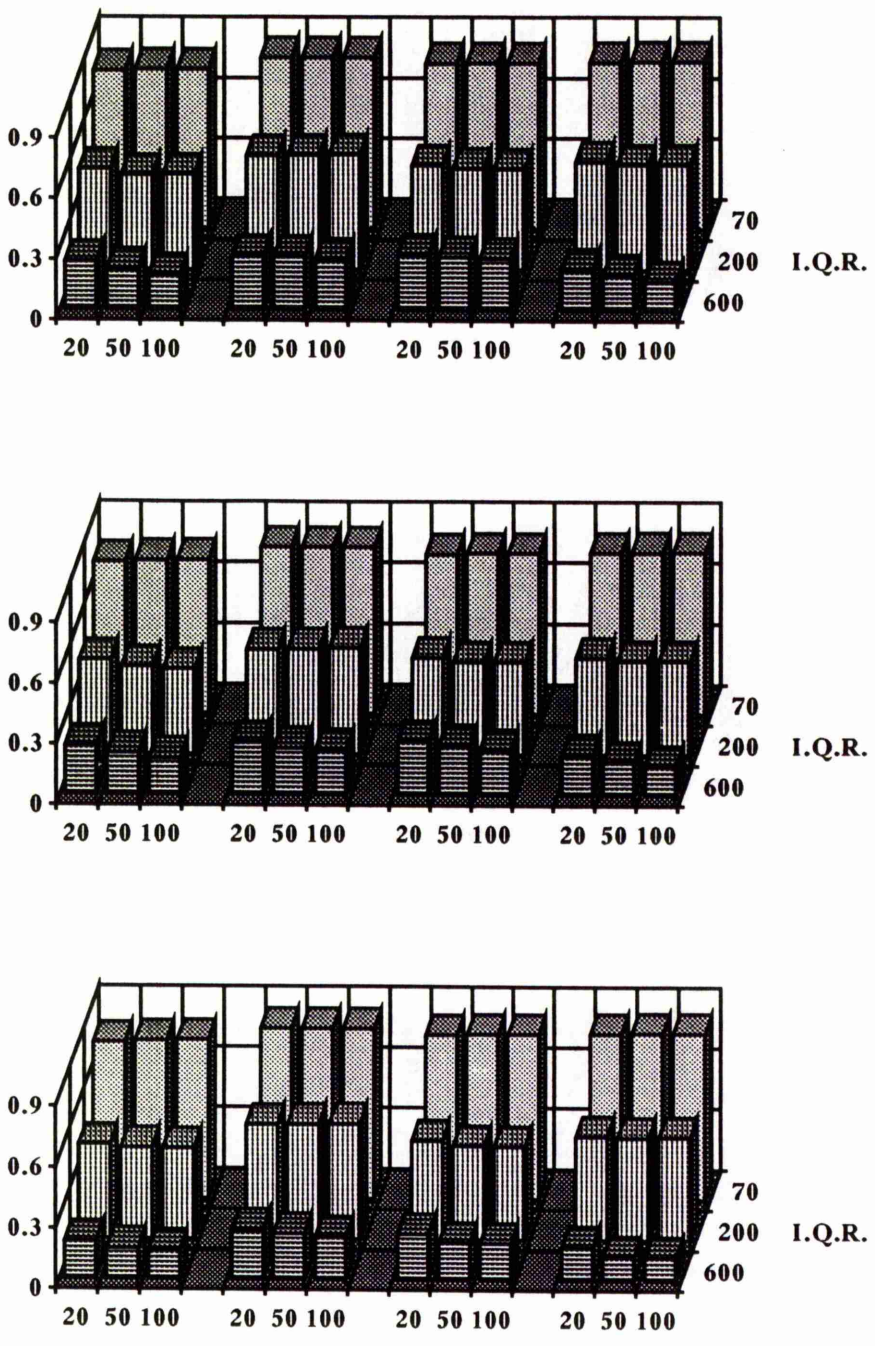

Figure 4.13 : Bar charts for the ***median*** of the ***Wastage*** of method ***B*** from a 1000 simulations.

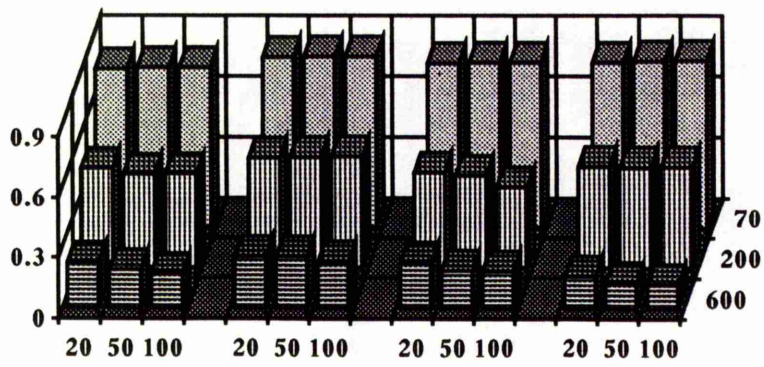

Normal Distribution

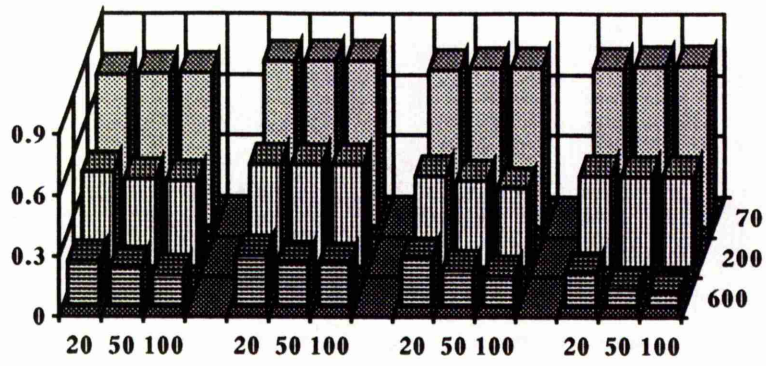

Skewed Distribution

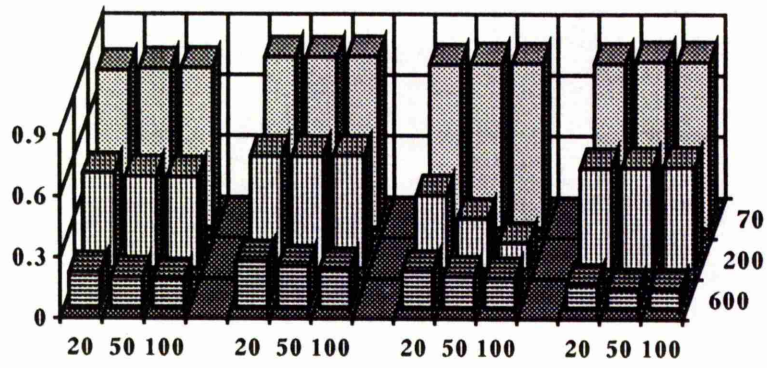

Bimodal Distribution

Years 700 AD 500 BC 2850 BC 3200 BC

Figure 4.14 : Bar charts for the ***median*** of the ***Wastage*** of method ***C*** from a 1000 simulations.

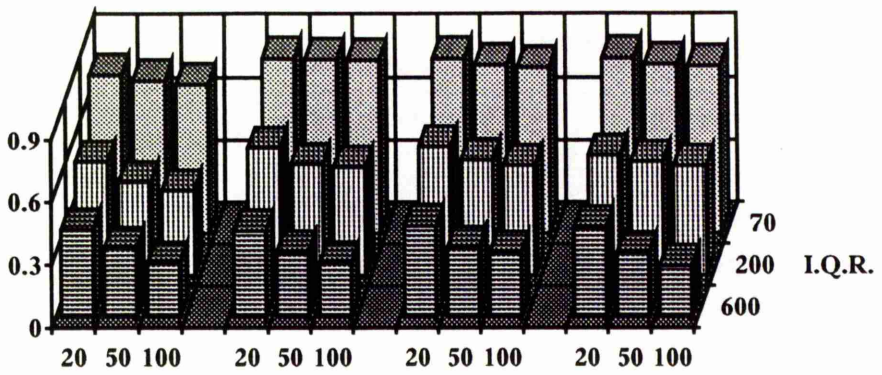

Normal Distribution

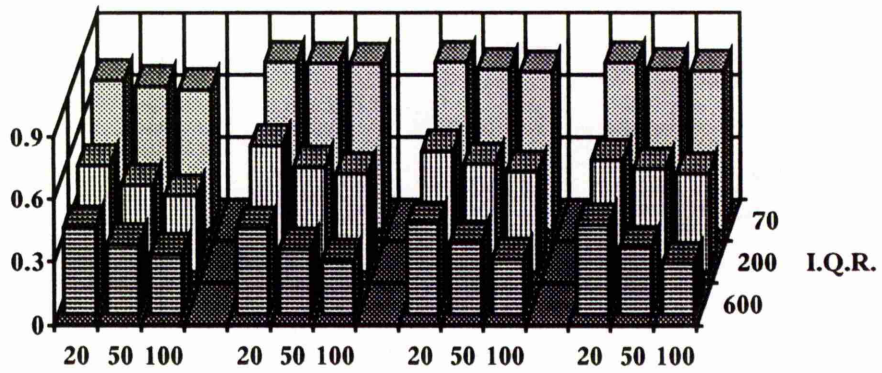

Skewed Distribution

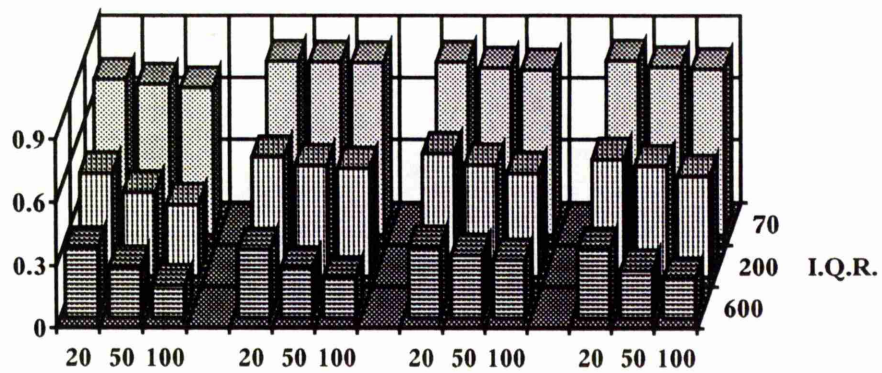

Bimodal Distribution

Years 700 AD 500 BC 2850 BC 3200 BC

Figure 4.15: Bar charts for the ***median*** of the ***Wastage*** of method ***D*** from a 1000 simulations.

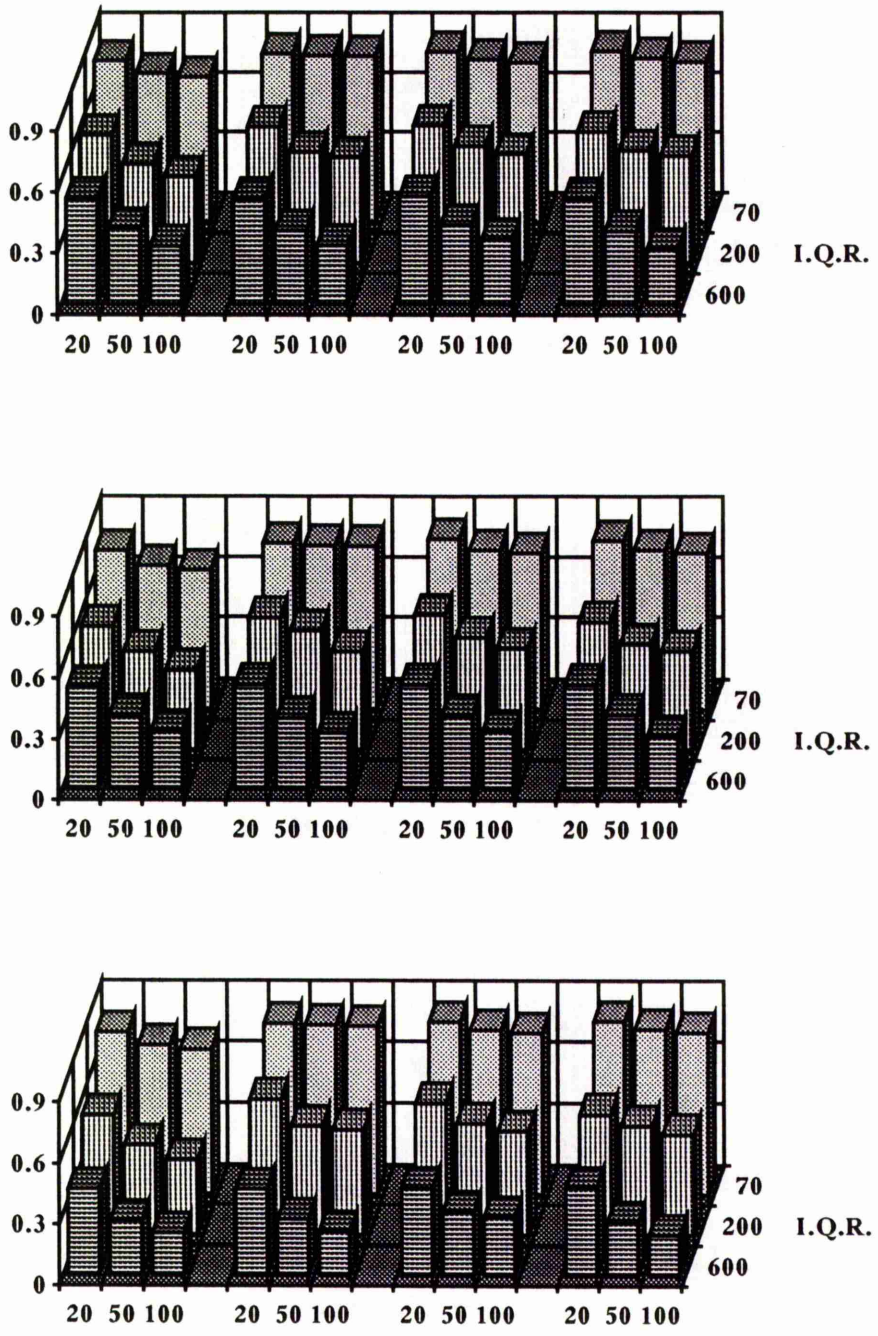

Figure 4.16 : Bar charts for the ***median*** of the ***Wastage*** of method ***E*** from a 1000 simulations.

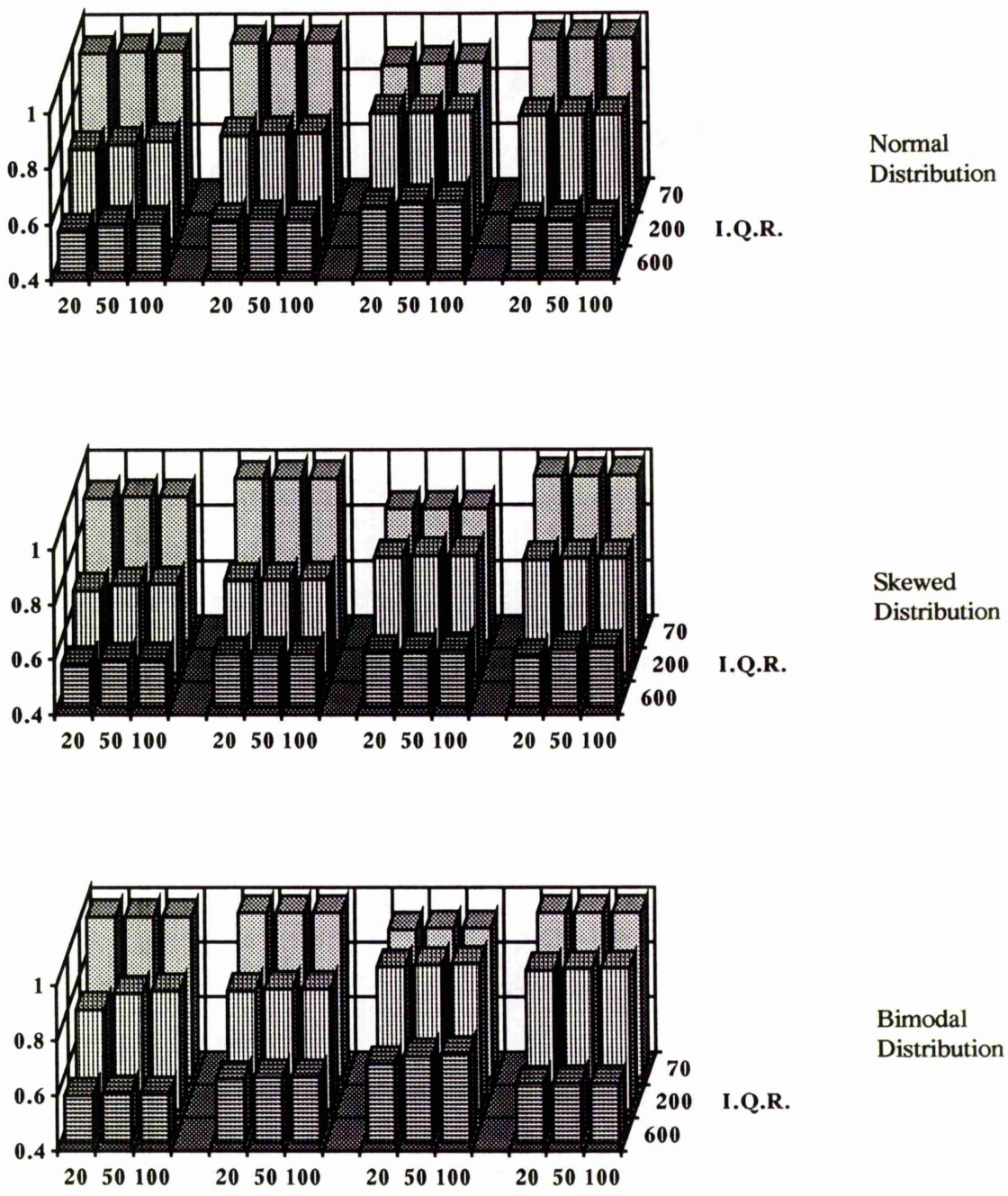

Figure 4.17 : Bar charts for the ***median*** of the ***Population Coverage*** of method ***A*** from a 1000 simulations.

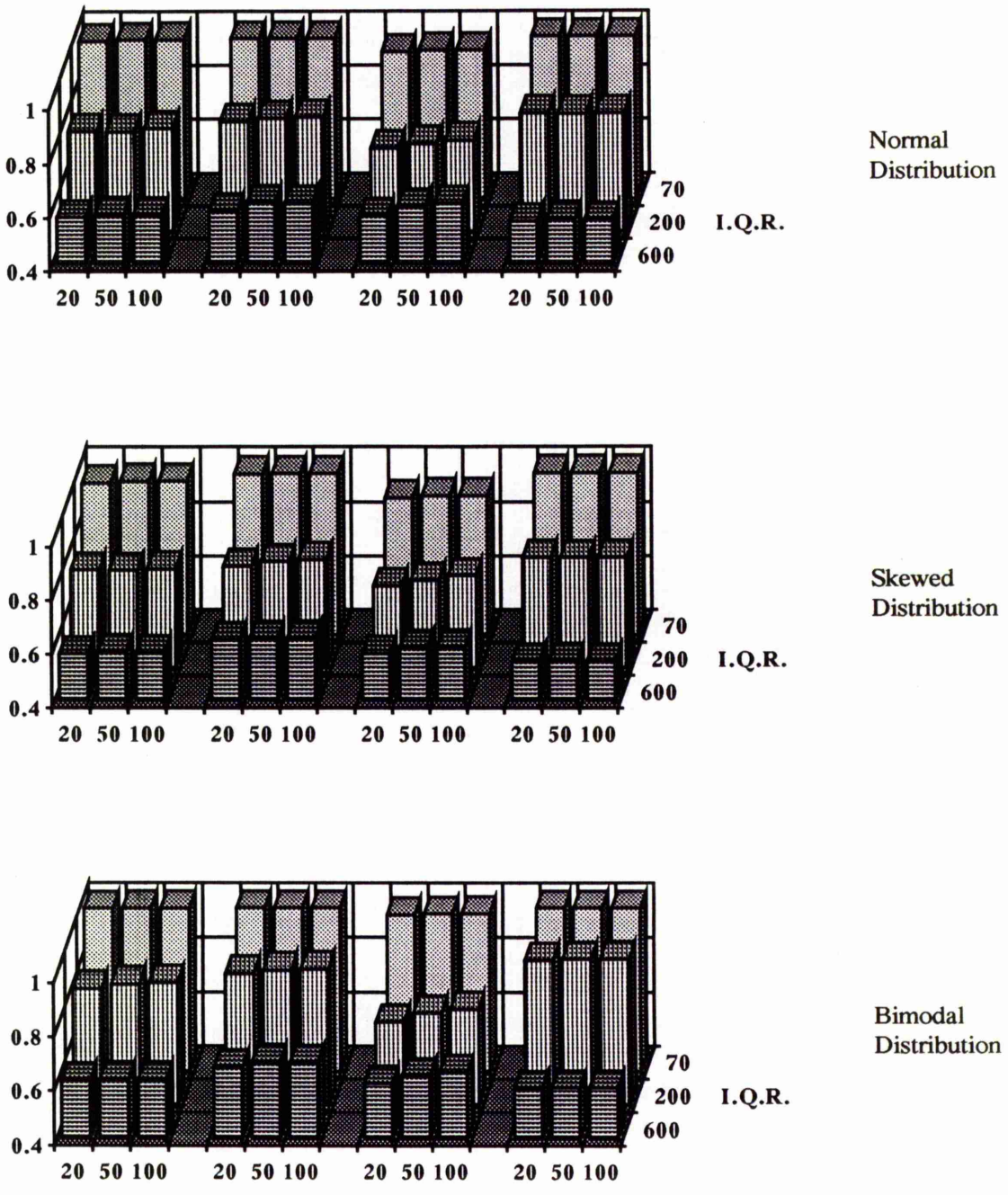

Figure 4.18 : Bar charts for the ***median*** of the ***Population Coverage*** of method ***B*** from a 1000 simulations.

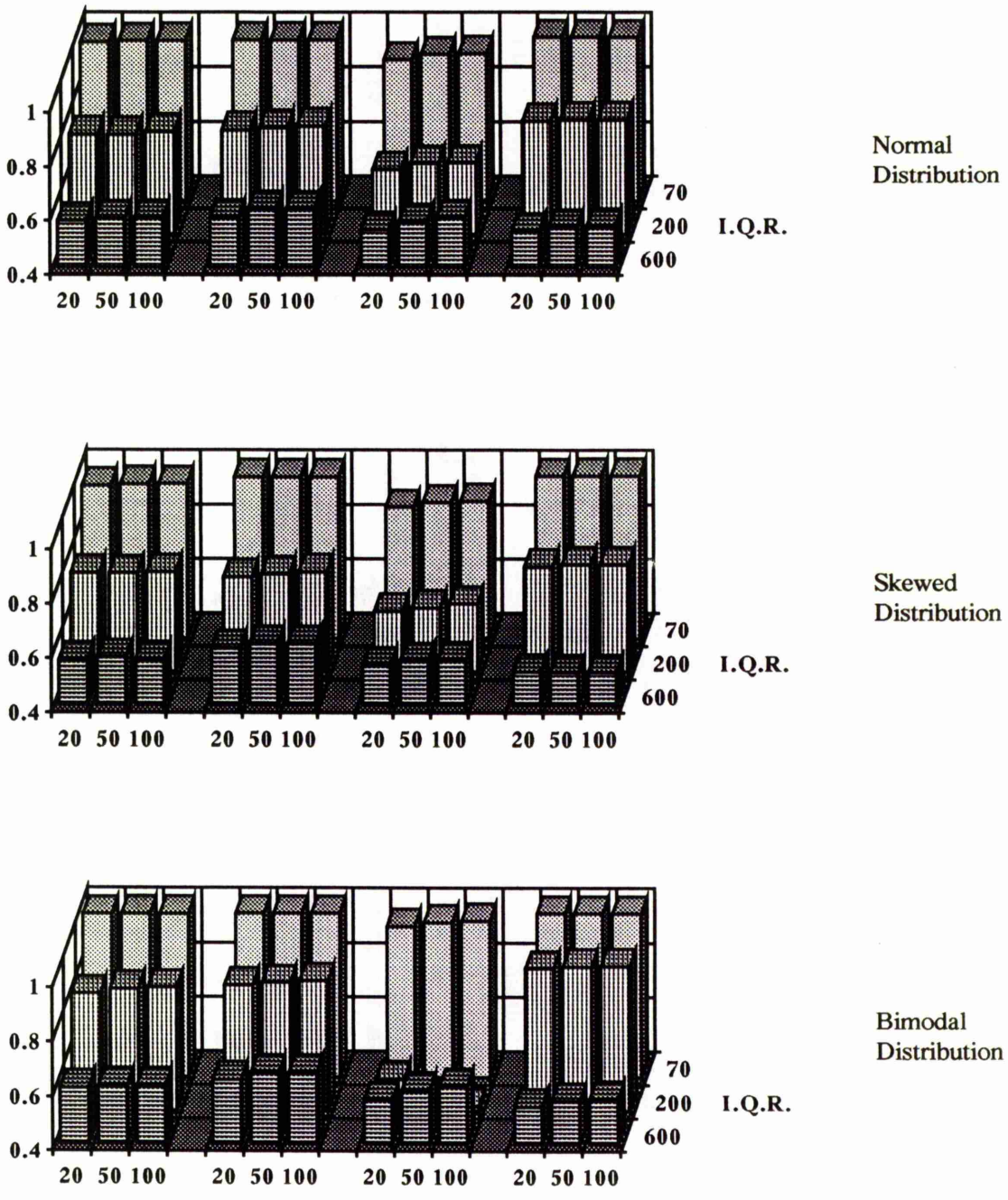

Figure 4.19 : Bar charts for the ***median*** of the ***Population Coverage*** of method ***C*** from a 1000 simulations.

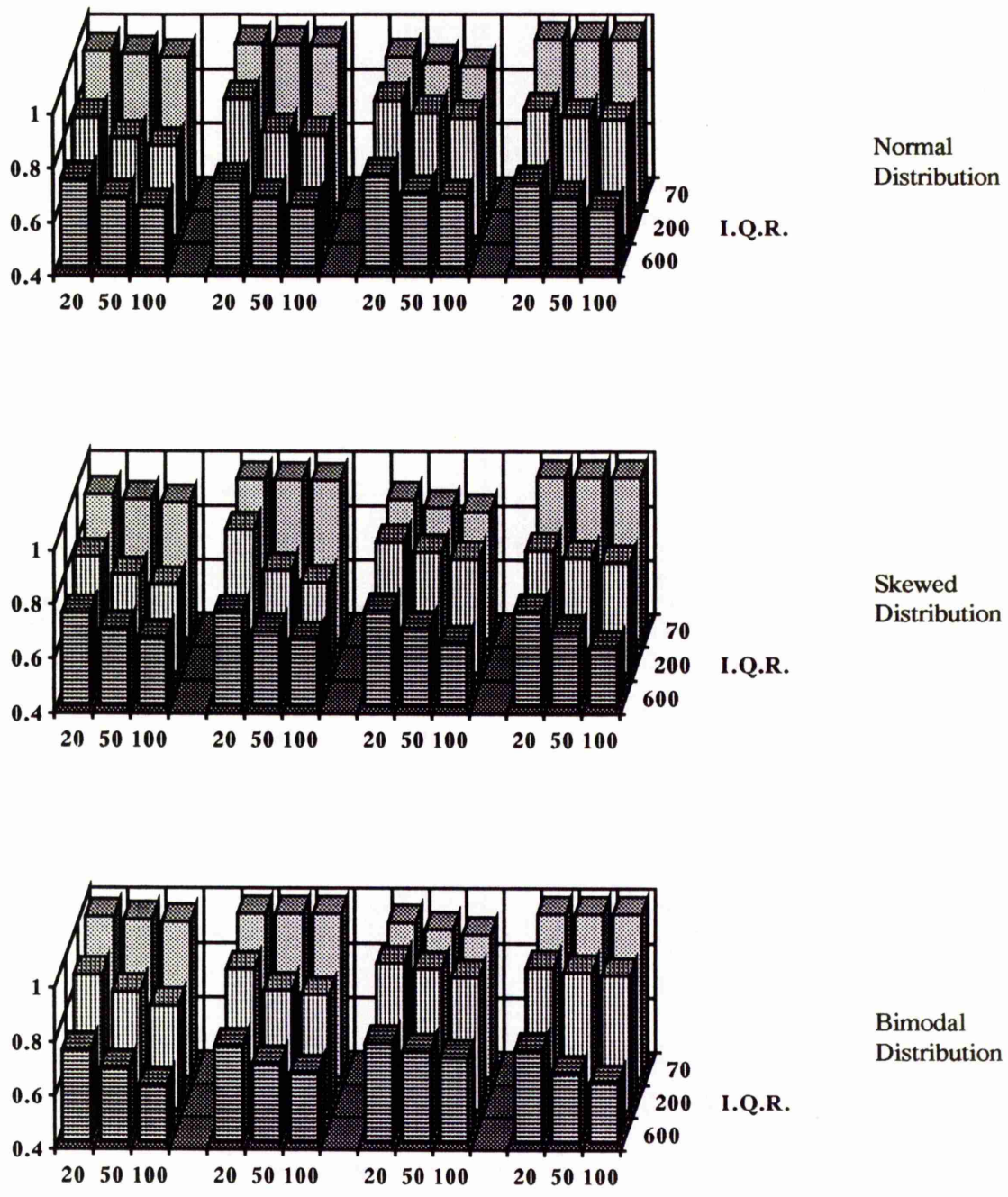

Figure 4.20 : Bar charts for the ***median*** of the ***Population Coverage*** of method ***D*** from a 1000 simulations.

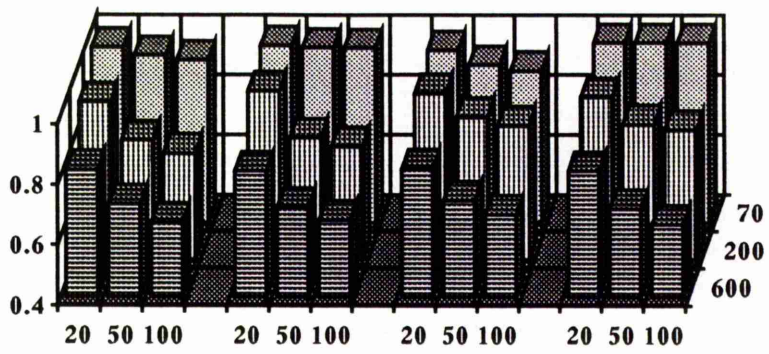

Normal Distribution

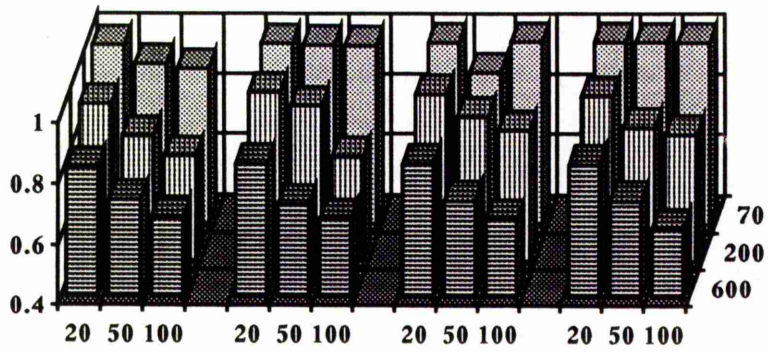

Skewed Distribution

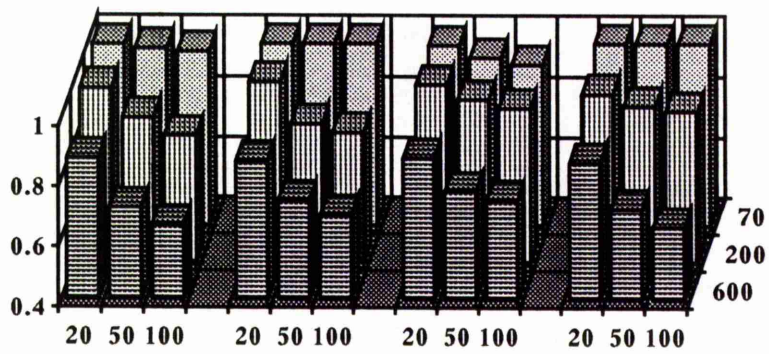

Bimodal Distribution

Years 700 AD 500 BC 2850 BC 3200 BC

Figure 4.21 : Bar charts for the ***median*** of the ***Population Coverage*** of method ***E*** from a 1000 simulations.

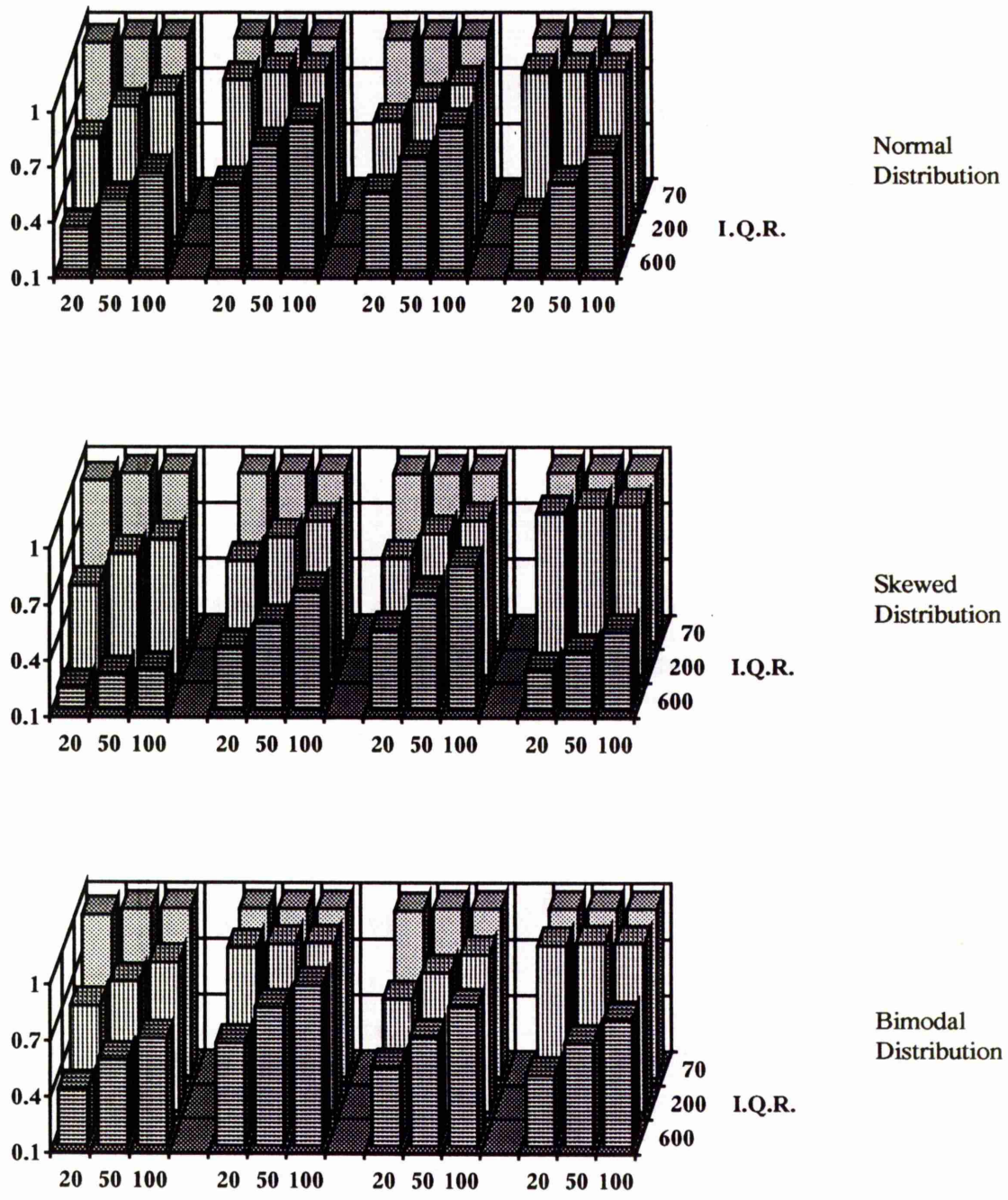

Figure 4.22 : Bar charts for the estimated ***Confidence*** for method ***A*** from a 1000 simulations.

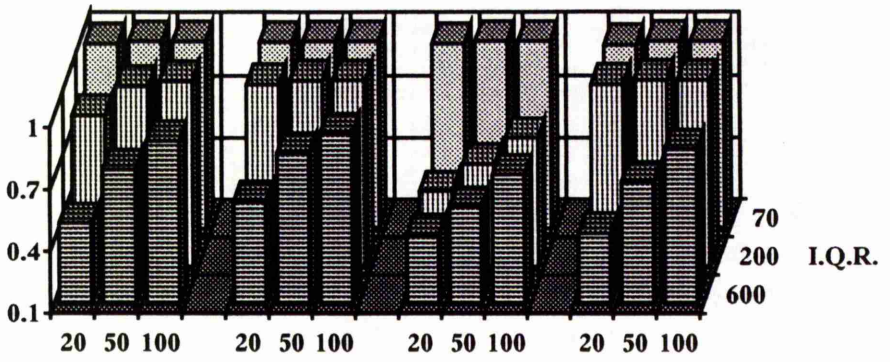

Normal Distribution

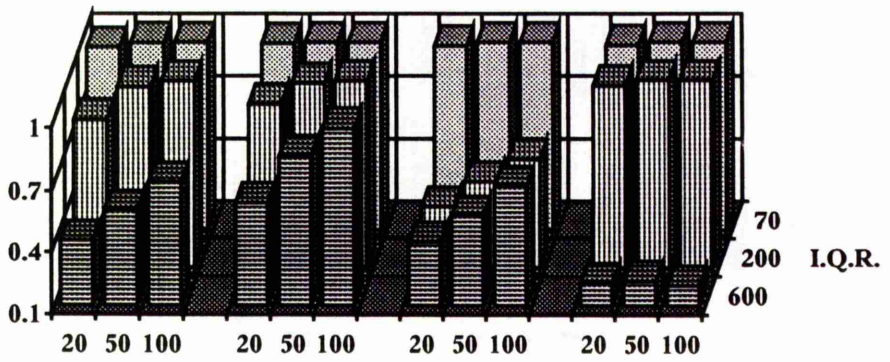

Skewed Distribution

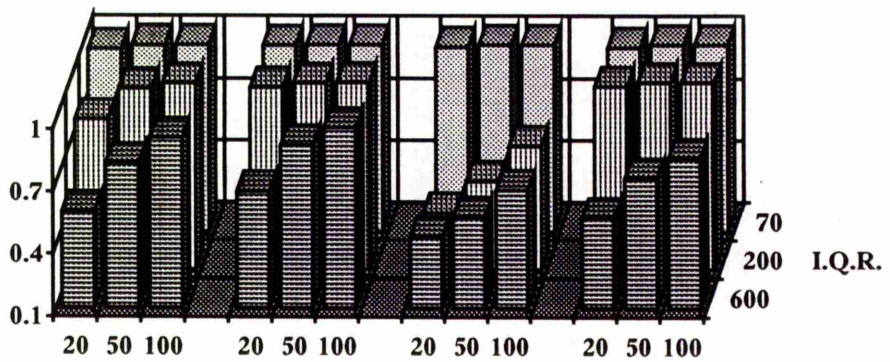

Bimodal Distribution

Years 700 AD 500 BC 2850 BC 3200 BC

Figure 4.23 : Bar charts for the estimated ***Confidence*** for method ***B*** from a 1000 simulations.

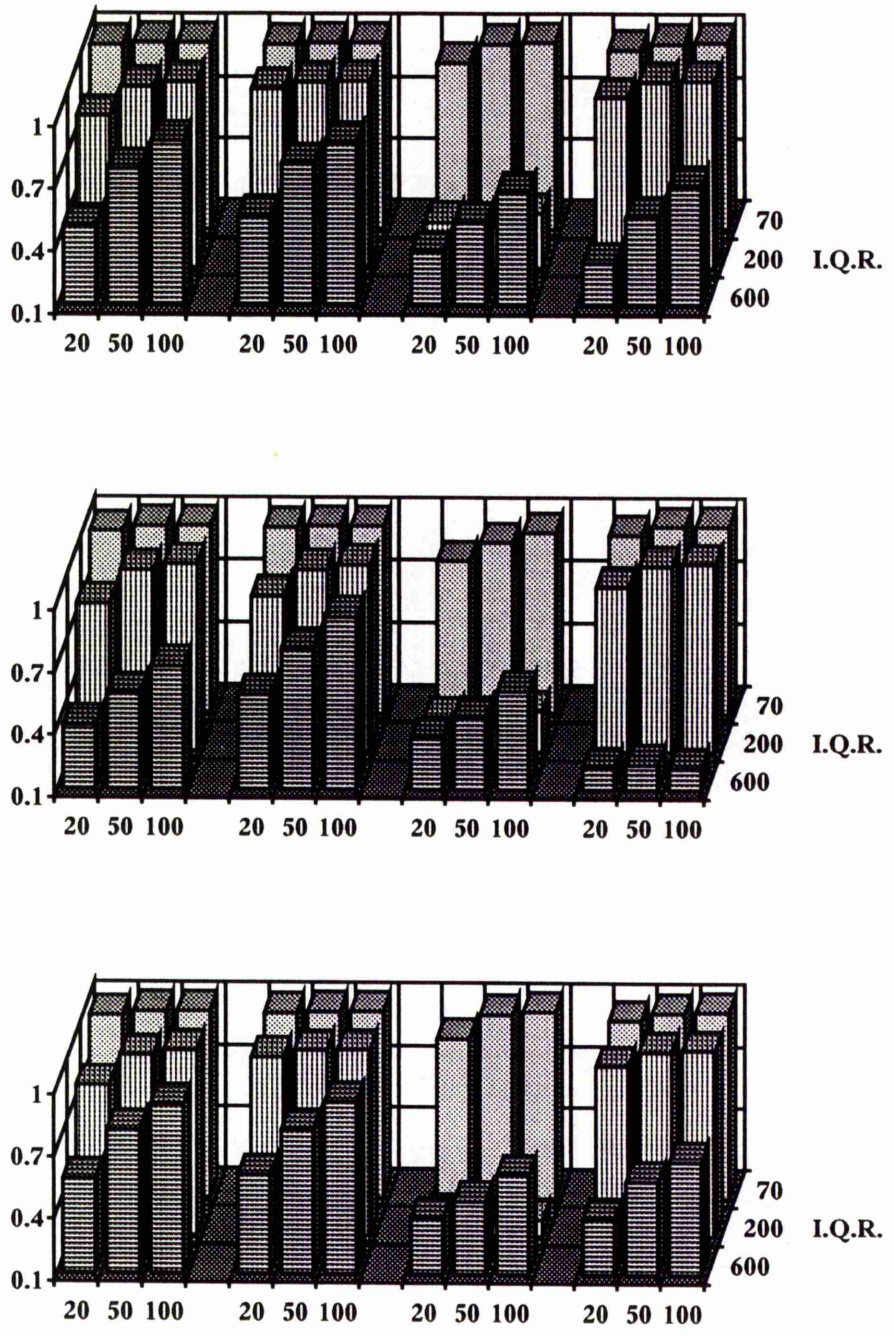

Figure 4.24 : Bar charts for the estimated ***Confidence*** for method ***C*** from a 1000 simulations.

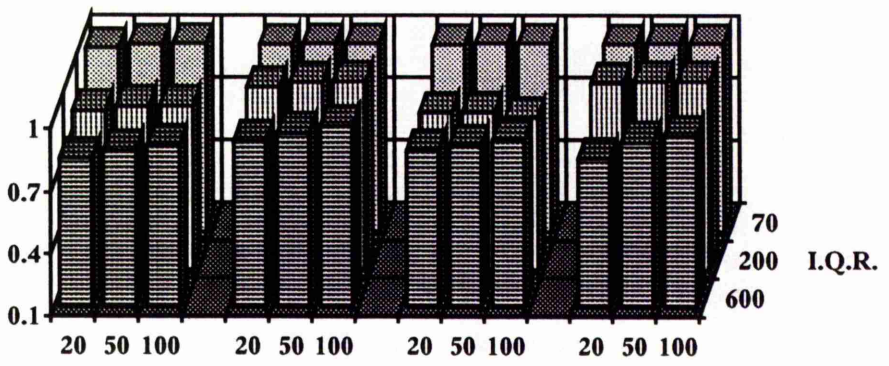

Normal Distribution

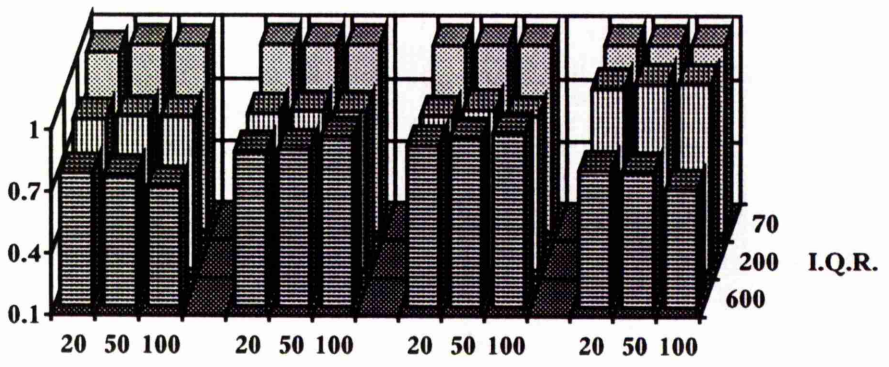

Skewed Distribution

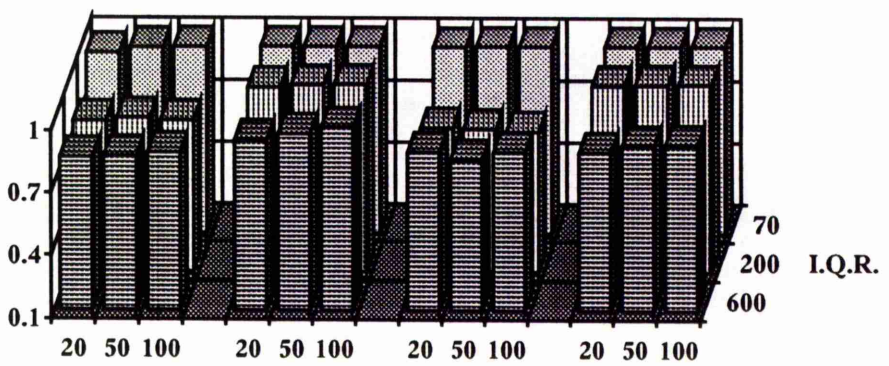

Bimodal Distribution

Years 700 AD 500 BC 2850 BC 3200 BC

Figure 4.25 : Bar charts for the estimated ***Confidence*** for method ***D*** from a 1000 simulations.

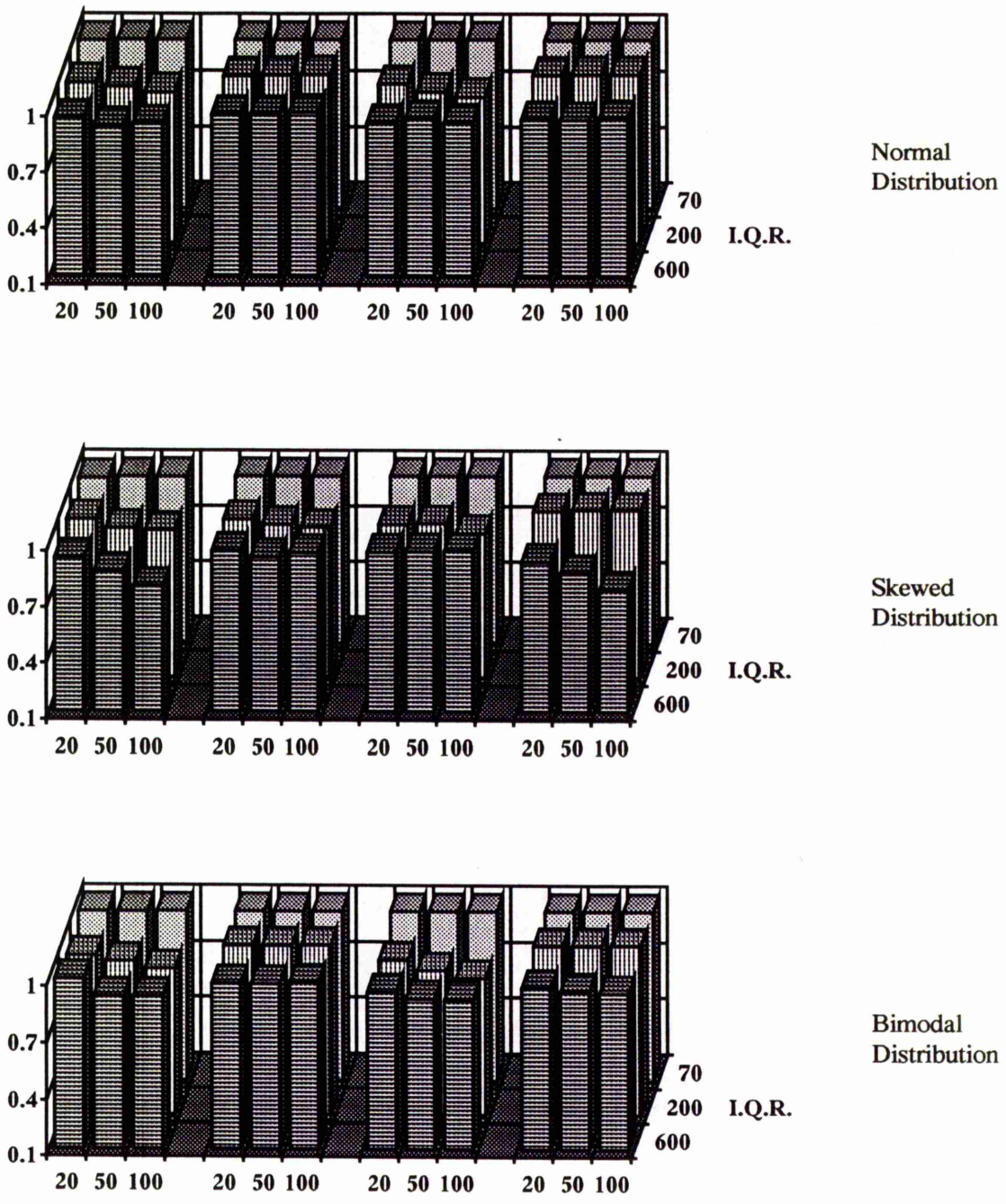

Figure 4.26 : Bar charts for the estimated ***Confidence*** for method ***E*** from a 1000 simulations.

4.5 Discussion of the Simulation Results

In this section the results of the simulation presented in section 4.4 are discussed and the performance of the five methods compared according to the chosen criteria. In summarising the results the median of the 1000 simulations for each criterion separately is used as the major factor. This will certainly give an indication of the long-run average performance of the criterion for a given method but some consideration should still be made of the underlying distribution of the criterion - perhaps through the quartiles.

Each of the four criteria are considered in turn by first of all looking at the performance separately for each choice of Inter-Quartile range (*i.e.* 70, 200 and 600 years) and then pool all conclusions on that criterion.

4.5.1 The Coverage

The median coverage over all simulation combinations are represented diagrammatically in figures 4.27 - 4.29 and the details in tables 4.1 - 4.5.

- ***When the I.Q.R.=70***

Over all four parts of the calibration curve and for all three types of distribution, the five methods all produce complete Coverage (i.e. Coverage=1) for all the sample sizes (see figure 4.27).

- ***When the I.Q.R.=200***

As can be seen in figure 4.28 for the three distributions, most of the methods have in general complete coverage except method B for n=20 when the median drops about and method C at 2850 BC when the performance can be very poor. The coverage of method B is greater than the coverage in method C. This happens because the shape of the curve at this point is steep on the right side and very wiggly on the left side which means the steep part allows the upper quartile of the calibrated dates to fall inside the true I.Q.R. while the

wiggles on the left can affect the quartiles estimate by shifting the lower quartile of the calibrated dates outside the true I.Q.R. in method B and inside the true I.Q.R. in method C. Method B has improved when the sample size increased while method C did not.

- ***When the I.Q.R.=600***

It can be seen from figure 4.29 that at any point and for all sample sizes, both methods D and E have produced a complete coverage. For the three methods A, B and C the complete coverage has been produced only at 500 BC. The reason behind this is that the large standard errors for the calibrated dates resulting from calibration on a flat part of the curve make the quartile interval produced wide enough to provide a high coverage for methods B and C, while the wiggles, in this part as well as in part centred at 2850 BC, play a role in producing a conservative quartile interval estimate and hence a high coverage for method A.

Over the other parts of the calibration curve, while the coverage of method A at 2850 BC is much better than the coverage of methods B and C, the coverage of methods B and C is higher than the coverage of method A at 700 AD.

Due to the wiggles at the true quartiles for the 3200 BC centred distribution, the coverage of method C is lower than the coverage in A and B which appear similar.

In the data generated from the Normal and Bimodal distributions the values of the coverage for these methods are higher than values of the coverage for these methods in the data generated from the Skewed distribution. All coverage increased with sample size.

4.5.1.1 Overall View

All methods produced coverages which are more than adequate (equal or close to 1.0) except for method C at certain combinations of location and I.Q.R.. Method A seems to have a high coverage in the parts of the calibration curve where wiggles are found and not in the parts where the curve is linear. On the other hand, Methods B and C work better in the linear parts than the wiggly parts of the calibration curve. There is no problem with methods D and E both of which have complete coverage in all cases. All five methods work properly in the flat parts of the calibration curve.

Although the coverage values are improved when sample size increased for all methods, methods E and D are the best in terms of coverage.

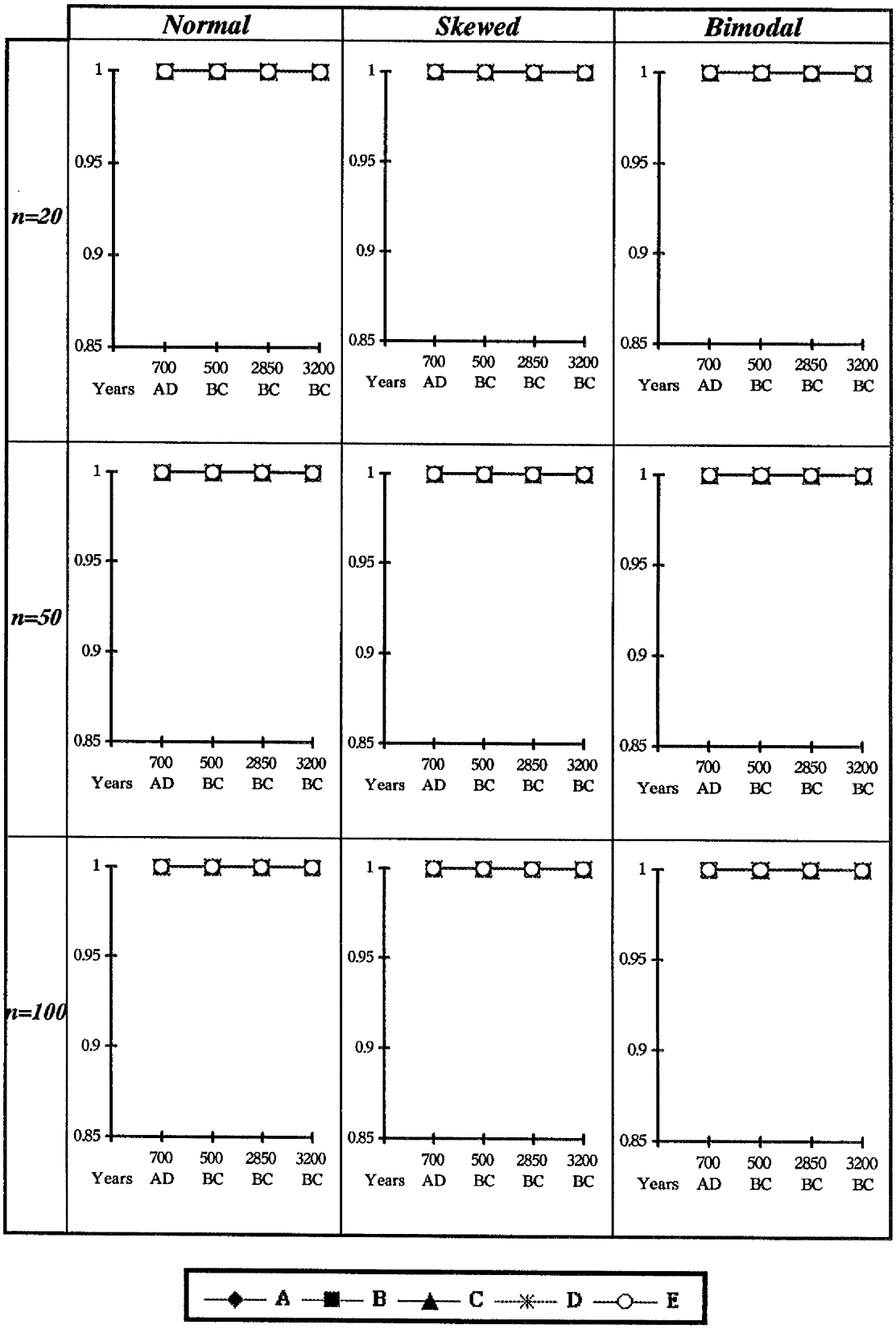

Figure 4.27 : Plots of the median values for the ***Coverage*** when ***I.Q.R.=70*** to compare the performance of the floruit interval estimation methods over the different parts of the calibration curve.

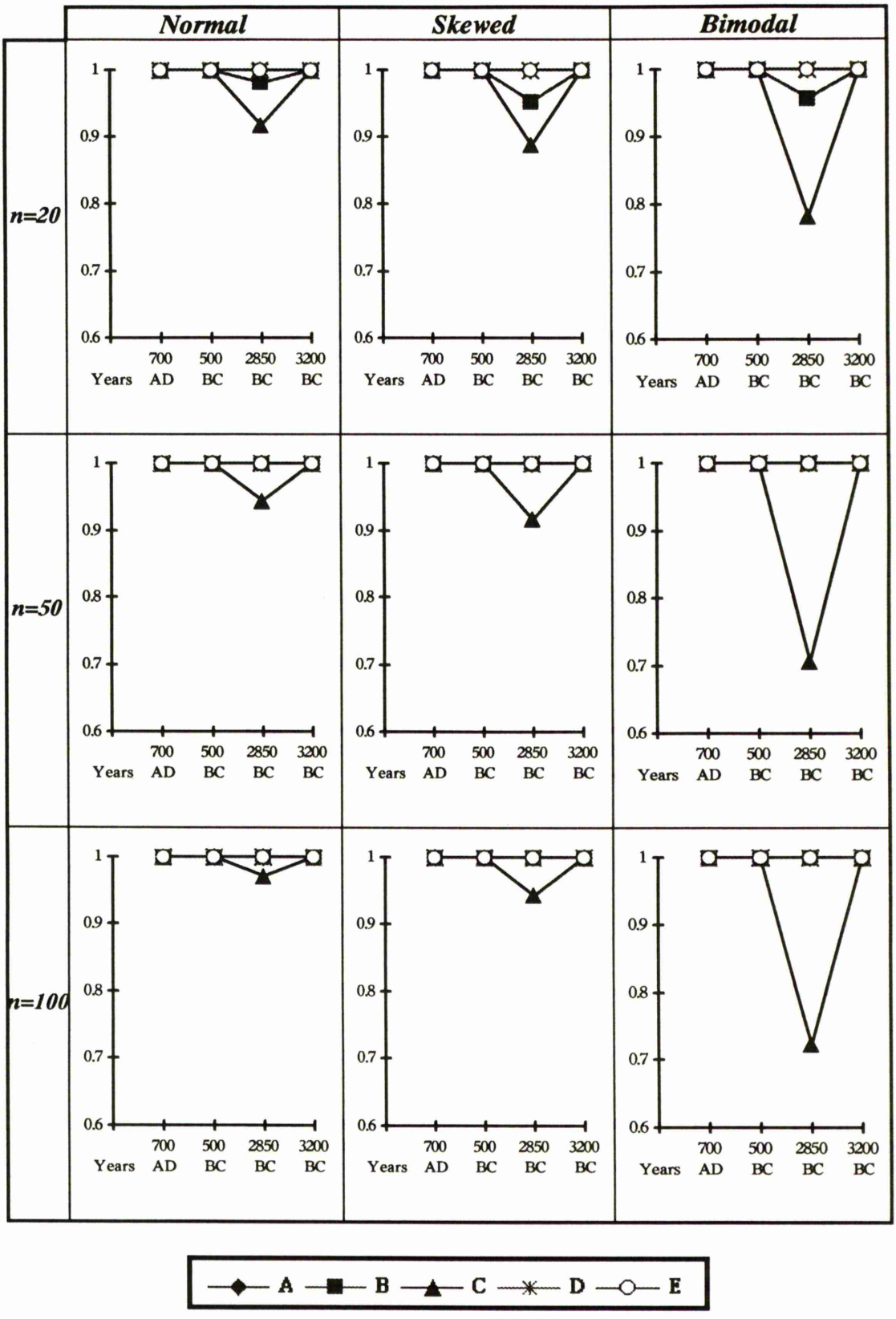

Figure 4.28 : Plots of the median values for the ***Coverage*** when ***I.Q.R.=200*** to compare the performance of the floruit interval estimation methods over the different parts of the calibration curve.

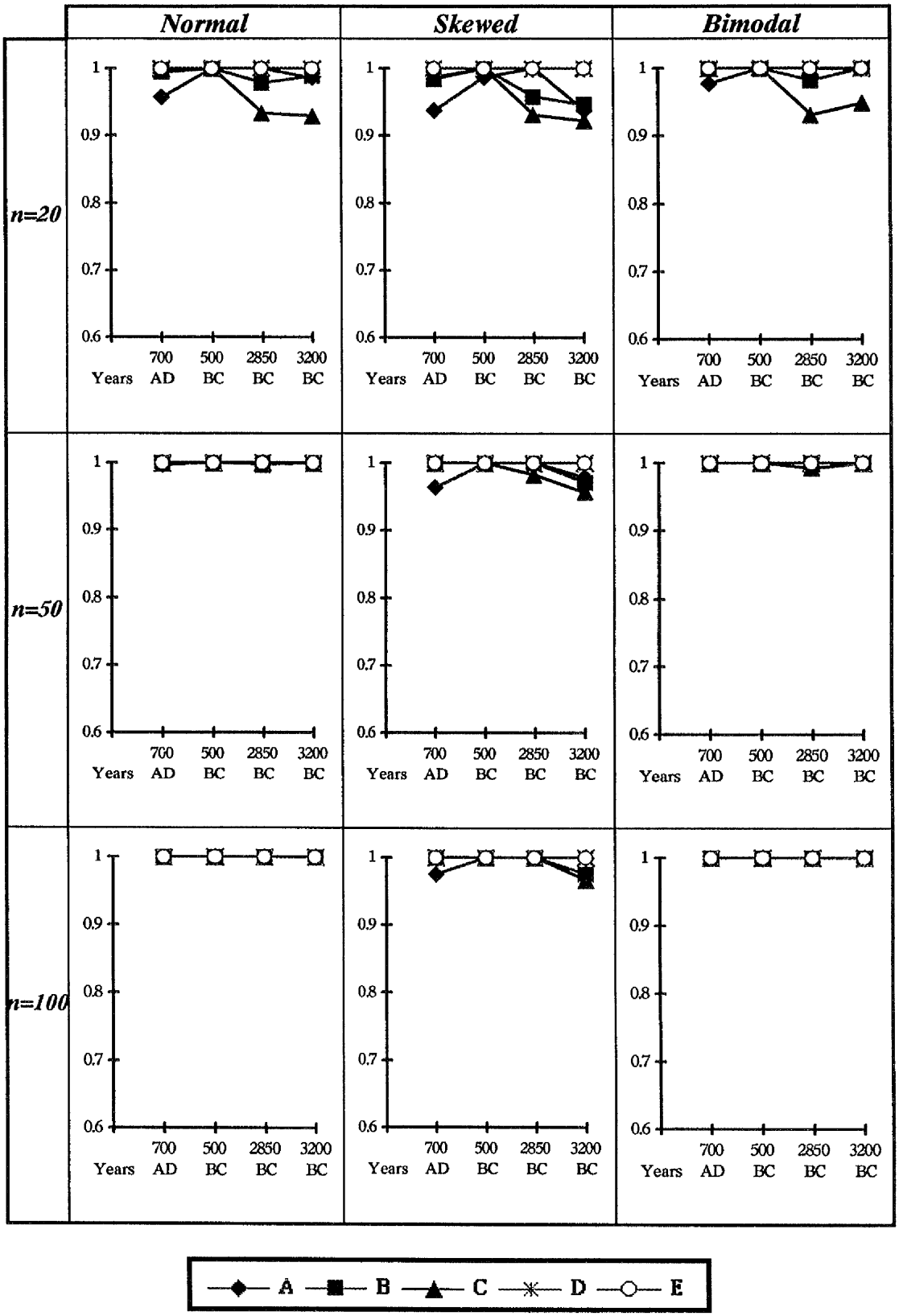

Figure 4.29 : Plots of the median values for the ***Coverage*** when ***I.Q.R.=600*** to compare the performance of the floruit interval estimation methods over the different parts of the calibration curve.

4.5.2 The Wastage

Diagrams of the median wastage over all simulation combinations are shown in figures 4.30 - 4.32 and the details given in tables 4.6 - 4.10.

- ***When the I.Q.R.=70***

For all five methods the wastage is rather unstable and very high - over 0.69 - (figure 4.30). While the wastage of methods D and E decrease with sample size, there is a slight increase (less than 0.01) with sample size in methods A, B and C (except for method A at 2850 BC because of the bump on the left side of the true I.Q.R.).

The lowest wastage for all the five methods occur at 700 AD where the curve seems to be linear. For the most part the highest wastages for the five methods occur at 500 BC where the curve is flat.

For n=20 method E performs poorest (*i.e.* has highest wastage) with no clear distinction universally among the other four methods.

At the large sample sizes (*i.e.* n=50 and 100) method B looks to be the worst (*i.e.* highest wastage) whereas methods D and E are best with method D very slightly the better of these two.

- ***When the I.Q.R.=200***

The plots in figure 4.31 indicate that the lowest wastage (0.126) and the highest wastage (0.682) are for methods C and E respectively, both occurring at 2850 BC where the curve is steep and wiggly.

There is no obvious relationship between the sample size and the wastage for methods A, B and C. There is a little change in the wastage (about 0.03) across sample sizes for all three methods.

Method E is again the poorest for n=20 and no clear best method is apparent among A, B and C. For n=50 and 100 no clear pattern emerges although method C performs well in terms of wastage at 2850 BC.

If the part of the calibration curve contains some wiggles then method C tends to have less wastage than methods A and B. The amount of difference depends on how wiggly the curve is. If there are no wiggles on the curve then method A produces less wastage than both methods B and C.

- ***When the I.Q.R.=600***

From figure 4.32 one can see that the wastage in methods D and E is high compared to that in methods A, B and C. Both D and E have the same pattern with higher wastage in E. For all five methods wastage has decreased with increasing sample size and in particular for methods D and E.

Due to wiggles on the curve method C has the lowest wastage at all the points except at 500 BC where method A has the lowest. This is because the curve tends to be linear at the edges of the *I.Q.R.* at this point.

The largest wastage for method A occurred when the curve was wiggly in the periods 2850 BC and 3200 BC.

4.5.2.1 Overall View

Except for methods D and E the wastage is rather unstable. In the wiggly parts of the calibration curve method A has its largest wastage while methods B and C have their lowest wastage. In general there is less wastage in method C than in B with the amount of difference depending on how wiggly the curve is at that part. On the other hand, methods B and C will have the same amount of wastage if there are no wiggles on the curve while method A will have its lowest wastage there.

For small sample size and wide I.Q.R. the wastage is too high for methods D and E relative to A, B and C. The wastage for all methods gets smaller as I.Q.R. increases. The wastage for method D and E decreases with increasing sample size. Method C looks to have the lowest wastage in general (certainly in the Bimodal case).

Across the board, method C appears to be the best in terms of wastage.

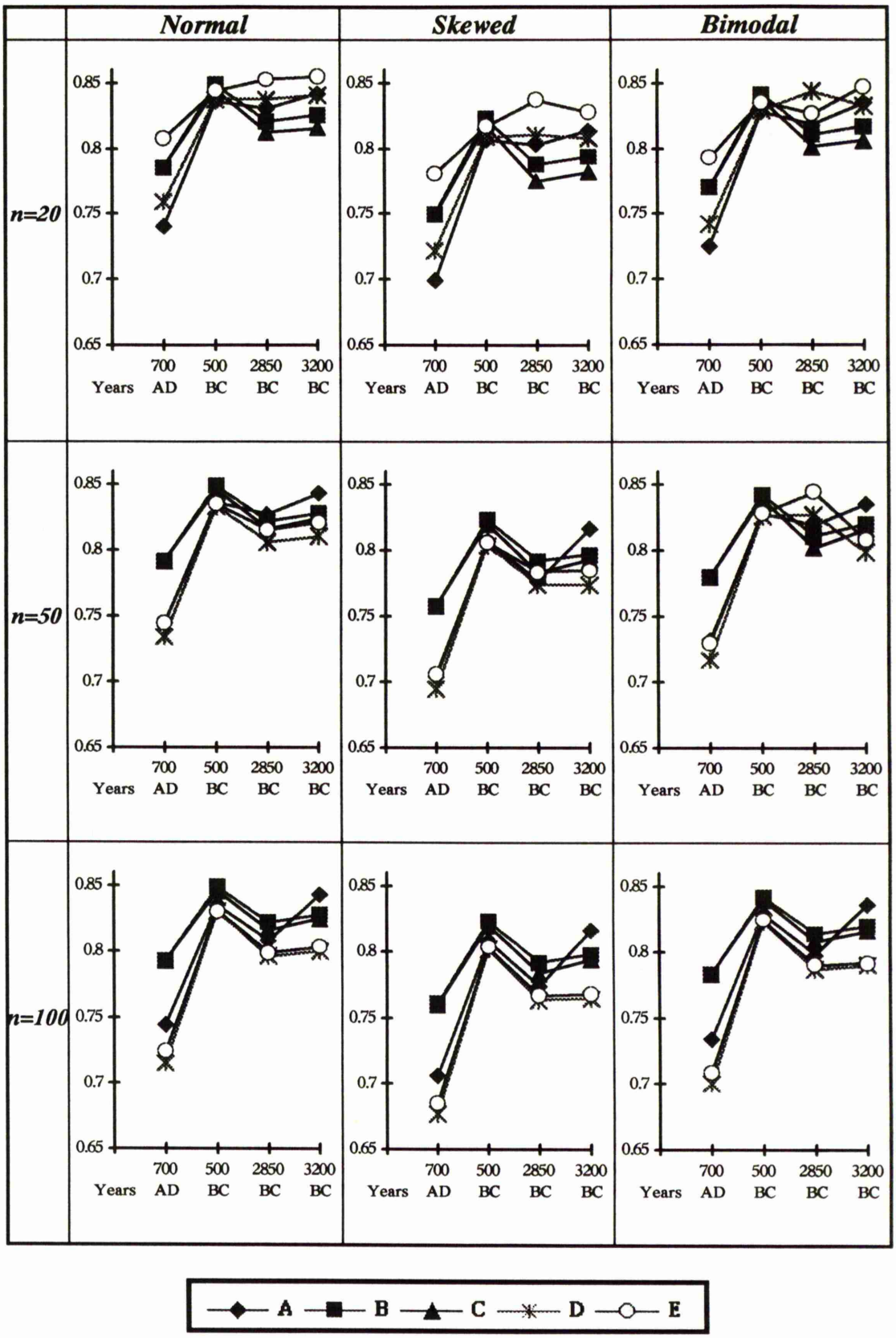

Figure 4.30: Plots of the median values for the ***Wastage*** when ***I.Q.R.=70*** to compare the performance of the floruit interval estimation methods over the different parts of the calibration curve.

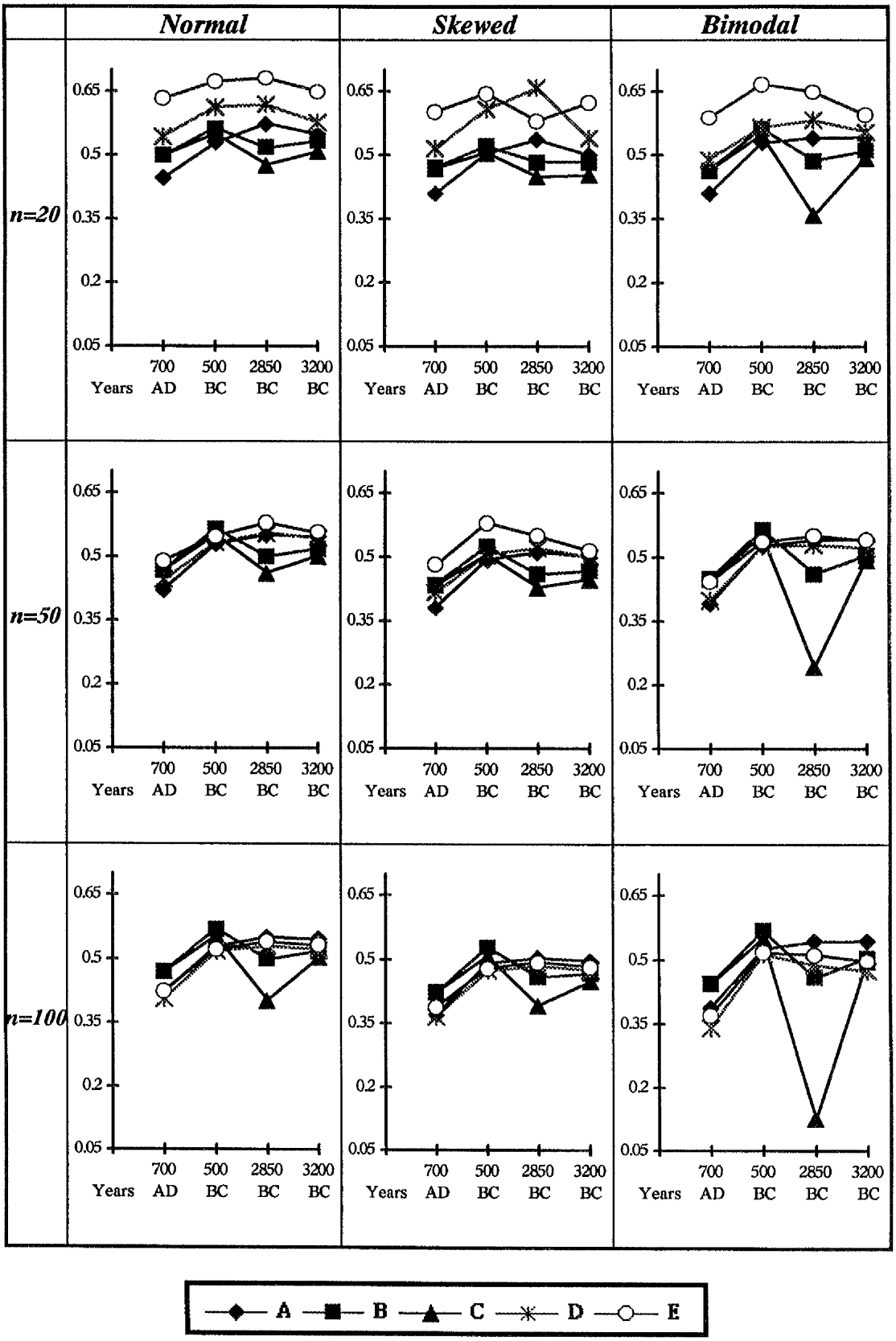

Figure 4.31 : Plots of the median values for the ***Wastage*** when ***I.Q.R.=200*** to compare the performance of the floruit interval estimation methods over the different parts of the calibration curve.

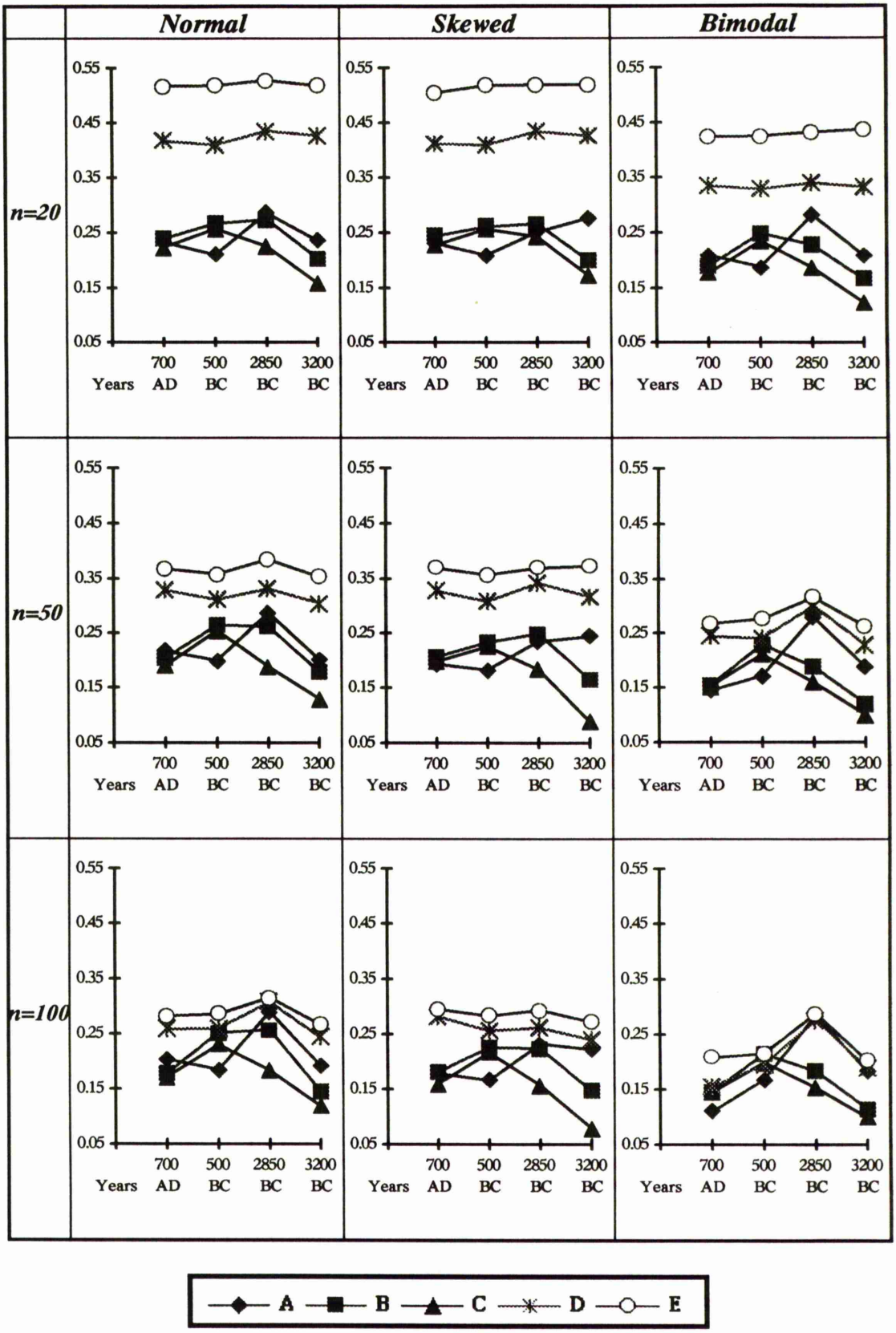

Figure 4.32 : Plots of the median values for the ***Wastage*** when ***I.Q.R.=600*** to compare the performance of the floruit interval estimation methods over the different parts of the calibration curve.

4.5.3 The Population Coverage

Plots of the median values for the population coverage over all simulation combinations are shown in figures 4.33 - 4.35 while the details are in tables 4.11 - 4.15.

- ***When the I.Q.R.=70***

As a result of complete coverage and high wastage for all the five methods at this range, the population coverage is very high representing at least 87% of the population (figure 4.33). The lowest population coverage occurred at steep parts of the calibration curve such as at years 2850 BC (where the curve is very steep inside this range). The flat parts of the calibration curve produce virtually complete population coverage for example at 3200 BC.

The population coverage in all methods does not behave consistently with sample size. While there is a slightly increase (less than 0.02) in methods A, B and C, there is a slightly decrease (in most cases less than 0.03) in methods D and E. Generally there is no clear distinction among the five methods since they all produce high and unstable population coverage.

- ***When the I.Q.R.=200***

There is a considerable reduction in population coverage at this range for all the five methods compared to that at the I.Q.R. of 70 as can be seen in figure 4.34. At the parts where the curve is very wiggly, methods A, D and E tend to have their highest population coverage, whereas methods B and C have their lowest population coverage. The flat parts of the curve cause high population coverage for all methods. The population coverages for methods B and C are very close at the times where the calibration curve is linear or steep.

While population coverage decreases with sample size for methods D and E, there is no obvious relationship between sample size and population coverage in methods A, B and C.

Except for method C the population coverage is higher in the Bimodal case than in the Normal and Skewed cases which seem to be close.

- ***When the I.Q.R.=600***

The plots in figure 4.35 indicate that, for small sample size (*i.e.* 20) population coverage seems too high for methods D and E relative to methods A, B and C.

It can be seen that methods A, B and C have very similar population coverage at 700 AD where the curve is linear, whereas differences occurred at 2850 BC where the curve is very wiggly. The population coverage for method A is greater than the population coverage for methods B and C at the parts where the curve is wiggly and less if there are no wiggles on that part of the curve.

The population coverage for methods D and E is still rather high (representing at least 60% of the population) with their lowest population coverages produced at the flat parts of the calibration curve. The highest population coverages occur at the wiggly parts of the calibration curve. Both methods have the same pattern with higher population coverage in E than in D.

4.5.3.1 Overall View

One would expect population coverage to tend to 0.5 as $n \to \infty$ since the target is to estimate the quartiles (*i.e.* middle 50%). Methods A, B and C do not exhibit this but increase with sample size. On the other hand, the population coverages for methods D and E tend to decrease with sample size but are still someway from 0.5 at $n=100$.

Methods D and E generally have larger population coverage than methods A, B and C.

In general, population coverage for all methods in all distributions is smaller for larger I.Q.R.. The Bimodal distribution seems to cause major problems at 2850 BC for I.Q.R.≥ 200. Method D performs best overall for smaller I.Q.R. (*i.e.* 70) and large sample size (*i.e.* 50 and 100), while methods A, B and C, with no clear distinction, are the best in terms of population coverages in the sense that their population coverages tend to converge to 0.5 with increasing sample size particularly for the large values of I.Q.R..

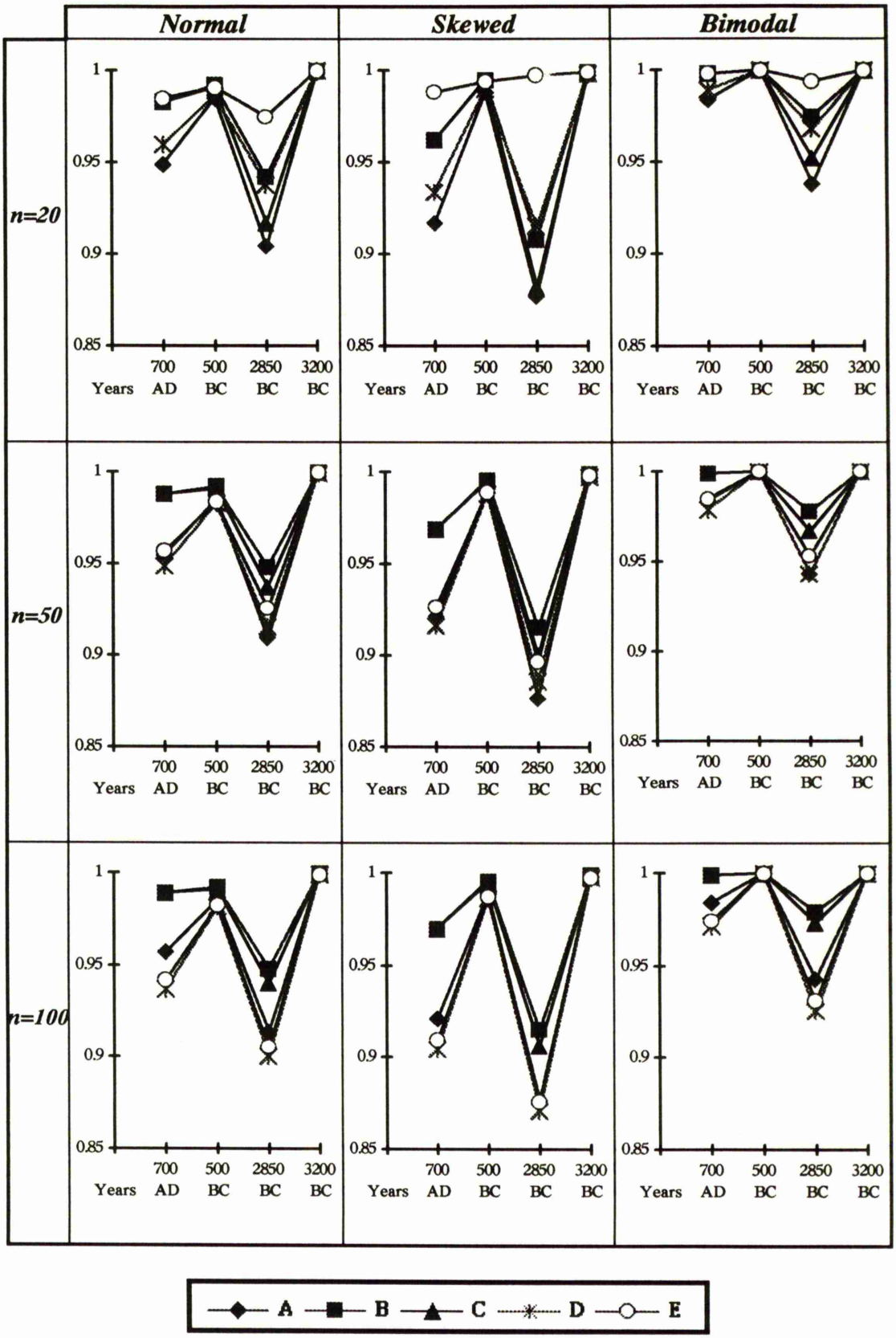

Figure 4.33 : Plots of the median values for the ***Population Coverage*** when ***I.Q.R.=70*** to compare the performance of the floruit interval estimation methods over the different parts of the calibration curve.

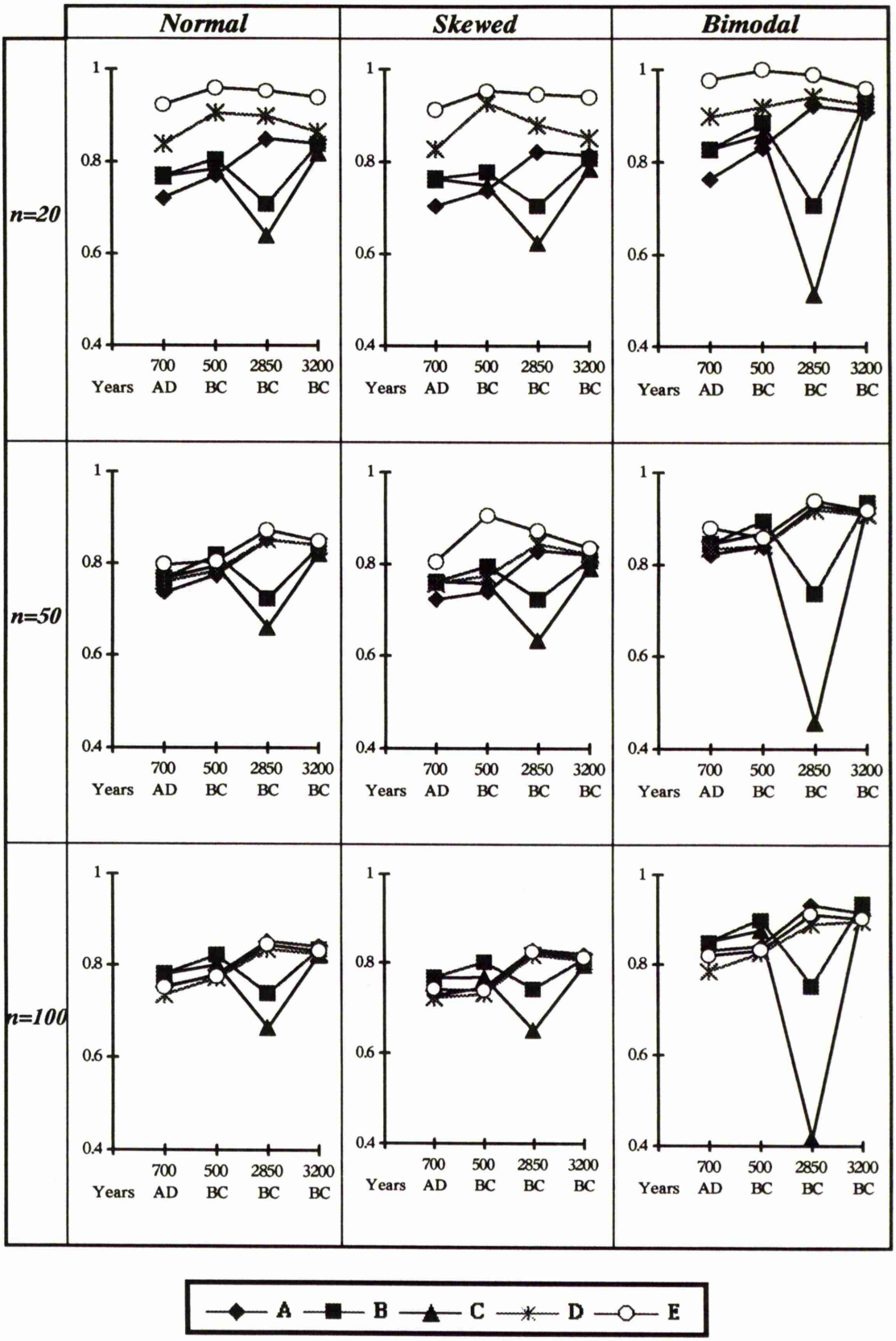

Figure 4.34 : Plots of the median values for the ***Population Coverage*** when ***I.Q.R.=200*** to compare the performance of the floruit interval estimation methods over the different parts of the calibration curve.

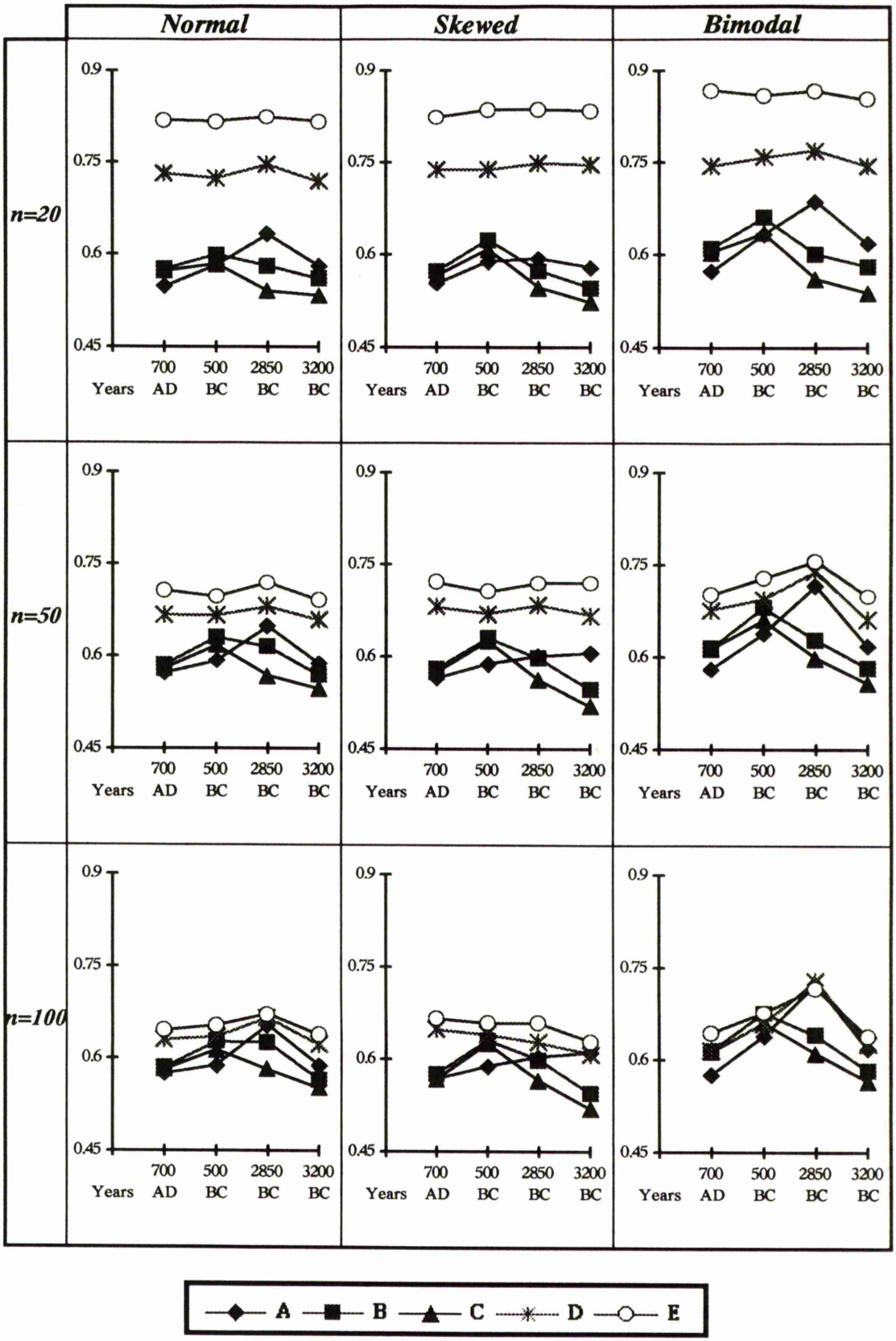

Figure 4.35 : Plots of the median values for the ***Population Coverage*** when ***I.Q.R.=600*** to compare the performance of the floruit interval estimation methods over the different parts of the calibration curve.

4.5.4 The Confidence

Figures 4.36 - 4.38 show the plots of the estimated confidence over all simulation combinations. Since the confidence is the fraction of times in the 1000 simulations performed when complete coverage occurred, there are similarities here with the results for coverage.

- ***When the I.Q.R.=70***

All methods do well and have a very high confidence (at least 95%) over the four parts of the calibration curve considered (see figure 4.36) except for method C which has the lowest confidence (not less than 83%) for all distributions at 2850 BC where the curve is very wiggly. All five methods have their highest confidence at 500 BC where the curve is flat, whereas the lowest confidence (except for method C) at 700 AD where the curve is linear.

All methods reach 100% confidence when the sample size was increased to n=100. This is clearly too conservative.

- ***When the I.Q.R.=200***

As shown in figure 4.37 for all methods and in all distributions the confidence is lower compared to that for the I.Q.R. of 70. The highest confidence occurs at the flat parts of the calibration curve such as 500 BC and 3200 BC, while the lowest is at the wiggly parts such as 2850 BC.

Except at 3200 BC where the confidence increases with sample size to 100% for all methods and distributions, there are some cases where methods D and E show little change in confidence with sample size. These occurred mostly at 700 AD and 2850 BC where the curve is linear or steep and wiggly.

In most cases the confidence achieved in cases of Skewed distributions is less than that from Normal or Bimodal distributions.

- ***When the I.Q.R.=600***

It can be seen from figure 4.38 that all the five methods have less confidence here than for an I.Q.R. of 200 except method C at 2850 BC. The apparent explanation for this is that the curve shape for the I.Q.R. of 200 is very wiggly which produces smaller coverage and hence lower confidence. However at an I.Q.R. of 600 the curve shape has less wiggles at the edges than at the centre which produces higher coverage and hence larger confidence .

For small sample sizes the confidence based on methods D and E is very high relative to that for methods A, B and C. The confidence for method A seems to be very unstable.

In general the confidence for all methods and all distributions improved with sample size except for some situations for methods D and E.

4.5.4.1 Overall View

In most cases the confidence for all methods gets lower with increasing I.Q.R. and higher as sample size increases. Data from Skewed distributions produce confidences lower than those from Normal or Bimodal distributions which appear roughly similar.

All five methods have their highest confidence at the flat parts of the calibration curve. Methods B and C have their lowest confidence on the wiggly parts of the curve, whereas method A has its lowest confidence on the linear parts of the curve. There tend to be poor performance for methods A, B and C at small/moderate sample sizes and high I.Q.R..

As with coverage, methods D and E have the highest confidence. Method E seems to perform best overall in the sense that confidence is high and generally close to 0.95.

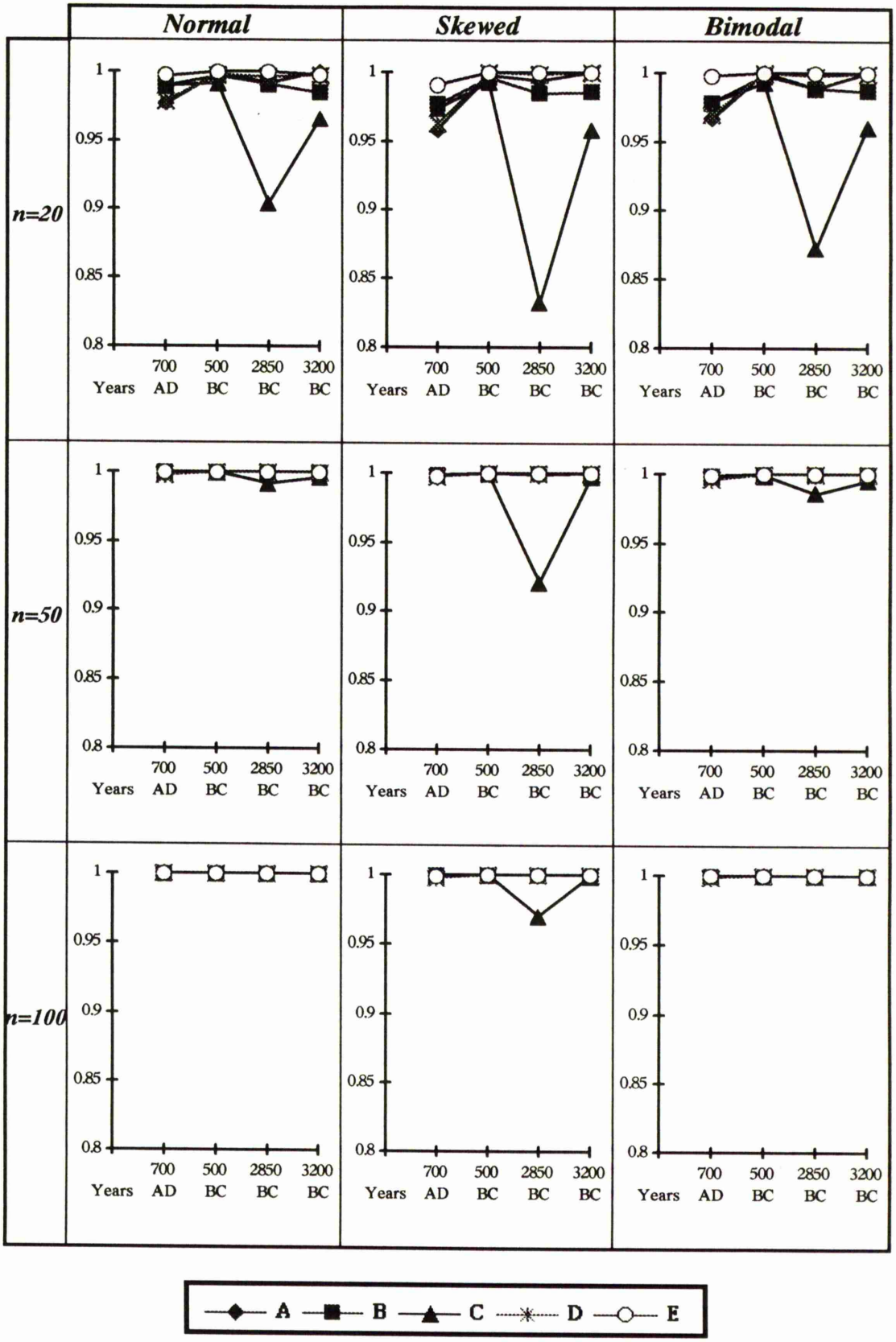

Figure 4.36 : Plots of the estimated values for the ***Confidence*** when ***I.Q.R.=70*** to compare the performance of the floruit interval estimation methods over the different parts of the calibration curve.

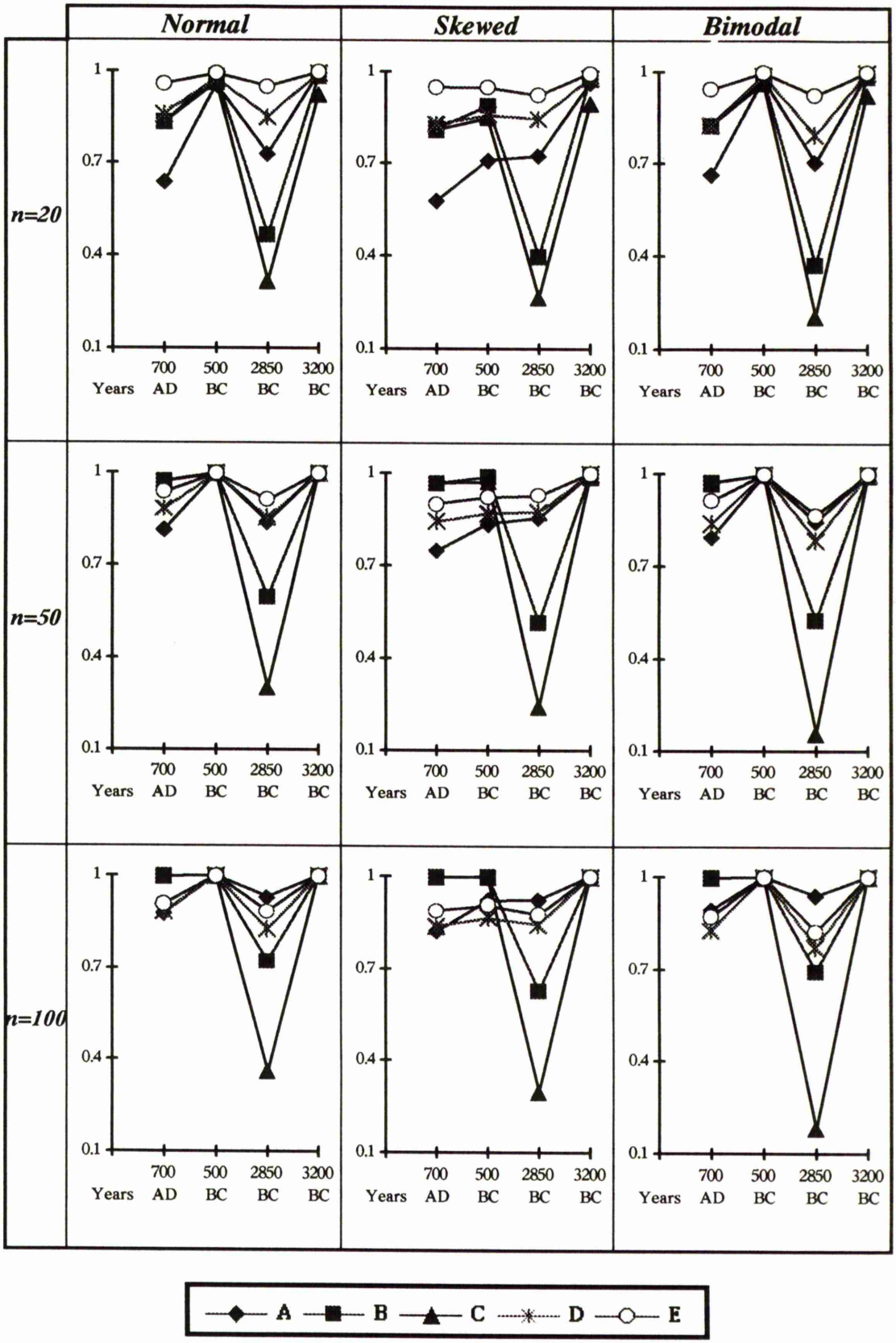

Figure 4.37 : Plots of the estimated values for the ***Confidence*** when ***I.Q.R.=200*** to compare the performance of the floruit interval estimation methods over the different parts of the calibration curve.

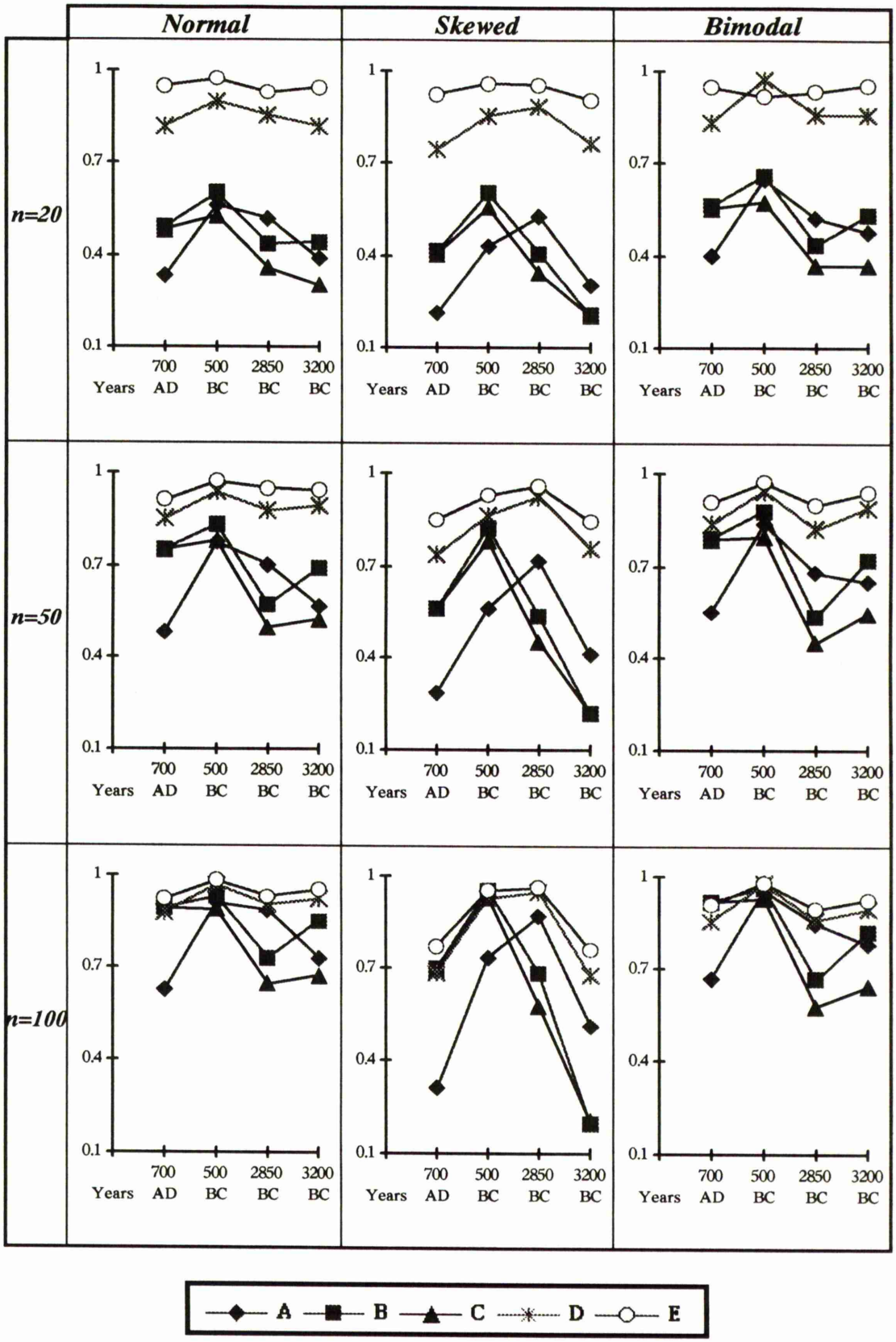

Figure 4.38 : Plots of the estimated values for the ***Confidence*** when ***I.Q.R.=600*** to compare the performance of the floruit interval estimation methods over the different parts of the calibration curve.

4.6 Comparison of the Five Methods

Based on these four criteria some methods work better than others on different parts of the calibration curve. The simplest way to compare and judge the methods is to pool together the results discussed in the previous four sections and point out the advantages and disadvantages for the five floruit interval estimation methods. As the calibration curve clearly plays such an enormous role in the whole procedure the five methods of floruit estimation are compared at each of the distinct parts of the curve introduced in the simulations.

4.6.1 Comparison of the Floruit Interval Estimation Methods at the Different Parts of the Calibration Curve

- ***At Year 700 AD***

The calibration curve at this point is relatively ***linear*** which means that every radiocarbon date calibrated on this part corresponds to a single historical date.

For an I.Q.R. of 70 years, the high population coverage produced for all the methods gives an impression that the floruit estimates are too wide. This results in high coverage and confidence but at the expense of high wastage. Although no one method was consistently superior, method D seemed to be the best in that it tended to have the smallest wastage. For an I.Q.R. of 200 years and small sample size, method A had the advantage that it has the lowest wastage but was the poorest in respect of confidence for all sample sizes. In general method A was poorer than B and C which were fairly similar. Compared to the other methods, D and E have the advantage that wastage and population coverage decrease with sample size. For an I.Q.R. of 600 years, method A was the worst regarding coverage and confidence but, together with

methods B and C, was better than methods D and E regarding wastage and population coverage.

- ***At Year 500 BC***

This is a ***flat*** part of the calibration curve which produces large standard errors on the calibrated dates.

For an I.Q.R. of 70 years, there were no significant differences among the five methods. They were all high in coverage, population coverage, confidence and unfortunately wastage. Methods B and C were slightly worse than the rest in the sense that they had the largest wastage, whereas method D was slightly betters than the rest in the sense that it had the smallest wastage.

For an I.Q.R. of 200 years and for Normal or Bimodal distributions all five methods produced similar results. However when Skewed distributions were used differences occurred. For small sample size methods A, B and C have the advantage on D and E in respect of wastage and population coverage, but this advantage was reversed as sample size increased. For Skewed distributions, method A was consistently poorer than methods B and C both of which perform well in terms of confidence.

For an I.Q.R. of 600 years, methods D and E are certainly better than A, B and C overall. While the differences in confidence came out in favour of methods D and E, the differences in wastage and population coverage were in favour of A, B and C. This seemed to be less as sample size increased to suggest method A was best overall.

- ***At Year 2850 BC***

The very ***wiggly*** parts of the calibration curve are represented by this time where multiple historical dates are likely to correspond to each radiocarbon date.

For an I.Q.R. of 70 years, even for method C for n=20 which has the smallest confidence, all methods have high confidence with too high wastage and population coverage. Methods D and E are better than the others in respect of minimising the wastage and population coverage with sample size.

For an I.Q.R. of 200 years, methods B and C have the poorest coverage and confidence. Method A was poorer than D and E for small sample sizes but better for large sample sizes in the sense that it had the highest confidence. Method C was better than the rest in respect of wastage and population coverage and worst with respect to coverage and confidence. Methods A, D and E all performed well in terms of coverage and confidence but at the expense of wastage and population coverage. When sample size increased, methods D and E have the advantage that they showed considerable decrease in wastage where there was little such for method A. Method A however showed substantially high confidence.

For an I.Q.R. of 600 years, methods D and E produced similar results with E slightly better and both methods clearly better than the rest. Method C was the poorest in confidence and the best in wastage and population coverage whatever the sample size or distribution. For all three underlying probability distributions, method A nearly had stable wastage for all sample size, while other methods improved with sample size.

- ***At Year 3200 BC***

The calibration curve at this point is ***flat*** and ***wiggly*** which is likely to produce multiple historical dates with large standard errors for a single radiocarbon date calibrated on this part.

Classification in the case of I.Q.R. of 70 years becomes difficult since all five methods produced very high population coverage (nearly 100%) which

result in high coverage, wastage and confidence. When sample size increased method D had superiority over the rest since it had the smallest wastage while still retaining high confidence.

All methods produced very high confidence for an I.Q.R. of 200 years, method E was the poorest in the sense that it had the largest wastage and population coverage. Although no one method seemed consistently superior, method C particularly in terms of wastage appeared best.

For an I.Q.R. of 600 years, there was considerable difference in methods A, B and C compared to methods D and E in terms of wastage, population coverage and confidence. Methods A, B and C were poor in coverage and confidence but were better in wastage and population coverage. Methods D and E were superior in respect of coverage and confidence. Results in confidence for A, B and C were even worse if the distribution is Skewed. Methods D and E had improved with sample size relative to wastage and population coverage but not to confidence. Methods A, B and C improved in confidence with increasing sample size.

4.6.2 Overall Comparison of the Floruit Interval Estimation Methods

Here an overall comparison of the five floruit interval estimation methods is made. First though remember that method A has the computational advantage that it is the simplest method as it only requires the radiocarbon dates with their associated errors to calculate the extended quartiles and then calibrate them conservatively to get the floruit estimate. The other methods require the calibration of all the radiocarbon dates and evaluation of all possible historical dates with their standard errors to evaluate the floruit estimate.

Of methods A, B and C, no one method seemed consistently superior to the others. Methods B and C generally produced similar results with B slightly

better than C with respect to coverage and confidence but poorer in respect of wastage and population coverage. While all the methods perform more than adequately at the flat parts of the calibration curve, methods B and C work better than method A in the linear parts but poorer in the wiggly parts. Method C is extremely poor at the very wiggly parts.

In most cases method D and E have the highest coverage and confidence whatever the sample size and the I.Q.R. but this occurs at the expense of wastage and population coverage. They have the advantages that in all cases wastage is decreasing with sample size and their population coverage tends to 0.5 as $n \rightarrow \infty$.

Overall method D seems to be the better of these two and thus would be the choice of optimal method although if only a paper, pencil and calibration curve are available method B is worth consideration as a first order approximation.

4.7 Summary

This chapter was entirely devoted to a simulation study investigating the performance of the floruit interval estimation methods. The study was prepared to investigate their performance over markedly different forms of the calibration curve. Data were simulated from three types of distribution functions (Normal, Skewed and Bimodal) for different combinations of sample sizes and Inter-Quartile Ranges.

Four statistical criteria (Coverage, Wastage, Population coverage and Confidence) were defined and used in the study to judge and compare the performance of the five methods. Simulation results were summarised and presented numerically and graphically.

For each of the four criteria the simulation results were discussed according to each choice of I.Q.R. separately and then pooled overall conclusions. Finally the performances of the five methods over the different parts of the calibration curve were compared. Overall it appeared that the best method was, not surprisingly perhaps, method D.

Chapter 5

Real Data Applications

5.1 Introduction

In the previous chapter a simulation study compared the performance of the five floruit estimation methods presented in chapter three. In this chapter, attention will focus on a wide selection of examples from archaeologically interesting cultures which will illustrate the applicability of the five methods to such groups of radiocarbon dates. This can be achieved by applying the five methods on each group of radiocarbon dates taken from an archaeological culture and providing point and interval estimates for its floruit on the historical timescale.

The primary concern in these applications is to compare the results from the five methods for floruit estimation and discuss whether there are many practically important differences among the methods. Unfortunately there is no guarantee that if a certain method provides the narrowest point and interval

estimates for the floruit of a certain archaeological culture, it will then always provide the narrowest estimate for the floruit of any archaeological culture. The reason behind this is mainly linked to the 'wiggly' nature of the non-homogeneous calibration curve at different time periods and the distribution of the radiocarbon dates from any given sample.

It is important to realise that there are various factors which may affect the floruit estimates of any archaeological culture. In the first instance, the *calibration procedure* which turns a radiocarbon date into a historical age represents an essential step in order to provide a floruit estimate for the archaeological culture from which the sample of radiocarbon dates were collected. This means that the *shape* of the calibration curve (whether linear, wiggly, steep or flat) will have some considerable effect on the floruit estimate. Also the *degree of smoothing* on the calibration curve may have considerable effect on the floruit estimate. On this basis, the effect of the calibration curve on the floruit estimate of a culture regarding the shape of the calibration curve at the particular time period for the culture and the degree of smoothing on the curve will be considered here. The effect of the degree of smoothing on the calibration curve will be assessed by comparing the floruit estimate obtained from the data calibrated on the unsmoothed calibration curve of Pearson *et al* (1986) with the floruit estimate obtained from the data calibrated on what is considered the more sensible alternative of a smoothed calibration curve where the data determine the amount of smoothing.

From the simulation study described in the previous chapter it has been seen that, as *sample size* increased, the width of the interval estimates has narrowed or the confidence attached to normal 95% confidence interval has increased *i.e.* with more artefacts or materials sampled from a culture, a more accurate estimate for the floruit can be obtained. But this usually, in practice,

costs time and money. On account of this, the effect of sample size on the floruit estimate will be under consideration.

Another important factor in the comparison of floruit estimation is the *spread* of radiocarbon dates in the sample from any one culture. The effects of influential *outlier* dates and their influence on the estimation procedure is also considered in these applications.

Since the quoted errors of the radiocarbon dates contribute to the historical dates by influencing the uncertainty on the fitted calibration curve and by determining the uncertainty on the date to be calibrated, the magnitude of the *quoted errors* will have some considerable effect on the floruit estimate for a culture and this will be taken into consideration to ascertain its effect .

In summary, the factors of the archaeological data sets under consideration which may influence the floruit estimate are :-

- The shape and the degree of smoothing of the calibration curve.
- The sample size of the collected radiocarbon dates from the archaeological culture.
- The spread of the radiocarbon dates in the sample from the culture.
- The magnitude of the reported error on each radiocarbon date in the sample.

For certain methods (the highly computational methods **D** and **E**) which require the estimation of density and distribution functions in the provision of floruit estimates, the effect of the degree of smoothing on the density function and hence on the floruit estimate will also be illustrated by the examples in this chapter.

5.2 Data used in the applications

The data considered in this application consist of a group of radiocarbon dates collected from each of ***seven*** cultures situated across different countries and time periods. Six of these groups (*Pfyn, Horgen, Childers, Cham, Cortaillod* and *Sâone-Rhône*) were provided by *Professor Barbara Ottaway* from the Department of Archaeology and Prehistory, Sheffield University, UK. The seventh group, the *Nok* culture, was provided by *Professor Susan McIntosh* from the Department of Anthropology, Rice University, USA.

The *Pfyn, Horgen, Cortaillod* and *Sâone-Rhône* cultures are situated in Switzerland. The *Childers* culture is situated in Australia. The *Cham* culture is a culture from the Late Neolithic of southern Germany. The *Nok* culture is situated in Nigeria, west Africa. The radiocarbon dates from these cultures are as usual expressed in radiocarbon years relative to AD 1950. For each culture, the radiocarbon dates, x_i, and the quoted errors, σ_i, are given in tables 5.1 to 5.7 together with the laboratory number in which the measurement was carried out and the site from which the date was taken.

Site	Lab. No.	Radiocarbon Date ± Error
Thayngen-Weier	B-43	4690 ± 150
Thayngen-Weier	B-44	4690 ± 200
Thayngen-Weier	GrN-241	4735 ± 130
Thayngen-Weier	K-539	4750 ± 100
Niedrewil	GrN-4202	4750 ± 60
Niedrewil	GrN-4204	4750 ± 60
Niedrewil	GrN-6486	4755 ± 40
Niedrewil	GrN-6484	4765 ± 40
Thayngen-Weier	B-45	4780 ± 150
Niedrewil	GrN-6483	4790 ± 40
Niedrewil	GrN-6485	4800 ± 40
Thayngen-Weier	B-459	4850 ± 150
Niedrewil	GrN-7179	4875 ± 50
Thayngen-Weier	K-540	4910 ± 100
Niedrewil	GrN-6482	4915 ± 40
Zürich-Bauschanze	UCLA-1765A	4930 ± 70
Feldmeilen-Vorderfeld	UCLA-1691H	4940 ± 70
Pfyn	GrN-5958	4965 ± 40
Niedrewil	GrN-7090	4980 ± 70
Niedrewil	GrN-4203	4990 ± 60
Pfyn	GrN-5957	5020 ± 40
Thayngen-Weier	KN-I.597	5030 ± 45
Zürich-Bauschanze	UCLA-1765B	5040 ± 60
Thayngen-Weier	H-313/283	5060 ± 100
Greifensee-Storen	UCLA-1825	5100 ± 70
Feldmeilen-Vorderfeld	UCLA-1766A	5100 ± 70
Thayngen-Weier	H-61/149	5140 ± 130
Zürich-Enge	B	5160 ± 120
Feldbach	UCLA-1809A	5170 ± 70
Thayngen-Weier	H-313/283	5180 ± 170
Greifensee-Storen	UCLA-1824	5180 ± 70
Feldmeilen-Vorderfeld	UCLA-1691G	5200 ± 70
Meilen-Obermeilen	UCLA-1835E	5280 ± 60
Zürich-Wollishofen	UCLA-1785	5320 ± 60
Feldmeilen-Vorderfeld	UCLA-1691F	5415 ± 60

Table 5.1 : Group of radiocarbon dates (years BP) were collected from different Sites in ***Pfyn*** culture in Switzerland.

Site	Lab. No.	Radiocarbon Date ± Error
Meilen-Obermeilen	UCLA-1835B	4040 ± 70
Zürich-Kleiner Haffner	UCLA-1654B	4060 ± 100
Männedorf	UCLA-1833	4180 ± 60
Feldmeilen-Vorderfeld	UCLA-1691D	4250 ± 65
Feldmeilen-Vorderfeld	UCLA-1766B	4320 ± 65
Zürich-Kleiner Haffner	UCLA-1764B	4350 ± 60
Fällanden	UCLA-1823	4370 ± 60
Uetikon	UCLA-1847	4380 ± 60
Meilen-Obermeilen	UCLA-1835C	4390 ± 65
Feldmeilen-Vorderfeld	UCLA-1691E	4450 ± 65
Feldmeilen-Vorderfeld	UCLA-1691C	4450 ± 65
Feldbach	UCLA-1809B	4450 ± 60
Meilen-Obermeilen	UCLA-1835D	4480 ± 70
Twann	B-3231	4490 ± 90
Twann	B-3229	4500 ± 80
Feldmeilen-Vorderfeld	UCLA-1691B	4500 ± 65
Twann	B-3228	4530 ± 60
Twann	B-2954	4570 ± 70
Twann	B-3230	4600 ± 80
Twann	B-2956	4650 ± 90
Twann	B-2955	4660 ± 90
Twann	B-3233	4720 ± 90
Twann	B-3232	4770 ± 70

Table 5.2 : Group of radiocarbon dates (years BP) were collected from different Sites in ***Horgen*** culture in Switzerland.

Site	Lab. No.	Radiocarbon Date ± Error
Fontenu-Lac Chalain	GrN-672	4180 ± 130
Auvernier-Port	B-2557	4360 ± 110
Seeberg-Burgaschisee-S	B-114	4390 ± 80
Auvernier-Port	B-2558	4390 ± 70
Seeberg-Burgäschisee-S	B-118A	4490 ± 90
Seeberg-Burgäschisee-S	B-120	4500 ± 100
Seeberg-Burgäschisee-S	B-126	4500 ± 110
Seeberg-Burgäschisee-S	B-123	4530 ± 100
Seeberg-Burgäschisee-S	B-125	4550 ± 100
Fontenu-Lac Chalain	GrN-970	4590 ± 80
Seeberg-Burgäschisee-S	B-118B	4630 ± 180
Seeberg-Burgäschisee-S	B-245	4630 ± 120
Zürich-Großer Haffner	UCLA-1722C	4640 ± 70
Seeberg-Burgäschisee-S	B-121	4680 ± 100
St. Léonard	B-232	4750 ± 100
Seeberg-Burgäschisee-S	B-119A	4750 ± 100
Seeberg-Burgäschisee-S	B-122	4750 ± 100
Seeberg-Burgäschisee-S	B-244	4790 ± 120
Twann	B-2958	4790 ± 120
Twann	B-2957	4790 ± 70
Seeberg-Burgäschisee-S	B-119B	4800 ± 130
Zürich-Großer Haffner	UCLA-1654A	4800 ± 100
Schenkon	B-882	4830 ± 150
Seeberg-Burgäschisee-S	B-116	4840 ± 110
Twann	B-2959	4870 ± 60
Twann	B-2960	4880 ± 70
Vallon-des-Vaux	GrN-5601	4930 ± 40
Seeberg-Burgäschisee-S	B-115	4950 ± 90
Twann	B-2965	4950 ± 50
Twann	B-2961	4960 ± 70
Auvernier-Port	B-2561	4980 ± 110
Schenkon	B-881	4980 ± 120
Twann	B-2962	4990 ± 70
Egolzwil 4	H-227/277	5040 ± 100
Seeberg-Burgäschisee-S	LJ-1293	5060 ± 35
Egolzwil 4	KN-I.21	5080 ± 70
Twann	B-2964	5090 ± 120
Auvernier-Port	B-2560	5100 ± 80
Sion-Petit Chasseur	B-2111	5100 ± 70
Vallon-des-Vaux	B-659B	5120 ± 120
Twann	B-2963	5120 ± 130
Auvernier-Port	B-2559	5130 ± 120
Sion-Petit Chasseur	B-2110	5130 ± 100
Zürich-Großer Haffner	UCLA-1722B	5145 ± 70
Egolzwil 4	H-228/276	5150 ± 100
Vallon-des-Vaux	B-659A	5150 ± 120
Montilier	Lv-625	5170 ± 130
Vallon-des-Vaux	B-659	5180 ± 120
Twann	B-2698	5200 ± 90
Thielle-Mottaz	Lv-623	5280 ± 110
Egolzwil 4	VRI-29	5360± 150

Table 5.3 : Group of radiocarbon dates (years BP) were collected from different Sites in ***Cortaillod*** culture in Switzerland.

Site	Lab. No.	Radiocarbon Date ± Error
Yverdon	B-2200	3900 ± 100
Yverdon	B-2202	3900 ± 100
Auvernier, La Saunerie	B-646	3960 ± 120
Yverdon	B-2213	3970 ± 100
Auvernier, La Saunerie	B-687	3990 ± 100
Auvernier, La Saunerie	B-685	4000 ± 120
Auvernier, La Saunerie	B-644	4000 ± 150
Yverdon	B-2198	4000 ± 100
Yverdon	B-2203	4010 ± 100
Sion-Petit Chasseur	B-2480	4020 ± 100
Yverdon	B-2205	4030 ± 100
Yverdon	B-2197	4060 ± 100
Auvernier, La Saunerie	LJ-1808	4077 ± 70
Yverdon	B-2201	4080 ± 100
Yverdon	B-2204	4080 ± 100
Yverdon	B-2212	4090 ± 90
Sion-Petit Chasseur	B-2478	4100 ± 90
Yverdon	B-2207	4100 ± 120
Auvernier, La Saunerie	LJ-1765	4103 ± 70
Auvernier, La Saunerie	LJ-1774	4129 ± 70
Auvernier, La Saunerie	B-689	4130 ± 100
Auvernier, La Saunerie	B-688	4140 ± 140
Yverdon	B-2210	4140 ± 100
Auvernier, La Saunerie	B-686	4160 ± 100
Auvernier, La Saunerie	B-643	4160 ± 120
Yverdon	B-2209	4160 ± 110
Yverdon	B-2208	4170 ± 100
Auvernier, La Saunerie	B-645	4180 ± 120
Auvernier, La Saunerie	LJ-1806	4191 ± 70
Yverdon	B-2217	4200 ± 110
Yverdon	B-2199	4210 ± 100
Yverdon	B-2216	4230 ± 110
Yverdon	B-2214	4260 ± 100
Sion-Petit Chasseur	B-2477	4280 ± 160
Sion-Petit Chasseur	B-2479	4290 ± 120
Yverdon	B-2215	4300 ± 100
Yverdon	B-2206	4300 ± 110
Yverdon	B-2211	4320 ± 110

Table 5.4 : Group of radiocarbon dates (years BP) were collected from different Sites in ***Sâone-Rhône*** culture in Switzerland.

Site	Lab. No.	Radiocarbon Date ± Error
Hienheim	GrN-7159	3885 ± 40
Galgenbreg	GrN-12563	4150 ± 60
Galgenbreg	GrN-12564	4210 ± 60
Hienheim	GrN-5732	4220 ± 55
Galgenbreg	GrN-12700	4225 ± 30
Galgenbreg	GrN-12561	4255 ± 40
Galgenbreg	GrN-12701	4280 ± 35
Galgenbreg	UB-2551	4285 ± 85
Galgenbreg	GrN-12562	4290 ± 45
Hienheim	GrN-8689	4305 ± 35
Hienheim	GrN-6425	4340 ± 40
Galgenbreg	GrN-12702	4385 ± 35
Hienheim	GrN-7556	4430 ± 45
Galgenbreg	GrN-12699	4510 ± 30
Galgenbreg	GrN-14426	4420 ± 35
Galgenbreg	GrN-14427	4245 ± 50
Galgenbreg	GrN-14428	4500 ± 80
Galgenbreg	GrN-14429	4310 ± 60
Oberschneiding	H 7415-7443	4170 ± 70
Oberschneiding	H 7415-7442	4350 ± 40

Table 5.5 : Group of radiocarbon dates (years BP) were collected from different Sites in ***Cham*** culture in Soutern Germany.

Lab. No.	Radiocarbon Age±Error	Lab. No.	Radiocarbon Age±Error
SMU-2223	1250 ± 65	B-22789	1610 ± 90
SMU-2224	1380 ± 70	B-27276	2060 ± 60
SMU-2254	1440 ± 70	B-27277	1450 ± 80
SMU-2269	1300 ± 65	B-27278	1660 ± 70
SMU-2270	1470 ± 110	B-27279	1470 ± 80
B-22397	1330 ± 80	B-27280	1580 ± 70

Table 5.6 : Group of radiocarbon dates (years BP) were collected from ***Childers*** culture of Austrailia.

Lab. No.	Radiocarbon Age±Error	Lab. No.	Radiocarbon Age±Error
BM-532	2042 ± 126	BM-942	2291 ± 133
BM-533	2269 ± 143	I-1459	2230 ± 120
BM-534	2121 ± 116	I-2960	2390 ± 140
BM-938	2541 ± 74	I-3400	2250 ± 100
BM-940	2488 ± 84	I-4913	2160 ± 95
BM-941	2541 ± 104		

Table 5.7 : Group of radiocarbon dates (years BP) were collected from ***Nok*** culture in Nigeria.

Each of these groups of radiocarbon dates were collected from different sites in the specific culture. The complete set of radiocarbon dates in each culture will be analysed to provide the point and interval estimates for the floruit of the culture. For *individual sites* within cultures consideration will be confined to two examples; these are respectively the two sites (*Seeberg-Burgäschisee-S* and *Twann*) of the *Cortaillod* culture and the two sites (*Auvernier La Saunerie* and *Yverdon*) of the *Sâone-Rhône* culture. The data from these sites will be analysed separately to provide the point and interval estimates for the floruit of each site. The resultant estimates will be discussed and compared to assess the plausibility of the contemporary nature of the sites from the same alleged culture.

Histograms for each group of the radiocarbon dates of these cultures and the chosen sites are plotted in figures 5.1-5.11 to show the nature of the variation within the radiocarbon dates of each group.

The reason for using all of these examples is that each has different features in terms of the number of observations, the shape of the part of the calibration curve used to calibrate the radiocarbon dates and the existence of the outliers in the group. Table 5.8 shows the individual features for each culture and site used in the applications. These different features will help to illustrate the problems which have been faced throughout the applications and will indicate the effect of the various factors on floruit estimate.

Individual Cultures			
Application	*Number of observations*	*Outliers?*	*Shape of the part of the calibration curve at the particular time period*
Pfyn	35	no	Monotonic with some wiggles
Horgen	23	no	Wiggly at the edges
Cortaillod	51	no	Monotonic with many wiggles
Sâone-Rhône	38	no	Steep at edges and flat in the middle with some wiggles
Cham	20	yes	Wiggly, steep and flat
Childers	12	yes	Linear
Nok	11	no	Linear, steep and flat
Sites within cultures			
The two sites within the Cortaillod culture			
Seeberg-Burgäschisee-S	16	no	Monotonic with many wiggles
Twann	10	no	Monotonic with few wiggles
The two sites within the Sâone-Rhône culture			
Yverdon	21	no	Steep at edges and flat in the middle with some wiggles
Auvernier La Saunerie	13	no	Steep at edges and flat in the middle with some wiggles

Table 5.8 : Individual features for each culture and site used in the applications.

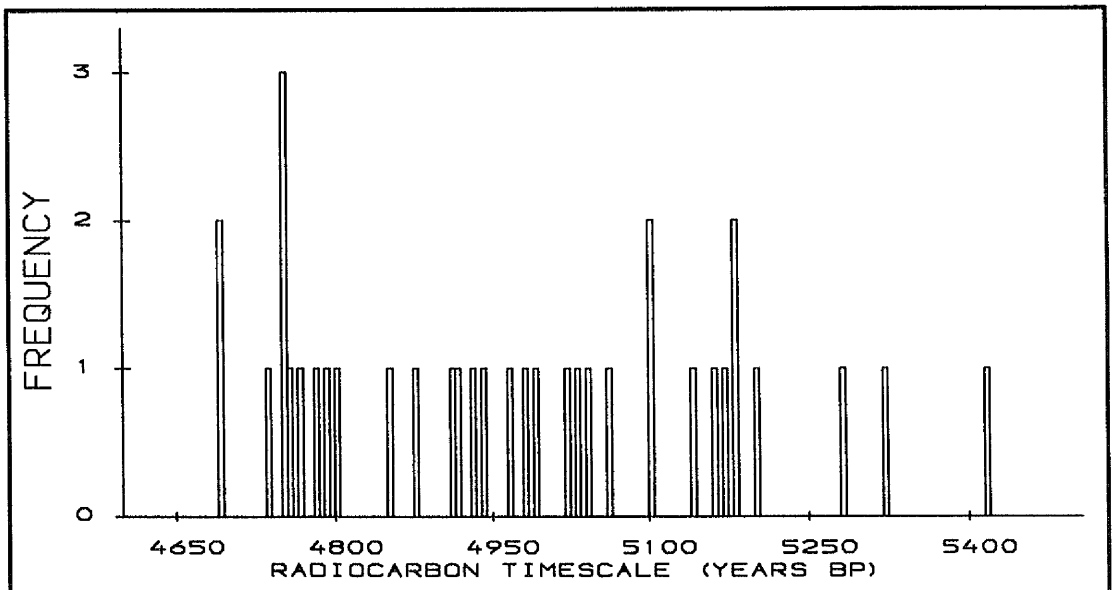

Figure 5.1 : Histogram plot for the radiocarbon dates collected from ***Pfyn*** culture.

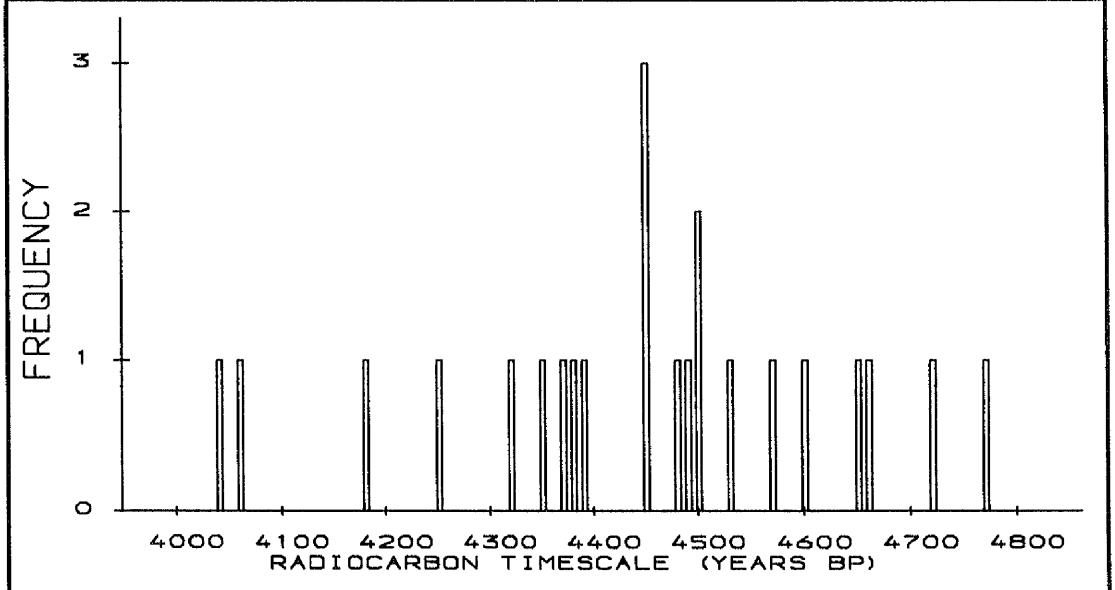

Figure 5.2 : Histogram plot for the radiocarbon dates collected from ***Horgen*** culture.

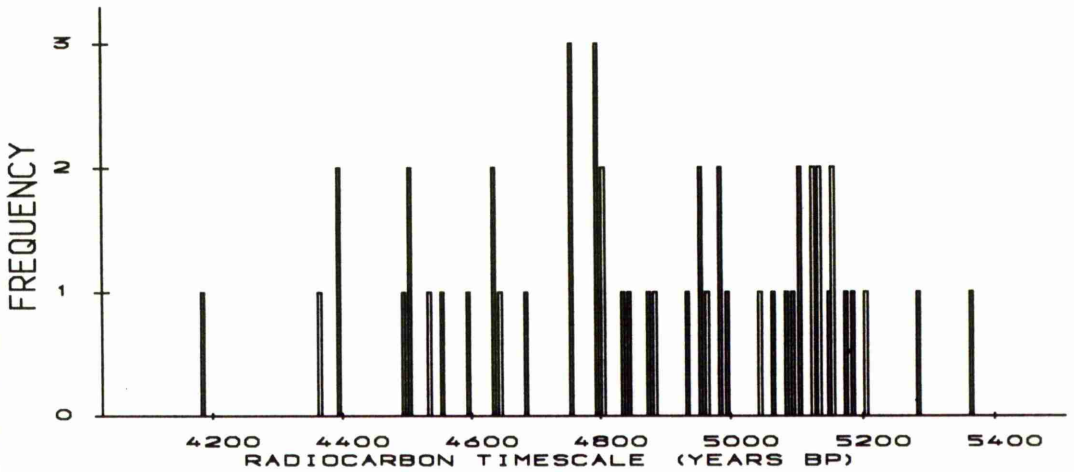

Figure 5.3 : Histogram plot for the radiocarbon dates collected from ***Cortaillod*** culture.

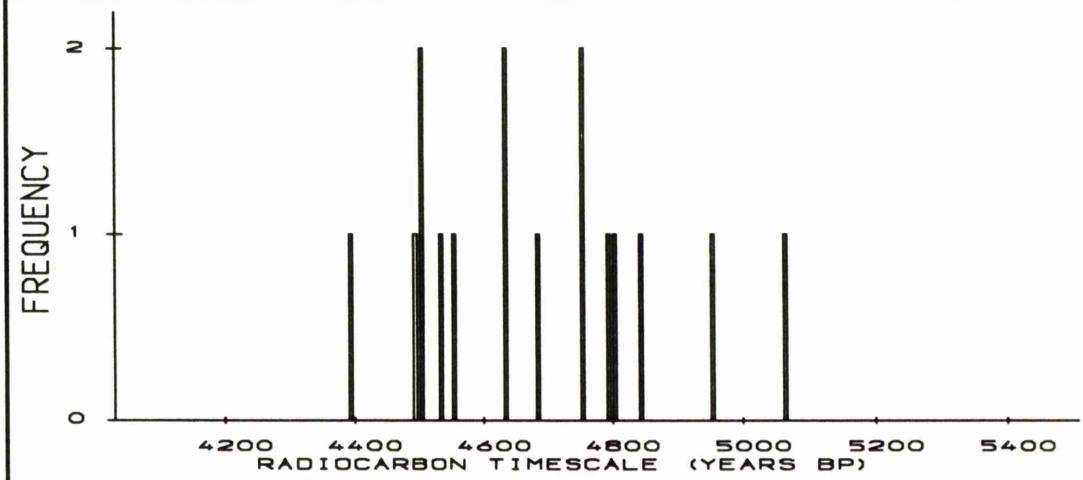

Figure 5.4 : Histogram plot for the radiocarbon dates collected from ***Seeberg-Burgaschisee-S*** site of ***Cortaillod*** culture.

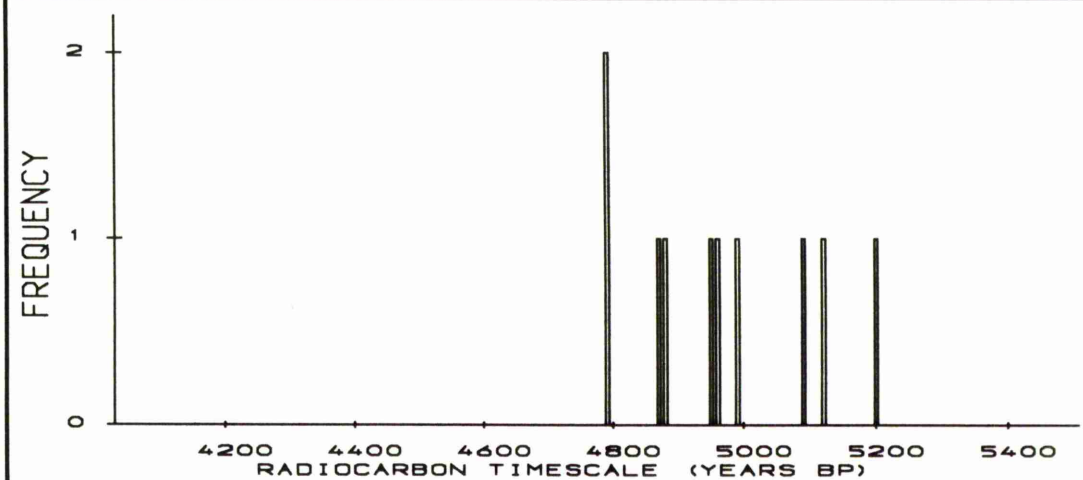

Figure 5.5 : Histogram plot for the radiocarbon dates collected from ***Twann*** site of ***Cortaillod*** culture.

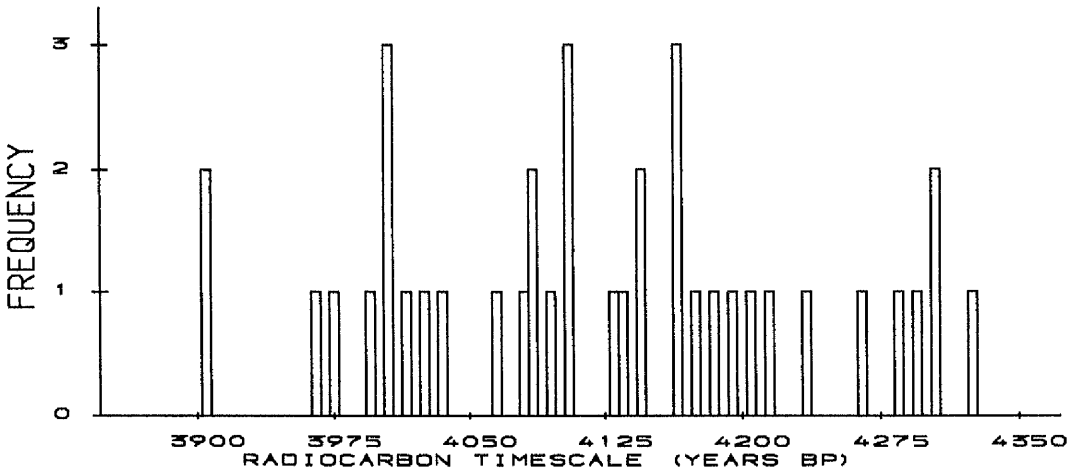

Figure 5.6 : Histogram plot for the radiocarbon dates collected from ***Sâone-Rhône*** culture.

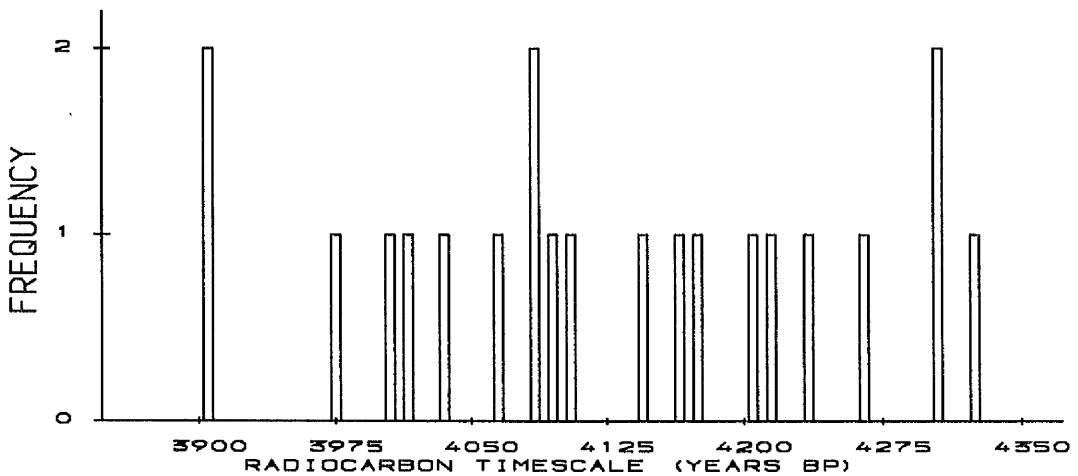

Figure 5.7 : Histogram plot for the radiocarbon dates collected from ***Yverdon*** site of ***Sâone-Rhône*** culture.

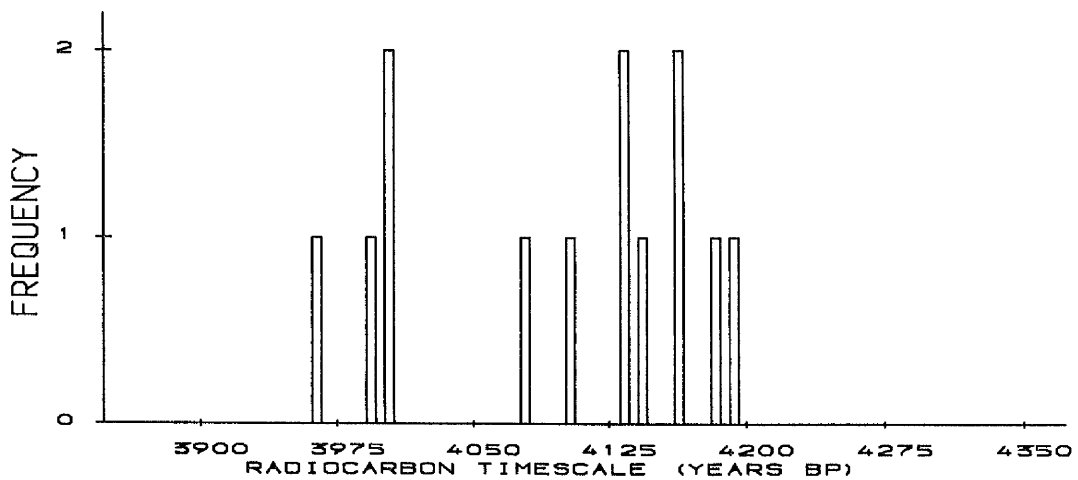

Figure 5.8 : Histogram plot for the radiocarbon dates collected from ***Auvernier La Saunerie*** site of ***Sâone-Rhône*** culture.

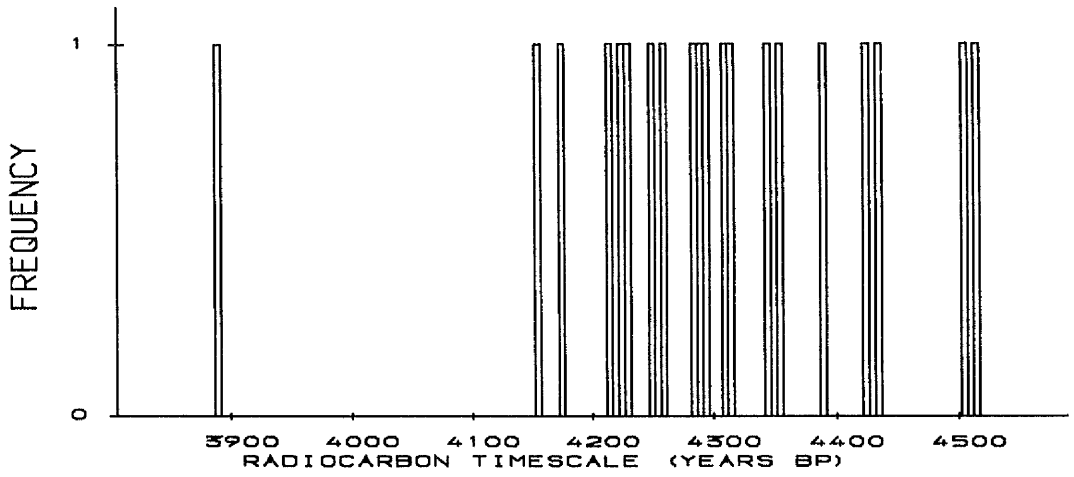

Figure 5.9 : Histogram plot for the radiocarbon dates collected from ***Cham*** culture.

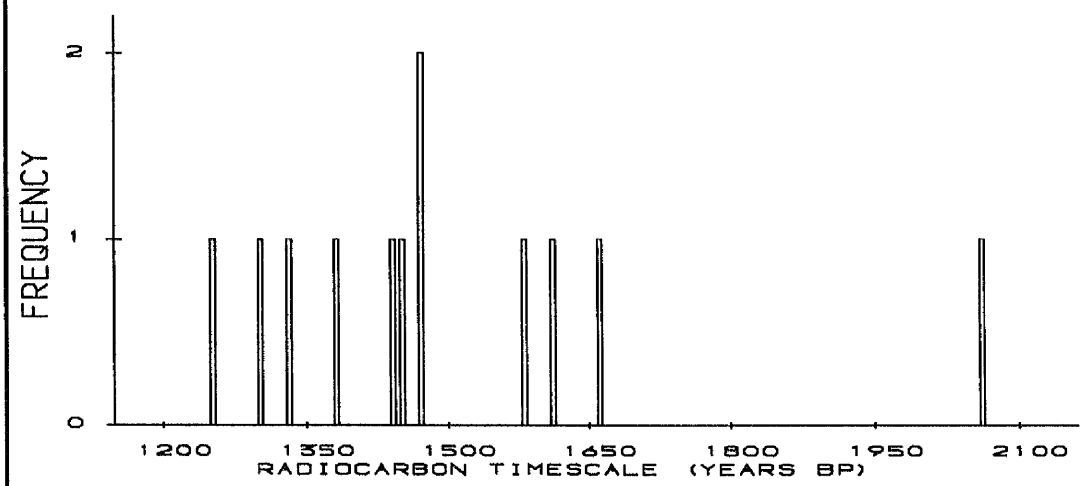

Figure 5.10 : Histogram plot for the radiocarbon dates collected from ***Childers*** culture.

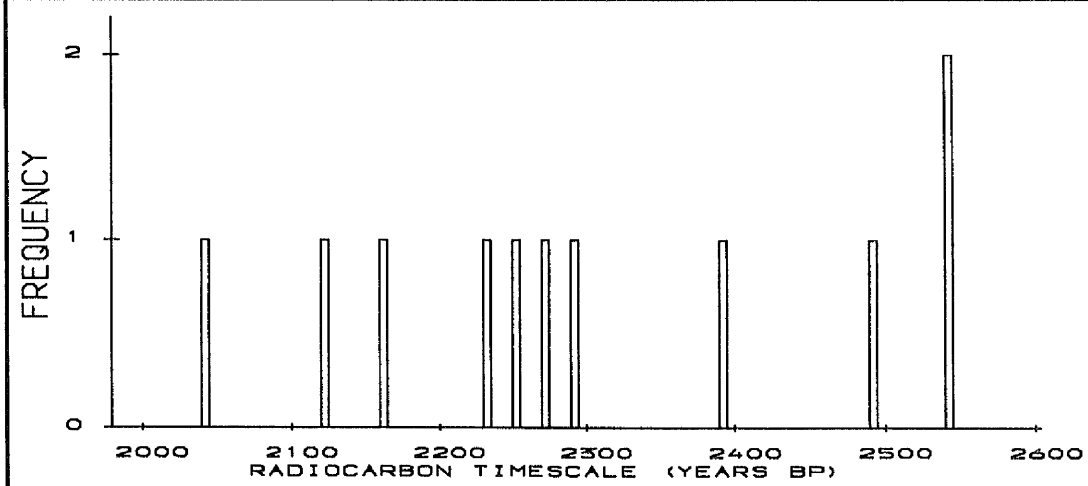

Figure 5.11 : Histogram plot for the radiocarbon dates collected from ***Nok*** culture.

5.3 The Analysis

This analysis does not aim to report technical details of how a group of radiocarbon dates were collected nor how they were measured nor to provide a holistic review of the archaeological perspective of all cultures and sites. The purpose of this analysis is the application of the five floruit estimation methods (introduced in chapter three) to each available data set for each culture and then the investigation of the effect of the various factors likely to influence floruit estimation.

Unfortunately it was difficult to separate out the different effects of influential factors on the floruit estimate through classification of the applications (cultural groups) into various categories according to the features given in table 5.8 *i.e.* it was difficult to classify the applications under categories such as data from linear part of the curve, data from wiggly part of the curve, the effect of sample size and the effect of the outlier date. This was because of the mixed set of factors relevant to each data set, and hence each group of dates covers a variety of the factors of interest.

So rather than considering the effects of each factor individually, the applications are divided into two main sections. In section (5.4) the ***individual cultures*** (*Pfyn, Horgen, Childers, Cham and Nok*) are dealt with and in section (5.5) the ***sites within cultures*** (*Cortaillod* culture with the two sites *Seeberg-Burgäschisee-S* and *Twann* and *Sâone-Rhône* culture with the two sites *Auvernier La Saunerie* and *Yverdon*) are considered in terms of the temporal comparability of the two sites within each culture.

5.4 Individual Cultures

This section is divided into sub-sections to consider the applications of the five methods of floruit estimation on each of the five cultural groups (*Pfyn, Horgen, Childers, Cham* and *Nok*) individually. The resultant estimates for

each culture will be summarised and compared. The effect of the various factors on the floruit estimate for each culture will be assessed throughout the applications.

Since the analytic process for each cultural group is basically the same, only the details of the first culture (*i.e. Pfyn*) are given. (For the rest of this chapter the terms '**smoothed data** and **unsmoothed data**' will be used instead of the terms '**historical dates calibrated on the smoothed curve** and **historical dates calibrated on the unsmoothed curve**' respectively).

5.4.1 Pfyn Cultural Group

This data group consists of 35 radiocarbon dates from archaeological samples collected from different sites in the *Pfyn* culture of Switzerland. These radiocarbon dates , x_i and their quoted errors, σ_i , are given in table 5.1 together with the laboratory number in which the measurement was carried out and the site from which the date was taken.

The part of the calibration curve which was used to calibrate the radiocarbon dates is shown in figures 5.12a&b for both smoothed and unsmoothed calibration curves. This part takes a monotonic form with more wiggles in the unsmoothed case. Most of these wiggles are dampened and in some cases removed by the smoothing procedure. One can see the result of this when the possible true historical dates, $\hat{t}_{ij}$, that might have generated the observed x_i are obtained (see table 5.9). For example, when the calibration carried on the unsmoothed curve, a radiocarbon date of x_i=5280 BP corresponds to five possible historical dates in calibrated years BC. These are

$\hat{t}_{i1}$= 4045 , $\hat{t}_{i2}$= 4120 , $\hat{t}_{i3}$= 4138 , $\hat{t}_{i4}$= 4207 and $\hat{t}_{i5}$= 4215.

When the calibration of the same radiocarbon date carried on the smoothed curve, it corresponds to only one possible historical date in the calibrated years BC. This date is $\hat{t}_{i1}$= 4050.

Each radiocarbon date, x_i , is calibrated separately. The full set of $\hat{t}_{ij}$ calibrated from both smoothed and unsmoothed calibration curve are given in table 5.9, together with the corresponding standard errors of such which are based on the methods of section 2.9 and involve the quoted errors of the radiocarbon dates and the slope of the calibration curve at the appropriate timespan. Histogram plots of the calibrated dates are given in figure 5.13a to show the nature of the variation within the calibrated dates.

The smoothing on the calibration curve has rounded out the peaks visible in the unsmoothed calibration curve. Consequently the slope of the smoothed calibration curve is fairly stable on the long term scale but the rounding nature of the peaks produces local slopes which are close to zero in some instances giving rise to considerably higher numerical values for the estimated standard errors of the $\hat{t}_{ij}$ in the smoothed case than in the unsmoothed. An example of this is the comparison of the estimated standard errors for the three historical dates correspond to the radiocarbon date of x_i=4750 BP. The standard errors for $\hat{t}_{i1}$ are identical in both the smoothed and unsmoothed cases since the curve seems unaffected by the smoothing at this point, while the standard errors for $\hat{t}_{i2}$ and $\hat{t}_{i3}$ have increased in the smoothed case when the calibration curve has been affected by the smoothing to produce a very flat area in the period 3500 - 3630 years BC. This is illustrated graphically in figure 5.12c.

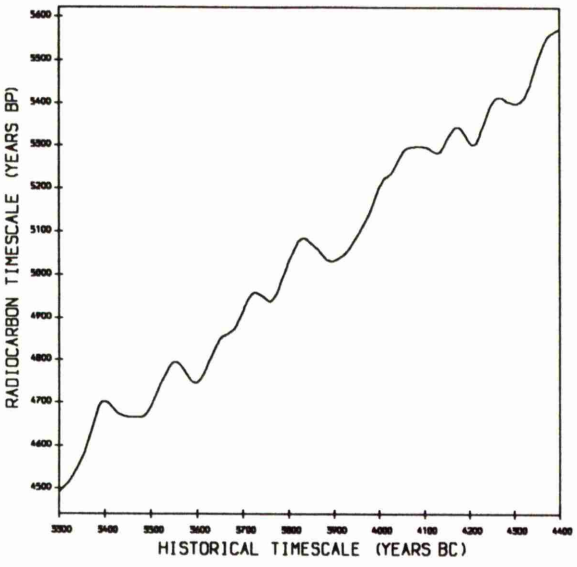

*Figure 5.12 :*a)
Part of the smoothed calibration curve used to calibrate the radiocarbon dates from ***Pfyn*** culture

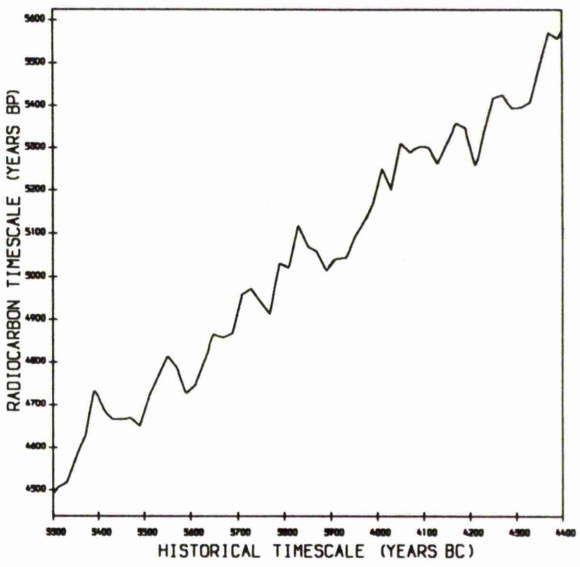

*Figure 5.12 :*b)
Part of the unsmoothed calibration curve used to calibrate the radiocarbon dates from ***Pfyn*** culture

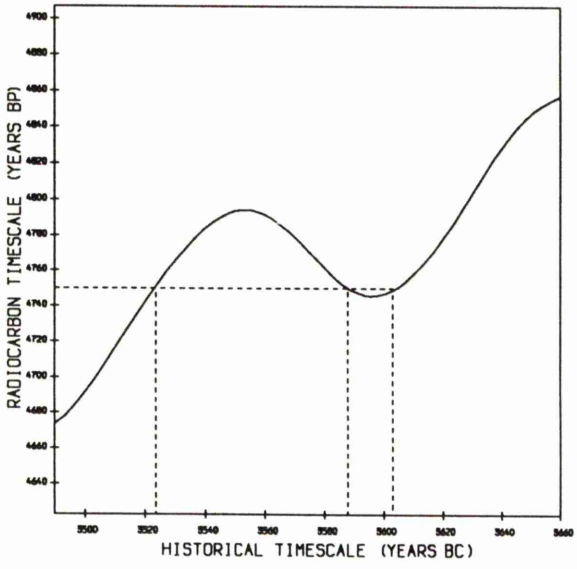

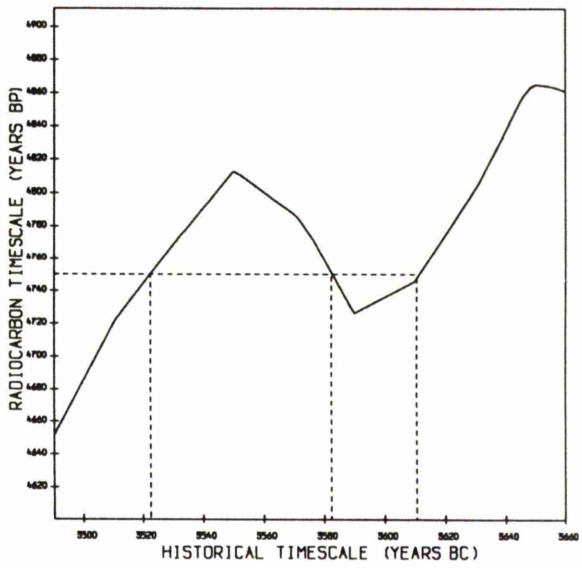

*Figure 5.12 :*c:
Graphical illustration of the three historical dates which may have generated the radiocarbon date of 4750 BP showing the effect of the smoothing procedure on the slope of the calibration curve.

#	Radiocarbon Date ± Error (Years BP)	Corresponding historical dates (years BC) calibrated from smoothed curve.			Corresponding historical dates (years BC) calibrated from unsmoothed curve.		
		number of $\hat{t}_{ij}$	estimated $\hat{t}_{ij}$	estimated standard errors $se(\hat{t}_{ij})$	number of $\hat{t}_{ij}$	estimated $\hat{t}_{ij}$	estimated standard errors $se(\hat{t}_{ij})$
1	4690 ± 150	3	3387	114	3	3382	45
			3414	190		3412	189
			3499	111		3501	70
2	4690 ± 200	3	3387	152	3	3382	60
			3414	256		3412	210
			3499	147		3501	93
3	4735 ± 130	1	3517	82	3	3516	87
						3587	69
						3599	94
4	4750 ± 100	3	3524	67	3	3523	67
			3588	153		3582	53
			3603	184		3611	58
5	4750 ± 60	3	3524	41	3	3523	41
			3588	93		3582	32
			3603	112		3611	36
6	4750 ± 60	3	3524	41	3	3523	41
			3588	93		3582	32
			3603	112		3611	36
7	4755 ± 40	3	3526	29	3	3525	28
			3584	46		3581	22
			3608	48		3613	25
8	4765 ± 40	3	3530	31	3	3529	29
			3578	38		3577	22
			3614	34		3617	24
9	4780 ± 150	3	3538	149	3	3535	107
			3568	152		3571	79
			3621	100		3622	86
10	4790 ± 40	3	3545	70	3	3540	30
			3560	82		3567	54
			3625	26		3626	25
11	4800 ± 40	1	3629	25	3	3544	30
						3560	52
						3629	25
12	4850 ± 150	1	3653	160	1	3645	77
13	4875 ± 50	1	3682	56	1	3690	37
14	4910 ± 100	1	3699	59	1	3699	35
15	4915 ± 40	1	3701	24	1	3700	15
16	4930 ± 70	1	3707	46	3	3704	25
						3758	79
						3773	19
17	4940 ± 70	3	3711	55	3	3707	25
			3754	64		3751	80
			3761	67		3774	19
18	4965 ± 40	1	3778	24	3	3719	103
						3733	44
						3779	11
19	4980 ± 70	1	3783	38	1	3781	19
20	4990 ± 60	1	3786	33	1	3783	17
21	5020 ± 40	1	3798	28	3	3789	12
						3889	30
						3895	51
22	5030 ± 45	1	3802	32	3	3809	139
						3883	34
						3902	57
23	5040 ± 60	3	3806	42	3	3813	20
			3881	89		3878	44
			3915	144		3914	39
24	5060 ± 100	3	3815	70	3	3818	33
			3864	147		3867	87
			3935	110		3938	53

continued/next page

#	Radiocarbon Age (Years BP)	Corresponding historical dates (years BC) calibrated from smoothed curve.			Corresponding historical dates (years BC) calibrated from unsmoothed curve.		
		number of $\hat{t}_{ij}$	estimated $\hat{t}_{ij}$	estimated standard errors $se(\hat{t}_{ij})$	number of $\hat{t}_{ij}$	estimated $\hat{t}_{ij}$	estimated standard errors $se(\hat{t}_{ij})$
25	5100 ± 70	1	3958	65	3	3826 3838 3957	23 46 68
26	5100 ± 70	1	3958	65	3	3826 3838 3957	23 46 68
27	5140 ± 130	1	3979	90	1	3979	99
28	5160 ± 120	1	3987	66	1	3988	92
29	5170 ± 70	1	3990	37	1	3991	27
30	5180 ± 170	1	3994	89	1	3994	63
31	5180 ± 70	1	3994	37	1	3994	27
32	5200 ± 70	1	4001	45	1	3998	26
33	5280 ± 60	1	4050	57	5	4045 4120 4138 4207 4215	18 50 43 23 24
34	5320 ± 60	3	4154 4194 4222	46 49 39	3	4155 4196 4225	40 22 24
35	5415 ± 60	1	4324	55	3	4252 4276 4330	17 29 16

Table 5.9 : Estimates of historical dates corresponding to each observed radiocarbon age, and their estimated standard errors from both smoothed and unsmoothed calibration curve for the group of radiocarbon dates taken from ***Pfyn*** culture.

The effect of the magnitude of the quoted radiocarbon errors on the calibrated historical dates can be seen by comparing the calibration of two distinct radiocarbon dates of x_i=4690 with quoted errors of 150 and 200 years respectively. This radiocarbon date corresponds to three dates in the historical timescale . These dates (taken from the smoothed case) are 3387, 3414 and 3499 years BC with estimated standard error equal to 114, 190 and 111 respectively in the first case and equal to 152, 256 and 147 respectively in the second case. Obviously therefore larger radiocarbon errors produce larger standard error in the calibrated dates which will tend to spread out the effect of the $\hat{t}_{ij}$ on the estimate of the floruit of culture on the historical timescale.

The essential requirements for this data to apply the pen and paper methods (A, B and C) are now available to provide the corresponding floruit

estimates(point and interval) for the *Pfyn* culture. One is also in a position to move towards those based on the highly computational methods (D and E) which require the estimates of the probability density function and hence the cumulative distribution function of artefacts for the *Pfyn* culture.

The estimates of the probability density function (p.d.f.) of the true frequency distribution for both smoothed and unsmoothed calibrated historical dates have been constructed using the procedure outlined in section (3.7.2). The estimated functions are graphed in figures 5.13 for both cases and for the different methods of choice of smoothing parameter.

Finally, one integrates the estimated density function to provide the estimate of the cumulative distribution function (c.d.f.) which is necessary for the estimation of the floruit. These estimated c.d.f.'s are shown in figure 5.14 (the middle band) together with the corresponding 95% confidence interval estimates.

Resulting estimates for the floruit of the *Pfyn* culture from the five floruit estimation methods are summarised in table 5.10 and plotted in figure 5.15 for all the methods.

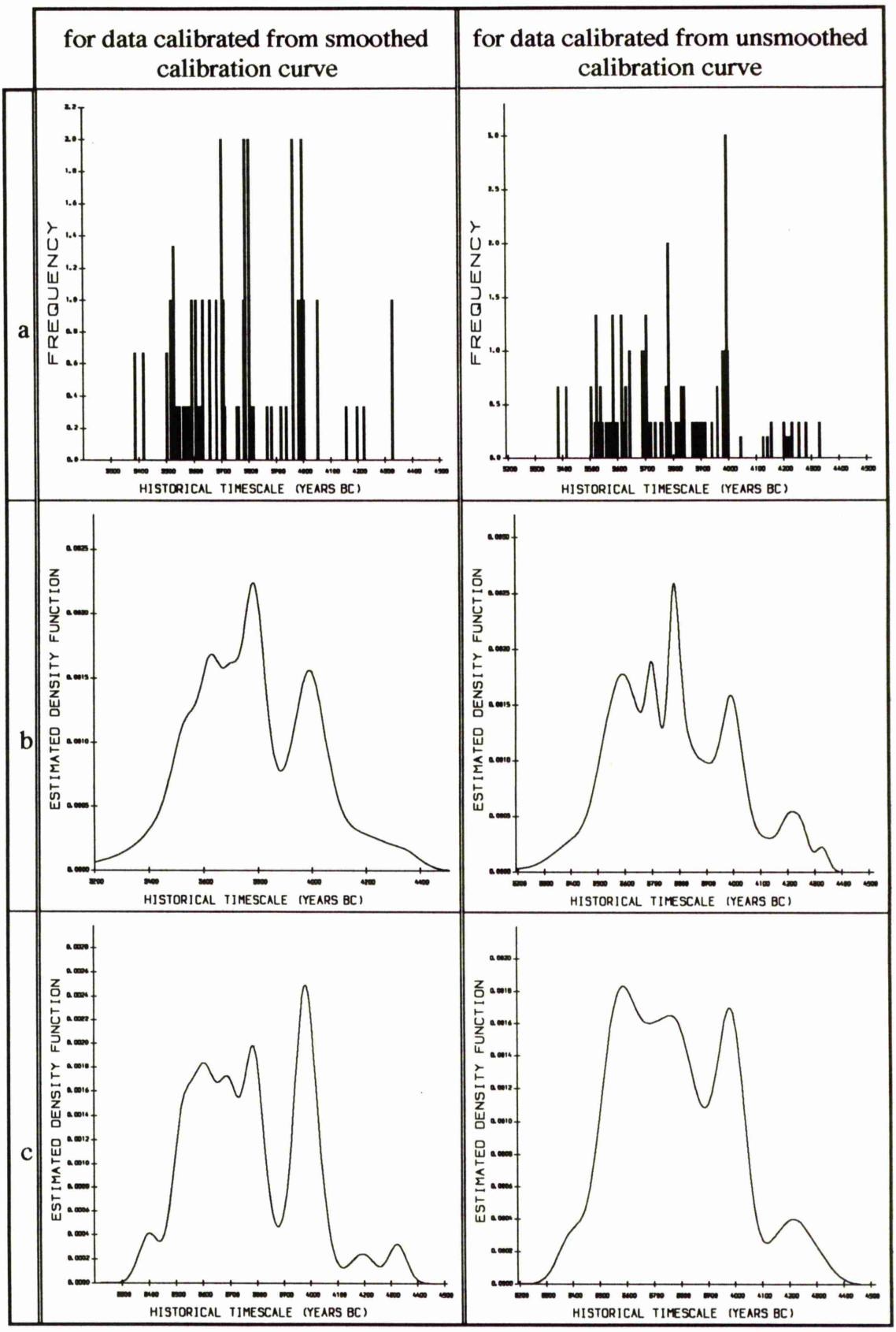

Figure 5.13 : a)Histogram plots for the calibrated historical dates for ***Pfyn*** culture and the plots of estimated density functions, b) smoothed by cross-validation method and c) smoothed by weighting method.

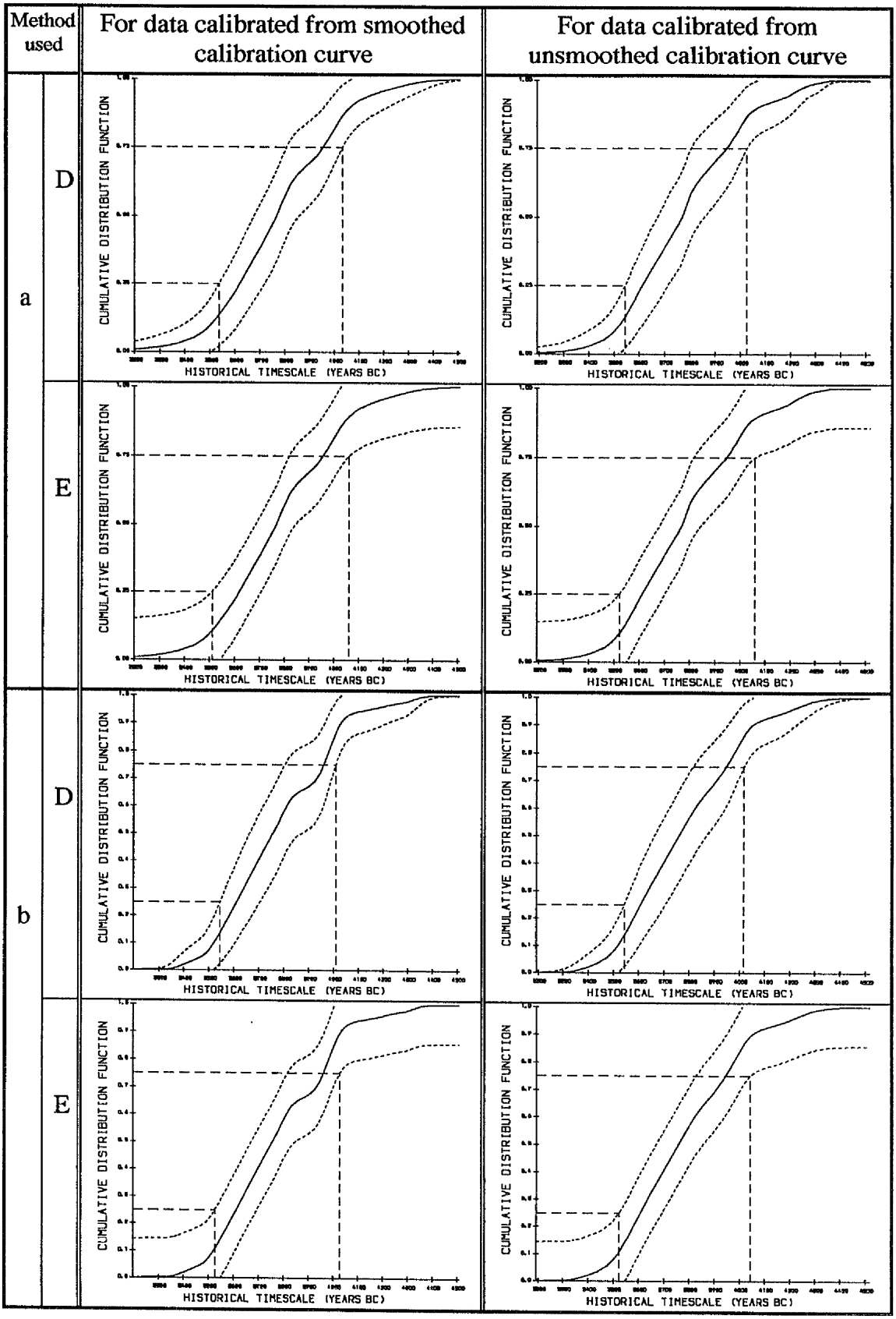

Figure 5.14 : Plots of estimated cumulative distribution functions for calibrated historical dates for ***Pfyn*** culture a) smoothed by cross-validation method, b) smoothed by weighting method.

Floruit Estimation (years BC)					
Method used		For data calibrated from smoothed calibration curve.		For data calibrated from unsmoothed calibration curve.	
		Point	Interval	Point	Interval
A		3541 - 3974	3519 - 4001	3538 - 3974	3518 - 3998
B		3612 - 3974	3553 - 4014	3611 - 3973	3583 - 4008
C		3594 - 3974	3549 - 4012	3583 - 3955	3571 - 3983
D	Cross-Validation	3620 - 3956	3538 - 4034	3612 - 3947	3546 - 4027
	Weighting Method	3610 - 3962	3545 - 4010	3609 - 3947	3545 - 4018
E	Cross-Validation	3620 - 3956	3511 - 4062	3612 - 3947	3524 - 4061
	Weighting Method	3610 - 3962	3526 - 4027	3609 - 3947	3525 - 4044

Table 5.10 : Point and Interval estimates for the floruit of ***Pfyn*** culture obtained from the five methods.

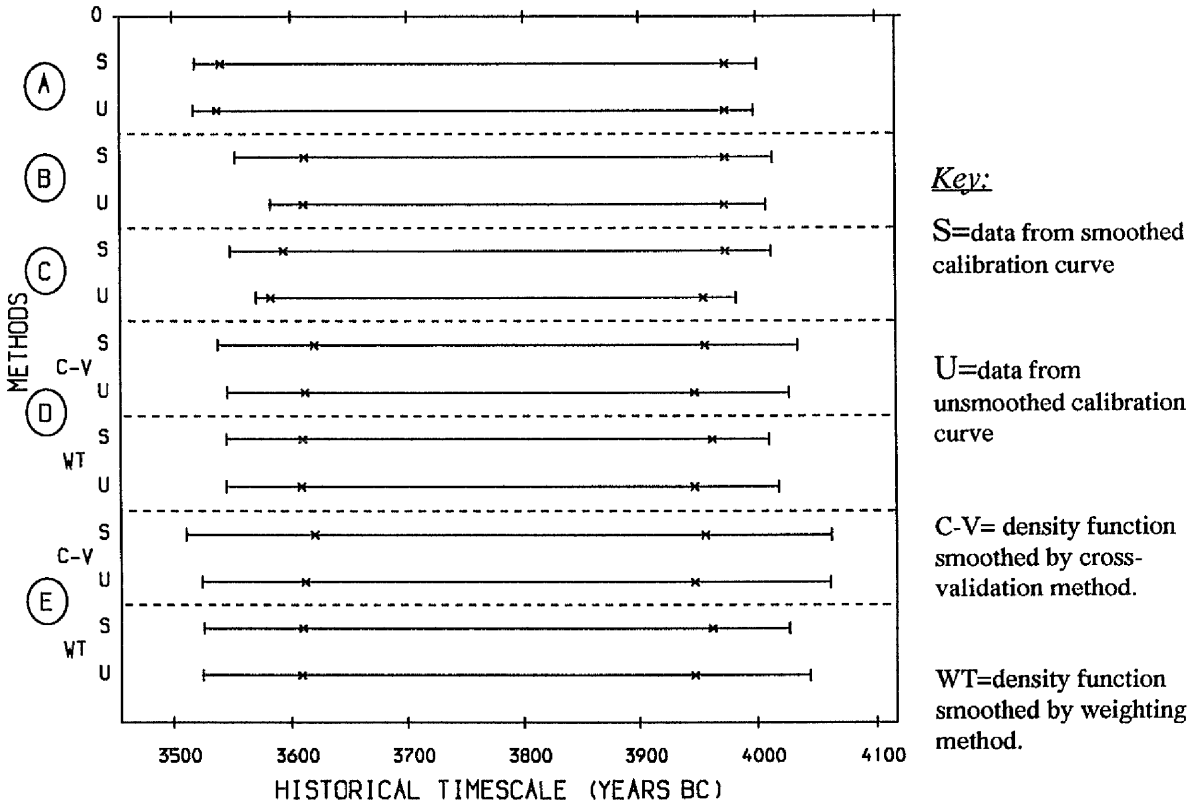

Figure 5.15 : Plots of point (x---x) and interval (|---|) estimates for the floruit of ***Pfyn*** culture.

For the estimates obtained from the smoothed data, at the older end of the floruit, all the pen and paper methods have produced exactly the same point estimate (3974 BC) and generally close interval estimates with slightly wider with methods B and C than A. Taking into account the younger end of the floruit however it is apparent that method A has produced the widest point and interval estimates for the floruit. This has happened since the calibration of the lower quartile of the radiocarbon dates occurred on a wiggly segment of the curve at the younger end (*i.e.* on the wiggle in the period 3520-3620 BC), while the calibration of the upper quartile of the radiocarbon dates occurred on a steep segment of the curve at the older end (*i.e.* in the period 3950-4050 BC).

The resulting estimates of the floruit from method A in the smoothed case are almost identical to those in the unsmoothed case. The point estimate of the floruit obtained from method B is identical in both smoothed and unsmoothed cases, but the interval estimate is wider in the smoothed case which was influenced by the large standard errors estimated for the calibrated dates compared with those for the unsmoothed case particularly for the younger dates. Due to more wiggles on the unsmoothed calibration curve, method C has shifted the point and interval estimates by 19 and 29 years respectively towards the younger end compared with the estimates obtained when the smoothed calibration curve used. Again the large standard errors for the calibrated dates in the smoothed case widen the interval estimate obtained from smoothed data compared with the interval estimate obtained from the unsmoothed data.

For the two methods based on density functions, D and E, the amount of smoothing on the density function has influenced the floruit estimates. As can be seen in figure 5.13b the cross-validation method smoothed the probability density function more using the data from the smoothed calibration curve than from the unsmoothed curve. This leads to a wider interval estimate for the

floruit obtained from the smoothed curve. Conversely, the weighting method gave less smoothing to the density function from the smoothed curve (figure 5.13c) and resulted in a slightly narrower floruit interval estimate than that obtained from the unsmoothed curve.

Comparing these two methods, one finds that method E produces wider interval estimates than method D whether the density function was smoothed by cross-validation or the weighting method. This is possibly due to the approximation of constant variance of the cumulative distribution function used in method E.

Overall the point estimates of the floruit tend to be wider in the cases of the pen and paper methods compared to those based on density estimation while conversely the interval estimates are narrower. This suggests, in line with the simulations of chapter four, that the pen and paper methods possibly should not have as much as 95% confidence attached to them.

5.4.2 Horgen Cultural Group

This group of radiocarbon dates contains 23 dates of samples collected from different sites of the *Horgen* culture of Switzerland. These were listed in table 5.2 together with their quoted errors and the laboratory number where they were measured and the sites of the culture from which they were collected.

The particular parts of the smoothed and unsmoothed calibration curve used to calibrate the radiocarbon dates of this group are shown in figures 5.16a&b respectively. From Table 5.11 where the calibrated historical dates (years BC) are listed together with their estimated standard error, one can see that there are in general a much greater number of $\hat{t}_{ij}$ in the unsmoothed case as a result of wiggles on the unsmoothed calibration curve compared with the smoothed case where most of these wiggles have been eased out. Histogram plots of the calibrated historical dates are given in figure 5.17a.

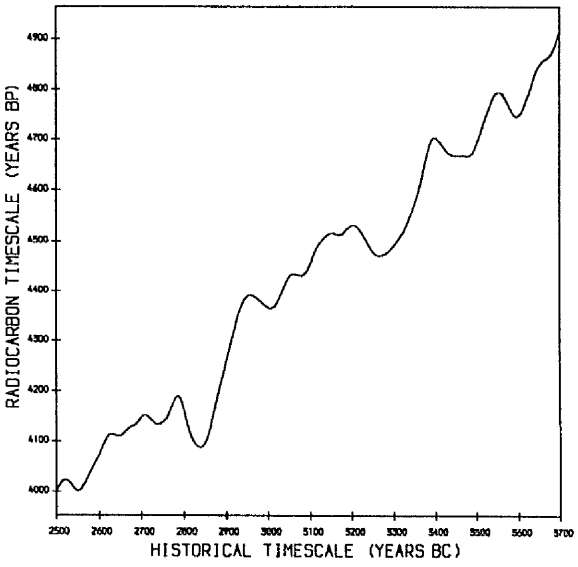

*Figure 5.16 :*a)
Part of the smoothed calibration curve used to calibrate the radiocarbon dates from ***Horgen*** culture

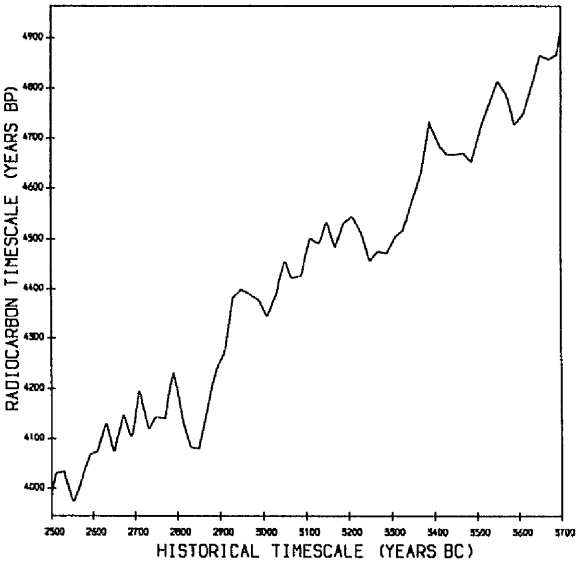

*Figure 5.16 :*b)
Part of the unsmoothed calibration curve used to calibrate the radiocarbon dates from ***Horgen*** culture

#	Radiocarbon Date ± Error (years BP)	Corresponding historical dates (years BC) calibrated from smoothed curve.			Corresponding historical dates (years BC) calibrated from unsmoothed curve.		
		number of $\hat{t}_{ij}$	estimated $\hat{t}_{ij}$	estimated standard errors $se(\hat{t}_{ij})$	number of $\hat{t}_{ij}$	estimated $\hat{t}_{ij}$	estimated standard errors $se(\hat{t}_{ij})$
1	4040 ± 70	1	2581	69	1	2580	42
2	4060 ± 100	1	2594	98	1	2589	60
3	4180 ± 60	3	2777	52	5	2706	21
			2794	48		2707	21
			2877	24		2778	20
						2802	20
						2875	26
4	4250 ± 65	1	2897	36	1	2897	60
5	4320 ± 65	1	2920	30	1	2919	19
6	4350 ± 60	1	2929	32	3	2924	18
						3007	61
						3011	49
7	4370 ± 60	3	2937	46	3	2930	18
			2992	133		2994	61
			3015	94		3023	49
8	4380 ± 60	3	2942	67	3	2933	16
			2980	119		2985	42
			3022	57		3027	49
9	4390 ± 65	3	2954	28	3	2940	19
			2963	32		2966	32
			3028	52		3031	30
10	4450 ± 65	1	3097	55	3	3048	30
						3051	61
						3096	29
11	4450 ± 65	1	3097	55	3	3048	30
						3051	61
						3096	29
12	4450 ± 60	1	3097	51	3	3048	28
						3051	56
						3096	27
13	4480 ± 70	3	3112	61	3	3104	31
			3249	103		3242	40
			3288	160		3295	67
14	4490 ± 90	3	3118	105	5	3107	40
			3241	101		3167	56
			3300	140		3168	56
						3239	52
						3301	85
15	4500 ± 80	3	3127	132	5	3133	62
			3234	86		3163	50
			3309	112		3177	52
						3235	46
						3307	76
16	4500 ± 65	3	3127	108	5	3133	51
			3234	70		3163	41
			3309	91		3177	42
						3235	38
						3307	62
17	4530 ± 60	3	3201	83	3	3192	79
			3206	85		3219	65
			3331	56		3334	21
18	4570 ± 70	1	3350	47	1	3348	38
19	4600 ± 80	1	3361	41	1	3360	55
20	4650 ± 90	1	3374	37	1	3375	27
21	4660 ± 90	1	3377	39	3	3377	27
						3480	83
						3493	42
22	4720 ± 90	1	3511	55	3	3390	73
						3396	73
						3511	61
23	4770 ± 70	3	3532	56	3	3531	51
			3575	63		3576	38
			3616	53		3619	41

Table 5.11 : Estimates of historical dates corresponding to each observed radiocarbon age, and their estimated standard errors from both smoothed and unsmoothed calibration curve for the group of radiocarbon dates taken from ***Horgen*** culture.

As the main step for applying methods D and E, estimates of the p.d.f. of the frequency distribution of artefacts for the culture have been constructed using both cross-validation and weighting methods to smooth the p.d.f.. Figures 5.17b&c show the plots of the p.d.f.'s for the data in the two cases for the smoothed or unsmoothed curve. It is clear from these plots that, the degree of smoothing on the p.d.f based on cross-validation produces a smoother version of the estimated p.d.f.. The c.d.f.'s based upon these density estimates are shown in figure 5.18 with approximate 95% confidence intervals.

The five methods of floruit estimation have been applied with the resulting point and interval estimates of the floruit summarised in table 5.12 and presented graphically in figure 5.19.

Generally speaking there is agreement among the five methods on the point estimate particularly in the case of data calibrated on the smoothed calibration curve. Whether the calibration was carried on the smoothed or unsmoothed curve, method A produces identical estimates for the floruit. This was because the calibration of the quartiles and the extended quartiles of the radiocarbon dates occurred on two steep parts of both curves (*i.e.* in the two periods 2890-2940 BC and 3320-3370 BC). With a wider interval in B than in C both methods have produced a wider interval estimates when using the smoothed calibration curve than with the unsmoothed calibration curve. This happened as a result of the larger estimated standard errors involved with each historical date based on the smoothed calibration curve.

For the two methods based on density estimation, the weighting method tends to under-smooth the p.d.f. and hence the resulting estimate of the floruit is narrower than that produced by cross-validation. Both methods produced wider interval estimates for the floruit than the pen and paper methods. For method D the interval estimates obtained from the unsmoothed data are quite a bit wider than those based on the smoothed data particularly at the younger end

of the culture. The reason behind this is primarily due to the larger number of possible historical dates in the unsmoothed case in addition to the degree of smoothing on the density function there.

Comparing the two methods, D seems to provides more reasonable interval estimates than the wide interval estimates provided by method E. This again, is likely to be, due to the approximation of constant variance used in method E and its effect can be seen clearly in figure 5.18.

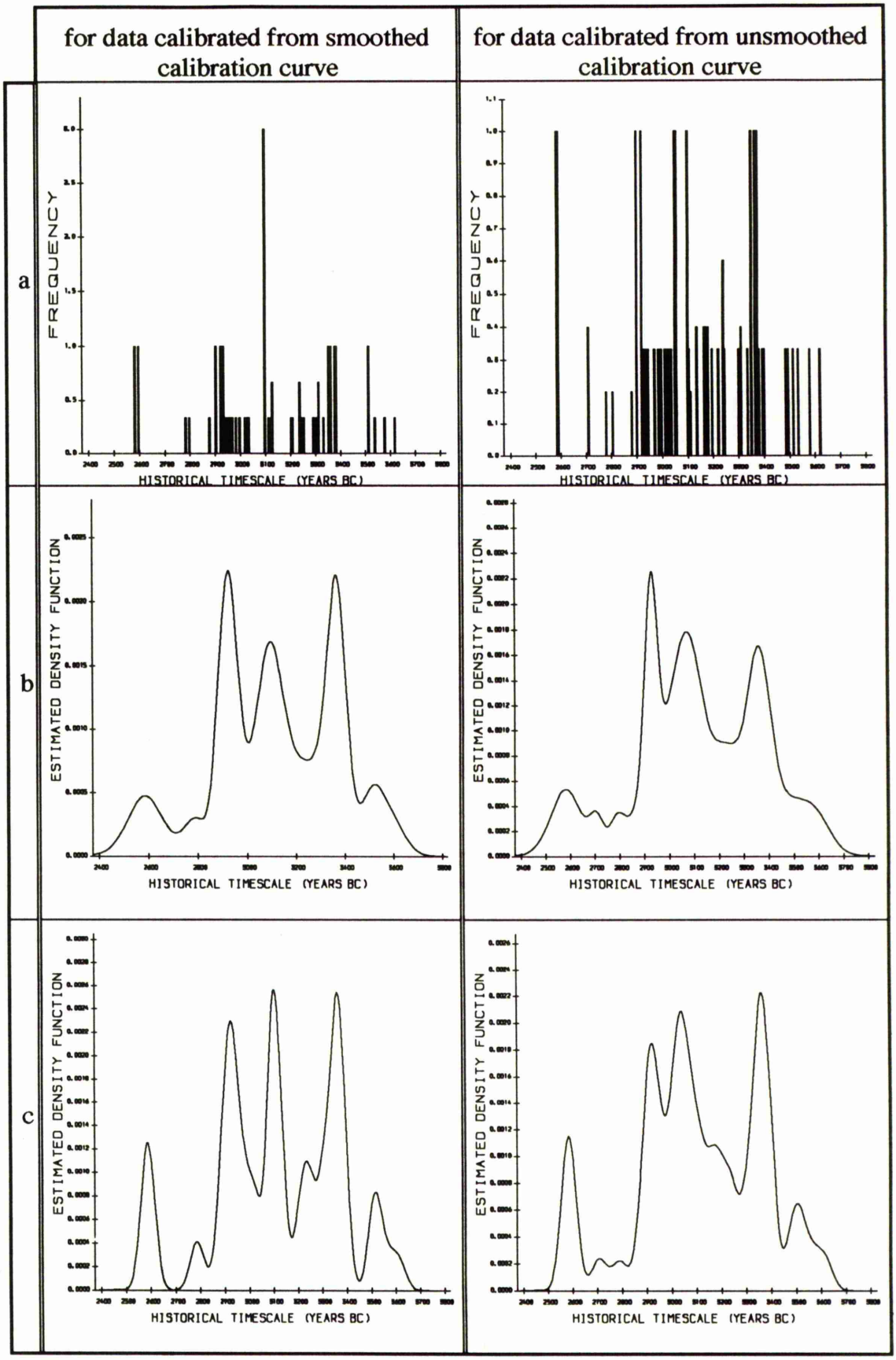

Figure 5.17 : a)Histogram plots for the calibrated historical dates for ***Horgen*** culture and the plots of estimated density functions, b) smoothed by cross-validation method and c) smoothed by weighting method.

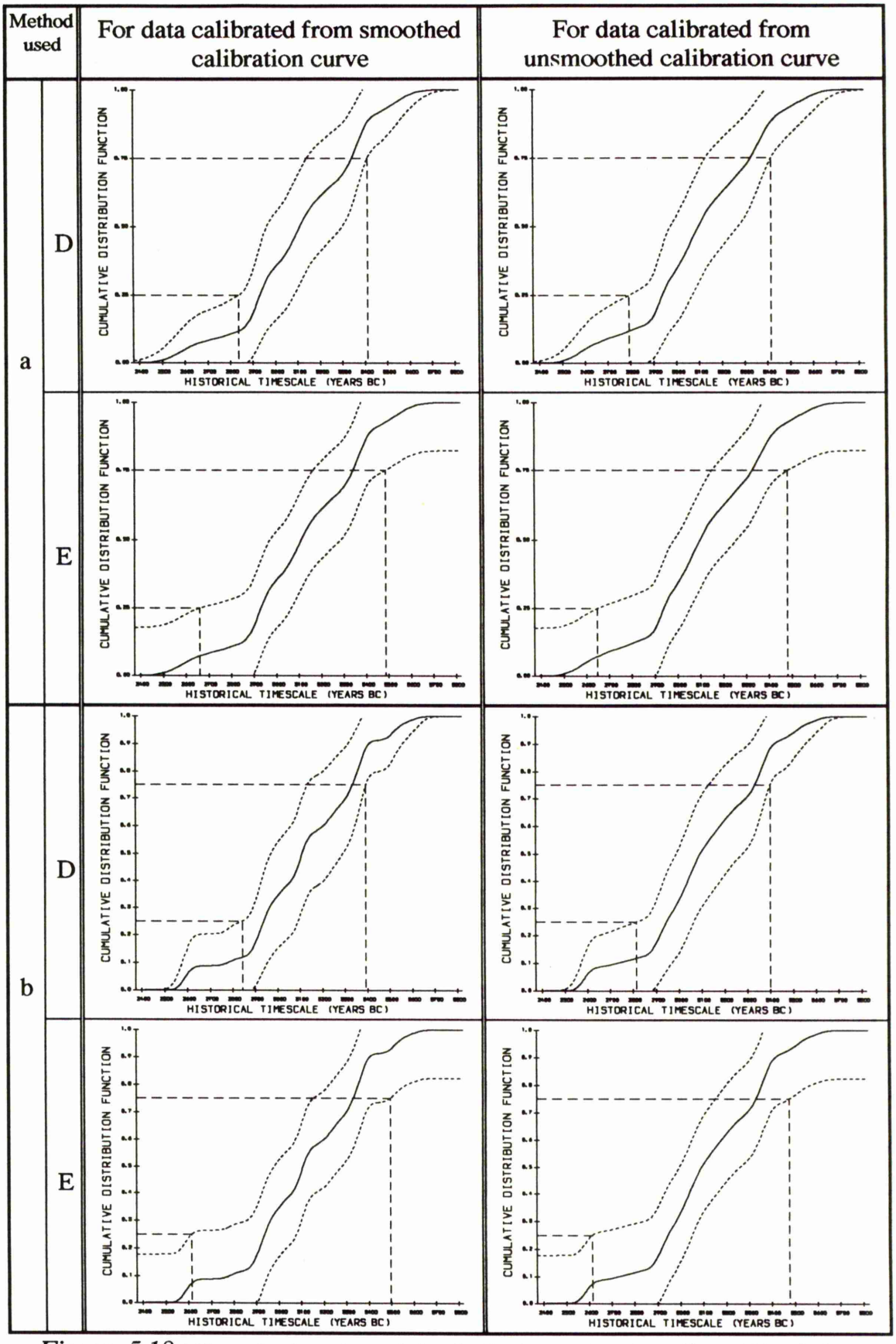

Figure 5.18 : Plots of estimated cumulative distribution functions for calibrated historical dates for ***Horgen*** culture **a)** smoothed by cross-validation method and **b)** smoothed by weighting method.

Floruit Estimation (years BC)					
Method used		for data calibrated from smoothed calibration curve.		for data calibrated from unsmoothed calibration curve.	
		Point	Interval	Point	Interval
A		2931 - 3345	2918 - 3362	2925 - 3344	2918 - 3362
B		2935 - 3345	2906 - 3385	2938 - 3344	2926 - 3370
C		2935 - 3330	2913 - 3361	2941 - 3340	2930 - 3362
D	Cross-Validation	2931 - 3342	2838 - 3411	2938 - 3326	2794 - 3415
	Weighting Method	2937 - 3334	2844 - 3393	2944 - 3332	2814 - 3399
E	Cross-Validation	2931 - 3342	2661 - 3484	2938 - 3326	2649 - 3482
	Weighting Method	2937 - 3334	2615 - 3497	2944 - 3332	2614 - 3478

Table 5.12 : Point and Interval estimates for the floruit of ***Horgen*** culture obtained from the five methods.

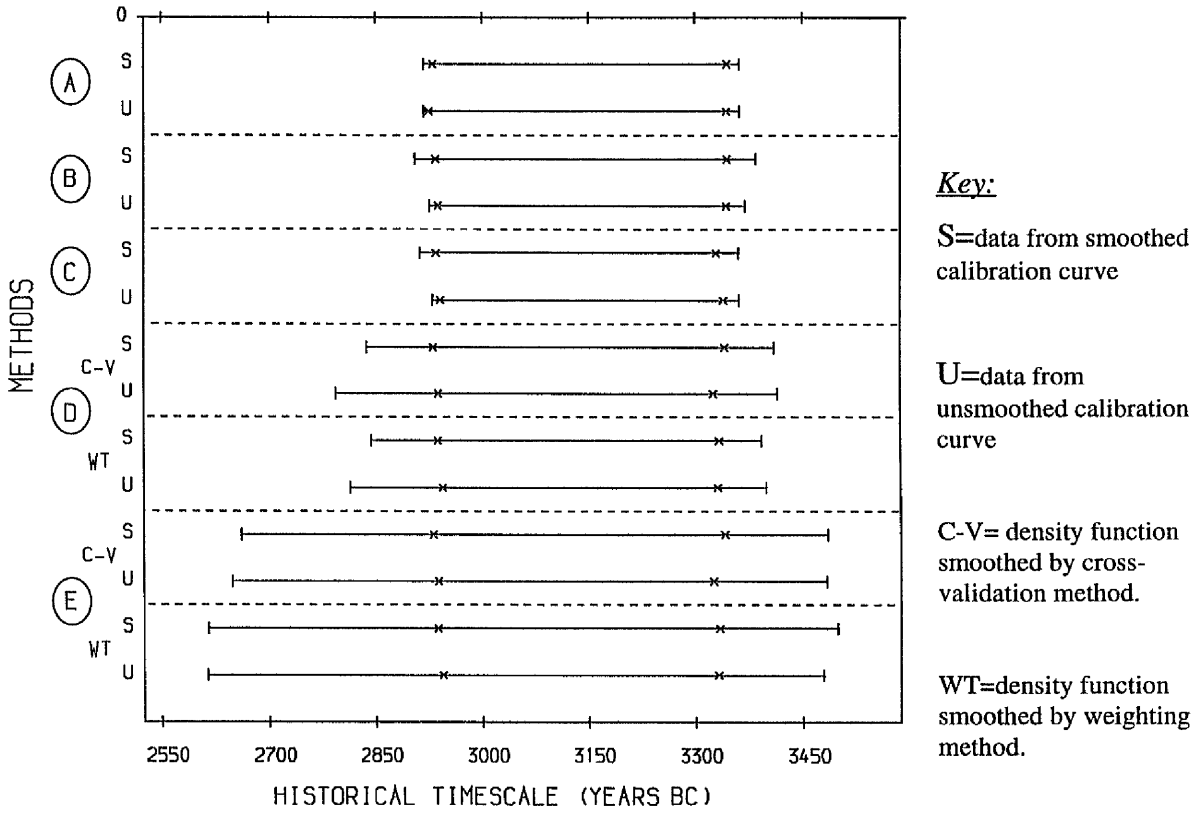

Figure 5.19 : Plots of point (x---x) and interval (|---|) estimates for the floruit of ***Horgen*** culture.

5.4.3 Childers Cultural Group

Twelve radiocarbon dates were collected from the *Childers* culture of Australia (table 5.6). The particular parts of the smoothed and unsmoothed calibration curves (figures 5.20 a&b) used to calibrated these radiocarbon dates are nearly linear with only a few wiggles on the unsmoothed curve. Due to this there is therefore only a single possible historical date corresponding to each radiocarbon date in the smoothed case and allmost all dates in the unsmoothed case. The full set of the calibrated historical dates with their estimated standard errors are given in table 5.13. Histogram plots of these calibrated dates are shown in figure 5.21a for both the smoothed and unsmoothed cases.

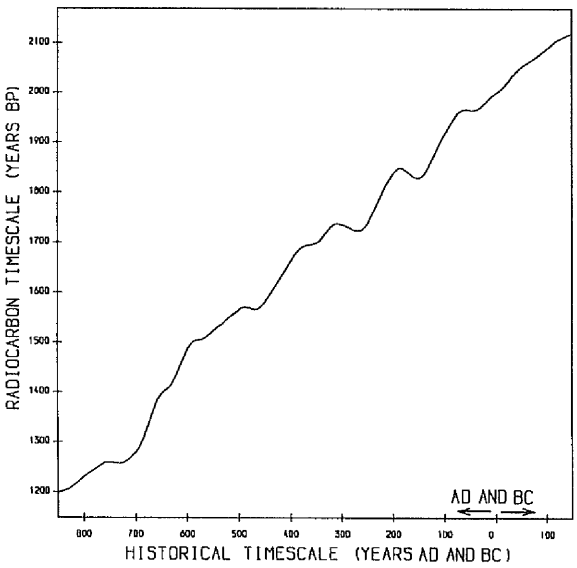

*Figure 5.20 :*a)
Part of the smoothed calibration curve used to calibrate the radiocarbon dates from ***Childers*** culture

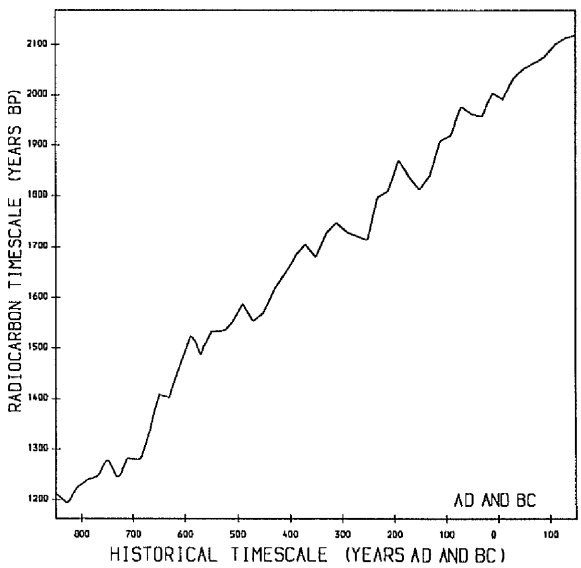

*Figure 5.20 :*b)
Part of the unsmoothed calibration curve used to calibrate the radiocarbon dates from ***Childers*** culture

# i	Radiocarbon Date ± Error (Years BP) $x_i \pm \sigma_i$	Corresponding historical dates (years AD) calibrated from smoothed curve.			Corresponding historical dates (years AD) calibrated from unsmoothed curve.		
		number of $\hat{t}_{ij}$	estimated $\hat{t}_{ij}$	estimated standard errors $se(\hat{t}_{ij})$	number of $\hat{t}_{ij}$	estimated $\hat{t}_{ij}$	estimated standard errors $se(\hat{t}_{ij})$
1	1250 ± 65	1	773	61	3	768 729 728	69 59 59
2	1380 ± 70	1	659	56	1	657	29
3	1440 ± 70	1	618	45	1	618	37
4	1300 ± 65	1	687	47	1	682	42
5	1470 ± 110	1	606	71	1	608	58
6	1330 ± 80	1	677	40	1	670	52
7	1610 ± 90	1	432	81	1	433	64
8	2060 ± 60	1	63 BC	73	1	64 BC	70
9	1450 ± 80	1	614	49	1	614	43
10	1660 ± 70	1	402	72	1	402	63
11	1470 ± 80	1	606	52	1	608	43
12	1580 ± 70	1	450	83	3	494 489 447	63 66 50

Table 5.13 : Estimates of historical dates corresponding to each observed radiocarbon age, and their estimated standard errors from both smoothed and unsmoothed calibration curve for the group of radiocarbon dates taken from ***Childers*** culture of Australia.

This group has one radiocarbon date (2060 ± 60 BP) which appears to be an outlier since it is 400 years away from the remaining dates and this may accordingly have a major influence on the floruit estimate. To investigate this, two analysis were carried out - one with and one without this possible outlier - and the resulting estimates compared in terms of floruit estimates.

Firstly, the whole data set has been analysed (*i.e.* including the outlier date) and the estimated p.d.f.'s are shown in figures 5.21b&c. Unfortunately, neither of the two methods of choice of smoothing parameter seems to provide sufficient smoothing for the density functions - particularly the weighting method. The corresponding estimates of cumulative distribution functions are given in figure 5.22.

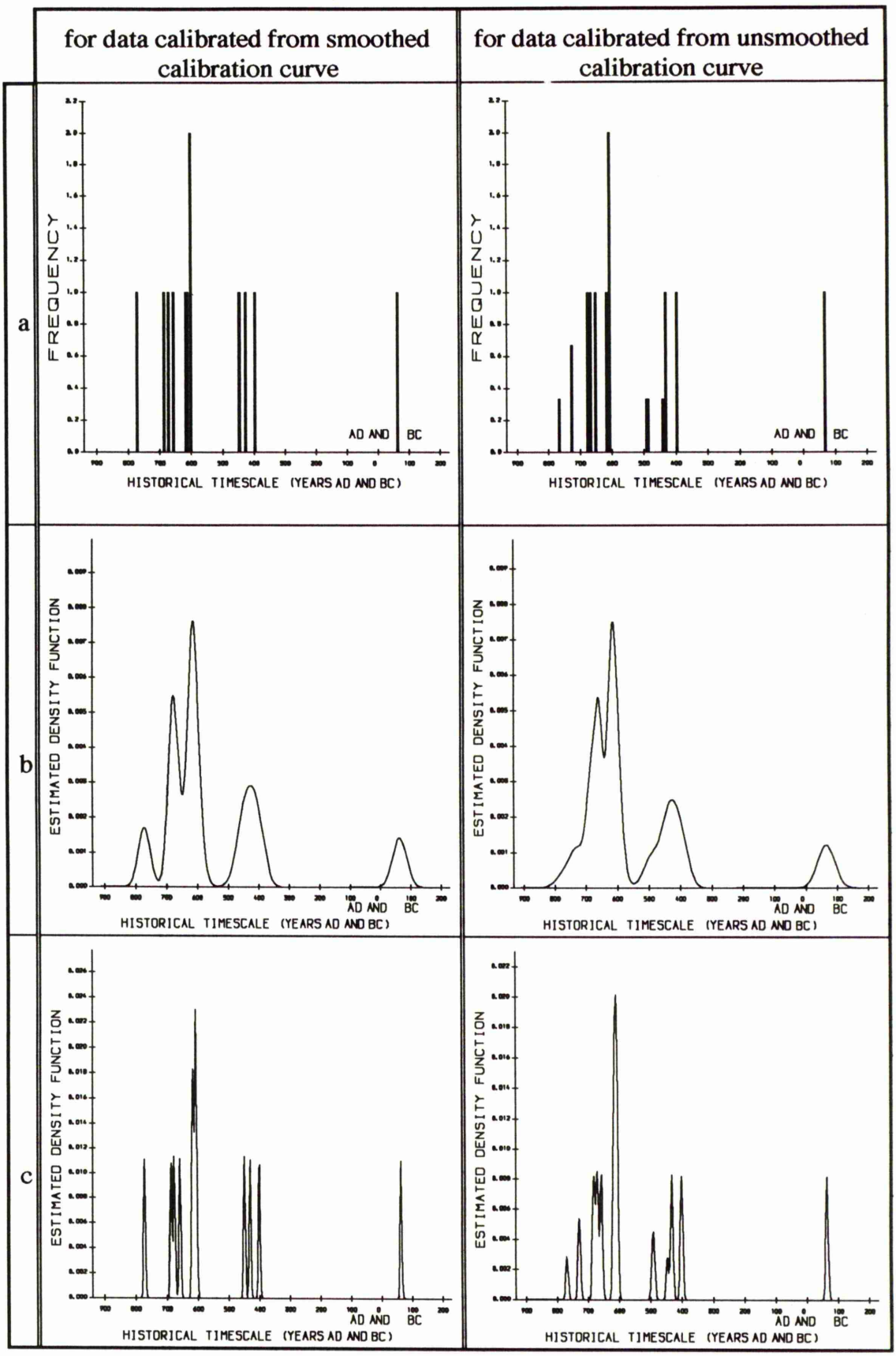

Figure 5.21 : a)Histogram plots for the calibrated historical dates for ***Childers*** culture and the plots of estimated density functions including the outlier date, b) smoothed by the cross-validation method and c) smoothed by the weighting method.

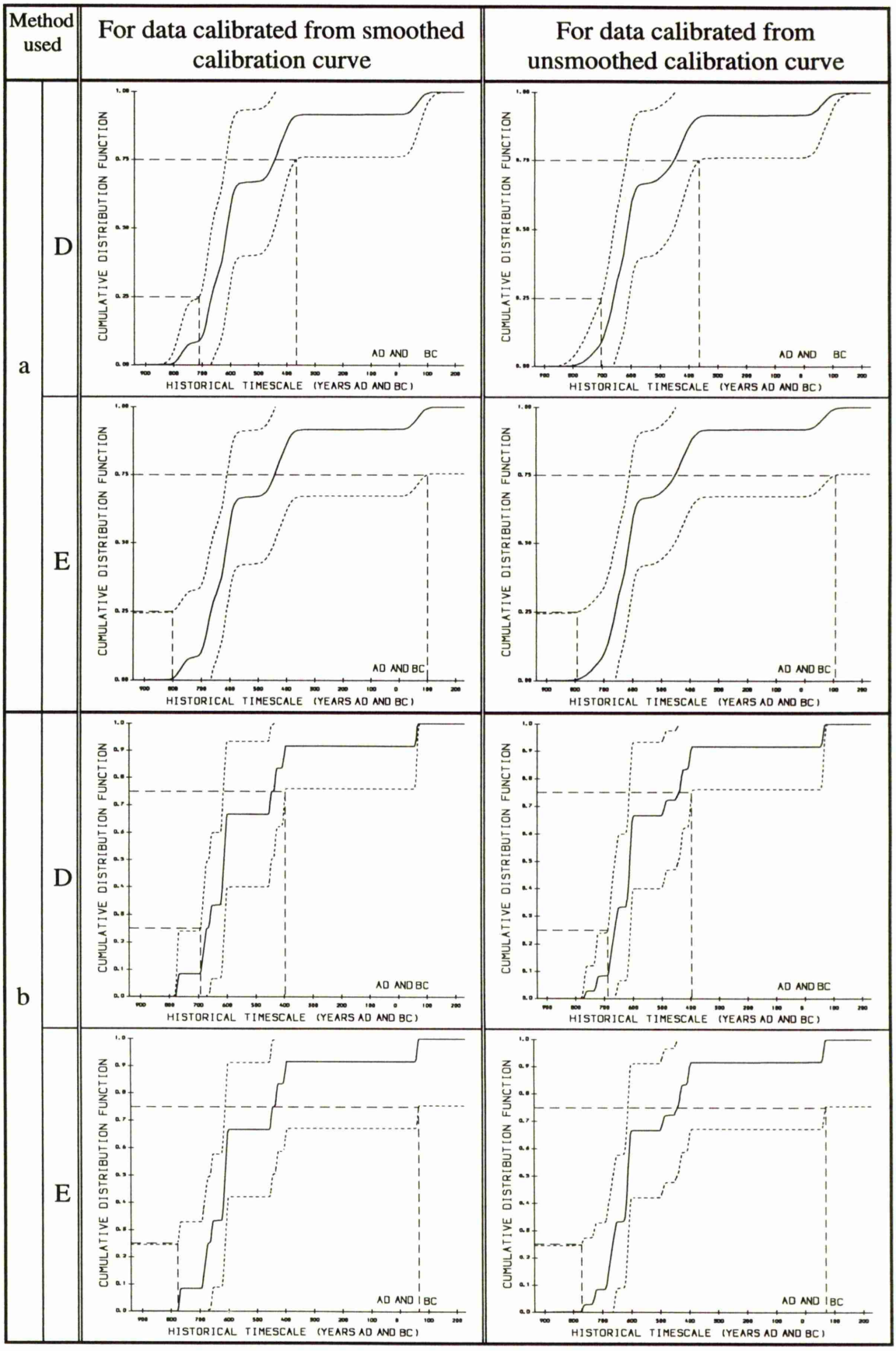

Figure 5.22 : Plots of estimated cumulative distribution functions for calibrated historical dates including the outlier date for ***Childers*** culture **a)** smoothed by cross-validation method, and **b)** smoothed by the weighting method.

The floruit estimates obtained from all five methods are given in table 5.14 and plotted in figure 5.23. It is quite clear there is an overall agreement between the five methods on the point estimate of the floruit particularly in the case of the smoothed calibration curve. Where there are no wiggles on the smoothed calibration curve, methods B and C provide similar results wider than that obtained from method A. When the unsmoothed calibration curve is used the results obtained from method C are narrower than those from both methods A and B due to presence of the wiggles on this unsmoothed curve.

The effect of the degree of smoothing of the density function on the floruit estimates can be seen when comparing the estimates from the two density estimation methods. Clearly the degree of smoothing given by the cross-validation method is greater than the degree of smoothing given by the weighting method for both the smoothed and unsmoothed data. As a result of this the estimates provided by methods D and E are wider when using cross-validation than the weighting procedure. The huge interval estimate produced by method E is due to the inflated value of the approximate constant variance of the c.d.f..

Floruit Estimation (years AD)					
Method used		For data calibrated from smoothed calibration curve.		For data calibrated from unsmoothed calibration curve.	
		Point	Interval	Point	Interval
A		668 - 440	685 - 407	663 - 439	679 - 407
B		667 - 440	699 - 385	663 - 439	690 - 401
C		667 - 440	699 - 385	663 - 451	690 - 419
D	Cross-Validation	667 - 442	710 - 365	660 - 451	702 - 364
	Weighting Method	667 - 440	691 - 397	663 - 440	687 - 395
E	Cross-Validation	667 - 442	802 - 99 BC	660 - 451	793 - 106 BC
	Weighting Method	667 - 440	777 - 67 BC	663 - 440	771 - 70 BC

Table 5.14 : Point and Interval estimates for the floruit of ***Childers*** culture obtained from the five methods with the outlier date included.

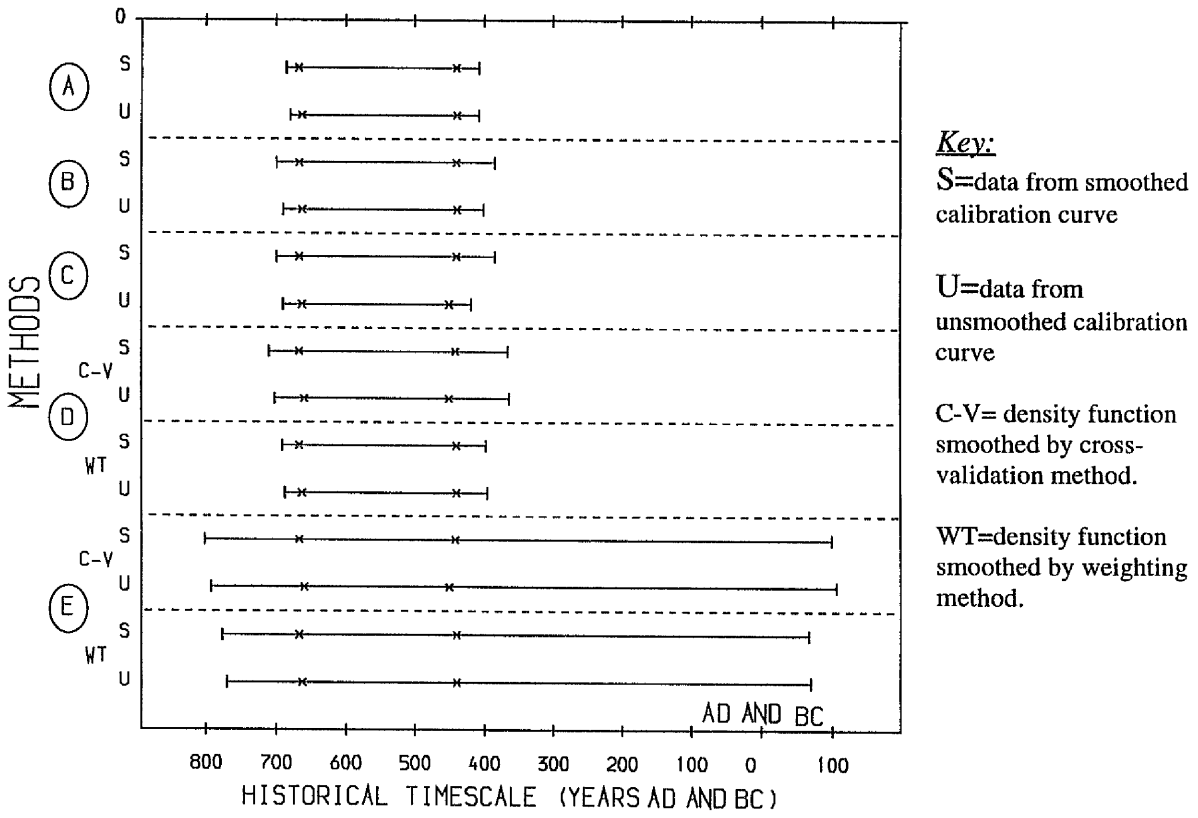

Figure 5.23 : Plots of point (x---x) and interval (|---|) estimates for the floruit of ***Childers*** culture with outlier date included.

Secondly, the outlier date has been removed and the data re-analysed. The p.d.f. estimates are shown in figure 5.24. These estimates have been smoothed more than those when the outlier included in particular when cross-validation used which seems over-smooth the p.d.f. estimates. The c.d.f estimates plotted in figure 5.25. The point and interval estimates for the floruit of the culture are given in table 5.15 and plotted in figure 5.26.

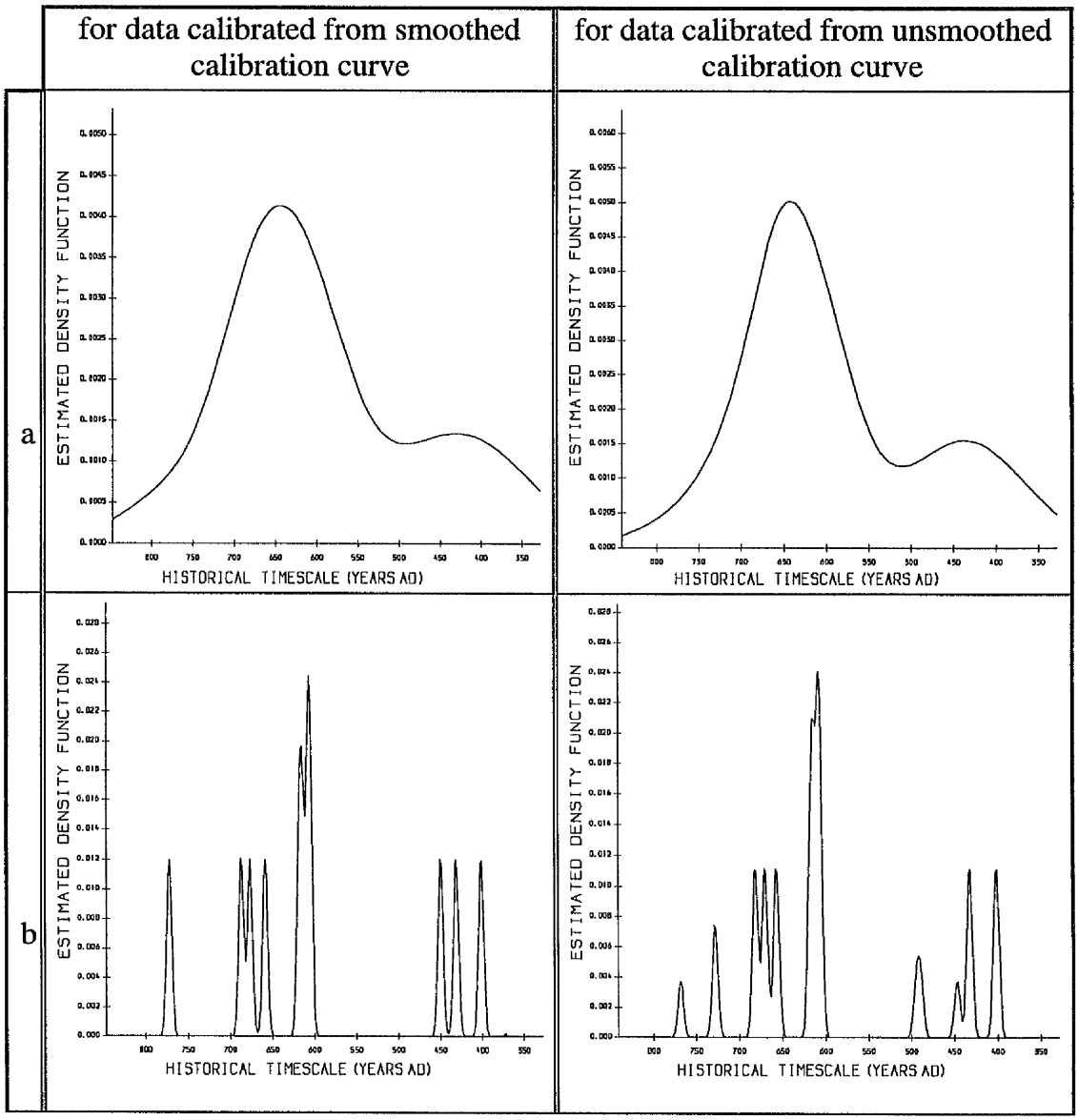

Figure 5.24 : Plots of estimated density functions for calibrated historical dates excluding the outlier date for ***Childers*** culture **a)** smoothed by cross-validation method and **b)** smoothed by the weighting method.

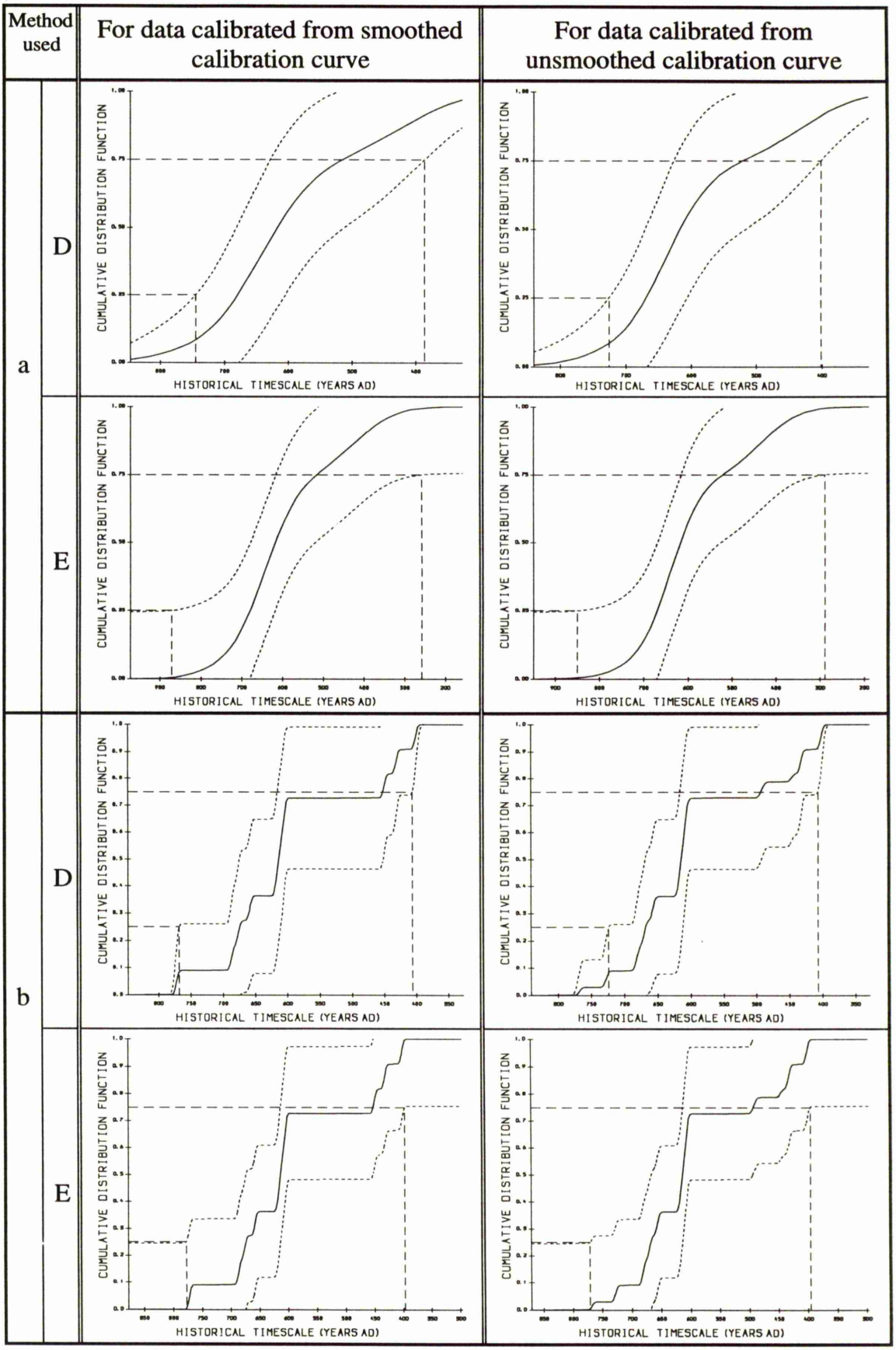

Figure 5.25 : Plots of estimated cumulative distribution functions for calibrated historical dates excluding the outlier date for ***Childers*** culture **a)** smoothed by cross-validation method, and **b)** smoothed by the weighting method.

Floruit Estimation (years AD)					
Method used		For data calibrated from smoothed calibration curve.		For data calibrated from unsmoothed calibration curve.	
		Point	Interval	Point	Interval
A		672 - 511	693 - 434	666 - 509	686 - 435
B		672 - 489	702 - 436	667 - 479	698 - 437
C		672 - 489	702 - 436	667 - 505	698 - 479
D	Cross-Validation	680 - 515	745 - 386	699 - 520	726 - 402
	Weighting Method	675 - 452	768 - 406	668 - 493	724 - 407
E	Cross-Validation	680 - 515	872 - 258	699 - 520	850 - 289
	Weighting Method	675 - 452	777 - 397	668 - 493	771 - 396

Table 5.15 : Point and Interval estimates for the floruit of ***Childers*** culture obtained from the five methods with the outlier date excluded.

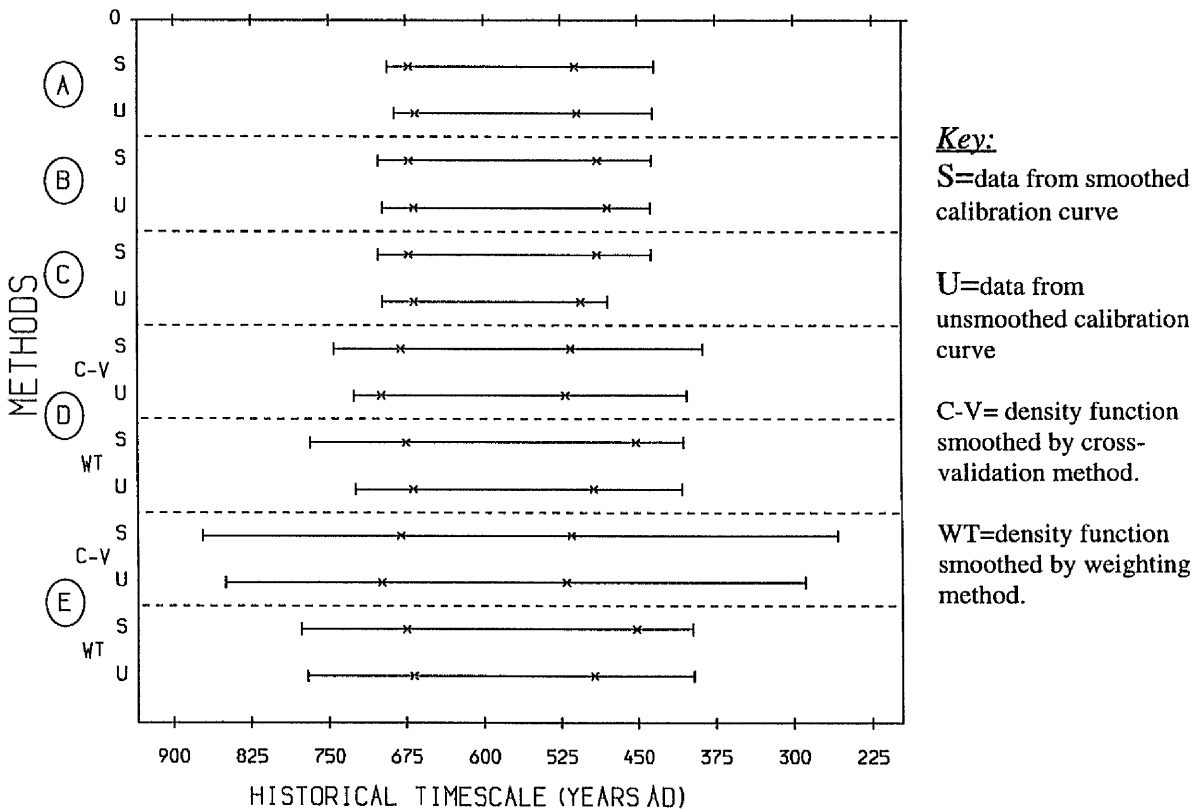

Figure 5.26 : Plots of point (x---x) and interval (|---|) estimates for the floruit of ***Childers*** culture with outlier date excluded.

The resulting estimates of the floruit from the pen and paper methods have, in general, similar pattern to those achieved when the potential outlier was included, while the estimates from the density estimation methods do not follow the same pattern since they are affected by degree of smoothing on the p.d.f.'s. For methods A, B and C the effect of omitting the potential outlier is to tighten the point and interval estimates of the floruit by differing amounts. For method D the effect is to tighten the point estimate and widen the interval estimate if the weighting method is used for the choice of smoothing parameter, while method E has tightened the interval estimate. This is due to the degree of smoothing on the density function being increased with the omission of the outlier.

Generally speaking, the effect of exclusion of the potential outlier is mainly to pull in the older end of the floruit estimate (both point and interval estimates) for all methods except in the case of method D which tends to shift the whole estimate to the younger end of the floruit (figure 5.27). Figure 5.27 and table 5.16 show the effect of the omission of the potential outlier date on the point and interval estimates of the floruit from the five methods. Obviously the most affected method was E which tightened the interval estimates by many years (not less than 287 years) compared to the other methods which tightened the interval estimates by no more than 52 years. One reason behind this is the inflation of the approximated constant variance for the c.d.f. of method E as a result of the small sample size of this group.

Effect (in years) of the outlier date on floruit estimation					
Method used		for data calibrated from smoothed calibration curve.		for data calibrated from unsmoothed calibration curve.	
		Point	Interval	Point	Interval
A		+4 , -71	+8 , -27	+3 , -70	+7 , -28
B		+5 , -49	+3 , -51	+4 , -40	+8 , -36
C		+5 , -49	+3 , -51	+4 , -54	+8 , -60
D	Cross-Validation	+13 , -73	+35 , -21	+39 , -69	+24 , -38
	Weighting Method	+8 , -12	+77 , -9	+5 , -53	+37 , -12
E	Cross-Validation	+13 , -73	+70 , -357	+39 , -69	+57 , -395
	Weighting Method	+8 , -12	0 , -464	+5 , -53	0 , -466

Table 5.16 : Effect of the omission of the potential outlier date in point and interval estimates for the floruit of the ***Childers*** culture obtained from the five methods (- sign means the effect is to pull in the estimate and + sign means the effect is to extend the estimate).

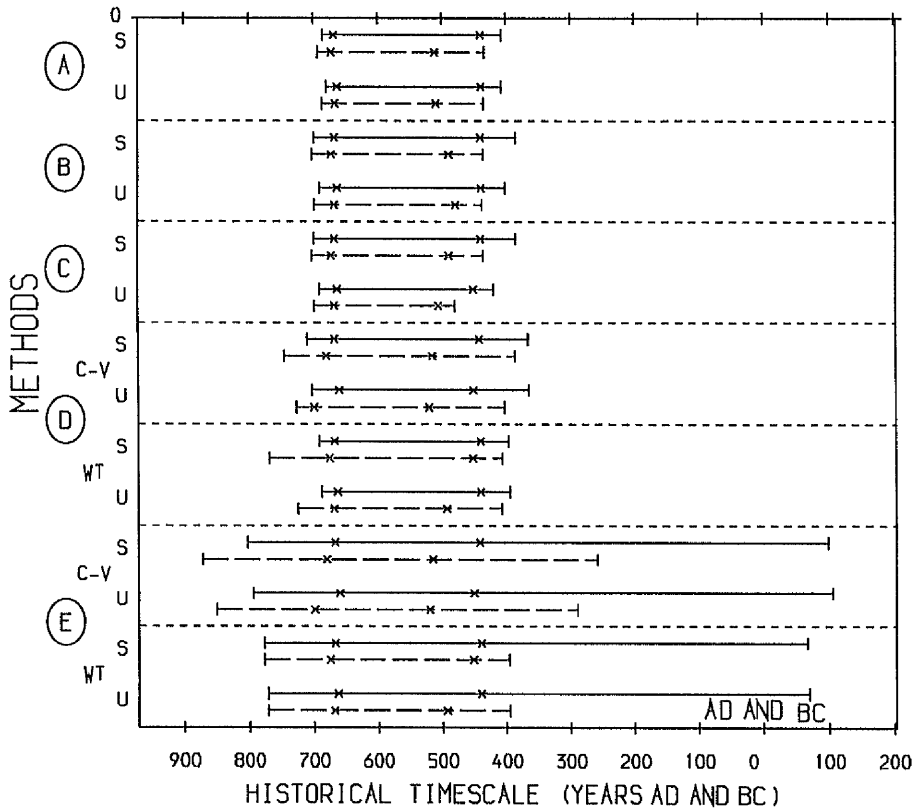

Key:
S=data from smoothed calibration curve

U=data from unsmoothed calibration curve

C-V= density function smoothed by cross-validation method.

WT=density function smoothed by weighting method.

Figure 5.27 : Comparison of point (x---x) and interval (|---|) estimates for the floruit of ***Childers*** culture with outlier date (solid line) and without outlier date (dotted line).

5.4.4 Cham Cultural Group

This group consists of 20 radiocarbon dates collected from different sites of the late Neolithic *Cham* culture of southern Germany. The individual dates were given in table 5.5 together with quoted errors, laboratory number and sites from which the dates were collected.

The parts of the smoothed and unsmoothed calibration curves used to calibrate this group are shown in figures 5.28a&b respectively. Each date was calibrated individually to the historical timescale. The full set of the calibrated dates are given in table 5.17 with their estimated standard errors. The histogram plots of the calibrated dates are shown in figure 5.29a.

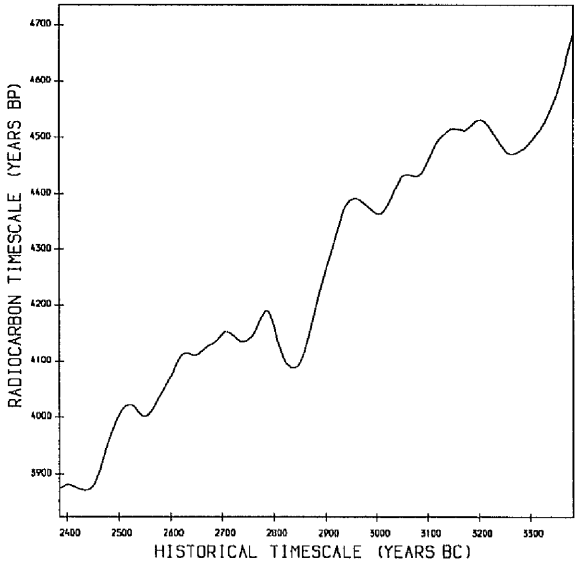

*Figure 5.28 :*a)
Part of the smoothed calibration curve used to calibrate the radiocarbon dates from ***Cham*** culture

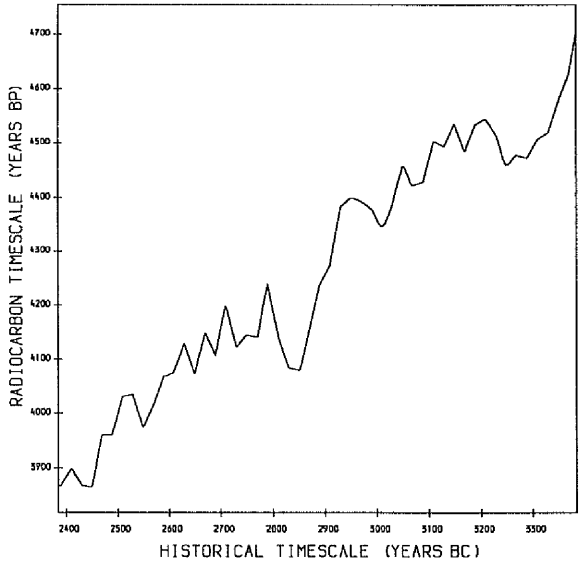

*Figure 5.28 :*b)
Part of the unsmoothed calibration curve used to calibrate the radiocarbon dates from ***Cham*** culture

#	Radiocarbon Date ± Error (Years BP) $x_i \pm \sigma_i$	Corresponding historical dates (years BC) calibrated from smoothed curve.			Corresponding historical dates (years BC) calibrated from unsmoothed curve.		
		number of $\hat{t}_{ij}$	estimated $\hat{t}_{ij}$	estimated standard errors $se(\hat{t}_{ij})$	number of $\hat{t}_{ij}$	estimated $\hat{t}_{ij}$	estimated standard errors $se(\hat{t}_{ij})$
1	3885 ± 40	1	2454	37	3	2401	41
						2419	42
						2454	14
2	4150 ± 60	5	2704	155	5	2699	21
			2714	148		2723	25
			2762	63		2772	21
			2804	27		2808	20
			2869	25		2867	24
3	4170 ± 70	3	2772	51	5	2704	25
			2798	38		2717	29
			2874	28		2776	24
						2804	23
						2872	30
4	4210 ± 60	1	2885	27	3	2786	20
						2796	20
						2883	26
5	4220 ± 55	1	2888	26	1	2886	24
6	4225 ± 30	1	2889	15	3	2788	11
						2793	11
						2887	14
7	4245 ± 50	1	2896	27	1	2895	47
8	4255 ± 40	1	2899	23	1	2900	38
9	4280 ± 35	1	2907	19	1	2910	34
10	4285 ± 85	1	2909	44	1	2912	25
11	4290 ± 45	1	2911	23	1	2913	14
12	4305 ± 35	1	2915	17	1	2916	11
13	4310 ± 60	1	2917	28	1	2917	18
14	4340 ± 40	1	2926	20	1	2923	12
15	4350 ± 40	1	2929	21	3	2924	12
						3007	42
						3011	34
16	4385 ± 35	3	2947	59	3	3934	65
			2973	80		3976	109
			3025	30		3029	30
17	4420 ± 35	1	3043	34	1	3040	16
18	4430 ± 45	1	3052	99	3	3043	21
						3065	42
						3087	30
19	4500 ± 80	3	3127	132	5	3133	62
			3234	86		3163	50
			3309	112		3177	52
						3235	46
						3307	76
20	4510 ± 30	3	3138	68	5	3139	24
			3227	36		3159	20
			3317	40		3181	21
						3231	18
						3318	84

Table 5.17 : Estimates of historical dates corresponding to each observed radiocarbon age, and their estimated standard errors from both smoothed and unsmoothed calibration curve for the group of radiocarbon dates taken from ***Cham*** culture.

Since one of the available radiocarbon dates (3885 ± 40 BP) is 265 years away from the remaining dates, it is potentially an outlier with considerable influence on the estimates of the floruit. Accordingly the analysis for this group will be carried out both with and without this date to consider its effect on the floruit estimation.

Firstly, all dates are included in the calculation of the floruit estimates. The p.d.f. estimates are graphed in figures 5.29b&c. Clearly the weighting method smoothed the density functions in both smoothed and unsmoothed calibration curves cases more than the cross-validation method. The effect of the outlier date on these estimates can be seen in the form of bump in the younger tail of the distribution. The corresponding c.d.f. estimates are plotted in figure 5.30.

The point and interval estimates for the floruit provided by the five methods are summarised in table 5.18 and plotted in figure 5.31.

The floruit estimates provided by the pen and paper methods are narrower than those of the density estimation methods. This can be explained by the very steep segment of the curve where more than 50% of the radiocarbon dates were calibrated on it. This actually narrows the floruit estimates obtained from the pen and paper methods since the technique used in these methods depends mainly on the calibrated dates close to the quartiles of the sample. On the other hand, the smoothing parameter involved in the density estimation methods and the standard errors of the cumulative distribution function have a remarkable effect on the floruit estimates particularly the widening of the interval estimates from method E (see figure 5.30).

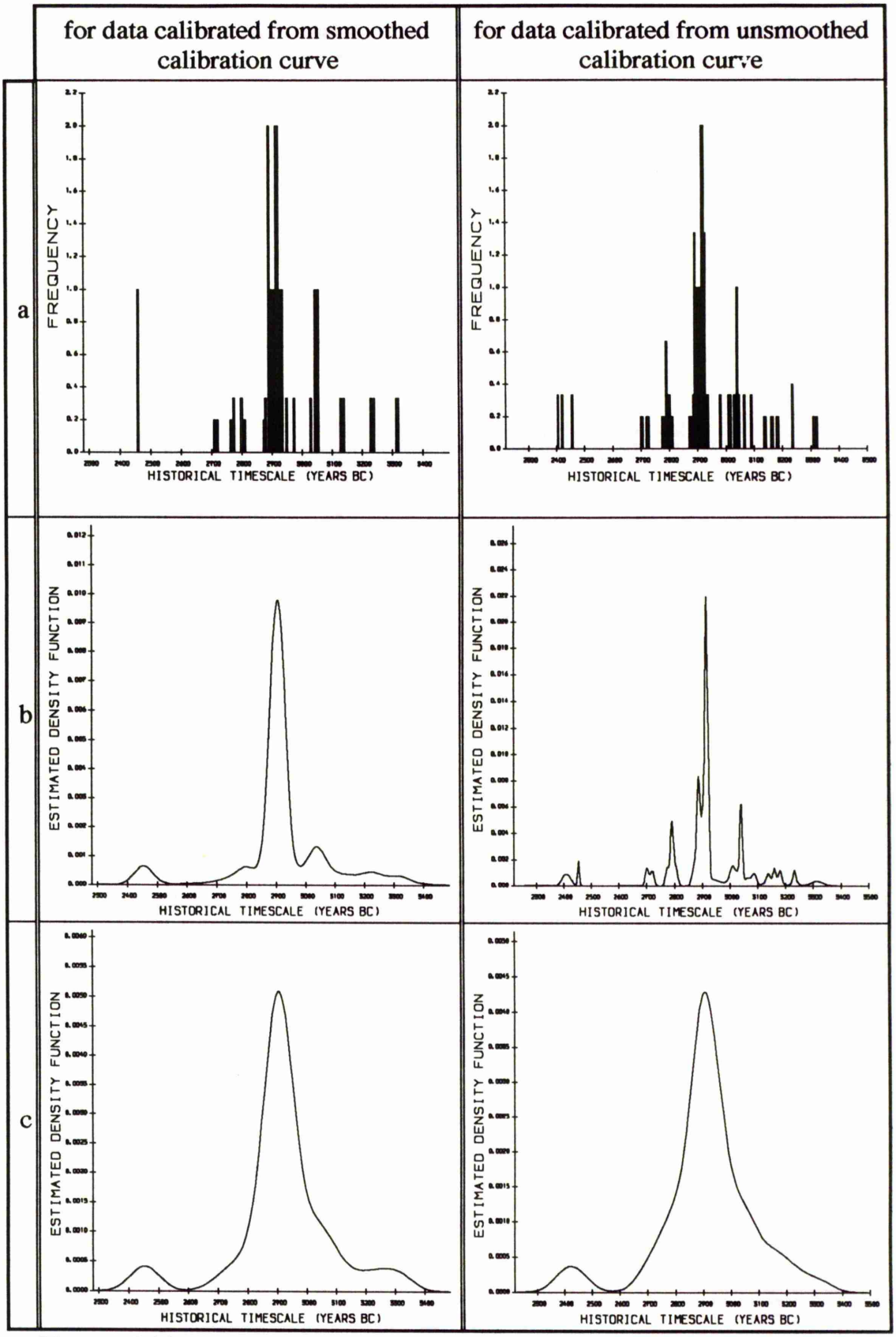

Figure 5.29 : a)Histogram plots for the calibrated historical dates for ***Cham*** culture and the plots of estimated density functions including the outlier date, b) smoothed by the cross-validation method and c) smoothed by the weighting method.

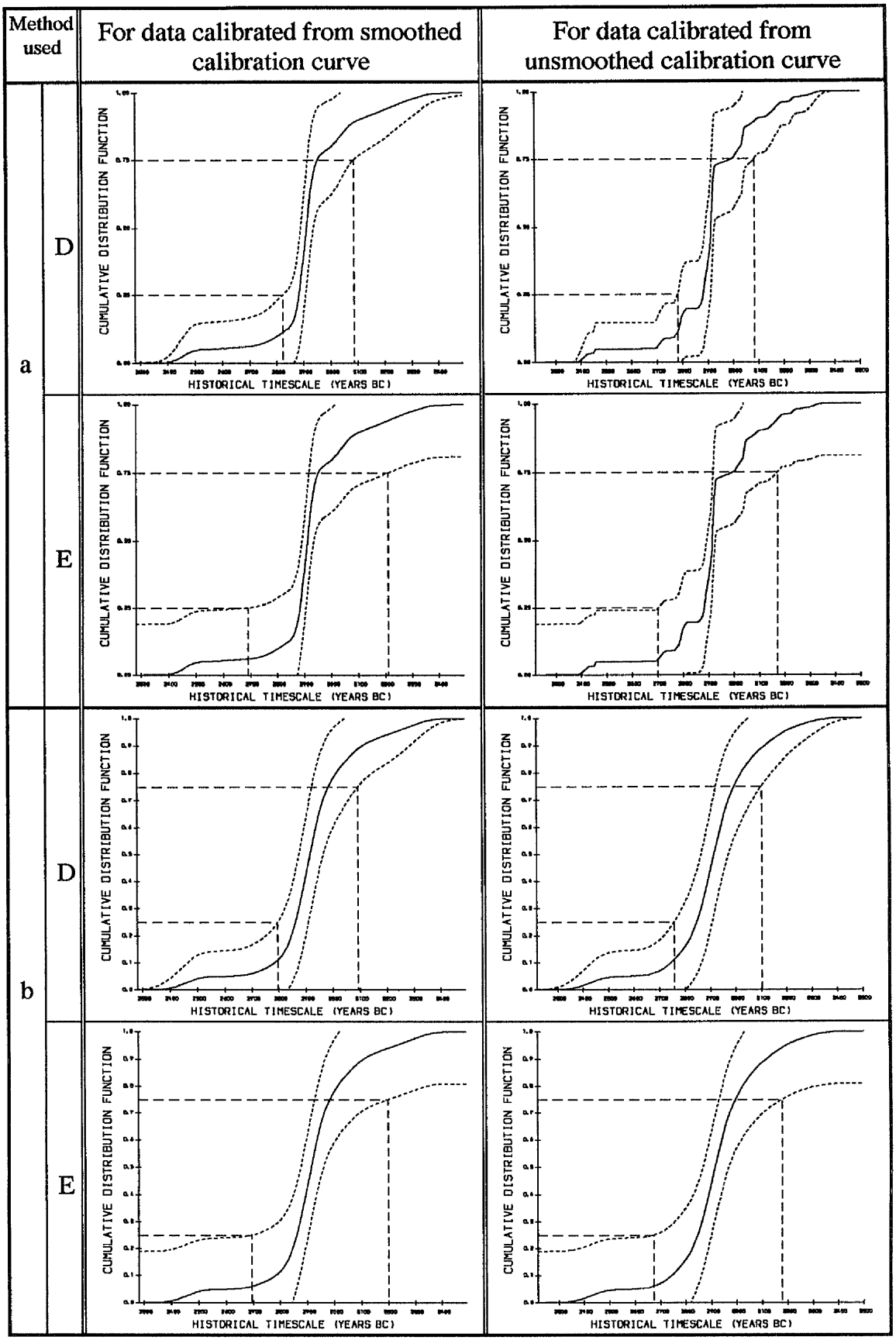

Figure 5.30 : Plots of estimated cumulative distribution functions for calibrated historical dates including the outlier date for ***Cham*** culture **a)** smoothed by cross-validation method, and **b)** smoothed by the weighting method.

Floruit Estimation (years BC)					
Method used		For data calibrated from smoothed calibration curve.		For data calibrated from unsmoothed calibration curve.	
		Point	Interval	Point	Interval
A		2889 - 3015	2881 - 3030	2788 - 3023	2781 - 3033
B		2888 - 2960	2874 - 3006	2885 - 3009	2864 - 3042
C		2888 - 2967	2874 - 2983	2849 - 2975	2836 - 2987
D	Cross-Validation	2883 - 2951	2822 - 3086	2883 - 2997	2782 - 3084
	Weighting Method	2863 - 2985	2797 - 3093	2847 - 2994	2758 - 3101
E	Cross-Validation	2883 - 2951	2691 - 3210	2883 - 2997	2701 - 3170
	Weighting Method	2863 - 2985	2696 - 3200	2847 - 2994	2673 - 3177

Table 5.18 : Point and Interval estimates for the floruit of ***Cham*** culture obtained from the five methods with the outlier date included.

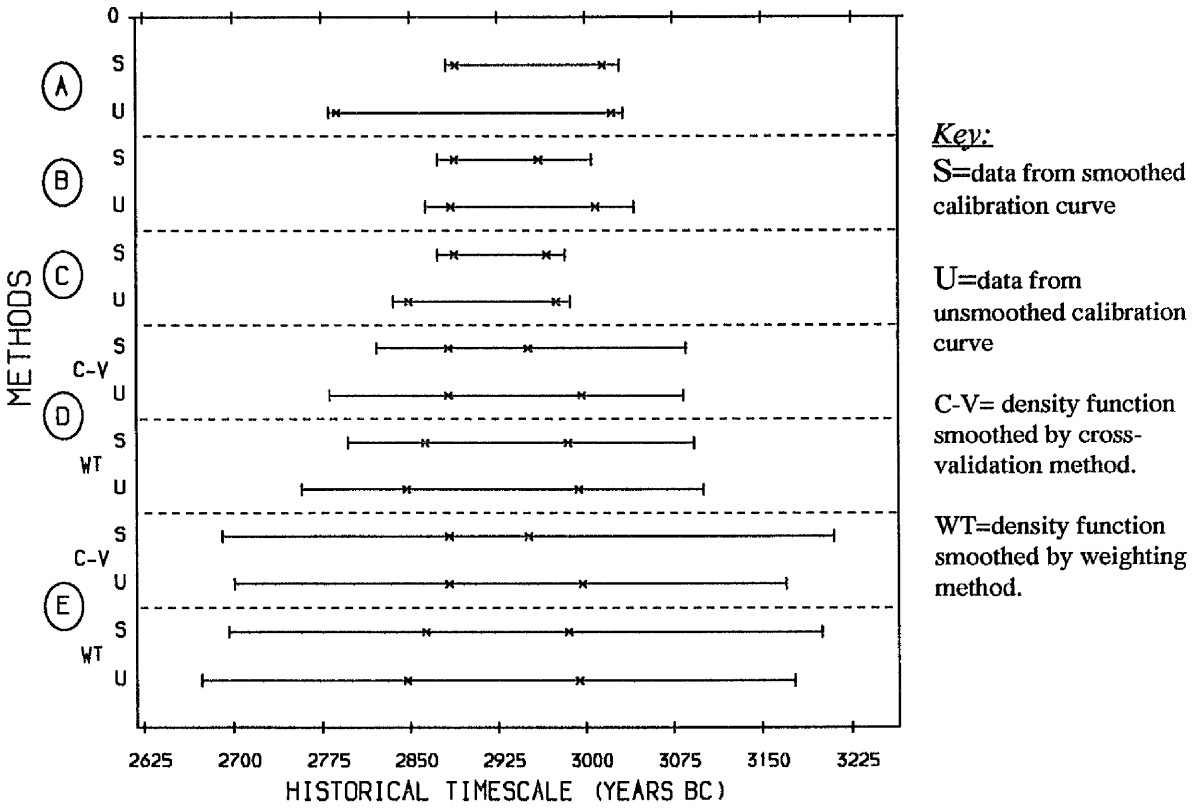

Figure 5.31 : Plots of point (x---x) and interval (|---|) estimates for the floruit of ***Cham*** culture with the outlier date included.

The assumed outlier date was then excluded from the group and re-analysed the remaining dates. The p.d.f. and c.d.f. estimates are graphed in figures 5.32 and 5.33 respectively. Since the cross-validation estimate clearly under-smoothes the p.d.f. only that obtained by the weighting method is considered. It is clearly noticeable the only change from figure 5.29 is that the bump in the tail of the distribution has been removed.

The resulting estimates for the floruit from the five methods are given in table 5.19 and plotted in figure 5.34. These estimates have a similar pattern to those when the outlier date was included wherefrom the estimates from pen and paper methods are narrower than those from the density estimation methods particularly interval estimates.

Investigating the effect of the omission of the potential outlier on the floruit estimate, it is found not to be the same for all five methods. But, in general, they all pulled in the younger end and extended the older end of the floruit with different amounts. Table 5.27 and figure 5.35 show the effect on the floruit estimates when the potential outlier date is omitted.

There is not much change in the estimates from method A except at the younger end of the point estimate which is pulled in by 101 years when the unsmoothed calibration curve was used. This happened because the calibration of the lower quartile of the sample occurred on the steep segment of the curve when the outlier date was omitted instead of the wiggly segment when it was included. Methods B and C have similar effects on the floruit estimates when the smoothed calibration curve was used as they both extended the older end. When the unsmoothed calibration curve was used (where there are more wiggles) the effect of omission of the outlier is more complicated. While method B has shifted the whole estimate and extended the older end for few

years, method C has tightened the estimate by pulling in the younger end more than extending the older end.

For the density estimation methods, the omission of the potential outlier has shifted the point estimate by a few years in the case of the smoothed calibration curve and pulled in the younger end more in the case of the unsmoothed calibration curve. More of an effect occurred in the interval estimates of both these two methods where the younger end has been pulled in more than the older end was extended.

Generally speaking, the omission of the potential outlier date does not materially influence the floruit estimates of the *Cham* culture except for method E when the interval estimate is influenced perceivably.

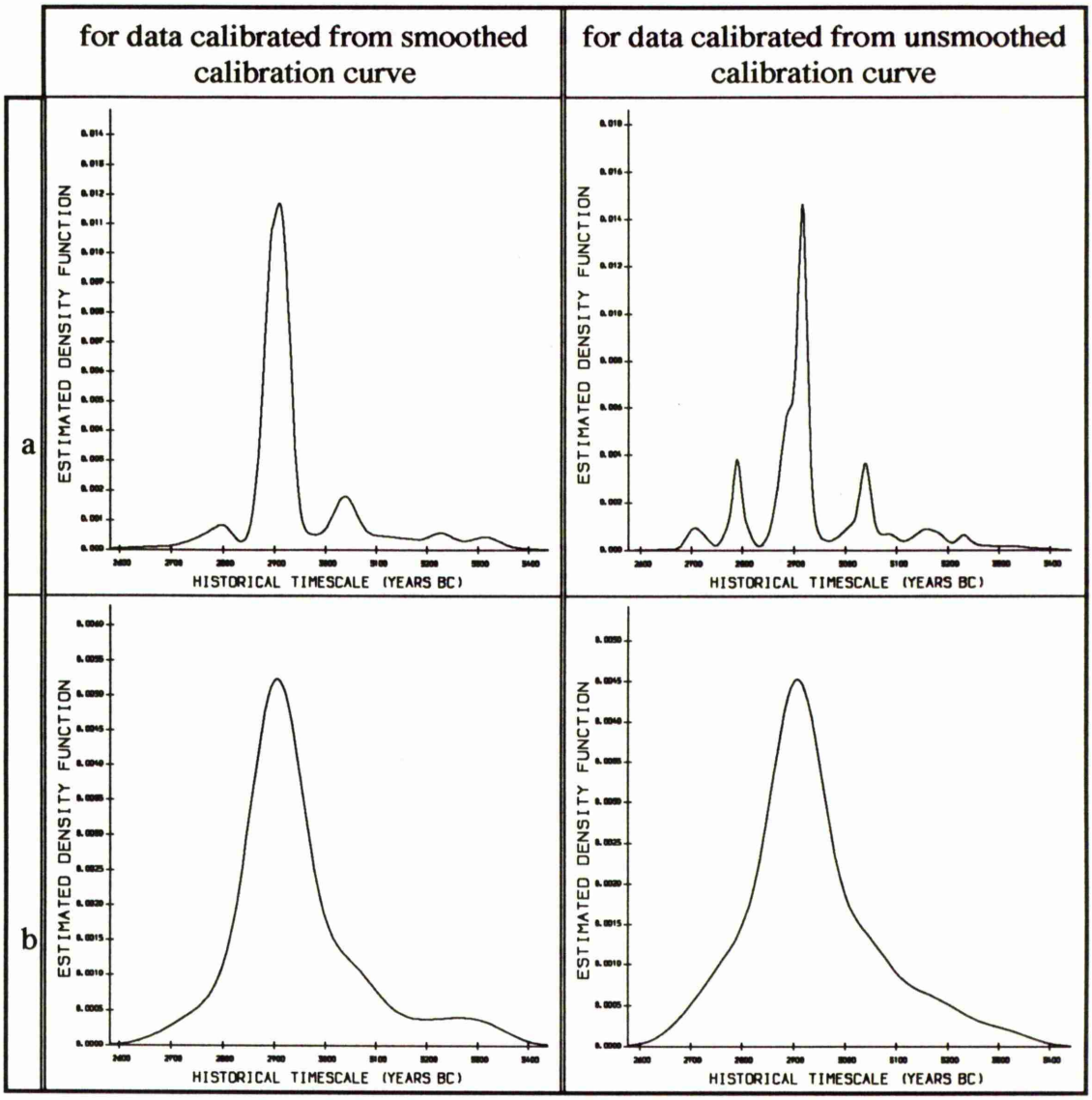

Figure 5.32 : Plots of estimated density functions for calibrated historical dates excluding the outlier date for ***Cham*** culture **a)** smoothed by cross-validation method and **b)** smoothed by the weighting method.

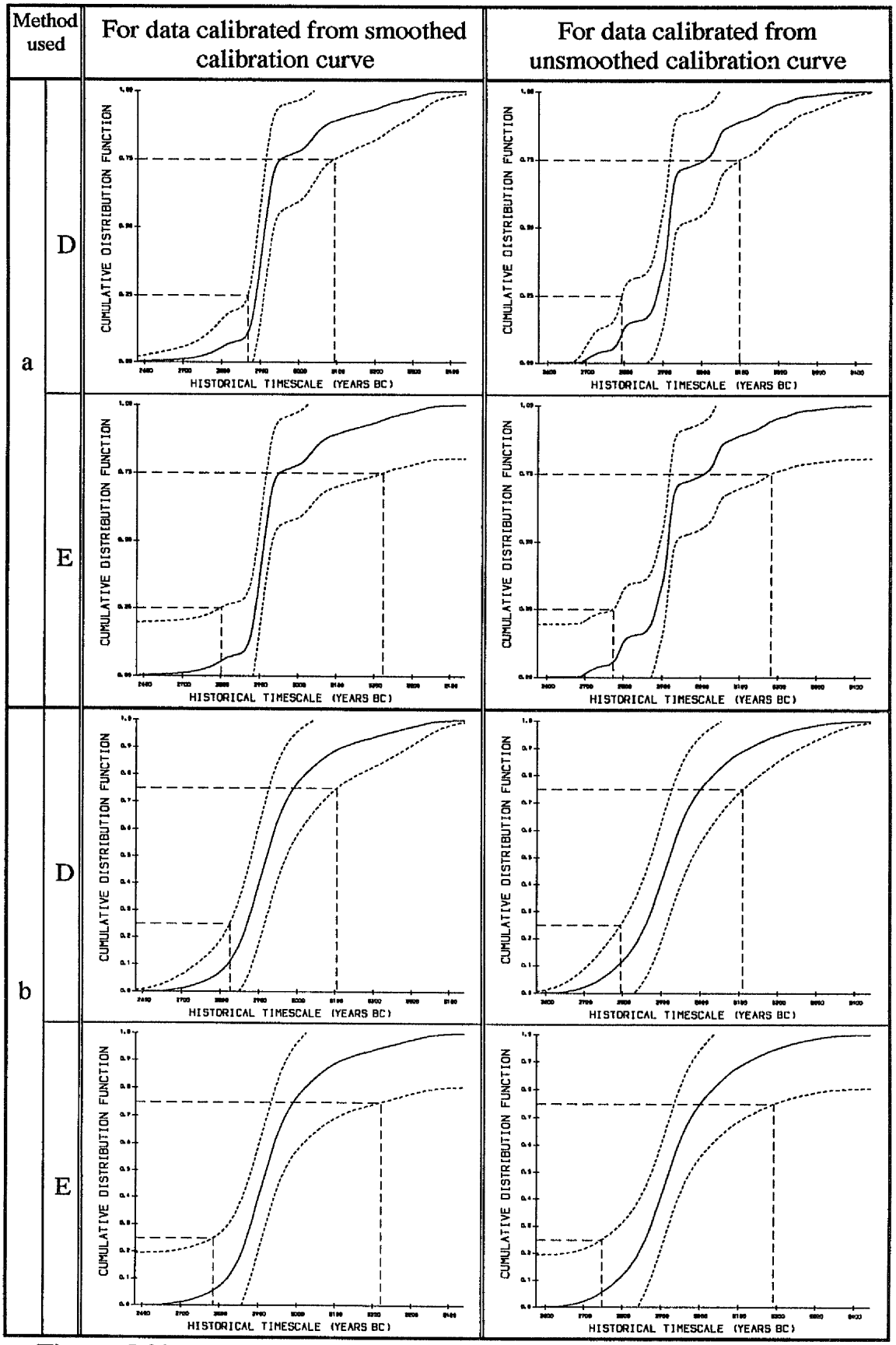

Figure 5.33 : Plots of estimated cumulative distribution functions for calibrated historical dates excluding the outlier date for ***Cham*** culture **a)** smoothed by cross-validation method and **b)** smoothed by the weighting method.

Floruit Estimation (years BC)					
Method used		For data calibrated from smoothed calibration curve.		For data calibrated from unsmoothed calibration curve.	
		Point	Interval	Point	Interval
A		2891 - 3020	2883 - 3033	2889 - 3025	2783 - 3034
B		2891 - 2986	2878 - 3031	2889 - 3016	2868 - 3049
C		2891 - 2986	2878 - 3003	2888 - 2993	2865 - 3008
D	Cross-Validation	2890 - 2953	2869 - 3094	2884 - 3008	2793 - 3099
	Weighting Method	2871 - 2992	2826 - 3104	2860 - 3001	2795 - 3111
E	Cross-Validation	2890 - 2953	2800 - 3224	2884 - 3008	2773 - 3182
	Weighting Method	2871 - 2992	2785 - 3221	2860 - 3001	2748 - 3191

Table 5.19 : Point and Interval estimates for the floruit of ***Cham*** culture obtained from the five methods with the outlier date excluded.

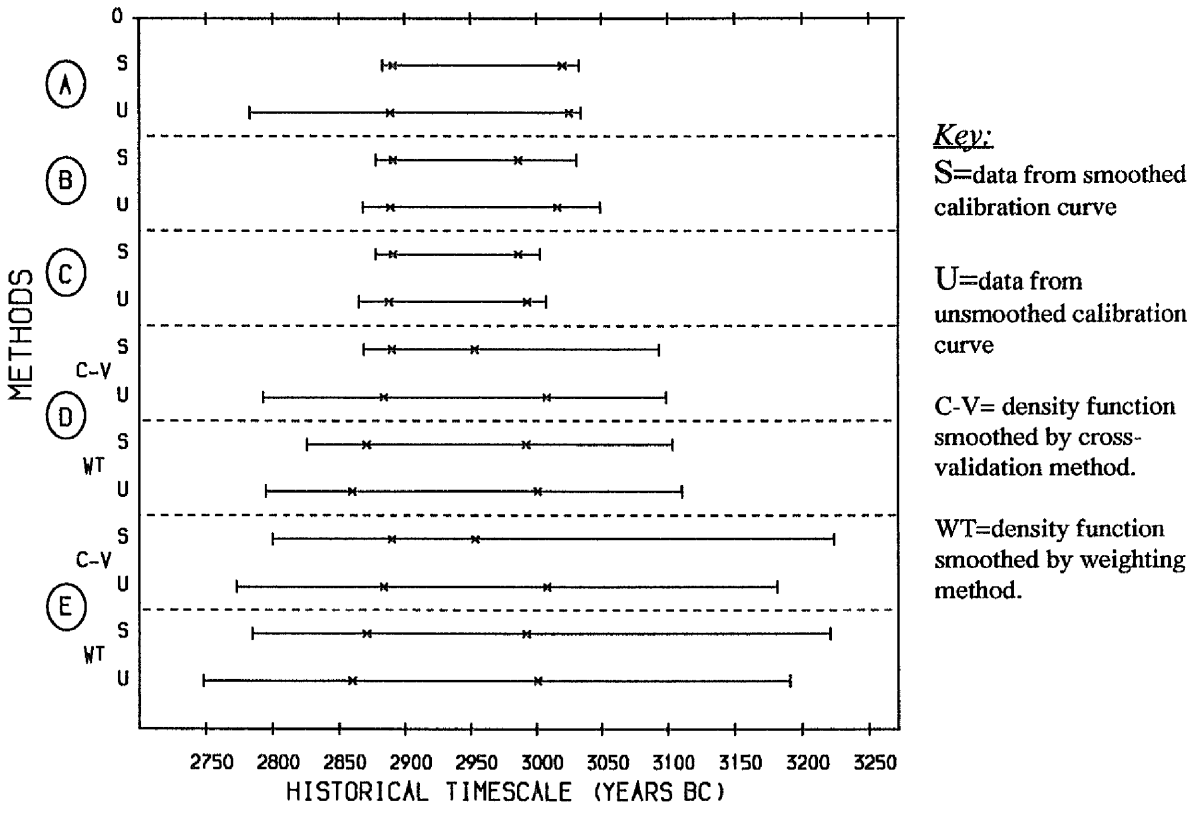

Figure 5.34 : Plots of point (x---x) and interval (|---|) estimates for the floruit of ***Cham*** culture with outlier date excluded.

Effect (in years) of the outlier date on floruit estimation					
Method used		for data calibrated from smoothed calibration curve.		for data calibrated from unsmoothed calibration curve.	
		Point	Interval	Point	Interval
A		-2 , +5	-2 , +3	-101 , +2	-2 , +1
B		-3 , +26	-4 , +25	-4 , +7	-4 , +7
C		-3 , +19	-4 , +20	-39 , +18	-29 , +21
D	Cross-Validation	-7 , +2	-47 , +8	-1 , +11	-11 , +15
	Weighting Method	-8 , +7	-29 , +11	-13 , +7	-37 , +10
E	Cross-Validation	-7 , +2	-109 , +14	-1 , +11	-72 , +12
	Weighting Method	-8 , +7	-89 , +21	-13 , +7	-75 , +14

Table 5.20 : Effect of the omission of the potential outlier date in point and interval estimates for the floruit of the ***Cham*** culture obtained from the five methods (- sign means the effect is to pull in the estimate and + sign means the effect is to extend the estimate).

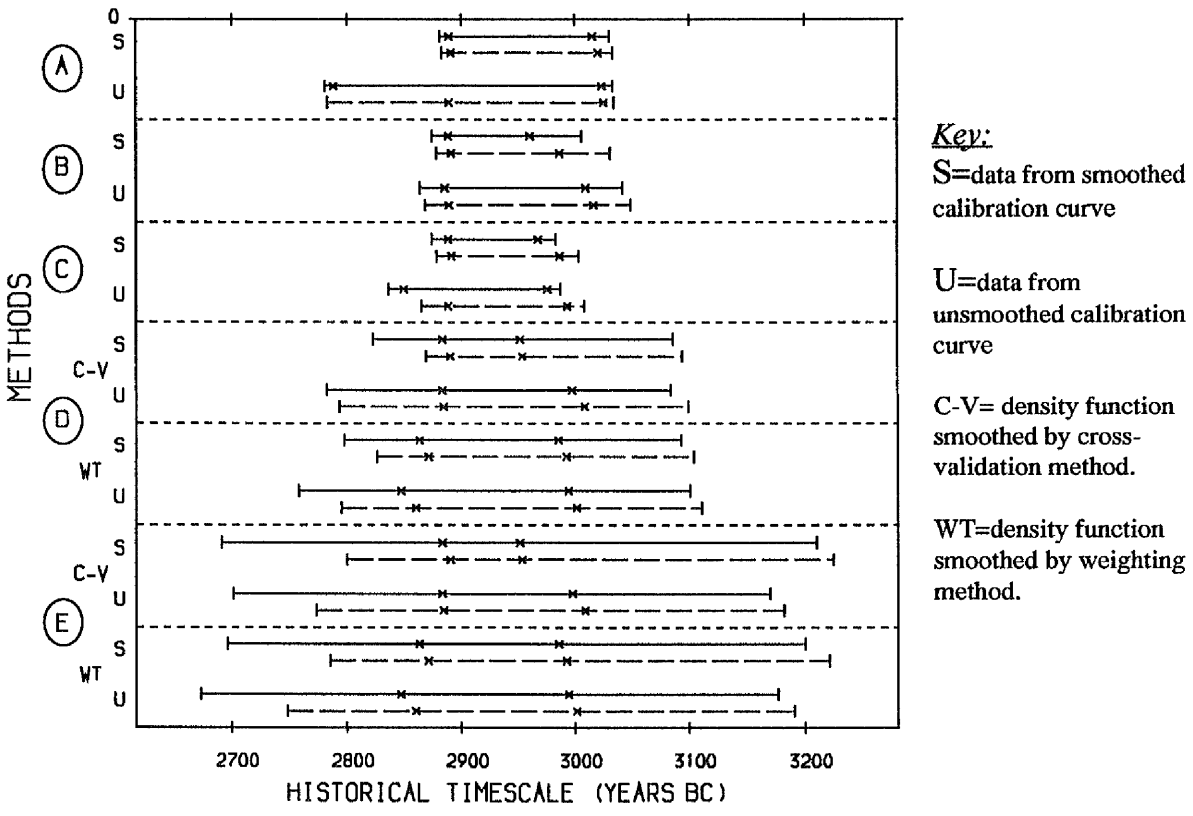

Figure 5.35 : Comparison of point (x---x) and interval (|---|) estimates for the floruit of ***Cham*** culture with outlier date (solid line) and without outlier date (dotted line).

5.4.5 Nok Cultural Group

This group is a series of 11 radiocarbon dates from the earliest Iron-smelting horizon in west Africa, the Nok culture of Nigeria. These dates were given in table 5.7 with the quoted errors and laboratory numbers.

The parts of the smoothed and unsmoothed calibration curves which were used to calibrate these dates are shown in figures 5.36a&b respectively. As can be seen, this part is a combination of linear, steep, flat and then steep segments.

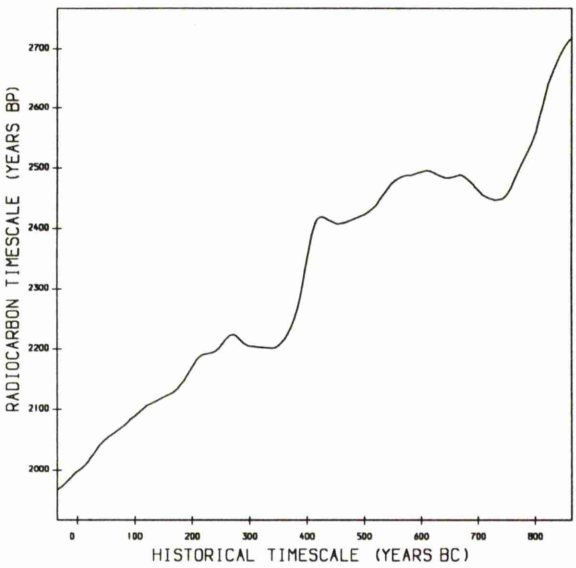

*Figure 5.36 :*a)
Part of the smoothed calibration curve used to calibrate the radiocarbon dates from ***Nok*** culture

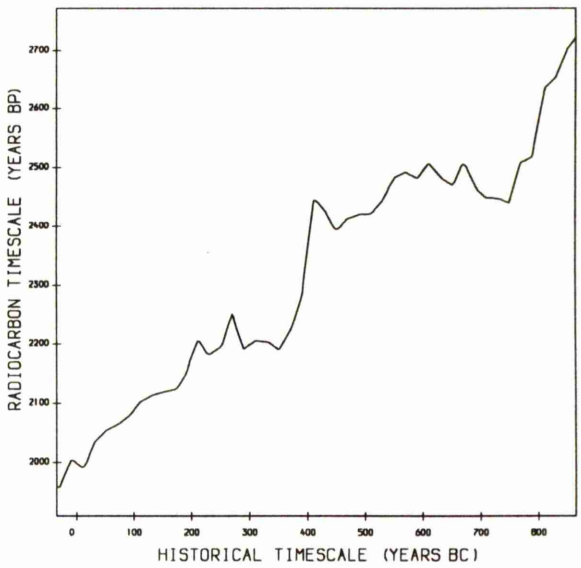

*Figure 5.36 :*b)
Part of the unsmoothed calibration curve used to calibrate the radiocarbon dates from ***Nok*** culture

Each radiocarbon date has been calibrated individually and the corresponding historical dates which might generate these radiocarbon dates are given with their estimated standard errors in table 5.21 and shown graphically in the histogram plots of figure 5.37a.

# i	Radiocarbon Date ± Error (Years BP) $x_i \pm \sigma_i$	Corresponding historical dates (years BC) calibrated from smoothed curve.			Corresponding historical dates (years BC) calibrated from unsmoothed curve.		
		number of $\hat{t}_{ij}$	estimated $\hat{t}_{ij}$	estimated standard errors $se(\hat{t}_{ij})$	number of $\hat{t}_{ij}$	estimated $\hat{t}_{ij}$	estimated standard errors $se(\hat{t}_{ij})$
1	2042 ± 126	1	39	134	1	37	137
2	2269 ± 143	1	384	64	1	386	81
3	2121 ± 116	1	151	128	1	157	124
4	2541 ± 74	1	794	52	1	794	21
5	2488 ± 84	3	588 627 769	98 103 60	5	597 625 661 678 764	104 117 77 73 39
6	2541 ± 104	1	794	73	1	794	29
7	2291 ± 133	1	389	48	1	389	75
8	2230 ± 120	1	369	88	3	263 277 372	69 64 68
9	2390 ± 140	1	410	59	1	403	27
10	2250 ± 100	1	378	60	1	380	56
11	2160 ± 95	1	194	92	1	194	54

Table 5.21 : Estimates of historical dates corresponding to each observed radiocarbon age, and their estimated standard errors from both smoothed and unsmoothed calibration curve for the group of radiocarbon dates taken from ***Nok*** culture.

The p.d.f. and the c.d.f. estimates are shown in figures 5.37b&c and 5.38 respectively. Although the cross-validation choice of smoothing parameter has slightly over-smoothed the p.d.f. estimates, it looks more realistic than the weighting method which under-smoothes the p.d.f. estimates.

The results of point and interval estimates for the floruit of the *Nok* culture obtained from the five methods are given in table 5.22 and plotted in figure 5.39.

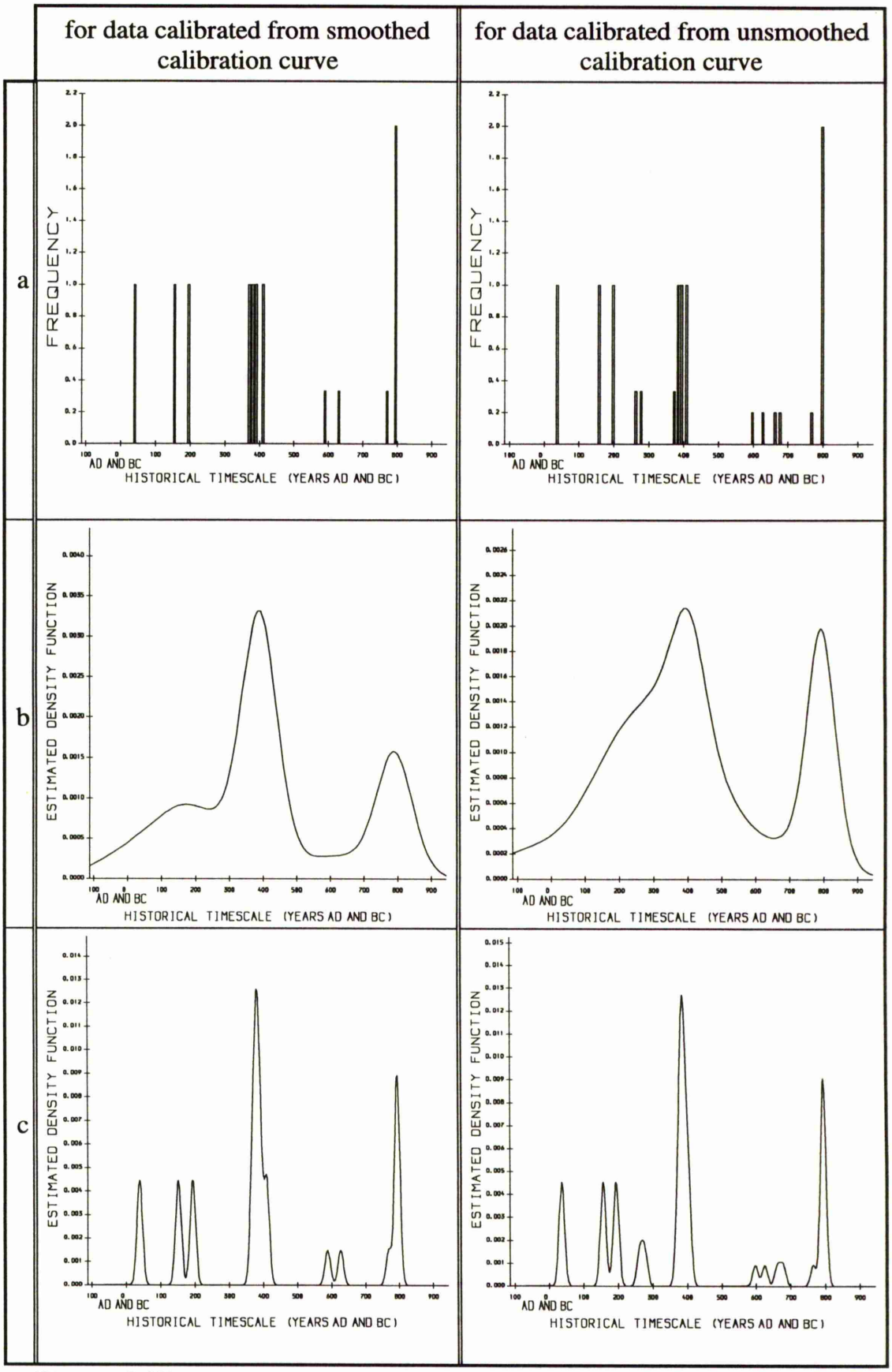

Figure 5.37 : **a)**Histogram plots for the calibrated historical dates for ***Nok*** culture and the plots of estimated density functions, **b)** smoothed by the cross-validation method and **c)** smoothed by the weighting method.

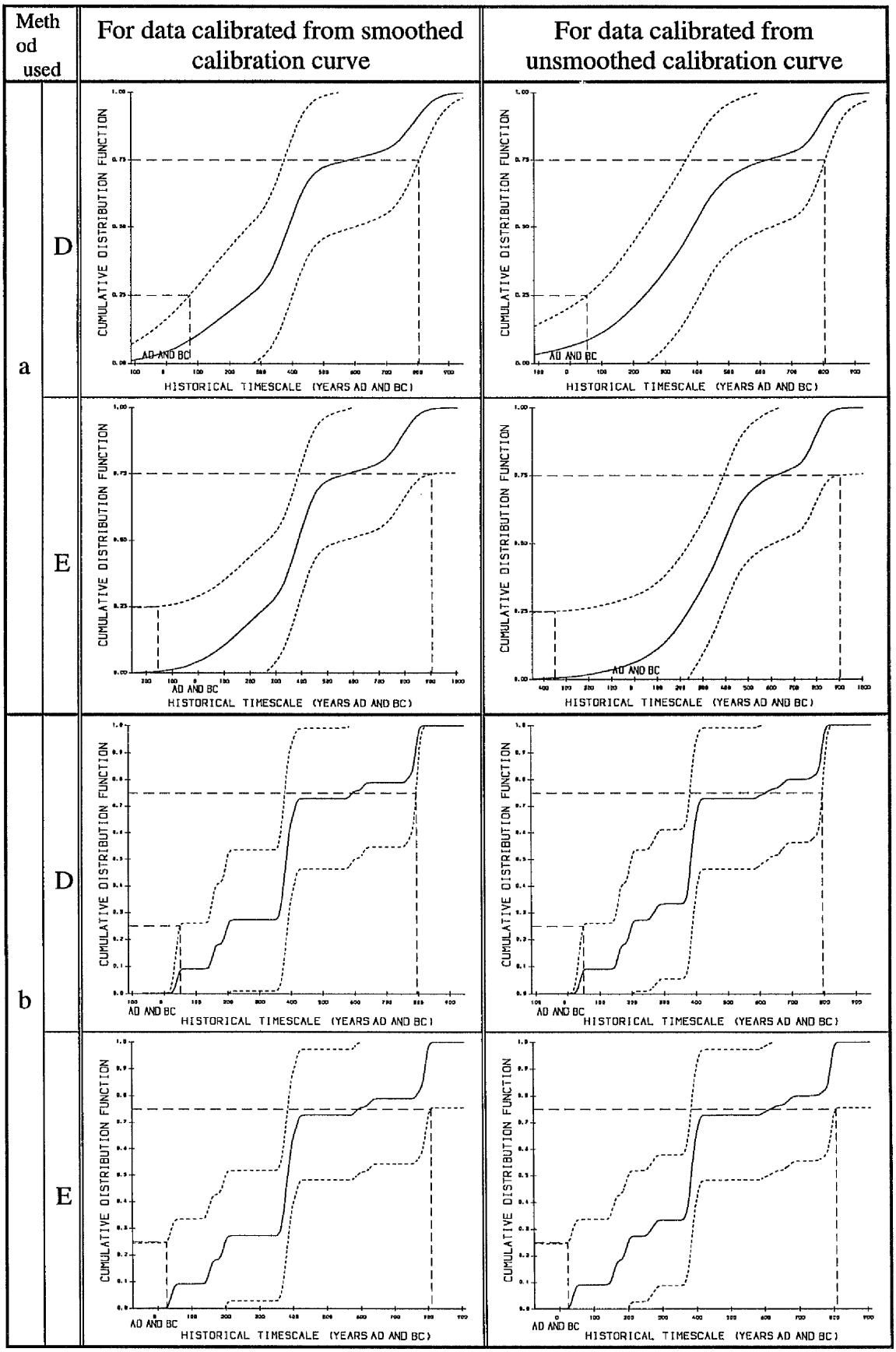

Figure 5.38 : Plots of estimated cumulative distribution functions for calibrated historical dates for the ***Nok*** culture **a)** smoothed by cross-validation method, and **b)** smoothed by the weighting method.

Floruit Estimation (years BC)					
Method used		For data calibrated from smoothed calibration curve.		For data calibrated from unsmoothed calibration curve.	
		Point	Interval	Point	Interval
A		207 - 756	129 - 789	201 - 757	125 - 792
B		237 - 662	176 - 724	245 - 674	202 - 724
C		237 - 628	176 - 661	221 - 636	188 - 660
D	Cross-Validation	265 - 580	74 - 805	236 - 622	54 - 806
	Weighting Method	199 - 594	51 - 795	199 - 620	49 - 794
E	Cross-Validation	265 - 580	155 AD - 905	236 - 622	350 AD - 904
	Weighting Method	199 - 594	26 - 810	199 - 620	24 - 809

Table 5.22 : Point and Interval estimates for the floruit of ***Nok*** culture obtained from the five methods.

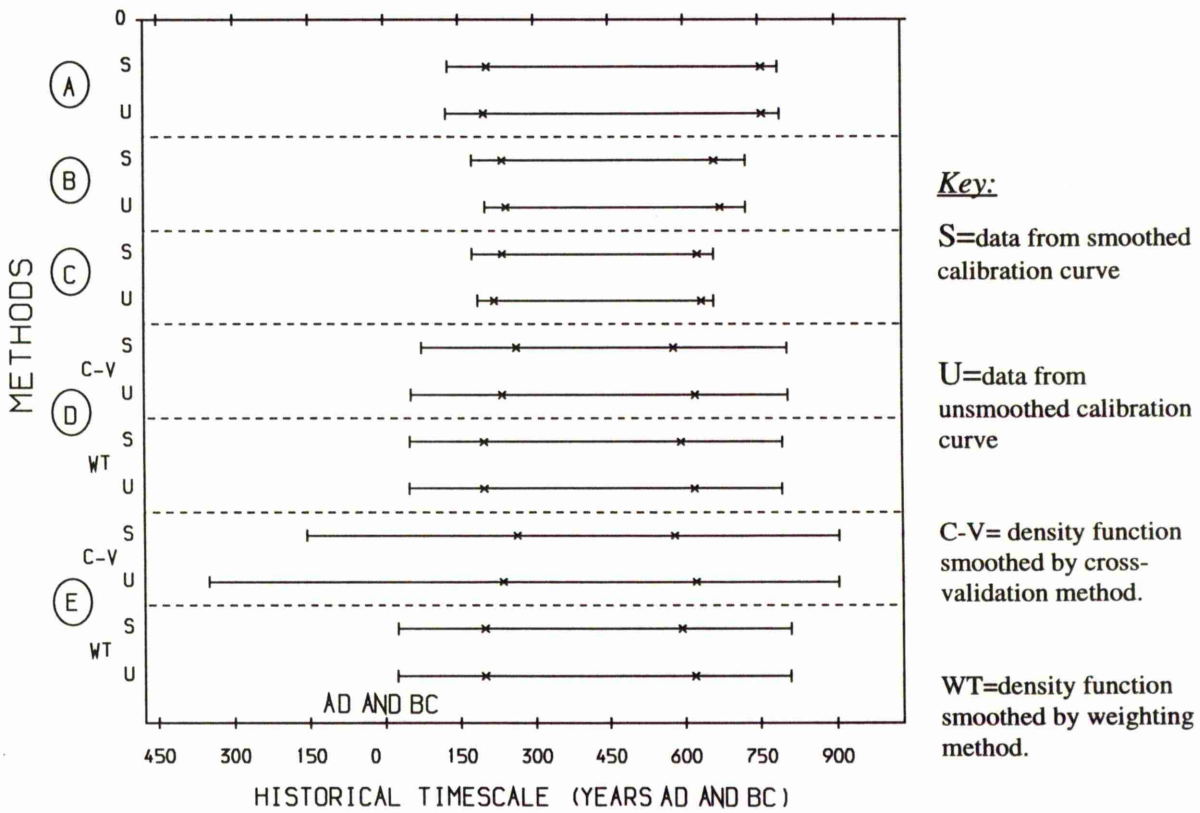

Figure 5.39 : Plots of point (x---x) and interval (|---|) estimates for the floruit of ***Nok*** culture.

Due to the wiggles at the bottom of the two steep segments, method A produced the wider estimates for the floruit compared with methods B, while the narrowest estimates were provided by method C. Comparing the two estimates of the floruit obtained from method D, it appears that the weighting method under-smoothed the density function and provided a wider floruit estimate. This happens very occasionally for small sample sizes and can be explained as a direct effect of the amount of smoothing on the density function. If the smoothing parameter is chosen too small the gaps between the spikes in the p.d.f. estimate causes discontinuities on the c.d.f. estimate (figure 5.38). The effect of this may be to produce sudden large changes in the interval estimate for very small changes in the data *i.e.* too little smoothing leaves the interval estimation procedure not at all robust.

Method E, as usual, provided the widest interval estimate for the floruit compared with the other methods and in particular when the p.d.f. smoothed by cross-validation

In this instance there is little difference in all of the interval estimates based on the smoothed or unsmoothed calibration curves. Generally speaking, the estimates of the floruit obtained from all the methods are wide which is due not only to the small sample size but also to the shape of the calibration curve at this horizon.

5.5 Sites within Culture

In this section, the five methods of floruit estimation will be applied to the two groups of radiocarbon dates taken from the *Cortaillod* and *Sâone-Rhône* cultures. Then the radiocarbon dates collected from two sites within each of these cultures (*Seeberg-Burgäschisee-S* and *Twann* sites of the *Cortaillod* culture and *Auvernier, La Saunerie* and *Yverdon* sites of the *Sâone-Rhône* culture) will be analysed for each site individually to consider, first, the temporal relation between the two sites within each culture and then the effect of reducing the sample size on the floruit estimate. The choice of these sites was based on the fact that most of the radiocarbon dates collected from each culture were collected from these two sites in the culture.

5.5.1 Cortaillod culture

This data group consists of 51 radiocarbon dates taken from twelve different sites in the *Cortaillod* culture of Switzerland. The radiocarbon dates , x_i and the quoted errors, σ_i , were given in table 5.3 together with the laboratory number in which the measurement was carried out and the site from which the date was taken.

The part of the calibration curve which was used to calibrate the radiocarbon dates is shown in figures 5.40a&b for both the smoothed and unsmoothed calibration curves. Most of the numerous wiggles appearing in the unsmoothed curve have been eased out in the smoothed curve.

Each radiocarbon date, x_i , is calibrated separately. The full set of $\hat{t}_{ij}$ calibrated from both smoothed and unsmoothed calibration curve are given in table 5.23, together with the corresponding standard errors of such.

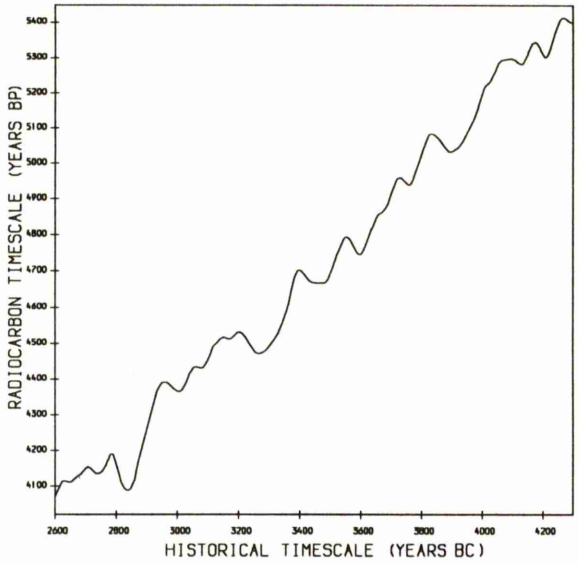

*Figure 5.40 :*a)

Part of the smoothed calibration curve used to calibrate the radiocarbon dates from ***Cortaillod*** culture

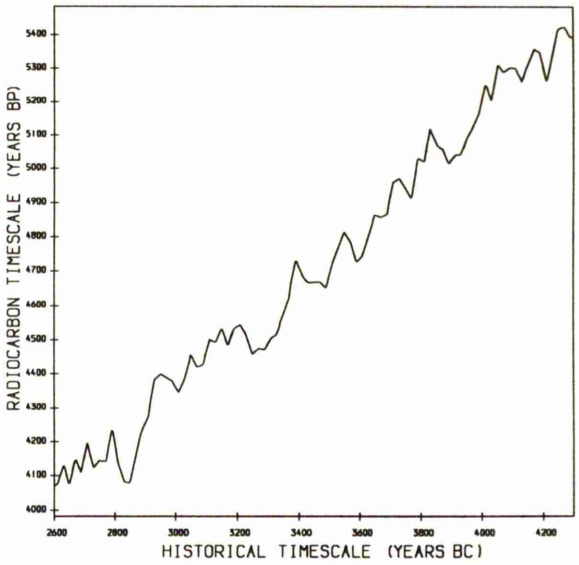

*Figure 5.40 :*b)

Part of the unsmoothed calibration curve used to calibrate the radiocarbon dates from ***Cortaillod*** culture

The histogram plots and the estimated p.d.f. of the true frequency distribution for the historical dates calibrated on both smoothed and unsmoothed calibration curve are shown in figure 5.41.

The estimated c.d.f. have been constructed and their plots (the middle band) are shown in figure 5.42 with the interval estimates for the true c.d.f. surrounding it for both methods D and E. Resulting estimates for the floruit of the *Cortaillod* culture obtained from the five floruit estimation methods are summarised in table 5.24 and plotted in figure 5.43.

#	Radiocarbon Age (Years BP)	Corresponding historical dates (years BC) calibrated from smoothed curve.			Corresponding historical dates (years BC) calibrated from unsmoothed curve.		
		number of $\hat{t}_{ij}$	estimated $\hat{t}_{ij}$	estimated standard errors $se(\hat{t}_{ij})$	number of $\hat{t}_{ij}$	estimated $\hat{t}_{ij}$	estimated standard errors $se(\hat{t}_{ij})$
1	4180 ± 130	3	2777 2794 2877	112 102 52	5	2706 2707 2778 2802 2875	45 45 44 43 56
2	4360 ± 110	1	2932	66	3	2927 3001 3018	33 110 88
3	4390 ± 80	3	2954 2963 3028	33 37 63	3	2940 2966 3031	26 40 37
4	4390 ± 70	3	2954 2963 3028	29 34 55	3	2940 2966 3031	22 35 32
5	4490 ± 90	3	3118 3241 3300	105 101 140	5	3107 3166 3167 3239 3301	40 56 56 52 85
6	4500 ± 100	3	3127 3234 3309	109 108 96	5	3133 3163 3177 3235 3307	77 62 65 57 95
7	4500 ± 110	3	3127 3234 3309	112 118 102	5	3133 3163 3177 3235 3307	84 68 71 63 104
8	4530 ± 100	3	3201 3206 3331	142 145 92	3	3192 3219 3334	138 107 54
9	4550 ± 100	1	3341	75	1	3341	54
10	4590 ± 80	1	3358	45	1	3356	55
11	4630 ± 180	1	3369	75	1	3370	123
12	4630 ± 120	1	3369	50	1	3370	83
13	4640 ± 70	1	3372	29	1	3372	22
14	4680 ± 100	3	3383 3423 3494	55 153 93	3	3381 3419 3498	30 129 47
15	4750 ± 100	3	3524 3588 3603	67 75 67	3	3523 3582 3611	67 53 58
16	4750 ± 100	3	3524 3588 3603	67 75 67	3	3523 3582 3611	67 53 58
17	4750 ± 100	3	3524 3588 3603	67 75 67	3	3523 3582 3611	67 53 58
18	4790 ± 120	3	3545 3560 3625	106 113 75	3	3540 3567 3626	86 149 69
19	4790 ± 120	3	3545 3560 3625	106 113 75	3	3540 3567 3626	86 149 69
20	4790 ± 70	3	3545 3560 3625	85 78 44	3	3540 3567 3626	51 89 41
21	4800 ± 130	1	3629	80	3	3544 3560 3629	93 113 75

continued / next page

#	Radiocarbon Age (Years BP)	Corresponding historical dates (years BC) calibrated from smoothed curve.			Corresponding historical dates (years BC) calibrated from unsmoothed curve.		
		number of $\hat{t}_{ij}$	estimated $\hat{t}_{ij}$	estimated standard errors $se(\hat{t}_{ij})$	number of $\hat{t}_{ij}$	estimated $\hat{t}_{ij}$	estimated standard errors $se(\hat{t}_{ij})$
22	4800 ± 100	1	3629	61	3	3544	72
						3560	124
						3629	58
23	4830 ± 150	1	3641	109	1	3639	77
24	4840 ± 110	1	3646	98	1	3642	56
25	4870 ± 60	1	3679	88	1	3687	42
26	4880 ± 70	1	3686	64	1	3693	25
27	4930 ± 40	1	3707	27	3	3704	15
						3758	46
						3773	12
28	4950 ± 90	3	3716	100	3	3709	32
			3742	147		3744	94
			3771	79		3776	25
29	4950 ± 50	3	3716	57	3	3710	18
			3742	83		3744	54
			3771	45		3776	14
30	4960 ± 70	1	3775	45	3	3714	41
						3738	46
						3778	19
31	4980 ± 110	1	3783	59	1	3781	30
32	4980 ± 120	1	3783	64	1	3781	32
33	4990 ± 70	1	3786	38	1	3783	19
34	5040 ± 100	3	3806	69	3	3813	33
			3881	75		3878	66
			3915	58		3914	48
35	5060 ± 35	3	3815	25	3	3818	12
			3864	52		3867	98
			3935	39		3938	25
36	5080 ± 70	3	3828	55	3	3822	23
			3841	61		3847	46
			3947	34		3947	48
37	5090 ± 120	1	3952	108	3	3824	39
						3842	79
						3951	117
38	5100 ± 80	1	3958	74	3	3826	26
						3838	53
						3957	78
39	5100 ± 70	1	3958	65	3	3826	23
						3838	46
						3957	68
40	5120 ± 120	1	3970	107	1	3969	117
41	5120 ± 130	1	3970	115	1	3969	127
42	5130 ± 120	1	3975	95	1	3974	92
43	5130 ± 100	1	3975	79	1	3974	77
44	5145 ± 70	1	3981	45	1	3981	54
45	5150 ± 100	1	3983	61	1	3983	77
46	5150 ± 120	1	3983	73	1	3983	92
47	5170 ± 130	1	3990	68	1	3991	49
48	5180 ± 120	1	3994	63	1	3994	45
49	5200 ± 90	1	4001	58	1	3998	34
50	5280 ± 110	1	4051	104	5	4045	32
						4120	91
						4138	77
						4207	40
						4215	44
51	5360 ± 150	1	4236	79	1	4235	62

Table 5.23 : Estimates of historical dates corresponding to each observed radiocarbon age, and their estimated standard errors from both smoothed and unsmoothed calibration curve for the group of radiocarbon dates taken from ***Cortaillod*** culture.

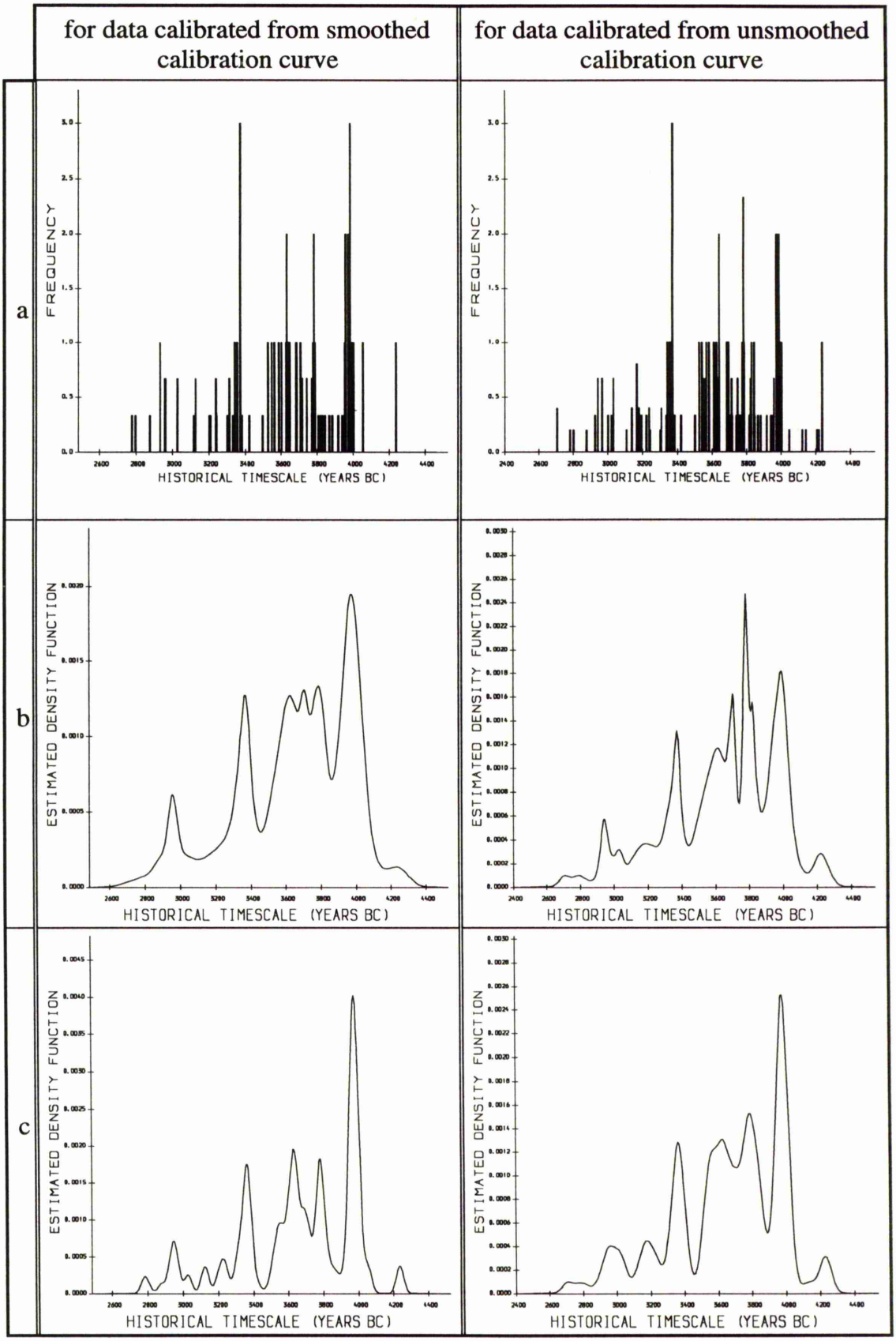

Figure 5.41 : a) Histogram plots for the calibrated historical dates for ***Cortaillod*** culture and the plots of estimated density functions, b) smoothed by cross-validation method and c) smoothed by weighting method.

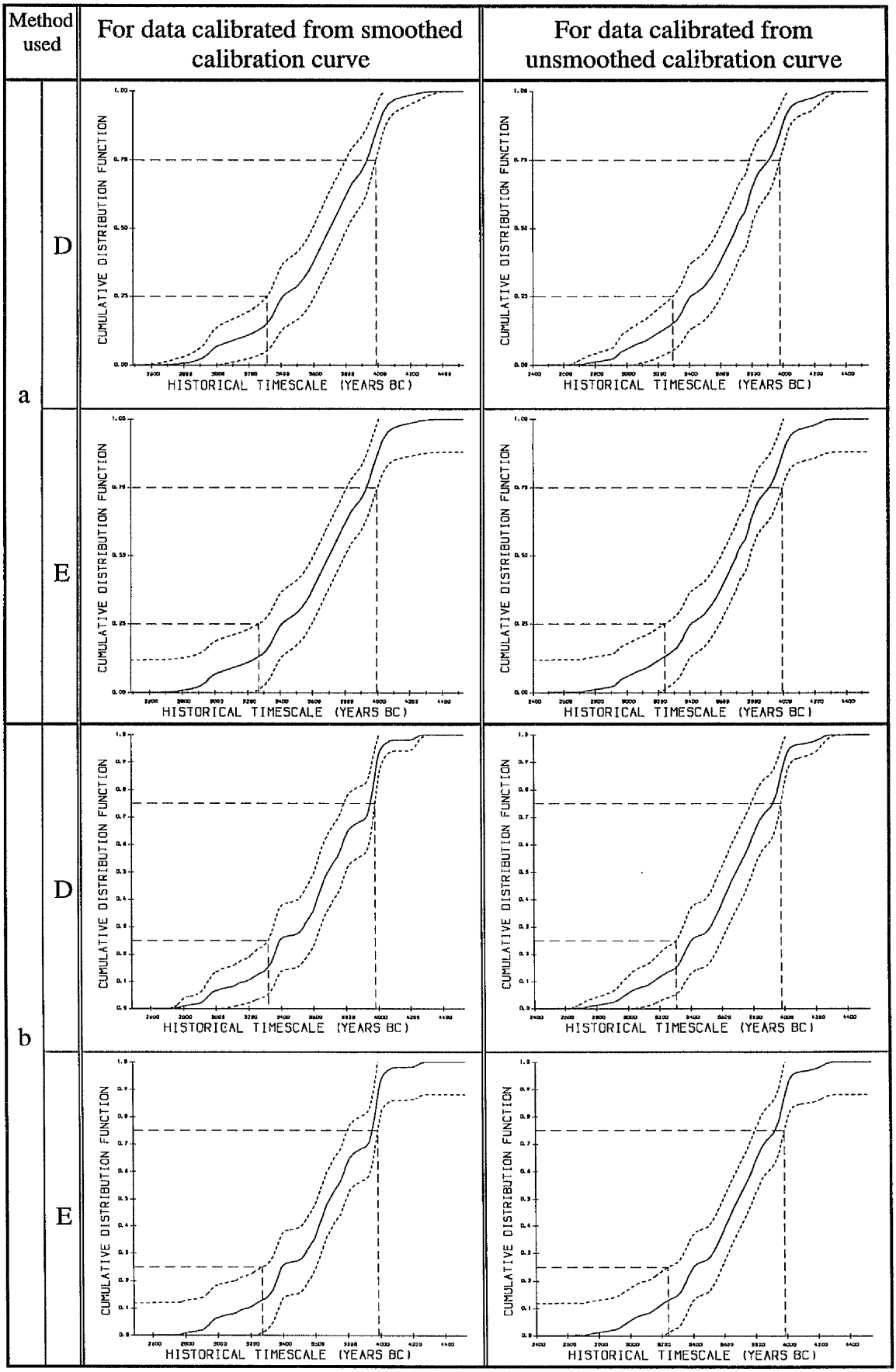

Figure 5.42 : Plots of estimated cumulative distribution functions for the calibrated historical dates for ***Cortaillod*** culture a) smoothed by cross-validation method and b) smoothed by the weighting method.

Floruit Estimation (years BC)					
Method used		For data calibrated from smoothed calibration curve.		For data calibrated from unsmoothed calibration curve.	
		Point	Interval	Point	Interval
A		3374 - 3958	3360 - 3988	3374 - 3957	3360 - 3989
B		3380 - 3958	3350 - 4011	3378 - 3957	3356 - 4010
C		3382 - 3958	3360 - 4011	3383 - 3849	3368 - 3865
D	Cross-Validation	3410 - 3931	3312 - 3985	3408 - 3909	3294 - 3982
	Weighting Method	3392 - 3953	3319 - 3980	3403 - 3928	3306 - 3978
E	Cross-Validation	3410 - 3931	3270 - 3996	3408 - 3909	3241 - 3993
	Weighting Method	3392 - 3953	3273 - 3985	3403 - 3928	3241 - 3986

Table 5.24 : Point and Interval estimates for the floruit of ***Cortaillod*** culture obtained from the five floruit estimation methods.

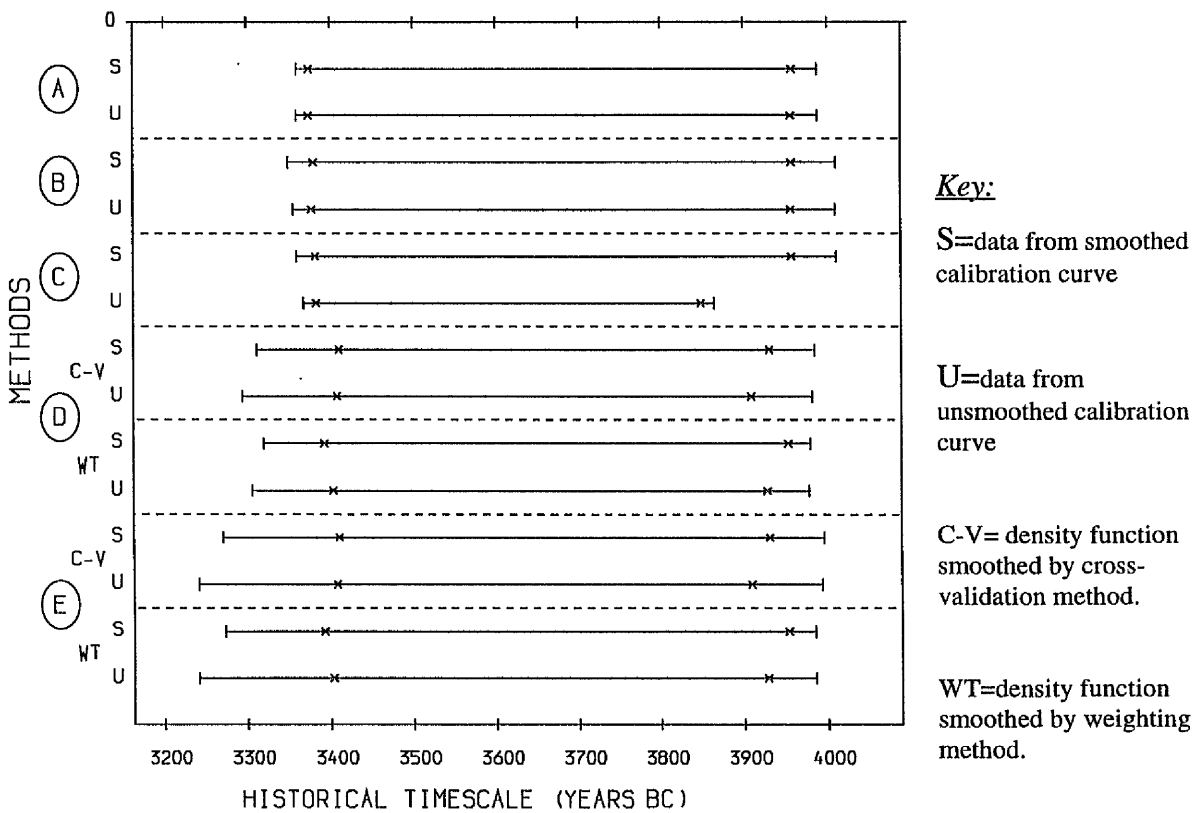

Figure 5.43 : Plots of point (x---x) and interval (|---|) estimates for the floruit of ***Cortaillod*** culture.

In general the results are all very similar both in terms of point and interval estimates. However some differences in the results occurred, particularly for method C when applied to the data calibrated on the unsmoothed calibration curve. This method provided a much narrower interval for the historical dates calibrated on the unsmoothed curve due to the wiggles at the period of 3800-4000 BC which affected the estimates by pulling the weighted average of the multiple dates calibrated in this period from the older end (4000 BC) to the younger end side 3800 BC reducing the resultant estimates in both point and interval estimates.

Methods A and B seem to produce almost identical estimates for the floruit whether the calibration was carried out on the smoothed or unsmoothed calibration curve. While method A provided a very slightly wider(6 years or less) point estimate for the floruit than method B in the two cases (smoothed and unsmoothed), method B provided a wider (nearly 30 years) interval estimate for the floruit than method A. The reason for this is that the standard errors of the calibrated dates are involved in the interval estimate provided by method B which takes into account the error on the calibration curve, the error in corresponding radiocarbon date and the slope of the calibration curve at the calibrated date, while method A takes only account of the error in the radiocarbon date.

Comparing the two methods based on the density estimation (D and E), one can find method E produced a marginally wider interval than method D particularly at the younger end of the interval whether the p.d.f. is smoothed by the cross-validation or weighting method. This is, as explained before, due to the approximation of the variance of the c.d.f. used in method E.

Furthermore, for each method, the resulting estimates for the floruit obtained from the data calibrated on smoothed or unsmoothed calibration curve are approximately identical at the older end of the floruit estimate and vary at the younger end of the floruit. This can be explained as a result of the amount of smoothing on the density function which is much more stable at the older end of the curve than at the younger end (figures 5.41b&c). This is caused by the multiple historical dates corresponding to each radiocarbon date at the younger end (see figure 5.41a).

Finally, the floruit estimates obtained from methods based on density estimation are shifted to the left (*i.e.* to the younger end (figure 5.43)) compared with the pen and paper methods. This again happened as a result of the amount of smoothing on the density function and the multiple historical dates caused by the 'wiggles' at the younger end of the calibration curve.

5.5.2 Seeberg-Burgäschisee-S site

The 16 radiocarbon dates collected from *Seeberg-Burgäschisee-S* site of the *Cortaillod* culture are analysed as a separate group. This group has been calibrated on the smoothed and unsmoothed calibration curves shown in figures 5.44a&b. The estimates of the historical dates corresponding to each radiocarbon date are given in table 5.25 together with their estimated standard errors. Due to the many wiggles on the curve, most of the radiocarbon dates correspond to multiple historical dates. The histogram plots for these calibrated dates are given in figure 5.45 with the estimated p.d.f. smoothed by cross-validation and weighting methods. It should be noted that the estimate with smoothing parameter chosen by cross-validation is over smoothed and perhaps tends to obscure the nature of the distribution, while the estimate with smoothing parameter chosen by the weighting method appears somewhat more realistic. The c.d.f.'s obtained from the integral of these estimated p.d.f.'s are graphed in figure 5.46.

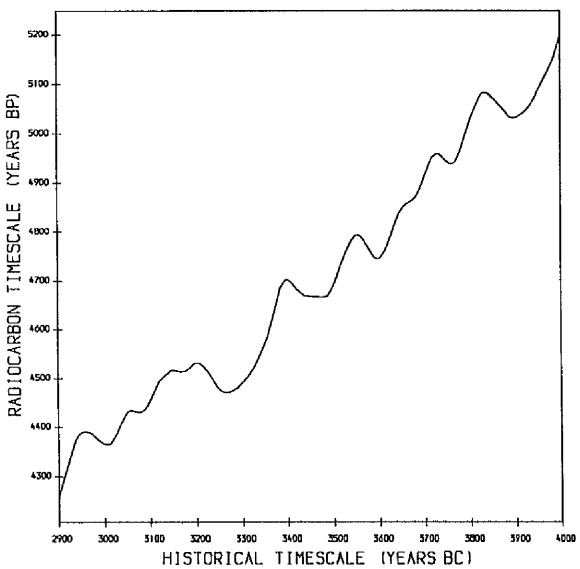

*Figure 5.44:*a)
Part of the smoothed calibration curve used to calibrate the radiocarbon dates from ***Seeberg-Burgäschisee-S*** Site in ***Cortaillod*** culture

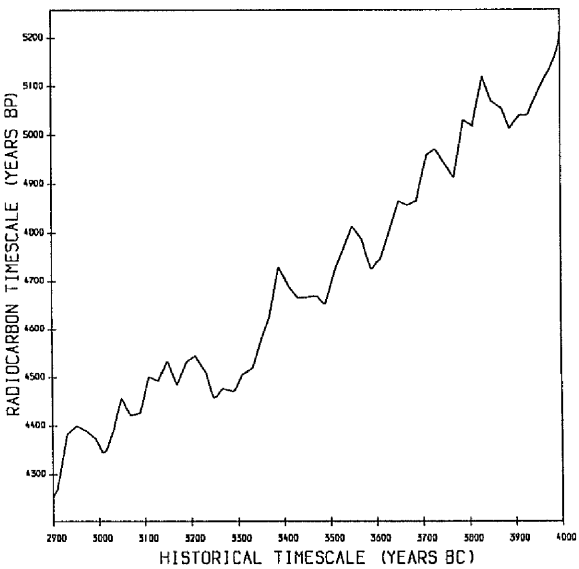

*Figure 5.44:*b)
Part of the unsmoothed calibration curve used to calibrate the radiocarbon dates from ***Seeberg-Burgäschisee-S*** Site in ***Cortaillod*** culture

#	Radiocarbon Date ± Error (Years BP)	Corresponding historical dates (years BC) calibrated from smoothed curve.			Corresponding historical dates (years BC) calibrated from unsmoothed curve.		
		number of $\hat{t}_{ij}$	estimated $\hat{t}_{ij}$	estimated standard errors $se(\hat{t}_{ij})$	number of $\hat{t}_{ij}$	estimated $\hat{t}_{ij}$	estimated standard errors $se(\hat{t}_{ij})$
1	4390 ± 80	3	2954	33	3	2940	26
			2963	37		2966	40
			3028	63		3031	37
2	4490 ± 90	3	3118	105	5	3107	40
			3241	101		3166	56
			3300	140		3167	56
						3239	52
						3301	85
3	4500 ± 100	3	3127	109	5	3133	77
			3234	108		3163	62
			3309	96		3177	65
						3235	57
						3307	95
4	4500 ± 110	3	3127	112	5	3133	84
			3234	118		3163	68
			3309	102		3177	71
						3235	63
						3307	104
5	4530 ± 100	3	3201	142	3	3192	138
			3206	145		3219	107
			3331	92		3334	54
6	4550 ± 100	1	3341	75	1	3341	54
7	4630 ± 180	1	3369	75	1	3370	123
8	4630 ± 120	1	3369	50	1	3370	83
9	4680 ± 100	3	3383	55	3	3381	30
			3423	153		3419	129
			3494	93		3498	47
10	4750 ± 100	3	3524	67	3	3523	67
			3588	75		3582	53
			3603	67		3611	58
11	4750 ± 100	3	3524	67	3	3523	67
			3588	75		3582	53
			3603	67		3611	58
12	4790 ± 120	3	3545	106	3	3540	86
			3560	113		3567	149
			3625	75		3626	69
13	4800 ± 130	1	3629	80	3	3544	93
						3560	113
						3629	75
14	4840 ± 110	1	3646	98	1	3642	56
15	4950 ± 90	3	3716	100	3	3709	32
			3742	147		3744	94
			3771	79		3776	25
16	5060 ± 35	3	3815	25	3	3818	12
			3864	52		3867	98
			3935	39		3938	25

Table 5.25 : Estimates of historical dates corresponding to each observed radiocarbon age, and their estimated standard errors from both smoothed and unsmoothed calibration curve for the group of radiocarbon dates taken from ***Seeberg-Burgäschisee-S*** Site in ***Cortaillod*** culture .

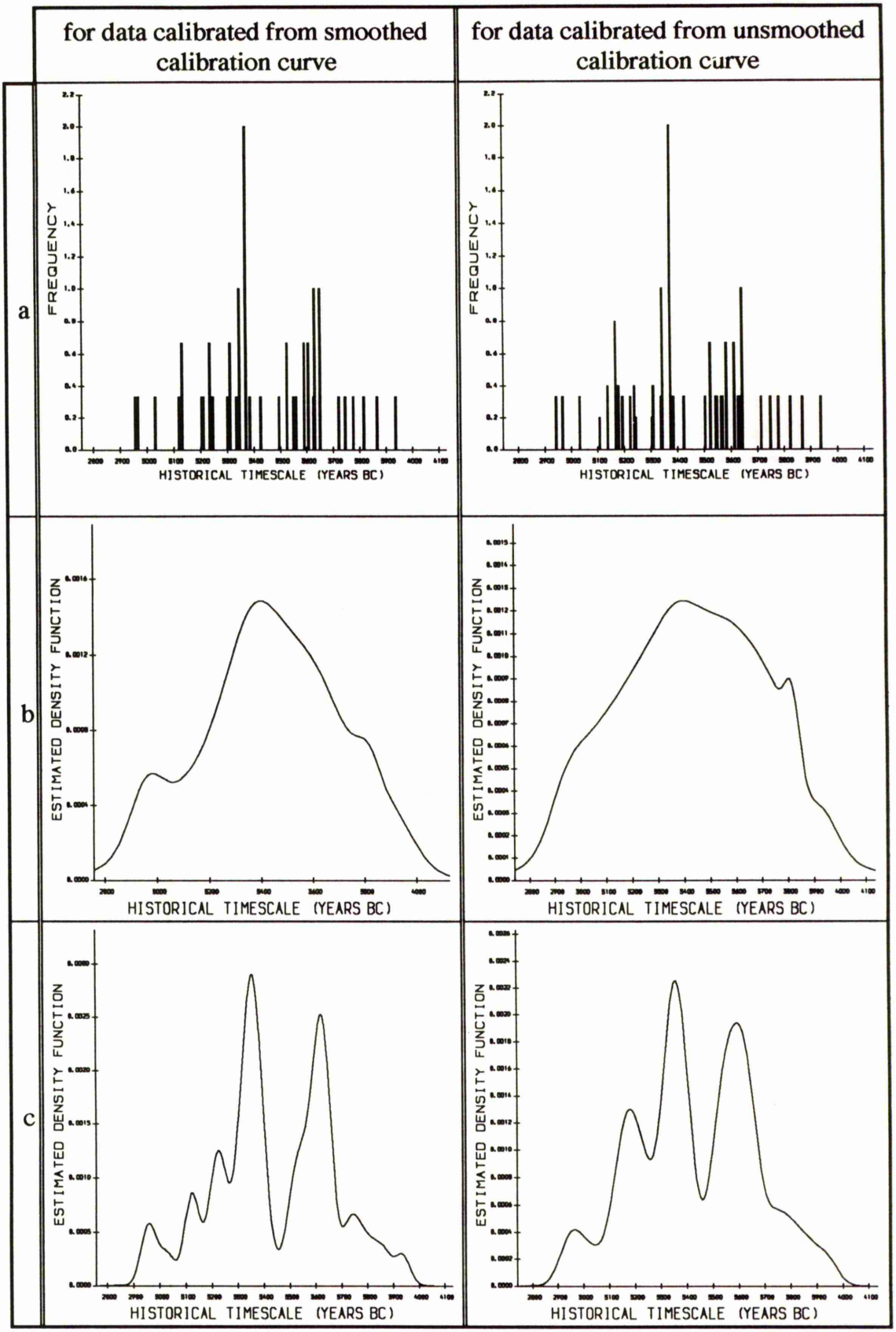

Figure 5.45 : a) Histogram plots for the calibrated historical dates for ***Seeberg-Burgäschisee-S*** Site in ***Cortaillod*** culture and the plots of estimated density functions, b) smoothed by cross-validation method and c) smoothed by the weighting method.

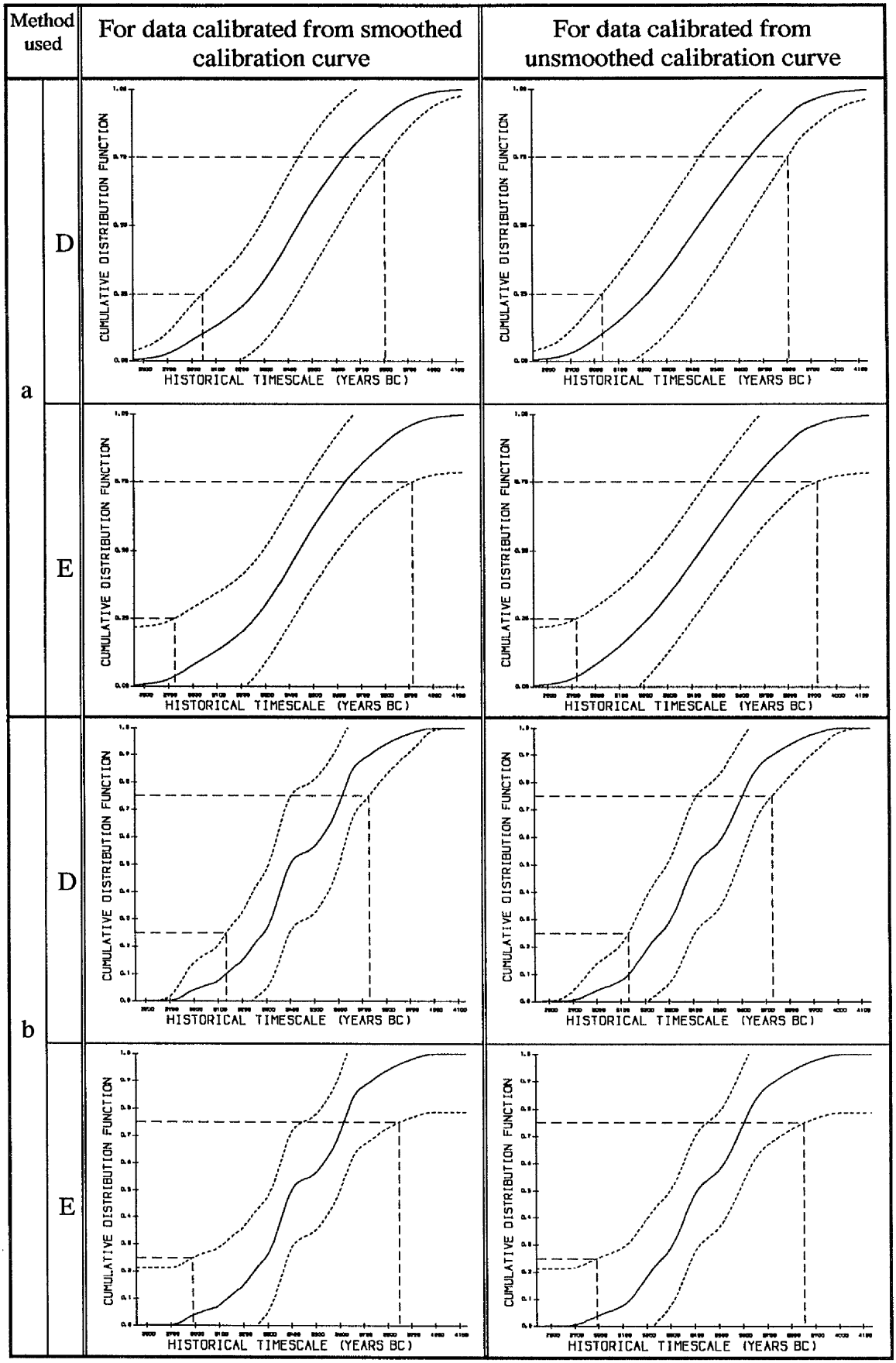

Figure 5.46 : Plots of estimated cumulative distribution functions for calibrated historical dates for ***Seeberg-Burgäschisee-S*** Site in ***Cortaillod*** culture a) smoothed by cross-validation method and b) smoothed by weighting method.

Floruit Estimation (years BC)					
Method used		For data calibrated from smoothed calibration curve.		For data calibrated from unsmoothed calibration curve.	
		Point	Interval	Point	Interval
A		3147 - 3627	3097 - 3686	3141 - 3627	3048 - 3693
B		3309 - 3627	3243 - 3679	3307 - 3618	3244 - 3669
C		3252 - 3609	3209 - 3654	3247 - 3589	3222 - 3623
D	Cross-Validation	3258 - 3636	3044 - 3806	3219 - 3650	3034 - 3807
	Weighting Method	3290 - 3618	3133 - 3731	3264 - 3605	3134 - 3729
E	Cross-Validation	3258 - 3636	2926 - 3916	3219 - 3650	2922 - 3923
	Weighting Method	3290 - 3618	2990 - 3849	3264 - 3605	2993 - 3855

Table 5.26: Point and Interval estimates for the floruit of ***Seeberg-Burgäschisee-S*** Site in ***Cortaillod*** culture obtained from the five floruit estimation methods.

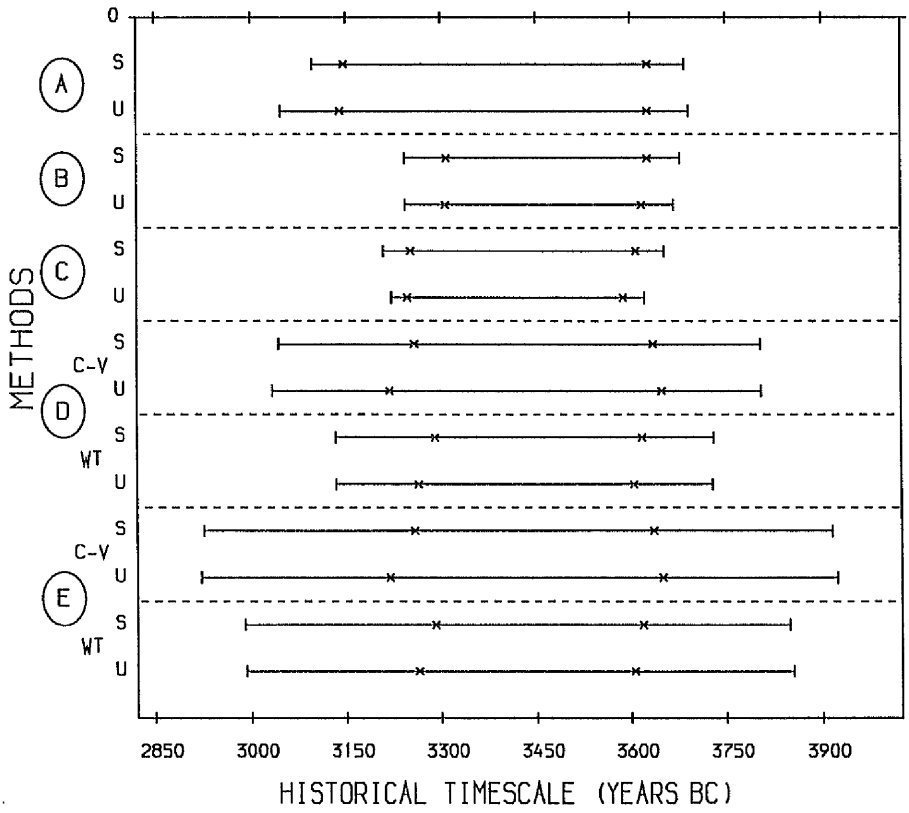

Figure 5.47: Plots of point (x---x) and interval (|---|) estimates for the floruit of ***Seeberg-Burgäschisee-S*** Site of Cortaillod culture.

The floruit estimates obtained from the five methods for the *Seeberg-Burgäschisee-S* site are summarised in table 5.6 and plotted in figure 5.8. These estimates show quite considerable differences.

For the pen and paper methods, while the wiggles widen the floruit estimate obtained from method A, their effect is to tighten the floruit estimate obtained from methods B and C. This is very clear when the results obtained from the data calibrated on the unsmoothed curve are compared with those obtained from the data calibrated on the smoothed curve.

For the density estimation methods, the effect of the degree of smoothing on the p.d.f. is quite different for each of the cross-validation and weighting methods. The p.d.f. is over smoothed by cross-validation which in turn influenced the floruit estimate by widening it more than that obtained by the weighting method. With a much wider interval estimate provided by E than D, both of these two methods have produced interval estimates from the data calibrated on the smoothed calibration curve similar to those from the data calibrated on the unsmoothed calibration curve.

Compared to the results from the whole of the *Cortaillod* culture group, these estimates of the floruit for the *Seeberg-Burgäschisee-S* site give some indication that this site represents the middle to late period of the *Cortaillod* culture.

5.5.3 Twann site

There are ten radiocarbon dates collected from this site. The specific smoothed and unsmoothed parts of the calibration curve used to calibrate this group of dates are plotted in figures 5.48a&b. This has less wiggles than that used for the *Seeberg-Burgäschisee-S* group of the same alleged culture. Accordingly there are less historical dates corresponding to most of the radiocarbon dates in this group (table 5.27). The histogram plots and estimated p.d.f.'s for these data are graphed in figure 5.49 with the estimated c.d.f.'s in figure 5.50. The point and interval estimates for the floruit of the *Twann* site obtained from the five methods are summarised in table 5.28 and plotted in figure 5.51.

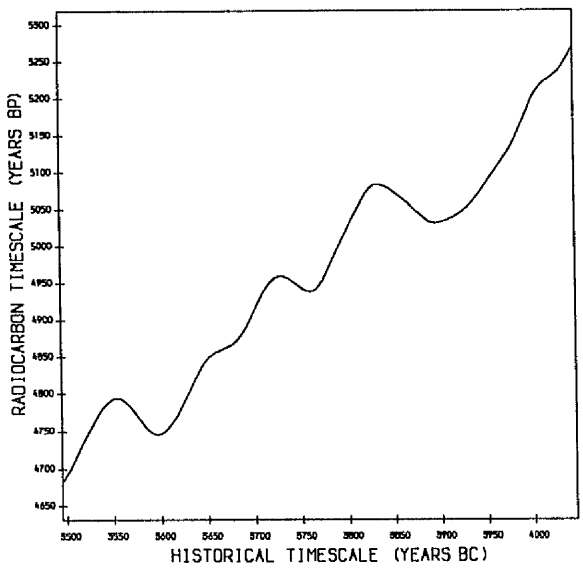

*Figure 5.48:*a)
Part of the smoothed calibration curve used to calibrate the radiocarbon dates from ***Twann*** Site in ***Cortaillod*** culture

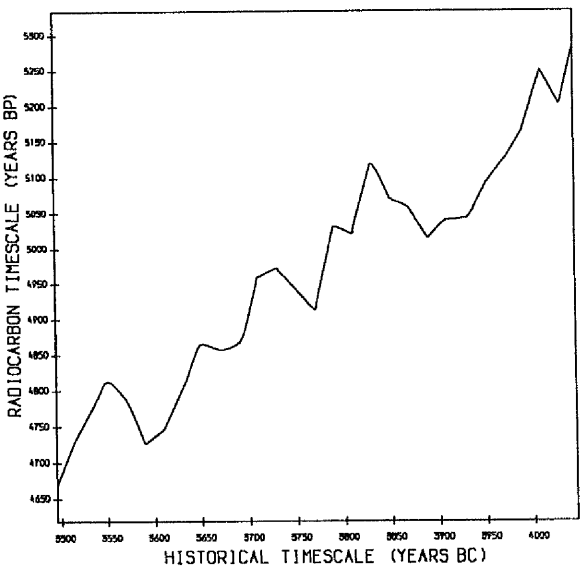

*Figure 5.48:*b)
Part of the unsmoothed calibration curve used to calibrate the radiocarbon dates from ***Twann*** Site in ***Cortaillod*** culture

# i	Radiocarbon Date ± Error (Years BP)	Corresponding historical dates (years BC) calibrated from smoothed curve.			Corresponding historical dates (years BC) calibrated from unsmoothed curve.		
		number of $\hat{t}_{ij}$	estimated $\hat{t}_{ij}$	estimated standard errors $se(\hat{t}_{ij})$	number of $\hat{t}_{ij}$	estimated $\hat{t}_{ij}$	estimated standard errors $se(\hat{t}_{ij})$
1	4790 ± 120	3	3545 3560 3625	106 113 75	3	3540 3567 3626	86 149 69
2	4790 ± 70	3	3545 3560 3625	85 78 44	3	3540 3567 3626	51 89 41
3	4870 ± 60	1	3679	88	1	3687	42
4	4880 ± 70	1	3686	64	1	3693	25
5	4950 ± 50	3	3716 3742 3771	57 83 45	3	3710 3744 3776	18 54 14
6	4960 ± 70	1	3775	45	3	3714 3738 3778	41 46 19
7	4990 ± 70	1	3786	38	1	3783	19
8	5090 ± 120	1	3952	108	3	3824 3842 3951	39 79 117
9	5120 ± 130	1	3970	115	1	3969	127
10	5200 ± 90	1	4001	58	1	3998	34

Table 5.27 : Estimates of historical dates corresponding to each observed radiocarbon age, and their estimated standard errors from both smoothed and unsmoothed calibration curve for the group of radiocarbon dates taken from ***Twann*** Site in ***Cortaillod*** culture .

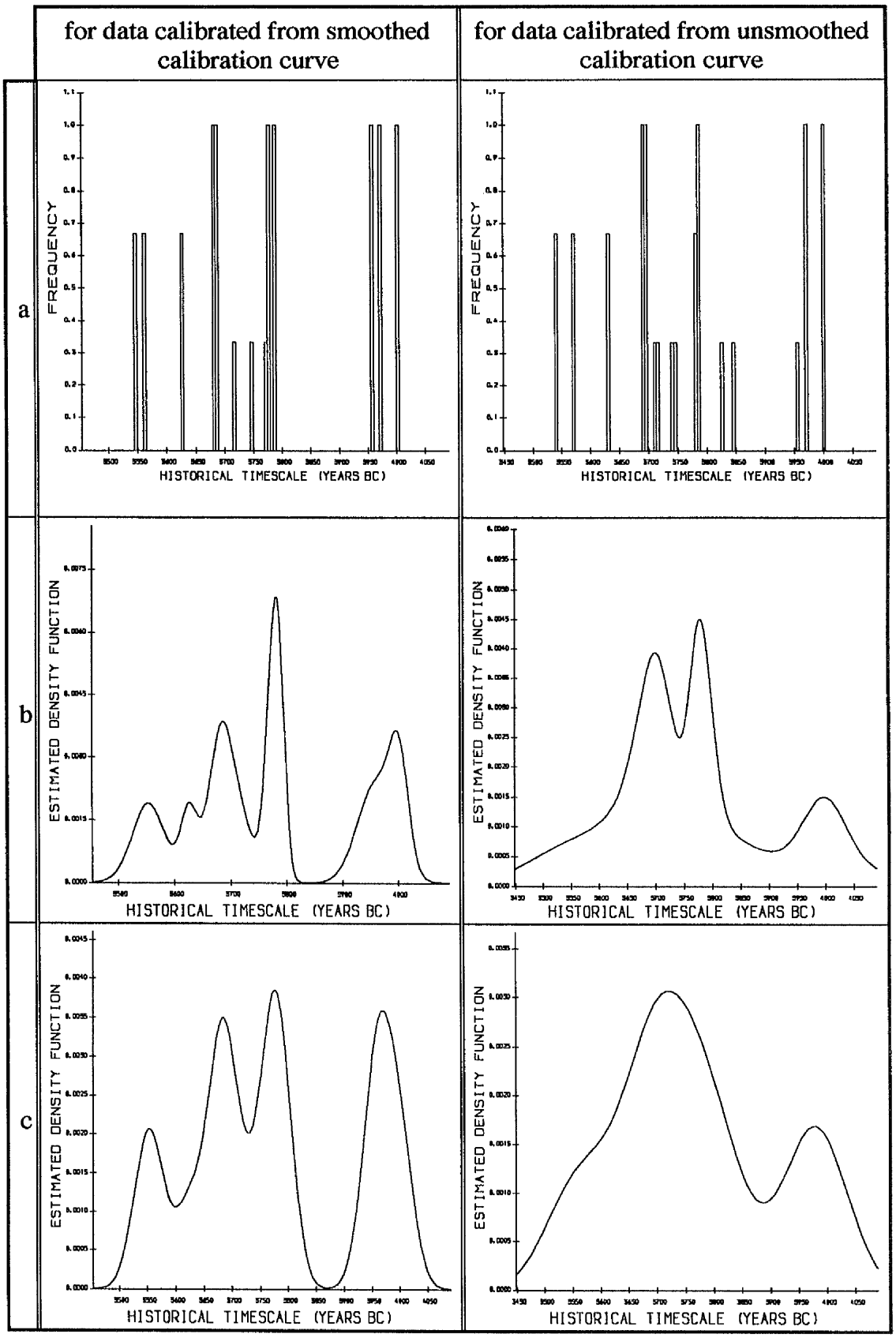

Figure 5.49 : a) Histogram plots for the calibrated historical dates for ***Twann*** site of ***Cortaillod*** culture and the plots of estimated density functions, b) smoothed by cross-validation method and c) smoothed by weighting method.

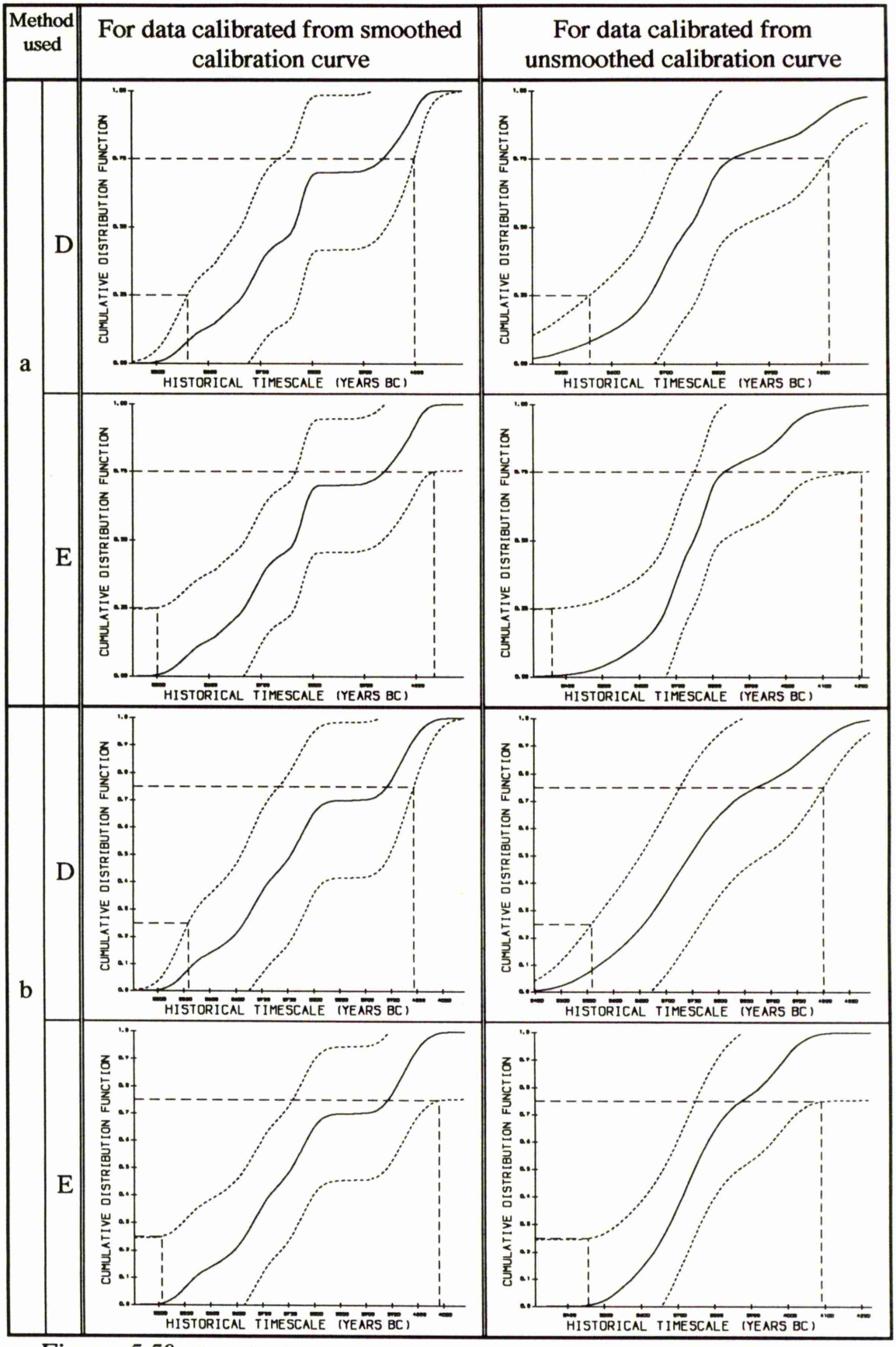

Figure 5.50: Plots of estimated cumulative distribution functions for calibrated historical dates for ***Twann*** Site in ***Cortaillod*** culture a) smoothed by cross-validation method and b) smoothed by the weighting method.

Floruit Estimation (years BC)					
Method used		For data calibrated from smoothed calibration curve.		For data calibrated from unsmoothed calibration curve.	
		Point	Interval	Point	Interval
A		3679 - 3952	3641 - 3990	3687 - 3951	3639 - 3991
B		3679 - 3952	3620 - 4025	3687 - 3951	3659 - 3937
C		3679 - 3952	3620 - 4025	3687 - 3838	3659 - 3860
D	Cross-Validation	3668 - 3938	3561 - 3999	3673 - 3832	3559 - 4015
	Weighting Method	3666 - 3943	3560 - 3994	3659 - 3872	3559 - 4001
E	Cross-Validation	3668 - 3938	3501 - 4035	3673 - 3832	3362 - 4206
	Weighting Method	3666 - 3943	3507 - 4042	3659 - 3872	3456 - 4091

Table 5.28 : Point and Interval estimates for the floruit of ***Twann*** Site of ***Cortaillod*** culture obtained from the five floruit estimation methods.

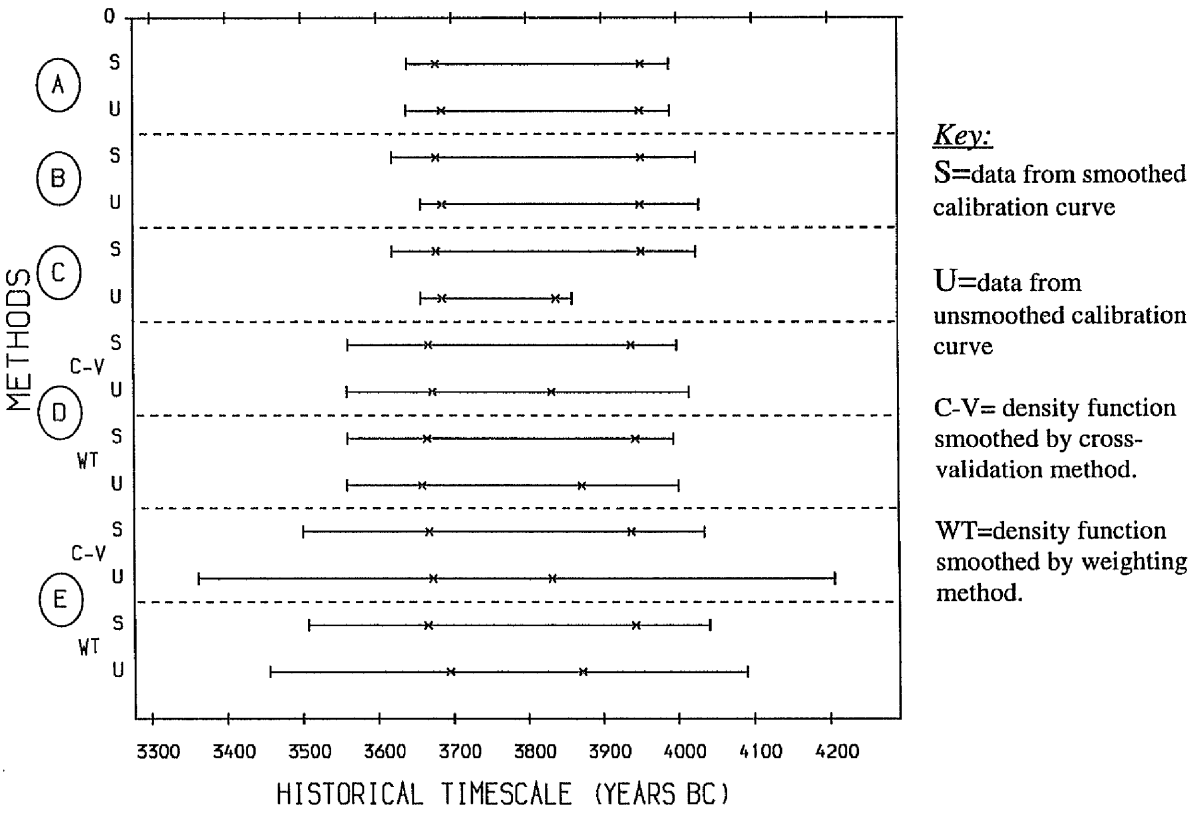

Figure 5.51: Plots of point (x---x) and interval (|---|) estimates for the floruit of ***Twann*** Site of ***Cortaillod*** culture.

In general all the five methods agree on the point estimate of the floruit when using the smoothed calibration curve whereas all the methods except A and B tend to substantially pull in the right-hand end (older end) of the point estimates. The explanation of this can be seen by looking at the histogram plots where there is a distinct gap between the three historical dates in the 3950-4000 BC period and the rest of the dates. This has influenced the estimation of the p.d.f.'s and produces a discontinuity in the estimated c.d.f. for the smoothed data (figure 5.50) which in turn widen the point estimate of the floruit compared with the point estimate for the unsmoothed data. Consequently, the estimated p.d.f. based on the unsmoothed data has a more realistic looking compared with that based on the smoothed data.

For method D whether cross-validation or the weighting method is used there is not much difference among the floruit interval estimates. For method E, the interval estimates obtained from the data calibrated on the unsmoothed calibration curve are much wider than those obtained when the smoothed curve is used. This is clearly because of the large degree of smoothing on the p.d.f. of the unsmoothed data. As usual method E has provided a much wider interval estimate for the floruit compared to the other methods perhaps due in part to this and to the small sample size involved in this example.

In comparison to the other major site (*Seeberg-Burgäschisee-S*) of the *Cortaillod* culture there appears to be a reasonable degree of overlap between the floruits of the two sites with the *Twann* site perhaps representing the earlier to middle part of the culture and the *Seeberg-Burgäschisee-S* site the middle to later part.

Formal consideration of the degree of overlap is made in chapter six which addresses the question of whether any overlap exists at all and, if so, then tries to quantify it.

5.5.4 Sâone-Rhône culture

This group consists of 38 radiocarbon dates collected from three sites in the *Sâone-Rhône* culture of Switzerland. The dates were given in table 5.4. As the majority of the dates came from two distinct sites (*Yverdon* and *Auvernier, La Saunerie*) the data will be analysed first collectively and then separately for each of these two sites.

The two plots in figures 5.52a&b represent the parts of the smoothed and unsmoothed calibration curves used to calibrate this group of radiocarbon dates. The curve shape tends to be steep at both ends but flat in the middle with more wiggles, of course, in the unsmoothed curve.

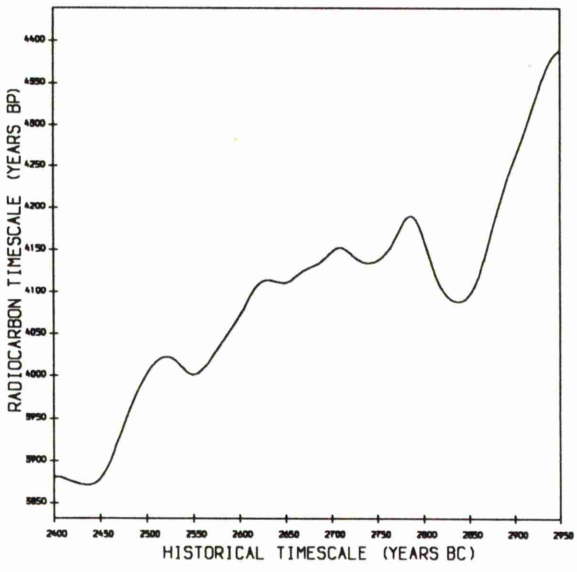

*Figure 5.52 :*a)
Part of the smoothed calibration curve used to calibrate the radiocarbon dates from ***Sâone-Rhône*** culture

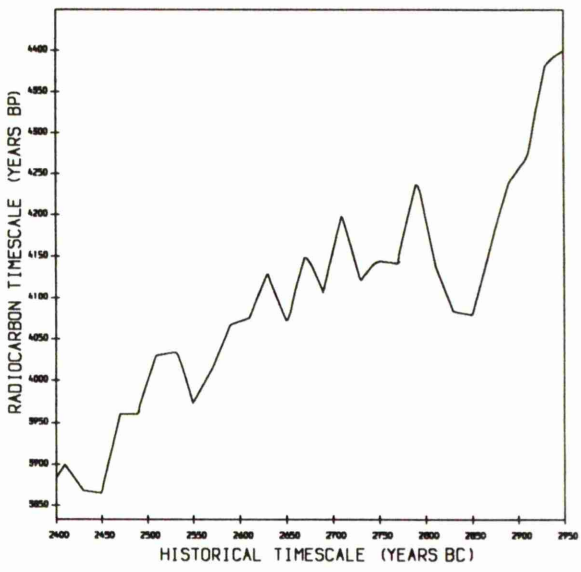

*Figure 5.52 :*b)
Part of the unsmoothed calibration curve used to calibrate the radiocarbon dates from ***Sâone-Rhône*** culture

The radiocarbon dates of this group have been calibrated individually on both smoothed and unsmoothed curves and the calibrated historical dates are given in table 5.29 together with their estimated standard errors. Figure 5.53a

shows the histogram plots of these calibrated dates. It should be noted that as a result of the shape of the curve the calibrated historical dates obtained from the smoothed curve are concentrated mainly at the two edges with only a few multiple dates in the middle. Almost the same phenomenon occurred with the historical dates calibrated from the unsmoothed curve but with more multiple dates in the middle due to more wiggles in the middle of the unsmoothed curve.

The estimated p.d.f.'s underlying the historical dates calibrated from both smoothed and unsmoothed curves have been constructed and graphed in figures 5.53b&c. With the smoothing parameter chosen by cross-validation (5.53b), the estimates are very noisy and have many spikes at the dates which are particularly noticeable in the unsmoothed case. These spikes have been eliminated in the estimates shown in figure 5.53c with the smoothing parameter chosen by the weighting method and a bimodal or even trimodal nature for the distribution can be noted especially in the smoothed case. The estimated c.d.f. integrated from these p.d.f. are graphed in figure 5.54 with an approximate 95% confidence interval for the true c.d.f. surrounding it.

Point and interval estimates for the floruit of *Sâone-Rhône* culture resulted from applying the five methods are summarised in table 5.30 and presented graphically in figure 5.55.

#	Radiocarbon Date ± Error (Years BP)	Corresponding historical dates (years BC) calibrated from smoothed curve.			Corresponding historical dates (years BC) calibrated from unsmoothed curve.		
		number of $\hat{t}_{ij}$	estimated $\hat{t}_{ij}$	estimated standard errors $se(\hat{t}_{ij})$	number of $\hat{t}_{ij}$	estimated $\hat{t}_{ij}$	estimated standard errors $se(\hat{t}_{ij})$
1	3900 ± 100	1	2461	62	1	2457	34
2	3900 ± 100	1	2461	62	1	2457	34
3	3960 ± 120	1	2482	73	1	2481	120
4	3970 ± 100	1	2485	65	1	2491	46
5	3990 ± 100	1	2494	75	3	2499	46
						2544	53
						2558	80
6	4000 ± 120	1	2499	104	3	2502	55
						2541	63
						2563	96
7	4000 ± 150	1	2499	130	3	2502	69
						2541	79
						2563	120
8	4000 ± 100	1	2499	87	3	2502	46
						2541	53
						2563	80
9	4010 ± 100	3	2506	114	3	2505	46
			2538	135		2538	53
			2562	127		2568	80
10	4020 ± 100	3	2515	112	3	2509	46
			2527	118		2534	53
			2569	102		2572	60
11	4030 ± 100	1	2575	96	3	2516	115
						2529	122
						2576	60
12	4060 ± 100	1	2594	98	1	2589	60
13	4077 ± 70	1	2602	57	1	2607	72
14	4080 ± 100	1	2604	77	3	2610	59
						2845	34
						2847	33
15	4080 ± 100	1	2604	77	3	2610	59
						2845	34
						2847	33
16	4090 ± 90	3	2610	68	5	2615	53
			2835	35		2644	50
			2842	31		2653	38
						2828	51
						2851	35
17	4100 ± 90	3	2615	83	5	2619	53
			2823	101		2640	50
			2852	86		2657	38
						2824	51
						2855	35
18	4100 ± 120	3	2615	110	5	2619	70
			2823	134		2640	66
			2852	114		2657	50
						2824	68
						2855	46
19	4103 ± 70	3	2618	80	5	2621	41
			2821	63		2639	39
			2855	52		2659	29
						2822	40
						2856	27
20	4129 ± 70	3	2678	93	7	2665	29
			2810	35		2679	54
			2864	20		2694	25
						2734	98
						2738	98
						2814	40
						2862	27

continued / next page

#	Radiocarbon Date ± Error (Years BP)	Corresponding historical dates (years BC) calibrated from smoothed curve.			Corresponding historical dates (years BC) calibrated from unsmoothed curve.		
		number of $\hat{t}_{ij}$	estimated $\hat{t}_{ij}$	estimated standard errors $se(\hat{t}_{ij})$	number of $\hat{t}_{ij}$	estimated $\hat{t}_{ij}$	estimated standard errors $se(\hat{t}_{ij})$
21	4130 ± 100	3	2678	108	7	2665	42
			2810	50		2679	77
			2864	29		2694	35
						2734	95
						2738	93
						2814	56
						2862	30
22	4140 ± 140	5	2693	168	7	2668	58
			2727	161		2670	58
			2752	148		2697	49
			2807	64		2725	58
			2867	60		2747	149
						2811	79
						2865	54
23	4140 ± 100	5	2693	113	7	2668	42
			2727	101		2670	42
			2752	87		2697	35
			2807	46		2725	41
			2867	29		2747	90
						2811	57
						2865	39
24	4160 ± 100	3	2767	79	5	2702	35
			2801	47		2720	41
			2872	40		2774	34
						2806	33
						2870	39
25	4160 ± 120	3	2767	95	5	2702	42
			2801	56		2720	49
			2872	48		2774	40
						2806	40
						2870	47
26	4160 ± 110	3	2767	87	5	2702	38
			2801	51		2720	45
			2872	44		2774	37
						2806	37
						2870	43
27	4170 ± 100	3	2772	72	5	2704	35
			2798	54		2717	41
			2874	40		2776	34
						2804	33
						2872	43
28	4180 ± 120	3	2777	103	5	2706	42
			2794	94		2707	42
			2877	48		2778	40
						2802	40
						2875	51
29	4191 ± 70	1	2879	29	3	2780	24
						2800	23
						2878	30
30	4200 ± 110	1	2882	47	3	2782	37
						2798	36
						2880	47
31	4210 ± 100	1	2885	45	3	2786	33
						2796	33
						2883	43
32	4230 ± 110	1	2891	56	1	2889	47
33	4260 ± 100	1	2901	56	1	2903	92
34	4280 ± 160	1	2907	84	1	2910	147
35	4290 ± 120	1	2911	61	1	2913	35
36	4300 ± 100	1	2914	48	1	2915	30
37	4300 ± 110	1	2914	53	1	2915	32
38	4320 ± 110	1	2920	51	1	2919	32

Table 5.29 : Estimates of historical dates corresponding to each observed radiocarbon age, and their estimated standard errors from both smoothed and unsmoothed calibration curve for the group of radiocarbon dates taken from ***Sâone-Rhône*** culture.

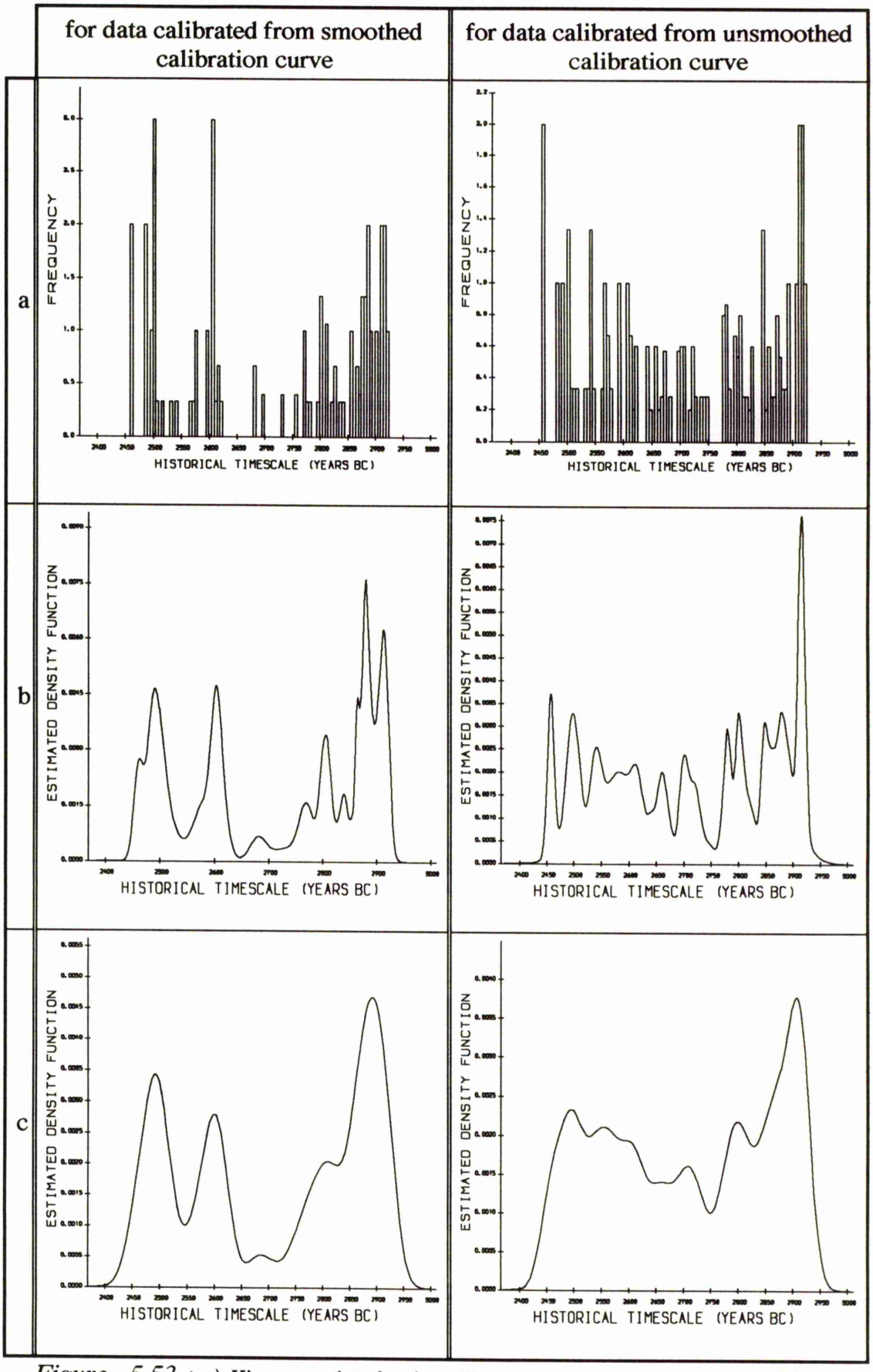

Figure 5.53 : a) Histogram plots for the calibrated historical dates for ***Sâone-Rhône*** culture and the plots of estimated density functions, b) smoothed by cross-validation method and c) smoothed by weighting method.

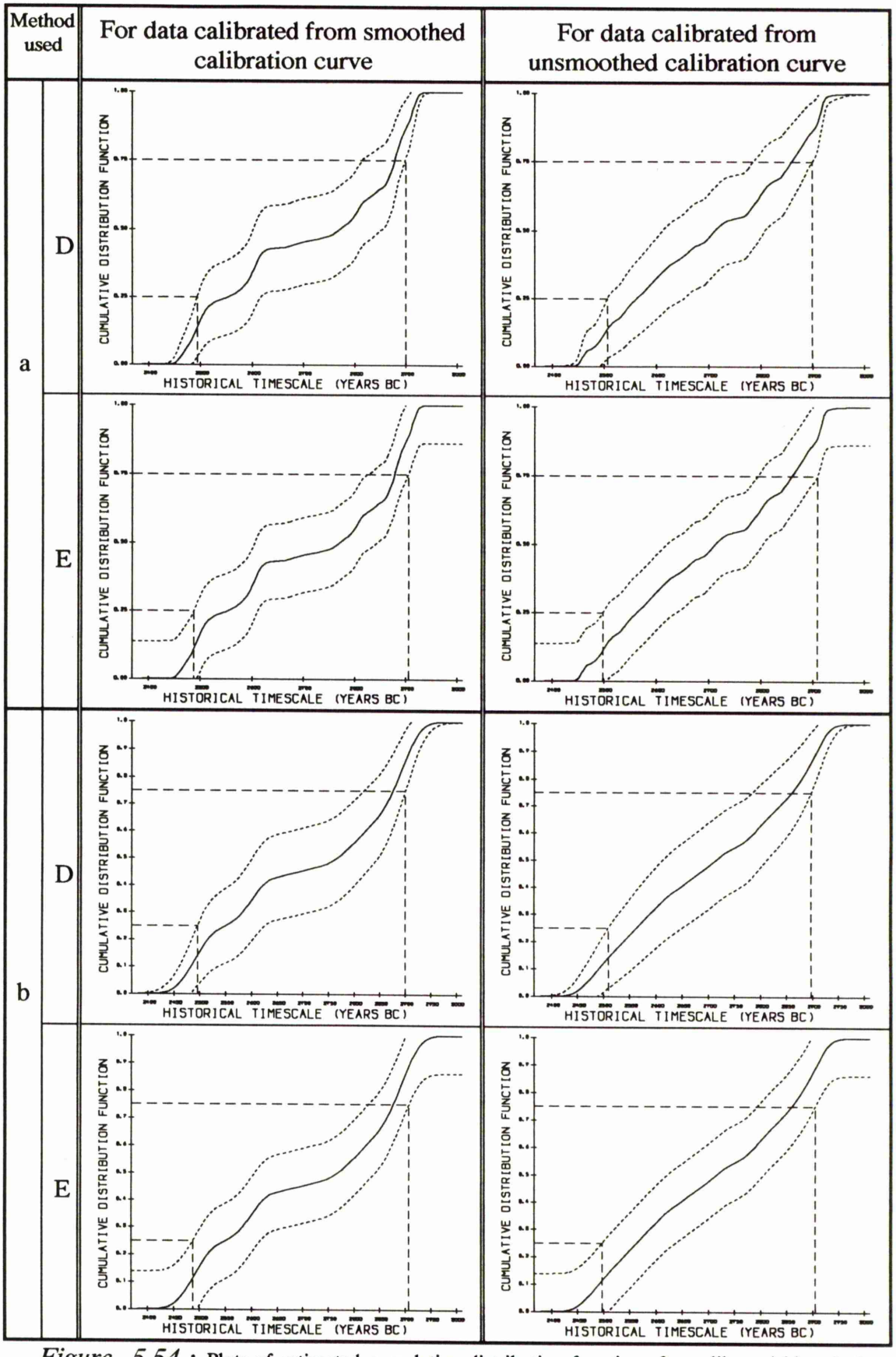

Figure 5.54 : Plots of estimated cumulative distribution functions for calibrated historical dates for ***Sâone-Rhône*** culture **a)** smoothed by the cross-validation method and **b)** smoothed by the weighting method.

Floruit Estimation (years BC)					
Method used		For data calibrated from smoothed calibration curve.		For data calibrated from unsmoothed calibration curve.	
		Point	Interval	Point	Interval
A		2515 - 2879	2480 - 2901	2509 - 2877	2473 - 2903
B		2569 - 2879	2501 - 2913	2563 - 2865	2510 - 2894
C		2539 - 2879	2497 - 2899	2533 - 2812	2513 - 2826
D	Cross-Validation	2555 - 2878	2493 - 2900	2563 - 2860	2507 - 2900
	Weighting Method	2551 - 2876	2495 - 2900	2563 - 2860	2509 - 2897
E	Cross-Validation	2555 - 2878	2488 - 2906	2563 - 2860	2498 - 2909
	Weighting Method	2551 - 2876	2487 - 2906	2563 - 2860	2497 - 2905

Table 5.30 : Point and Interval estimates for the floruit of ***Sâone-Rhône*** culture obtained from the five floruit estimation methods.

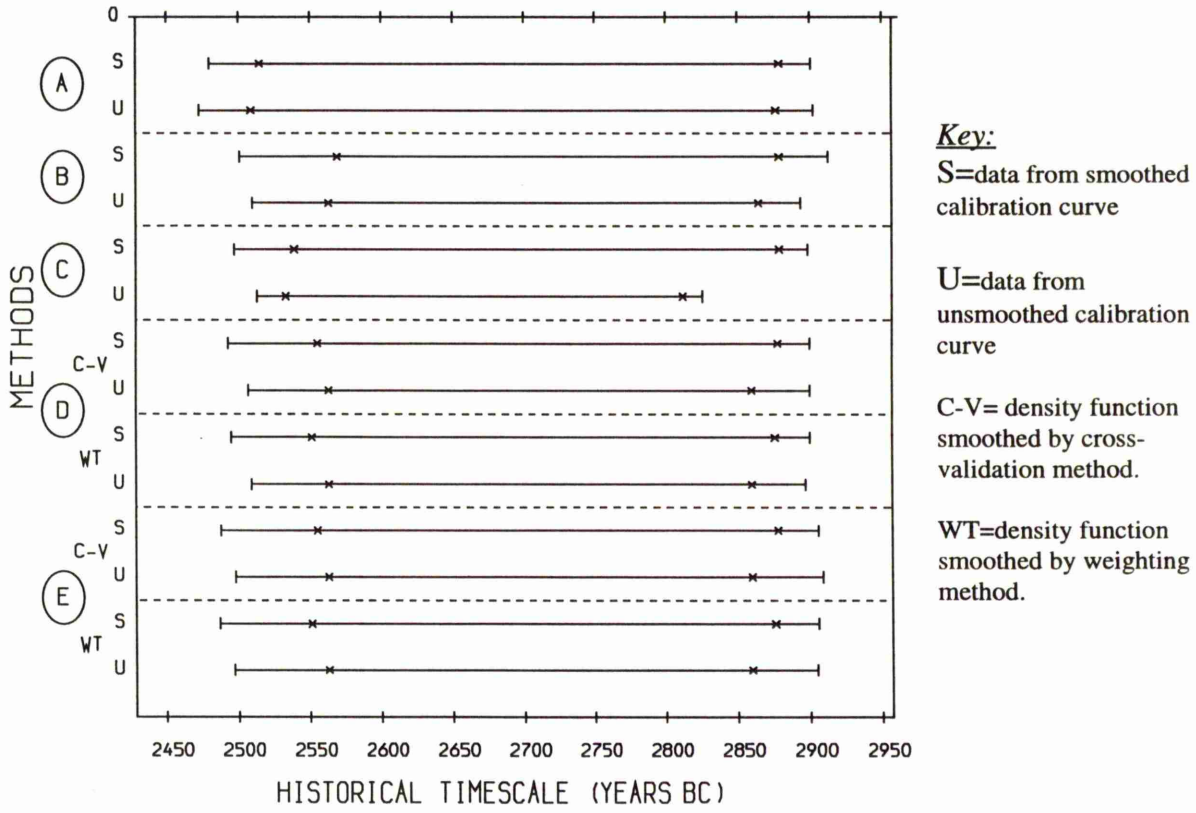

Figure 5.55 : Plots of point (x---x) and interval (|---|) estimates for the floruit of ***Sâone-Rhône*** culture.

Since the calibration of the last ten dates (4191-4320 BP) occurred on the very steep segment of the smoothed curve then all the five methods have significant agreement on the older end of the point and interval estimates. Comparing the floruit estimates produced from smoothed data with the estimates produced from the unsmoothed data, it can be seen how the distribution shape of the smoothed data spread out the floruit estimates on the historical timescale for all the methods except method A which deals with the raw radiocarbon dates and then calibrates the result. Method A provided the widest estimates from the younger end side because of the wiggle in the curve at the period 2500-2575 BC. Due to this wiggle the point estimate for the floruit obtained from method A is at least 25 years wider than the point estimate produced from the remaining methods. When the calibration of the extended lower quartile of the radiocarbon dates occurred on a non-wiggly segment of the curve, the difference in the interval estimates has been reduced. Comparing the estimates produced from method C when applied to both smoothed and unsmoothed data, it can be seen how the wiggles on the unsmoothed curve affected the floruit estimates by reducing it from both sides.

Methods D and E seem to have similar results for the floruit estimates with slightly wider estimates in method E than in D. This similarity may will be due to the effect of greater sample size here since the more data that is available the closer are the estimates from both methods.

5.5.5 Yverdon site

There are 21 radiocarbon dates collected from the *Yverdon* site of the *Sâone-Rhône* culture (*i.e.* most of the 38 radiocarbon dates on the *Sâone-Rhône* culture came from this site).

As the *Yverdon* site appears to cover the whole of the *Sâone-Rhône* culture this group of radiocarbon dates has been calibrated on the same parts of the smoothed and unsmoothed calibration curves as shown in figures 5.52a&b. The corresponding calibrated historical dates are listed with their estimated standard errors in table 5.31. The histogram plots, the estimated p.d.f.'s and c.d.f.'s are displayed in figures 5.56 and 5.57.

Table 5.32 summarises the point and interval estimates for the floruit of *Yverdon* site obtained from applying the five methods and figure 5.58 represents these estimates graphically.

The floruit estimates for the *Yverdon* site appear very similar to the floruit estimates for the whole of the *Sâone-Rhône* culture data with wider estimates for the *Yverdon* site floruit due to reduction of sample size from 38 to 21 dates. It should be noted that the point estimate at the younger end obtained from method A when applied to the smoothed data has been pulled in compared with the estimate obtained when applied to the unsmoothed data. This has happened as the calibration of the lower quartile of the sample on the smoothed curve occurred on a linear segment of the curve but on a wiggle segment in the unsmoothed curve. Method E is the most affected method when the sample size reduced since it has widened the interval estimate of the floruit more than any other method.

#	Radiocarbon Date ± Error (Years BP)	Corresponding historical dates (years BC) calibrated from smoothed curve.			Corresponding historical dates (years BC) calibrated from unsmoothed curve.		
		number of $\hat{t}_{ij}$	estimated $\hat{t}_{ij}$	estimated standard errors $se(\hat{t}_{ij})$	number of $\hat{t}_{ij}$	estimated $\hat{t}_{ij}$	estimated standard errors $se(\hat{t}_{ij})$
1	3900 ± 100	1	2461	62	1	2457	34
2	3900 ± 100	1	2461	62	1	2457	34
3	3970 ± 100	1	2485	65	1	2491	46
4	4000 ± 100	1	2499	87	3	2502	46
						2541	53
						2563	80
5	4010 ± 100	3	2506	114	3	2505	46
			2538	135		2538	53
			2562	127		2568	80
6	4030 ± 100	1	2575	96	3	2516	115
						2529	122
						2576	60
7	4060 ± 100	1	2594	98	1	2589	60
8	4080 ± 100	1	2604	77	3	2610	59
						2845	34
						2847	33
9	4080 ± 100	1	2604	77	3	2610	59
						2845	34
						2847	33
10	4090 ± 90	3	2610	68	5	2615	53
			2835	35		2644	50
			2842	31		2653	38
						2828	51
						2851	35
11	4100 ± 120	3	2615	110	5	2619	70
			2823	134		2640	66
			2852	114		2657	50
						2824	68
						2855	46
12	4140 ± 100	5	2693	113	7	2668	42
			2727	101		2670	42
			2752	87		2697	35
			2807	46		2725	41
			2867	29		2747	90
						2811	57
						2865	39
13	4160 ± 110	3	2767	87	5	2702	38
			2801	51		2720	45
			2872	44		2774	37
						2806	37
						2870	43
14	4170 ± 100	3	2772	72	5	2704	35
			2798	54		2717	41
			2874	40		2776	34
						2804	33
						2872	43
15	4200 ± 110	1	2882	47	3	2782	37
						2798	36
						2880	47
16	4210 ± 100	1	2885	45	3	2786	33
						2796	33
						2883	43
17	4230 ± 110	1	2891	56	1	2889	47
18	4260 ± 100	1	2901	56	1	2903	92
19	4300 ± 100	1	2914	48	1	2915	30
20	4300 ± 110	1	2914	53	1	2915	32
21	4320 ± 110	1	2920	51	1	2919	32

Table 5.31 : Estimates of historical dates corresponding to each observed radiocarbon age, and their estimated standard errors from both smoothed and unsmoothed calibration curve for the group of radiocarbon dates taken from ***Yverdon*** site of ***Sâone-Rhône*** culture.

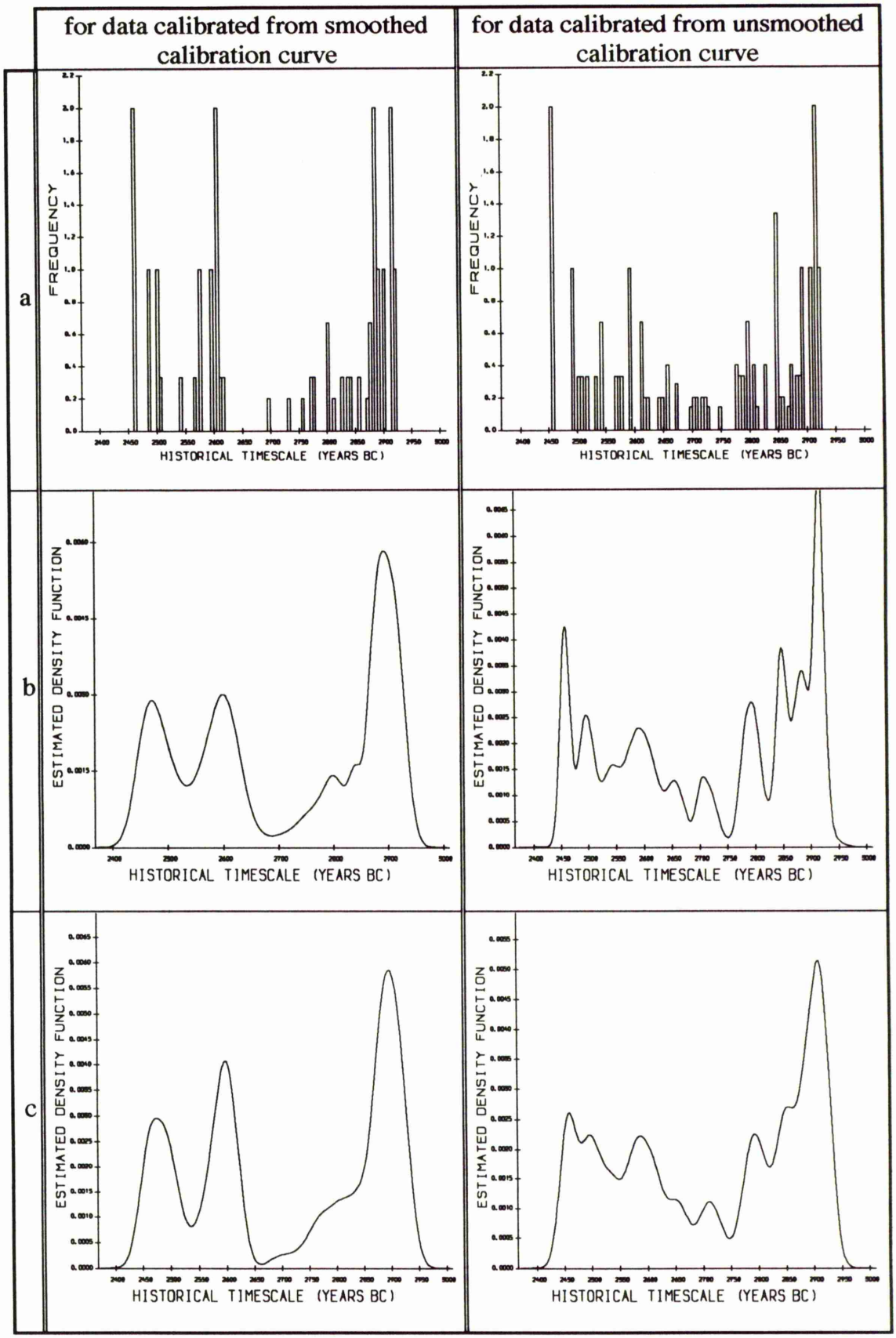

Figure 5.56 : **a)** Histogram plots for the calibrated historical dates for ***Yverdon*** site of ***Sâone-Rhône*** culture and the plots of estimated density functions, **b)** smoothed by cross-validation method and **c)** smoothed by weighting method.

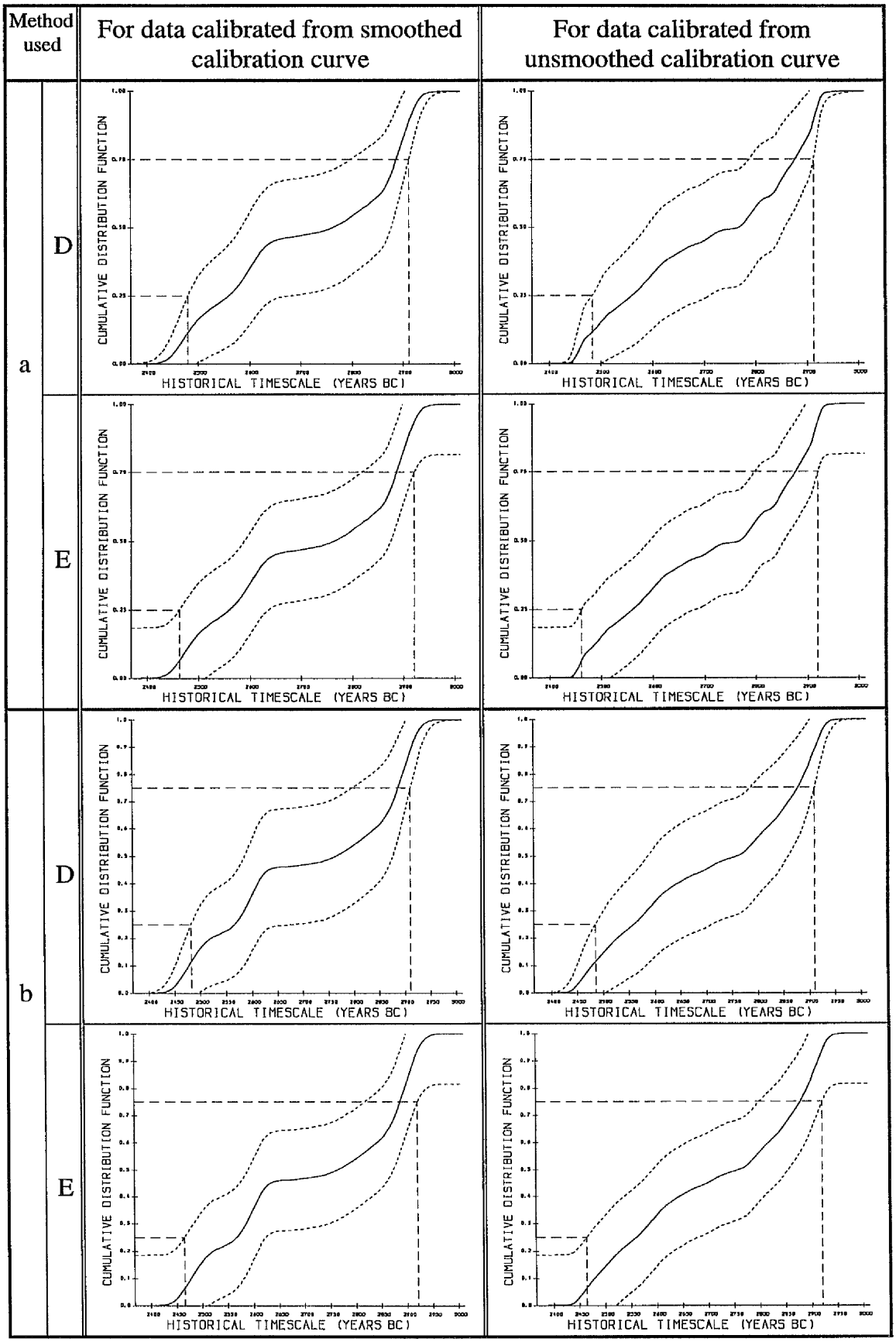

Figure 5.57: Plots of estimated cumulative distribution functions for calibrated historical dates for ***Yverdon*** site of ***Sâone-Rhône*** culture **a)** smoothed by cross-validation method and **b)** smoothed by weighting method.

Floruit Estimation (years BC)					
Method used		For data calibrated from smoothed calibration curve.		For data calibrated from unsmoothed calibration curve.	
		Point	Interval	Point	Interval
A		2572 - 2886	2482 - 2909	2509 - 2884	2478 - 2912
B		2572 - 2886	2502 - 2923	2570 - 2884	2520 - 2914
C		2565 - 2886	2504 - 2918	2550 - 2833	2520 - 2852
D	Cross-Validation	2559 - 2887	2479 - 2911	2561 - 2877	2484 - 2913
	Weighting Method	2566 - 2887	2482 - 2911	2560 - 2879	2486 - 2910
E	Cross-Validation	2559 - 2887	2462 - 2921	2561 - 2877	2461 - 2919
	Weighting Method	2566 - 2887	2465 - 2921	2560 - 2879	2464 - 2920

Table 5.32: Point and Interval estimates for the floruit of ***Yverdon*** site of ***Sâone-Rhône*** culture obtained from the five floruit estimation methods.

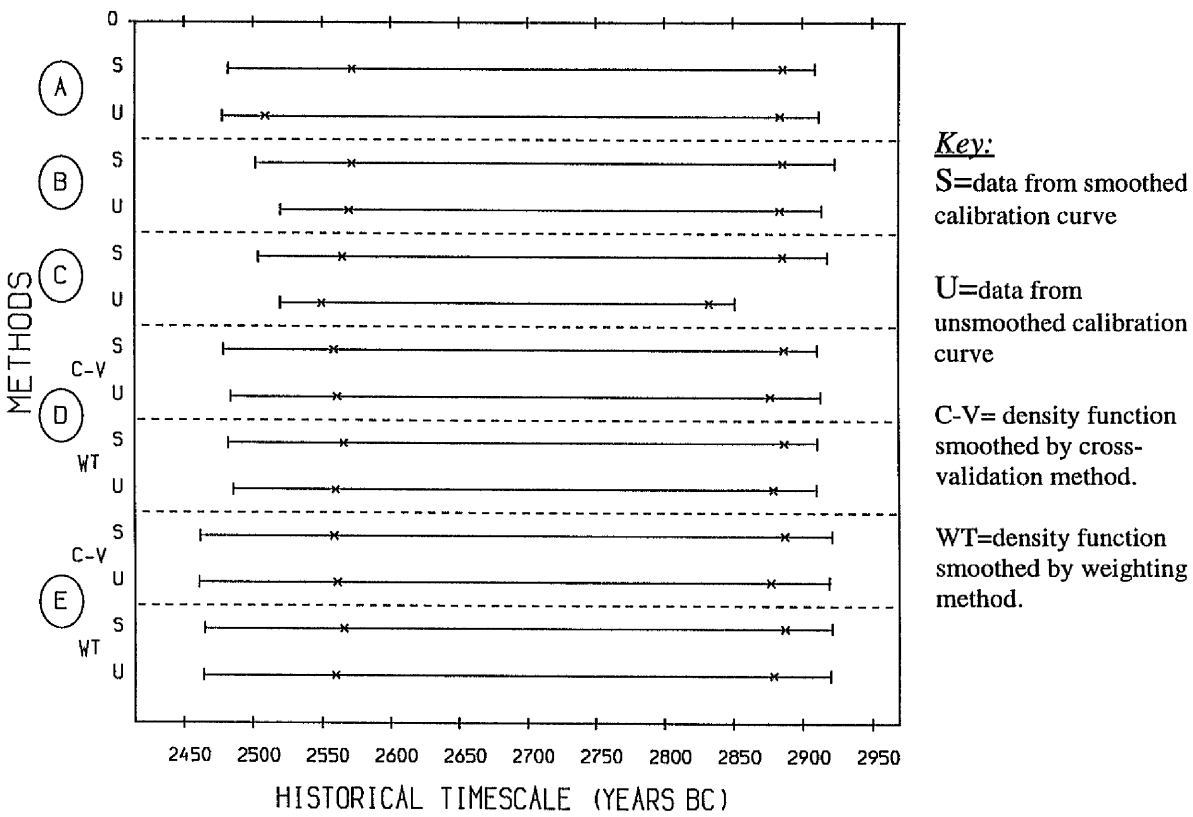

Figure 5.58: Plots of point (x---x) and interval (|---|) estimates for the floruit of ***Yverdon*** site of ***Sâone-Rhône*** culture.

5.5.6 Auvernier La Saunerie site

This group of thirteen radiocarbon dates collected from the *Auvernier La Saunerie* site of the *Sâone-Rhône* culture has been analysed in order to provide the floruit estimates for this site and to compare the resulting estimates with those for the complete data from the *Sâone-Rhône* culture.

The estimated historical dates correspond to each radiocarbon date in this site are given in table 5.33. Their histogram plots, estimated p.d.f.'s and c.d.f.'s are shown in figures 5.59 and 5.60.

The point and interval estimates for the floruit of the *Auvernier La Saunerie* site obtained from the five methods are summarised in table 5.34 and plotted in figure 5.61.

Since method A deals only with the radiocarbon dates and quoted errors, it has produced similar results whether the smoothed or unsmoothed calibration curve was used. The other four methods, which deal with the calibrated historical dates and their errors, have produced wider estimates (both point and interval) when the smoothed calibration curve used. This is primarily due to there being less historical dates, with larger standard errors, calibrated from the smoothed calibration curve.

Generally speaking, these estimates are disappointingly wide particularly for those obtained when the smoothed calibration curve used, but if the spread of the calibrated historical dates on the historical timescale is considered the influence on these estimates from the gaps between the dates can be seen. Also with such a small sample size it is difficult to get a very precise estimate of the floruit

Compared to the floruit estimates of the *Sâone-Rhône* culture, these estimates have extend the younger end and pulled in the older end by different amounts.

#	Radiocarbon Date ± Error (Years BP)	Corresponding historical dates (years BC) calibrated from smoothed curve.			Corresponding historical dates (years BC) calibrated from unsmoothed curve.		
		number of $\hat{t}_{ij}$	estimated $\hat{t}_{ij}$	estimated standard errors $se(\hat{t}_{ij})$	number of $\hat{t}_{ij}$	estimated $\hat{t}_{ij}$	estimated standard errors $se(\hat{t}_{ij})$
1	3960 ± 120	1	2482	73	1	2481	120
2	3990 ± 100	1	2494	75	3	2499	46
						2544	53
						2558	80
3	4000 ± 120	1	2499	104	3	2502	55
						2541	63
						2563	96
4	4000 ± 150	1	2499	130	3	2502	69
						2541	79
						2563	120
5	4077 ± 70	1	2602	57	1	2607	72
6	4103 ± 70	3	2618	80	5	2621	41
			2821	63		2639	39
			2855	52		2659	29
						2822	40
						2856	27
7	4129 ± 70	3	2678	93	7	2665	29
			2810	35		2679	54
			2864	20		2694	25
						2734	98
						2738	98
						2814	40
						2862	27
8	4130 ± 100	3	2678	108	7	2665	42
			2810	50		2679	77
			2864	29		2694	35
						2734	95
						2738	93
						2814	56
						2862	30
9	4140 ± 140	5	2693	168	7	2668	58
			2727	161		2670	58
			2752	148		2697	49
			2807	64		2725	58
			2867	60		2747	149
						2811	79
						2865	54
10	4160 ± 100	3	2767	79	5	2702	35
			2801	47		2720	41
			2872	40		2774	34
						2806	33
						2870	39
11	4160 ± 120	3	2767	95	5	2702	42
			2801	56		2720	49
			2872	48		2774	40
						2806	40
						2870	47
12	4180 ± 120	3	2777	103	5	2706	42
			2794	94		2707	42
			2877	48		2778	40
						2802	40
						2875	51
13	4191 ± 70	1	2879	29	3	2780	24
						2800	23
						2878	30

Table 5.33 : Estimates of historical dates corresponding to each observed radiocarbon age, and their estimated standard errors from both smoothed and unsmoothed calibration curve for the group of radiocarbon dates taken from ***Auvernier, La Saunerie site of Sâone-Rhône*** culture.

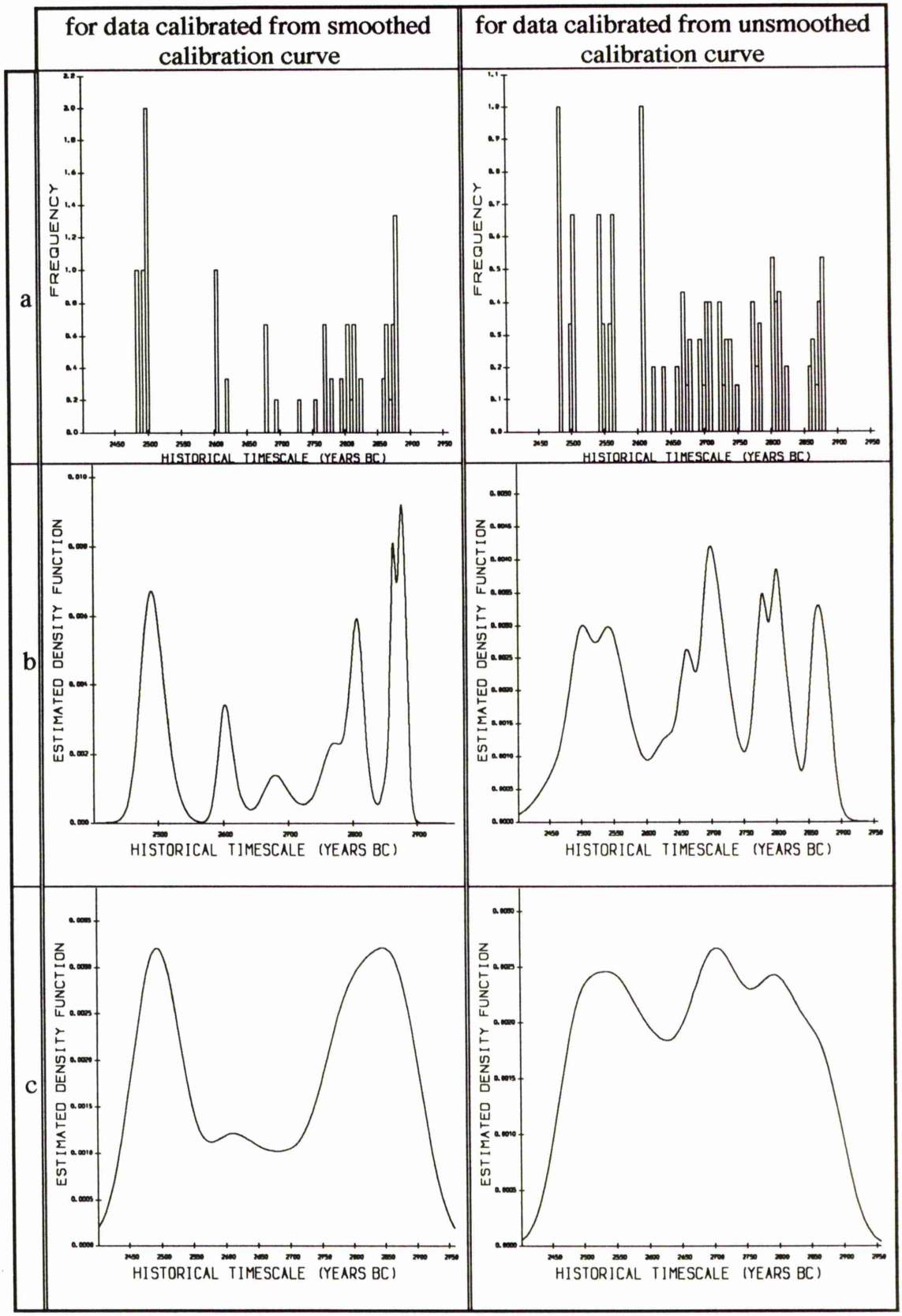

Figure 5.59: a) Histogram plots for the calibrated historical dates for ***Auvernier, La Saunerie*** site of ***Sâone-Rhône*** culture and the plots of estimated density functions, b) smoothed by cross-validation method and c) smoothed by weighting method.

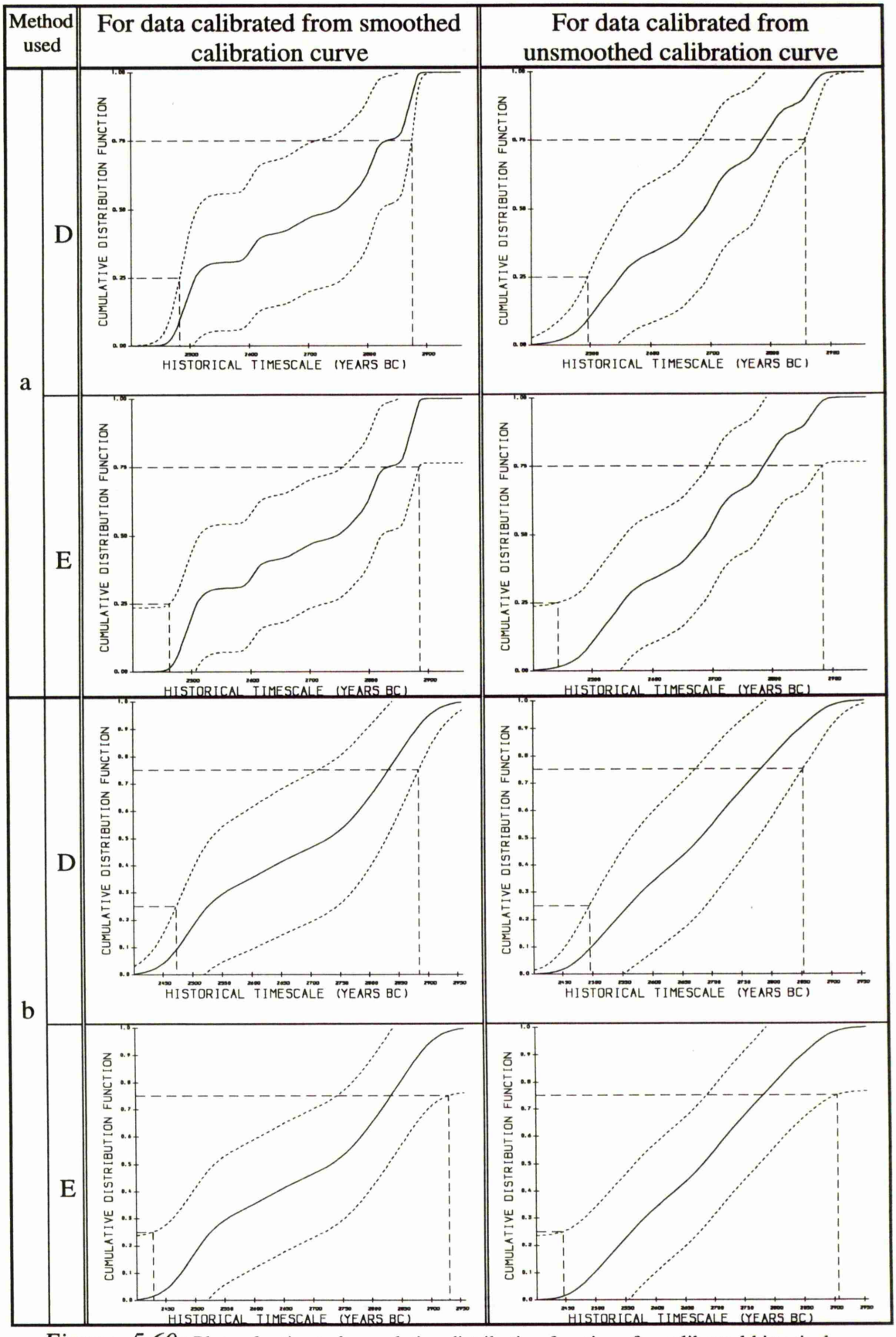

Figure 5.60: Plots of estimated cumulative distribution functions for calibrated historical dates for ***Auvernier, La Saunerie*** site of ***Sâone-Rhône*** culture **a**) smoothed by cross-validation method and **b**) smoothed by the weighting method.

Floruit Estimation (years BC)					
Method used		For data calibrated from smoothed calibration curve.		For data calibrated from unsmoothed calibration curve.	
		Point	Interval	Point	Interval
A		2499 - 2872	2468 - 2892	2501 - 2870	2462 - 2890
B		2499 - 2858	2441 - 2879	2563 - 2800	2491 - 2827
C		2499 - 2842	2441 - 2857	2526 - 2769	2499 - 2786
D	Cross-Validation	2510 - 2833	2483 - 2876	2551 - 2787	2496 - 2858
	Weighting Method	2527 - 2834	2474 - 2885	2561 - 2783	2496 - 2853
E	Cross-Validation	2510 - 2833	2464 - 2886	2551 - 2787	2443 - 2885
	Weighting Method	2527 - 2834	2429 - 2931	2561 - 2783	2447 - 2907

Table 5.34: Point and Interval estimates for the floruit of ***Auvernier, La Saunerie*** site of ***Sâone-Rhône*** culture obtained from the five floruit estimation methods.

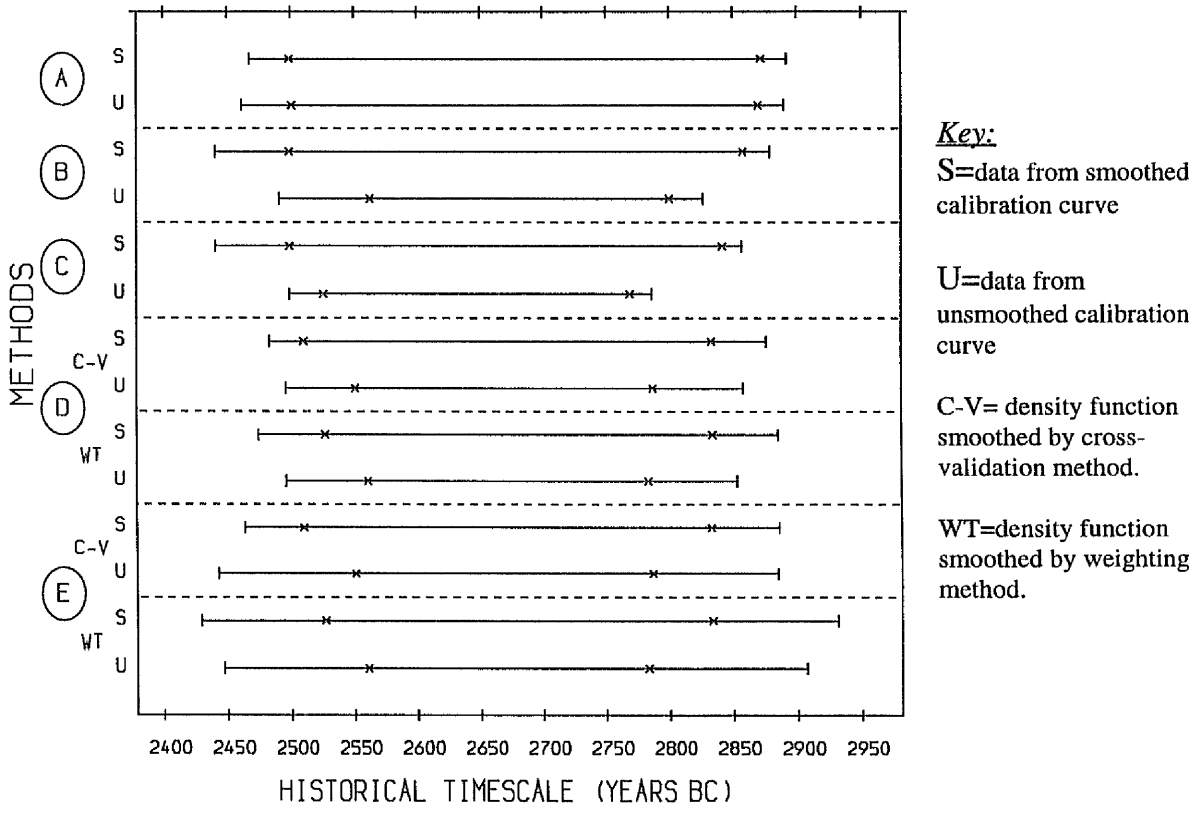

Figure 5.61: Plots of point (x---x) and interval (|---|) estimates for the floruit of ***Auvernier, La Saunerie*** site of ***Sâone-Rhône*** culture.

5.6 Discussion

As the five methods of floruit estimation have been applied on various groups of radiocarbon dates from different archaeological cultures, it is important to provide an overall summary of the performance of each of the methods on these data sets of real archaeological interest.

To do this the features which appear to influence the performance of each method on the various data sets are considered individually, and then the performances of each of the five methods are compared in overall conclusion.

5.6.1 The Shape and the Degree of Smoothing of the Calibration Curve

The influence of this factor on the performances of the five methods varied from one method to another. While a huge influence occurred in some methods for some applications (for A as in *Cham* culture and for C as in *Cortaillod* culture and *Twann* site), little effect occurred for different applications such as in A for *Nok* culture. Accordingly the influence of this factor on each method will be highlighted and discussed individually.

- ***Effect of the Calibration Curve on the Performance of Method A***

Since this method deals only with the raw radiocarbon dates and their quoted errors to provide the floruit estimates (in the sense of calibrating the quartiles and their extended values to the historical timescale), it is quite clear that, for this method, the shape of the calibration curve has a direct effect on the obtained results. While the results obtained from using the smoothed and unsmoothed calibration curve were identical for most data sets, differences occasionally occurred as with the *Cham* culture and the interval estimate of the floruit of the *Seeberg-Burgäschisee-S* site of the *Cortaillod* culture. This was particularly clear when the calibration curve was very wiggly in part and especially when it was wiggly at the extreme of the data set where the two

quartiles or their extended values were calibrated. Further, with many wiggles on the edges, the estimates for the floruit tend to become wider.

The results obtained using both smoothed and unsmoothed calibration curves were identical when the curve contained small wiggles or the calibration of the two quartiles or their extended values occurred on non-wiggly segments in both curves. Conversely, differences occurred between the results obtained from smoothed and unsmoothed calibration curves when the curve had large wiggles or the calibration of the two quartiles or their extended values occurred on wiggly segments of the curve. An explicit examples showed these situations *(i.e.* when the point estimates of the floruit obtained using smoothed and unsmoothed calibration curves were identical and their interval estimate were different and vice versa as a result of existence or not of the wiggles on the curves) in the applications of the *Cham* culture (without the outlier date), *Seeberg-Burgäschisee-S* site and *Yverdon* site of *Sâone-Rhône* culture.

- ***Effect of the Calibration Curve on the Performance of Method B***

The effect of the shape of the calibration curve on the performances of this method emerges from its effect on the calibrated dates and their estimated errors. For most cultures, the point estimates of the floruit obtained from the historical dates calibrated on the smoothed and unsmoothed curves are similar. However this similarity does not extend to interval estimates of the floruit. On the whole, the interval estimates of the floruit obtained using historical dates calibrated on the smoothed calibration curve are wider than those obtained when using the historical dates calibrated on the unsmoothed calibration curve as happened in the *Pfyn* culture, the *Horgen* culture, the *Nok* culture and the *Twann* site of the *Cortaillod* culture. This is mainly due to the much larger values of the estimated standard errors for the estimated historical dates calibrated on the smoothed curve, as an effect of the smoothing procedure on

the slope of the calibration curve, compared with those based on the unsmoothed calibration curve.

- ***Effect of the Calibration Curve on the Performance of Method C***

As this method takes the weighted average of multiple historical dates calibrated from a single radiocarbon date, its results were affected mostly by the wiggles on the unsmoothed calibration curve as seen in the *Cortaillod* culture, the *Twann* site of the *Cortaillod* and the *Sâone-Rhône* culture. Generally speaking, the results obtained from the estimated historical dates calibrated on the smoothed curve are wider than those obtained on the unsmoothed curve. This is due to there being more wiggles on the unsmoothed calibration curve which tighten the results obtained using the unsmoothed calibration curve and to the large values of the estimated standard errors corresponding to the estimated historical dates calibrated on the smoothed curve which widen the results obtained using the smoothed calibration curve. This was very clear in the application of the *Twann* site.

- ***Effect of the Calibration Curve on the Performance of Method D***

Influence of the shape and degree of smoothing of the calibration curve on the performance of this method can not be distinguished easily from that effect of the degree of smoothing of the density function used in this method. Differences between the results obtained using smoothed and unsmoothed calibration curve occurred for most applications. The degree of these differences depends on the shape of the calibration curve. The results became nearly identical when the calibration curve was effectively monotonic with small wiggles or linear as in the cases of the *Pfyn* and *Childers* cultures but vary when the curve was wiggly particularly at the extremes of the curve as seen in the *Cham* and *Horgen* cultures.

One would notice that, when the calibration curve was wiggly as in the *Cham* and *Horgen* cultures the results based on the unsmoothed calibration curve were wider than those when the smoothed curve was used. On the other hand, the results obtained using the smoothed calibration curve were wider when the shape of the curve was monotonic or steep as happened in the *Auvernier La Saunerie* site of the *Sâone-Rhône* culture.

- ***Effect of the Calibration Curve on the Performance of Method E***

From the previous applications there was no clear evidence of the influence of the shape of the calibration curve on the performance of this method. The reason behind this is because this method had influenced mostly by other factors particularly the degree of smoothing of the density function and the sample size which involved in the approximation of the constant variance used for the cumulative distribution function.

5.6.2 Effect of the Sample Size on the Performances of the Five Methods

As with the simulations the sample size has a remarkable effect on the performances of the five methods. In general, the performances of the five methods improved with sample size as the results obtained for the applications (*i.e.* the estimated quartile interval) converge to the true quartile interval. With small sample sizes the performances of the five methods tended to be poor and the obtained results became wider particularly for method E which is substantially affected by this factor as can be seen in the *Childers* culture. All methods gave better performances in providing interval estimates for the floruit as can be noticed in the applications of the *Pfyn*, *Cortaillod* and *Sâone-Rhône* cultures. Also, whenever sample size increased the results obtained from the two methods D and E became closer.

5.6.3 Effect of the Outliers on the Performances of the Five Methods

The effect of the outliers on the results can be noticed for both applications (the *Cham* and the *Childers* cultures) when the outlier date was included in the analyses. The results obtained were shifted towards the outlier compared with those when it was excluded. The magnitude of this effect varied across the five methods.

A single outlier date had only a small effect on the results obtained from method A in the case of *Cham* culture but a much more considerable effect on the results obtained in the case of *Childers* culture. This can be ascribed to the shape of the calibration curve and the distance of the outlier from the remaining dates (sample size also plays a significant role).

For method B, the effect of the outlying date on the results was to tighten the estimates in the case of *Cham* culture and widen the estimates in the case of *Childers* culture. This effect is mainly due to the spread of the calibrated historical dates for each group. While the historical dates in *Cham* group were close to each other at the estimated lower quartile, the historical dates in the *Childers* group were separated at the estimated upper quartile (*i.e.* influenced by the gap in the data in the period 600-550 AD).

When method C was applied, the effect of the outlier was to widen the estimates except in the smoothed case of *Cham* group where the very steep and wiggly segment of the curve narrowed the estimates as in method B but of course by a different amount.

While method D has been affected by the outlier date more than methods A, B and C, method E is the most affected. The reasons behind this are the shape of the calibration curve, the degree of smoothing of the estimated p.d.f. and the sample size.

5.6.4 Effect of the Degree of Smoothing for the Density Function on the Performances of the Non-Parametric Density Estimation Methods

The degree of smoothing for the density function underlying the estimated historical dates has the foremost effect on the results of the floruit estimates produced from the two methods D and E. In general, wider estimates were obtained for the floruit when there was more smoothing on the density function as occurred in the *Cham* and *Horgen* cultures except in a few cases where too little smoothing caused a discontinuity on the cumulative function and hence widened the estimates of the floruit as happened with the *Nok* culture.

5.6.5 Overall Conclusions

The conclusions drawn from the previous applications were that the floruit estimates obtained from the pen and paper methods were influenced by the shape of the calibration curve more than those obtained from the highly computational methods which themselves were influenced, mostly, by the degree of smoothing of the density function.

All five methods were very similar when the calibration curve contained few wiggles as occurred in the *Horgen* and *Childers* cases. For pen and paper methods, method A produced the widest estimates for the floruit compared with the other methods when the calibration curve was very wiggly (*e.g.* with the *Cham* data set). Comparing proportionally the interval estimates produced from method B with the interval estimates produced from method A, it was found that the interval estimates obtained from method B were wider than those from A. The reason for this is that method A took account of the radiocarbon dates errors only to provide the interval estimates, while method B took account of the estimated standard errors for the calibrated historical dates which in turn took account of radiocarbon dates errors, calibration curve errors and the slope of the calibration curve. The presence of wiggles in the

calibration curve tends to narrow the floruit estimates obtained from method C more than any other method.

In most cases, the floruit estimates obtained from the density estimation methods were wider than the estimates obtained from pen and paper methods with a major contribution to this due to smoothing the density function.

The effect of the outlier date on the floruit estimates depends, mainly, on the shape of the calibration curve for the results obtained from methods A, B and C, while the amount of smoothing on the density function played an extra role in the effect of the outlier (in addition to the calibration curve and sample size) on the floruit estimates obtained from density estimation methods particularly E.

Finally in the choice of the optimal method, these applications seemed to be agreed with the conclusions of the simulation study of the previous chapter that method D would be optimal among the highly computational methods, while method B would be best among the pen and paper methods.

5.7 Summary

The main aim of this chapter was to illustrate and compare the applicability of the five methods of floruit estimation (presented in chapter three) on real data applications. Various groups of radiocarbon dates, with different features, collected from different archaeological cultures were used in these applications. Features of each group, such as sample size and shape of the calibration curve, were highlighted.

The majority of this chapter was concerned with the analysis of each group individually and the comparison of the performances of the five methods. The effect of several factors on the floruit estimates has been considered and highlighted throughout the applications.

The major emphasis in this chapter has been to focus on the factors which may influence the performances of the five methods. The effect of each factor on the performances of the five methods was discussed. The major factors affected the floruit estimates were found to be the shape of the calibration curve, for the pen and paper methods, and the smoothing degree of the density function for the highly computational methods.

On the whole method D has been concluded to be the best of all five methods while B was the alternative choice if only a paper, pencil and calibration curve are available.

Chapter 6

Overlap of Archaeological Cultures

6.1 Introduction

In chapter two attention was focused on the problem of calibration of a single radiocarbon date. This was extended in chapter three to cover the case of a set of radiocarbon dates from a single archaeological phenomenon in order to provide an interval estimate for a summary measure (*i.e.* the floruit) of the historical timespan of the underlying archaeological culture. This chapter will be devoted to the problem of whether or not two archaeological cultures or sites ***overlap*** on the historical timescale and, indeed, to ***quantify the degree of overlap*** on the basis of sets of radiocarbon dates from each culture.

In the archaeological literature, the comparison of neighbouring archaeological cultures describes, in general, the structure and development of each culture and highlights common features with other cultures. An important aspect of the comparison is to identify patterns of cultural changes and

associations among various archaeological cultures and to decide whether cultural transmission between them has occurred or not. The quantity and diversity of materials from comparative cultures allow for recovery of their settlement patterns, investigation of their characterisation and determination of their chronology, which altogether, play significant roles in the assessment of temporal and cultural linkage between the cultures.

As the prime interest of this chapter is in assessing the degree of temporal overlap between two neighbouring cultures (neighbouring in the chronological sense rather than in the geographical sense), there is no attempt here to provide a holistic review of the archaeological comparison between cultures or sites since there exist several archaeological articles comparing archaeological cultures, their chronology, artefacts, settlements, economy,....etc. - see for examples Gimbutas (1965), Telegin (1987), Dergachev (1989) and Rimantiene (1992).

In the next section a formal definition of the overlap between two archaeological cultures will be produced and some possible approaches to the estimation of such an overlap will be provided. These approaches will then be applied to archaeological data to illustrate their applicability.

6.2 Definition of the Overlap

The overlap of two cultures, in the archaeological sense, is to be interpreted as the period of time where the two cultures have coincided with each other and hence have a possibility of cultural influence on one another. To define the overlap in mathematical terms, it is convenient to recall the two assumptions stated earlier in section 1.3 which assumed that, for an archaeological phenomenon/culture, there exists a frequency distribution (with respect to the historical timescale) of all possible artefacts or materials from the phenomenon which might be sampled by an archaeologist and the actual

artefacts sampled can be assumed to be a reasonably representative sample from this frequency distribution.

This provides an effective basis for the definition of the temporal overlap between two archaeological cultures in terms of these frequency distributions. Thus to assess whether or not two distinct cultures were contemporaneous with each other consider the overlap between the two frequency distributions underlying them. If there is temporal overlap between two cultures, then the degree of overlap will be shown as an intersection between their frequency distributions. On this basis, there is one of the following three possibilities of the degree of overlap between two archaeological cultures:-

1) There is ***No Overlap*** at all between the two cultures. This occurs when the two frequency distributions fail to overlap as shown in figure 6.1a.

2) There is a ***Partial Overlap*** between the two cultures when their frequency distributions do overlap as shown in figure 6.1b.

3) There is a ***Complete Overlap*** between the two cultures if the range of one of the frequency distributions falls inside the range of the other as illustrated in figure 6.1c.

The second of these, ***Partial Overlap***, is the practically relevant case and represents the real problem which is concentrated on here *i.e.* attempt to measure the degree of overlap (**OL**) between two partially overlapping archaeological cultures.

In practice, the collected radiocarbon dates from the two cultures are the data which can provide inferences about the temporal overlap between them. Assume that one archaeological culture, say the '***x***' culture, has produced a group of radiocarbon dates $x_1, x_2, \ldots\ldots, x_n$, in increasing order of age in years BP so that x_1 is the youngest date of culture '***x***', with quoted errors $\sigma_{x_1}, \sigma_{x_2}, \ldots\ldots, \sigma_{x_n}$. A different and distinct archaeological culture, say the '***y***'

culture, has produced a group of radiocarbon dates $y_1, y_2, \ldots\ldots, y_m$ with quoted errors $\sigma_{y_1}, \sigma_{y_2}, \ldots\ldots, \sigma_{y_m}$. Also without loss of generality assume that the 'x' culture is "younger" than the 'y' culture *i.e.* effectively that $x_n < y_m$. Although this is clearly not an explicit definition it is sufficient for explaining the underlying basic ideas of overlap estimation.

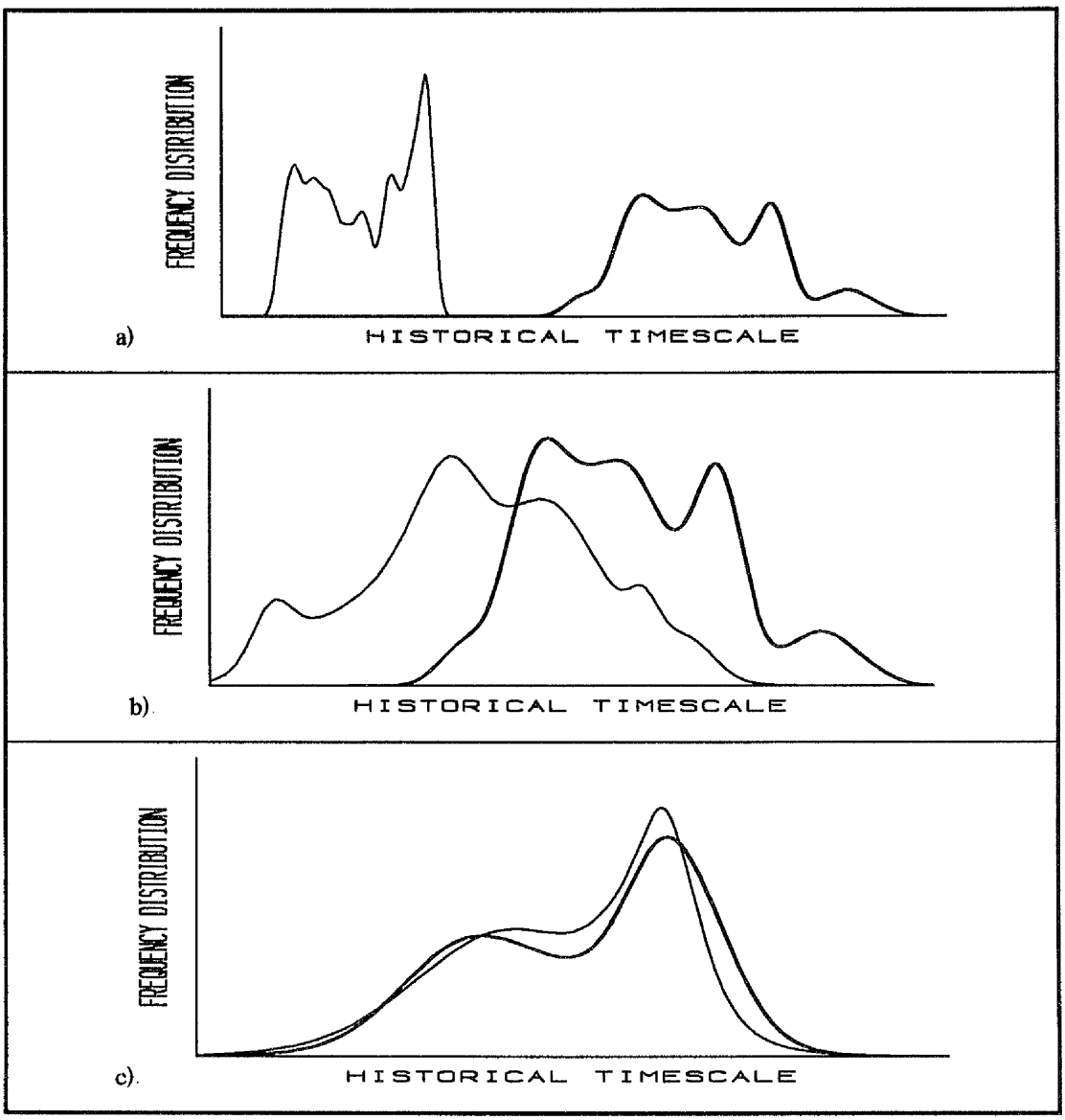

Figure 6.1 :Diagrammatic representation of the three possibilities of the degree of overlap between two frequency distributions for two distinct archaeological cultures **a)** No Overlap between the two cultures, **b)** Partial Overlap between the two cultures and **c)** Complete Overlap between the two cultures.

One possible and simple way to check the overlap using the radiocarbon dates is to represent the range of the sample of dates from each culture graphically with a bar. If the two bars overlap, this will gives an indication of possible overlap between the two cultures as illustrated in figure 6.2. However this method does not show the concentration of radiocarbon dates for each culture in the overlap area nor indeed allow for the errors associated with each radiocarbon date. A simple alternative method which overrides this problem is to construct back-to-back histogram plot for the cultures as in figure 6.3.

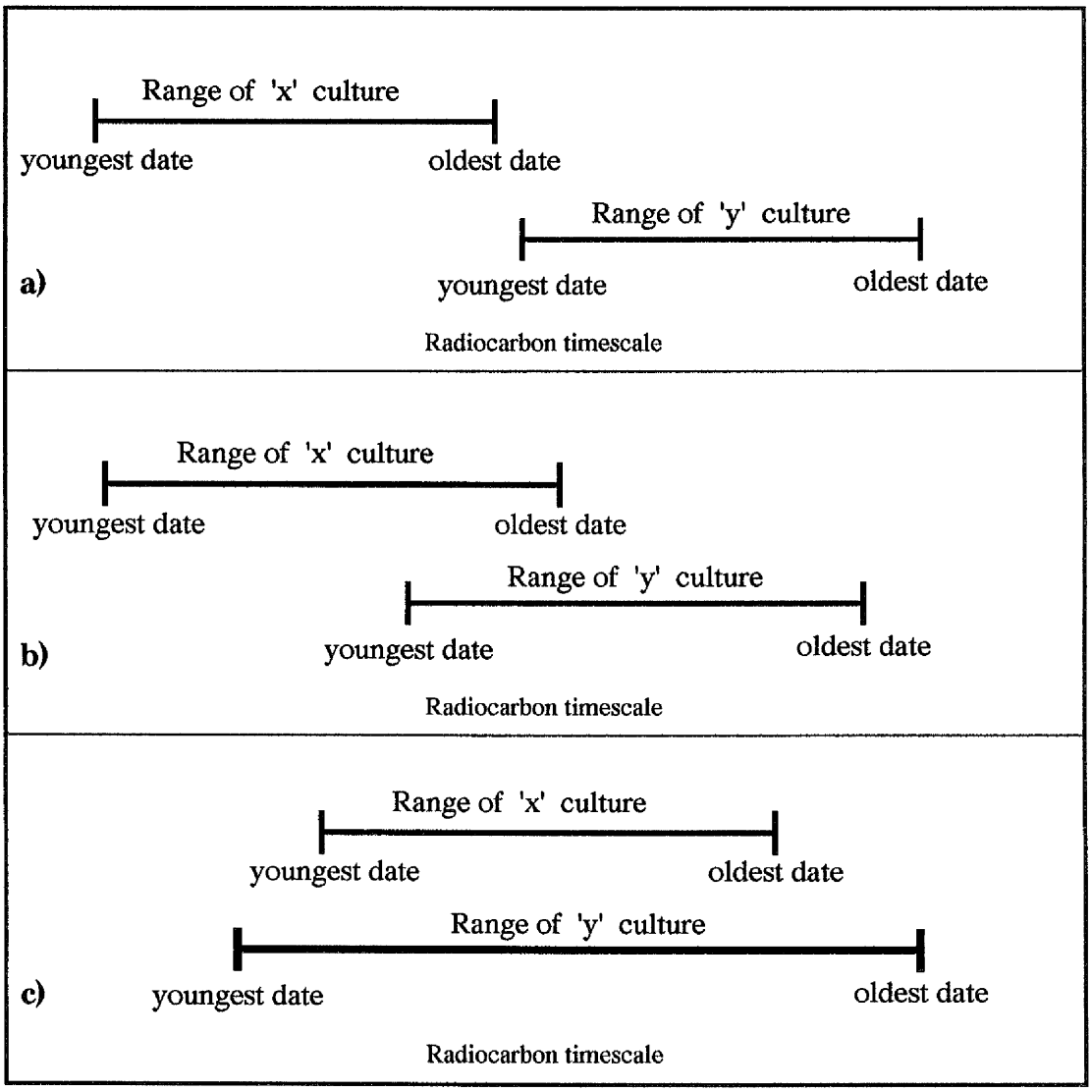

Figure 6.2 :Diagrammatic representation of the three possibilities of the degree of overlap between two distinct archaeological cultures represented by the ranges of the sample of dates from each culture a) No Overlap between the two cultures,.b) Partial Overlap between the two cultures. and c) Complete Overlap between the two cultures.

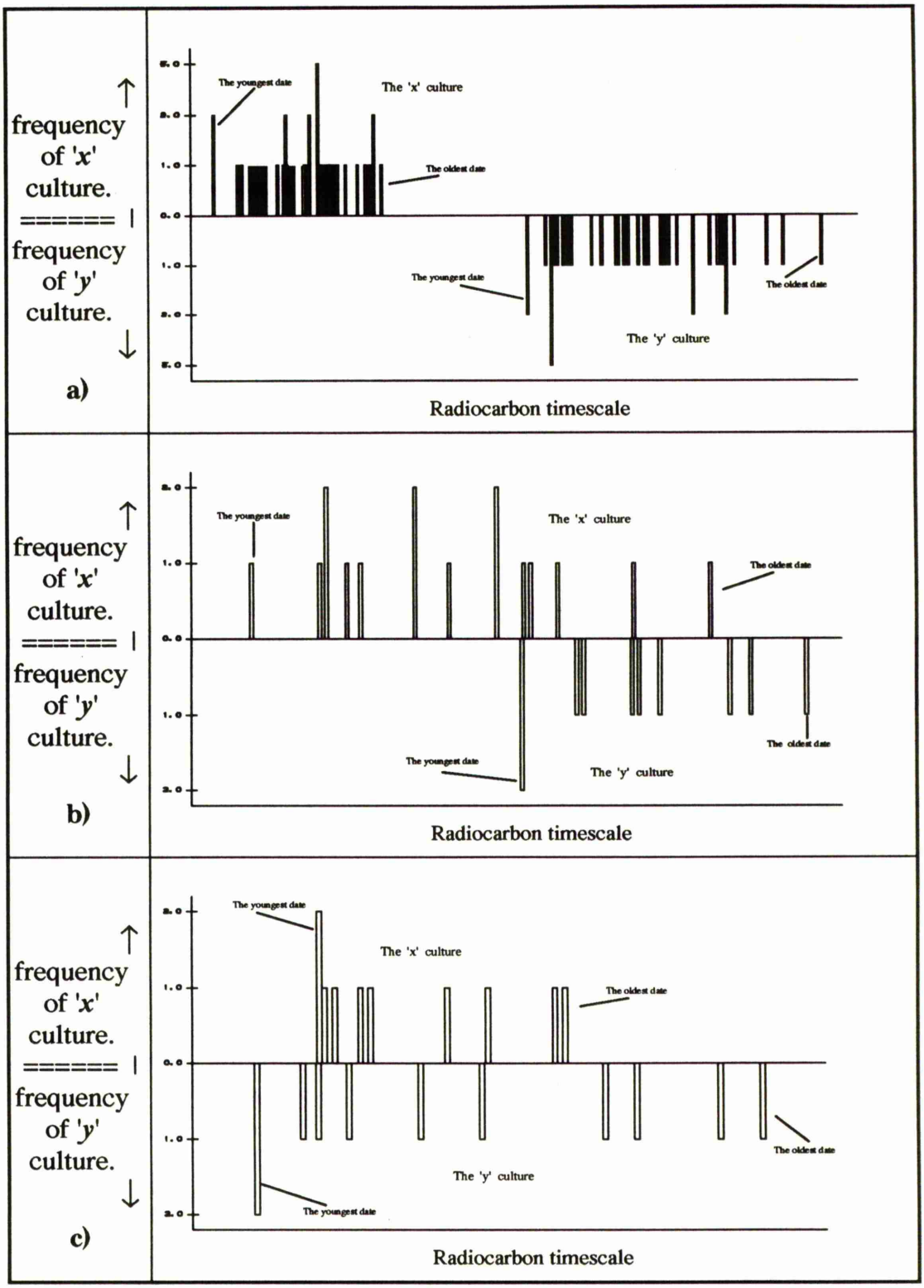

Figure 6.3 : Illustrations of histograms plots for two groups of radiocarbon dates collected from two cultures showing the three possibilities of overlap **a)** No Overlap between the two cultures, **b)** Partial Overlap between the two cultures and **c)** Complete Overlap between the two cultures.

6.3 Measurement of Overlap

The degree of overlap (OL) between two archaeological cultures can be measured in different ways. Here, attention is restricted to two such choices. The first of these is based on the Proportional overlap (POL) between their frequency distributions and the second is based on the time overlap between the two floruits of the archaeological cultures *i.e.* Floruit overlap (FOL).

6.3.1 Proportional Overlap (POL)

The POL between two archaeological cultures is a measure on the scale of **0** to **1** of the common timespan (on the historical timescale) of the two cultures. Mathematically it is defined as the common proportion (intersection area) between the two frequency distributions, say $p_1(t)$ and $p_2(t)$, underlying the two cultures, and therefore is such that

$$0 \leq POL \leq 1$$

which means the three possibilities of overlap are as follow:-

If there is No overlap, then $POL=0$

If there is Partial overlap, then $0<POL<1$

and If there is Complete overlap, then $POL=1$

As the practical problem relates to the case of partial overlap, the remainder of this chapter will be devoted to its estimation but there are two types of partial overlap which can occur between the two cultures.

The first and simplest one is ***single overlap*** which can occur only when there is a single point of intersection between the two frequency distributions and is shown as the shaded area in figure 6.4a.

The second case is a situation of ***multi-modal*** overlap where there is more than one point of intersection between the two frequency distributions as illustrated in figure 6.4b. In this chapter attention is restricted to the case of

single overlap and the multi-modal situation is not considered here although there are obvious simple extensions to the single overlap case which can be easily pursued.

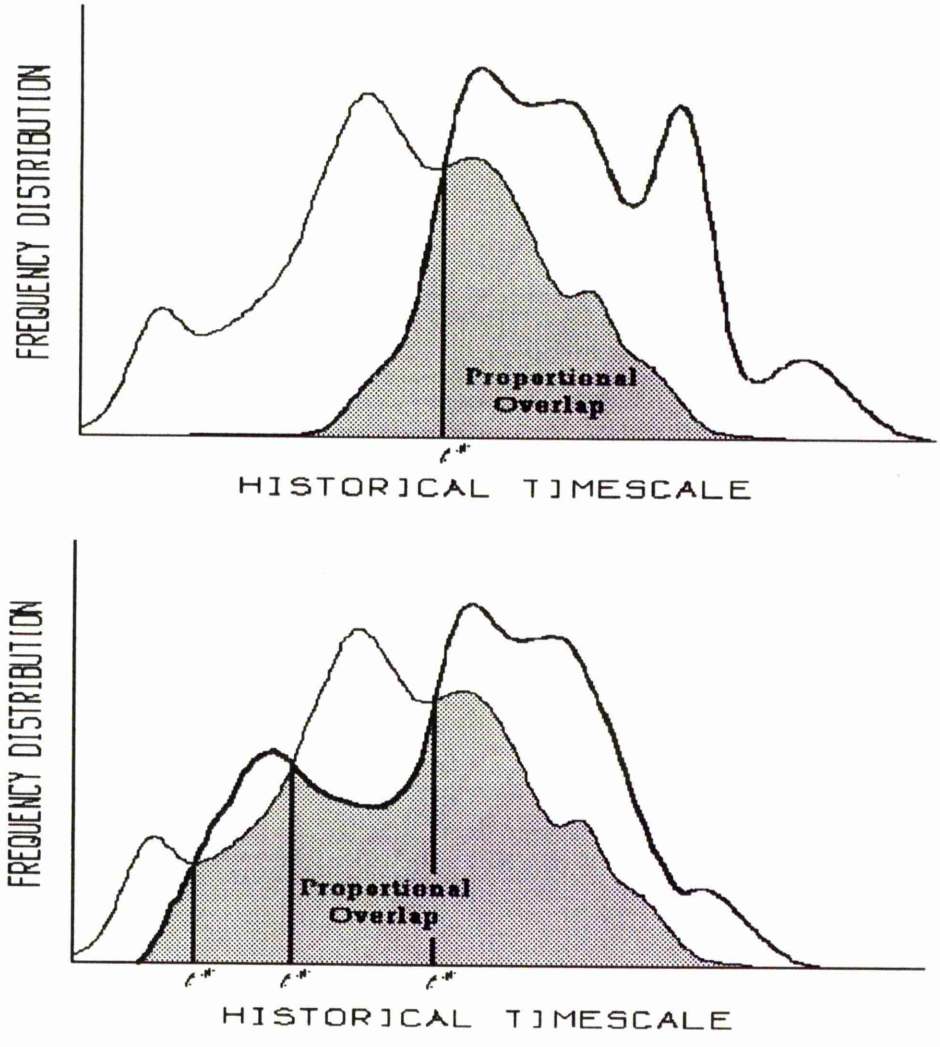

Figure 6.4 : Diagrammatic representation of the definition of Proportional Overlap between the frequency distributions of two archaeological cultures a) single partial overlap, and b) Multi-modal partial overlap.

6.3.1.1 Estimating the Proportional Overlap

In the case of single overlap the first essential step in the estimation of the POL is to estimate the intersection point of $p_1(t)$ and $p_2(t)$. If t^* is the single point of intersection then it can in principle be obtained by solving

$$p_1(t^*) = p_2(t^*) \qquad \text{for } t^* .$$

In practice, replace $p_1(t)$ and $p_2(t)$ by their estimates $\hat{p}_1(t)$ and $\hat{p}_2(t)$ and solve

$$\hat{p}_1(t^*) = \hat{p}_2(t^*) \qquad \text{for } t^* .$$

This is computationally awkward to solve and is perhaps best achieved through a computer search over a sensible range of historical ages from both cultures. Once the point of intersection, t^*, is estimated by $\hat{t}^*$, then the degree of POL is estimated by

$$\hat{POL} = \int_{\hat{t}^*}^{\infty} \hat{p}_1(t)dt + \int_{-\infty}^{\hat{t}^*} \hat{p}_2(t)dt \qquad .....(6.1)$$

$$= 1 - \hat{F}_1(\hat{t}^*) + \hat{F}_2(\hat{t}^*)$$

Of course, there is uncertainty associated with any point estimate and there are two main factors involved in this uncertainty, and in the uncertainty of t^* as well, which should be taken into account in order to derive an interval estimate for the POL. The first factor is the *degree of smoothing* involved in the estimation of the frequency distributions underlying the two cultures, while the second factor is the *variability in the estimation* of the cumulative distribution function of each culture given an appropriate amount of smoothing. The effect of the degree of smoothing on the estimation of POL results from its crucial importance in the determination of the shape of the frequency distribution underlying each culture and, consequently, plays an important role in the estimation of the intersection point t^*. Furthermore, it has an effect on the determination of the type of overlap (*i.e.* single or multi-modal) in that changing the degree of smoothing may move one from a single to a multi-modal case.

Given the specific degree of smoothing, the uncertainty in the estimation of POL results from the variability in the cumulative distribution function which can be utilised to derive a standard error for the POL. This has already been dealt with for a single culture effectively in chapter 3.

Accordingly, an approximate 95% confidence interval for the POL can be obtained, for given smoothing parameters, say $\hat{\lambda}_1$ and $\hat{\lambda}_2$ for each culture, in the form

$$\hat{POL} \pm 1.96\sqrt{Var\left(\hat{F}_1(\hat{t}^*)\right) + Var\left(\hat{F}_2(\hat{t}^*)\right)} \qquad .....(6.2)$$

where $Var\left(\hat{F}_1(\hat{t}^*)\right)$ and $Var\left(\hat{F}_2(\hat{t}^*)\right)$ were introduced in section 3.9.2 as the approximate variances of $F_1(t)$ and $F_2(t)$ evaluated at the estimate of historical time $\hat{t}^*$ respectively, with

$$\sqrt{Var\left(\hat{F}_1(\hat{t}^*)\right) + Var\left(\hat{F}_2(\hat{t}^*)\right)} = \sqrt{\frac{\hat{F}_1(\hat{t}^*)\left\{1-\hat{F}_1(\hat{t}^*)\right\}}{n_1} + \frac{\hat{F}_2(\hat{t}^*)\left\{1-\hat{F}_2(\hat{t}^*)\right\}}{n_2}}$$

Since none of the methods for choosing the smoothing parameter can be guaranteed to be optimal for such data, it is important here to extend our 95% confidence interval for the POL to spread over a sensible choice of smoothing parameters for λ_1 and λ_2. This brings up the question of what is the sensible range for the smoothing parameter and this is considered in the following sub-section.

6.3.1.2 Choosing the Smoothing Parameters Range for the Extension of the Interval Estimation of the POL

The aim of this sub-section is to provide a sensible range for the smoothing parameter and to apply this to a natural extension of the confidence interval for the degree of overlap (*i.e.* the proportional overlap) between two archaeological cultures. The reasons behind this involve the important role played by the smoothing parameter in the determination of the degree of overlap and the lack of an automatic means of choosing an optimal method for the smoothing parameter.

It has already been shown in previous applications (chapter 5) on empirical criteria that, of the cross-validation and weighting method, the cross-validation

was the optimal choice for choosing the smoothing parameter of the density estimate in some applications while the weighting method was the optimal choice for other applications. Thus, for the applications where the cross-validation provided the optimal smoothing, the weighting method was chosen as the method which provided the minimum degree of smoothing of these applications. Conversely, the cross-validation method was chosen to provide the minimum degree of smoothing for the applications where the weighting method was the optimal choice.

So, with the minimum degree of smoothing chosen by either the cross-validation or weighting method, an ad hoc approach is considered here in order to provide the maximum degree of smoothing required to restrain the density estimate from being over-smoothed.

The ad hoc approach adopted here to choose the maximal amount of smoothing is to restrict both tails of the density estimate from getting "too large" i.e. by ensuring they are less than a prescribed value dependent upon the calibrated historical dates, $\hat{t}_{ij}$, and their estimated standard errors, $Se(\hat{t}_{ij})$.

The actual prescription used here is

- *Step 1* Compute

$$t_L^* = \underset{all_{i,j}}{Min}\{\hat{t}_{ij} - 3 \times Se(\hat{t}_{ij})\}$$

and denote by t_L and s_L the appropriate values of the calibrated historical date and standard error where this minimisation is achieved.

Similarly compute

$$t_U^* = \underset{all_{i,j}}{Max}\{\hat{t}_{ij} + 3 \times Se(\hat{t}_{ij})\}$$

with corresponding historical date, t_U, and standard error, s_U.

• *Step 2* By means of a search procedure increase the choice of smoothing parameter, λ, from the optimal choice until the density estimate, $\hat{p}_\lambda(\bullet)$, is such that

$$Min\left\{\hat{p}_\lambda(t_L^*) - \frac{1}{s_L}\phi(3)\ ,\ \hat{p}_\lambda(t_U^*) - \frac{1}{s_U}\phi(3)\right\} \geq 0$$

where $\phi(\bullet)$ is the standard normal density function

i.e. effectively ensuring that the maximal amount of smoothing is (just) more than the corresponding ordinate of a point three standard deviations away from the most extreme cases of all $N\{\hat{t}_{ij}\ ,\ Se^2(\hat{t}_{ij})\}$ density functions (see figure 6.5).

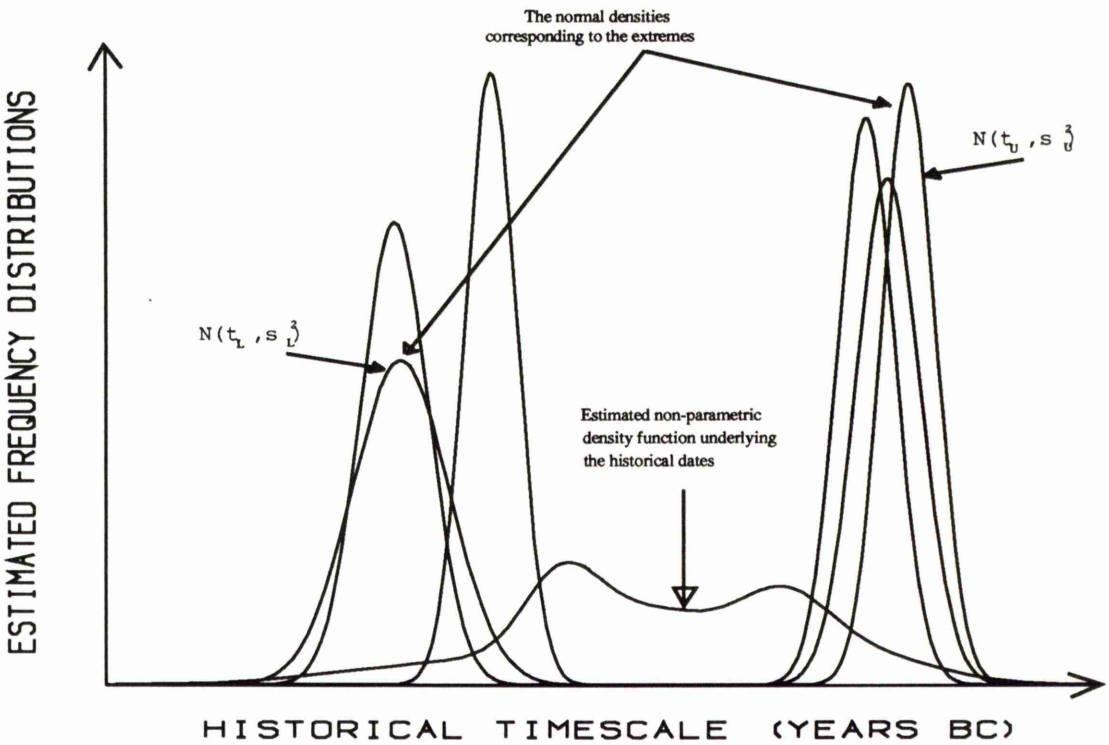

Figure 6.5 : Diagrammatic representation for the non-parametric density estimate with its tail ordinates constrained by the most extreme tail ordinates of normal densities centred at every single historical date.

Now the smoothing parameter obtained by this procedure will be taken as the maximum plausible degree of smoothing considered in the production of the confidence interval for the overlap between two archaeological cultures. Two examples from the previous data sets presented in chapter five are used here as illustrations of this approach. Figure 6.6 shows the estimated density

functions of the *Pfyn* and *Sâone-Rhône* cultures with the minimum, optimal and maximum degrees of smoothing chosen respectively by the weighting method, cross-validation and the ad hoc approach for the density estimate of the *Pfyn* culture and by cross-validation, the weighting method and the ad hoc approach respectively for the density estimate of the *Sâone-Rhône* culture.

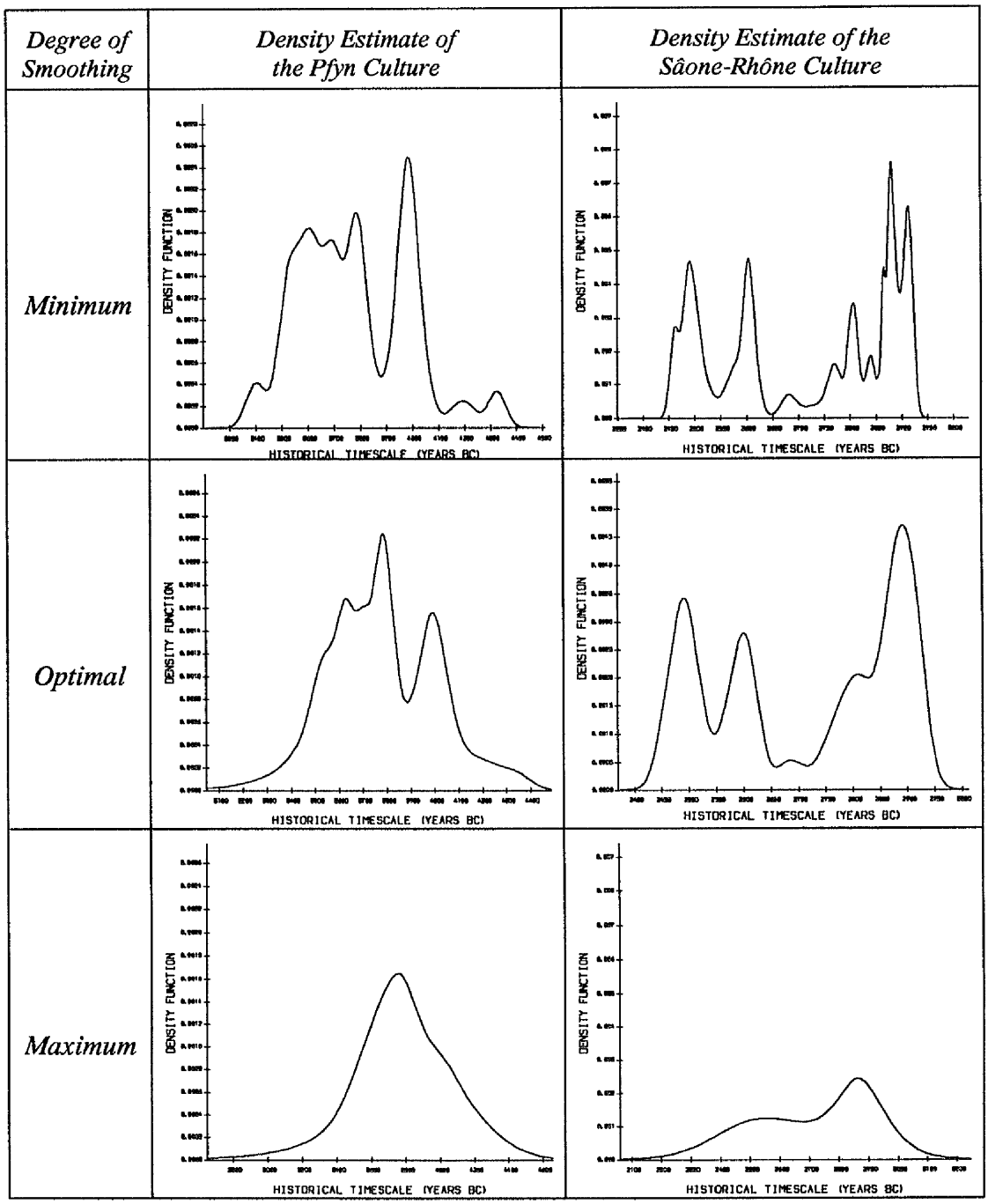

Figure 6.6 : Plots of the estimated density functions for the *Pfyn* and *Sâone-Rhône* cultures with the minimum, optimal and maximum degree of smoothing.

6.3.2 Time Overlap — Floruit Overlap (FOL)

An alternative but possibly equally useful summary measure of overlap on the historical timescale is the degree of overlap between the floruits of the two cultures. Clearly there is a significant temporal overlap between two archaeological cultures if their floruits overlap significantly. Floruit overlap (FOL) occurs only when there is POL of more than 50% and can be defined as the number of common years to the two floruits. It is readily evaluated by calculating the difference between the upper quartile of the frequency distribution of the younger culture and the lower quartile of the frequency distribution of the older culture. That is, if LQ_1 and UQ_1 represent the floruit of the younger culture and LQ_2 and UQ_2 represent the floruit of the older culture, then the difference between UQ_1 and LQ_2 represents the time overlap between the two floruits *i.e.*

$$FOL=UQ_1 - LQ_2$$

This is illustrated graphically in figure 6.7 for the case of "single value" partial overlap.

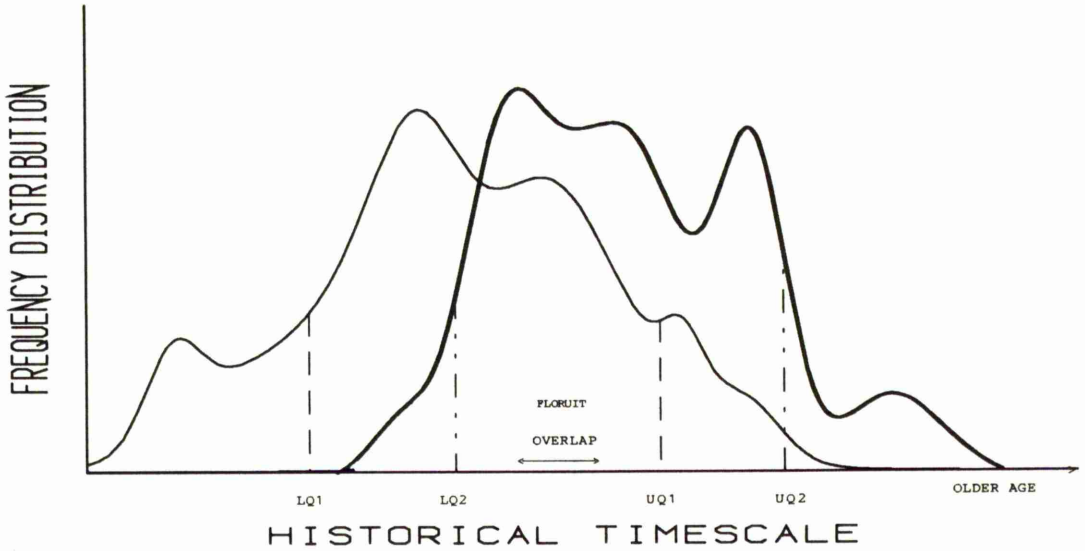

Figure 6.7 : Diagrammatic representation of the definition of Floruit Overlap between two archaeological cultures.

In practice estimate UQ_1 by $\hat{UQ}_1$ and LQ_2 by $\hat{LQ}_2$ *i.e.* the appropriate sample quartiles.

6.3.2.1 Interval Estimate for the FOL

Again the main approach is in constructing an interval estimate to account for the uncertainty in the estimation procedure. Recall the approach derived in chapter 3 (sections 3.5.1b and 3.9.2), where it was shown how to find a joint C.I. for the population quartiles and hence a C.I. for the floruit. This will be adapted here to construct a C.I. for the FOL. In effect, if a joint C.I. for UQ_1 and LQ_2 is constructed, then a derived C.I. for their difference (i.e. for the FOL) can be obtained.

6.3.2.2 Conservative Interval Estimate for the FOL

A simple way to construct a joint C.I. for UQ_1 and LQ_2 is to use the individual confidence intervals previously obtained for UQ_1, say $(L\hat{U}Q_1 , U\hat{U}Q_1)$ and LQ_2, say $(L\hat{L}Q_2 , U\hat{L}Q_2)$ which can be formed as before *i.e.* of the form

$$P\left(L\hat{U}Q_1 < UQ_1 < U\hat{U}Q_1\right) = 1-\alpha \qquad .....(6.3)$$

$$P\left(L\hat{L}Q_2 < LQ_2 < U\hat{L}Q_2\right) = 1-\alpha \qquad .....(6.4)$$

where $1-\alpha$ is a choice of confidence coefficient.

The region displayed in figure 6.8 which is the intersection of these two intervals gives a joint confidence region for UQ_1 and LQ_2 with confidence coefficient equal to $(1-\alpha)^2$ since they are independent events. Thus the confidence coefficients in 6.3 and 6.4 will be replaced and taken to be equal to $\sqrt{1-\alpha}$ instead of $(1-\alpha)$ in order to get an approximate $(1-\alpha)$ joint confidence region (**J.C.R.**) for UQ_1 and LQ_2. Then one takes tangents to this region to provide an interval estimate for UQ_1 - LQ_2 with $(1-\alpha)$ confidence coefficient.

Of course this J.C.R. is a conservative confidence region, and hence the interval estimate will be a very conservative interval, but it has the advantage that it is easier to construct than the region of minimum area which is likely to be roughly elliptical in shape.

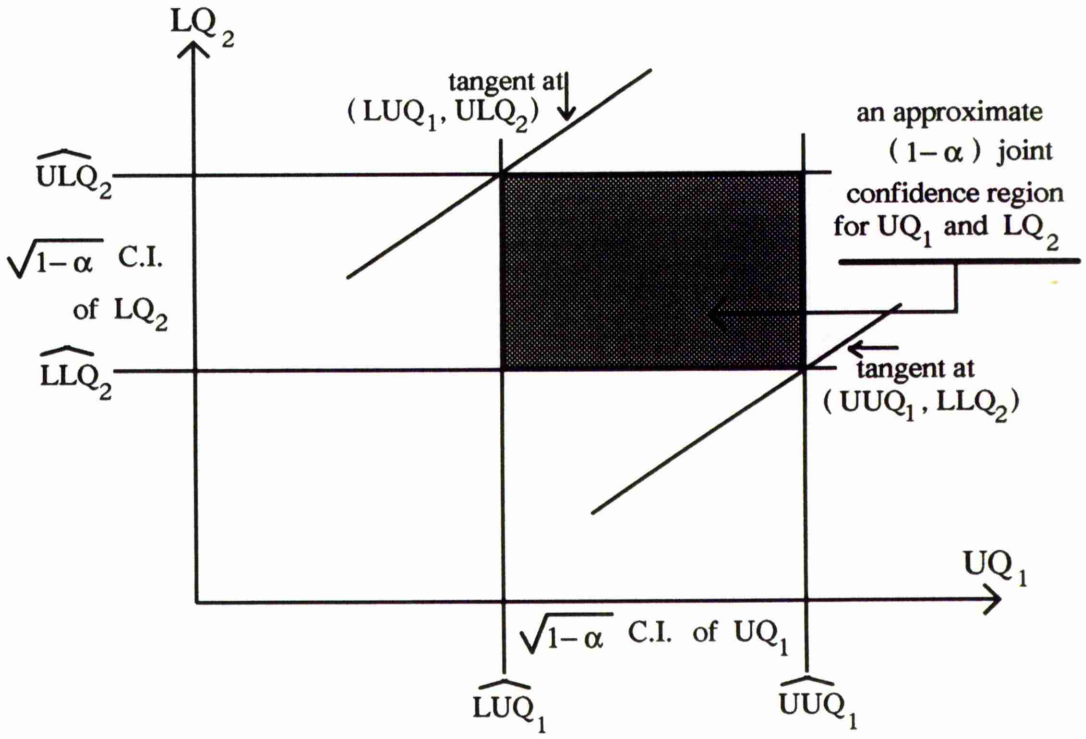

Figure 6.8 : Diagrammatic representation for the conservative joint confidence region of UQ_1 and LQ_2.

It is worth noting that one can only be sure of a true overlap between two cultures if the joint confidence region lies to the right of the line $UQ_1=LQ_2$ which means $L\hat{U}Q_1$ must be greater than $U\hat{L}Q_2$. In other words if 0 lies inside the interval there may be no overlap.

To obtain an approximate 95% confidence interval for FOL construct an approximate $\sqrt{0.95}$ confidence interval for UQ_1 and an approximate $\sqrt{0.95}$

confidence interval for LQ_2. One approximation to obtain $L\hat{U}Q_1$ is the solution of

$$0.75 = \hat{F}_1(t) + 2.24\sqrt{\frac{\hat{F}_1(t)\{1-\hat{F}_1(t)\}}{n_1}}$$

for t and $U\hat{U}Q_1$ is obtained by solving for t

$$0.75 = \hat{F}_1(t) - 2.24\sqrt{\frac{\hat{F}_1(t)\{1-\hat{F}_1(t)\}}{n_1}}$$

Similarly $L\hat{L}Q_2$ and $U\hat{L}Q_2$ can be obtained by solving the following equations respectively for t

$$0.25 = \hat{F}_2(t) + 2.24\sqrt{\frac{\hat{F}_2(t)\{1-\hat{F}_2(t)\}}{n_2}}$$

and

$$0.25 = \hat{F}_2(t) - 2.24\sqrt{\frac{\hat{F}_2(t)\{1-\hat{F}_2(t)\}}{n_2}}$$

That is for an approximate $\sqrt{0.95}$ confidence interval for UQ_1, one has

$$P\left(L\hat{U}Q_1 < UQ_1 < U\hat{U}Q_1\right) \overset{\cdot}{\underset{\cdot}{\approx}} \sqrt{0.95}$$

and for an approximate $\sqrt{0.95}$ confidence interval for LQ_2, one has

$$P\left(L\hat{L}Q_2 < LQ_2 < U\hat{L}Q_2\right) \overset{\cdot}{\underset{\cdot}{\approx}} \sqrt{0.95}$$

Based on these marginal intervals and hence the J.C.R. tangents to the rectangle can be taken and hence

$$P\left(L\hat{U}Q_1 - U\hat{L}Q_2 < FOL < U\hat{U}Q_1 - L\hat{L}Q_2\right) \overset{\cdot}{\underset{\cdot}{\approx}} 0.95 \qquad \text{.....(6.6)}$$

provides an approximate 95% conservative confidence interval for the time overlap between the two floruits of the two archaeological cultures.

6.3.2.3 Interval Estimate of Minimum area for the FOL

The interval based on the conservative J.C.R. is likely to be very wide and hence it is advisable to provide an interval more attuned to considering linear combinations of UQ_1 and LQ_2.

One such approach is to considers the rough Normal approximations

$$\hat{F}_1(t_1) \overset{\cdot}{\underset{\cdot}{\approx}} N\left(F_1(t_1),\ \frac{F_1(t_1)\{1-F_1(t_1)\}}{n_1}\right)$$

and

$$\hat{F}_2(t_2) \overset{\cdot}{\underset{\cdot}{\approx}} N\left(F_2(t_2),\ \frac{F_2(t_2)\{1-F_2(t_2)\}}{n_2}\right)$$

then, both pivotal functions

$$\frac{\hat{F}_1(t_1)-F_1(t_1)}{\sqrt{\frac{\hat{F}_1(t_1)\{1-\hat{F}_1(t_1)\}}{n_1}}} \quad \text{and} \quad \frac{\hat{F}_2(t_2)-F_2(t_2)}{\sqrt{\frac{\hat{F}_2(t_2)\{1-\hat{F}_2(t_2)\}}{n_2}}}$$

have approximately a standard normal distribution, and

$$\left\{\left(\frac{\hat{F}_1(t_1)-F_1(t_1)}{\sqrt{\frac{\hat{F}_1(t_1)\{1-\hat{F}_1(t_1)\}}{n_1}}}\right)^2+\left(\frac{\hat{F}_2(t_2)-F_2(t_2)}{\sqrt{\frac{\hat{F}_2(t_2)\{1-\hat{F}_2(t_2)\}}{n_2}}}\right)^2\right\}$$

has approximately a chi-square distribution with 2 degrees of freedom.

Therefore, for $F_1(t_1)=0.75$ and $F_2(t_2)=0.25$, the probability statement

$$P\left\{\left(\frac{\hat{F}_1(t_1)-0.75}{\sqrt{\frac{\hat{F}_1(t_1)\{1-\hat{F}_1(t_1)\}}{n_1}}}\right)^2+\left(\frac{\hat{F}_2(t_2)-0.25}{\sqrt{\frac{\hat{F}_2(t_2)\{1-\hat{F}_2(t_2)\}}{n_2}}}\right)^2<\chi^2_{(2,\,1-\alpha)}\right\}=(1-\alpha)\ldots..(6.5)$$

provides the basis for the appropriate J.C.R of minimum area for UQ_1 and LQ_2 with confidence coefficient equal to $(1-\alpha)$. Then the two tangents to the "ellipse" of form (UQ_1 - LQ_2) would be the end points of the required interval for FOL. This is illustrated graphically in figure 6.9.

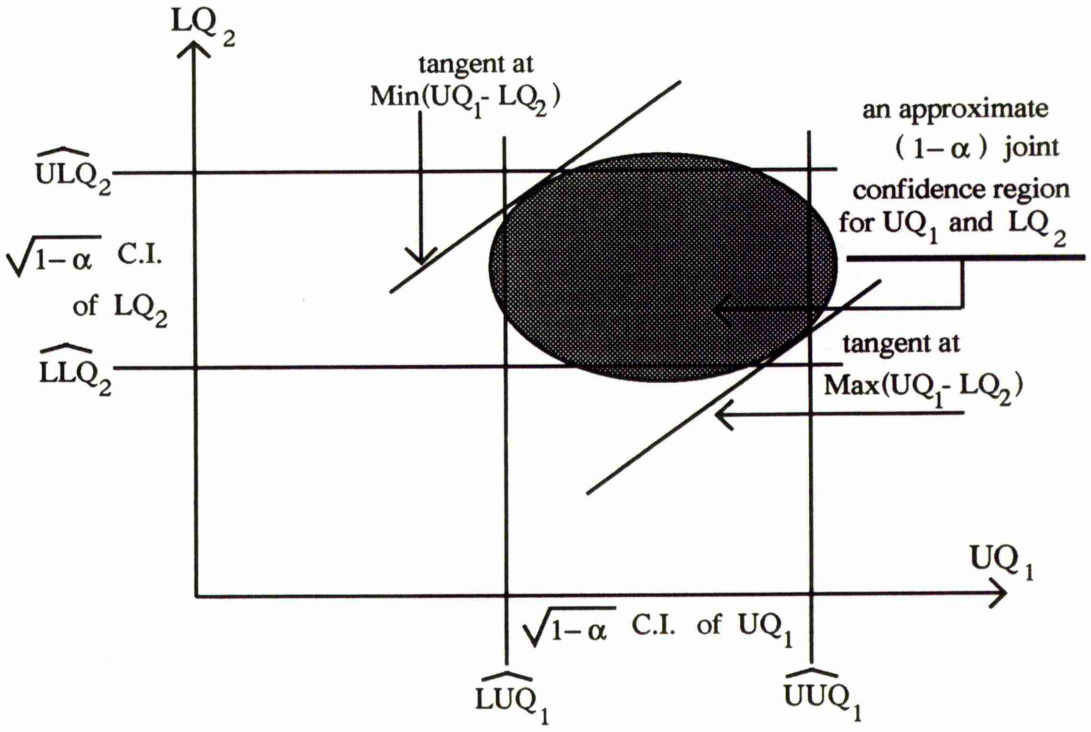

Figure 6.9 : Diagrammatic representation for the joint confidence region of minimum area for UQ_1 and LQ_2.

Now, an approximate 95% J.C.R. of minimum area for UQ_1 and LQ_2 can be constructed by replacing α in 6.5 with 0.05 and obtaining all possible combinations of values of t_1 and t_2 to satisfy

$$\left\{\left(\frac{\hat{F}_1(t_1)-0.75}{\sqrt{\frac{\hat{F}_1(t_1)\{1-\hat{F}_1(t_1)\}}{n_1}}}\right)^2+\left(\frac{\hat{F}_2(t_2)-0.25}{\sqrt{\frac{\hat{F}_2(t_2)\{1-\hat{F}_2(t_2)\}}{n_2}}}\right)^2\right\}<5.99 \qquad .....(6.7)$$

Thus, one can construct an approximate 95% C.I. for the FOL by taking the minimum and maximum differences of t_1 and t_2 for all combinations. In

other words, the two tangents , say C_1 and C_2, to the "ellipse" would constitute the required approximate 95% confidence interval for the FOL.

i.e. (C_1,C_2) is an approximate 95% C.I. for FOL

where the lines $C_1=t_1-t_2$ and $C_2=t_1-t_2$ are tangents to the J.C.R. for t_1 and t_2 based on 6.5.

Similar to the POL some account of the effect of smoothing on the floruit estimate should be taken and this interval extended to cover a sensible range of smoothing parameters.

6.4 Illustrative Examples

The aim of this section is to look at the two measurements of overlap (POL and FOL) applied to some examples of the data sets presented in chapter five and known to be geographically close. These examples are chosen to exemplify three situations of overlap as follows :-

a) The first example is the overlap of the *Horgen* and *Pfyn* cultures which reflects the case of ***little*** overlap.

b) The second example considers the case of ***moderate*** overlap between the *Sâone-Rhône* and *Cham* cultures and also highlights on the *effect of an outlier date* (which exist in the *Cham* culture) on the degree of overlap.

c) The final example of these illustrations is the case of ***significant*** overlap between the *Cortaillod* and *Pfyn* cultures.

The major emphasis in these examples is to take into account the uncertainty in smoothing parameters of the two cultures to consider their effect on the overlap between the two cultures. In order to achieve this, the overlap of the two cultures will be estimated with the minimum, optimal and maximum degree of smoothing for both frequency distributions of the two cultures. Then for the two cultures, the influence of the degree of smoothing (from minimum to maximum) of one culture on the overlap will be considered separately with the minimum and maximum degree of smoothing of the other culture.

6.4.1 Example 1 : The Case of Little Overlap

This example is considered to give a measure of overlap, on the historical timescale, between the *Horgen* and *Pfyn* cultures of Switzerland. The lists of uncalibrated radiocarbon dates collected from these two cultures were reported early in tables 5.11 and 5.9 respectively, together with their corresponding calibrated historical dates.

For a quick assessment of the overlap of these two cultures, back-to-back histogram plots are displayed in figure 6.10a for the radiocarbon dates and in figure 6.10b for the corresponding calibrated historical dates. There appears to be an overlap of nearly 80 years on the radiocarbon timescale since only 2 out of 23 radiocarbon dates from the *Horgen* culture overlap with 8 out of 35 radiocarbon dates from the *Pfyn* culture. Due to the calibration procedure this number is extended to nearly 230 years on the historical timescale when 4 out of 43 historical dates from the *Horgen* culture have overlapped with 26 out of 61 historical dates from the *Pfyn* culture.

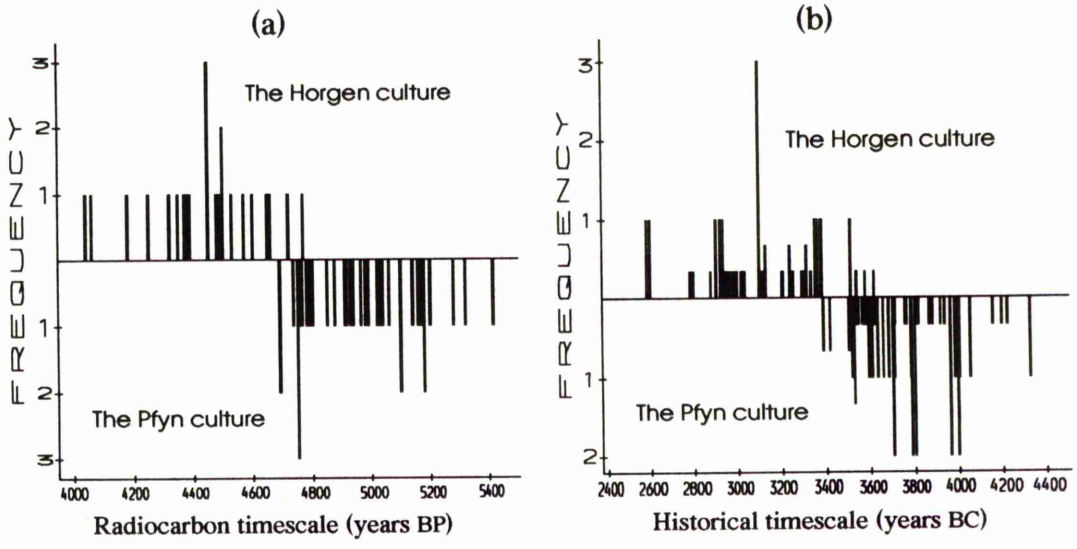

Figure 6.10 : back-to-back histogram plots for **a)** the radiocarbon dates, and **b)** the historical dates of the *Horgen* and *Pfyn* cultures.

The next step is to estimate the POL of the two cultures by first estimating the true frequency distribution of the overlap. The density estimate with optimal choice of smoothing parameter is shown in figure 6.11a. To consider the influence of the degree of smoothing on the overlap, the density estimates are graphed in figures 6.11b&c respectively for the least and most smoothing that would be required for these two cultures.

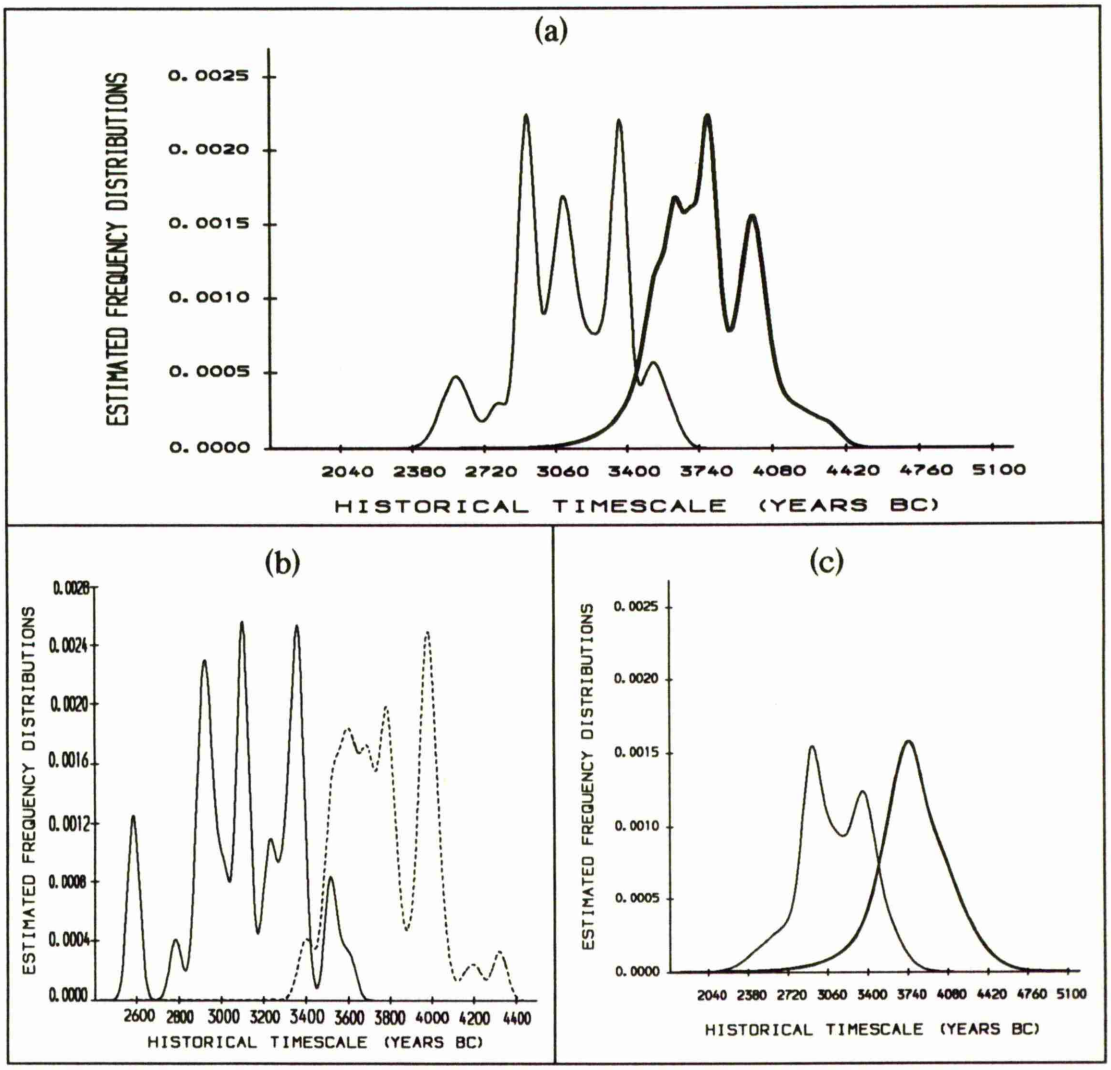

Figure 6.11 : Estimated frequency distribution of the overlap of the *Horgen* (thin) and *Pfyn* (thick - dotted) culture for a) the optimal, b) the least, and c) the most smoothing that would be necessary for these two cultures.

For the three cases, the optimal, least and most smoothing, the intersection point is evaluated and then the POL of the two cultures is estimated using formulae 6.1 and 6.2 for the point and interval estimates respectively.

The point estimates of the POL with an approximate 95% C.I. are given in the following table for the optimal, minimum and maximum smoothing of these two cultures

Degree of smoothing	Point estimate	95% confidence interval
Optimal smoothing	18%	3 - 34%
Minimum smoothing	15%	1 - 29%
Maximum smoothing	24%	7 - 41%

These results indicate that the estimated POL is influenced by the degree of smoothing of the frequency distributions as the optimal estimate of the POL has changed when the smoothing parameters of these two cultures are moved about. Therefore, it would be of interest to consider the individual influence of the smoothing parameter of each frequency distribution on the estimated POL and then to consider the simultaneous influence of both smoothing parameters of the two cultures.

The effect of the smoothing parameter of the frequency distribution of the *Horgen* culture, from the minimum to the maximum, on the point and interval estimates of the POL is plotted in figure 6.12a against the least and the most smoothing of the frequency distribution of the *Pfyn* culture. This plot shows that the estimated POL is increased when the smoothing parameter of the frequency distribution of the *Horgen* culture is increased. A similar effect occurs for the POL as the smoothing parameter of the frequency distribution of the *Pfyn* culture varies (figure 6.12b).

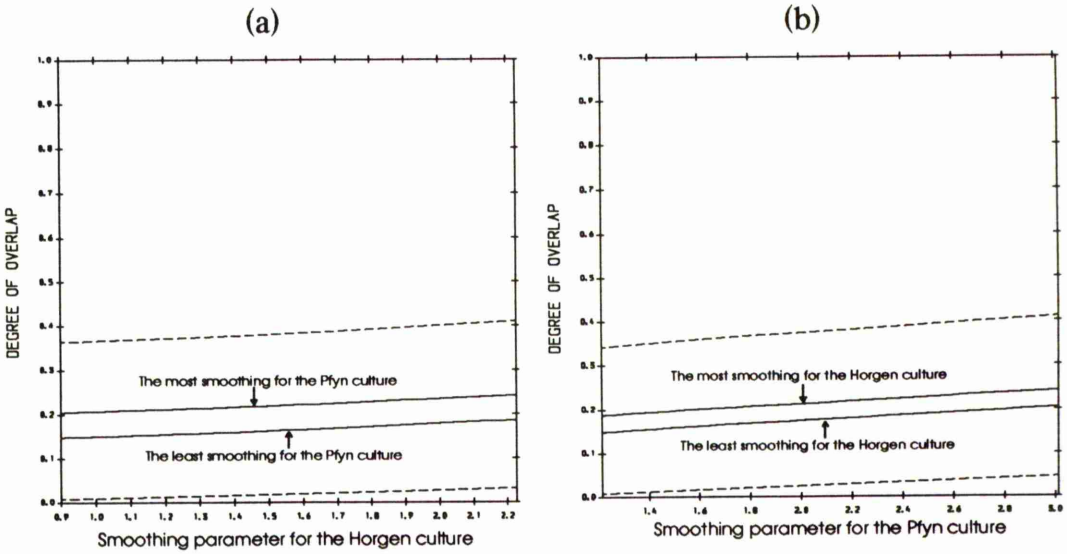

Figure 6.12 : Effect of the degree of smoothing on the point (solid) and interval (dotted) estimates of the POL between the *Horgen* and *Pfyn* cultures.

An overall illustration of the effect of varying the smoothing parameter of the frequency distribution on the POL is given in a 3-Dimensional plot shown in figure 6.13 for the simultaneous influence of the smoothing parameter for the two cultures. It is clear that, in this example, the estimated POL has a direct relationship with degree of smoothing of the frequency distributions *i.e.* the estimated POL between the *Horgen* and *Pfyn* culture increases as either smoothing parameter of the frequency distributions increases.

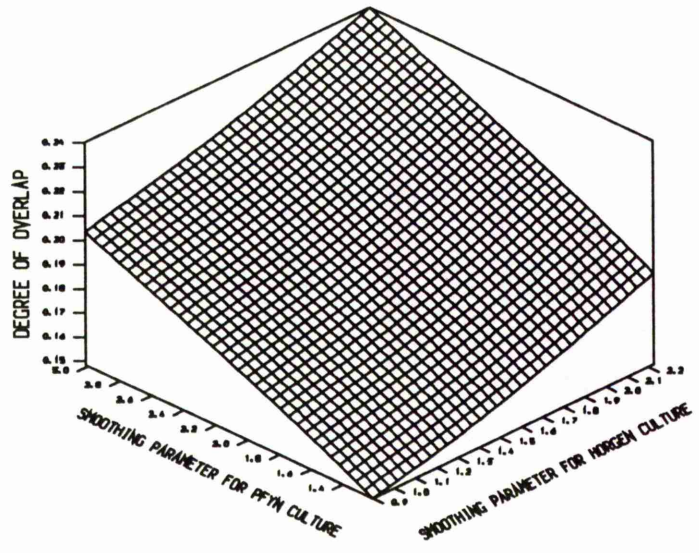

Figure 6.13:
An inclusive illustration for the effect of the degree of smoothing on the estimated POL between the *Horgen* and *Pfyn* cultures.

Finally, from the above results, one can conclude an overall estimate for the POL between the *Horgen* and *Pfyn* cultures to cover the effect of the degree of smoothing on the POL over the specified range by taking the point estimate (rounded to the nearest 5%) of **20%** with an interval estimate of between **1** and **40%**.

In order to estimate the FOL between two cultures, the estimated POL must be greater than 50%. Accordingly, in examples such as this where the estimated POL is 24% with maximum smoothing, it is not possible to construct an estimate for the FOL since there is no floruit overlap.

6.4.2 Example 2 : Effect of an Outlier date in the Case of Moderate Overlap

This example considers the case of moderate overlap between the *Sâone-Rhône* culture of Switzerland and the *Cham* culture of southern Germany. The lists of uncalibrated radiocarbon dates which were collected from these two cultures were given earlier in tables 5.29 and 5.17 respectively, together with the corresponding calibrated historical dates.

For the two cultures back-to-back histogram plots are shown in figures 6.14a&b for the radiocarbon and historical dates respectively. It is clear from these histograms that, with the existence of very probable outlier date of the *Cham* culture, all dates (radiocarbon and historical) from the *Sâone-Rhône* culture overlap with over half the number of dates from the *Cham* culture which gives a rather spurious impression that complete overlap may have occurred between these two cultures. However, when the assumed outlier date is removed from the *Cham* culture, the *Sâone-Rhône* culture overlap with the *Cham* culture with less than half the number of its dates.

Hence the main thrust of this example will be to demonstrate the influence of the assumed outlier date, of the *Cham* culture, on the POL of the two cultures. The analysis will therefore be carried out twice - once **with** and once **without** the assumed outlier date.

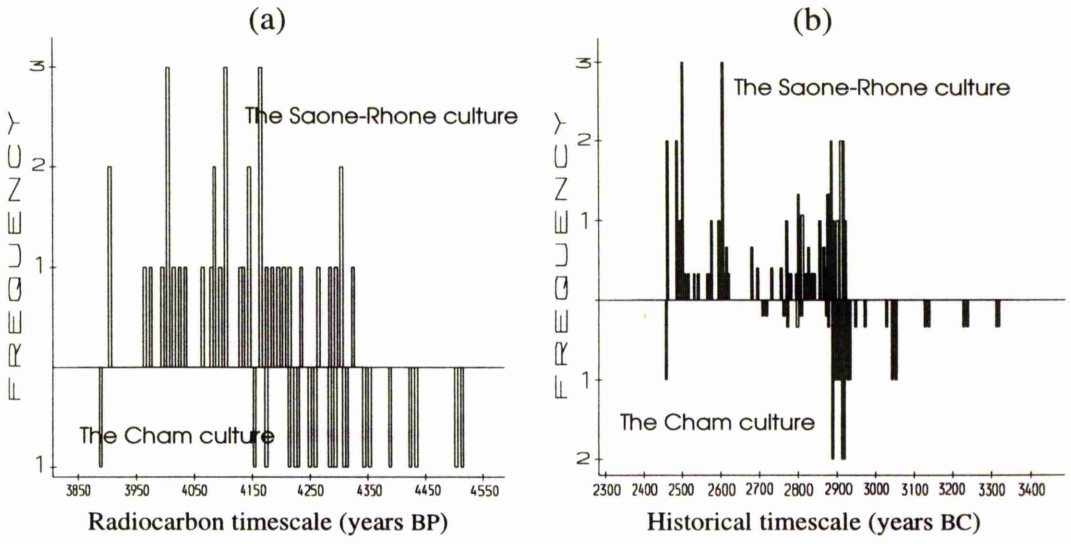

Figure 6.14 : back-to-back histogram plots for **a)** the radiocarbon dates, and **b)** the historical dates of the *Sâone-Rhône* and *Cham* cultures.

- ***With the Outlier Date***

To estimate the optimal POL between these two cultures, the optimal estimate of the frequency distribution of the overlap is constructed with the outlier date being included and plotted in figure 6.15a. Also, to consider the effect of the degree of smoothing on the estimated overlap, the frequency distributions of the overlap across the range of possible smoothing parameters for the *Sâone-Rhône* and *Cham* cultures are graphed in figures 6.15b&c. From these plots it should be noticed that, for the optimal and minimum smoothing, there is more than one point of intersection due to the possibility of under smoothing the frequency distribution of the *Sâone-Rhône* culture. In practice the chosen point of intersection in both cases is that which is closest to the one estimated in the case of maximum smoothing *i.e.* in the period of 2800 – 2890 BC.

The point estimates of the POL with approximate 95% C.I., based on the optimal, least and most smoothing that would be required for these two cultures, are given in the following table:-

Degree of smoothing	Point estimate	95% confidence interval
Optimal smoothing	52%	28 - 75%
Minimum smoothing	47%	24 - 70%
Maximum smoothing	59%	35 - 82%

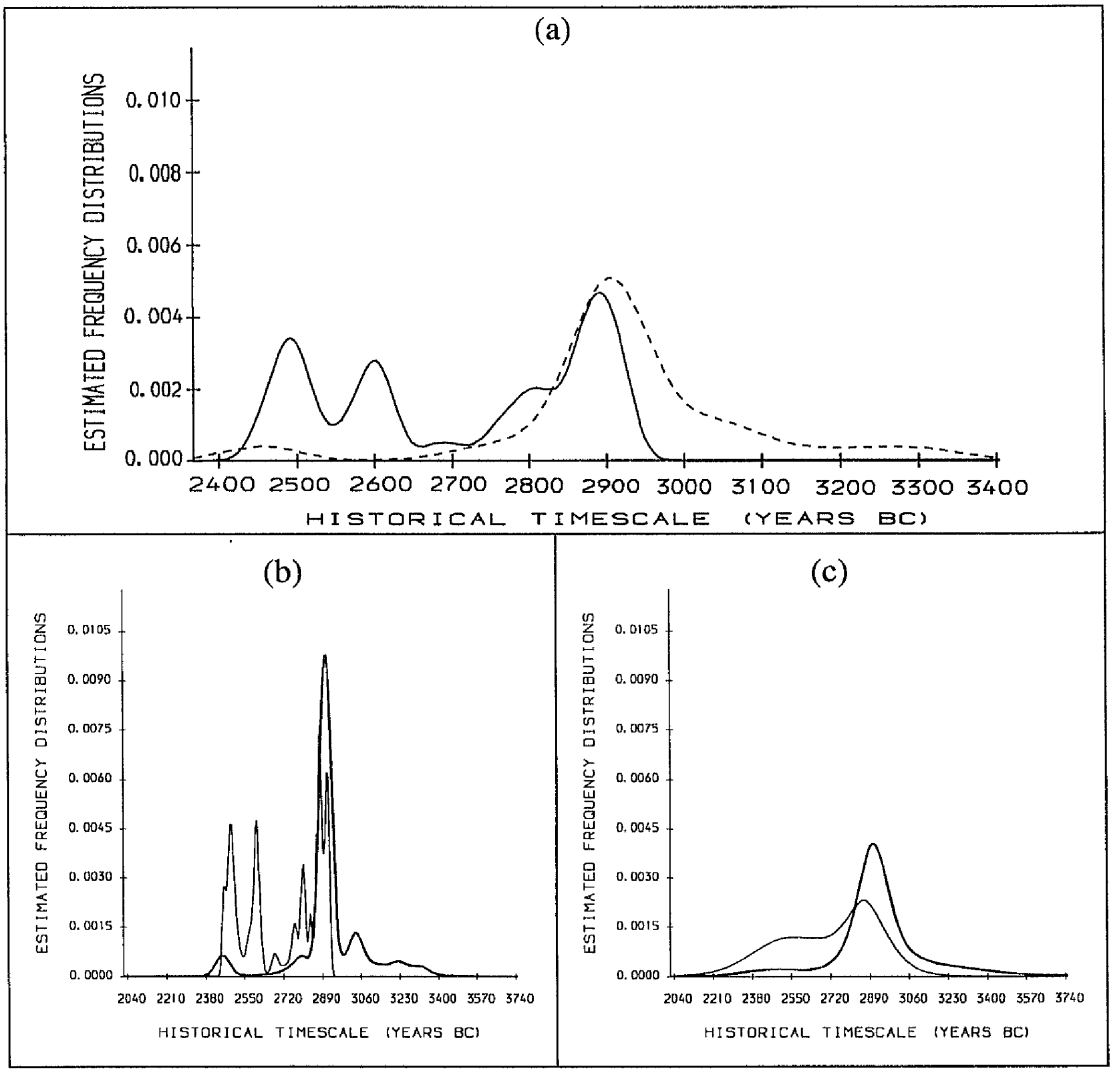

Figure 6.15 : Estimated frequency distribution of the overlap of the *Sâone-Rhône* (thin) and *Cham* (thick - dotted) culture with the assumed outlier date for a) the optimal, b) the least, and c) the most smoothing that would be necessary for these two cultures .

For the specified range of smoothing of the *Sâone-Rhône* culture *i.e.* from the least to the most, the effect of the degree of smoothing on the estimated POL is not consistent for the minimum and maximum of the *Cham* culture. As can be seen in figure 6.16a for the least smoothing of the *Cham* culture the

estimated POL decreases with more smoothing of the *Sâone-Rhône* culture and then starts to increase again as the smoothing parameter moves past the value 1, while the inverse to this occurred at the maximum smoothing of the *Cham* culture. On the other hand the estimated POL always increased with smoothing of the *Cham* culture except when it became nearly stable for the combinations of smoothing parameters over 2.4 for the *Cham* culture and the minimum smoothing of the *Sâone-Rhône* culture as shown in figure 6.16b. The overall influence of both smoothing parameters on the estimated POL can be seen in the 3-Dimensional plot displayed in figure 6.17 which indicates that, generally speaking, the estimated POL increases when both of the smoothing parameters increase.

As in the previous example, if one wishes to conclude an overall estimate for the POL between the *Sâone-Rhône* and *Cham* (with the outlier date) cultures to cover the effect of the degree of smoothing on the POL over the specified range, then it would be the point estimate of **50%** (rounded to the nearest 5%) with an interval estimate of between **25** and **80%**.

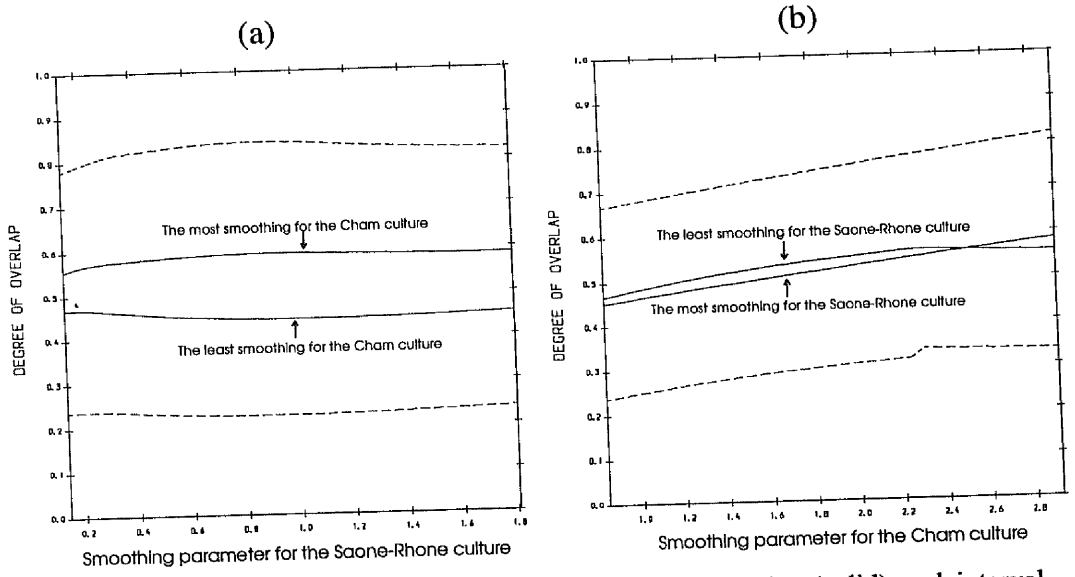

Figure 6.16 : Effect of the degree of smoothing on the point (solid) and interval (dotted) estimates of the POL between the *Sâone-Rhône* and *Cham* cultures.

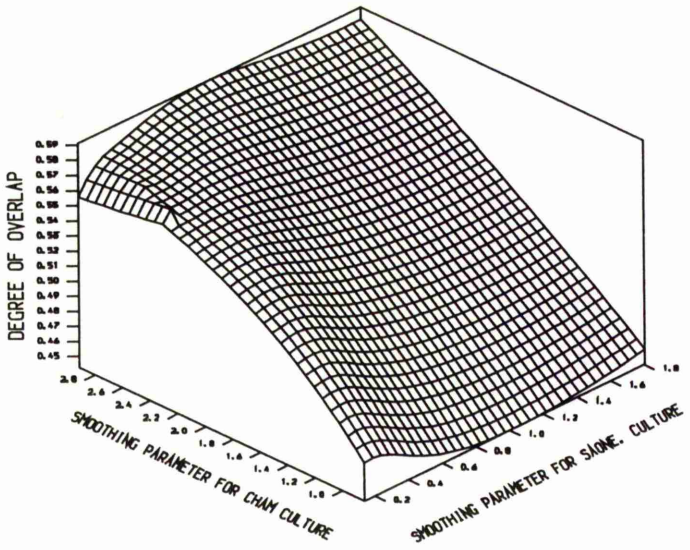

Figure 6.17:
An inclusive illustration for the effect of the degree of smoothing on the estimated POL between the *Sâone-Rhône* and *Cham* cultures.

- ***Without the Outlier Date***

The process of measuring the POL of the *Sâone-Rhône* and *Cham* cultures is repeated here with the assumed outlier date being **excluded** from the radiocarbon dates of the *Cham* culture in order to consider its effect on the estimated POL.

The resulting estimates for the frequency distribution of the overlap are displayed in figure 6.18a for the optimal and in figures 6.18b&c for the least and most smoothing of these cultures. Generally speaking, they are similar to those estimates obtained when the outlier date was included except that bump in the tail of the estimated frequency distribution of the *Cham* culture has been removed particularly noticeably in the optimal and least smoothing cases.

The POL of the two cultures is then estimated and the results of point estimates with approximate 95% C.I. are given below for the optimal, least and most smoothing that would be required.

Degree of smoothing	Point estimate	95% confidence interval
Optimal smoothing	48%	25 - 70%
Minimum smoothing	43%	20 - 65%
Maximum smoothing	54%	32 - 77%

Here the influence of the degree of smoothing on the estimated POL is almost identical to the previous case as can be seen in figures 6.19 and 6.20. An overall estimate for the POL of these two cultures which covers the effect of the degree of smoothing over the specified range (rounded to the nearest 5%) would be **50%** for the point estimate with an interval estimate of between **20** and **75%**.

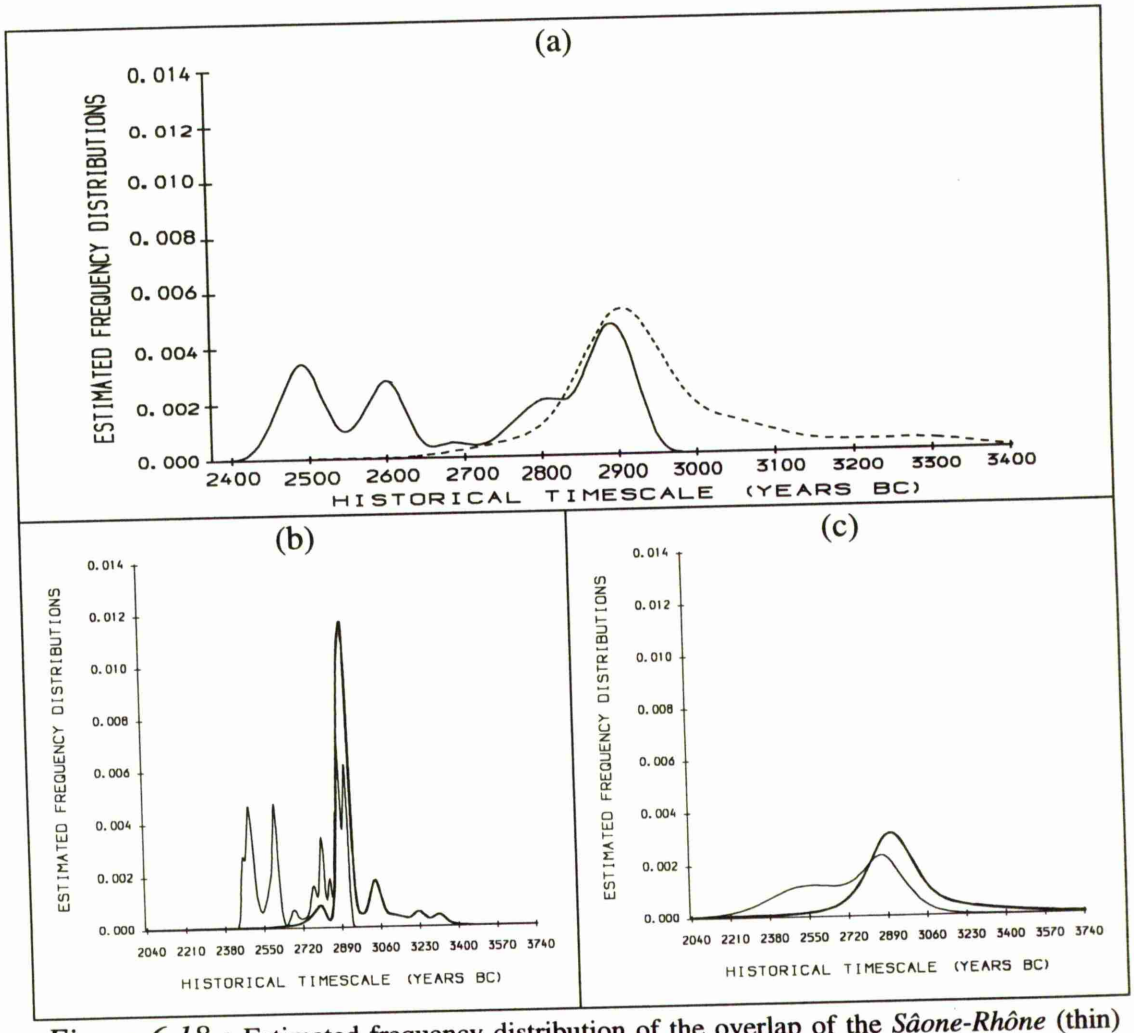

Figure 6.18 : Estimated frequency distribution of the overlap of the *Sâone-Rhône* (thin) and *Cham* (thick - dotted) cultures without the assumed outlier date for a) the optimal, b) the least and b) the most smoothing of these two cultures.

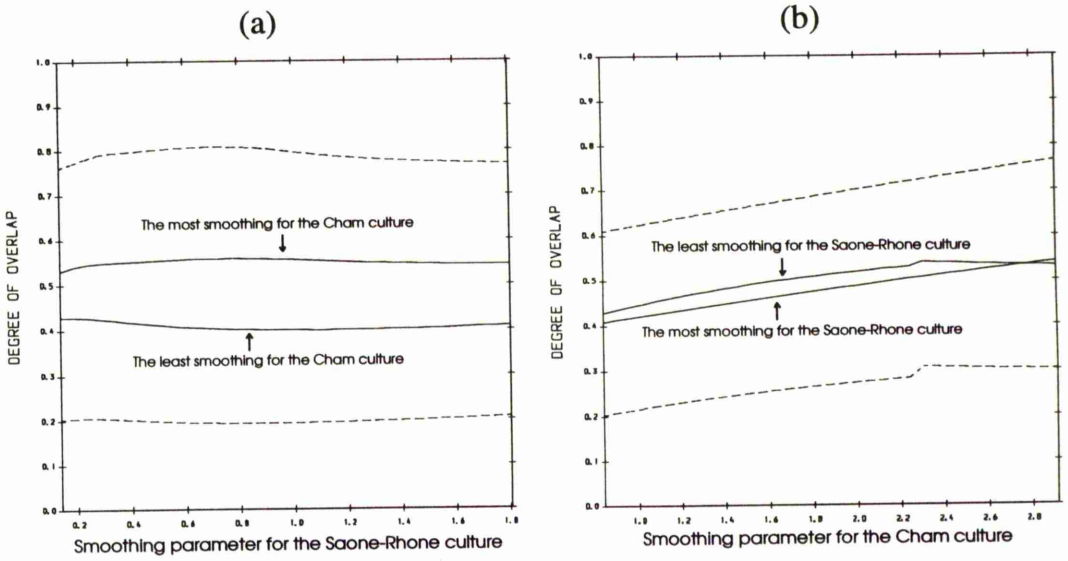

Figure 6.19 : Effect of the degree of smoothing on the point (solid) and interval (dotted) estimates of the POL between the *Sâone-Rhône* and *Cham* cultures.

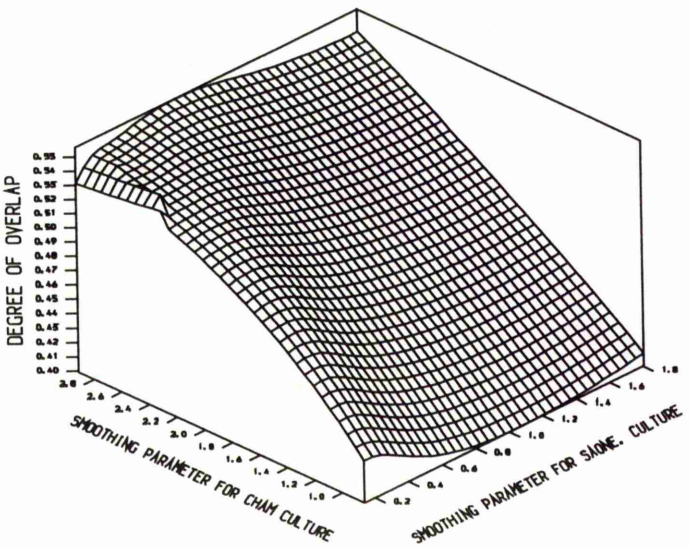

Figure 6.20:
An inclusive illustration for the effect of the degree of smoothing on the estimated POL between the *Sâone-Rhône* and *Cham* cultures.

The (assumed) outlier date has little effect on the results of the estimated POL, point and interval. They are slightly decreased (about 4%) compared with those obtained when the outlier date was included. This, in fact, consolidates that the use of the density estimation method in dampening out the effect of possible outliers on the density estimates and hence the estimate of POL.

6.4.3 Example 3 : The Case of Significant Overlap

In this final example the case of significant overlap between the *Cortaillod* and *Pfyn* cultures of *Switzerland* is considered in order to provide an estimate for proportional and floruit overlap of these two cultures. The data sets, radiocarbon and historical dates, of the *Cortaillod* and *Pfyn* cultures were reported early in tables 5.23 and 5.9 respectively.

As in the previous examples, the first step is the construction of two back-to-back histogram plots in order to check the magnitude of overlap of the radiocarbon dates of the two cultures which is displayed in figure 6.21a and between the historical dates as shown in figure 6.21b. These histograms show how significant the overlap is particularly for the *Pfyn* culture, which seems the older, where all of its dates except one have overlapped with most of the dates of the *Cortaillod* culture.

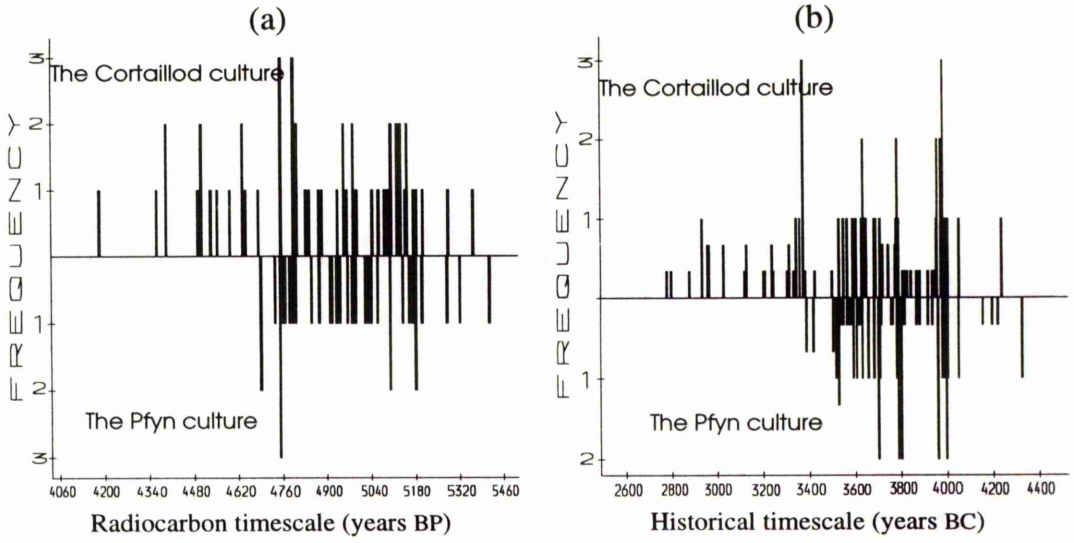

Figure 6.21 : back-to-back histogram plots for a) the radiocarbon dates, and b) the historical dates of the *Cortaillod* and *Pfyn* cultures.

The estimated frequency distributions used in the estimation of the overlap are graphed for the optimal, minimum and maximum smoothing that would be needed for these two cultures in figures 6.22a-c. From these plots it can be seen at once that the overlap is large, and it is quite possible, in this example, to provide an estimate for both of POL and FOL of these two cultures.

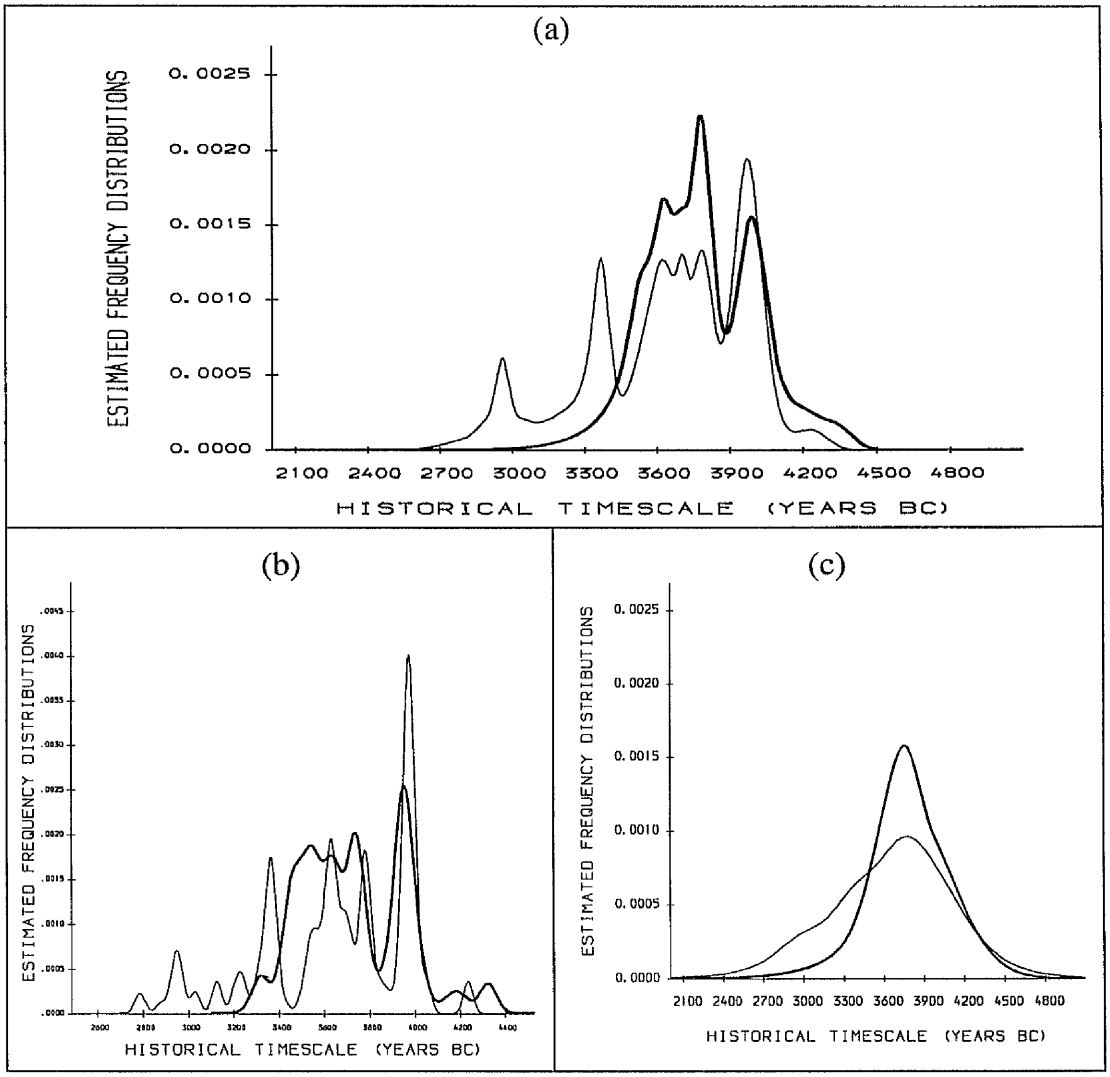

Figure 6.22 : Estimated frequency distribution of the overlap of the *Cortaillod* (thin) and *Pfyn* (thick) cultures for a) the optimal, b) the least, and c) the most smoothing that would be necessary for these two cultures.

- ***Estimation of the POL of the Cortaillod and Pfyn cultures***

Since the first step in measuring the POL is the estimation of the intersection point of the two frequency distributions and, because there is more than one point of intersection in the cases with minimum and optimal smoothing, then the intersection point in the minimum and optimal smoothing choice will be estimated close to that in the maximum smoothing choice *i.e.* in the period of 3300 - 3600 BC.

The following table gives the estimated POL with approximate 95% C.I. for the optimal, minimum and maximum degree of smoothing for the *Cortaillod* and *Pfyn* cultures :-

Degree of smoothing	Point estimate	95% confidence interval
Optimal smoothing	80%	64 - 95%
Minimum smoothing	79%	65 - 93%
Maximum smoothing	81%	63 - 98%

These results show that there is not much difference whether the minimum or maximum smoothing is considered. The influence of the degree of smoothing of each frequency distribution on the estimated POL is very clear in figure 6.23a as the estimated POL is decreased when the frequency distribution of the *Cortaillod* culture is smoothed more, while increased in figure 6.23b when the degree of smoothing of the frequency distribution of the *Pfyn* culture is increased. This contradictory influence makes the overall change in the estimated POL from the minimum to the maximum degree of smoothing very little as can be seen clearly in figure 6.24. Thus, in this example the chosen degree of smoothing of the frequency distribution is not crucial.

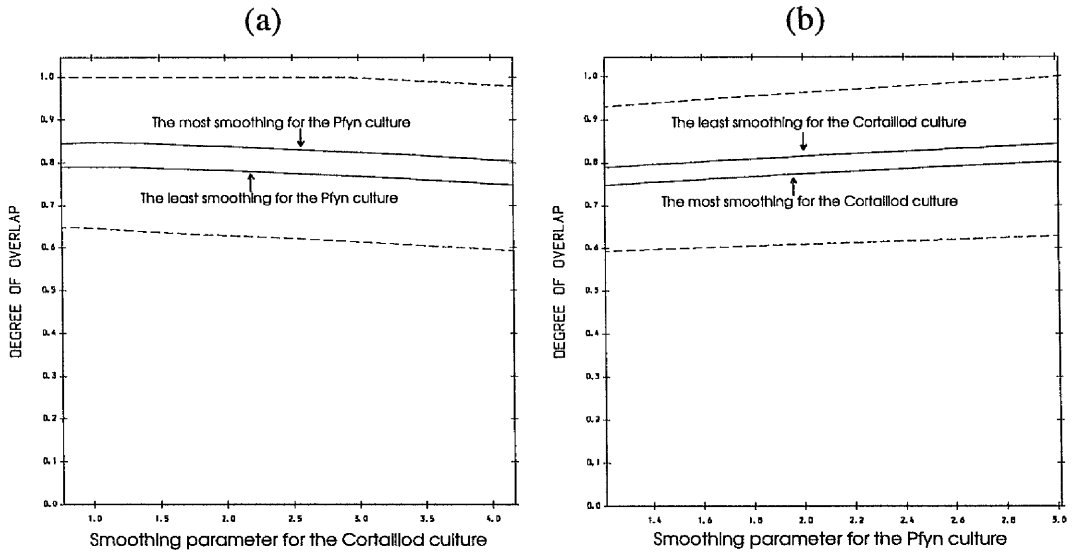

Figure 6.23 : Effect of the degree of smoothing on the point (solid) and interval (dotted) estimates of the POL between the *Cortaillod* and *Pfyn* cultures.

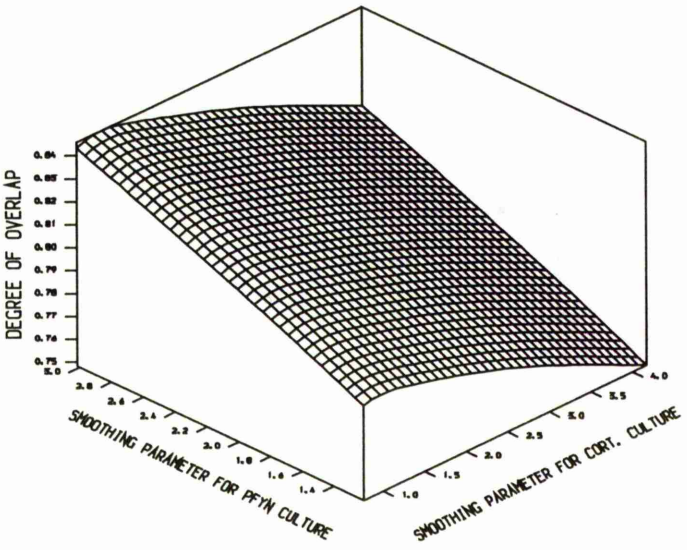

Figure 6.24:
An inclusive illustration for the effect of the degree of smoothing on the estimated POL between the *Cortaillod* and the *Pfyn* cultures.

To summarise the above results, an overall estimate for the POL of the *Cortaillod* and *Pfyn* cultures (rounded to the nearest 5%) would be **80%** for the point estimate with an interval estimate of between **65** and **95%**.

- ***Estimation of the FOL of the Cortaillod and Pfyn cultures***

The starting point in measuring the FOL of two cultures is the estimation of the floruit of each culture individually and in particular the estimation of point and interval estimates for both of upper quartile of the younger (*Cortaillod*) culture and lower quartile of the older (*Pfyn*) culture.

As, in the estimation of the POL, the influence of the degree of smoothing on the FOL will be considered by estimating the FOL for the least and most smoothing that would be necessary for each frequency distribution of these two cultures.

Both floruits are estimated and only the point and interval estimates for the upper quartile of the *Cortaillod* culture and for the lower quartile of the *Pfyn* culture are summarized, for the optimal, least and most smoothing, in the following table:-

Degree of Smoothing	The Upper quartile of the *Cortaillod* culture		The Lower quartile of the *Pfyn* culture	
	Point Estimate	Interval Estimate	Point Estimate	Interval Estimate
Optimal	3931	3780 - 3992	3620	3529 - 3735
Minimum	3953	3763 - 3985	3610	3537 - 3727
Maximum	3958	3789 - 4122	3602	3465 - 3738

From this table reading off the point estimate for the FOL give 311 years for the optimal, 343 years for the minimum and 356 years for the maximum degree of smoothing.

Now, to provide approximate 95% confidence intervals for each level of smoothing, an approximate 95% joint confidence region for the upper quartile of the *Cortaillod* culture and the lower quartile of the *Pfyn* culture is constructed using the approach outlined in section 6.3.2 and shown graphically in figures 6.25a-c for the optimal, minimum and maximum smoothing (note that the boxed intersection area represents the conservative confidence region while the shaded 'elliptical' region is that of "minimum" area).

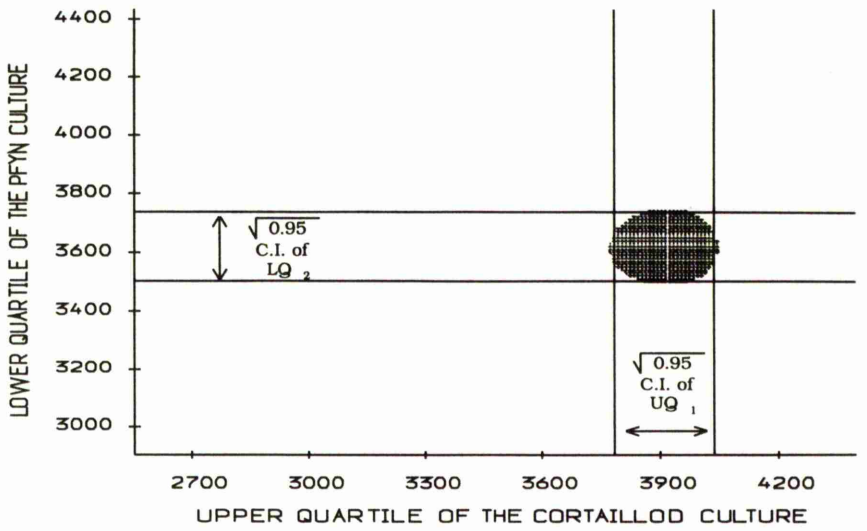

a)

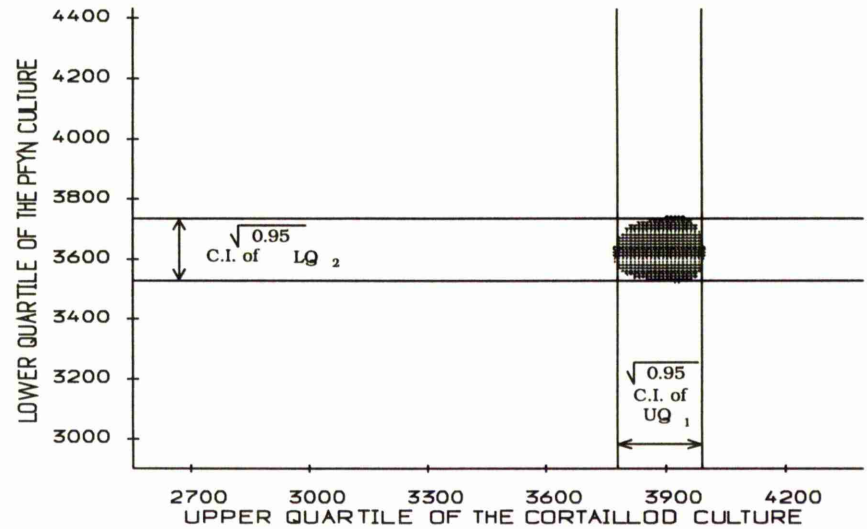

(b)

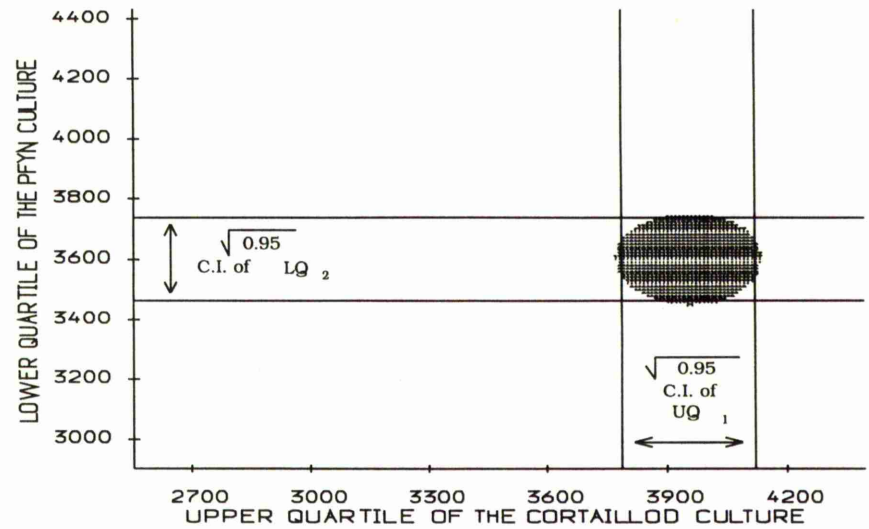

(c)

Figure 6.25 : An approximate 95% joint confidence region of the upper quartile of *Cortaillod* culture and the lower quartile of the *Pfyn* culture for a) the optimal, b) the minimum and c) the maximum degree of smoothing.

So if one wishes to provide an interval estimate for the FOL in a quick and easy way, formula 6.6 can be used to obtain an approximate 95% conservative confidence intervals of

45 - 463 years for the case of optimal smoothing,

36 - 448 years for the case of minimum smoothing

and 51 - 657 years for the case of maximum smoothing.

Based on the "elliptical" shaped regions an approximate 95% confidence intervals for the FOL are between

112 - 482 years for the case of optimal smoothing,

102 - 432 years for the case of minimum smoothing

and between 122 - 582 years for the case of maximum smoothing.

These intervals are narrower than the conservative intervals in each of the cases by 48, 82 and 146 years respectively.

From the above results the conservativeness of the first approach is clearly illustrated - especially for the maximal amount of smoothing. The influence of the degree of smoothing on the estimated FOL can be seen, graphically, in figures 6.26a&b for the individual influence of the degree of smoothing on the FOL for the *Cortaillod* and *Pfyn* cultures respectively while the simultaneous effect of the degree of smoothing of these two cultures is graphed in figure 6.27.

Similar to the POL, one can summarise the above results by concluding an overall estimate for the FOL between the *Cortaillod* and *Pfyn* cultures (rounded to the nearest 100 years) to be **300** years for the point estimate with an interval estimate of between **100** and **600** years.

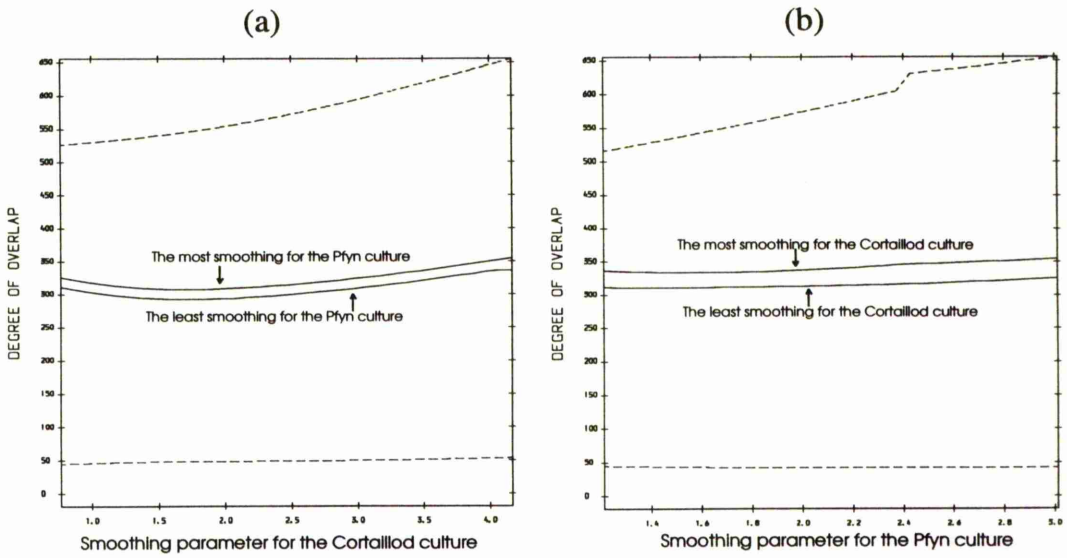

Figure 6.26 : Effect of the degree of smoothing on the point (solid) and interval (dotted) estimates of the FOL between the *Cortaillod* and *Pfyn* cultures.

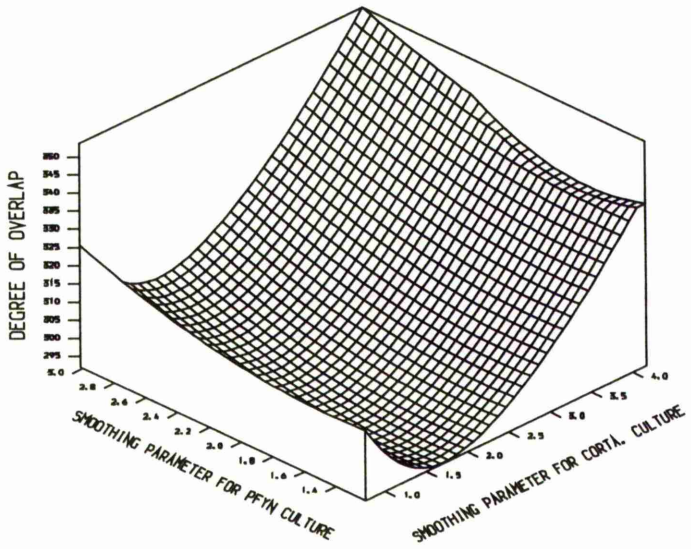

Figure 6.27:
An inclusive illustration for the effect of the degree of smoothing on the estimated FOL between the *Cortaillod* and *Pfyn* cultures.

6.5 Summary

This chapter has been devoted to the problem of overlap of archaeological cultures. The concept of the overlap in the archaeological sense was reviewed and a definition of overlap was given conceptually and mathematically. There are three situations worthing separete consideration *i.e.* where there is no overlap, partial overlap or complete overlap. Of these three situations, concentration was centred on the partial overlap since it is represents the practical problem.

One simple method of checking the overlap of two cultures using histograms has been presented and two formal methods of measuring the overlap have been considered.

The first method measures the proportional overlap (POL) which was defined to be a measure of the common timespan on the historical timescale of the two cultures. It was classified into single and multi-modal overlap and only the single overlap was considered. The second method measures the floruit overlap (FOL) between two cultures and was defined to be the number of common years to the two floruits of the cultures.

Approaches to provide point and interval estimates for both the POL and FOL have been given and ad hoc approach which provides an upper limit for the degree of smoothing was introduced to restrain the frequency distribution from being over-smoothed.

The chapter concluded with three illustrative examples representing the cases of little, moderate and significant overlap. In these examples the influence of the smoothing degree of the frequency distribution and the effect of an outlier (in the moderate case) on the estimated overlap were considered. The degree of smoothing was found to have a moderate whereas the outlier date had a negligible effect on the estimation of overlap.

Chapter 7

Conclusions and Further Work

7.1 Conclusions

The main concern in this work which has been described in the preceding chapters was to introduce and develop statistical approaches which would provide a statistical basis to the estimation of the duration of settlements in archaeological contexts by means of radiocarbon calibration. There are three distinct aspects of such work covered by this thesis.

The first of these was put forward in chapter 2 and dealt with the problem of the fitting of the radiocarbon calibration curve and the calibration procedure which turns a measure of single radiocarbon date into an estimate of a calendar/historical date. The calibration curve data used was the Irish oaks data (Pearson *et al*; 1986) and was fitted using a technique based on the kernel non-parametric regression estimator (Watson; 1964) with the smoothing parameter chosen by cross-validation. The main purpose here was to review

the procedures of calibration of a single radiocarbon date both from the view of point and interval estimation. It has been found that all the calibration methods reviewed provided effectively the same results and the major factors involved in the uncertainty of the true historical age were a realistic estimate of the error in the data, the error in the curve and the slope of the curve in the region of the calibration. The basic recommendation was the use of a graphical approach particularly when the calibration is carried out on flat parts of the curve. As many archaeologists may not have access to suitable software to carry out the calibration, the graphical method suggested by Neftel (1980) and revised by Aitchison and Scott (1987) is the graphical approach which would be recommended.

The second and main aspect of this thesis was presented in chapters 3-5 and dealt with problem of summarising a set of radiocarbon dates from a single archaeological phenomenon. Five methods based on the idea of using sample quartiles were set forth to provide point and interval estimates for the ***floruit*** of archaeological culture on a historical timescale by means of the calibration of the radiocarbon dates of a representative sample of artefacts or materials from the culture. These methods, which divided into simple pen and paper or highly computational methods, can provide a coherent summary of the full sample through estimation of the floruit. Such estimation procedures were found to converge with increasing sample size to the true underlying floruit *i.e.* the true quartiles. The simple methods have the advantage that they can be applied with only pencil, paper and the calibration curve while one advantage of the highly computational methods is the estimation of the density function underlying the culture to give an extremely useful guide to the full extent of the phenomenon on historical timescale.

In chapter 4 the performances of the five methods were investigated in a simulation study with data simulated from Normal, Skewed and Bimodal

distributions. Particular attention was paid to their performances over different parts of the calibration curve and for different combinations of sample size and inter-quartile range (I.Q.R.) of the underlying frequency distribution. Their performances were then compared according to four criteria (Coverage, Wastage, Population Coverage and Confidence) defined in section 4.3.

Simulation results revealed that, for small I.Q.R., there were no differences among the five methods and they were all high in terms of average coverage, population coverage, confidence and unfortunately wastage whatever the sample size and the parent distribution. For large I.Q.R., some methods were better than others on certain combinations but no particular method was consistently superior to the others. As was perhaps expected, it was found that, for all the five methods, any increase of coverage and confidence came out at the expense of increasing wastage and population coverage. In most cases the pen and paper methods were found to be the worst regarding the coverage and confidence but better than the highly computational (density estimation) methods regarding wastage and population coverage. It was also found that the density estimation methods have the advantages that they have the highest coverage and confidence whatever the sample size and the I.Q.R. and their wastages decreased with sample size. Further the population coverage tended to 50% as $n \to \infty$ *i.e.* the correct coverage for the true floruit.

The main conclusion drawn from the simulation results was that, of the five methods, the density estimation methods are best and among such, **D**, which provides the interval estimate for the floruit with variance of the estimated cumulative distribution function approximated by $\frac{\hat{F}(t)\{1-\hat{F}(t)\}}{n}$, was preferable. However if the choice is limited to pen and paper methods then method **B**, which provides the interval estimate for the floruit by using the

extended quartile interval for the calibrated/historical dates based on the fractional weighting scheme, is worth consideration as a first order approximation.

The performances of the five methods were then subjected to further investigation and comparison in chapter 5 where a number of real data applications, each with different features, were presented to illustrate the applicability of the five methods to such groups of radiocarbon dates and to discuss the effect of various factors on the resultant estimates.

It was difficult in the applications to appreciate the influence of each factor individually since each application generally covered a combination of different factors. Nevertheless, and without neglecting the effect of the other factors which exist, the results of the applications revealed that the shape of the calibration curve and the degree of smoothing on the density function had the most influence on the floruit estimates obtained from the five methods. Also, the results agreed with the simulation results regarding the effect of the sample size where the floruit estimates tended to be poor with small sample size particularly for the density estimation method **E**, where the variance of the estimated cumulative distribution function is approximated by $\frac{(0.25)(0.75)}{n}$, and is the substantially affected by the sample size. When the effect of a possible outlier date on the floruit estimate was considered, the results showed that these methods (except **E** with small sample size) dampen out its effect. Hence these are reasonably robust to the presence of a few outliers, eliminating the need to identify and eliminate suspected outliers. In the choice of optimal method the results of the different applications seemed to agree with the conclusions of the simulation results in that method **D** would be the best of all five methods and **B** would be the alternative choice among the pen and paper methods.

The third important aspect of the thesis was put forward in chapter 6 which considered the problem of overlap between two archaeological cultures. Of three situations of overlap (complete, partial and no overlap), attention was restricted to the practical problem of partial overlap involving a single point of intersection of the underlying density estimates.

An initial, simple approach was suggested for checking the overlap by constructing back-to-back histograms for both radiocarbon and historical dates of the two cultures. The density estimation technique was adapted to measure the overlap of two archaeological cultures in a formal manner. Two different measurements were proposed for this purpose involving measurement of proportional (POL) and floruit (FOL) overlap. The POL measures the common timespan, on the historical timescale, of the two cultures and defined mathematically to be the common proportion of the two frequency distributions underlying the two cultures. The FOL measures the number of common years to the two floruits and defined mathematically to be the difference between the upper quartile of the frequency distribution of the younger culture and the lower quartile of the frequency distribution of the older culture. The starting point in the measurement of POL was the estimation of the intersection point of the two density functions while it was the estimation of the floruit of each culture in the measurement of FOL. For both definitions the main factors involved in the uncertainty of the overlap were the degree of smoothing in the estimation of the density functions underlying each of the two cultures and the variability in the estimation of the cumulative distribution function of each culture. For investigation of the effect of smoothing degree on the overlap, an ad hoc approach was suggested to provide an upper limit for the degree of smoothing and to restrain the density estimate from being over-smoothed.

Three different archaeological applications were considered to cover the cases of little, moderate and significant overlap as well as the effect of an outlier date in the case of a moderate overlap. The results showed that the degree of smoothing of the density estimate has a reasonable influence on both POL and FOL while the effect of an outlier date seemed to be relatively small as the method of density estimation appeared to damp out the effect of a single outlier on the estimate of density function and hence on the estimate of overlap.

7.2 Further Work

As is always the case, the work described in the previous chapters could not possibly hope to answer all of the questions of interest in the area covered. Rather, it can be thought of as a starting point for more research. There is much scope for further work that could be done and here some points are given in which this work may be extended :-

- Extend the data set for calibration beyond the Irish oaks data, for instance fit a calibration curve for the Seattle data (Stuiver and Pearson; 1986) in order to consider the influence of using a different calibration curve on the floruit estimation.

- Although it has been mentioned in this thesis that, there is not much to choose, in terms of performance, between the different methods for constructing the calibration curve, nevertheless one method may be more suitable for a particular application. Thus, it would be a good idea to consider the use of different methods for fitting the calibration curve such as the use of smoothing splines (Wegman and Wright; 1983 and Silverman; 1985) or convoluted smoothing (Clark; 1977) in order to see how this will affect floruit estimation.

- Investigate extensions to the pen and paper methods to maintain coverage and confidence while not effecting a large increase in wastage and population coverage. It is not clear what this precise extension would be but it may include:-

  a) Calibration of the sample quartiles of the radiocarbon dates into the historical timescale and then provide an interval estimate for the calibrated quartiles.

  b) Using a different multiple than 0.6745 for the standard errors in the calculation of the extended series of the radiocarbon and historical dates.

- Further investigation of the density estimation methods would be worthwhile. This might involve:-

  a) A different method for the choice of optimal smoothing parameter which is a top priority requirement.

  b) A possible alternative to the kernel density estimation procedure such as the nearest neighbour method or the maximum penalized likelihood estimators (Silverman; 1986).

- Naylor and Smith (1988) have introduced a Bayesian method as an alternative approach for dealing with a set of radiocarbon dates. This approach, which considers some prior information about the conversion of the radiocarbon dates into calendar dates, has been outlined and discussed in depth by Litton and Leese (1991) and has seen much development during the last few years by several authors (Buck *et al*; 1991, Buck & Litton; 1991, Buck *et al*; 1992 and Christen; 1994). It is clear that the Bayesian approach to floruit estimation is different from that outlined in this thesis and thus a comparison between the two approaches would be worthwhile.

- The idea of estimating the overlap in the case of single point of intersection may be extended to cover the case of multi-modal partial overlap.

These points of further work are suggestions and might be supplemented and modified at a later stage by other ideas. Although the ideas for further research work are useful, the most important remaining task for the author of this thesis is the translation of the work done so far into appropriate software to be, easily, used by the archaeologists.

References

Aitchison; T.C., Leese; M., Michczynska; D.J., Mook; W.G., Otlet; R.L., Ottaway; B.S., Pazdur; M.F., Van der Plicht; J., Reimer; P.J., Robinson; S.W., Scott; E.M., Stuiver; M. and Weninger; B. **(1989).**

A comparison of methods used for the calibration of radiocarbon dates.

Radiocarbon, Vol 31, No. 3, pp. 846-864. Proceedings of the 13th International Radiocarbon Conference, Dubrovnik, 1988.

Aitchison; T.C., Ottaway; B.S. and Al-Ruzaiza; A.S. **(1991).**

Summarising a group of 14C dates on the historical time scale: with a worked example from the Late Neolithic of Bavaria.

Antiquity, Vol 65, No. 246, pp. 108-116.

Aitchison; T.C., Ottaway; B.S. and Scott; E.M. **(1990).**

Statistical treatment of groups of related radiocarbon dates.

Proceedings of the 2nd symposium on archaeology and ^{14}C, Groningen 1987.

Aitchison; T.C. and Scott; E.M. **(1987).**

A review of the methodology for calibrating radiocarbon dates into historical ages.

In: **Applications of Tree-ring Studies, Current Research in Dendrochronology and Related Subjects** (edited by R. Ward), Oxford: **BAR** international series 333, pp. 187-201.

Arnold; J.R. and Libby; W.F. **(1949).**

Age determinations by radiocarbon content: Checks with samples of known age.

Science 100, pp. 678-680.

Azzalini; A. **(1981).**

A note of the estimation of a distribution function and quantiles by a kernel method.

Biometrika 68, pp. 326-328.

Bowman; A.W. **(1981).**

Some aspects of density estimation by the kernel method.

Ph.D Thesis, University of Glasgow, Glasgow

Bowman; S. **(1990).**

Radiocarbon Dating - (Interpreting the Past).

British Museum Publications, London.

Bruns; M., Munnich; K.O. and Becker; B. **(1980).**

Natural radiocarbon variations from 200-800 AD.

Radiocarbon, Vol 31, No. 3, pp. 273-278.

Buck; C.E., Kenworthy; J.B., Litton; C.D. and Smith; A.F.M. **(1991).**

Combining archaeological and radiocarbon information : a Bayesian approach to calibration.

Antiquity, Vol 65, pp. 808 - 821.

Buck; C.E.and Litton; C.D **(1991).**

Applications of the Bayesian paradigm to archaeological data analysis.

Actes du XII congres international des sciences prehistoriques et protohistoriques (ed. J. Pacvuk). Bratislava, pp. 367-374.

Buck; C.E., Litton; C.D. and Smith; A.F.M. **(1992).**

Calibration of radiocarbon results pertaining to related archaeological events.

Journal of Archaeological Science, 19, pp. 497 - 512.

Christen; J. A. **(1994).**

Summarizing a set of radiocarbon determinations: a robust approach.

Applied Statistics, Vol 43, No. 3, pp. 489 - 503.

Clark; R.M. **(1975).**

A calibration curve for radiocarbon dates.

Antiquity, Vol 49, pp. 251-266.

Clark; R.M. **(1977).**

Non-parametric estimation of a smooth regression function.

Journal of the Royal Statistical Socity, Vol 39(B), pp.107-113.

Clark; R.M. **(1979).**

Calibration, Cross-validation and carbon-14, I.

Journal of the Royal Statistical Society, Ser. A, 142, Part 1, pp.47-62.

Conover; W.J. **(1971).**

Practical Nonparametric Statistics.

John Wiley & sons, New York.

Damon; P.E., Ferguson; C.W., Long; A. and Wallick; E.I. **(1974).**

Dendrochronologic calibration of the radiocarbon timescale.

American Antiquity, Vol 39, pp. 350-366.

Dergachev; V. **(1989).**

Neolithic and Bronze Age Cultural Communities of the Steppe Zone of the USSR.

Antiquity, Vol. 63, No. 241, pp. 793 - 802.

Duin; R.P.W. **(1976).**

On the choice of smoothing parameters for Parzen estimators of probability density functions.

I.E.E.E. Trans. Comput., C-25, pp. 1175-1179.

Epanechnikov; V.A. **(1969).**

Nonparametric estimation of a multivariate probability density.

Theory Prob. Applic. 14, pp. 153-158.

Fleming; S. **(1976).**

Dating in Archaeology: A Guide to Scientific Techniques.

J. M. Dent & Sons Ltd., London.

Geyh; M. and de Maret; P. **(1982).**

Histogram evaluation of 14C dates applied to the first Iron Age sequence from west Central Africa.

Archaeometry 24, pp. 158-163.

Gibbons; J.D. **(1971).**

Nonparametric Statistical Inference.

McGraw-Hill Book company, New York.

Gimbutas; M. **(1965).**

The Relative Chronology of Neolithic and Chalcolithic Cultures in Eastern Europe, North of the Balkan Peninsula and the Black Sea.

In: **Chronologies in Old World Archaeology** (edited by R. Ehrich), pp. 459 - 502, The University of Chicago press: Chicago and London.

Godwin; H. **(1962).**

Half-life of radiocarbon.

Nature 195, pp. 984.

Habbema; J.D.F., Hermans; J. and Van der Broek; K. **(1974).**

A stepwise discrimination program using density estimation.

In: **Bruckman; G. (ed.)**, Compstat 1974. Vienna: Physica Verlag, pp. 100-110.

Harkness; D.D. **(1975).**

The role of the archaeologist in C-14 age measurement.

In: **Radiocarbon: Calibration and prehistory** (edited by Trevor Watkins), appendix II, pp. 128 - 135, Edinburgh University press.

Houtermans; J.C. **(1971).**

Geophysical interpretations of Bristlecone pine radiocarbon measurements using a method of Fourier analysis for unequally spaced data.

Ph.D Thesis, University of Bern, Switzerland.

International Study Group **(1982).**

An inter-laboratory comparison of radiocarbon measurements in tree rings.

Nature 298, pp. 619-623.

International Study Group **(1983).**

An international tree ring replicate study.

In: **Radiocarbon and Archaeology**, PACT 8, pp. 123-133.

Klein; J., Lerman; J.C., Damon; P.E. and Linick; T.W. **(1980).**

Radiocarbon concentrations in the atmosphere: 8000 year record of variations in tree rings. First results of a USA workshop.

Radiocarbon, Vol 22, No. 3, pp. 950-961.

Klein; J., Lerman; J.C., Damon; P.E. and Ralph; E.K. **(1982).**

Calibration of radiocarbon dates : Tables based on the concensus data of the Workshop on calibration of the radiocarbon timescale.

Radiocarbon, Vol 24, No. 2, pp. 103-151.

Libby; W.F. **(1955).**

Radiocarbon Dating (2nd ed.).

University of Chicago press, Chicago.

Lindley; D.V. **(1965).**

Introduction to Probability and Statistics from a Bayesian Viewpoint (Part 1 Probability).

Cambridge University press, Cambridge.

Litton; C. D. and Leese; M. N. **(1991).**

Some statistical problems arising in radiocarbon calibration.

In: **Computer Applications and Quantitative Methods in Archaeology** (edited by K. Lockyear and S. Rahtz), Oxford: **BAR** international series 565, pp. 101-109.

Michels; J. **(1973).**

Dating Methods In Archaeology.

Seminar press, New York

Mood; A.M., Graybill; F.A. and Boes; D.C. **(1974).**

Introduction to the theory of statistics (3rd ed.).

McGraw-Hill International Book Company, Tokyo.

Naylor; J. C. and Smith; A. F. M. **(1988).**

An archaeological inference problem.

Journal of the American Statistical Association, Vol 83, No. 403, pp.47-62.

Neftel; A. **(1980).**

The construction of a radiocarbon calibration curve based on radiocarbon measurements of absolutely dated American tree ring samples.

Unpuplished report, University of Bern, Switzerland.

Neustupny; E. **(1968).**

Absolute chronology of the Neolithic and Aeneolithic periods in Central and SE Europe.

Archaeol Kozhl 21, pp. 783-809.

Noether; G.E. **(1967).**

Elements of Nonparametric Statistics.

John Wiley & Sons, inc, New York.

Olsson; I.U. **(1991).**

Conventional Radiocarbon Dating and Some Problems of ^{14}C Dating.

In: **Scientific Dating Methods** (H.Y. Goksu et al. eds.), pp. 15-35, ECSC, EEC, EAEC, Brussels and Luxembourg, Printed in the Netherlands.

Ottaway; B.S. **(1973).**

Dispersion diagrams: a new approach to the display of 14C dates.

Archaeometry, Vol 15(1), pp. 5-12.

Ottaway; B.S. **(1986).**

Is radiocarbon dating obsolescent for archaeologists?.

Radiocarbon, Vol 28, No. 2A, pp. 732-738.

Ottaway; B.S. **(1988).**

The Galgenberg, a Late Neolithic enclosure in Bavaria.

In: **Enclosures and defences in the Neolithic of Western Europe** (edited by C. Burgess, P. Topping, C. Mordant and M. Maddison), Oxford: **BAR** international series 403, pp. 391 - 418.

Pardi; R. and Marcus; L. **(1977).**

Non-counting errors in radiocarbon dating.

Annals New York Academy of Sciences, 288, pp. 174-180.

Park; B.U. and Marron; J.S. **(1990).**

Comparison of data-driven band width selectors.

Journal of the American Statistical Association, Vol 85, No. 409, Theory and methods, pp. 66-72.

Parzen; E. **(1962).**

On estimation of a probability density function and mode.

Annals Mathematical Statistics 33, pp. 1065-1076.

Pearson; G.W., Pilcher; J.R. and Baillie; M.G.L. **(1983).**

High precision radiocarbon measurement of Irish oaks to show natural radiocarbon variations from 200 BC to 4000 BC.

Radiocarbon, Vol 25, No. 2, pp. 179-186.

Pearson; G.W., Pilcher; J.R., Baillie; M.G.L., Corbett; D.M. and Qua;F. **(1986).**

High precision radiocarbon measurement of Irish oaks to show natural radiocarbon variations from AD 1840 to 5210 BC.

Radiocarbon, Vol 28, pp. 911-934.

Pearson; G.W., Pilcher; J.R., Baillie; M.G.L. and Hillam; J. **(1977).**

Absolute radiocarbon dating using a low altitude European tree ring calibration.

Nature, 270, pp. 25-28.

Prakasa Rao; B.L.S. **(1983).**

Nonparametric Functional Estimation.

Academic Press, New York.

Quitta; H. **(1967).**

The C-14 chronology of the Central and SE European Neolithic.

Antiquity, XLI, pp.263-270.

Ralph; E.K. **(1971).**

Carbon-14 Dating.

In: **Dating Techniques for the Archaeologist** (H.N. Michael and E.K. Ralph eds.), pp. 1 - 48, Cambridge, Massachusetts: The MIT press.

Rimantiene; R. **(1992).**

The Neolithic of the Eastern Baltic.

Journal of World Prehistory, Vol. 6, No. 1, pp. 97 - 143.

Rosenblatt; M. **(1956).**

Remarks on some nonparametric estimates of a density function.

Annals Mathematical Statistics 27, pp. 832-837.

Scott; D.W., Tapia; R.A. and Thompson; J.R. **(1977).**

Kernel density estimation revisited.

Nonlinear Analysis 1, pp. 339-372.

Silverman; B.W. **(1985).**

Some aspects of the spline smoothing approach to nonparametric regression curve fitting.

Journal of the Royal Statistical Society, Vol 46(B), pp. 1 - 52.

Silverman; B.W. **(1986).**

Density Estimation for Statistics and Data Analysis.

Chapman and Hall, London.

Stone; M. **(1974).**

Cross validatory choice and assessment of statistical predictions.

Journal of the Royal Statistical Society, Vol 36(B), pp. 111 - 147.

Stuiver; M. **(1982).**

A high precision calibration of the AD timescale.

Radiocarbon, Vol 24, No. 1, pp. 1-27.

Stuiver; M. and Pearson; G.W. **(1986).**

High-Precision Calibration of the Radiocarbon Time Scale, AD 1950-500 BC.

Radiocarbon, Vol 28, No. 2B, pp. 805 - 838.

Telegin; D.J. **(1987).**

Neolithic Cultures of the Ukraine and Adjacent Areas and their Chronology.

Journal of World Prehistory, Vol. 1, No. 3, pp. 307 - 331.

Titterington; D.M. **(1980).**

A comparative study of kernel-based density estimates for categorical data.

Technometrics 22, pp. 259-268.

Ward; G.K. and Wilson; S.R. **(1981).**

Evaluation and clustering of radiocarbon age determinations : Procedures and paradigms.

Archaeometry, Vol 23, No. 1, pp.19-39.

Waterbolk; H.T. **(1971).**

Working with radiocarbon dates .

Actes du VIII congres international des sciences prehistoriques et protohistoriques 1, pp. 11-25.

Watson; G.W. **(1964).**

Smooth regression analysis.

Sankhya A, 26, pp. 359-372.

Wegman; E.J. and Wright; J.W. **(1983).**

Splines in Statistics.

Journal of the American Statistical Association, Vol. 78, pp. 351-365.

Whittle; P. **(1958).**

On the smoothing of probability density functions.

Journal of the Royal Statistical Society, Vol 20 (B), pp. 334-343.

GLASGOW UNIVERSITY LIBRARY